NASA Conference Publication 2093

Workshop on Thrust Augmenting Ejectors

Cosponsored by NASA-Ames Research Center
Naval Air Development Center
Air Force Flight Dynamics Laboratory
Held at
Ames Research Center
Moffett Field, California
June 28-29, 1978

September 1979

NASA
National Aeronautics and
Space Administration

NASA Conference Publication 2093

Workshop on Thrust Augmenting Ejectors

Cosponsored by NASA-Ames Research Center
Naval Air Development Center
Air Force Flight Dynamics Laboratory
Held at
Ames Research Center
Moffett Field, California
June 28-29, 1978

Edited by
A. E. Lopez
D. G. Koenig, Ames Research Center, Moffett Field, California
D. S. Green, Naval Air Development Center, Warminster, Pennsylvania
K. S. Nagaraja, Air Force Flight Dynamics Laboratory
Wright-Patterson Air Force Base, Dayton, Ohio

National Aeronautics and
Space Administration

Ames Research Center
Moffett Field, California 94035

ERRATA

NASA Conference Publication 2093

WORKSHOP ON THRUST AUGMENTING EJECTORS

Edited by
A. E. Lopez and D. G. Koenig, Ames Research Center, Moffett Field, California
D. S. Green, Naval Air Development Center, Warminster, Pennsylvania
K. S. Nagaraja, Air Force Flight Dynamics Laboratory
Wright-Patterson Air Force Base, Dayton, Ohio

September 1979

Insert the attached References (pp. 6a-6b) between pages 6 and 7.

Insert amended page 512.

PREFACE

The proceedings of the Workshop on Thrust Augmenting Ejectors held at Ames Research Center, Moffett Field, California, on June 28 and 29, 1978, are reported in this Conference Publication. This workshop was sponsored by NASA/Ames Research Center, Naval Air Development Center, and Air Force Flight Dynamics Laboratory.

The purpose of this workshop was the dissemination of progress and to point the desired direction of future studies in all aspects of Ejector Thrust Augmenting Systems. Following the presentation of the formal papers a panel composed of some advocates of Ejector Thrust Technology Development presented their impression of the workshop, reviewed briefly the state of the art in ejector technology, and pointed out the desired direction of future research.

Contributions to this workshop were made by representatives from NASA Ames and Lewis Research Centers, Boeing Aircraft Company, Rockwell International, Air Force, Navy, George Washington University, Wright State University, Duvvuri Associates, Vought Corporation, Jet Propulsion Laboratory, University of Calgary, Flight Dynamics Research Corporation, Lockheed California Company, The de Havilland Aircraft of Canada, Ltd., University of Queensland, and University of Virginia.

TABLE OF CONTENTS

RECENT DEVELOPMENTS IN EJECTOR TECHNOLOGY IN THE AIR FORCE: AN OVERVIEW

K. S. Nagaraja

Air Force Flight Dynamics Laboratory, Aero Mechanics Division
Wright-Patterson Air Force Base, Ohio

As one of those who believe in the potential usefulness of thrust augmenting ejectors in flight, I feel honored to be here to speak a little on the ejector development that took place at Wright-Patterson Air Force Base. A great deal of fundamental and applied work (see the Bibliography) was performed in the course of the last fifteen to twenty years, and a considerable amount of the results has been published.

Initially, a systematic fundamental study was undertaken at the Aerospace Research Laboratories (ARL) at WPAFB under the direction of Hans Von Ohain. Subsequently, an applied study was initiated in the early 1970's at the Air Force Flight Dynamics Laboratory, and the specific task of completing the design of an ejector thrust augmented V/STOL aircraft was completed.

The basic studies at ARL conducted over a period of about ten years yielded several significant results (refs. 1-5). Extensive in-house studies at ARL and several contracted studies provided considerable information on ejector characteristics and on the design aspects of practical ejector for aircraft applications.

Following are some of the significant and fundamental developments in thrust augmenting ejectors that resulted from ARL's studies (ref. 6).

1. Development of hypermixing nozzles for mixing enhancement was achieved. This provided a basis for designing a more compact ejector (refs. 4, 5, 7-10).

2. Demonstration that mixing and diffusion of flows could be done simultaneously with performance advantage was accomplished. Previously, it was believed that performance advantage would result if diffusion is preceded by the accomplishment of complete mixing.

3. An incompressible ejector analysis which will parametrically evaluate an ejector performance was performed (ref. 5).

4. Thrust augmentation of the order of two in an ejector of inlet area ratio 23 was successfully achieved experimentally (ref. 7).

5. Good thrust augmentation for V/STOL purposes was also realized by using full-scale multichannel ejectors (ref. 11). Bypass air from a turbofan engine was diverted by suitable valving into the ejectors installed in a wing. Test data confirmed that an aircraft-installed ejector would perform satisfactorily.

6. It was demonstrated that diffusion normal to the plane of the velocity profile always leads to improved mixing in contrast to diffusion in the plane of the velocity profile (refs. 6, 12).

7. An ejector-wing model (6 ft model) was designed, fabricated and tested (under an ARL sponsored study which was performed by the Bell Aerospace Company in a wind tunnel (ref. 13). The tests showed that the resulting favorable supercirculation effects due to the ejector flow would enable transitioning from hover to cruise condition even when the lift due to the thrust component is drastically reduced. This supercirculation effect resulting from an ejector wing in flight points out the inherent shortcoming of an ejector incorporated in the fuselage of an aircraft (as was done in the case of the Hummingbird).

8. Further compactness of the ejector was realized by the utilization of a device that combines efficient boundary-layer energization with a configured diffusion device, that is, trapped vortex cavity (ref. 14). This work was performed under contract by the Advanced Technology Center, Inc. of the Vought Corporation, Dallas, Texas.

A few of ARL's publications and others which describe the fundamental ejector developments are indicated in the bibliography which also includes the reports resulting from other AF projects on thrust augmenting ejectors.

Air Force Flight Dynamics Laboratory of WPAFB undertook some exploratory study in the ejector area in the late 1960's. A more systematic design study of a V/STOL demonstrator aircraft was initiated in the early 1970's.

Initial exploratory studies supported under AFFDL contract led to the development of the so-called Jet Flap Diffuser Ejector (JFDE). Although jet flap diffuser concept had been proposed earlier in France, no systematic effort was undertaken then to develop an effective configuration. Hans Von Ohain's suggestion regarding the orientation of the primary jet injection relative to the inlet geometry proved successful, and the subsequent tests performed on the jet diffuser ejector at the Flight Dynamics Research Corporation in California showed that relatively high thrust augmentation could be realized in a compact ejector.

In support of the design study of a V/STOL demonstrator vehicle trailing-edge ejectors on wings were fabricated and tested (refs. 15, 16). One of the wind-tunnel models (ref. 15) was fabricated and tested in the 7- by 10-ft low speed tunnel at NASA-Ames. This wind-tunnel model was a constant chord two-dimensional 30-in. span and 44.5-in. chord (with the flaps up) model. The tests assessed the lift off and low speed transition phases of flight. The results of the tests showed that in an aircraft configuration, with sufficient BLC provided, a trailing-edge ejector system could provide predicted levels of thrust augmentation. Some insight was also gained about optimal flap settings for transitioning the aircraft from hover to cruise condition.

Preliminary design of an ejector thrust augmented aircraft required a theoretical methodology which could evaluate the performance of the ejectors subject to a wide range of variation in the thermodynamic parameters of the

injected and entrained fluids. A compressible ejector flow analysis was developed by assuming that the primary and the secondary streams mixed in a constant area duct (ref. 17). The schematic of the single-stage ejector is shown in figure 1. The analysis was performed in steps as shown below:

1. Pressures were prescribed incrementally at station 1, and the other flow quantities were determined from the thermo fluid dynamic relations.

With choked primary flow, the static pressure of the secondary flow was allowed to take on values less than the primary static pressure. The computations were cut off just before the secondary Mach number reached unity.

The analysis was extended to include the ejector flight velocities in the performance calculations. While in flight, the static pressure at station 1 was allowed to take on values greater than the ambient air static pressure, but less than the ambient stagnation pressure. It was noted in some instances from the results that the ejector performance reached optimum levels whenever the entrained air was compressed as it entered the injection station 1. This characteristic requires some further examination.

2. The momentum balance equation in the constant area mixing duct also included the total ejector flow losses evaluated empirically from the test results of ARL.

The velocity of the mixed flow at station 2 was provided by a quadratic equation — one solution corresponding to mixed subsonic flow, and the other corresponding to mixed supersonic flow. Only the subsonic solution was considered, and the supersonic solution was ignored.

3. Diffuser flow was evaluated isentropically. However, any diffuser loss that arises has been accounted for empirically in the momentum equation.

4. Considerations to the thermodynamic constraints (i.e., no entropy decrement as the flow moves forward) were given in the computations.

Typical results of the calculations are shown in figure 2. It is worth noting that the net thrust augmentation reaches a peak value around 2 for the diffuser area ratio and then begins to drop. This indicates that the flow in the diffuser is separating from the walls. Further, the net thrust augmentation decreases as the primary air stagnation temperature is increased. In fact, the performance degradation with increasing primary stagnation temperature was consistently demonstrated by the computed data for all cases of inlet area ratio, temperature conditions and pressure ratio. It should, however, be noted that experiments have also shown that the effect of temperature is minimal on an incompletely mixed flow (ref. 18). Regarding the pressure ratio effect on the ejector performance, the situation is quite complicated. The pressure ratio effect seems to depend on the inlet area ratio, the primary stagnation temperature and the static pressure at the injection plane (i.e., the diffuser area ratio).

The effect of ejector forward velocity on the thrust augmentation ratio is quite conceivable. As the forward velocity increases, the net thrust

augmentation decreases due to ram drag. The results shown in figure 3 illustrate typically the ejector performance in flight. However, as will be shown later, an ejector with a different operating thermodynamic condition in the shroud would provide a different performance characteristic (ref. 19). This will be discussed subsequently in some detail.

The sensitivity of ejector performance to inlet conditions is illustrated in figure 4. In fact, an operating ejector in an aircraft may well require a variable inlet geometry for yielding optimal performance. Inlet design is a significant factor in optimal ejector designs, for it is the effect of the pressure forces acting on the inlet that determines the thrust magnitude. However, the performance may become sensitive to other ejector components also, for example, at higher forward velocities. Sensitivity of the ejector components as well as of the ejector itself will have to be carefully evaluated, especially when the ejector is installed in an airplane.

It is worth making reference to the performance calculation of a two-stage ejector. A schematic of a two-stage ejector being considered is shown in figure 5. The performance calculations are illustrated in figure 6. It is seen that with smaller inlet area ratios in the two staging process, augmentations which correspond to those of high inlet area ratios in single-stage ejector can be achieved. The potential usefulness of staging may also be realized if a staged ejector becomes necessary due to the packaging problems in an airframe.

Based on the data obtained from the analysis, preliminary design study of a V/STOL demonstrator vehicle was conducted (ref. 20). An RPV vehicle having a canard wing arrangement with a trailing-edge ejector, balanced by a forward fuselage ejector was designed (figure 7). The injection area ratio of the ejectors was an optimum 13.5 which was designed to produce a thrust augmentation ratio of 1.66 or a VTOL gross weight of 896 lb. The design configuration was powered by the Williams F107-WR-100 engine which in turn fed the fuselage and wing trailing-edge ejectors. At the maximum VTOL weight, the vehicle was designed with fuel capacity of 205 lb, and with full control capability. Further, it had hover acceleration margin of 1.02, radius of 100 n. mi. and loiter time of 100 min. Internal ducting characteristics were evaluated based on the pressure losses due to the internal aerodynamics (ref. 21). A digital computer program for calculating the internal gas ducting system weight of the ejector thrust augmented vehicle was developed for the vehicle sizing determination (ref. 22). This program is capable of generating a large and consistent amount of trade-off data for achieving an optimum vehicle.

Aside from the design studies performed at AFFDL, some theoretical studies on augmentors and augmentor wings were also performed. Particularly, Hasinger's investigations (refs. 23-26) were noteworthy. Although the objective of the investigations is to design a jet pump which would yield the lowest possible primary plenum pressure to achieve a given pressure ratio (of the ejector exhaust stagnation pressure to the secondary stagnation pressure) at a given mass flow ratio (of the primary mass flux to the entrained mass flux), the analysis which deals with both subsonic as well as supersonic mixed flow cases is capable of yielding information that will be relevant to thrust augmenting ejector designs as well. The analysis also indicates the inlet flow conditions

which determine whether the mixed flow is coming subsonically or supersonically at the exit of the mixing duct.

High lift characteristics of an ejector-flapped wing was theoretically evaluated by Woolard (ref. 27) for a two-dimensional wing section with a point sink located aft of the wing chord for simulating the ejector intake flow. The work also treated the matching problem of the airfoil external flow with the ejector internal flow and derived the overall ejector-flapped wing section aerodynamic performance. Comparisons of the lift characteristics of an ejector-flapped wing with those of a jet augmented flapped wing show the superior performance of the former at low forward speeds. Significant items in the analytical approach and evaluation of the results are presented in the author's paper presented elsewhere in this volume.

A three-dimensional calculation method for determining the aerodynamic characteristics of arbitrary ejector-jet-flapped wings was developed under AFFDL contract by the McDonald-Douglas Aircraft Company. The computer program which is user oriented is capable of generating the aerodynamic coefficients including the ground effect of arbitrary wing-ejector configurations. The analysis program is based on the linear theory, and compressible ejector flow program is coupled with the wing aerodynamic program of Douglas.

A trailing-edge ejector installed on a wing was fabricated and tested in the AAFDL subsonic tunnel whose test section measures one square meter (ref. 28). The wind-tunnel model was provided with an upper door at the inlet which in cruise flight condition would fold down as the ejector flaps would fold up to provide the conventional cruise wing. The upper door which captured the external flow and directed the flow into the ejector shroud was designed to be set at different angles relative to the wing plane. It was possible also to set the ejector flaps at desired angles. The semispan wing ejector model was one fourth the scale of the wing ejector designed for the AFFDL V/STOL demonstrator vehicle. Lift, drag, and pitching-moment data were taken over a range of upper door setting angles, the ejector flap angles and at several angles of attack as the wind-tunnel airspeed was varied from 20 to 60 ft/sec. The test result showed, for example, that the wing stall angle was substantially larger compared to the unpowered (or the unaugmented) case. Flow visualization tests were also performed utilizing helium bubbles. These tests showed the separated flow region on the exterior side of the aft flap of the ejector for certain configuration positions. The tests demonstrated again the favorable lift characteristics that would result in the ejector augmented case.

Recent theoretical calculations of ejector performance have shown that under certain conditions, it appears to be possible to achieve relatively high thrust augmentation values in forward flight (ref. 19). Based on the results obtained from a simple, incompressible evaluation of the ejector performance (fig. 8), it became clear that proper aerothermodynamic matching of the ejector flows (also including the ejector geometric characteristics) would play a significant role in optimal ejector designs. An effort on a more systematic evaluation of ejector performance was undertaken under AFFDL contract by the Flight Dynamics Research Corporation, Van Nuys, California. The investigations utilized one-dimensional compressible flow equations much the same way as was done in reference 20, and these equations, without accounting for ejector

losses, were solved by incrementally assigning values to the inlet flow Mach number M_1 of the entrained stream at the injection plane. In reference 20, the solution process was explicitly started by assigning values incrementally to the static pressure at the injection plane.

Loss effects were not analytically accounted for in the initial studies primarily because all the realistic losses could be estimated only after the geometric and other related flow parameters were fixed based on the objectives of the specific ejector mission roles. However, the analysis that would account for the incomplete mixing effects as well as the skin-friction effects was performed in a general sense.

The calculations in reference 33 were performed by imposing the thermodynamic constraint that the entropy did not decrease as the flow progressed in the ejector toward the exit. This ensured that only physically acceptable solutions were utilized in the ejector performance calculations. The present investigations considered mixed supersonic flow conditions also, unlike those reported in reference 17. The ejector performance was evaluated based on both the first solution (corresponding to the subsonic mixed flow) and the second solution (corresponding to the supersonic mixed flow).

The results of the calculations are shown in figures 9-16. The results shown in figure 9 pertain to the same ejector as indicated in figure 10. The plus and minus signs in parentheses indicate that the results correspond to supersonic and subsonic mixed flows respectively at the end of the mixing duct. Propulsive efficiency, if defined in the classical manner where the reference jet energy is purely mechanical, can exceed one in certain thermodynamic situations because the thermal energy of the primary jet can also contribute along with the jet kinetic energy to the useful work produced by the system. However, if the reference jet energy is the total jet energy (including mechanical and thermal components), then the propulsive efficiency will be less than unity.

The data in the figures 9-16 indicate that ejectors, based on the so-called second solution, exhibit a great deal of potential usefulness as thrust augmentors. It is necessary to pursue further the design aspects of such practical ejectors. A great deal of parametric analysis as well as design optimization studies will be required before new ejector configurations can be defined. However, the possibility of deriving new ejector concepts for thrust augmentation purposes is clearly indicated by the recent AFFDL studies.

REFERENCES

1. Fancher, R. B.: A Compact Thrust Augmenting Ejector Experiment. ARL 70-0137 (AD 713634), Aug. 1970.

2. Fancher, R. B.: Low-Area Ratio Thrust Augmenting Ejectors. J. Aircraft, vol. 9, March 1972 (Also AIAA Paper 71-576, June 1971).

3. Eastlake, C. N.: The Macroscopic Characteristics of Some Subsonic Nozzles and the Three-Dimensional Jets They Produce. ARL 71-0058, March 1971.

4. Quinn, Brian: Compact Ejector Thrust Augmentation. J. Aircraft, vol. 10, no. 8, Aug. 1973.

5. Quinn, Brian: Recent Developments in Large Area Ratio Thrust Augmentors. AIAA Paper 72-1174, Nov. 1972.

6. Viets, Hermann: Thrust Augmenting Ejectors. ARL 75-0024, June 1975.

7. Quinn, Brian: Experiments with Hypermixing Nozzles in an Area Ratio 23 Ejector. ARL 72-0084, June 1972.

8. Quinn, Brian: Wind Tunnel Investigations of the Forces Acting on an Ejector in Flight. ARL 70-0141, July 1970.

9. Bevilaqua, P. M.: An Evaluation of Hypermixing for V/STOL Aircraft Augmentors. AIAA Paper 73-654, July 1973.

10. Bevilaqua, P. M.: An Analytic Description of Hypermixing and Test of an Improved Nozzle. AIAA Paper 74-1190, Oct 1974.

11. Campbell, David R.; and Quinn, Brian: Full Scale Tests of an Augmentor VTOL Concept. AIAA Paper 73-1185, Nov. 1973.

12. Viets, Hermann; and Quinn, Brian: Concurrent Mixing and Diffusion in Three-Dimensions. AIAA Paper 75-873, June 1975.

13. Ryan, P. E.; and Breidenstein, R. M.: Wind Tunnel Test Data Report for a Powered 1/5 Scale ARL/Bell V/STOL Aircraft Model. Bell Aero Space Company Report No. 2353-921002, June 1969.

14. Haight, Charles H.; and O'Donnell, R. M.: Experimental Mating of Trapped Vortex Diffusers with Large Area Ratio Thrust Augmentors. ARL 74-0115, Sept. 1974.

15. Brown, Squire L.; and Murphy, Ronald D.: Design and Test of Ejector Thrust Augmentation Configurations. AGARD CPP-143, April 1974.

16. Clark, Rodney L.: Ejector Blown Lift/Cruise Flap Wind Tunnel Investigation. AFFDL-TR-73-132, Nov. 1973.

17. Nagaraja, K. S.; Hammond, David L.; and Graetch, J. E.: One-Dimensional Compressible Ejector Flows. AIAA Paper 73-1184, Nov. 1973.

18. Quinn, Brian: Ejector Performance at High Temperatures and Pressures. J. Aircraft, vol. 13, no. 12, Dec. 1976, pp. 948-954.

19. Alperin, Morton; and Wu, Jiunn-Jeng: High Speed Ejectors. (To be published as an AFFDL Technical Report).

20. Byrnes, J. M.; Murphy, R. D.; Ball, R. F.; Nagaraja, K. S.; Hammond, D. L.; Langleben, E. A.; and English, R. B.: V/STOL Demonstrator Vehicle for Thrust Augmentation Technology. AIAA Paper 74-995, Aug. 1974.

21. Ball, Raymond F.: Internal Ducting Design Methodology for Applications to V/STOL Systems. AFFDL-TM-74-183-PTB, 1974.

22. Langleben, Edward A.: Digital Computer Program for Computing Total Internal Gas Ducting System Weights for an Ejector Thrust Augmented Vehicle. AFFDL-TM-74-181-PTB, 1974.

23. Hasinger, Siegfried H.: Simplified Lay-Out of Supersonic, Heterogeneous Ejectors. ARL 73-0149, Nov. 1973.

24. Hasinger, Siegfried H.: Performance Characteristics of Ejector Devices. ARL TR-75-0205, June 1975.

25. Hasinger, Siegfried H.; and Fretter, Earnest F.: Comparison of Experiment and Analysis for a High Primary Mach Number Ejector. AFFDL-TR-77-38, May 1977.

26. Hasinger, Siegfried, H.: Ejector Optimization. AFFDL-TR-78-23, June 1978.

27. Woolard, Henry W.: Thin-Airfoil Theory of an Ejector — Flapped Wing Section. J. Aircraft, vol. 12. Jan. 1975 (Also AIAA Paper 74-187).

28. Nagaraja, K. S.; and Clark, G. W.: A Wind Tunnel Study of the Effect of Free Stream Capture Area on the Aerodynamic Forces of a Thrust Augmenting Ejector-Wing. (To be published).

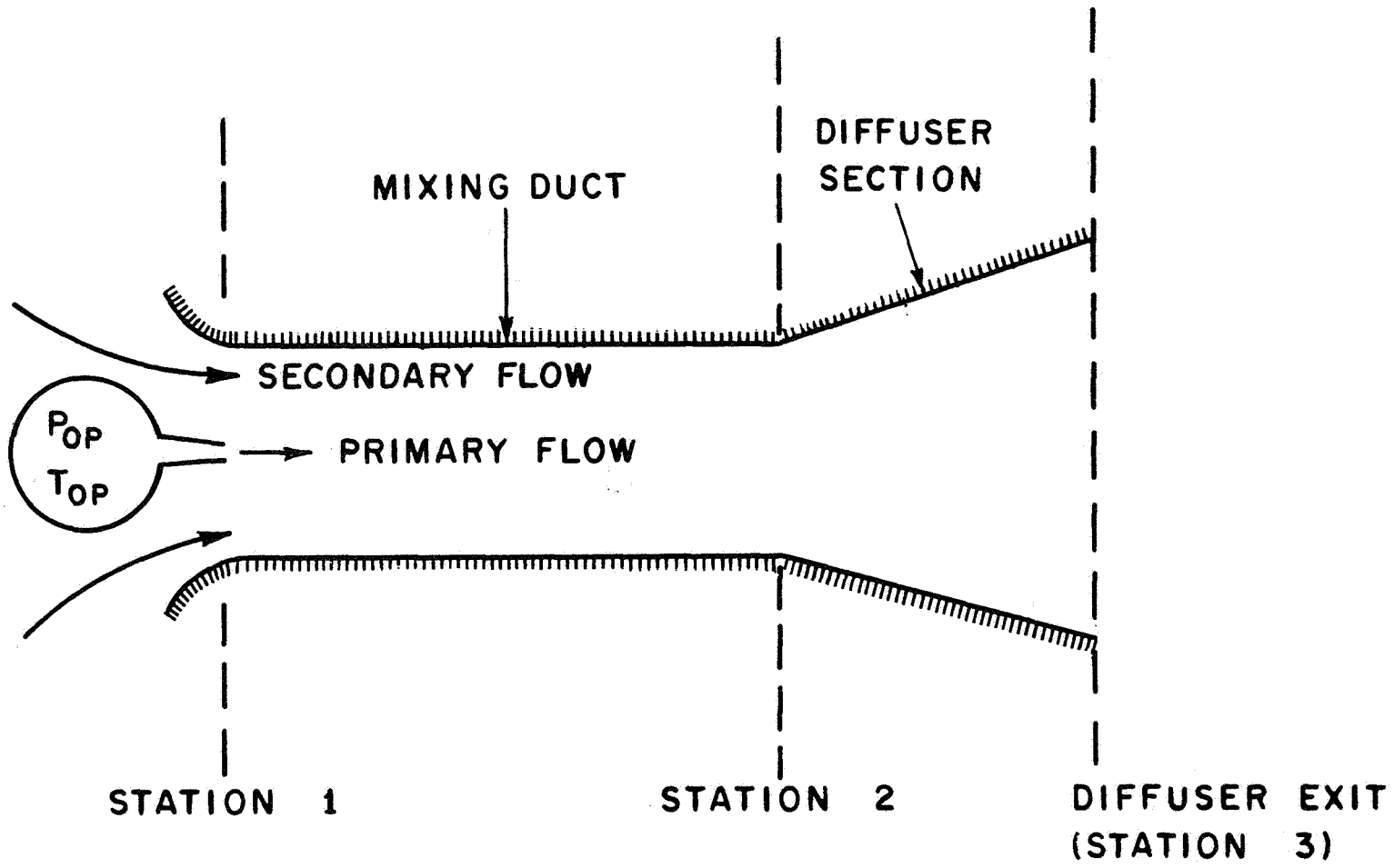

Figure 1.- Schematic of a single-stage ejector.

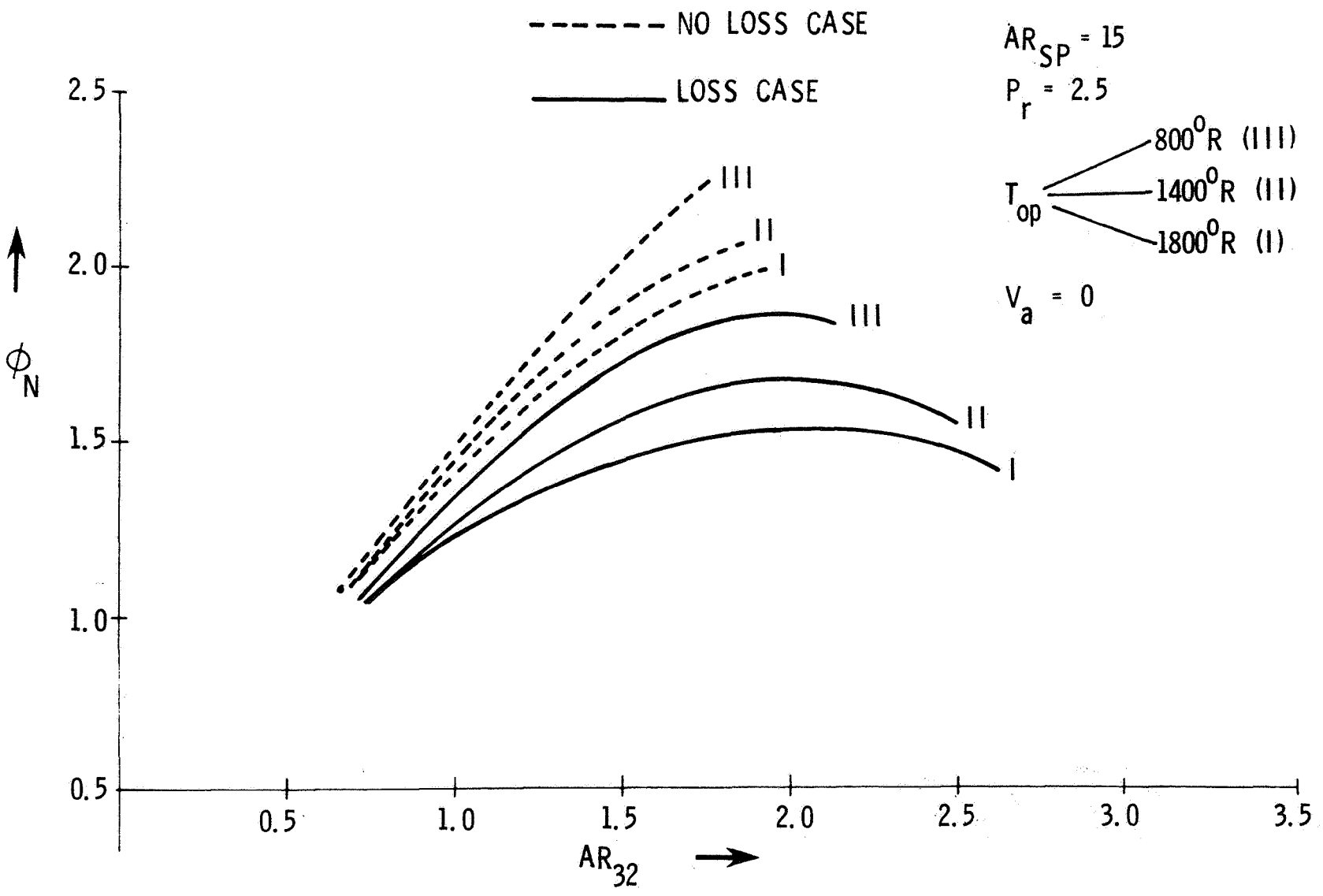

Figure 2.- Thrust augmentation ratio vs diffuser area ratio.

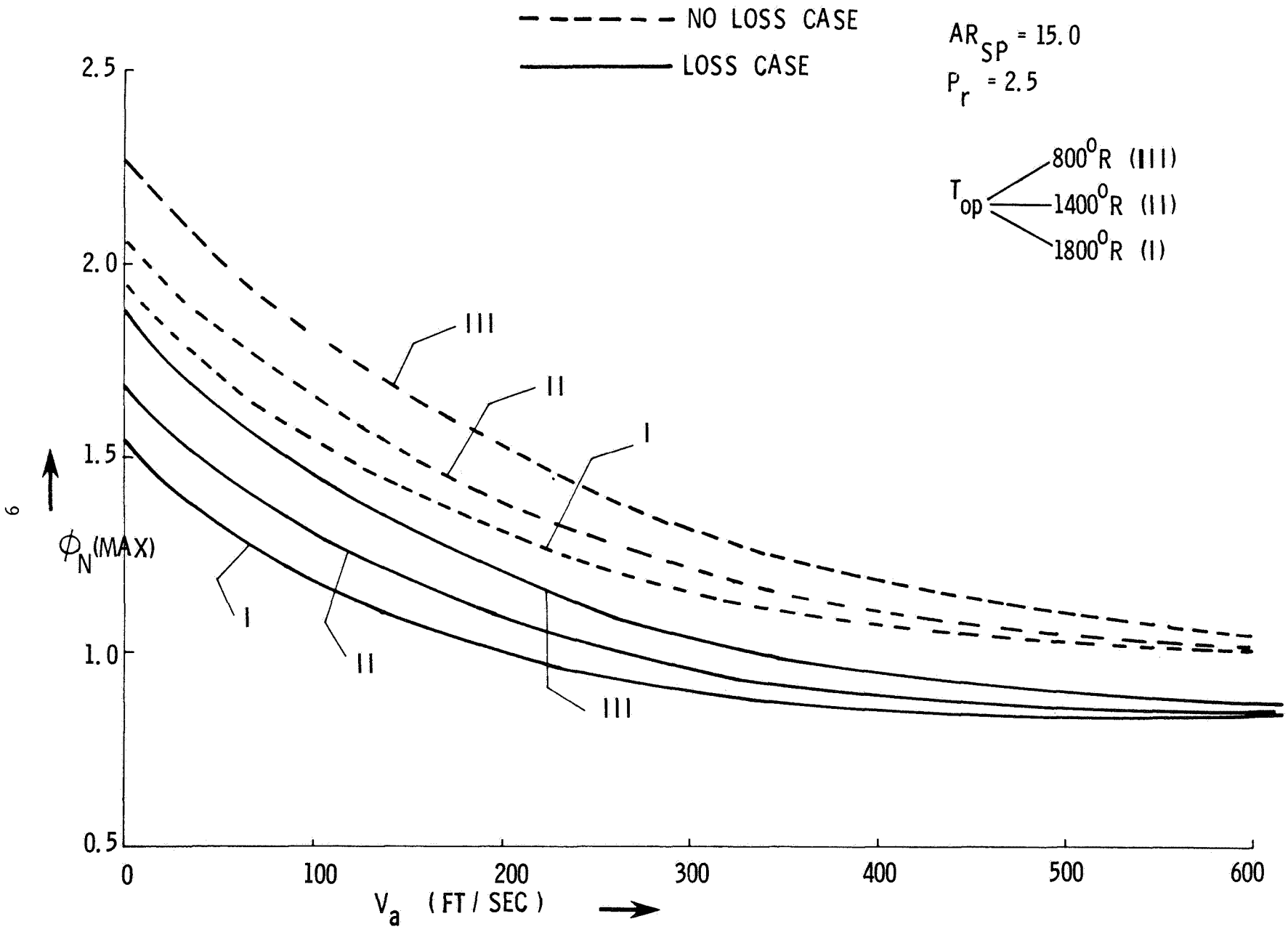

Figure 3.- Distribution of ϕ_N(max) vs V_a(forward velocity).

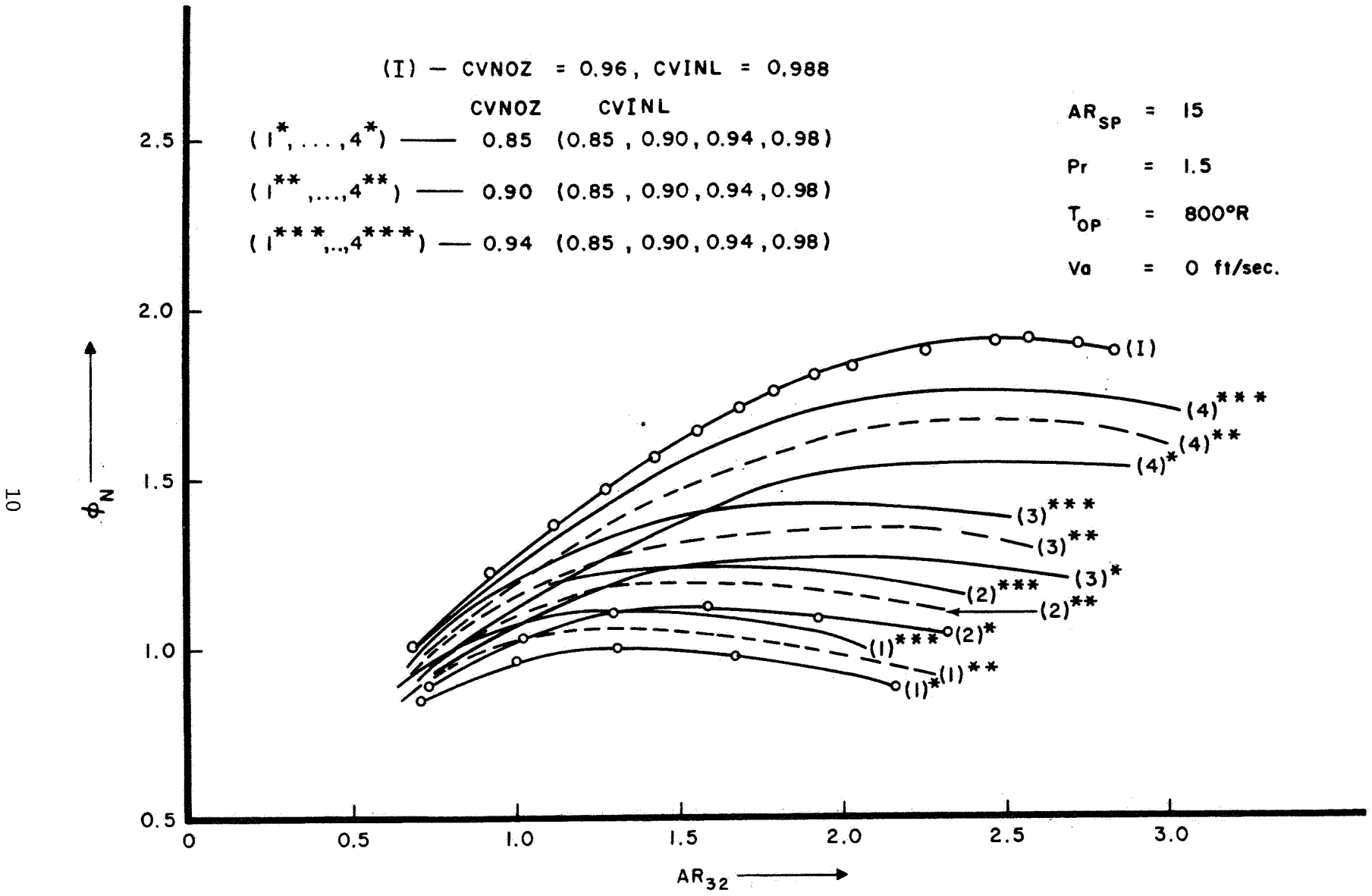

Figure 4.- Thrust augmentation characteristics for several nozzle and inlet losses.

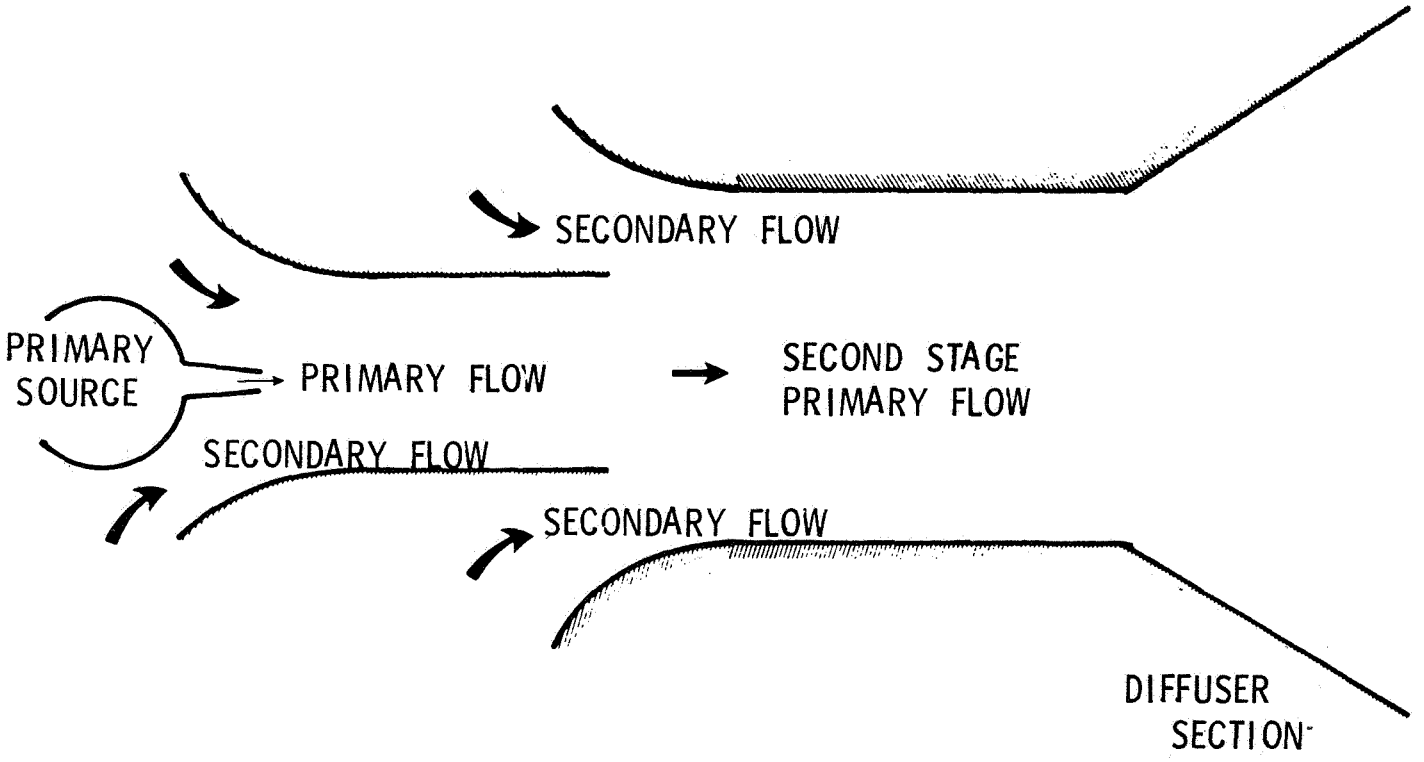

Figure 5.- Schematic of a two-stage ejector.

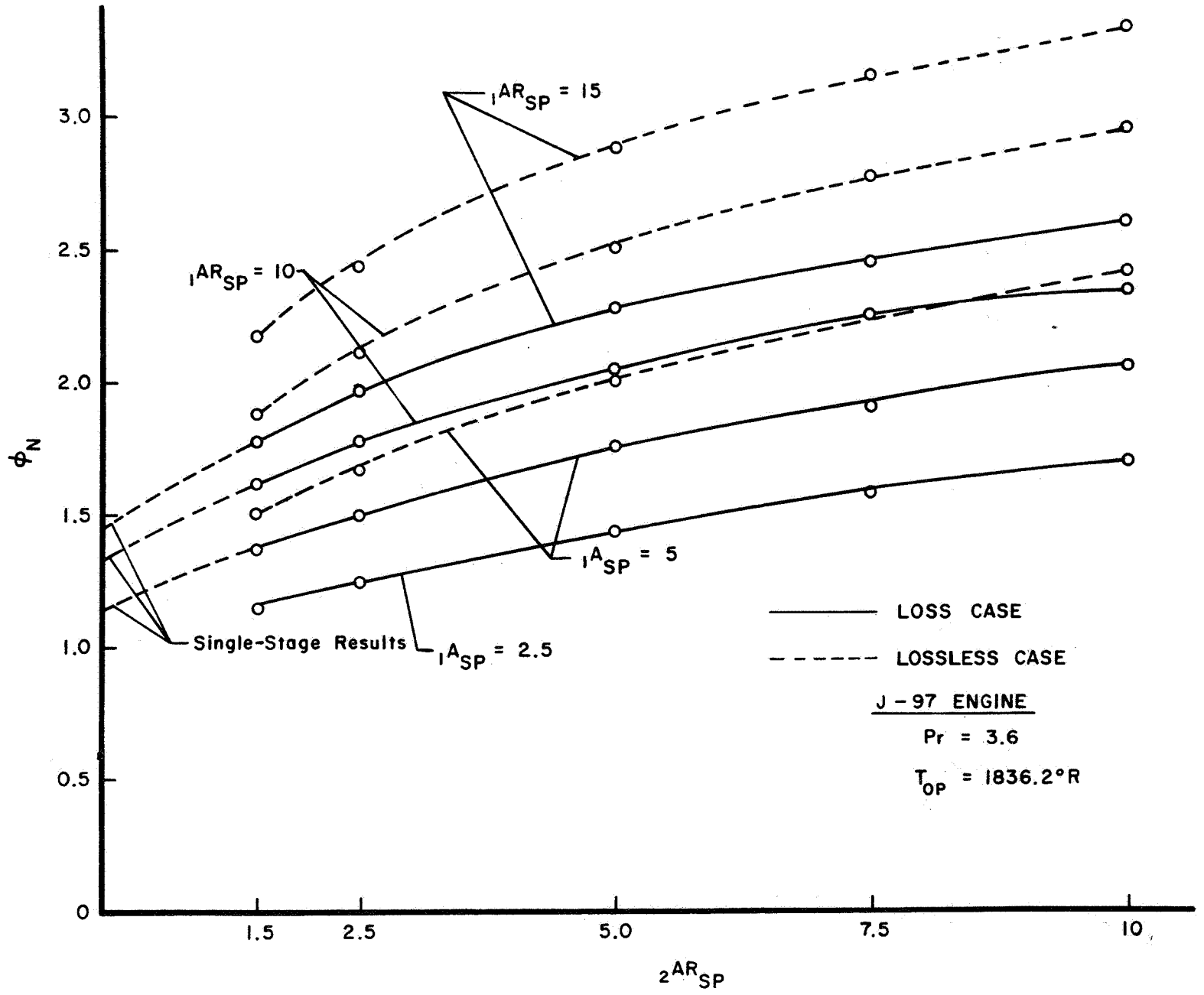

Figure 6.- Thrust augmentations in two-stage ejector flows.

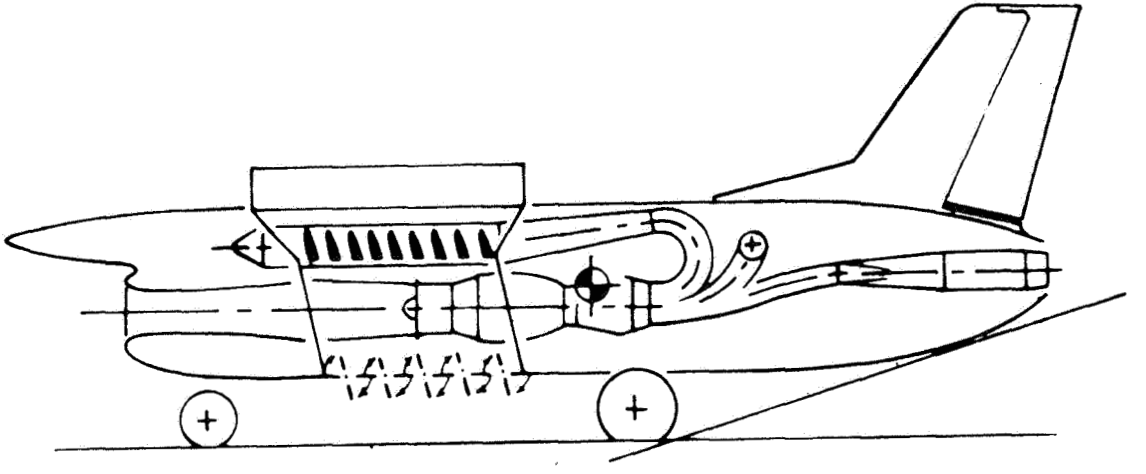

F107-WR-100 DEMO ENGINE

- 600 LBT CLASS

121 LB WEIGHT

GAS DUCTING SYSTEM

6.25% PRESSURE LOSS

210 LB WEIGHT

EJECTOR STATIC PERFORMANCE

OPTIMUM IAR = 13.5

OPTIMUM Φ = 1.66

Figure 7.- Propulsion system.

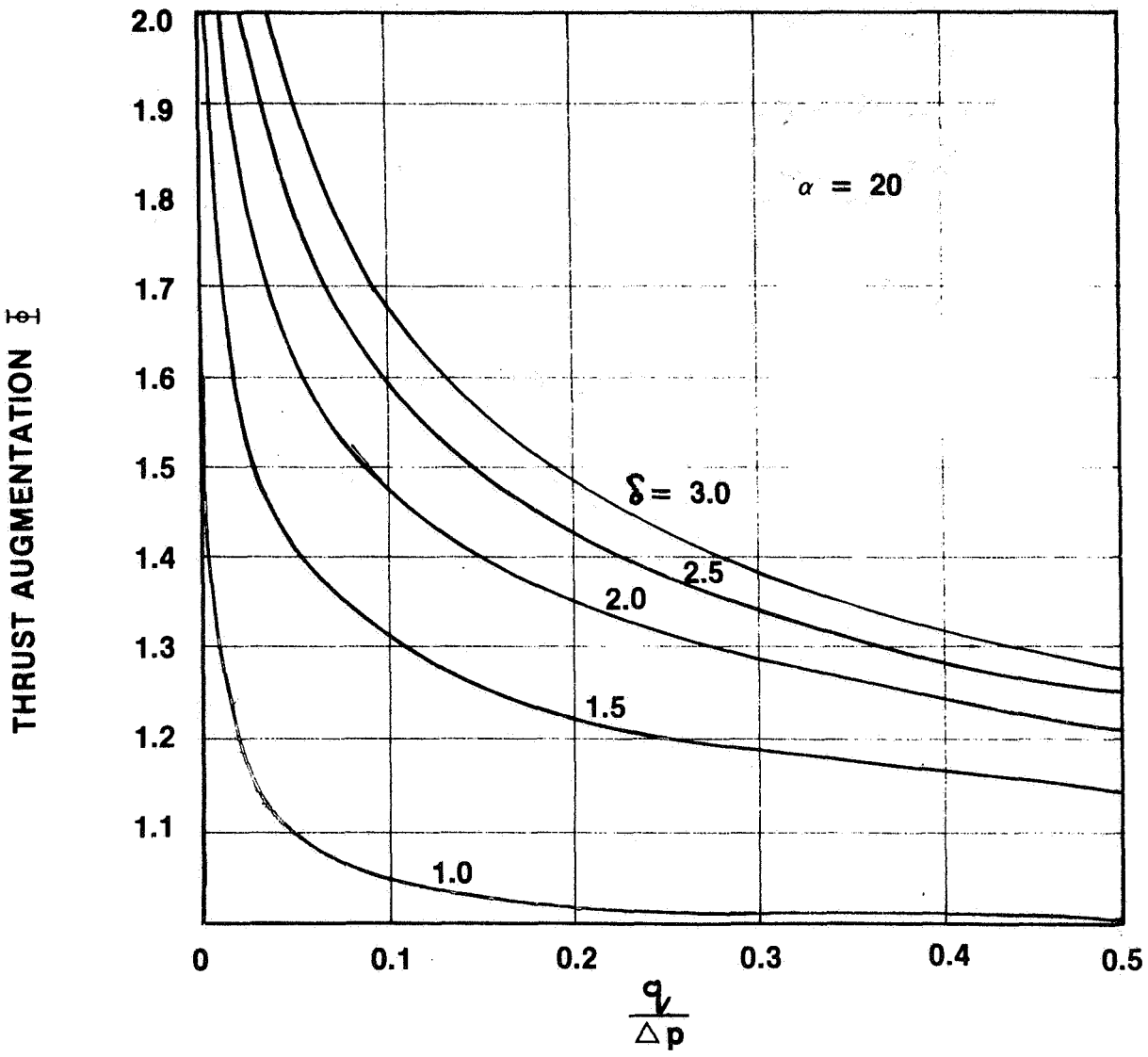

q · DYNAMIC PRESSURE

Δp · INCREMENTAL STAGNATION PRESSURE = $P_{op} - P_\infty$

α · INLET AREA RATIO

δ · DIFFUSER AREA RATIO

Figure 8.- Variation of thrust augmentation with $q/\Delta p$.

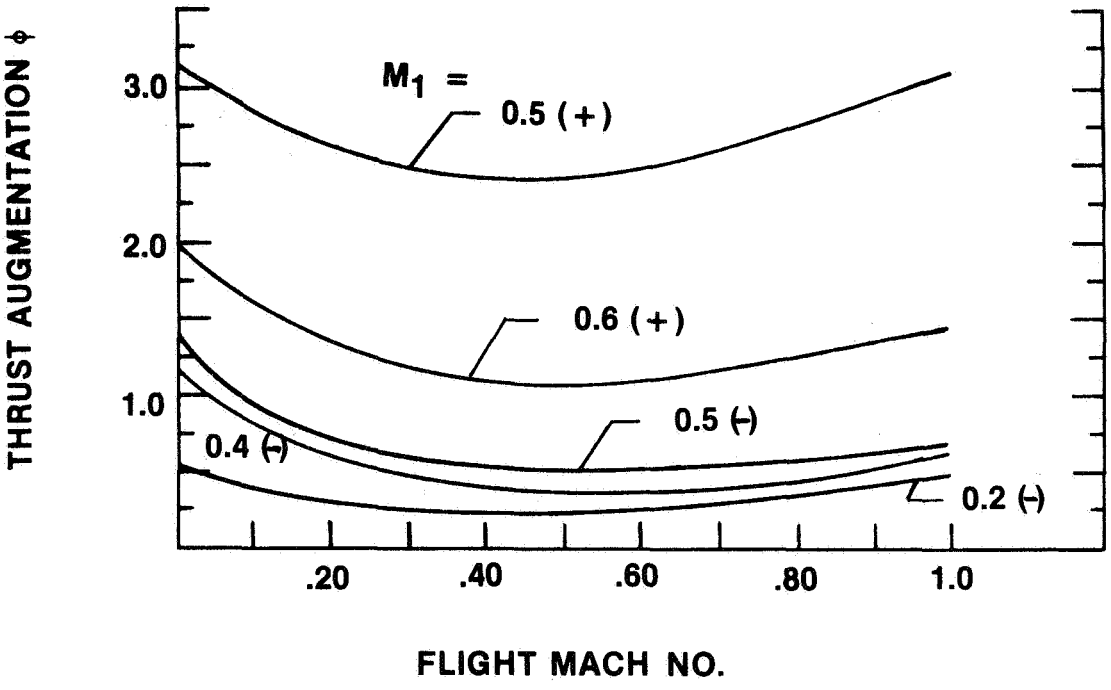

Figure 9.- Variation of thrust augmentation flight Mach number.

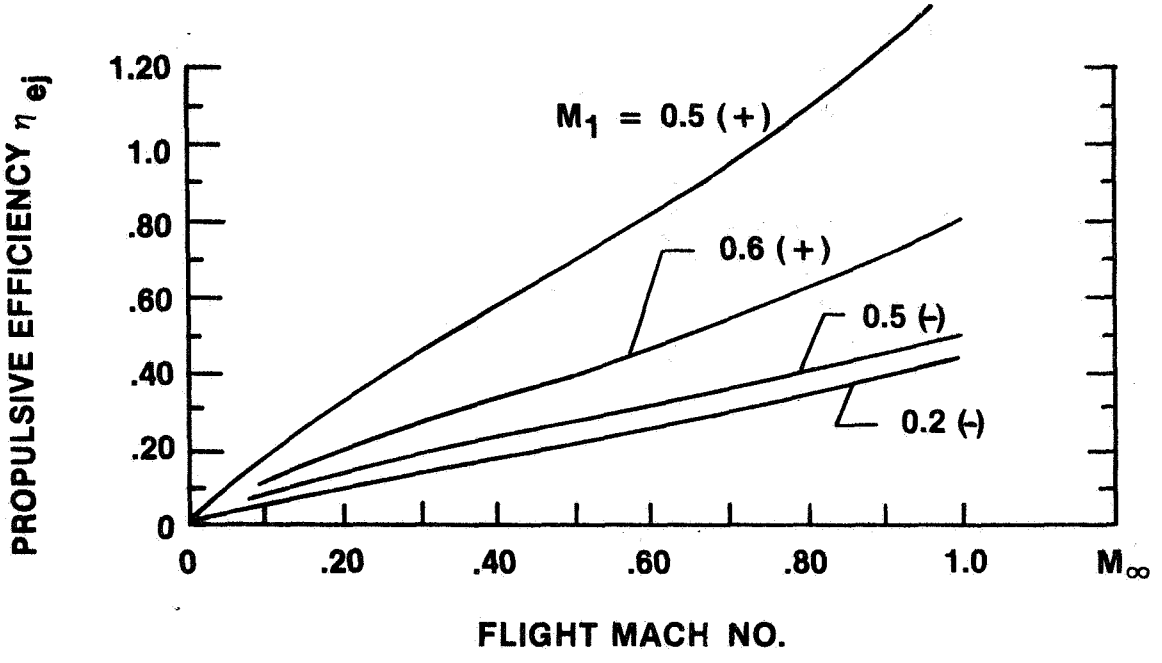

Figure 10.- Solid diffuser ejector performance; $\alpha_\infty = 20$, $\Delta T/T_\infty = 5.0$, $\Delta P/p_\infty = 3.0$, $C_{di} = C_F = C_\mu = 0$.

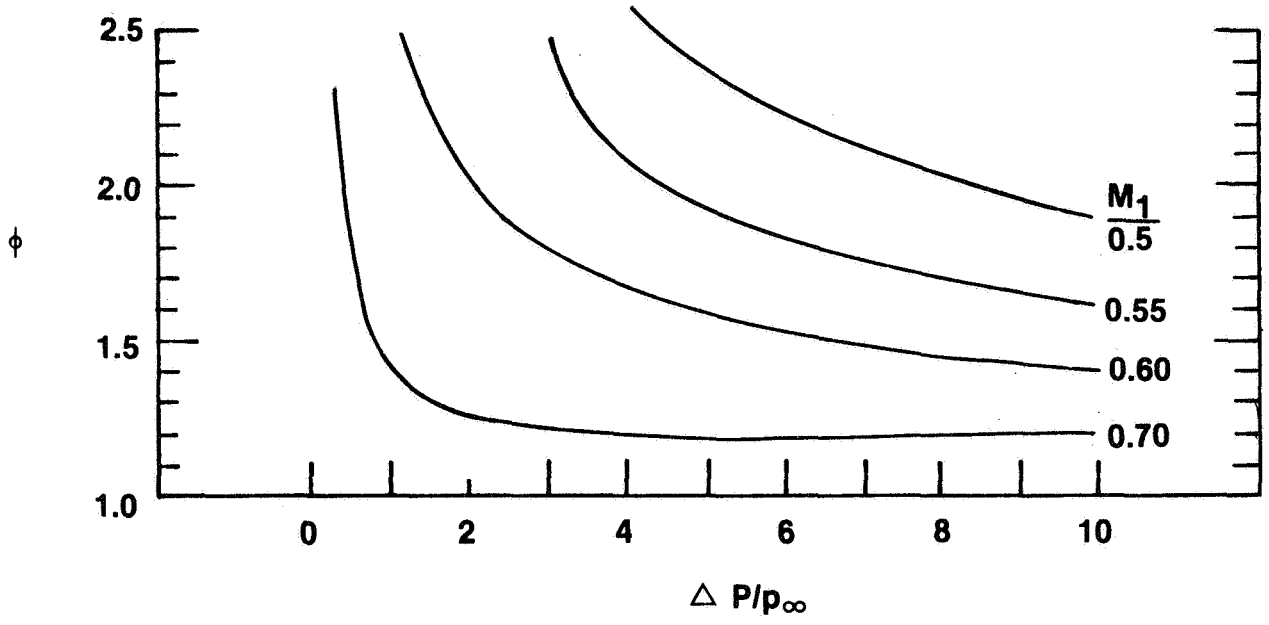

Figure 11.- Ideal high-speed ejector; $M_\infty = 0.5$, $\alpha_\infty = 20$, $\Delta T/T_\infty = 3.0$; second solution.

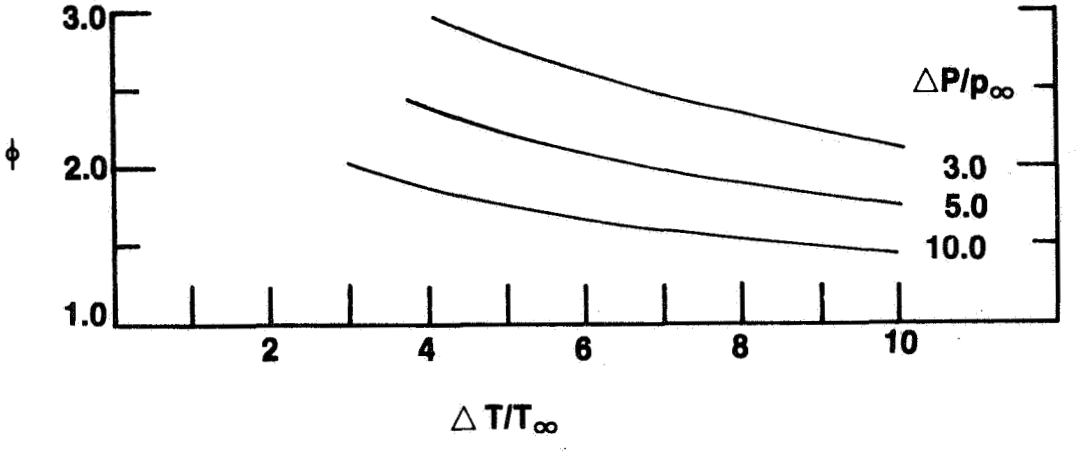

Figure 12.- Ideal high-speed ejector; $M_\infty = 0.8$, $\alpha_\infty = 20$, $M_1 = 0.5$; second solution.

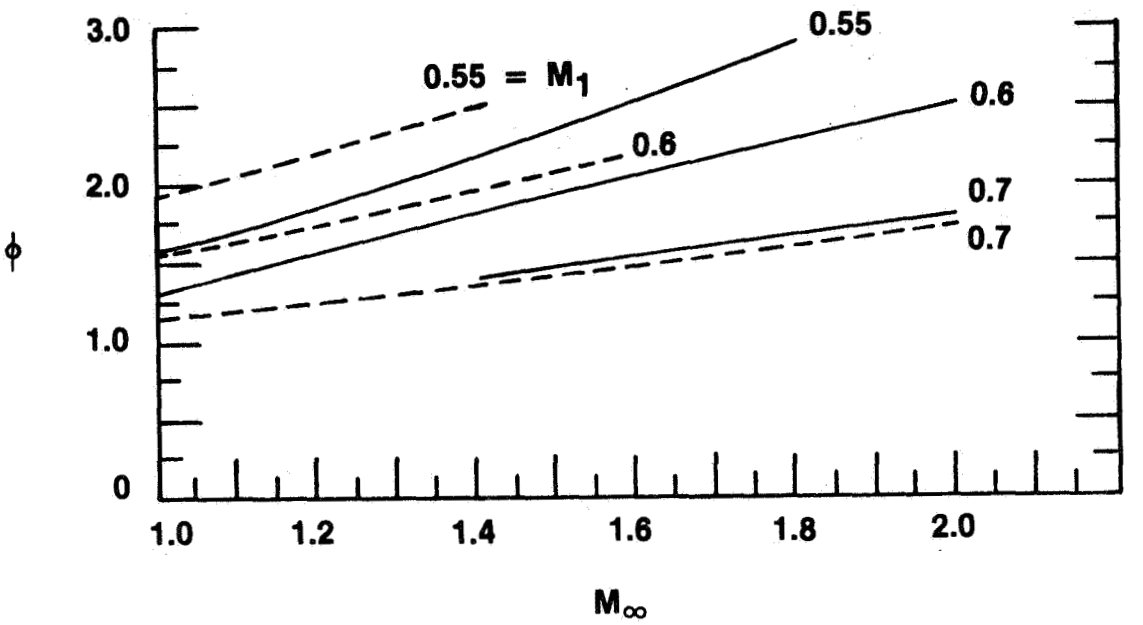

Figure 13.- Supersonic ejector performance; $\alpha_\infty = 20$, $P/p_\infty = 5.0$, $\frac{\Delta T}{T_\infty} = \begin{cases} \text{——} & 10.0 \\ \text{- - - -} & 5.0 \end{cases}$; second solution.

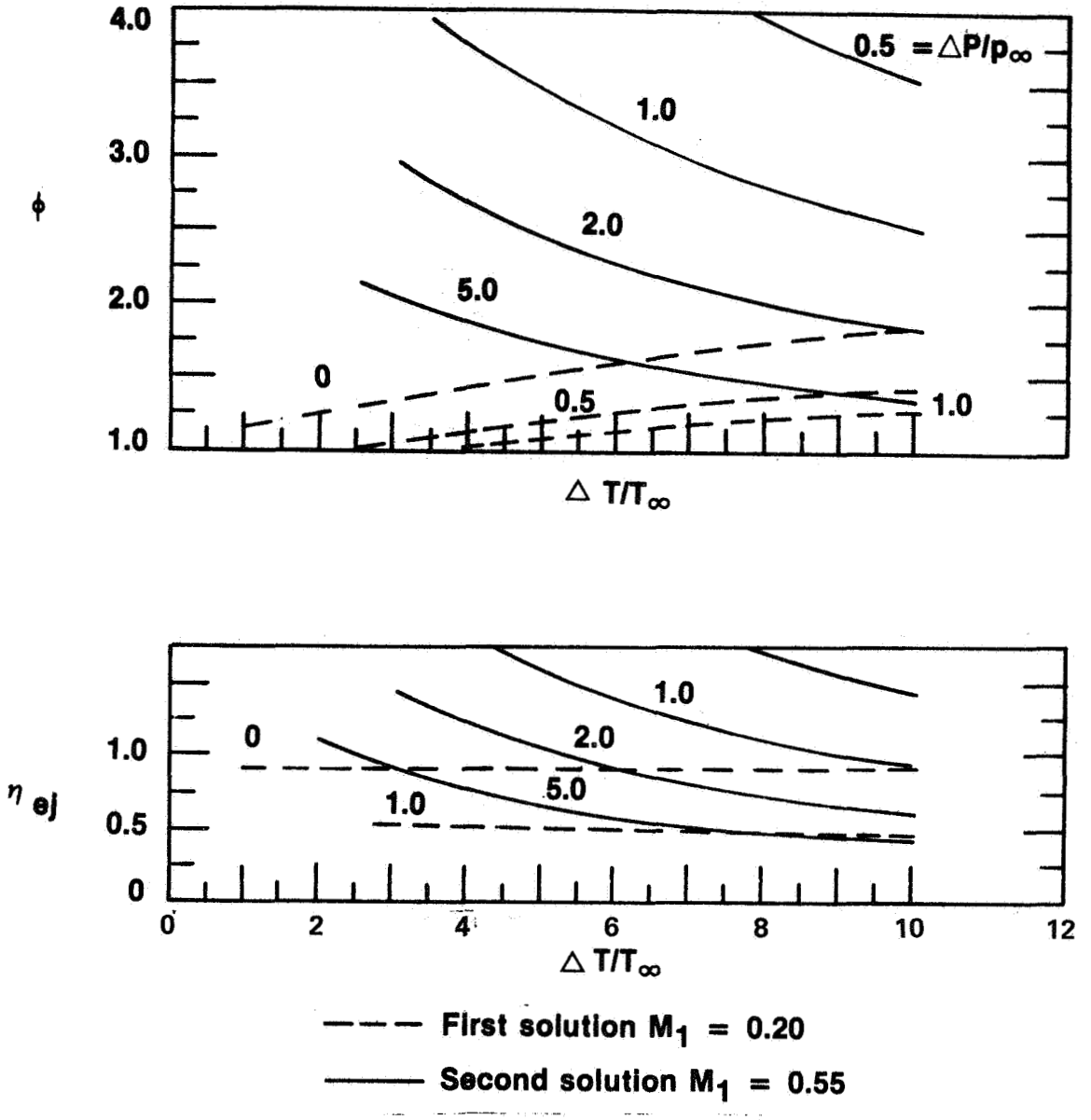

Figure 14.- Ideal high-speed ejector; $M_\infty = 0.8$, $\alpha_\infty = 20$, $s_\infty/a_\infty = 0$.

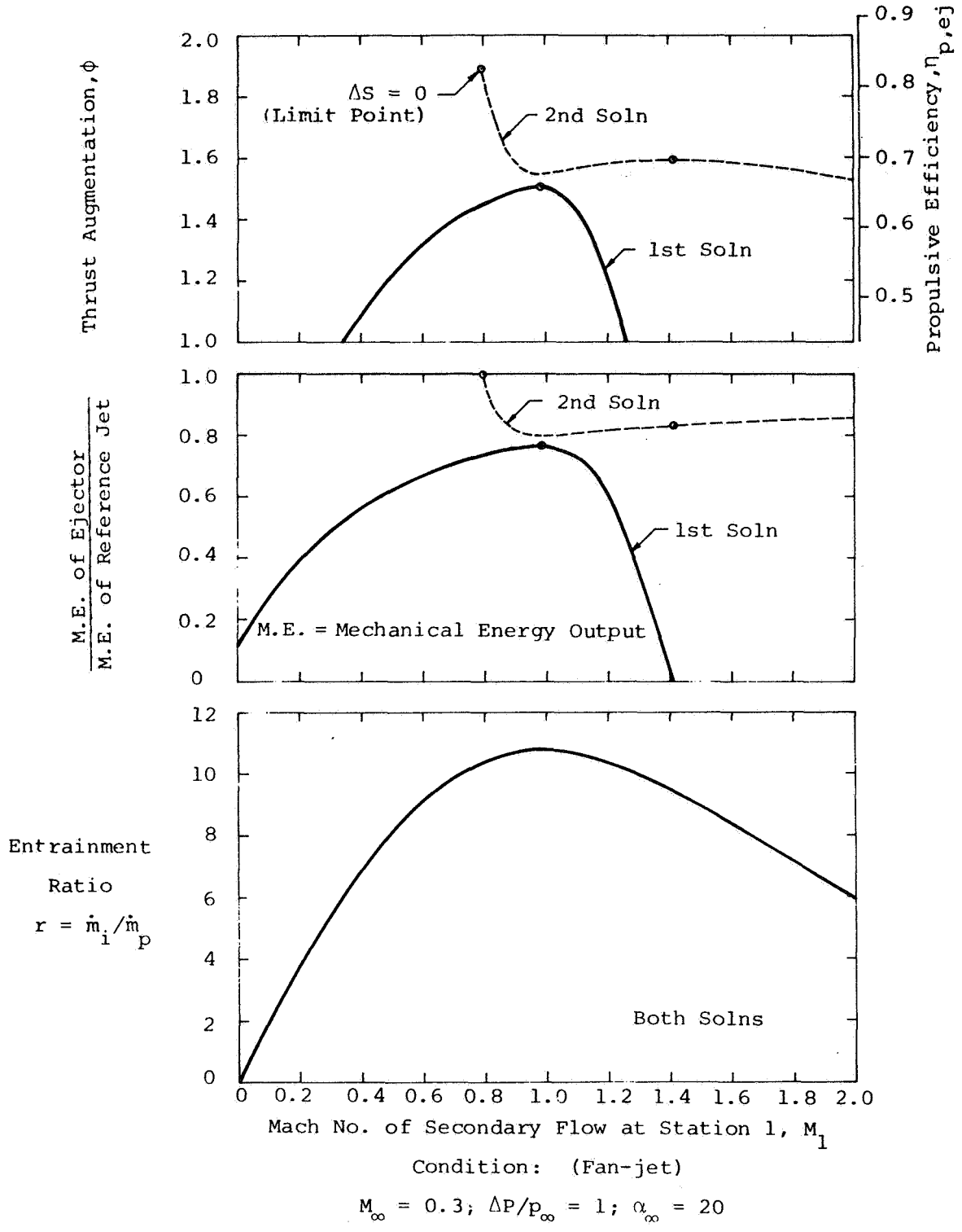

Figure 15.- Ejector in low-speed flight.

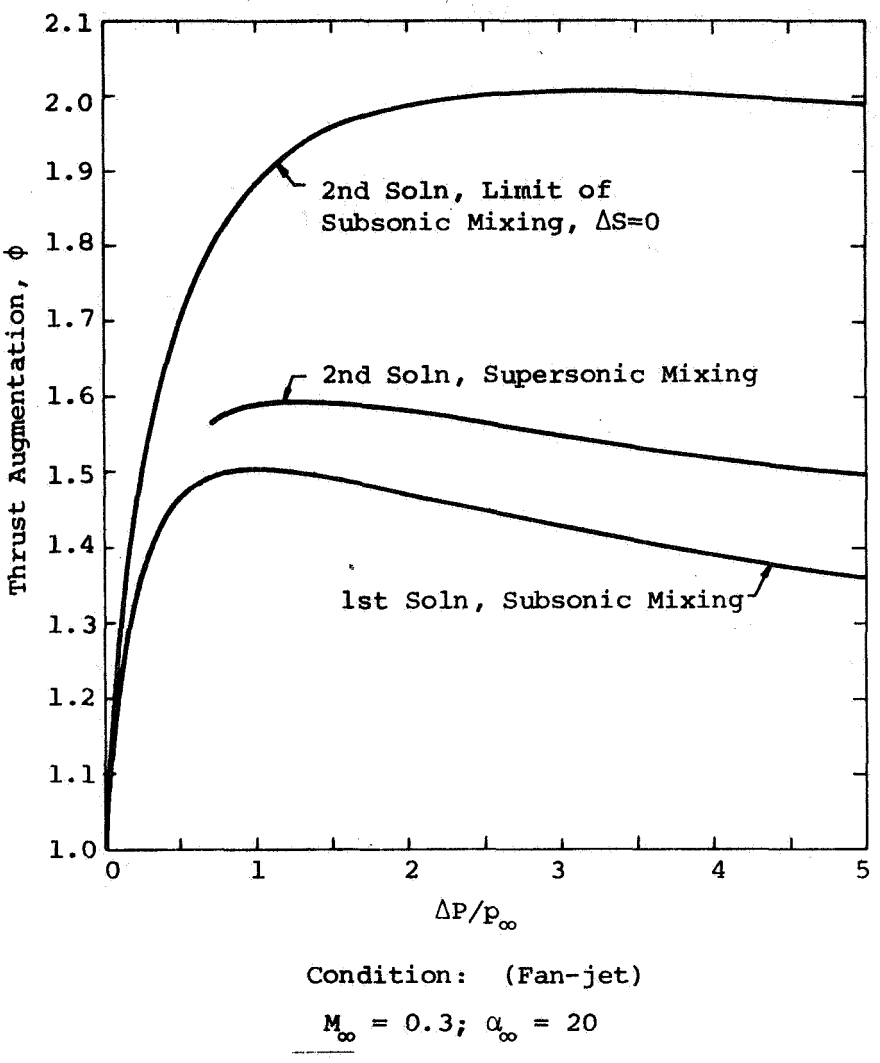

Figure 16.-Influence of pressure on low-speed ejector performance.

NASA OVERVIEW

David G. Koenig

Ames Research Center
Moffett Field, Calif. 94035

INTRODUCTION

This review as outlined in figure 1 will be a summary of effort at Ames Research Center in researching performance and application of thrusting augmentors. It represents the major portion of the NASA-wide effort in recent years. Ames got started in 1965 when a large-scale testing program on STOL application, which was sponsored jointly with the Canadian Government, was initiated. The investigation has culminated in the publication of references 1 and 2 and the continuing study of the augmentor wing at forward speed which is presently still funded by the Canadians. The early part of this effort resulted in using the augmentor wing in the NASA Research Aircraft C8A which is still being flown. More description of this effort is documented in references 3 through 6 including Ames in-house research. Specific application to VTOL was initiated with a joint Air Force NASA program in 1972 and resulted in Ames 7- by 10-Foot Wind-Tunnel tests, some of which are reported in reference 7, and a report by NASA currently in preparation. Support of research in the application of thrusting ejectors to V/STOL will continue until maximum installed performance has been achieved.

OBJECTIVES

The objectives of this effort have and will continue to be those listed in figure 2. In all studies, there is a concentrated effort to understand configuration effects on performance resulting in a general parametric description of thrust augmentors for effective application to STOL and V/STOL. Everyone tries to obtain as much theoretical as empirical data to apply to this objective but, at present, the latter is by far more abundant than pertinent theoretical results. All the objectives in figure 2 are very much related but must support the principal objective of application or "Key Design Considerations" which, in our current target, are not only high uninstalled performance or large thrust augmentation numbers in the laboratory but assuring that these numbers come from configurations which can be packaged into V/STOL aircraft — "fighter" or otherwise.

TEST FACILITIES

To study installed performance, Ames will rely on several test facilities which take both small- and large-scale models for static and wind-tunnel tests. An installation in the Ames 7- by 10-Foot Wind Tunnel is shown in figure 3.

The configuration is the Air Force design — reference 7 in a semispan model which yield both static and wind-on data. Figure 4 shows the Ames 11-foot wind-tunnel test section with a semispan model of the deHavilland "Cruise Augmentor." This installation allowed study of the performance of the augmentor wing at high subsonic speeds. The Large-Scale Static Test Stand is shown in figure 5 with the Ames wind tunnels shown in the background. An additional building is now being located to the right of the stand but will not interfere with operation of the test stand. Figure 6 shows the de Havilland fuselage-mounted ejector model in the 40- by 80-foot wind tunnel. For this model the ejector is powered by a J-97. More will be said about the configuration and the test results by a later speaker. An updated data reduction system and a high pressure air supply is being added to the latter two facilities.

An additional facility, the 80- by 120-foot wind tunnel will be ready for use in three years and should be included in plans for developmental testing. It will share power systems with an "overhauled" 40 by 80 foot wind tunnel and will be a through-flow no-return part of the complex extending out the right (toward the northwest) of the 40- by 80-foot wind tunnel shown in figure 5. Also seen in figure 5, a large full-scale model or aircraft can be tested on the test stand, put on a trailer and transported to the 40 by 80 or 80 by 120 foot wind tunnel over a very short distance.

EJECTOR PERFORMANCE EVALUATION

Through testing both at small- and large-scale numbers on augmentor performance are summarized in figure 7. This collection of data has been shown previously and parts of it published last year in reference 8. The gross augmentation is defined as the ratio of total actual thrust to the actual thrust of primary nozzle. For evaluating the primary thrust, this actual or measured value must often be derived from the thrust based on isentropic expansion from the nozzles using correction factors representative of nozzle efficiency. The mixing length is the average distance from the primary nozzles to the end of the diffuser and is nondimensionalized by the average nozzle width $\bar{t}$. (Total nozzle area divided by ejector throat length.) The lower performance ejectors are either STOL application for low entrainment or were poorly optimized.

It is certainly possible that both the values for the XFV-12A and the de Havilland model (fuselage ejector) can be or already has been further optimized. The use of $\ell/\bar{t}$ as a parameter in the figure was an arbitrary choice but was used for many years as a means of "collapsing" data for slotted and simple lobed nozzles to the faired lines. The spread in performance for given mixing lengths illustrates the effects of both types of entrainment and mixing as well as ejector configuration differences.

The challenge in sorting out the differences in ejector performance shown in figure 7 must be met by evaluating some of and more than the parameters listed in figures 8, 9, and 10 which have been separated into geometric, performance, and operating definition, respectively. For geometry, one can organize these into nozzle, shroud or diffuser, and general configuration.

What is, obviously, absent is the type or specific design or "scheme" such as whether or not the configuration promotes strictly turbulent mixing or is the entrainment accomplished through shear alone. For each ejector configuration, the performance evaluated, using some or all of the parameters listed in figure 9, must be documented for as many of the geometric parameters as possible. Tests must be made at the operating conditions (parameters) in figure 10. A primary problem in the experimental study of the potential of a given ejector concept is not just the complexity of the hardware required but the amount and sophistication of the instrumentation needed to document this performance and operation.

INVESTIGATIONS AT LARGE SCALE

Many of the operating or test conditions can be obtained only by installing the ejector in an aircraft configuration and testing it both statically and at airspeed. It seems essential to investigate installation effects with a particular ejector configuration even though the isolated ejector is still not completely optimized in order to insure that all performance parameters have been evaluated properly. To do this, a significant amount of basic research using smaller models (cold or hot air supply) and analytical development should be continued vigorously, however, large-scale testing is a valuable tool in evaluating installation effects.

Current experimental and theoretical programs are being carried out on the V/STOL fighter configuration shown in figures 11 and 12. The NASA XV-12A static tests are complete and some of the results will be discussed here. The wind-tunnel tests on a large-scale model of the wing root or fuselage-mounted ejectors (installation shown in fig. 6) were completed in February and will be discussed in this workshop by Mr. D. C. Whittley. Installation of the short diffuser or Alperin ejector will be studied using the fighter design shown in figure 12.

It is intended that this be a parallel program with large-scale tests on a RALS plus deflector nozzle configuration. This latter program will be initiated next February with test in Ames 40- by 80-Foot Wind Tunnel on the STOL configuration having blowing over a deflected flap plus spanwise blowing. All of these models will be powered by J-97's. As shown in figure 12 an alternate configuration might be the combination of an ejector with the VEO or vectored direct thrust in the rear.

A more detailed sketch of the ejector fighter configuration is shown in figure 13. Except for the strakes, it is a configuration that is meeting requirements of the Navy and Air Force supersonic fighter, particularly for subsonic high maneuverability needs. A strake is a natural spot to place the ejector but the ejector diffuser must be short, or, if not, diffuser scheme must be designed into the aircraft such that it can be retracted for cruise. For the latter option, a primary emphasis on the complete model tests will be one of integration into the aircraft mission both mechanically and aerodynamically. The program is being started with both NASA and Contractual work using isolated and small-scale ejector models. This will be followed by

large-scale static tests (at the scale of the complete model) using the complete ejector propulsion system. And only after acceptable installed ejector performance is obtained statically will the complete model be tested.

CONCLUDING REMARKS

Ames Research Center will continue to take the lead in NASA's effort to explore several applications of the thrusting ejector. Figure 14 lists areas in future effort where research and development will be supported both in-house and contractually. It seems evident that the major application will be to the V/STOL fighter and our large-scale testing is currently organized on this basis. However, it is felt that other applications such as that of control thrustors, and augmenting circulatory lift in the STOL mode should be continually considered.

REFERENCES

1. Koenig, David G.; and Falarski, Michael D.: Wind-Tunnel Investigation of the Thrust Augmentor Performance of a Large-Scale Swept Wing Model, NASA TM X-73,239, 1978.

2. Garland, D. B.; and Whittley, D. C.: Thrust Performance of a Large Scale Augmentor Wind Tunnel Model NASA CR-152170, 1978.

3. Whittley, D. C.; and Cook, W. L.: Comparison of Model and Flight Test Data for an Augmentor-Wing STOL Research Aircraft. Presented at the AGARD Flight Mechanics Symposium on "Flight/Ground Testing Facilities Correlations," June 9-12, 1975.

4. Farbridge, J. E.: The Transonic Multi-Foil Augmentor-Wing, AIAA Paper 77-606. Presented at 1977 AIAA/NASA Ames V/STOL Conference, 1977.

5. Aiken, Thomas N.: Aerodynamic and Noise Measurements on a Quasi-Two Dimensional Augmentor Wing Model with Lobe-Type Nozzles, NASA TM X-62,237, 1974.

6. Aiken, Thomas N.; Falarski, M. D.; and Koenig, David G.: Aerodynamic Characteristics of a Large-Scale Semispan Model with a Swept Wing and an Augmented Jet Flap with Hypermixing Nozzles, NASA TM X-73,236, 1979.

7. Brown, S. L.; and Murphy, R. D.: Design and Test of Ejector Thrust Augmentation Configurations Paper No. 19, AGARD CP-143, April 1974.

8. Aiken, Thomas N.: Thurst Augmentor Application for STOL and V/STOL, NASA TM X-73,241, 1977; also AIAA Paper 77-605, 1977.

- AMES RESEARCH CENTER OBJECTIVES
- TEST FACILITIES
- SUMMARY OF DEVELOPMENTS AND EJECTOR PERFORMANCE
- PARAMETERS
- V/STOL FIGHTER APPLICATION

Figure 1.- Outline of NASA overview.

- PARAMETRIC DESCRIPTION OF THRUST AUGMENTOR APPLICATION TO STOL AND V/STOL
- USE OF THEORETICAL AND EMPIRICAL DATA
- AIRCRAFT–AUGMENTOR INTEGRATION
- KEY DESIGN CONSIDERATIONS:
  - •STOL TRANSPORTS
  - √ •V/STOL FIGHTER

Figure 2.- Current objectives of thrust augmentor development at Ames Research Center.

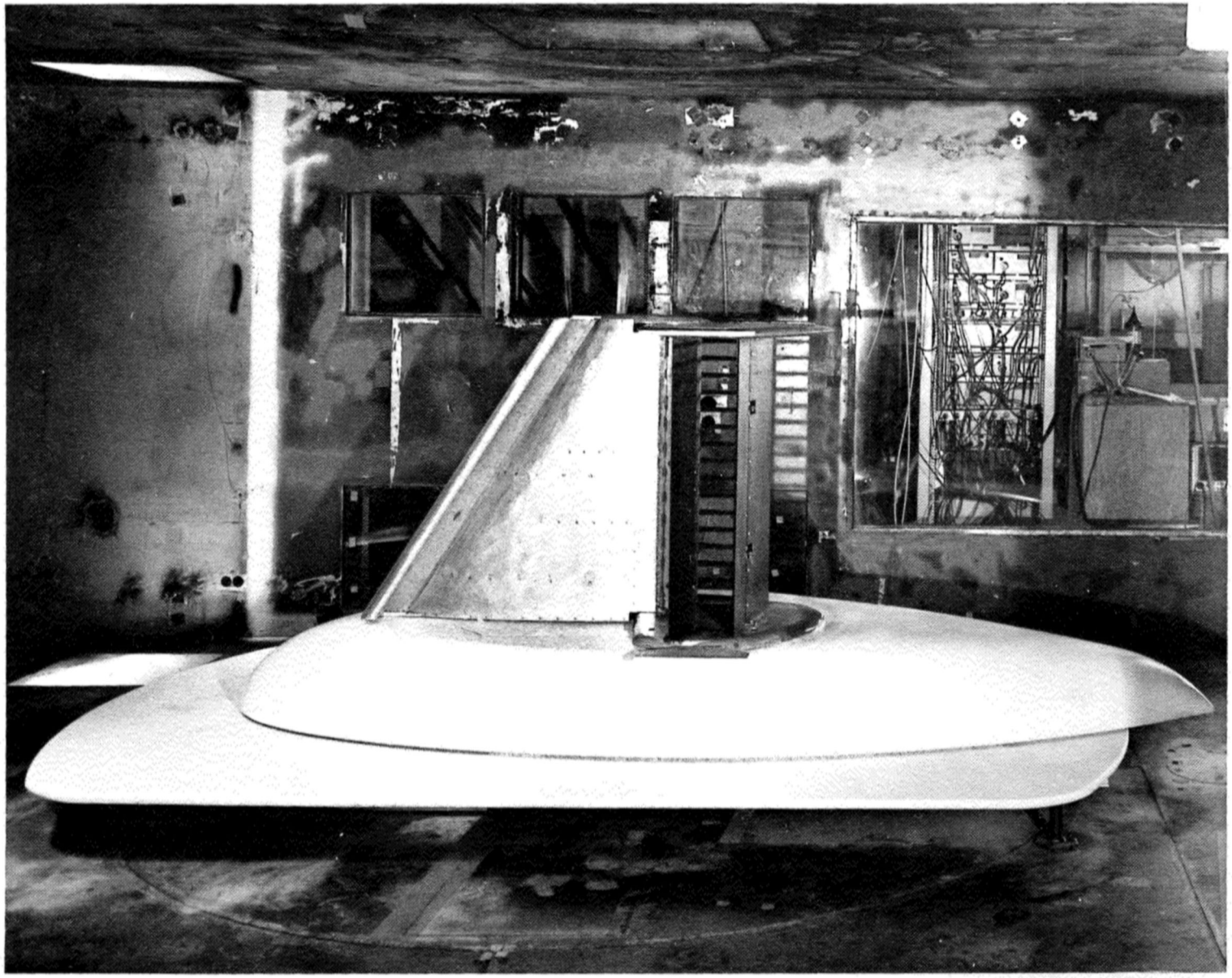

Figure 3.- Ejector powered model in Ames 7- by 10-Foot Wind Tunnel.

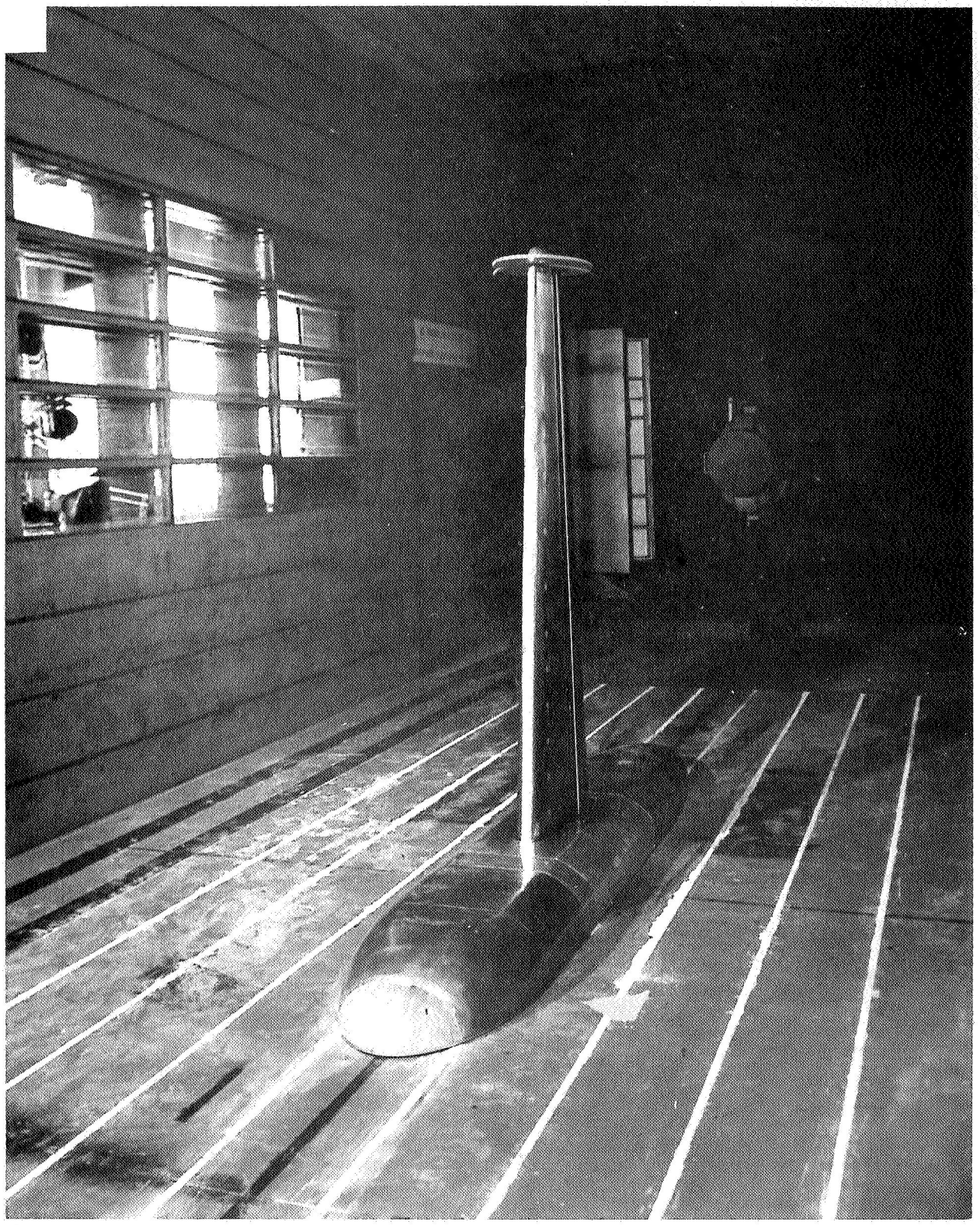

Figure 4.- de Havilland cruise model in Ames 11-Foot Wind Tunnel.

Figure 5.- AV-8B model in Ames Static Test Facility.

Figure 6.- de Havilland fuselage ejector model in Ames 40- by 80-Foot Wind Tunnel.

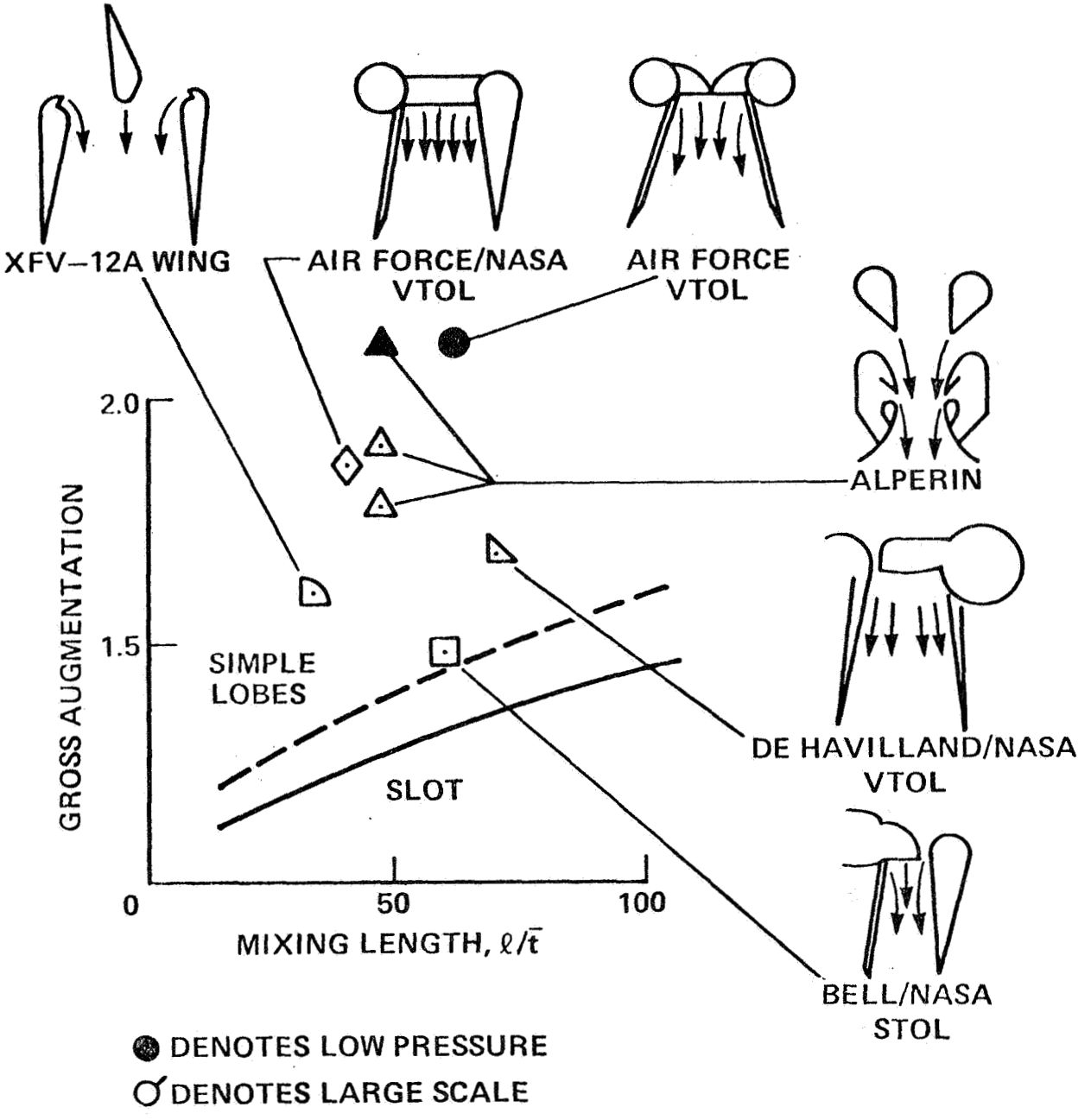

Figure 7.- Thrust augmentor performance.

DUCT AREA RATIO	A_d/A_n
THROAT AREA RATIO	A_t/A_n
DIFFUSER AREA RATIO	A_e/A_t
EXIT AREA RATIO	A_e/A_n
MIXING LENGTH	$\ell/\bar{t}$
NOZZEL TYPE	
NOZZEL ASPECT RATIO, NAR	h/t
NOZZEL PITCH, NP	p/t
TURNING ANGLE, θ_T	
VENTILATION	
AUGMENTOR ASPECT RATIO	

Figure 8.- Thrust augmentor geometry parameters.

DUCT PRESSURE LOSS, $\Delta P/P$	$(P_{IN}-P_{OUT})/P_{IN}$
NOZZEL VELOCITY COEFFICIENT, C_V	$(T/m_n V_{JI})$ SHROUD OFF
TURNING EFFICIENCY, η_T	T/T_{OT}
CIRCULATION LIFT COEFFICENT, C_{L_i}	$C_L - C_L$ POWER OFF
GROSS AUGMENTATION, ϕ_G	$T_{SHROUD\ ON}/T_{SHROUD\ OFF}$
ISENTROPIC AUGMENTATION, ϕ_I	$(T/m_n V_{J_I})$ SHROUD ON
ENTERTAINMENT RATIO	m_S/m_n
NET AUGMENTATION, ϕ_N	$\theta_G-(m_S V_\infty)/T_{SHROUD\ OFF}$

Figure 9.- Thrust augmentor performance parameters.

DUCT MACH NUMBER, M_D	
NOZZEL PRESSURE RATIO, NPR	$(P_N)_{TOTAL}/P_\infty$
NOZZEL TEMPERATURE RATIO,	$(T_n)_{TOTAL}/T_\infty$
THRUST LOADING, T/S	$(T_n)_a/S$
VELOCITY RATIO, V_∞/V_J	$V_\infty/(V_{J_a}$ OR $V_{J_1})$
THRUST COEFFICIENT, C_J	$(T_n)_a/qS$

Figure 10.- Thrust augmentor operating parameters.

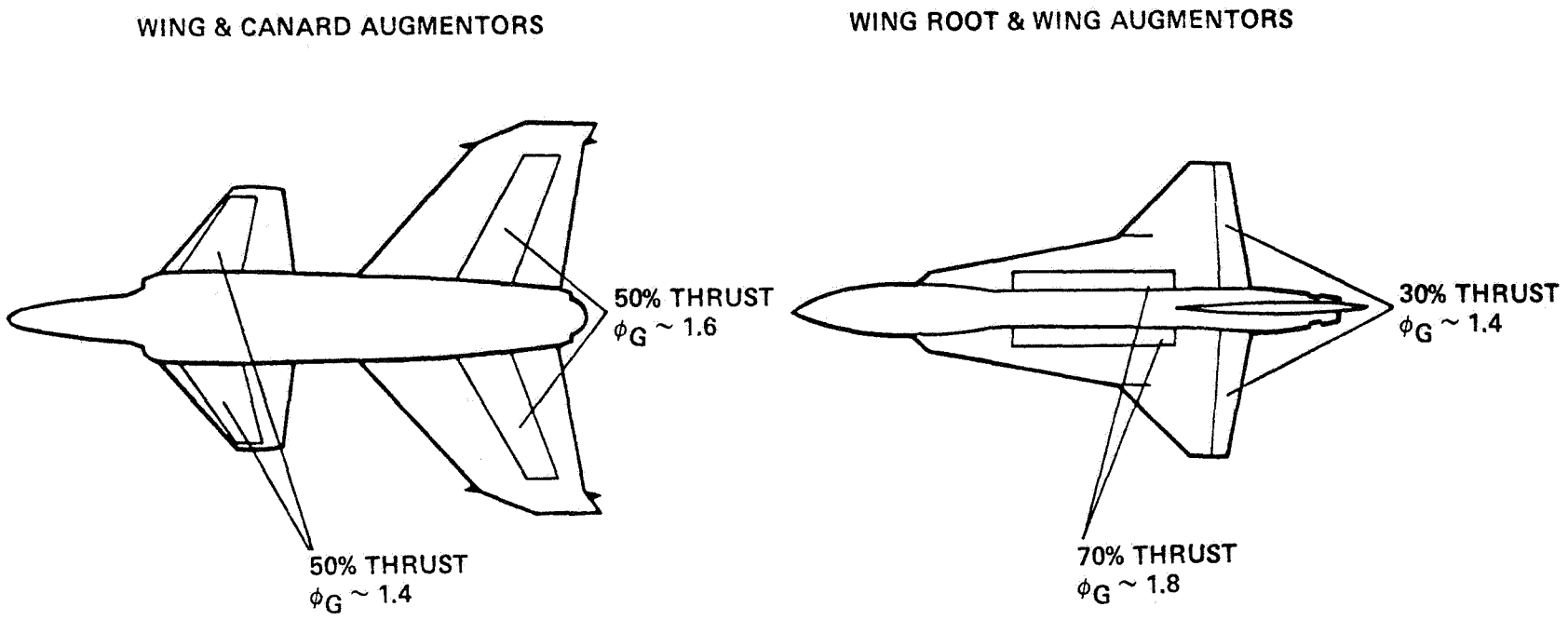

Figure 11.- V/STOL fighter-augmentor integration concepts.

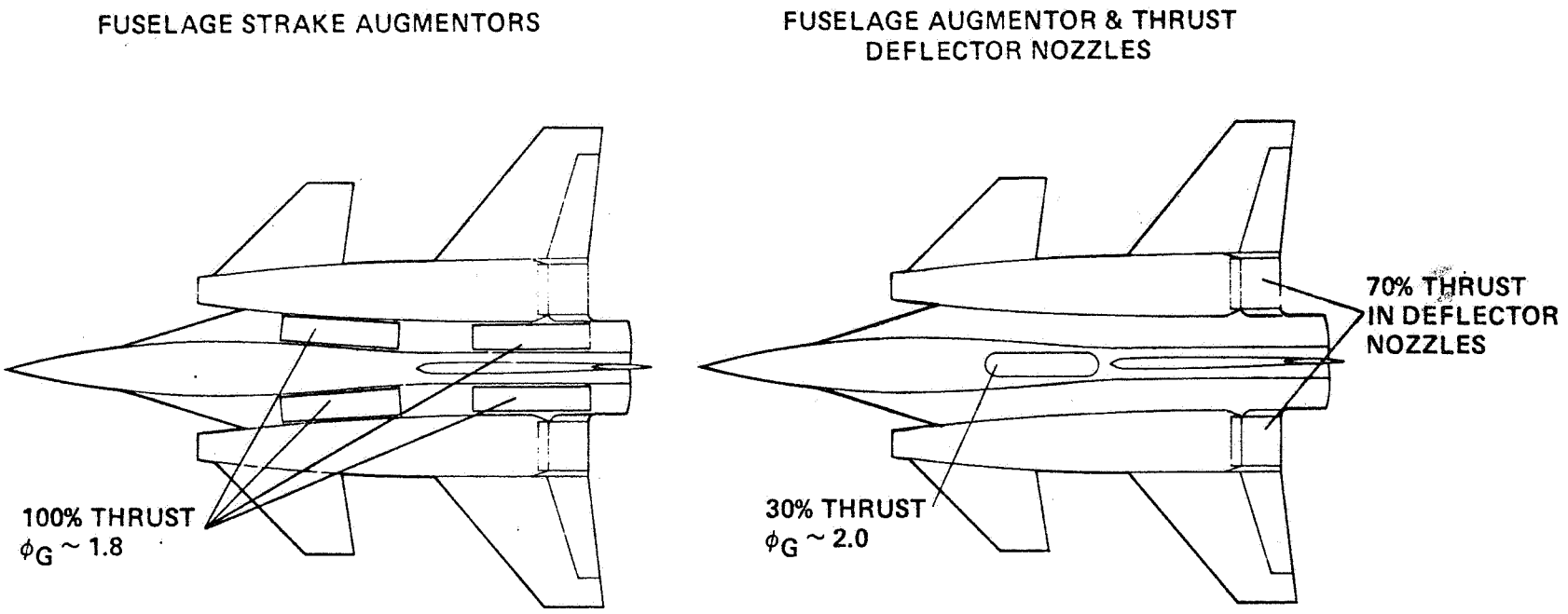

Figure 12.- V/STOL fighter-augmentor integration concepts.

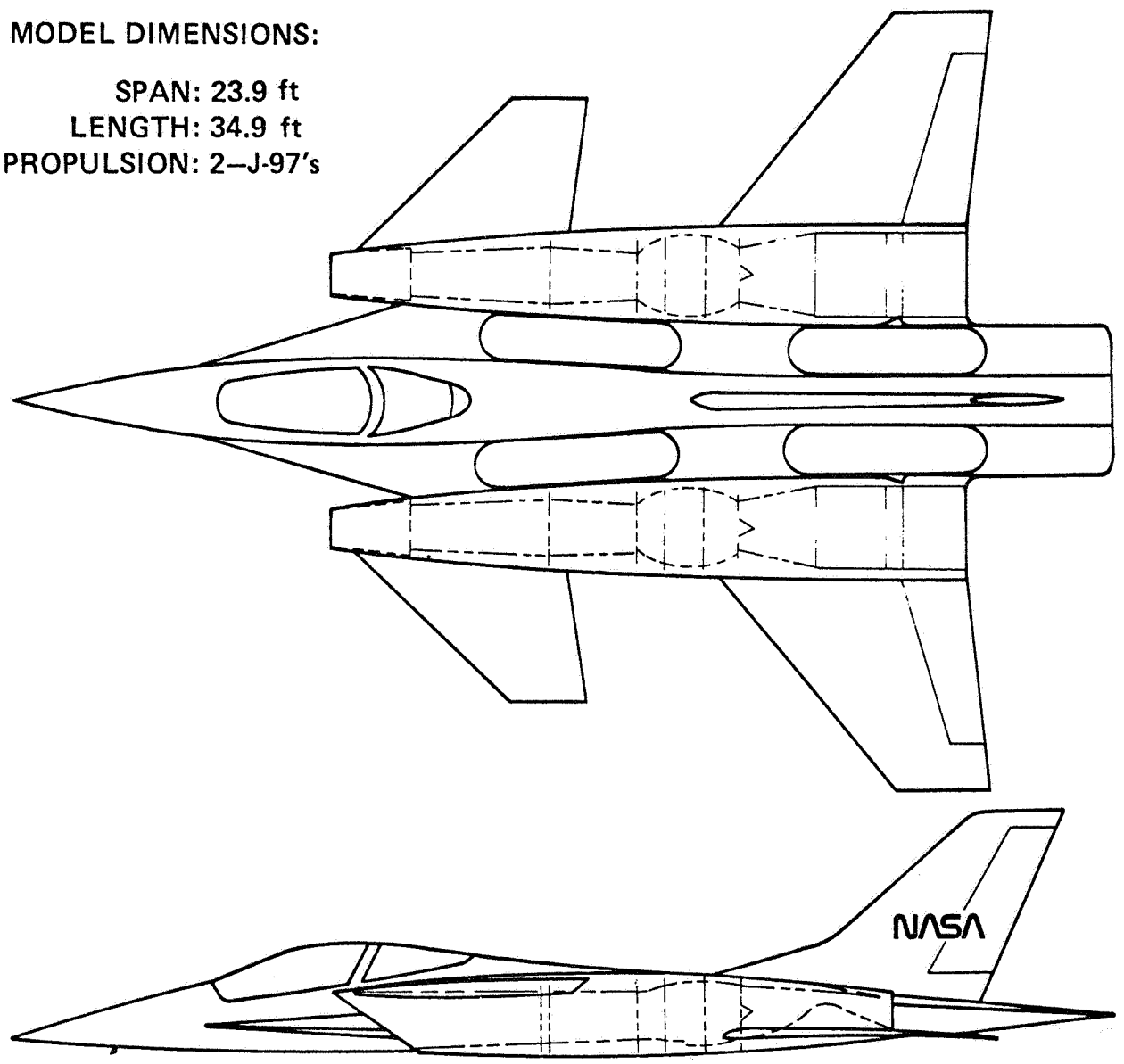

Figure 13.- Sketch of model under consideration for tests in the Ames 40- by 80-Foot Wind Tunnel.

- BASIC STUDIES—(EXPERIMENTAL)
  - SHORT DIFFUSER AUGMENTOR
  - FUSELAGE OR NACELLE MOUNTED
  - STOWAGE PROBLEMS
- THEORY DEVELOPMENT
- LARGE-SCALE V/STOL FIGHTER
  - FUSELAGE MOUNTED
  - NACELLE MOUNTED
- CONTROL THRUSTERS

Figure 14.- Areas of future effort in thrusting ejector research and development.

An Overview of Current Navy Programs to Develop Thrust Augmenting Ejectors

K. A. Green
Naval Air Development Center

Abstract

A brief description of current basic research and exploratory development programs related to thrust augmenting ejectors within the Navy is given. The individual pieces of work are related to an overall direction of effort with the objective of developing improved augmenter designs for both lift and control applications.

Introduction

The Navy has been examining the possibilities for a Vertical/Short Take-off and Landing (V/STOL) aircraft since the early 1950's to maintain its sea control capability while enhancing the dispersal of these aircraft within the fleet. Although many propulsion concepts for V/STOL aircraft have been proposed, the particular concept of interest in this paper is the ejector/augmenter. The ejector concept for vertical take-off and landing aircraft has been under consideration for many years. To date, however, a successful aircraft using this concept has not been demonstrated. This fact has been attributed primarily to the low values of augmentation ratio achieved in the aircraft configurations.

During the past 10 to 12 years a significant effort has been applied to developing a thrust augmenting ejector design that produces a high augmentation ratio. The Air Force Aerospace Research Laboratories (ARL) appears to be the primary source of recent basic information on these designs. The work conducted at ARL was summarized by Viets in reference (a).

Based on the ground work set down by ARL and particularly the hypermixing primary nozzle design developed at ARL (references (b) and (c)) the Navy and the Rockwell International Corporation (Columbus Aircraft Division) launched into the development of a high speed aircraft technology demonstrator using thrust augmenting ejectors in the wings to provide lift in the vertical mode. This aircraft, designated the XFV-12A, is now undergoing its initial testing and evaluation.

The purpose of this paper is to briefly outline current on-going basic research and exploratory development programs related to thrust augmenting ejectors being supported by the Navy and to show how these efforts fit into an overall plan or direction of work. The XFV-12A aircraft is not included in this category and its status will not be discussed in this paper.

Background

During the past several years numerous Navy Laboratories and installations have been involved in supporting in-house and/or contractural efforts in many different aspects of ejector/augmenter design (figure 1). Some of these labs are not currently funding ejector work but they remain interested in the technology.

Rather than start by listing and describing the currently funded work, an effort is made to describe the general technology development program goals, how these goals are being approached and how previous, current and planned programs are interrelated. Figure 2 is an attempt to summarize this information and illustrates three main flows or directions of work. The flow of primary interest is the one with direct application to the end goal of developing an improved augmenter for V/STOL applications. This effort starts with the expansion and optimization of those areas that have indicated promise for substantial increases in augmentation ratio, proceeds with a design phase, laboratory model testing, full scale testing and finally aircraft installation and testing. Although the basic research and exploratory development is primarily involved in the data base development, it has become increasingly clear that specific design and installation effects are very important. The design phase and laboratory model testing, therefore, should be broached early in the total plan. Iteration on specific pieces of the data base may be required after the design configuration and requirements are established.

In support of this main program effort there are two additional flows of work. The first is to develop an accurate prediction capability that will not only impact on the main program at a number of points, but will be of value in future years in evaluating a variety of ejector designs. The second area of work that will impact on the main program flow is a general technology development of ejectors and associated effects. This technology development, as it presently exists, is split into the more specific areas of lift and control, since thrust augmenting ejectors may be suitable for both areas.

Figure 2 indicates not only the general goals and the approach being used, but also shows specific areas of interest for which work has been done in the recent past, is currently underway, or is being considered for future studies. This figure is not intended to be all inclusive but hopefully will provide a clear and concise overview of the current ejector technology program within the Navy. The remainder of this paper will briefly discuss the currently funded programs, who is doing the work and which Navy installation is funding the effort.

Advanced Diffuser and End Wall Design

The jet-diffuser ejector was a concept developed by the Flight Dynamics Research Corporation under a Naval Weapons Center contract as part of the STAMP (Small Tactical Aerial Mobility Platform) program (reference (d)). Figure 3 illustrates this ejector design in the STAMP configuration. One of the unique features of this device is the high velocity jet that not only provides boundary layer control for the highly diverging diffuser but also extends the diffuser action beyond the physical walls. High values of augmentation ratio ($\phi \simeq 2.0$) have been obtained with this device in the laboratory at low pressure and temperature ratios. Recent testing of the STAMP configured ejector at the Naval Air Propulsion Center has shown the device to be relatively insensitive to pressure ratio (up to NPR = 2.1) but indicated approximately a 0.15 reduction in ϕ at a nozzle temperature ratio of 2.4.

During the development of the jet-diffuser ejector, it was found that significant differences in augmentation ratio could be obtained with changes in end wall design. Work has been completed by the Flight Dynamics Research Corporation, under contract to the Naval Air Development Center, to shorten and optimize the design of the end walls as well as maximize the augmentation ratio with the new diffuser configuration. Results to date have shown that the end walls can be reduced in length such that they are no longer than the side walls of the original STAMP configuration and are also flaired out to provide additional diffusion. The configuration has been fabricated and tested, showing good flow stability and high values for augmentation ratio ($\phi \simeq 2.0$) at NPR $\simeq$ 1.3 and NTR $\simeq$ 1.0.

A second area of concern with the jet-diffuser ejector is the detached primary nozzles. These present significant installation and packaging difficulties in aircraft applications. The Naval Air Development Center in conjunction with NASA Ames is initiating an effort with the Flight Dynamics Research Corporation to integrate the primary nozzles into the ejector shroud. That is, develop attached nozzles for the ejector while maintaining high augmentation ratio.

Advanced Primary Nozzles

The Rockwell International Corporation supported by the Naval Air Systems Command has studied a wide variety of primary nozzle configurations and designs (figure 4) to enhance the mixing and entrainment process within an ejector (reference (e)). Currently, Rockwell is investigating advanced configurations of hypermixing nozzles both analytically and experimentally.

The development of the advanced hypermixing design is based on a three dimensional mixing code. With this code a wide variety of nozzle configurations can be examined for possible improved mixing characteristics. Having found a computer predicted design that shows promise, it is then planned to fabricate and test this configuration. Current thinking is toward a combination of hypermixing and cross-slot nozzles (figure 5).

A second concept for increasing the primary nozzle entrainment is the use of unsteady flow. Work in this area is presently underway at the Naval Post Graduate School in a joint effort with the University of Queensland (reference (f)). Two basic concepts are being examined in these studies. The first involves a time varying jet deflection with a constant mass flow (fluidic nozzle). The second is a time varying mass flow with no variation in direction (fully pulsed primary and a pulsed core axisymmetric primary nozzle). Figure 6 illustrates the test results for the three different nozzle designs. In this case the entrainment function (Q/Q_E) is plotted against the non-dimensionalized downstream distance. All of these tests, however, were conducted at rather low pressure ratios (NPR $\simeq$ 1.13) and into quiescent air. Although these results appear encouraging, it remains to be determined if similar results can be obtained at the higher pressure ratios necessary for practical application and if high nozzle thrust efficiencies can be obtained.

The previously discussed basic research and exploratory development work is directed to improving the augmentation ratio and stability of ejectors and allowing for the orderly progression to a design phase and eventual aircraft application. Supporting this main effort, as mentioned earlier, are two additional paths of work. One is directed to developing improved predictive capability and the second is a general technology development.

Analytical Studies

There are several programs currently underway to develop an improved predictive capability with the ultimate goal of being able to estimate installed ejector performance. This, of course, will not only impact the main thrust or direction of effort but will also be useful for future evaluations.

Work is currently underway at the Naval Air Development Center to build an in-house predictive capability and understanding of various loss mechanisms and their sensitivity to overall augmenter performance. Several computer codes of varying degrees of sophistication are being exercised and applied to several different ejector configurations of interest. Figure 7 examines the ARL configuration "C" ejector showing the no loss situation, the effects of various losses, and a comparison with experimental data.

Viscous wall jets in a co-flowing field with finite cross flows are being studied analytically by the Rockwell International Corporation (Science Center) under contract to the Naval Air Development Center. Although this particular study is of interest for numerous applications, the application of primary interest is related to secondary stream cross flows within an augmenter having Coanda wall jets. These cross flows are particularly strong for ejectors having a tapered trailing edge as illustrated in figure 8. The spanwise flow is always toward the wide side of the augmenter and is probably due to the lower pressure being maintained for a longer distance at the point when the diffuser flaps are long. Figure 8 also schematically illustrates the mathematical problem being studied for the purpose of examining the evolution of velocity profiles, shear stress, sideslip angles and separation.

As a first step in developing a unified theory to include the effects of external flow on ejector augmentation ratio, the Rockwell International Corporation (Columbus Division), under contract to the Office of Naval Research, has described the ejector in terms of a lifting surface as illustrated in figure 9. The technique makes use of a parabolic, two dimensional analysis utilizing a turbulence kinetic energy model for inner jet mixing. By using a vortex lattice description for the shrouds and wing surfaces an elliptic outer potential solution can be developed that will provide a method of feedback from the ejector exit to the inlet conditions.

The augmenter wing in transition also provides a fertile area for analytical as well as experimental work. Figure 10 indicates three programs currently underway to study the jet path, vortex distribution, entrainment characteristics as well as pressure distribution on surrounding surfaces caused by a high aspect ratio rectangular nozzle in a cross flow. The first approach indicated in figure 10 is being conducted by the Vought Corporation and is jointly funded by the Naval Air Development Center and NASA Langley. Although this is primarily an experimental study, its ultimate goal is to develop empirical models. In any case, this data will be very useful in verifying and providing a reference point for the other two purely analytical methods.

The second approach to the augmenter wing in transition is being conducted by Neilson Engineering and is jointly supported by the Naval Air Systems Command and NASA Ames. This approach makes use of vortex "rings" and quadralaterals and does require some experimental data as input. The objective is to determine final jet position and pressure distribution on a wing type surface.

The third approach is the most sophisticated and as a result the most risky. This study is being undertaken by Computational Mechanics Consultants, Inc. and is supported by the Naval Air Development Center. The technique being used here is to solve the parabolic form of the Navier-Stokes equations for the viscous jet and match the solution to a potential free stream. The objective is to determine the final jet position and configuration as well as determine the effect on wing loading in and out of ground effect. The advantage of this approach is that it requires no experimental data input.

General Technology Development

As mentioned previously, efforts in this area are directed to both lift and control applications. Although a number of items are listed in figure 2 as areas of interest, not all of them are currently funded. The one area that is presently being funded is that using ejector concepts to augment reaction control systems (RCS). That is, amplify the control thrust for the same engine bleed flow or produce the same thrust for a reduced bleed flow. A near term possibility for this application is the Harrier RCS. Two approaches are presently being examined in this regard.

The first involves a high pressure annular nozzle design with a variable area ratio valve-in-nozzle concept shown schematically in figure 11. This work is being conducted by the David Taylor Naval Ship Research and Development Center (Carderock). The secondary flow for this device enters through a central core as well as around the primary head. The sliding ring valve that moves in and out on the cylindrical core controls the flow. Static tests with this device have indicated a 23% increase in specific thrust over a simple primary nozzle alone at a pressure ratio 9.0 and mixer length to diameter of 2.25. Work is currently underway to examine the system dynamically. Input parameters to be used and output parameters desired for this study are shown in figure 11.

A second concept that is being examined for possible application to reaction control systems is the crypto-steady or rotary augmenter concept shown in figure 12. Both analytical and experimental studies are being conducted with this device as a joint effort of the U.S. Naval Academy and the George Washington University. The device consists of a rotating primary nozzle assembly which is centrally supplied by a high pressure/energy primary fluid. The slot nozzles, having an inclination to the spin axis, discharge the fluid into the primary-to-secondary duct interaction zone as primary jet sheets. Reaction forces cause the primary nozzles to rotate, thus defining helical pseudo blades which accelerate the ambient secondary flow. As can be seen from figure 12, significant augmentation ratios are predicted analytically for this concept.

Summary

Research and exploratory development programs on ejector technology are being conducted in a number of areas by the Navy. Figure 2 attempts to summarize these efforts and show their relationship to an overall direction of work.

Symbols

A_o, A'_p	Primary nozzle area
A_2, A_i	Ejector throat area
A_3	Diffuser exit area
d	Hydraulic diameter of nozzle
F	Lifting force on shroud
L_D	Diffuser length
L_M	Mixer length
NPR	Nozzle pressure ratio
NTR	Nozzle temperature ratio
$P^o_{p_i}$	Primary nozzle pressure
Q	Volumetric flow rate at position X
Q_E	Volumetric flow rate at nozzle exit
RCS	Reaction control system
T	Thrust from primary nozzle
X	Distance from nozzle exit
U, V, W	Velocities in coordinate directions
U_∞	Free-stream velocity
$\hat{U}_i$	Velocity vector of jet
β'_i	Nozzle inclination angle
ϕ	Augmentation ratio (ejector measured thrust/ideal thrust available from all nozzles due to an isentropic expansion of the same mass flow to ambient conditions)

References

a. Viets, H., "Thrust Augmenting Ejectors," Aerospace Research Laboratories Report ARL75-0224, June 1975.

b. Quinn, B., "Recent Developments in Large Area Ratio Thrust Augmentors," AIAA Paper No. 72-1174, November 1972.

c. Bevilaqua, P. M., "An Analytical Description of Hypermixing and Tests of an Improved Nozzle," AIAA Paper No. 74-1190, October 1974.

d. Alperin, M., Wu, J. J., and Smith, C. A., "The Alperin Jet-Diffuser Ejector (AJDE) Development, Testing, and Performance Verification Report," Flight Dynamics Research Corporation Final Report prepared for the Naval Weapons Center, NWC-TP-5853, 1976.

e. Schum, E., "A Study of Potential Techniques for Increasing Jet Entrainment Rates in Ejector Augmenters," Rockwell International Final Report prepared for the Naval Air Systems Command, October 1975.

f. Platzer, M. F., Simmons, J. M. and Bremhorst, K., "On the Entrainment Characteristics of Unsteady Subsonic Jets". AIAA Journal, March 1978.

- NAVAL AIR SYSTEMS COMMAND
- NAVAL AIR DEVELOPMENT CENTER
- NAVAL AIR PROPULSION CENTER
- NAVAL WEAPONS CENTER
- OFFICE OF NAVAL RESEARCH
- NAVAL POST GRADUATE SCHOOL
- NAVAL ACADEMY

FIGURE 1. NAVY LABORATORIES AND INSTALLATIONS WHICH HAVE SUPPORTED OR CONDUCTED WORK WITH THRUST AUGMENTING EJECTORS FOR AIRCRAFT APPLICATIONS IN THE RECENT PAST.

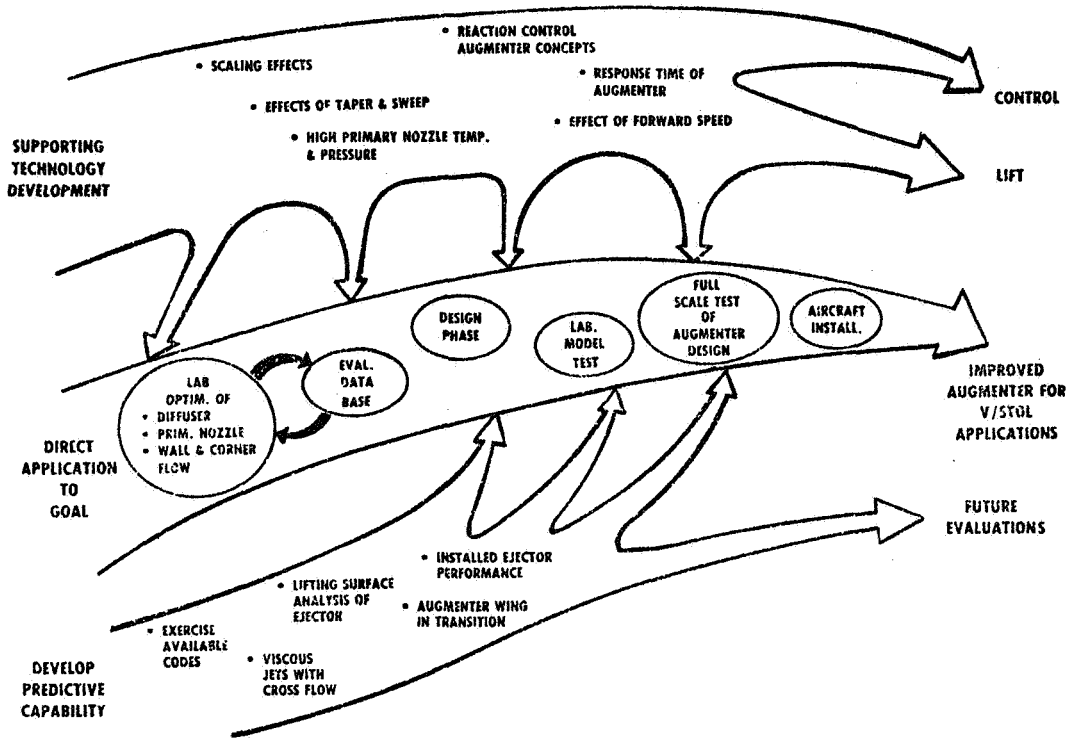

FIGURE 2. EJECTOR TECHNOLOGY DEVELOPMENT.

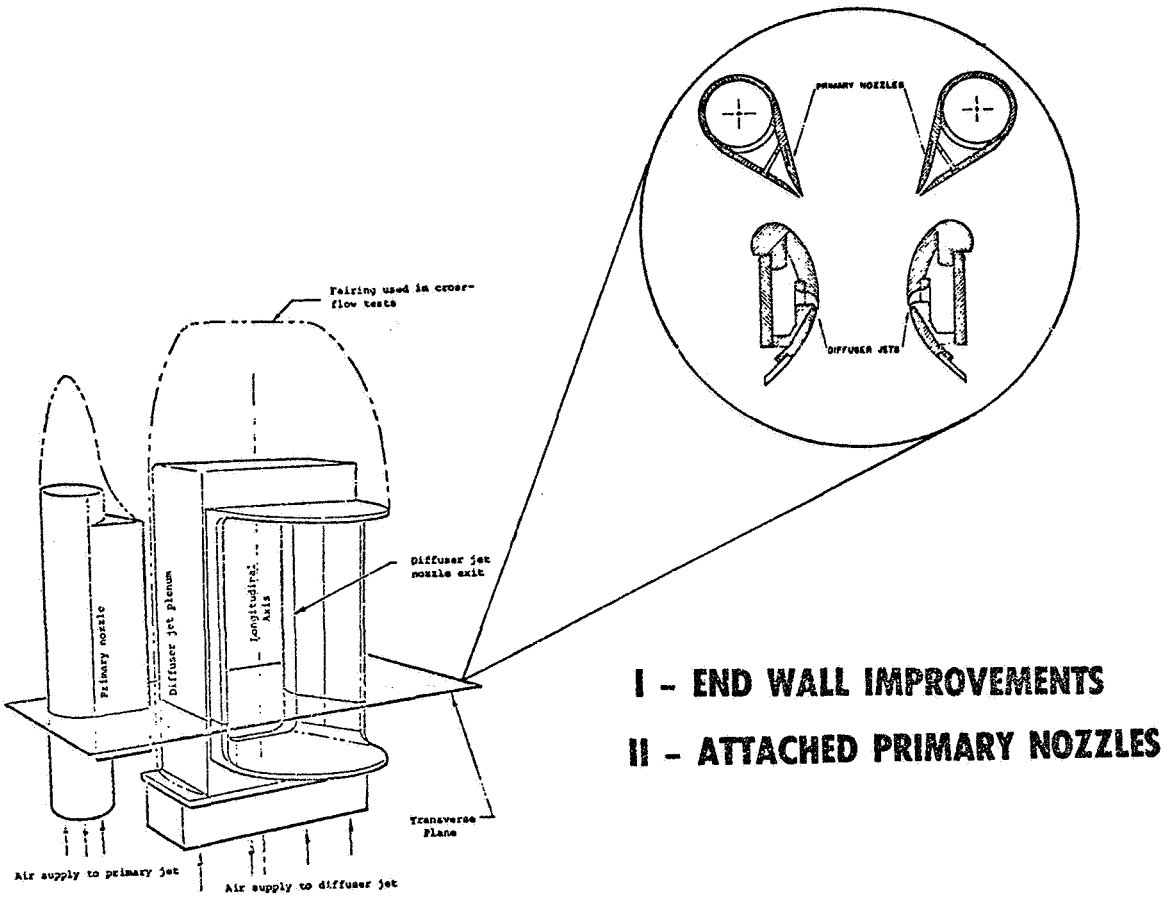

FIGURE 3. IMPROVEMENTS TO ALPERIN JET-DIFFUSER EJECTOR.

- HYPERMIXING NOZZLE
- SWIRL FLOW
- JET DISTURBANCES
- ACOUSTIC INTERACTION
- FORCED PULSATIONS
- JET INTERACTION
- BASE FLOW TURBULENCE

FIGURE 4. POTENTIAL PRIMARY NOZZLE DESIGNS FOR INCREASING ENTRAINMENT.

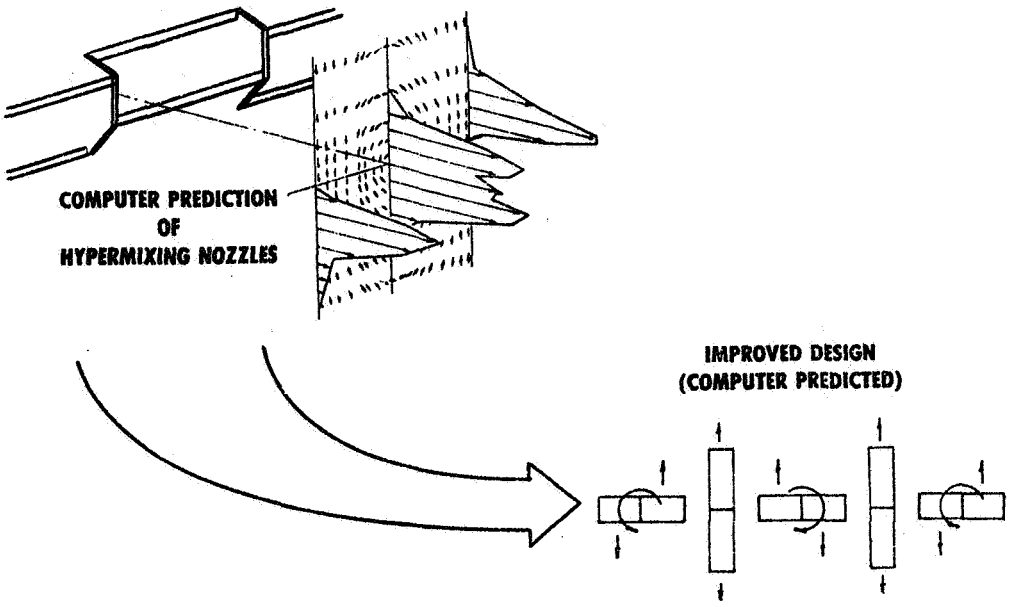

FIGURE 5. DEVELOPMENT OF ADVANCED HYPERMIXING NOZZLES.

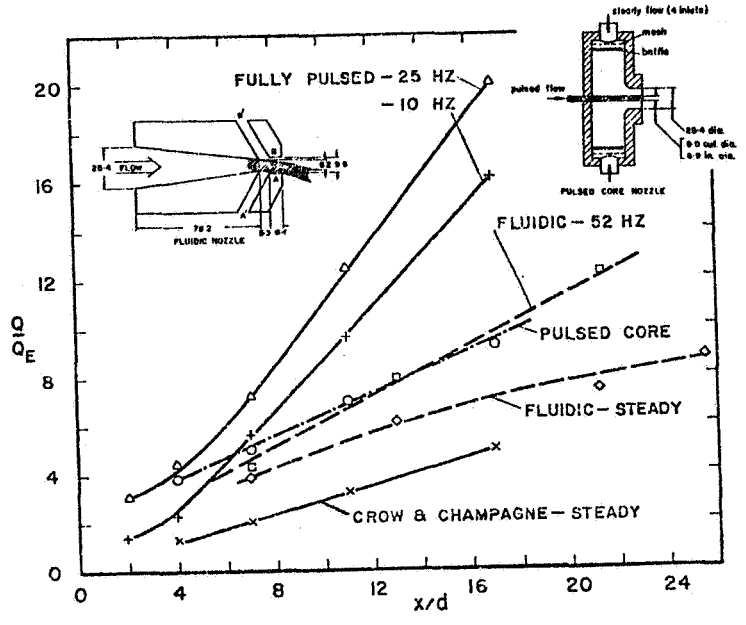

FIGURE 6. INCREASED ENTRAINMENT DUE TO UNSTEADY FLOW.

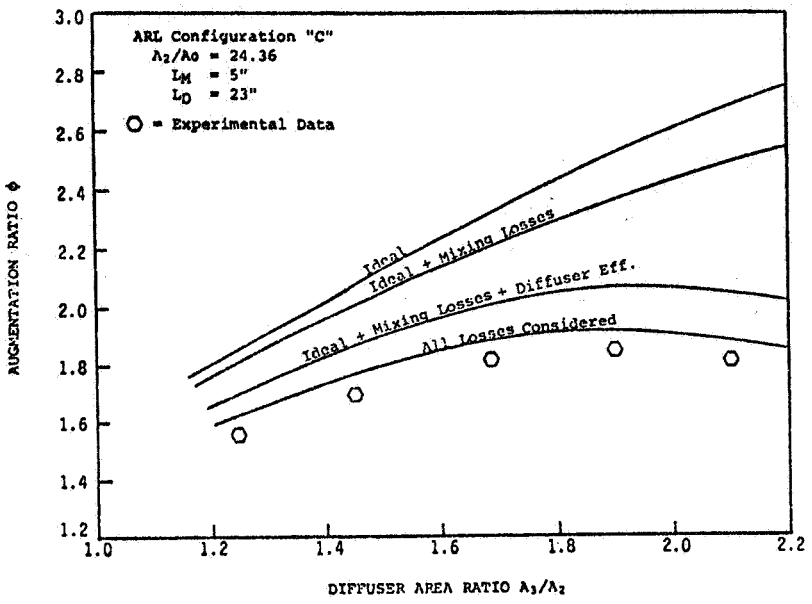

FIGURE 7. EXERCISE SEVERAL EJECTOR COMPUTER CODES AND COMPARE TO AVAILABLE EXPERIMENTAL DATA.

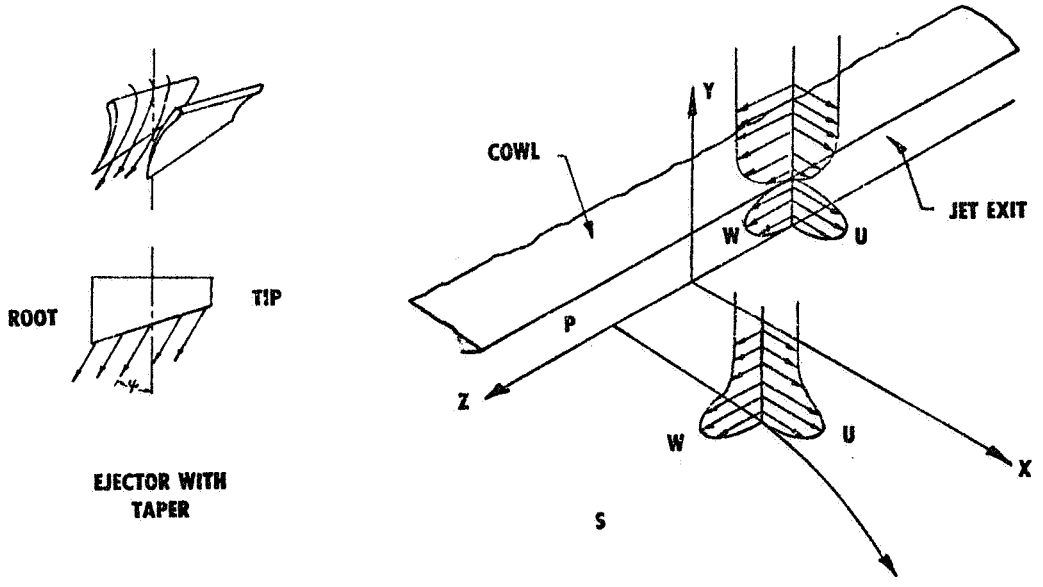

FIGURE 8. THREE-DIMENSIONAL WALL JETS WITH CROSS FLOWS.

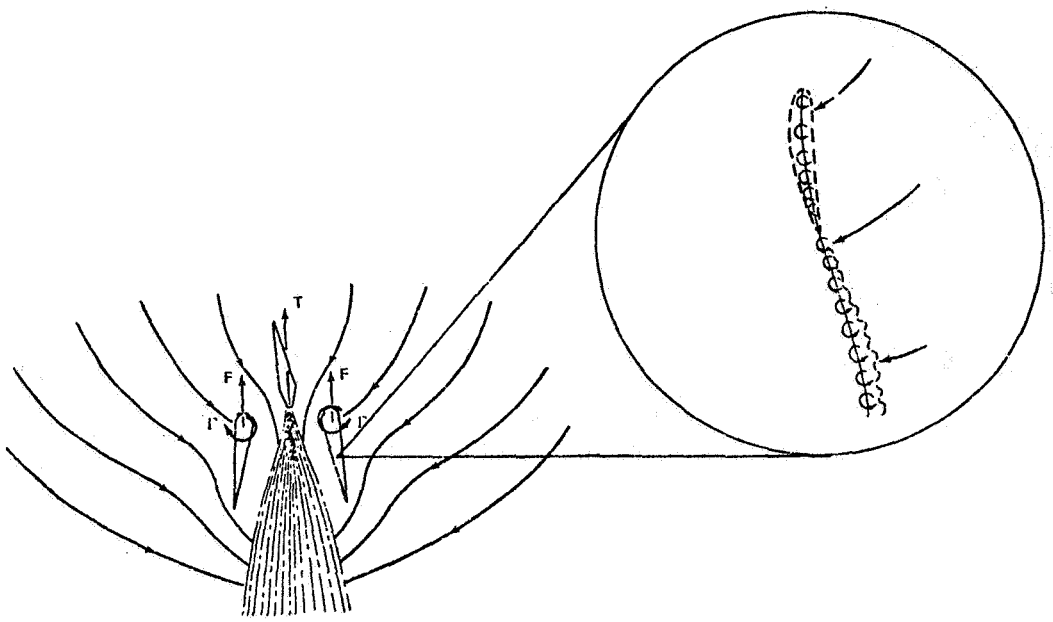

FIGURE 9. LIFTING SURFACE THEORY FOR THRUST AUGMENTING EJECTORS.

APPROACHES

- **EXPERIMENTAL (AR = 4)**
  - **DEVELOP EMPIRICAL MODEL FOR**
    JET PATH
    VORTEX DISTRIBUTION
    ENTRAINMENT
- **ANALYTICAL**
  - **VORTEX "RING" APPROACH**
  - **DETERMINE FINAL JET POSITION**
  - **DETERMINE WING LOADING**
- **ANALYTICAL**
  - **VISCOUS JET**
  - **POTENTIAL FREE STREAM**
  - **DETERMINE FINAL JET POSITION & CONFIGURATION**
  - **DETERMINE WING LOADING IN AND OUT OF GROUND EFFECT**

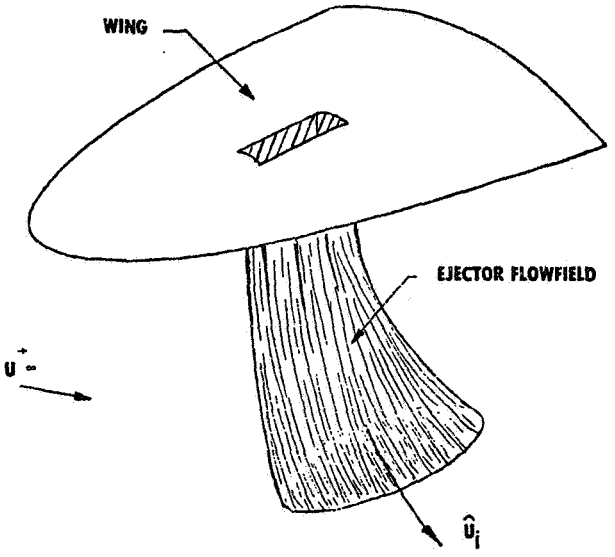

FIGURE 10. AUGMENTER WING IN TRANSITION.

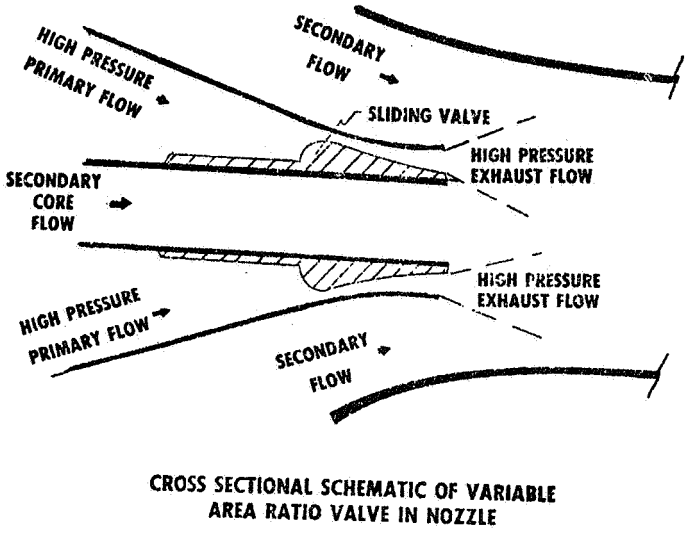

CROSS SECTIONAL SCHEMATIC OF VARIABLE AREA RATIO VALVE IN NOZZLE

DYNAMIC EXPERIMENTATION

- **INPUTS**
  - STEP & SINUSOIDAL
  - AMPLITUDE = 10, 50 & 90% OF MAXIMUM
  - FREQUENCY RANGE = 0-20 HZ
  - INCREASING & DECREASING THRUST
- **OUTPUT**
  - THRUST AMPLITUDE
  - RESPONSE RATE
  - PHASE LAG

FIGURE 11. AUGMENTATION OF REACTION CONTROL SYSTEMS.

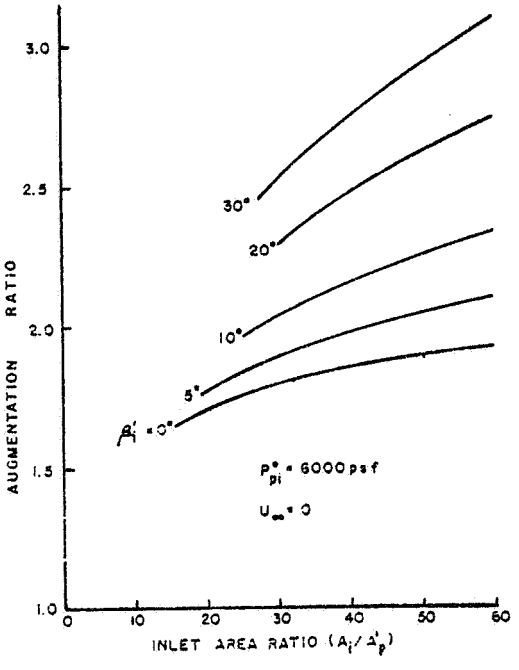

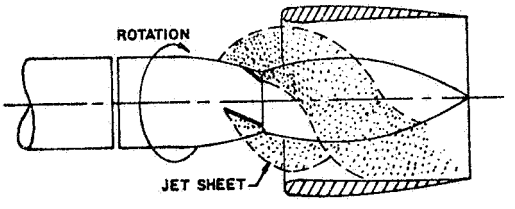

FIGURE 12. CRYPTO STEADY AUGMENTER PERFORMANCE (THEORETICAL).

NUMERICAL PREDICTION OF 3-D EJECTOR FLOWS

Donald W. Roberts
Gerald C. Paynter

Boeing Military Airplane Development
Mail Stop 41-52
P.O. Box 3999
Seattle, Washington 98124

NUMERICAL PREDICTION OF 3-D EJECTOR FLOWS

Introduction

Ejectors are devices that present numerous complex flow problems to the design engineer. One obvious problem is that complex three-dimensional geometries can be of interest. Another problem is that local regions of supersonic flow can occur. Effects associated with three-dimensional boundary layers and regions of strong curvature can also be important, as shown in Figure 1. The performance of the ejector is a strong function of the mixing process between the primary nozzle flow and the secondary flow. The turbulence levels and the turbulence-driven secondary flows can influence the mixing process and thus the ejector performance. The design engineer is confronted with the difficult task of managing a number of complex flow phenomena when designing an ejector. The current design procedure, based on parametric model scale testing, can be substantially improved through the use of available flow analyses to reduce the required test matrix and to improve the designer's understanding of flow phenomena which have a strong influence on ejector performance.

In the traditional or test based design procedure, parametric model scale tests are conducted to obtain gross performance parameters, such as mass flow rates and thrust. These tests are not aimed at getting flow details and they are thus usually of little use in providing an understanding of the complex ejector flow phenomena. In this approach, a design concept and simple analysis are used to define a baseline geometry. Important geometric features are varied parametrically to obtain a test matrix. These tests are often very expensive which limits the number of parameters that can be examined in a given study. Without detailed flowfield measurements during these tests, one really doesn't understand what flow phenomena are important to the performance of the ejector. Another problem with this approach is that model scale test results may not scale well. This is often because of the poor control of the

upstream flow conditions in the model test. The final result of a test based approach is typically a design that is not optimum and not well understood. This can lead to unpleasant surprises in the full scale validation phase of the design process.

The approach advocated in this paper is based on the use of parametric flow analysis rather than parametric model scale testing* to support the design of an ejector system. This approach offers a number of potential advantages. Analysis allows one to closely examine the details of the flow. Analyses can be fast and inexpensive compared to parametric model scale tests. One can afford to look at a larger number of parameters, can vary them parametrically over a wider range, and can precisely control the flow conditions. Experimental testing may still be used, but its main purpose would be to confirm the analysis for just the final design. This can give us more confidence in the design, and enhance the chance for success.

Analysis Objectives

The objective of this paper is to describe how available 3-D flow analyses might be applied to the design of ejectors. This problem can be subdivided into several key analysis elements. These are numerics, turbulence modeling, data handling and display, and testing in support of analysis development.

With the recent developments in numerics and computer technology, the capability exists to develop a useful analysis based design procedure. There are a number of numerical tools available; many of these have been developed in the basic research centers such as Ames and other Government laboratories and in the private sector. The analysis problem can be simplified by looking at the ejector flow. The flow can be naturally divided into an elliptic region that is basically inviscid and a

---

* A model scale test of a given configuraion may be desirable to validate the analysis. In contrast to the test based approach, however, this test must provide detailed flow properties to be useful for analysis validation.

parabolic or partially parabolic region which is dominated by viscous effects. The idea then is to use available flow analysis tools and couple them together to yield one analytical tool for analyzing the ejector flow. Another important feature in the numerics category is the use of automated computational mesh generation. To keep the computational costs within reason, one must make optimum use of the available computational mesh. This can be accomplished most efficiently by tailoring the mesh to the geometry and to the flow.

Turbulence modeling can often make or break an analytical method. We advocate the use of the Bradshaw classification system (Ref. 1) for complex flows. It is based on the selection of a turbulence model for the actual turbulence phenomena that occur in the flow as opposed to selecting or developing a model for the geometries that are present. Two-equation turbulence models for mixing type flows have been shown to be a good compromise between accuracy and simplicity (Ref. 2, 3, 4). These models also have direct extensions to more complex models such as the algebraic Reynolds stress models which show promise for analyzing flows with turbulence-driven secondary flows (Refs. 5, 6).

Data handling and display is important since a large computer program is going to provide a vast amount of output. One wants to be able to look at it rapidly and make quick decisions. Boeing uses dedicated minicomputers with the associated video hardware which allow one to look at large amounts of data in a short amount of time.

Testing in support of the analysis development will always be necessary to provide a means for validating the analysis. Government sponsored bench mark experiments which would be valuable for developing an improved understanding of turbulent flows could lead to better turbulence models. One could also obtain the detailed flow properties necessary for analysis validation from applied technology experiments by just adding more instrumentation.

Coupling Procedure

The basic coupling procedure proposed in this paper would divide the flow into four basic regions, Figure 2. Three of these regions are dominated by viscous effects; the other region is essentially inviscid. Initially, boundary layers on the shrouds would be neglected. An ejector system design study usually assumes a given engine operating at a "match point" or given operating condition. Therefore, the flow at (1) is fixed, and it is assumed that the nozzle ejector geometry can be varied such that the engine follows a known operating line. In other words the engine must be able to pass the mass flow rate dictated by the operating line. One must solve for the viscous flow in Region I to obtain flow conditions at B. Assuming that an initial plume shape can be determined, one can solve for the flow in the inviscid region (Region IV) to get a match at B. Then the mixing internal flow (Region II) is solved with a parabolic analysis. Finally, the jet flow (Region III), which has boundaries that overlap into the inviscid region such that the flow properties can be used for boundary conditions, is predicted. From the jet calculation a new plume shape is derived. This procedure is then iterated until a converged solution is obtained. Coupling procedures similar to this have been successfully developed. Several inviscid analyses are available for predicting the flow in Region IV. This analysis component could be a linearized potential flow code such as PANAIR or the full transonic potential flow codes which are being developed currently. Boeing has developed two 3-D parabolic viscous flow analyses. One of these has been well-documented for mixing types of flows (Refs. 3, 4). The other code has been developed for the analysis of parabolic flows in ducts with arbitrary cross sections (Ref. 7). This code solves the compressible three-dimensional parabolized Navier-Stokes equations. The Boeing viscous codes use a two-equation turbulence model which can be directly extended to the algebraic Reynolds stress model. The flow equations have been transformed and are solved in a body fitted coordinate system which allows one to tailor the mesh to the geometry and to the flow. The parabolic analysis could be extended to a partially parabolic analysis which has the fully elliptic pressure coupling necessary when strong

curvature of the flow is present (Ref. 8). This code has been used to predict turbulent flows in diffusers which transition in cross section from rectangular to round.

Our experience has shown that parabolic analyses are useful and accurate for predicting mixing and jet flows. A flow that is similar to the mixing process you find in ejectors is the mixing between a primary flow and a fan flow, Figure 3. The predictions (Ref. 3) of the total temperature contours at the exit plane are shown in Figure 4. The peak values of these total temperature contours show good agreement with the experimental data. The one exception is that the contours in the experimental data tend to be round where the predicted ones are more elliptical. This was also indicated in the model scale results. This difference in the shape of the total temperature contours could be due to a problem with initial conditions in the predicted results or it could be a problem with the turbulence model. An algebraic Reynolds stress model was recently developed which could yield a better simulation of this effect. Another example of a complex mixing flow is the interaction of the residual swirl in the turbine exhaust with the turbine support strut which generates a distorted flow in the exhaust jet. This asymmetric nozzle flow was not expected in an axisymmetric nozzle, but it is what was found experimentally. The prediction of this flow using our parabolic analysis provided good agreement with the experimental data, Figure 5.

The 3-D viscous jet analysis has been applied to several complex free jet flows (Ref. 4). One of these, the interaction of the three jets on a 727, also has an interaction with the ground plane, Figure 6. Figure 7 presents the predicted velocity contours which show the merging of the jets and the interaction with the runway. It is a biplaner solution so it is only necessary to look at one and a half jets. The jet peak velocity decay is compared with the only experimental data that is available in Figure 8. The prediction falls along the line of the experimental data. If this flow is computed assuming an axisymmetric single free-jet, the peak velocity decay of the jet is missed by a large margin. The 3-D analysis was essential in this particular case.

Conclusions

3-D flow analysis technology exists that could be used to develop an analysis based design procedure for ejectors. The key 3-D viscous and inviscid component analyses are currently available. The coupling procedures for these analyses are well understood, and they have been used in the past. A primary requirement now is to demonstrate computational efficiency so that the overall analysis procedure can be used for design work. The ability to select a suitable turbulence model or models may prove to be the factor which controls the effectiveness of an analysis based design procedure for ejectors.

References

1. Bradshaw, P., "Review - Complex Turbulent Flows", Journal of Fluids Engineering, Trans. ASME, June 1975.

2. Launder, B., and Spalding, D. B., "The Numerical Computation of Turbulent Flows", Computer Methods in Applied Mechanics and Engineering, 3, 269-289, 1974.

3. Birch, S. F., Paynter, G. C., Spalding, D. B., and Tatchell, D. G., "Numerical Modeling of 3-D Flows in Turbofan Engine Exhaust Nozzles", J. of Aircraft, 15, 8, 1978.

4. Barton, J. M., Birch, S. F., Paynter, G. C., and Crouch, R. W., "An Experimental and Numerical Study of Three-Dimensional Turbulent Jets", AIAA Paper No. 78-994, 1978.

5. Tatchell, D. G., "Convection Processes in Confined Three-Dimensional Boundary-Layers", Ph.D. Thesis, University of London, July 1975.

6. Gessner, F. B., and Emery, A. F., "A Reynolds Stress Model for Turbulent Corner Flows -- Part I: Development of the Model", Journal of Fluids Engineering, 261-268, June 1976.

7. Roberts, D. W., and Forester, C. K., "Parabolic Procedure for Flows in Ducts with Arbitrary Cross-Sections", AIAA Journal, Vol. 17, No. 1, January 1979.

8. Pratap, V. S., "Flow and Heat Transfer in Curved Ducts", Ph.D. Thesis, Imperial College, University of London, 1975.

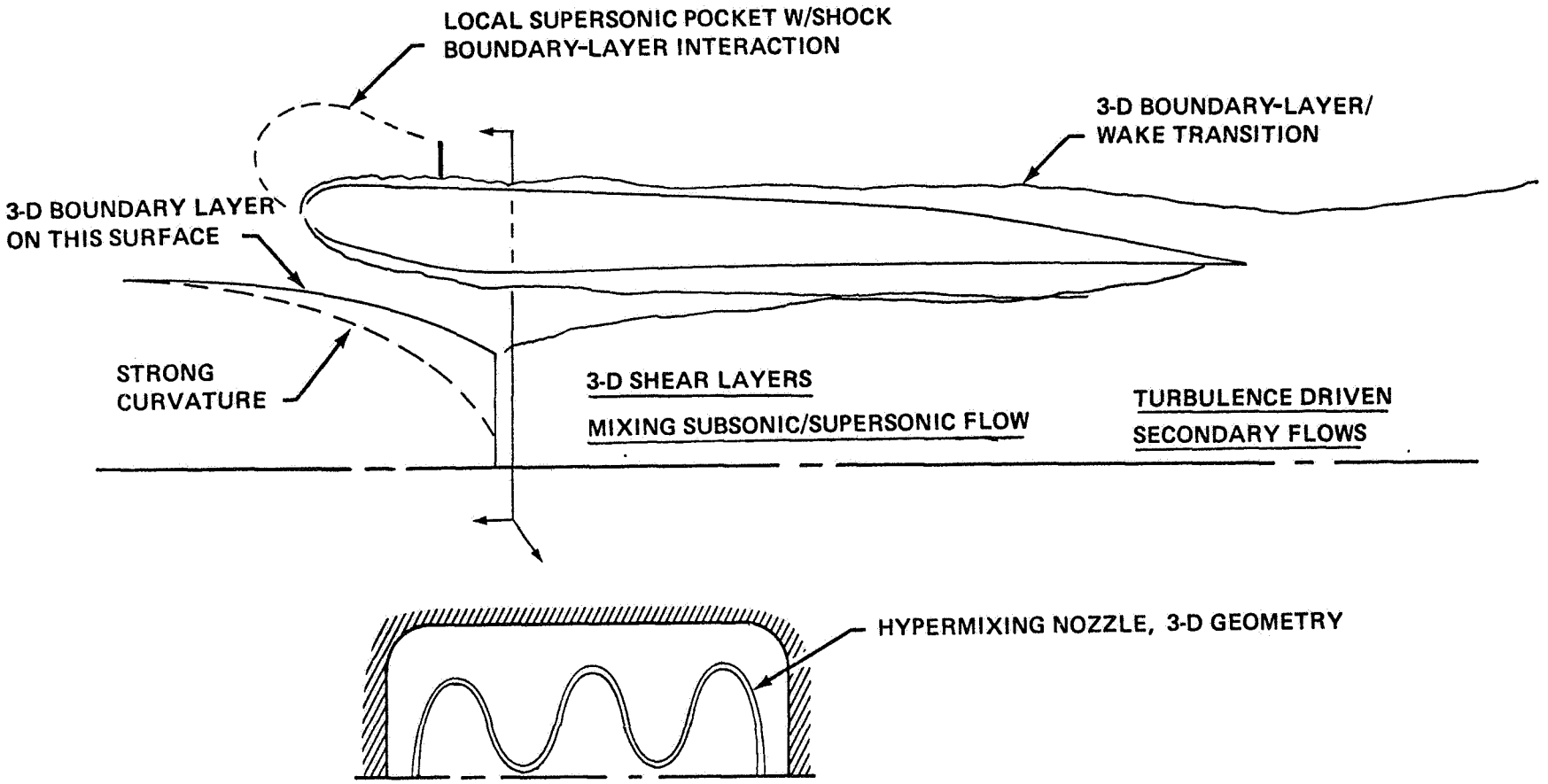

Figure 1. Flow Problems Associated with 3-D Ejectors.

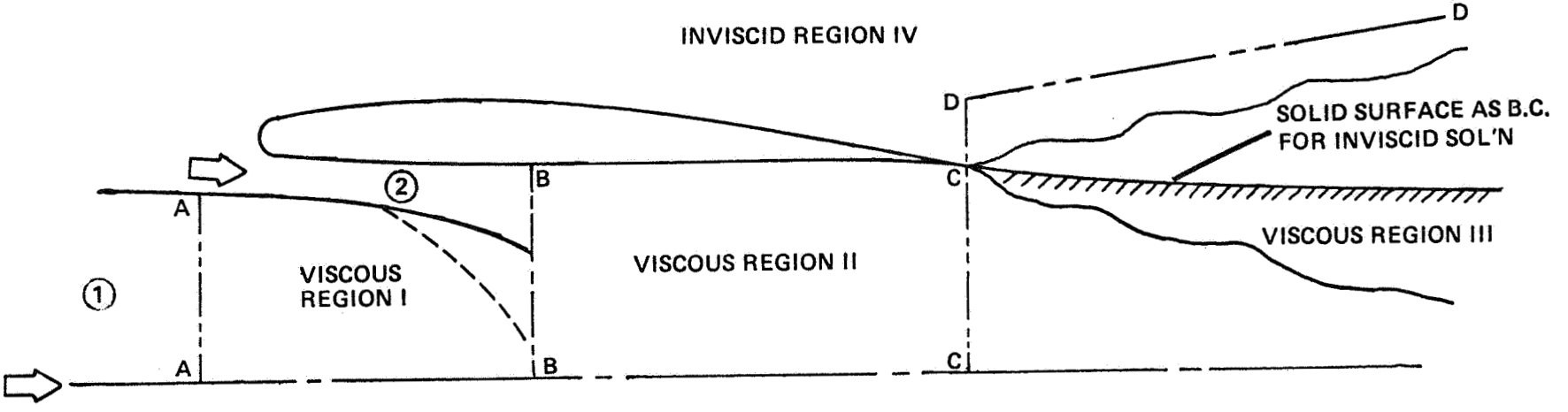

ASSUMPTIONS

- FLOW (1) IS KNOWN AND FIXED
- THE ENGINE NOZZLE GEOMETRY IS ADJUSTABLE

COUPLING PROCEDURE

1. ASSUME PRIMARY NOZZLE EXIT AREA – SOLVE REGION I
2. SOLVE REGION IV, ITERATING MASS FLOW (2) UNTIL PRESSURE CONTINUITY BETWEEN VISCOUS AND INVISCID SOLUTIONS IS OBTAINED IN PLANE B - B
3. SOLVE VISCOUS REGIONS II & III ITERATE STEPS 1, 2 & 3 UNTIL CONVERGENCE IS OBTAINED FOR PROPERTIES ON LINES C-D & D-D

Figure 2. Coupling Procedure for Viscous and Inviscid Flow Regions.

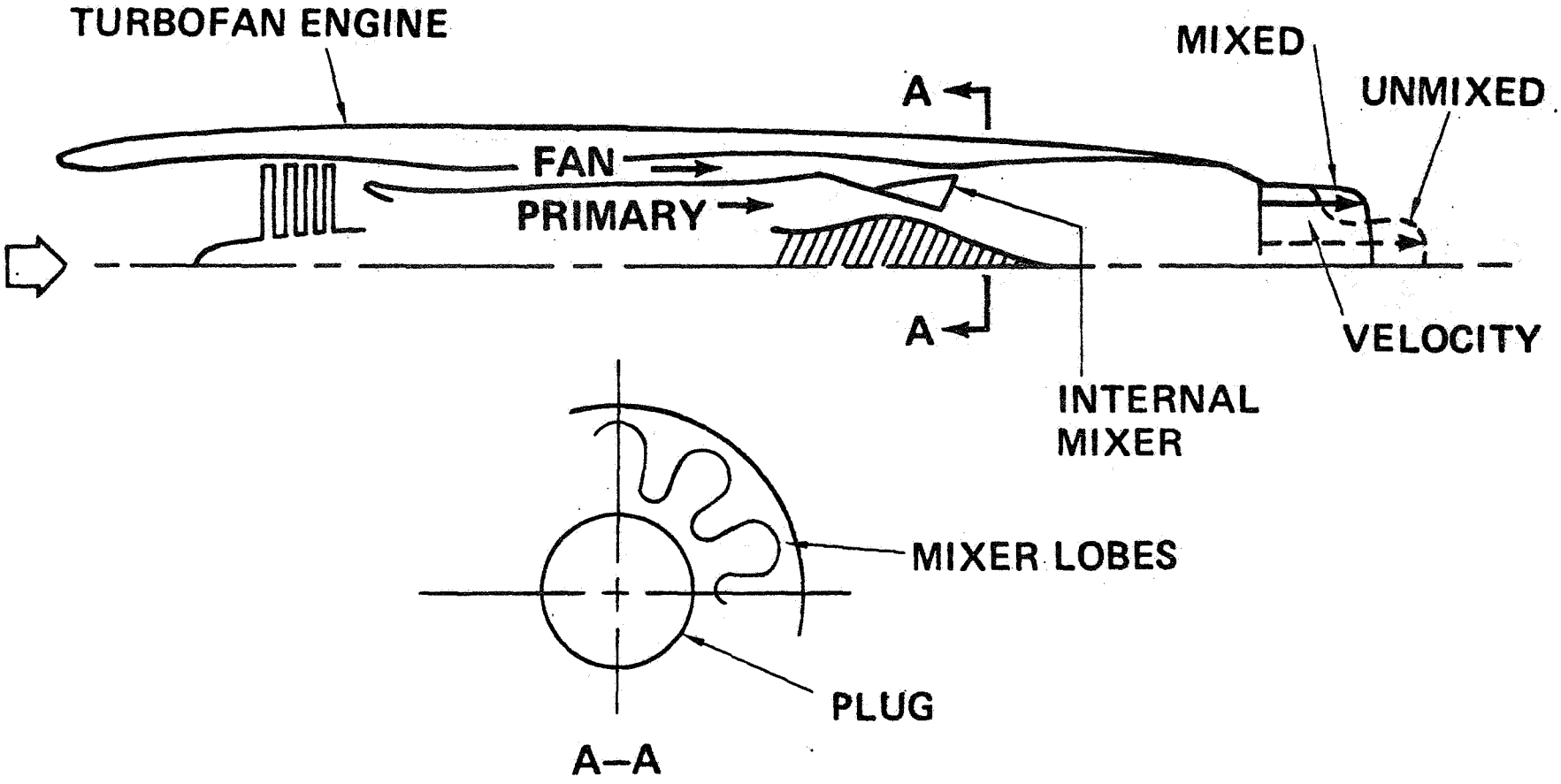

Figure 3. Cross-Section of Turbofan Engine with Lobed Mixer.

NOZZLE EXIT TOTAL TEMPERATURE MAP FROM TEST OF THE FULL SCALE FORCED MIXER

P_{tP}/P_A = 1.791
P_{tF}/P_A = 1.789
T_{tP}/T_{tF} = 2.148

CONTOUR	T_t/T_{tF}
1	1.90
2	1.80
3	1.70
4	1.60
5	1.40
6	1.20
7	1.00

COMPUTED NOZZLE EXIT TOTAL TEMPERATURE MAP FOR THE FULL SCALE FORCED MIXER, CASE 5 , **REF. 3**

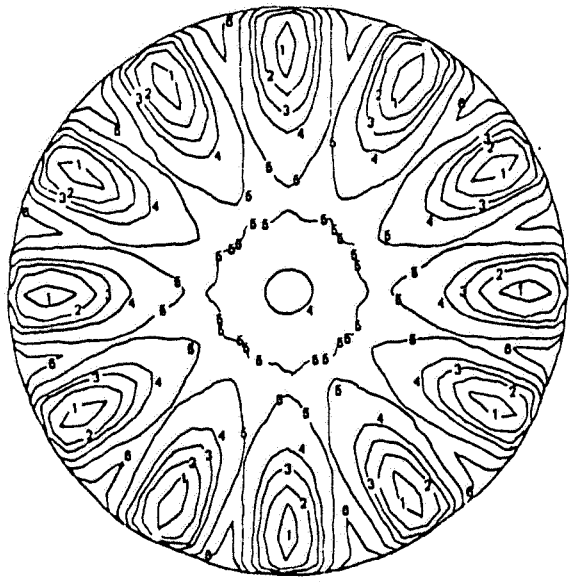

Figure 4. Experimental and Predicted Total Temperature Contours.

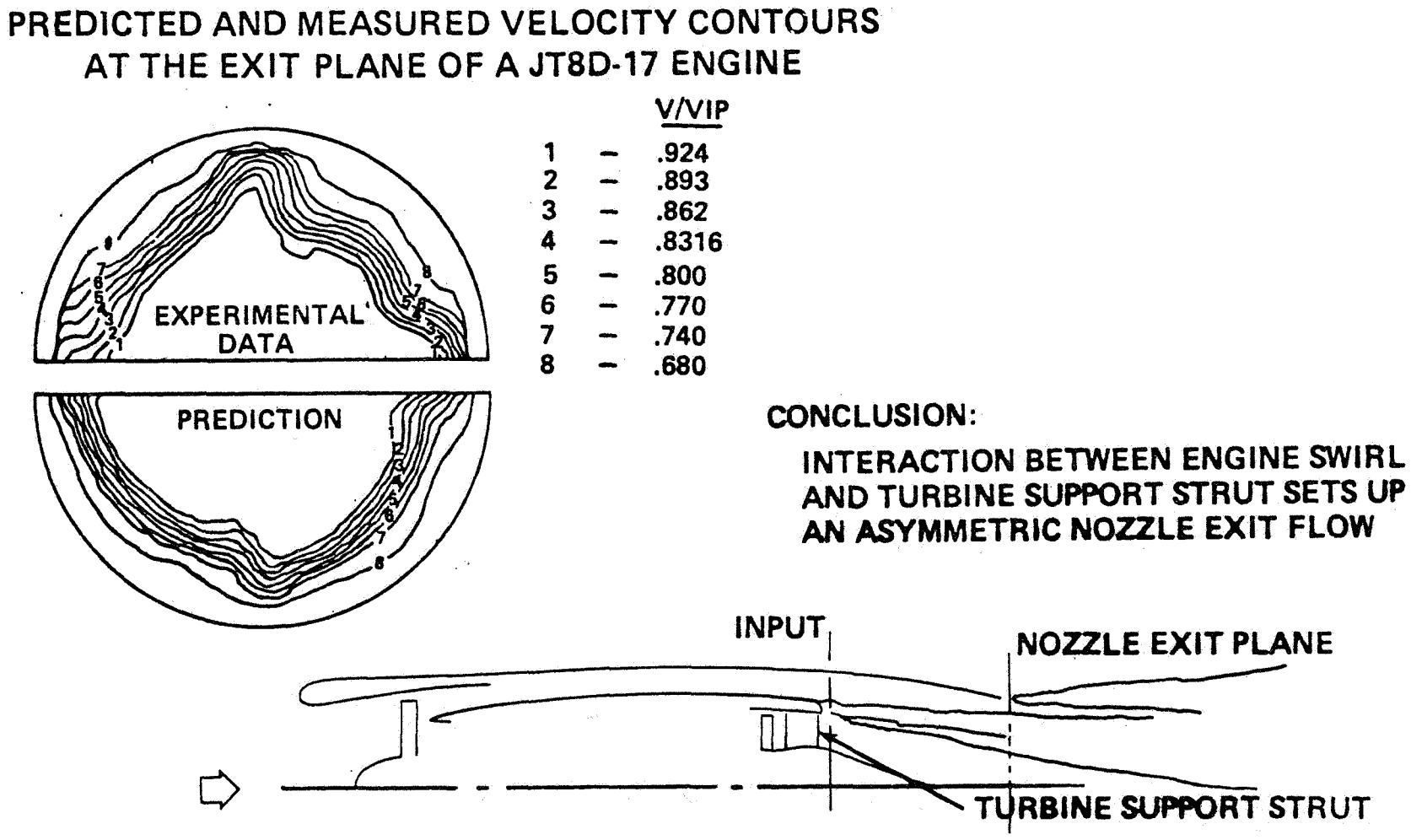

Figure 5. Experimental and Predicted Velocity Contours for Asymmetric Nozzle Flow.

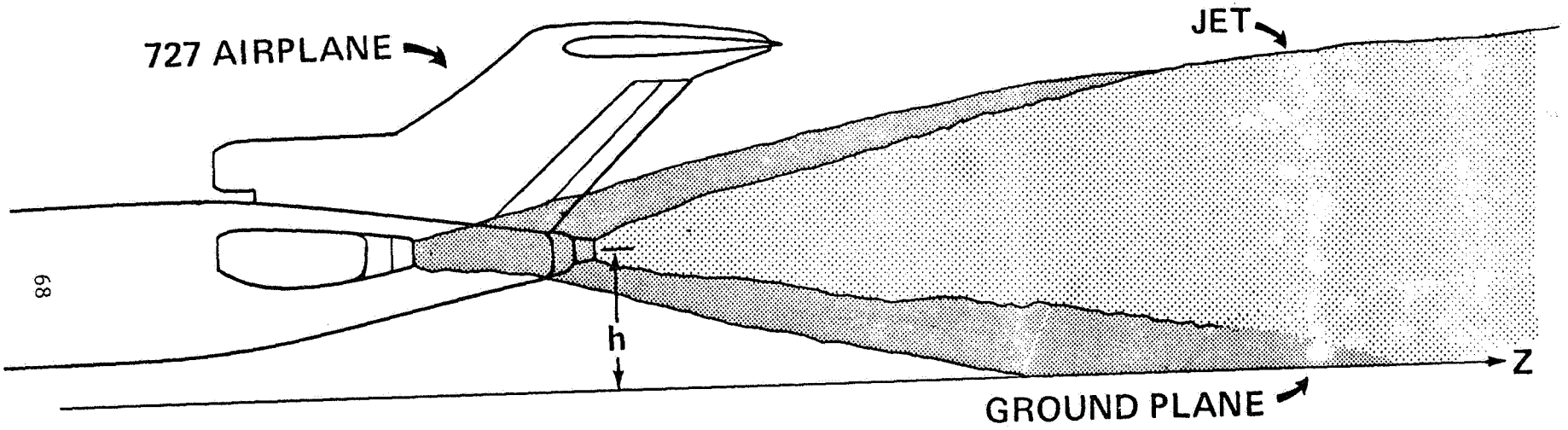

Figure 6. Schematic of 727 Jet Exhaust Interacting with Runway.

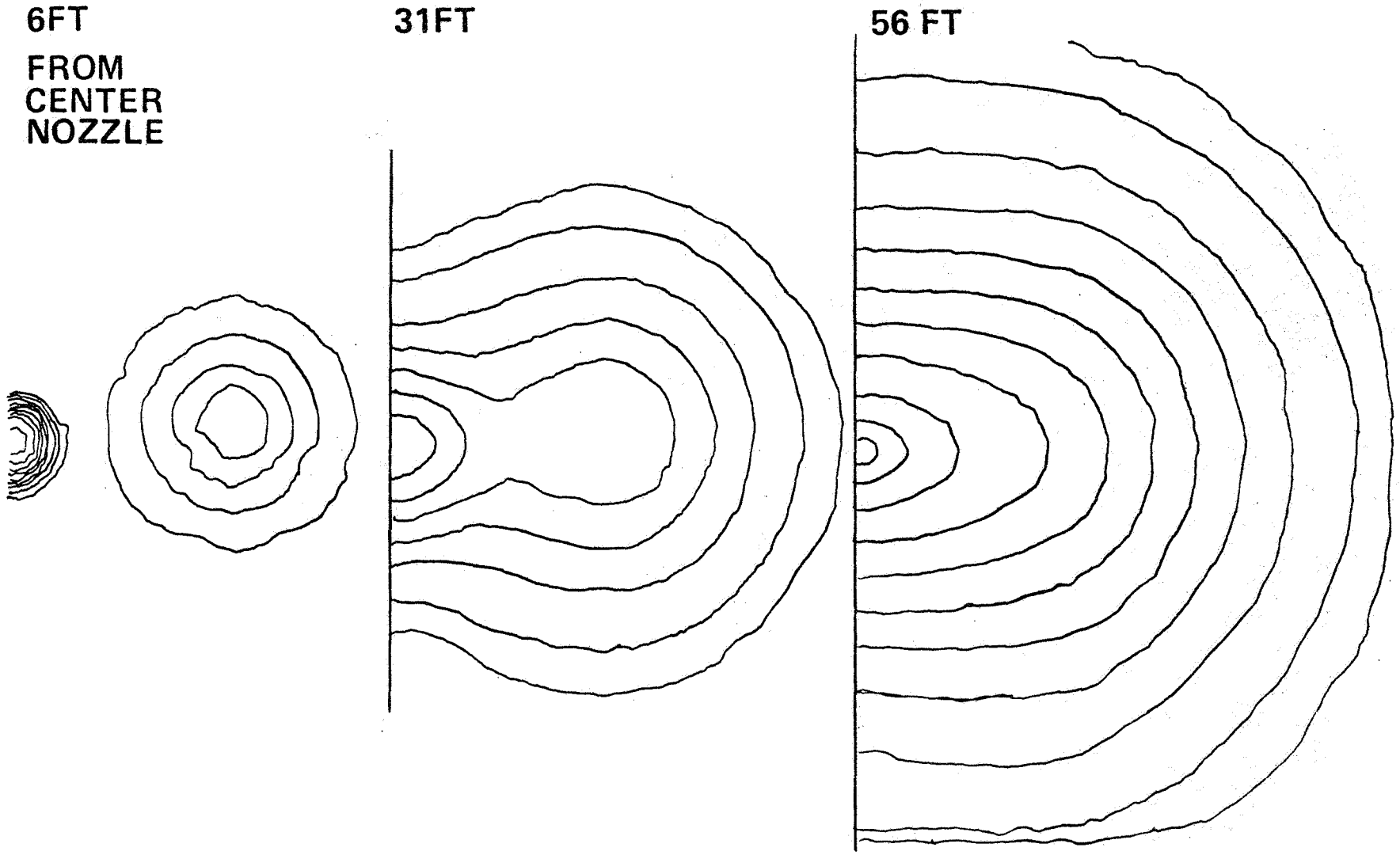

Figure 7. Predicted 727 Jet Exhaust Development.

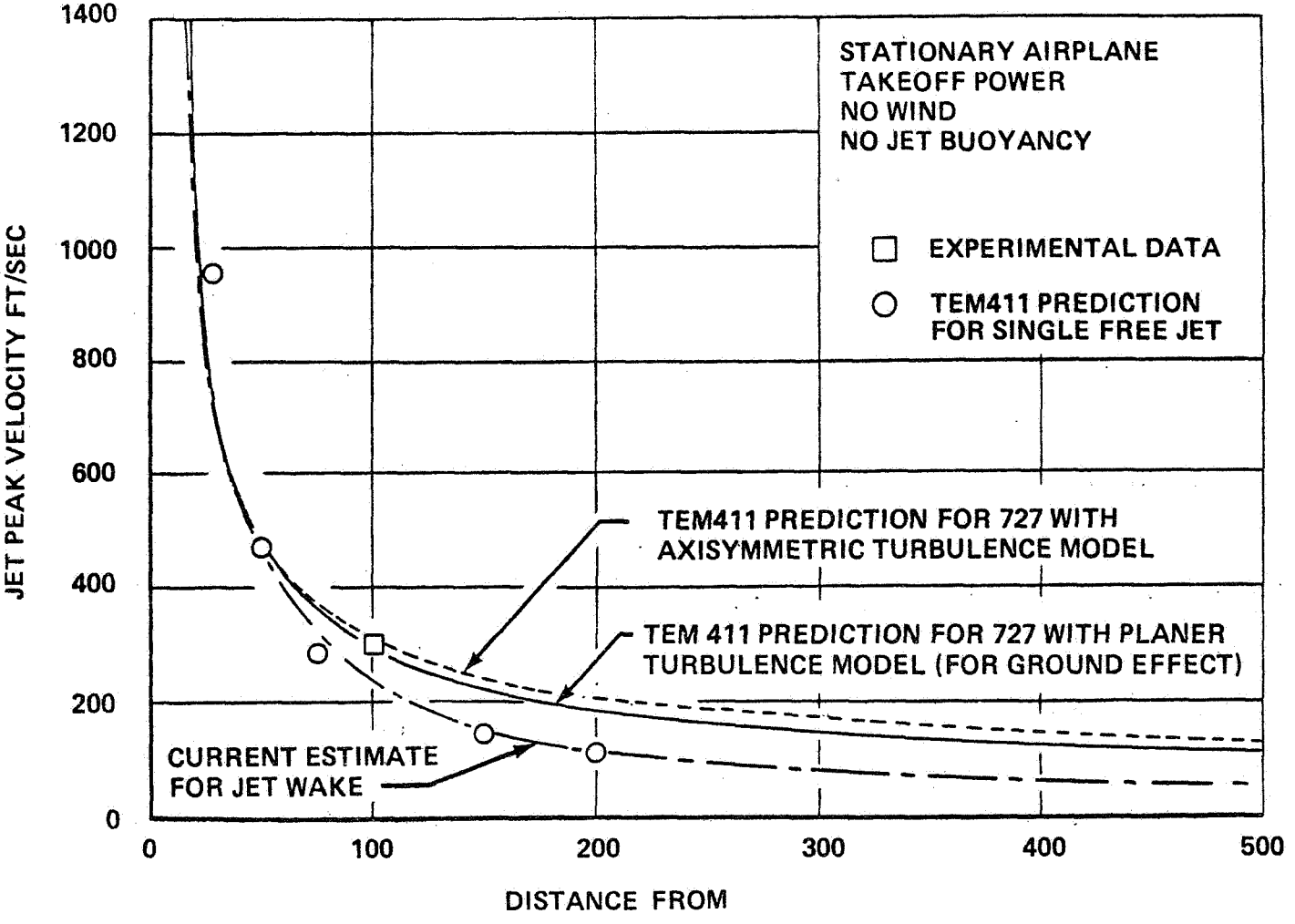

Figure 8. Predicted and Experimental peak Velocity Decay for 727 Jet Exhaust on Runway.

VISCID/INVISCID INTERACTION ANALYSIS OF THRUST AUGMENTING EJECTORS

P. M. Bevilaqua and A. D. DeJoode
Rockwell International
Columbus Aircraft Division

- Abstract -

A method has been developed for calculating the static performance of thrust augmenting ejectors by matching a viscous solution for the flow through the ejector to an inviscid solution for the flow outside the ejector. A two-dimensional analysis utilizing a turbulence kinetic energy model is used to calculate the rate of entrainment by the jets. Vortex panel methods are then used with the requirement that the ejector shroud must be a streamline of the flow induced by the jets to determine the strength of circulation generated around the shroud. In effect, the ejector shroud is considered to be "flying" in the velocity field of the jets. The solution is converged by iterating between the rate of entrainment and the strength of the circulation. This approach offers the advantage of including external influences on the flow through the ejector. Comparisons with data are presented for an ejector having a single central nozzle and Coanda jet on the walls. The accuracy of the matched solution is found to be especially sensitive to the jet flap effect of the flow just downstream of the ejector exit.

Sponsored by the Office of Naval Research under Contract N00014-77-C-0271.

INTRODUCTION

Analytic procedures for calculating ejector performance are necessary to guide research and for preliminary design studies. The analytic methods that have been developed to date are based broadly on von Karman's now classical momentum analysis.[1] These methods[2-4] deal only with the flow inside the ejector. The thin shear layer approximations are applied to reduce the governing elliptic equations to a parabolic set, which can be solved by marching through the ejector in the streamwise direction. This approach has been useful in identifying some of the factors that affect the level of augmentation and in predicting the results of particular changes in the ejector geometry. However, since elliptic effects are neglected, these solutions are limited to cases in which the ejector is relatively long and the diffuser angle is small.

The purpose of this paper is to present an ejector analysis not subject to these limitations. The primary elliptic effects are included by iterating between a parabolic solution for the flow through the ejector and an elliptic solution for the flow outside the ejector. This technique is similar to that used in coupling a solution for the displacement thickness of a wing boundary layer to a solution for the external flow. In the next section an outline of ejector theory is presented to introduce the mathematical models used in this analysis. The solution algorithms and the method of iteration are described in the following sections. The predictions of this new model are compared with classical solutions and experimental data in the final section.

PRINCIPLE OF THRUST AUGMENTATION

Although ejector thrust augmentation may seem to utilize a new principle of lift generation, it actually involves no more than a novel application of the familiar circulation theorem of aerodynamic lift. An isolated jet induces an essentially lateral flow of entrained air, as sketched in Figure 1. However,

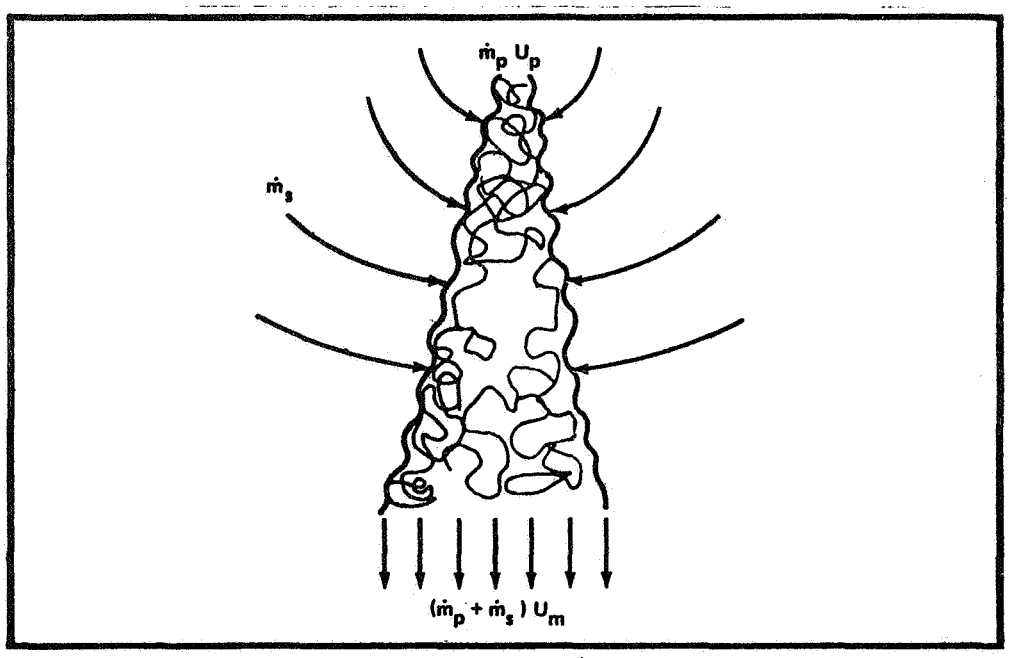

Figure 1. Streamlines of the Flow Induced by a Free Jet.

the distributions of pressure and velocity in the flow outside the ejector are altered by the shroud. A circulation which redirects the entrained flow through the ejector is generated around each of the shroud sections, as shown in Figure 2. The shroud can therefore be considered to be "flying" in the

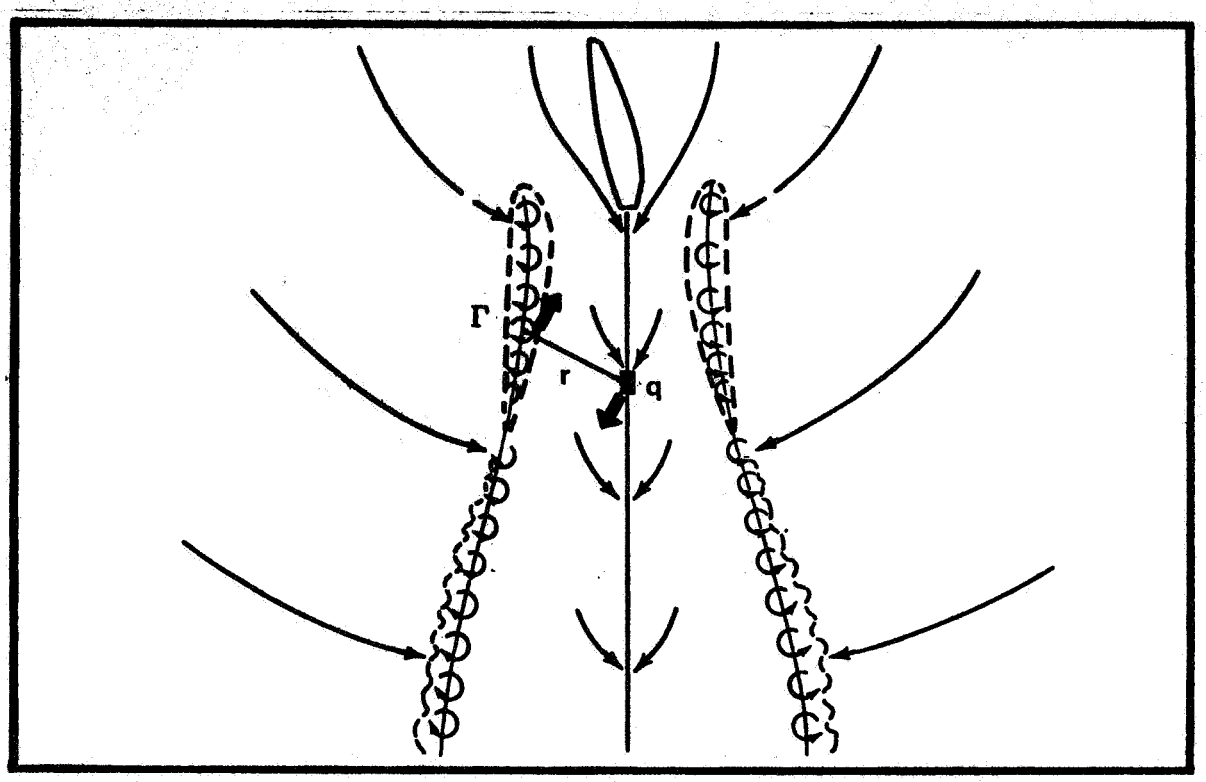

Figure 2. A Circulation Redirects the Flow through the Ejector.

velocity field of the flow entrained by the jet, and it experiences a force analogous to the lift developed on a wing fixed in a moving stream. According to this lifting surface theory,[5] the thrust augmentation ϕ can be defined as the ratio of the primary jet thrust T plus the "lift" on the shroud F to the isentropic thrust of the primary mass:

$$\phi = \frac{T + F}{\dot{m}V} \tag{1}$$

The thrust augmentation results from the fact that the interaction between the flow induced by the entrainment of the jet and the vorticity bound in the sections of the shroud generates a pair of equal and opposite forces. The origin of these forces can be understood by a consideration of the interaction between a sink of strength Q, which represents a section of the jet, and a vortex of strength Γ, which represents a segment of the vortex sheet in the shroud. These singularities are a distance r apart, as shown in Figure 2.

At the vortex, the sink induces a velocity of magnitude $Q/2\pi r$, directed along r. The vortex therefore experiences a force $\rho\Gamma Q/2\pi r$, perpendicular to r. At the sink, the vortex induces a velocity of magnitude $\Gamma/2\pi r$, perpendicular to r. The sink therefore experiences a force $\rho Q\Gamma/2\pi r$, also perpendicular to r, but opposite to the force on the vortex. The net effect of the interactions between all the sinks and vortices is a force which increases the thrust of the jet, and an equal but opposite reaction on the shroud.

The force on the shroud can be recognized as the vortex force given by the Kutta-Joukowski theorem for airfoil lift. This force appears in the pressure distribution on the surface of the shroud, primarily as a leading edge suction. The thrust on the jet sinks is conceptually similar to the ram drag that develops on an aircraft inlet. However, it must be remembered that the sink/vortex interaction, as described, only applies to irrotational flows. The flow through the ejector actually includes regions of interacting irrotational and turbulent fluid, subject to lateral straining and streamwise curvature, with variations of temperature and density. In the following section a method of calculating these forces in a real fluid will be developed from the principles outlined in this section.

VISCOUS, INNER SOLUTION

Governing Equations

The entrainment of the jets is calculated from a solution for the turbulent mixing within the ejector. It is possible to calculate the rate of entrainment without solving the complete three-dimensional mixing problem, by taking advantage of the flow geometry. Since there is a primary direction of flow (through the ejector) it is assumed that the thin shear layer approximation can be applied. This approximation means that the gradients of the normal stress are negligible, and the pressure P is constant in each plane normal to the direction of flow. Thus, only shear stresses caused by velocity gradients across the flow are significant. An additional assumption that the fluid density ρ is uniform was also made. Under these assumptions, the equation for the conservation of mass and momentum through the ejector become:

$$\text{Continuity:} \quad \rho \frac{\partial u}{\partial x} = 0 \tag{2}$$

$$\text{Momentum:} \quad \rho u \frac{\partial u}{\partial x} = \frac{\partial \tau}{\partial y} - \frac{dP}{dx} \tag{3}$$

Here, u is the time averaged velocity in the streamwise direction, and τ is the turbulent shear stress. Laminar stresses are assumed to be negligible.

In order to provide accurate calculations of the turbulent stresses in each region of the flow (initial and developed sections of the free jet, inner

and outer layers of the wall jet, and the merged region) the two equation turbulence model described by Launder and Spalding[6] was used for turbulence closure. According to the usual eddy viscosity assumption, the turbulent stress is first expressed in terms of a turbulent viscosity μ_t and the velocity gradient in the cross stream direction:

$$\tau = \mu_t \frac{\partial u}{\partial y} \tag{4}$$

The two-equation turbulence model gives the turbulent viscosity in terms of two parameters, for which two differential equations are solved. The expression for turbulent viscosity is:

$$\mu_t = \frac{c_\mu \rho k^2}{\epsilon} \tag{5}$$

where c_μ is a constant, k is the kinetic energy of turbulence, and ϵ is the rate of its dissipation. In two-dimensional parabolic flows, the governing equations for k and ϵ are:

$$\rho u \frac{\partial k}{\partial x} = \frac{\partial}{\partial y}\left(\frac{\mu_t}{\sigma_k} \frac{\partial k}{\partial y}\right) + G - \rho\epsilon \tag{6}$$

$$\rho u \frac{\partial \epsilon}{\partial x} = \frac{\partial}{\partial y}\left(\frac{\mu_t}{\sigma_\epsilon} \frac{\partial \epsilon}{y}\right) + (c_1 G - c_2 \rho\epsilon) \frac{\epsilon}{k} \tag{7}$$

The procedure used to solve the governing equations is very similar to the method devised by Patankar and Spalding.[7] It is basically a finite-difference marching procedure; from known conditions at an upstream cross section, x, the flow field at the downstream cross section, $x + \Delta x$, is computed. This marching process is continued until the domain of interest is covered. The initial conditions are determined from the velocities induced in the ejector inlet by the vorticity distribution obtained in the outer solution on the previous iteration. The finite-difference equations are formed by integrating the differential equations over a small control volume surrounding each grid point. The resulting non-linear equations are linearized by using upstream values of the flow variables to evaluate coefficients involving cross stream convection and diffusion. The equations are solved by the use of the tri-diagonal matrix algorithm.

Jet Entrainment Rate

The sink strengths that will represent the effect of the jets in the inviscid calculation are determined from the entrainment of each jet. An entrainment velocity, U_e, is derived from the mass entrained between successive stations, $\dot{m}_e$, according to the definition,

$$U_e = \dot{m}_e / \rho \Delta x \tag{8}$$

in which Δx is the distance between stations. The entrainment of the central jet is represented by a series of overlapping, triangular sink distributions on the axis of the ejector. Each distribution is identified by the index of its central point, where the strength of the sink is q_j; every panel is the same length, 2s. The horizontal and vertical components of velocity induced at an arbitrary point P(x,y) by such a distribution are

$$u_s = \frac{q_j}{2\pi}\left\{\frac{y}{s}\left[\tan^{-1}\left(\frac{sy}{x^2 + sx + y^2}\right) + \tan^{-1}\left(\frac{-sy}{x^2 - sx + y^2}\right)\right]\right.$$

$$\left. + \left(\frac{x}{c} + 1\right)\ln\left(\frac{(x + s)^2 + y^2}{x^2 + y^2}\right)^{1/2} + \left(\frac{x}{s} - 1\right)\ln\left(\frac{(x - s)^2 + y^2}{x^2 + y^2}\right)^{1/2}\right\} \quad (9)$$

and

$$v_s = \frac{q_j}{2\pi}\left\{\left(\frac{x}{s}+1\right)\tan^{-1}\left(\frac{sy}{x^2+sx+y^2}\right) + \left(\frac{x}{s} - 1\right)\tan^{-1}\left(\frac{-sy}{x^2 - sy + y^2}\right)\right.$$

$$\left. - \frac{y}{s}\left[\ln\left(\frac{(x + s)^2 + y^2}{x^2 + y^2}\right)^{1/2} + \ln\left(\frac{(x - s)^2 + y^2}{x^2 + y^2}\right)^{1/2}\right]\right\} \quad (10)$$

The strengths of the q_j are determined by setting the velocity induced at the midpoint of each triangular distribution equal to the entrainment velocity at that point.

The surface of the ejector shroud is represented by m source panels of different lengths, ℓ_j, and uniform strength, q_j. Because a single sheet of sinks cannot provide the jump in entrainment necessary to model the presence of a wall jet on the inner surface of the shroud only, both the inner and outer surfaces must be represented by source panels. The velocity components induced at an arbitrary point by a uniform source distribution are

$$u_s = \frac{q_j}{2\pi}\ln\left[\frac{(x - s)^2 + y^2}{x^2 + y^2}\right]^{1/2} \quad (11)$$

$$v_s = \frac{q_j}{2\pi}\tan^{-1}\left(\frac{sy}{x^2 - sx + y^2}\right) \quad (12)$$

The strengths of the q_j on the surface of the ejector shroud are determined by simultaneously satisfying the known entrainment (inflow) boundary condition due to the wall jet on the inner surface of the shroud, and the condition of zero flow through the outer surface. The solution yields sinks (negative sources) on the inner surface and positive sources on the outer surface.

INVISCID, OUTER SOLUTION

The circulation generated around each section of the ejector shroud is calculated by solving a system of equations which specify that the shroud must be a streamline of the flow induced by the entrainment of the jets. A vortex lattice method was used to determine the circulation density. The continuous vorticity distribution is replaced by n discrete vortices of strength Γ_j, located at x_j, the quarter chord of the panels shown in Figure 2. It was found that better results were obtained if the vortex sheet is placed on the inner surface of the shroud, rather than on the mean camber line. All the flow singularities which represent the shroud geometry and jet effects must induce the known entrainment (inflow) velocities on the surface of the shroud. However, the source/sink distribution on each surface already satisfies this boundary condition. Therefore, the resultant of the velocities induced by all the other singularities must be tangent to the inner surface of the shroud; that is, the normal velocity induced by the vortex sheet must be equal but opposite to the normal velocity induced by the central jet and opposite wall jet.

The vortex strengths are determined by satisfying this boundary condition at n points which correspond to the three quarter chord station on each panel. The horizontal and vertical components of velocity induced at a point $P(x_i, y_i)$ by the vortex pair of strength Γ_j at the points $P(x_j, y_j)$ and $P(x_j, -y_j)$ are

$$u(x_i, y_i) = \left(\frac{y_j - y_i}{2\pi r_{ij}^2} - \frac{y_j + y_i}{2\pi r_{i,-j}^2} \right) \Gamma_j \tag{13}$$

$$v(x_i, y_i) = \left(\frac{x_j - x_i}{2\pi r_{ij}^2} + \frac{x_j - x_i}{2\pi r_{i,-j}^2} \right) \Gamma_j \tag{14}$$

in which $r_{ij} = \left[(x_i - x_j)^2 + (y_i - y_j)^2 \right]^{1/2}$ is the distance between points. Thus, the contribution to the velocity normal to panel-i by both vortex sheets is

$$U_v = \sum_j \left(b_{ij} \cos \alpha_i - a_{ij} \sin \alpha_i \right) \Gamma_j \tag{15}$$

in which the influence coefficients, a_{ij} and b_{ij}, have the form given in Equations (13) and (14), and α_i is the angle of panel-i relative to the ejector axis. Similarly, the normal velocity induced by the central jet and the opposite wall jet is

$$U_S = \sum_j \left(d_{ij} \cos \alpha_i - c_{ij} \sin \alpha_i \right) q_j \tag{16}$$

in which the range of the index j is over both jets. Since the resultant of the normal velocities induced by the jet and vortex sheet must be zero, U_v is set equal but opposite to U_s at each control point. The resulting set of simultaneous equations is solved for the Γ_j by triangularization of the coefficient matrix.

SOLUTION MATCHING PROCEDURE

Method of Iteration

The inner and outer routines are incorporated into a single computer program which yields a matched solution by iterating between the rate of entrainment by the jets and the circulation around the shroud. The circulation determines the sink strengths by controlling the secondary velocity at the ejector inlet. Conversely, the sink distribution determines the circulation by controlling the velocity field in which the shroud "flies." A unique matched solution is established by satisfying the appropriate Kutta condition, which depends on the exhaust jet momentum, as follows.

When the ejector is short or the diffuser angle is large, curvature of the jet sheet leaving the trailing edge supports a low pressure region behind the ejector, as shown in Figure 3. Morel and Lissaman[8] noted that the effect

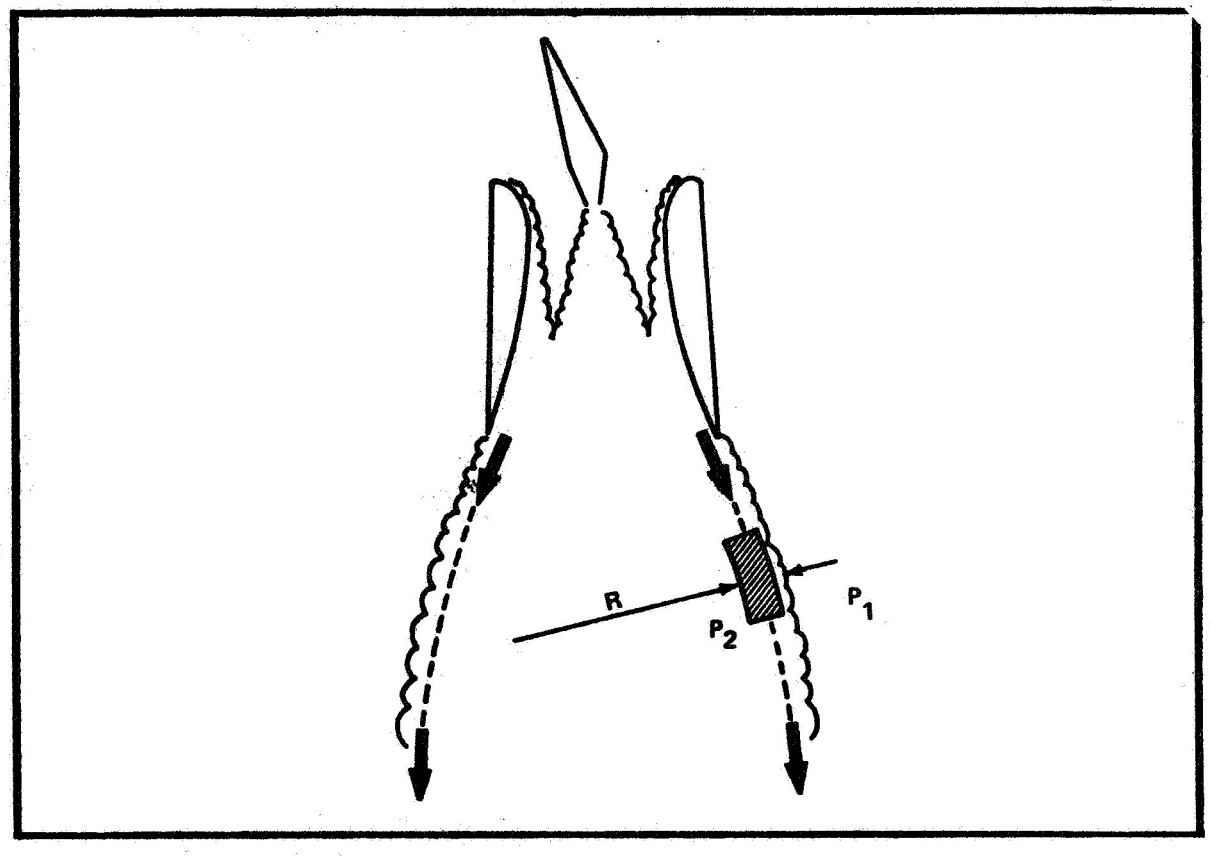

Figure 3. Curvature of the Trailing Jet Balances the Pressure Difference.

is similar to that of a jet flap and described the phenomenon as a "jet flap diffuser." The influence of the jet flap is calculated using an approach suggested by the classical jet flap theory of Spence.[9] Since the pressure difference is balanced by inertia forces due to curvature of the jet sheet, the radius of jet curvature, R, is given by

$$\frac{T}{R} = \Delta P \tag{17}$$

in which T is the thrust of the wall jet at the ejector exit. To a first approximation, both the jet thrust and radius of curvature can be assumed constant. The pressure difference across the trailing jet sheet is related to the strength of an equivalent vortex sheet,

$$\rho u \gamma = \Delta P \tag{18}$$

so that the basic mathematical problem becomes finding a vorticity distribution which makes the jet sheet a streamline of the flow.

These two additional boundary conditions for the shape and strength of the jet flap diffuser are satisfied as part of the iteration to match the inner and outer solutions. When the iteration converges and the solutions are matched, the pressure within the ejector reaches atmospheric pressure at the point where the jet sheets become parallel to each other and the axis of the ejector. In effect, the Kutta condition for the vorticity distribution is satisfied at the end of the jet flap diffuser, rather than at the trailing edge of the ejector shroud.

Evaluation of the Thrust Augmentation

The thrust of the ejector is evaluated by integrating the thrust of the mixed flow at the ejector exit. It is given by

$$\tau = \int_{Ae} u^2 dy - (P_a - P_e)A_e \tag{19}$$

in which P_e and A_e are the static pressure and area at the exit. Because the flow velocities are constant over a small control volume surrounding each grid point, integration of the stream thrust involves a simple summation of the thrust increment from each control volume. The static pressure is constant across the exit. It should be noted that even though the pressure force is negative, lowering the exhaust pressure, as with the jet flap diffuser, results in a net thrust increase. This is because the momentum flux is increased more than the pressure force is reduced.

RESULTS AND DISCUSSION

In order to evaluate the basic lifting surface theory that the force on the shroud is related to the lift on a wing, the prediction of this analysis will be compared to experimental data. A sketch of the test ejector is shown in Figure 4. It combines a single central nozzle with Coanda jets on the

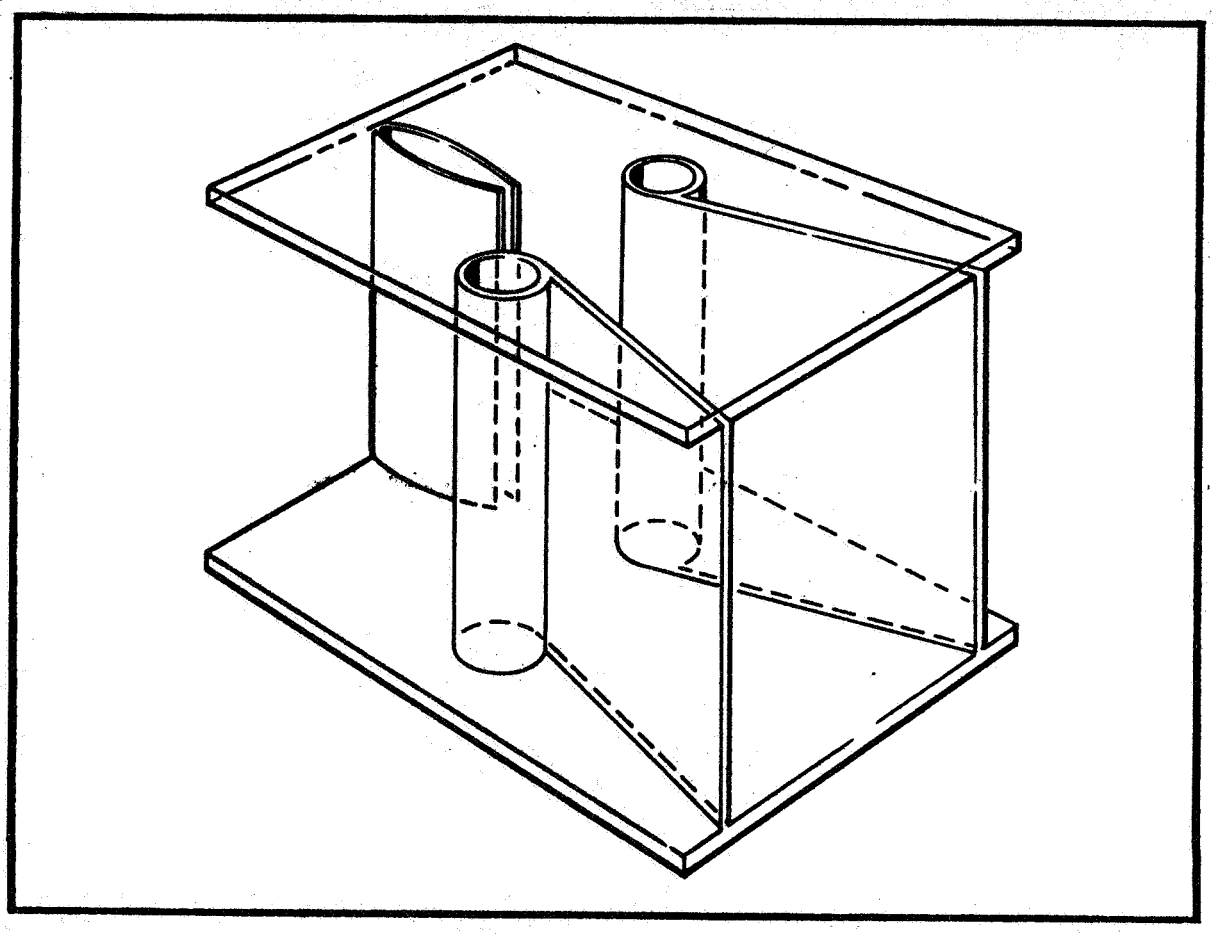

Figure 4. Sketch of the Experimental Ejector.

inner surface of the shroud. A slot in each endwall at the ejector throat provides a boundary layer control jet to prevent separation of the flow from these surfaces. In this configuration 60% of the primary flow is in the central jet, 17% goes to each of the Coanda jets, and the remaining 6% of the primary flow is divided between the two endwall jets. The ejector has a span of 36 cm, a length of 27 cm, and has a throat 12 cm wide. The inlet area ratio is approximately 11.

The calculated jet boundaries are compared with the measured boundaries in Figure 5. Since the turbulence constants were not adjusted for this case, but derived from other flows, the agreement is particularly good. The predictions of the shape and length of the jet flap diffuser are also satisfactory. In Figure 6 the calculated velocity distributions at three stations within the

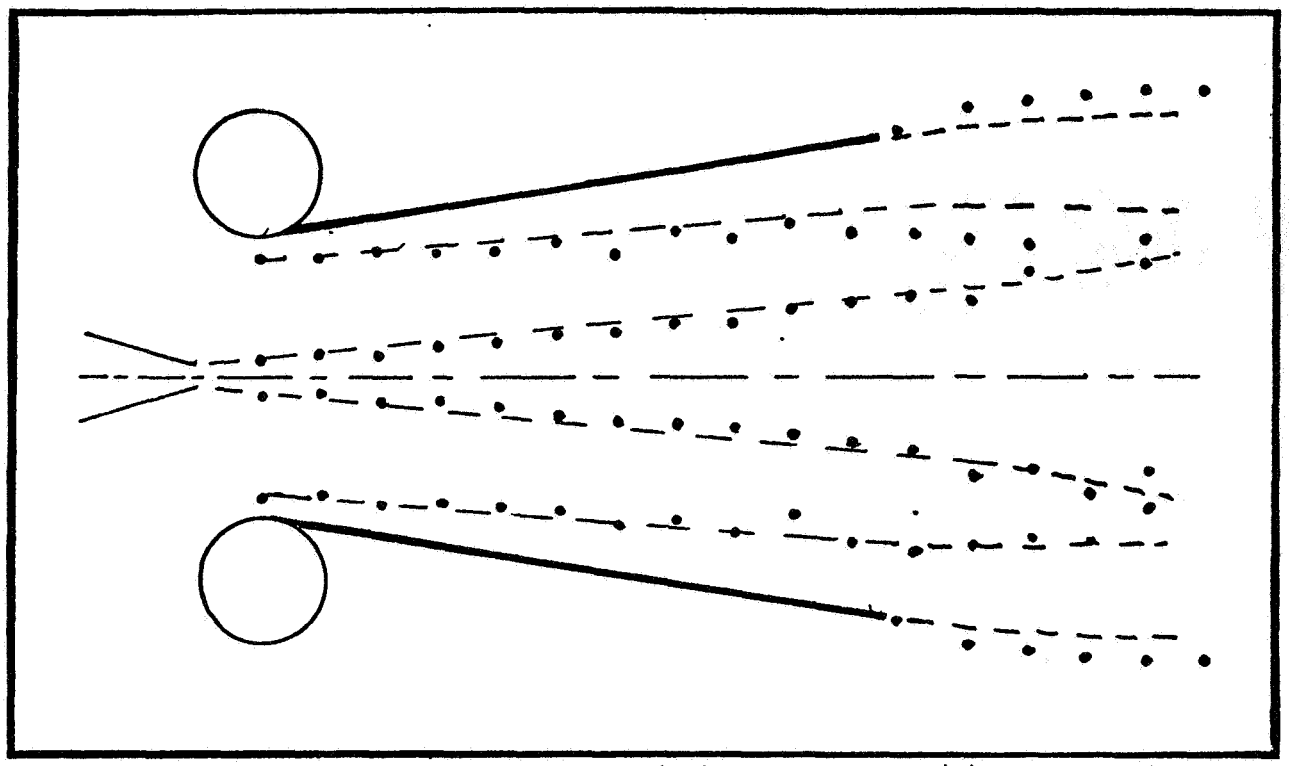

Figure 5. Comparison of Calculated (--) and Measured (•) Jet Spreading Rates.

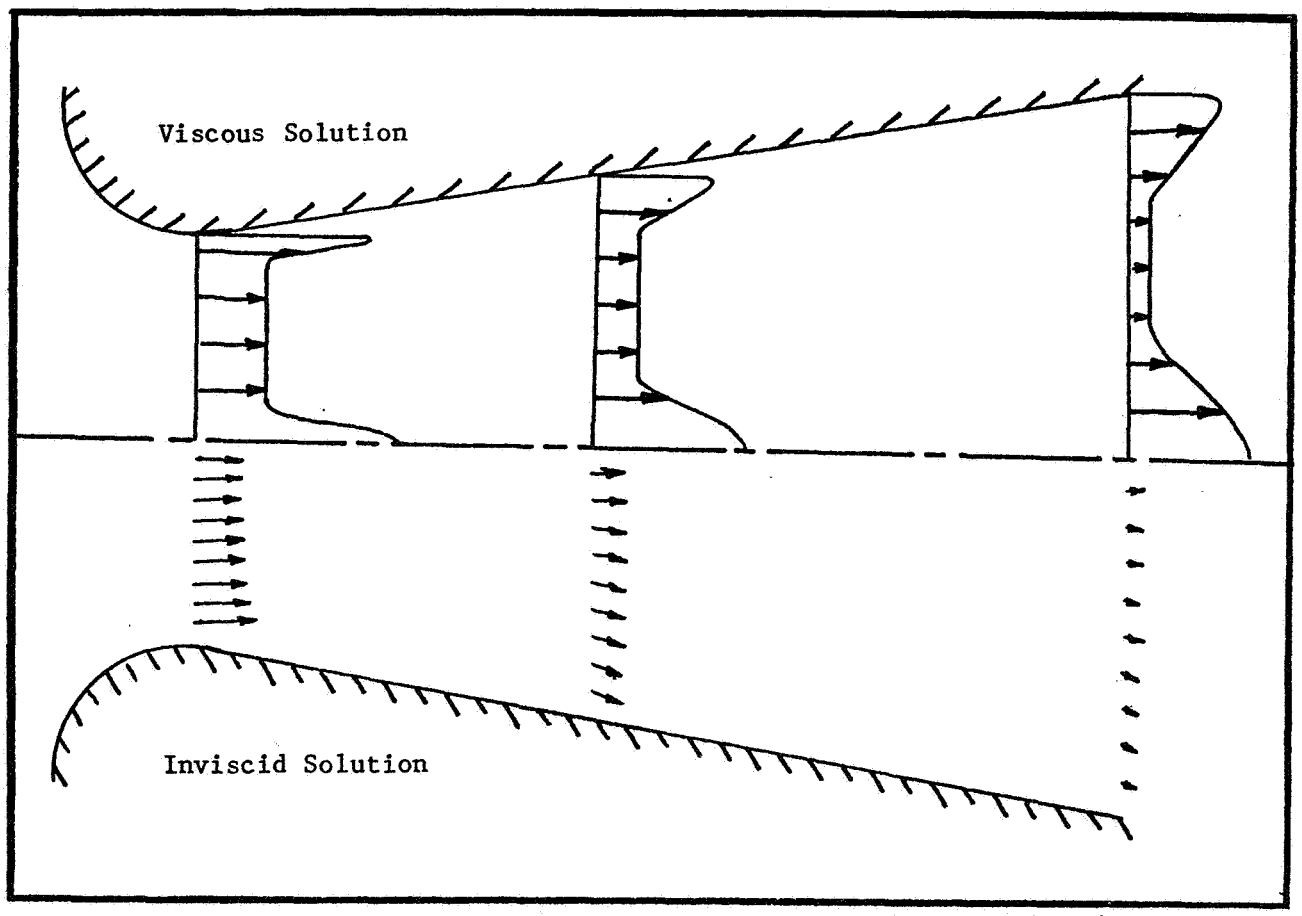

Figure 6. Comparison of Velocity Distributions Calculated by Viscous and Inviscid Solutions.

ejector are compared. The profiles from the inner, viscous solution show the spreading of the jets, as well as the reduction in secondary velocities. Due to the assumption that the static pressures are constant at each axial station, the secondary velocities in the viscous solution are uniform; further, there is no transverse velocity component. The inviscid velocity distributions, shown on the other side of the ejector, indicate the extent of the actual skewness and the magnitude of the transverse velocities. Since the jets are replaced by equivalent sinks in the inviscid solution, The jet profiles are not seen in this case.

In Figure 7 the calculated change in the thrust augmentation ratio with the diffuser area ratio is compared to experimental values. At low diffuser area

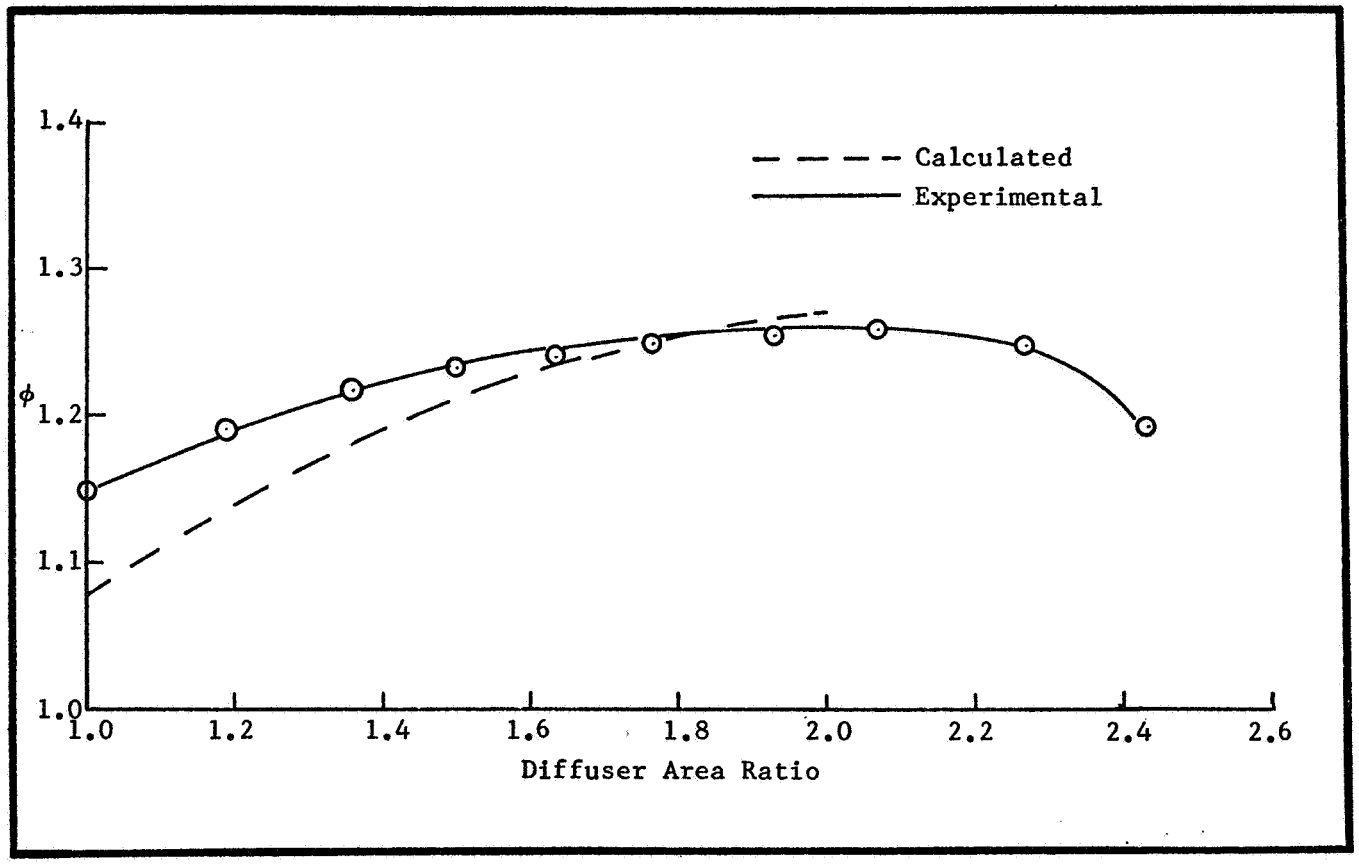

Figure 7. Comparison of the Effect of Calculated and Experimental Changes in the Diffuser Area Ratio.

ratios the thrust augmentation is underpredicted by approximately 6%, while good predictions of the maximum augmentation are obtained. This result is a consequence of the approach taken in calculating the jet flap effect. Because the length of the jet flap diffuser is defined by the point where

the jet sheets becomes parallel, the jet diffuser length goes to zero as the diffuser angle of the duct is reduced. Most of the discrepancy at the low diffuser area ratios can probably be attributed to this effect. With this perspective, the agreement between analysis and experiment can be judged satisfactory.

Figure 8 shows the predicted variation of the thrust augmentation ratio as a function of inlet area ratio, for a constant diffuser area ratio of 1.8.

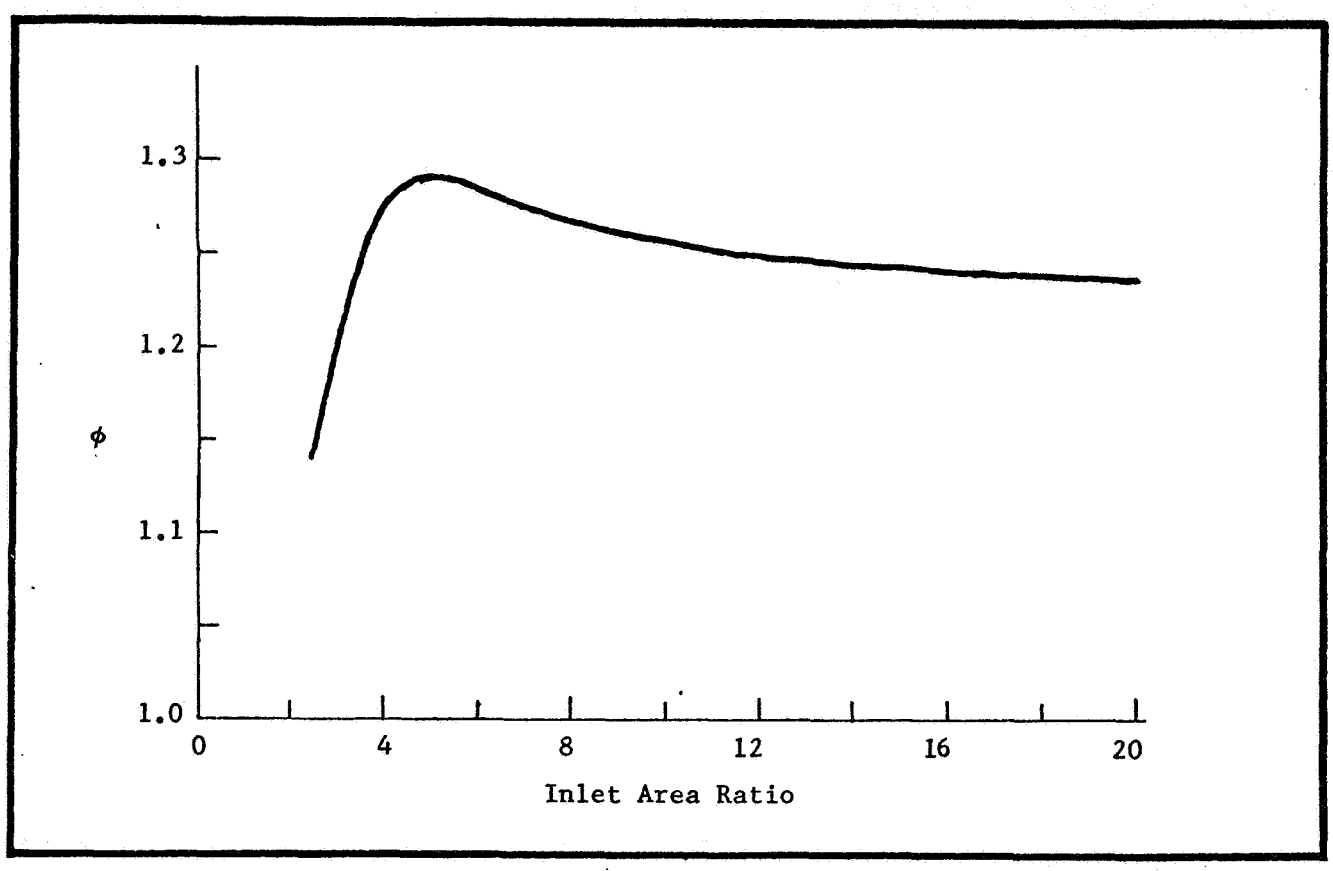

Figure 8. Predicted Effect of Inlet Area Ratio.

The length of the shroud was kept constant, so that the ejector becomes relatively long at low inlet area ratios. In this case the parabolic flow approximation is valid, and the augmentation is seen to initially increase with the inlet area ratio. This is as predicted by the momentum theories. As the sides of the shroud are moved further apart, the strength and influence of the circulation is diminished, and the augmentation begins to decrease. This is according to the lifting surface theory. Thus, the correct behavior has been predicted in each limit.

CONCLUSIONS

A viscous/inviscid interaction analysis has been used to extend classical momentum theories of ejector thrust augmentation. The primary elliptic effects have been included by iterating between a parabolic solution for the flow through the ejector and an elliptic solution for the flow outside the ejector. Briefly, a calculation of the rate of entrainment by the turbulent jets is used to determine the equivalent sink strengths. The requirement that the ejector shroud must be a streamline of the flow induced by these sinks is then used to evaluate the circulation generated around the shroud. The influence of the circulation is included in the next iteration for the rate of entrainment. Comparison of the calculated thrust augmentation with experimental data establishes confidence in the ability to predict the complex ejector flowfield with this approach. In addition, greater understanding of the principle of ejector thrust augmentation is obtained from the analysis.

REFERENCES

1. von Karman, T., "Theoretical Remarks on Thrust Augmentation," in Contributions to Applied Mechanics, Reissner Anniversary Volume, pub. by J. W. Edwards, Ann Arbor, Michigan, 1949, pp 461-468.

2. Gilbert, G. B. and Hill, P. G., "Analysis and Testing of Two-Dimensional Slot Nozzle Ejectors with Variable Area Mixing Sections," NASA CR-2251, 1973.

3. DeJoode, A. D. and Patankar, S. V., "Prediction of Three-Dimensional Turbulent Mixing in an Ejector," AIAA Journal, Vol. 16, No. 2, February 1978, pp 145-150.

4. Bevilaqua, P. M., "Evaluation of Hypermixing for Thrust Augmenting Ejectors," Journal of Aircraft, Vol. 11, No. 6, June 1974, pp 348-354.

5. Bevilaqua, P. M., "Lifting Surface Theory for Thrust Augmenting Ejectors," AIAA Journal, Vol. 16, No. 5, May 1978, pp 475-481.

6. Launder, B. E. and Spalding, D. B., "The Numerical Computation of Turbulent Flows," Computer Methods in Appl. Mech. and Eng., Vol. 3, No. 2, March 1974, pp 269-289.

7. Patankar, S. V. and Spalding, D. B., "Heat and Mass Transfer in Boundary Layers," International Textbook Company, Ltd, London, 1970.

8. Morel, J. P. and Lissaman, B. S., "The Jet Flap Diffuser, a New Thrust Augmenting Device," AIAA Paper No. 69-777, 1969.

9. Spence, D. A., "The Lift Coefficient of a Thin, Jet-Flapped Wing," Royal Society of London, Proceedings, Vol. 238, Jan. 1957, pp 46-68.

INTERNAL-EXTERNAL FLOW INTEGRATION FOR A THIN EJECTOR-FLAPPED WING SECTION

Henry W. Woolard

Flight Control Division
Air Force Flight Dynamics Laboratory
Wright-Patterson Air Force Base

SUMMARY

Some results from a thin-airfoil theory of an ejector-flapped wing section are reviewed briefly with particular attention given to the global matching of the external airfoil flow with the ejector internal flow and the overall ejector-flapped wing-section aerodynamic performance.

INTRODUCTION

Within the last two decades, considerable numbers of high-lift concepts for V/STOL aircraft have been proposed. One among these is the ejector-flapped wing (fig. 1) also known as the augmentor wing, the ejector wing, the augmented jet-flap wing, etc. The ejector-flapped wing operates on a principle similar to the ordinary jet-flapped wing in that use is made of a trailing jet sheet to increase the circulation about the wing itself. It differs from the jet-flapped wing in the presence of ejector air intakes and the existence of an augmented trailing-edge momentum flux resulting from the ejector action. Since the augmented trailing-edge momentum flux is an internal-flow phenomenon, the basic difference in the external aerodynamics of the two systems is due to the air-intake flows. The intake flows behave as sink flows and are not accounted for in the usual jet-flap theory (refs. 1 and 2).

Woolard, in reference 3, has performed a theoretical analysis of an ejector-flapped wing section based on a small-perturbation thin-airfoil mathematical model which takes into account the intake sink flows. Although much of the emphasis of reference 3 was on the thin-airfoil modeling of the external flow, the paper was also concerned with the global matching of the airfoil external flow with the ejector internal flow and the overall ejector-flapped wing-section aerodynamic performance. Since the theme of this workshop is thrust-augmenting ejectors, the principal emphasis in this overview of reference 3 will be on global matching and overall aerodynamic performance.

This paper is intended to be only a brief overview of reference 3. Greater detail may be found in the original document.

SYMBOLS

A	cross-sectional area
b_f	ejector-flap span
c	airfoil chord
c_f	flap chord
c_j	primary-jet installed momentum coefficient, $\rho U_j^2 \bar{h}_j / q_\infty c$
$\hat{c}_j$	primary-jet uninstalled momentum coefficient, $\rho \hat{U}_j^2 \bar{h}_j / q_\infty c$
c_j^*	primary-jet test momentum coefficient, $\rho U_j \bar{h}_j \hat{U}_j / q_\infty c$
c_J	ejector exit-flow momentum coefficient, $\rho U_E^2 h_E / q_\infty c$
c_ℓ	lift coefficient
c_{m_o}	airfoil nose-up pitching-moment coefficient about the leading edge
c_Q	thin airfoil suction coefficient, $Q/U_\infty c$
c_Q	ejector net suction coefficient, $(U_s - U_\infty)\bar{h}_s / U_\infty c$
$\check{c}_Q$	ejector gross suction coefficient, $U_s \bar{h}_s / U_\infty c$; $(\check{c}_q = c_q + \bar{h}_s/c)$
c_T	ejector net-thrust coefficient, $(\rho U_E^2 h_E - \rho U_s U_\infty \bar{h}_s / q_\infty c)$
$\hat{c}_t$	primary-jet uninstalled net-thrust coefficient, $\rho \hat{U}_j (\hat{U}_j - U_\infty) \bar{h}_j / q_\infty c$
h_e, h_E	heights at ejector diffuser inlet and exit, respectively
$\bar{h}_j$	mean height of ejector primary-jet nozzle, A_j / b_f
$\bar{h}_s$	mean height of ejector secondary flow passage at primary-jet A_s / b_f
p	static pressure
P	total pressure
q_∞	free-stream dynamic pressure, $(\rho/2) U_\infty^2$
Q	two-dimensional ideal-flow sink strength
U	mean local axial velocity within the ejector (except U_∞)
$\hat{U}_j$	primary-jet uninstalled isentropic velocity, $[(2/\rho)(P_j - p_\infty)]^{1/2}$

$\tilde{U}_x$ $U_x/\hat{U}_j$, where x = j, s, E, etc.

U_∞ free-stream velocity

$\tilde{U}_\infty$ forward-speed parameter, $U_\infty/\hat{U}_j$

x,y rectangular coordinates, see figure 2

x_s chordwise location of sink on airfoil of unit chord

α angle of attack

δ_f trailing-edge flap deflection angle, positive for trailing edge down

ρ density

σ $\sigma = 1$ for an upper-surface sink, $\sigma = -1$ for a lower-surface sink

Ω_D ejector diffuser area ratio, A_E/A_e

Ω_j ejector injection area ratio, A_s/A_j

$( )_D$ denotes the diffuser

$( )_e$ ejector station e, see figure 6

$( )_E$ ejector station E, see figure 6

$( )_{EF}$ denotes an ejector-flapped wing

$( )_f$ denotes the trailing-edge flap

$( )_j$ denotes station j and the ejector primary jet, see figure 6

$( )_{JF}$ denotes a jet-augmented-flapped wing

$( )_s$ denotes the ejector secondary flow (except x_s)

$( )_\infty$ denotes a free-stream quantity

$(\hat{})$ denotes quantities associated with isentropic flow from P_j to p_∞

$(\tilde{})$ denotes a velocity normalized by dividing by $\hat{U}_j$

$(\bar{})$ denotes a mean quantity

DISCUSSION

The External Aerodynamics

A thin-airfoil representation of an ejector-flapped wing section having an upper intake only is shown in figure 2. The main airfoil and flap are approximated by straight lines, the ejector net intake flow by a surface sink[1] (not necessarily at the flap knee, but usually taken there), and the actual jet sheet of finite thickness by an infinitesimally thin sheet having a finite internal momentum. In this approximation the ejector intake and exhaust openings are required to be small relative to the airfoil chord. The internal and external flow fields are not required to match in fine detail at their interface, but the values of the ejector intake net mass flow and ejector exhaust total momentum flux must match those used in external flow aerodynamics.

Although figure 2 is illustrative of the modeling for an ejector-flapped wing section with an upper intake only, the fundamental solution obtained in reference 3 is valid for any sink location on the wing upper or lower surface. Since the governing equations are linear for the small perturbation analysis of reference 3, solutions and boundary conditions are additive and a solution for an ejector-flapped wing section having both upper and lower intakes is obtained by adding the appropriate individual solutions for upper and lower surface sink flows.

The flow shown in figure 2 consists of three additive components as illustrated on the left-hand side of figure 3. These are: 1) the flow about a flat plate at angle of attack with trailing-edge tangential (regular) blowing; 2) the flow about a flapped airfoil at zero angle of attack with regular blowing; 3) the flow about a flat-plate suction airfoil at zero angle of attack with regular blowing, as shown in the bottom left-hand illustration of figure 3. Shown for comparison on the right-hand side of figure 3 is an idealized representation of a real-flow ejector-flapped wing having an ejector without a diffuser. Spense in references 1 and 2, respectively, has solved the aforementioned flow component cases 1 and 2. The solution for the flow about the flat-plate suction airfoil shown in figures 3 and 4 is given by Woolard in reference 3.

Although the external flow analysis of Woolard yields other aerodynamic details, only the lift and pitching moment coefficients will be discussed here. These characteristics are given by

$$c_\ell = (\partial c_\ell/\partial\alpha)\alpha + (\partial c_\ell/\partial\delta_f)\delta_f + (\partial c_\ell/\partial c_Q)c_Q \tag{1}$$

$$c_{m_o} = (\partial c_{m_o}/\partial\alpha)\alpha + (\partial c_{m_o}/\partial\delta_f)\delta_f + (\partial c_{m_o}/\partial c_Q)c_Q \tag{2}$$

where the component terms on the right-hand sides of equations (1) and (2) are the contributions of the various component flows illustrated on the left-hand

---

[1] A sink for which the flow enters a point from only one side of a surface.

side of figure 3. All the partial derivatives in equations (1) and (2) are functions of the jet-momentum coefficient, c_J. The derivatives with respect to δ_f and c_Q are also functions respectively of the flap chord to airfoil chord ratio and the sink (intake) chordwise location. It is the third term on the right-hand side of equations (1) and (2) that involves matching of the ejector flow characteristics, since for a given ejector geometry, ejector primary air-supply pressure ratio, and ejector forward speed, a specific relation exists for c_Q/c_j.

Curves showing $(\partial c_\ell/\partial c_Q)/\sigma$ and $(\partial c_{m_o}/\partial c_Q)/\sigma$ as a function of c_J for several sink locations are presented in figure 5. The parameter σ employed in the figure provides for the placement of a sink (intake) on the upper or lower surface or both. For an upper surface sink, $\sigma = -1$; while for a lower surface sink, $\sigma = -1$. It is seen in figure 5, that for a sink on the upper surface only, the sink effect alone (i.e., $c_J = 0$) contributes an incremental increase to the lift coefficient that becomes larger as the sink approaches the trailing edge. It is also seen that the interference effect of the jet sheet ($c_J \neq 0$) decreases the lift coefficient and increases the nose-up pitching moment.

The Suction Coefficient

The discussion thus far has been concerned with a thin-airfoil approximation in which the real airfoil and the ejector shroud (or shrouds) are taken to lie on a single skeletal line. A real ejector-flapped wing, however, has a finite-height intake (or intakes) and a question arises regarding the application of a limiting process in which the intake height is reduced to zero in a manner such that the thin-airfoil aerodynamics most appropriately represents the real-airfoil aerodynamics. Since the thin-airfoil approximation is an imperfect representation of the real flow, there cannot be a one-to-one correspondence between the real and theoretical flows and a decision must be made regarding which properties are to be matched in a thin-airfoil representation. Certainly the lift coefficient is an important quantity to be conserved. The thrust coefficient is of lesser importance in the thin-airfoil representation since it is easily determined from considerations of conservation of global momentum applied directly to the real flow. As an intermediate step to taking the limiting process, consider the "idealized real wing" shown in figure 6 representing a real ejector-flapped wing (with upper shroud only) at zero angle of attack and zero flap deflection. In this representation, the main airfoil and the shroud are of infinitesimal thickness, but the total airfoil is not a thin airfoil because of the small, but finite, intake height (exaggerated in the figure for clarity). For an arbitrary intake flow in figure 5 there is no formal procedure for applying a limiting process in which the lift coefficient is held constant. However, as will be shown subsequently, the appropriate limit can be obtained by inductive reasoning. On the other hand, the limit in which the intake mass flow is held constant while the intake height is reduced to zero is easily implemented by simply taking the theoretical sink mass flow equal to the gross intake mass flow of the real wing. In this case, the suction coefficient used in the

theoretical relations is the ejector gross suction coefficient, $\check{c}_Q$. Use of the gross suction coefficient is suggested by Chan (ref. 4) and Lopez (ref. 5). On the bases of the argument which follows and a comparison with other work, the present author maintains that the ejector net suction coefficient, c_Q, is the correct suction coefficient to use in the thin airfoil representation.

For the purposes of the present argument, the idealized real flow in figure 6 is taken to be the real flow since the intake has a finite height. Now consider a flow in which the intake capture streamline is parallel to the main airfoil as shown by the dashed line a'b in figure 6. For this situation, $c_Q = 0$ and $\check{c}_Q = h_s/c$. Since in this case all the streamlines of the idealized real flow are parallel there is no lift (or moment) on the real wing, hence the thin-airfoil theory should yield zero lift and moment. Use of the ejector net suction coefficient, $c_Q = 0$, in the thin-airfoil results of figure 5 for this case, yields the proper zero lift and moment; use of the ejector gross suction coefficient, $\check{c}_Q = h_s/c$, however, yields incorrect non-zero values for the lift and moment. It follows that the thin-airfoil lift and moment coefficients based on c_Q will be in error also for an arbitrary intake mass flow ($c_Q \neq h_s/c$).

Although matching of the thin-airfoil and real flows by means of the net suction coefficient yields the proper lift and pitching-moment coefficients in the thin-airfoil approximation, it fails to give the correct thrust coefficient. This latter property is easily obtained from the real flow as $c_T = c_J - 2\,(c_Q + \overline{h}_s/c)$. Inconsistencies of this type frequently occur in approximate representations of complicated flows, and generally are tolerated for the purposes of obtaining an engineering estimate of the problem being solved.

Although it is believed that the foregoing argument demonstrates that the ejector net suction coefficient, c_Q, is the proper coefficient to use in the thin-airfoil approximation, additional justification is provided by the following comparison with the work of Sidor (ref. 6).

Sidor has performed an analysis and digital-computer computation for the flow situation illustrated in figure 7. Sidor employs distributed vortices over the main airfoil, over the upper and lower ejector shroud surfaces, and over the upper and lower interfaces of the jet sheet. The flow momentum imparted by the ejector is represented by an actuator disk located at the aft end of the ejector shrouds as indicated in figure 7. For $\alpha = \delta_f = 0$, Sidors model is analogous to the flow situation of figure 4 and therefore can be used to obtain a rough check of how well the present sink-flow jet-flap model approximates the flow for a finite height shroud, and to provide also some insight regarding the selection of the proper suction coefficient.

For $\alpha = \delta_f = 0$, the variation of the lift coefficient with the jet-momentum coefficient, c_J, for the actuator-disk flow model (taken from ref. 6) is shown in figure 8. Also shown in figure 8 are the lift coefficient curves for the sink-flow jet-flap model based on the net and gross intake suction

coefficients corresponding to the relationship[2] between c_Q and c_j for the actuator disk. Since the curve based on the use of the net-suction coefficient agrees much more favorably with the actuator-disk flow model curve, it can be concluded from this agreement and the previously presented argument that the net-suction coefficient, c_Q, is the proper one to use in the present model.

One-Dimensional Ejector-Flow Relations

A schematic representation of an ejector flap is given in figure 9. The ejector internal flow is taken to be incompressible and is analyzed on the basis of assumptions that the flow properties are uniform at any given cross-sectional station and there are no flow losses except those due to mixing. It is recognized that this is an oversimplification for aircraft design purposes. The purpose here, however, is to delineate the general characteristics of the integrated external-internal aerodynamic system and this is best accomplished by keeping the mathematical modeling as simple as possible.

The primary air is injected at station j (see fig. 9), and mixing with the secondary air is assumed to be completed at the end of the constant cross-sectional area region extending between stations j and e. It is assumed also that the static pressures of the primary and secondary streams are equal at the injection station j and that the diffuser-exit static pressure is equal to the free-stream static pressure. In view of the assumption of loss-free flow in the intake, the primary nozzle, and the diffuser, Bernoulli's equation is applicable to these regions.

In the ejector analytics, flow velocities are nondimensionalized by dividing by $\hat{U}_j$, where $\hat{U}_j$ is the velocity attained by the primary nozzle exhausting isentropically to the free-stream static pressure. This velocity is a measure of the primary-air total pressure, the quantity most likely to be held constant during the major portion of a landing or take-off operation.

On the base of the aforementioned assumptions, the governing equations for the ejector internal flow are

$$2\tilde{U}_j^2 - \tilde{U}_s^2(1 - \Omega_j) - \tilde{U}_E^2(1 + \Omega_D^2)(1 + \Omega_j) + \tilde{U}_\infty^2(1 + \Omega_j) = 0 \tag{3}$$

$$\tilde{U}_j + \tilde{U}_s\Omega_j = \tilde{U}_E(1 + \Omega_j)\Omega_D \tag{4}$$

$$\tilde{U}_j^2 = \tilde{U}_s^2 - \tilde{U}_\infty^2 + 1 \tag{5}$$

Equations (3) and (4) are respectively expressions of conservation of momentum and mass between stations j and e in figure 9. These forms of the conservation equations were derived from the basic forms by appropriate use of Bernoulli's equation, continuity, and the previously mentioned assumptions.

---

[2]For the actuator disk, it is easily shown that the relation between the net-suction coefficient and the jet-momentum coefficient is given by $c_Q = [(h/c)c_J 2]^{1/2} - (h/c)$.

Equation (5) is a consequence of the equality of p_s and p_j and the use of Bernoulli's equation for the primary and secondary flows.

The quantities $\tilde{U}_j$ and $\tilde{U}_E$ may be eliminated from equation (1) through the use of equations (3) and (4), yielding the following quadratic equation in $\tilde{U}_s^2$

$$a_o\tilde{U}_s^4 + (b_o + b_2\tilde{U}_\infty^2)\tilde{U}_s^2 + c_o + c_2\tilde{U}_\infty^2 + c_4\tilde{U}_\infty^4 = 0 \tag{6}$$

where

$$a_o = (\Omega_j + 1)^2\,[\Omega_j^2 - 2(1 + 2\Omega_D^2)\Omega_j + 1] \tag{7}$$

$$b_o = -4\Omega_D^2\Omega_j^3 + 2(2\Omega_D^4 - 5\Omega_D^2 - 1)\Omega_j^2 + 4(\Omega_D^4 - 2\Omega_D^2)\Omega_j - 2\Omega_D^2 + 2 \tag{8}$$

$$b_2 = -2\Omega_D^2\Omega_j^4 + 4\Omega_D^4\Omega_j^3 + 2(2\Omega_D^4 + 3\Omega_D^2 + 1)\Omega_j^2 + 4\Omega_D^2\Omega_j - 2 \tag{9}$$

$$c_o = [\Omega_D^2 - (1 - 2\Omega_D^2\Omega_j)]^2 \tag{10}$$

$$c_2 = 2(1 + \Omega_D^2\Omega_j^2)[\Omega_D^2 - (1 - 2\Omega_D^2\Omega_j)] \tag{11}$$

$$c_4 = (1 + \Omega_D^2\Omega_j^2)^2 \tag{12}$$

Equation (6) may be solved for $\tilde{U}_s^2$ by the standard quadratic formula. For the sign options preceding the radical, the negative sign must be selected. The numerics are much more convenient, however, if equation (6) is divided through by a_o and then solved by the quadratic formula. In this case, the sign of the radical is given by $(-\text{sgn } a_o)$.

Solution of equation (6) yields $\tilde{U}_s$ as a function of the forward-speed parameter, $\tilde{U}_\infty$, the injection area ratio, Ω_j, and the diffuser area ratio, Ω_p. With $\tilde{U}_s$ known, $\tilde{U}_E$ and $\tilde{U}_j$ can be determined as functions of $\tilde{U}_\infty$, Ω_j, and Ω_D by means of equations (4) and (5). By appropriate substitutions, the ejector coefficients, $\hat{c}_j$, c_j^*, $\hat{c}_t$, c_Q, and c_Q (see symbols) also can be determined as functions of U, Ω_j, Ω_D.

Some selected ejector characteristics as functions of the forward-speed ratio are shown in figures 10 through 12 for a diffuser area ratio of unity. For aircraft high-lift operations, forward-speed ratios in the vicinity of 0.1 may be anticipated. For a primary nozzle speed of 1000 ft/sec, say, this corresponds to a flight speed of 100 ft/sec.

Shown in figure 10 is the exit-momentum ratio $c_J/\hat{c}_j$. This parameter has a value of unity for a jet flap and is a measure of the increase in the exit-momentum coefficient of an ejector flap over that of a jet flap having the same primary-air supply pressure ratio. The parameter, c_J/c_j is important to the lift. It is apparent from the figure that both forward speed and increased injection-area ratio are beneficial to increasing $c_J/\hat{c}_j$. The thrust, however, behaves differently with forward speed and injection-area ratio as may be seen in figure 11. It is seen in this figure that regardless of the injection-area ratio the thrust augmentation decreases with forward speed, reaching values of less than 1.1 for speed ratios in excess of 0.3. At small forward-speed ratios

the thrust augmentation increases with increasing injection-area ratio while at the high ratios the opposite occurs. In the region of potential interest for high-lift systems ($\hat{U}_\infty/U_j = 0.1$) the injection-area ratio has little effect except at very low area ratios.

Finally, the behavior of the net suction coefficient with forward speed ratio is shown in figure 12 which indicates that for a constant area ratio, A_s/A_j, the suction coefficient reaches a maximum value at a particular forward-speed ratio. The maximum suction coefficient and the corresponding speed ratio are seen to be a function of the injection-area ratio, although at the higher area ratios the variation of the maximum with speed ratio is slight. For area ratios of interest for high-lift systems ($A_s/A_j \cong 10$) the maximum coefficients occur at forward-speed ratios typical of high-lift systems. It is seen also from figure 12 that for the maximum suction coefficients and a c_J of unity, c_Q and δ_f are of the same order of magnitude for flap angles of approximately five degrees. Hence in this regime, for small flap-chord to airfoil-chord ratios at which $(\partial c_\ell/\partial c_Q)$ and $(\partial c_\ell/\partial \delta_f)$ are of approximately the same order of magnitude, the suction and flap lift contributions are also of approximately the same order of magnitude.

Relative Lift Performance

The lift performance of an ejector-flapped wing relative to that of a wing with a jet-augmented flap, based on the relations given in this paper, is shown in figure 13 for typical values of the pertinent parameters. It can be seen in the figure that for forward-speed ratios below 0.3 the ejector-flap lift is substantially superior and continues to increase in superiority as the forward speed is reduced. The superiority also increases with increasing ejector size as indicated by the gains accompanying the change in the relative nozzle height from 0.005 to 0.010. The lift superiority of the ejector-flapped wing also increases with decreasing flap deflection. As may be seen in figure 14, this effect is because the relative suction contribution to the lift of the ejector-flapped wing is larger at lower flap angles.

CONCLUDING REMARKS

On the basis of simple mathematical models of the external and internal flows, an integrated theoretical analysis of the aerodynamics of an ejector-flapped wing was developed in reference 3. The external aerodynamics was systemized for ease of application in the aforementioned reference by inclusion of a table of Fourier coefficients. The incompressible, idealized, forward-speed ejector-flow equations from reference 3 have been presented in this paper. The normalized form used for these equations is believed to be the most appropriate for interfacing with the external aerodynamics. Some parametric curves of ejector forward-speed characteristics have been also presented. Although forward-speed effects on exit momentum and net thrust of ejectors are generally well-known, it is believed to have been worthwhile to reemphasize these and cast them in a form appropriate for interfacing with the external aerodynamics. The delineation of the suction-flow coefficient

characteristics is believed to be new or at least relatively unfamiliar. The idealized lift performance of an ejector-flapped wing relative to a jet-augmented-flapped wing has been compared and the ejector-flapped wing was found to be substantially superior at low forward-speed ratios. Finally, it was determined that the suction effect on the lift is most significant at low flap angles.

Despite the idealized character of the flow model, it is believed that it adequately delineates the important trends. Because of its relative simplicity, it is easily amenable to empirical modification for use as a preliminary design tool.

REFERENCES

1. Spence, D. A.: The Lift Coefficient of a Thin Jet-Flapped Wing. Proceedings of the Royal Society of London, ser. A, vol. 238, no. 1212, Dec. 1956, pp. 46-48.

2. Spence, D. A.: The Lift of a Thin Aerofoil with a Jet-Augmented Flap. The Aeronautical Quarterly, vol. 9, pt. 3, Aug. 1958, pp. 287-299.

3. Woolard, Henry W.: Thin-Airfoil Theory of an Ejector-Flapped Wing Section. Journal of Aircraft, vol. 12, no. 1, Jan. 1975; also AIAA Paper 74-187.

4. Chan, Y. Y.: Lift Induced by Suction Flaps on Augmentor Wings. Canadian Aeronautics and Space Institute Transactions, vol. 3, no. 2, Sept. 1970, pp. 107-110.

5. Lopez, M. L.; and Wasson, N. F.: A Theoretical Method for Calculating the Aerodynamic Characteristics of Arbitrary Ejector-Jet-Flapped Wings. Air Force Systems Command, AFFDL-TR-74-72, June 1944, (AD-A-002319).

6. Sidor, Laurent B.: An Investigation of the Ejector-Powered Jet-Flap. Thesis for the Degree of Aeronautical Engineer, Calif. Inst. of Technology, 1974. Also published in "Theoretical and Experimental Study on the Ejector Augmented Jet Flap" by H. J. Stewart. NASA CR-136749, Aug. 1974 (N75-17296#).

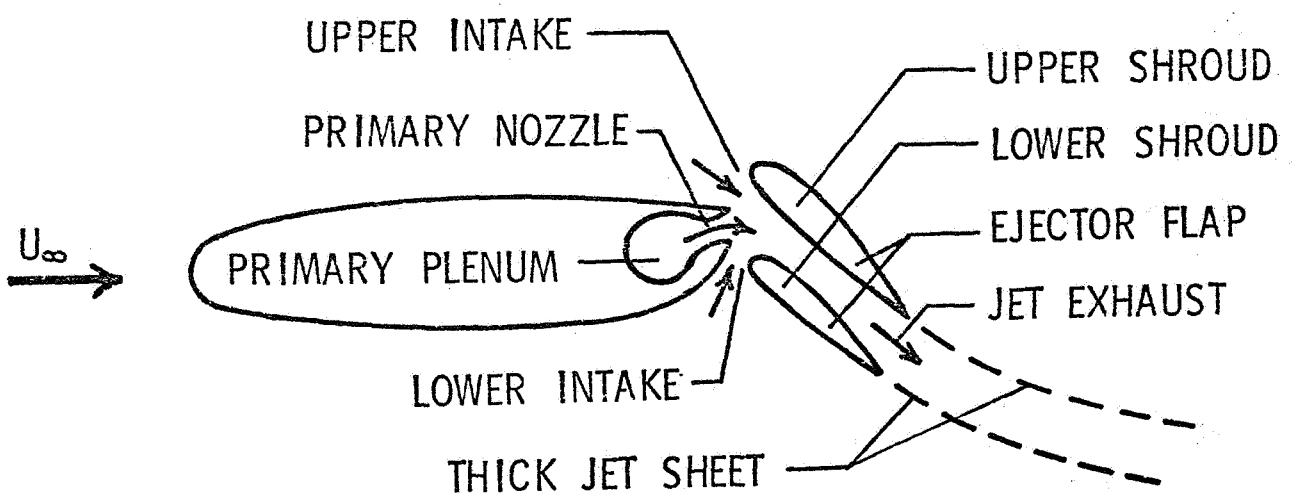

Figure 1.- Ejector-flapped wing section.

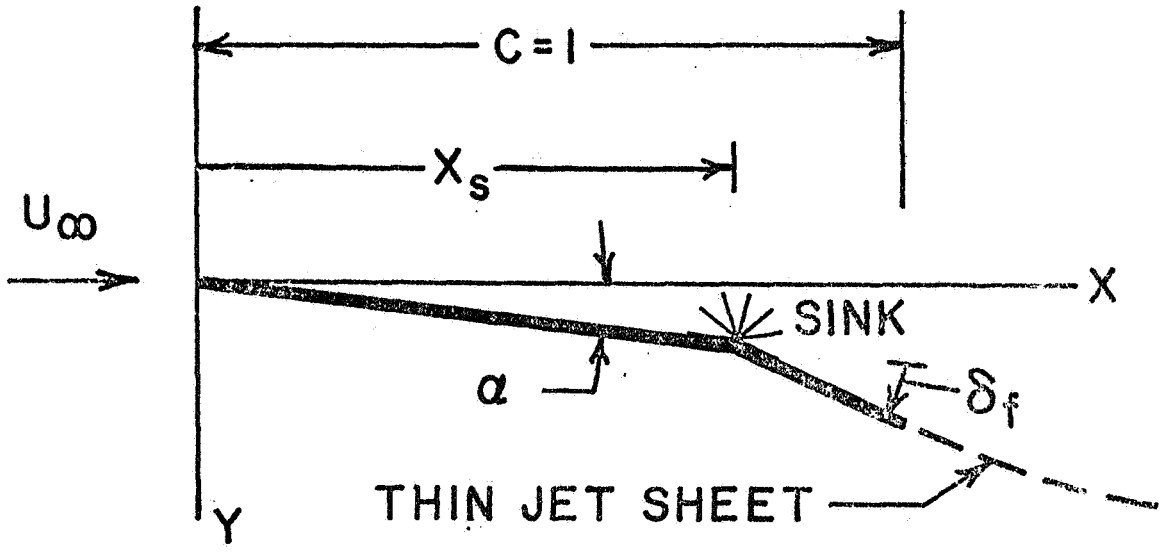

Figure 2.- Thin-airfoil representation of an ejector-flapped wing with an upper-surface intake only.

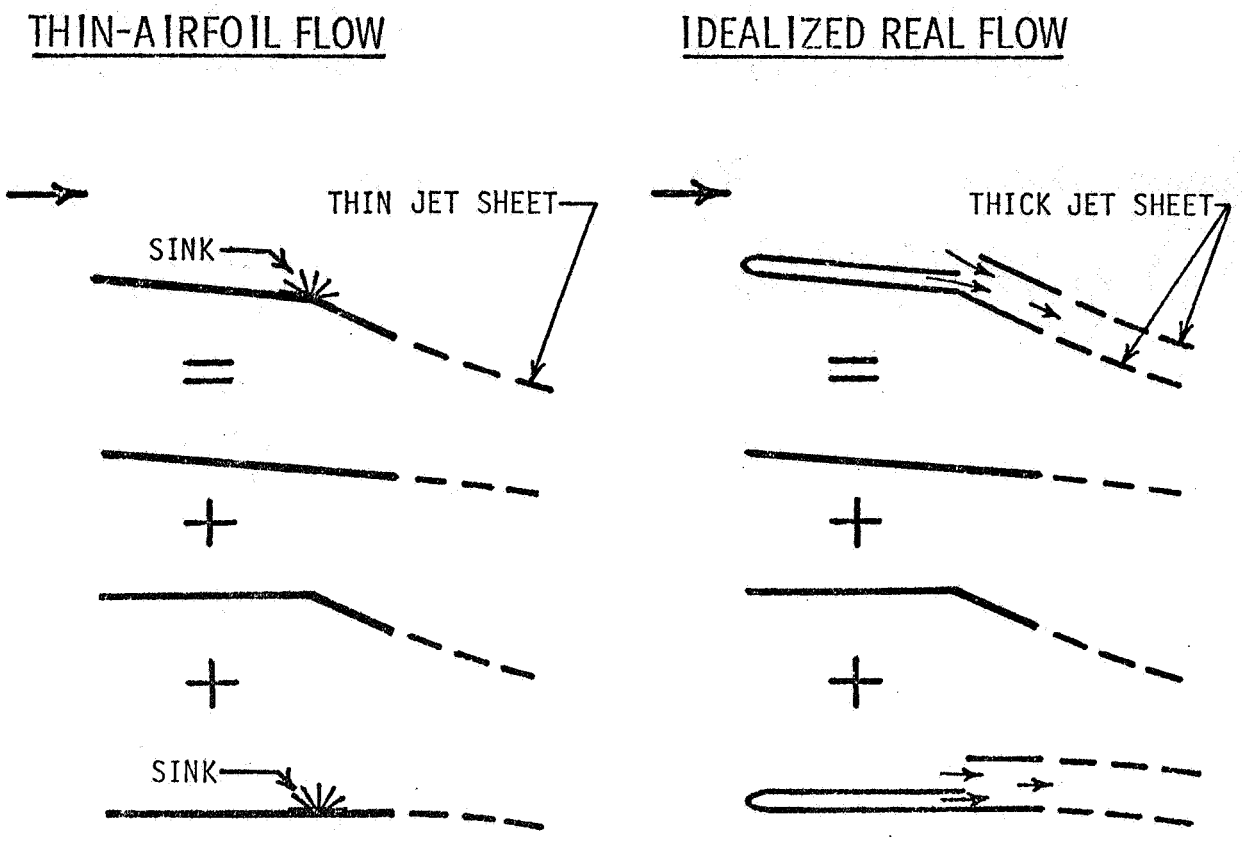

Figure 3.- Illustration of superposition principle.

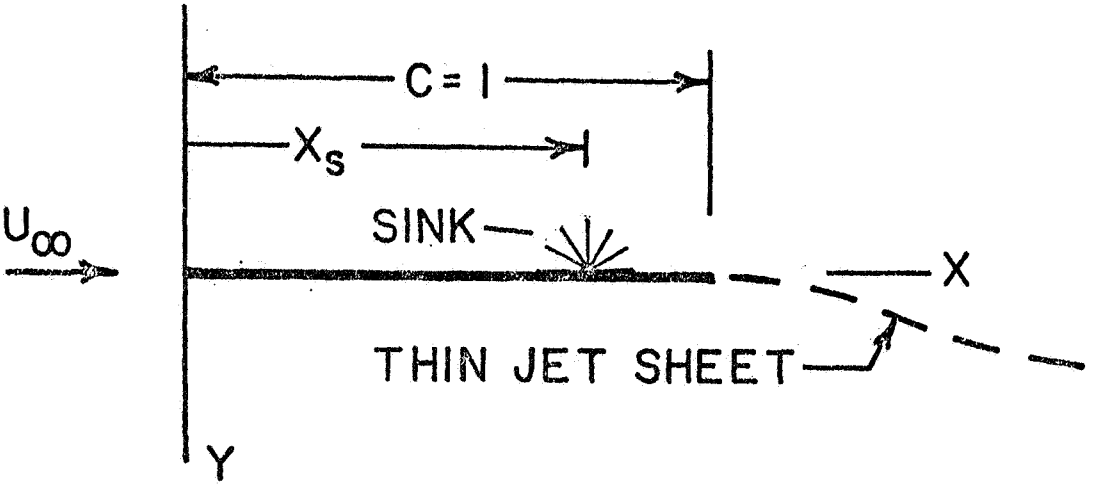

Figure 4.- Flat-plate suction airfoil with trailing-edge regular blowing.

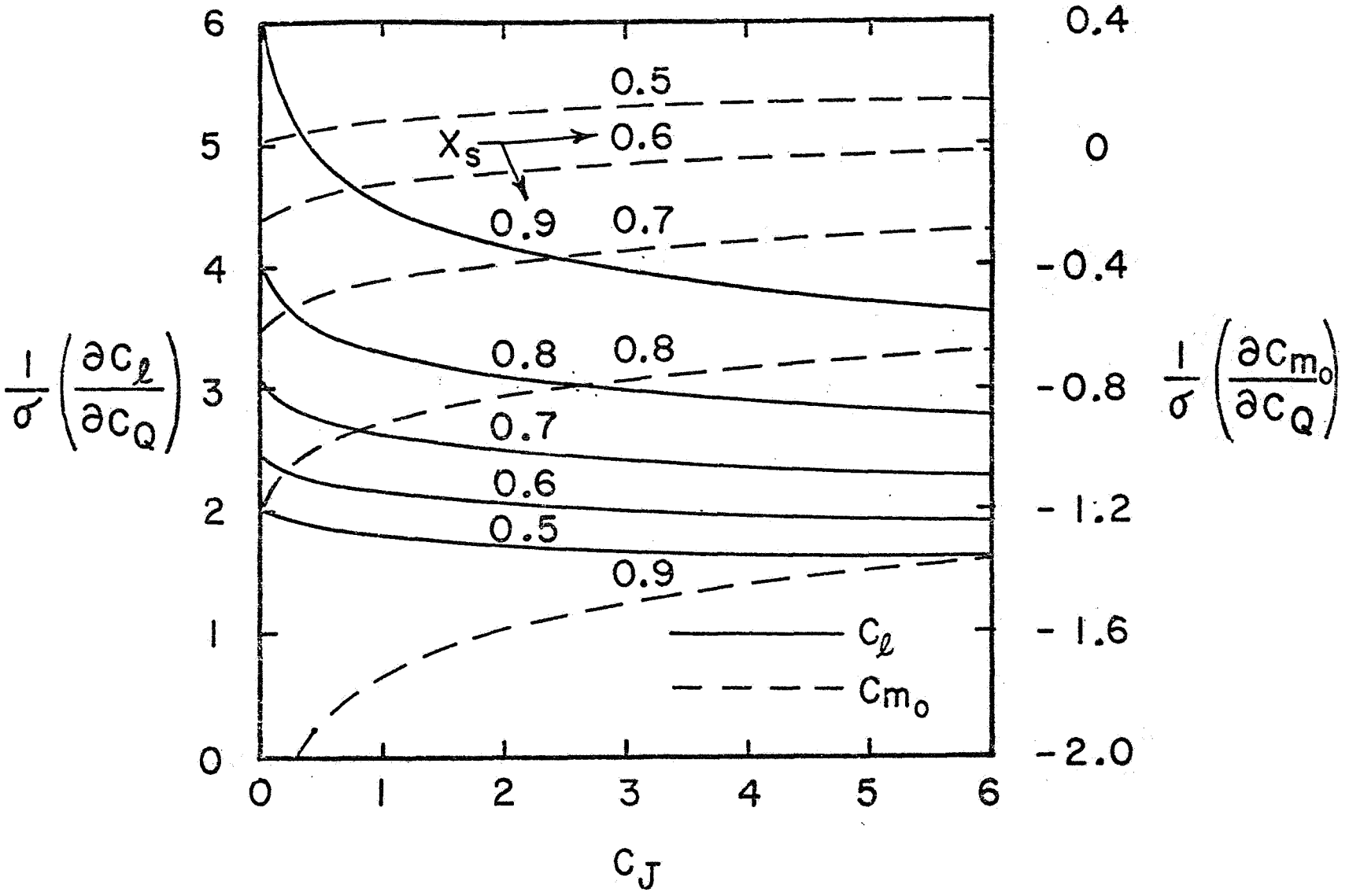

Figure 5.- Lift and pitching-moment characteristics of a flat-plate suction airfoil with trailing-edge regular blowing.

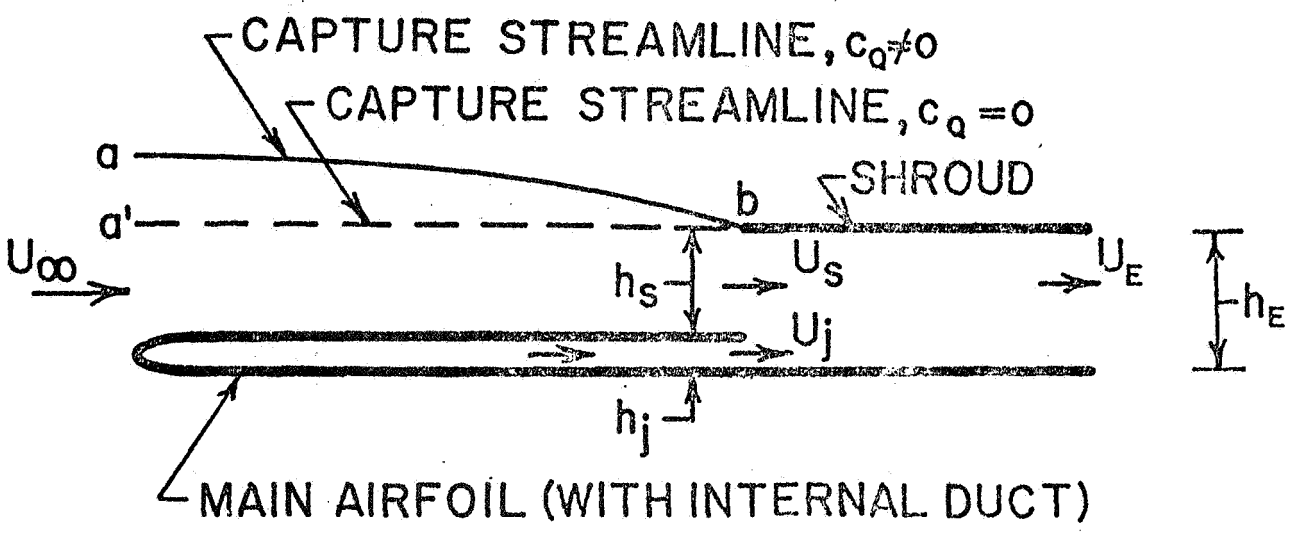

Figure 6.- Idealized ejector-flapped wing section defining $c_Q = 0$.

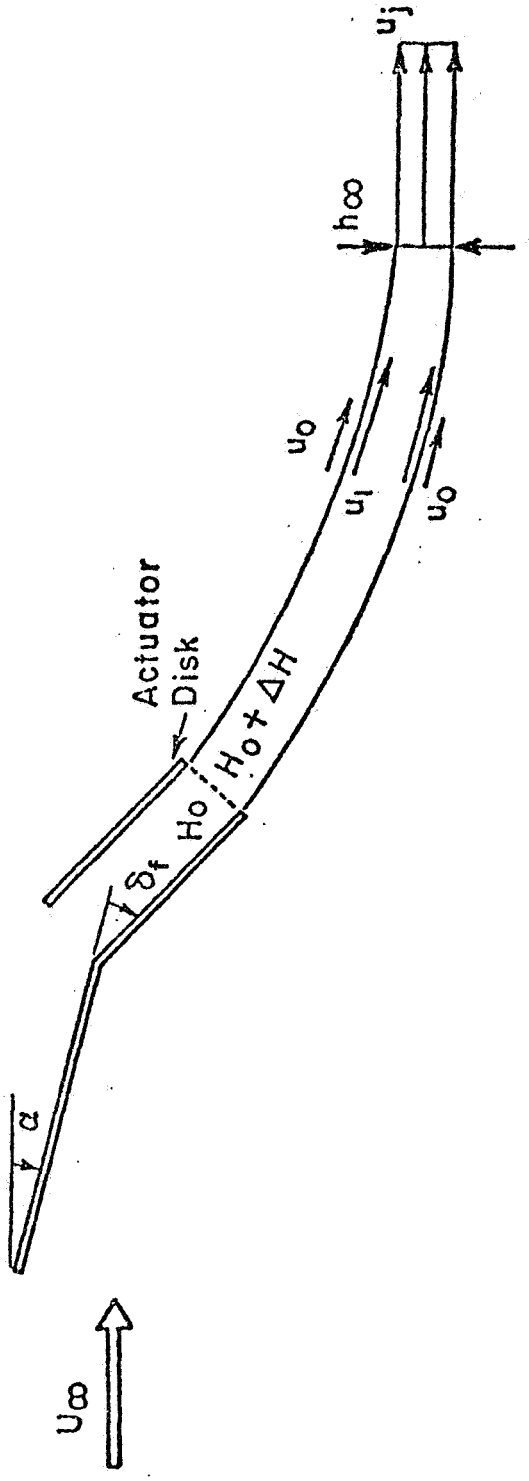

Figure 7.- Galcit actuator-disk flow model.

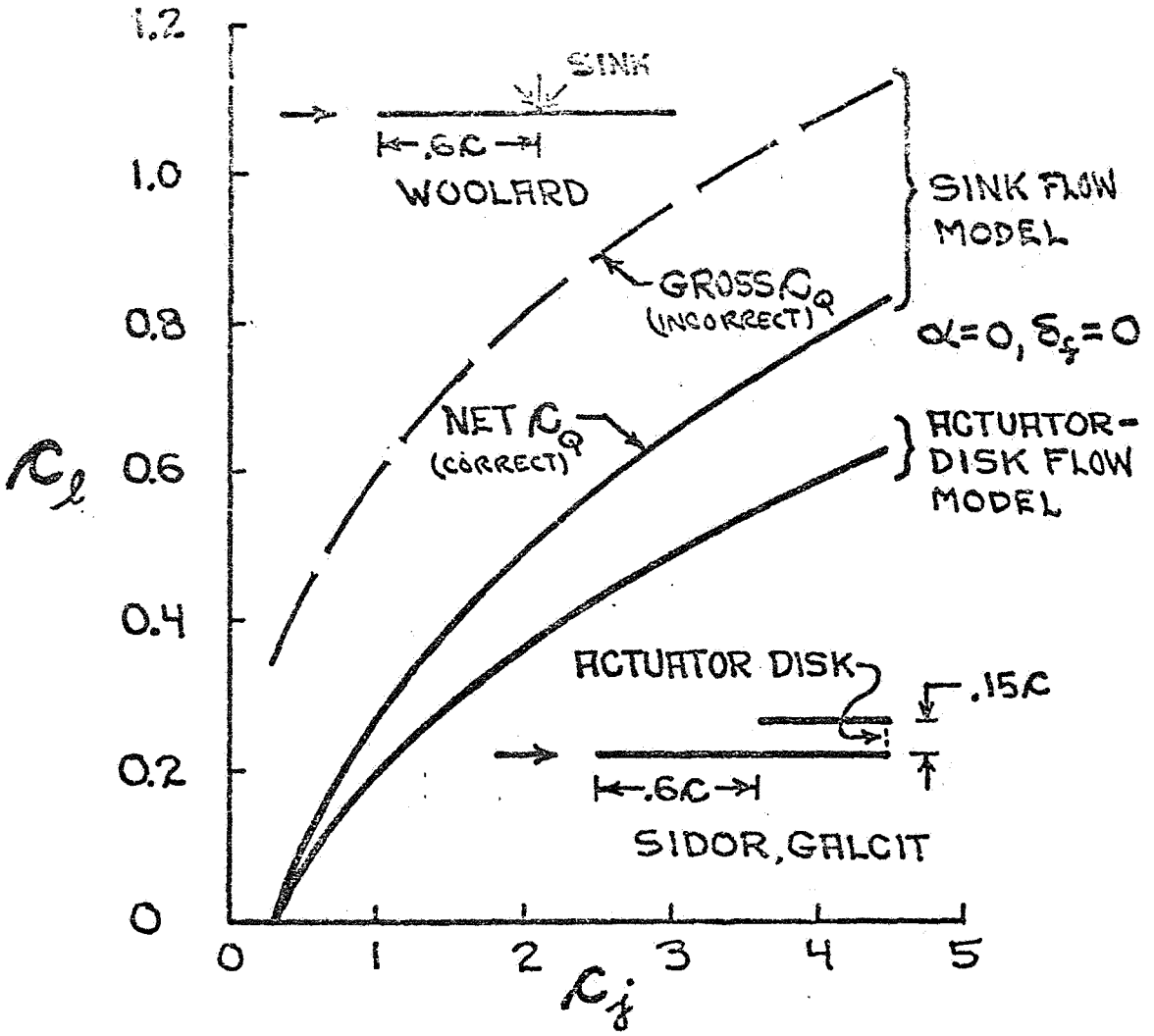

Figure 8.- Comparison of the suction-induced lift coefficients for several flow models.

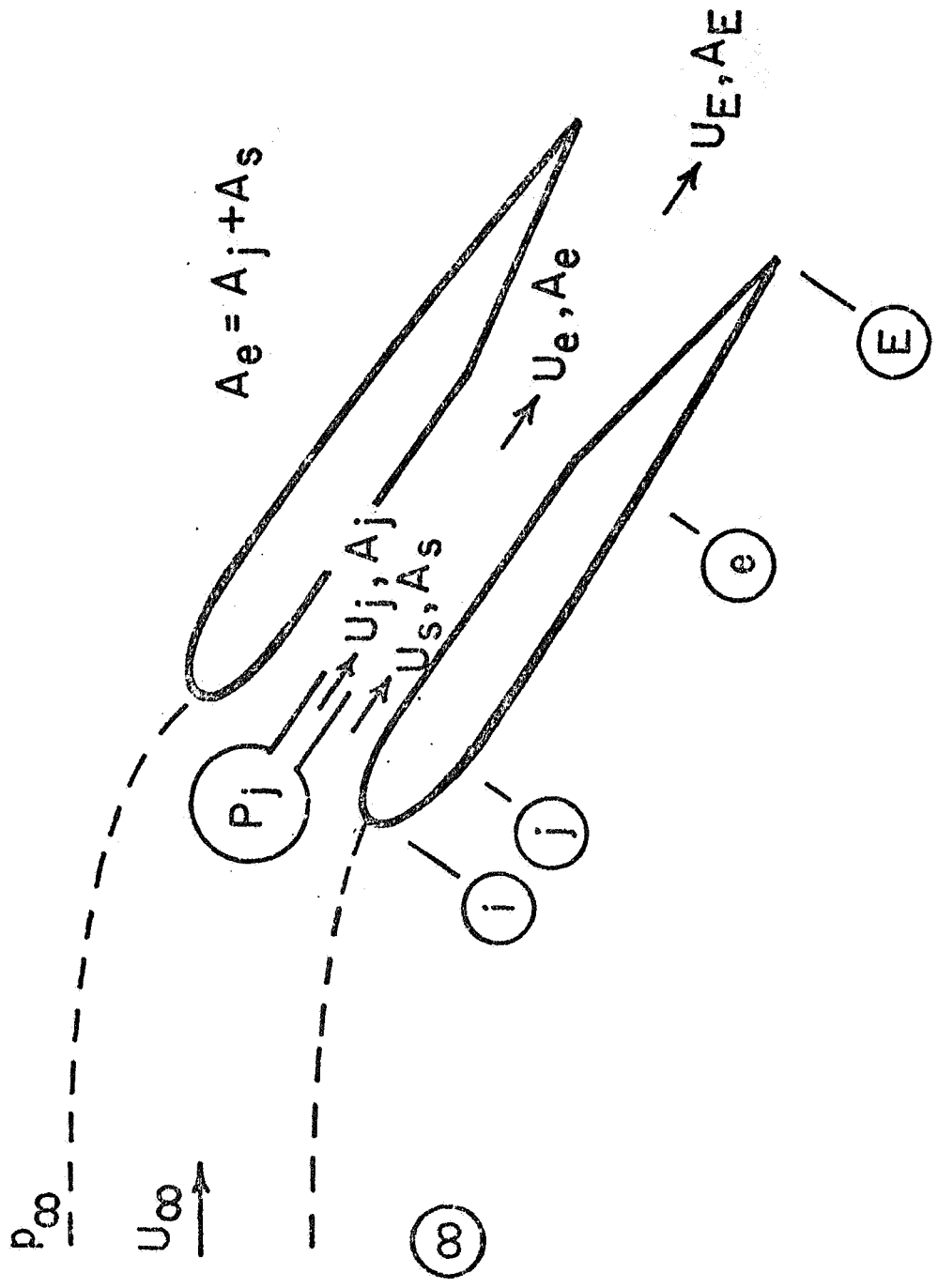

Figure 9.- Schematic representation of an ejector flap.

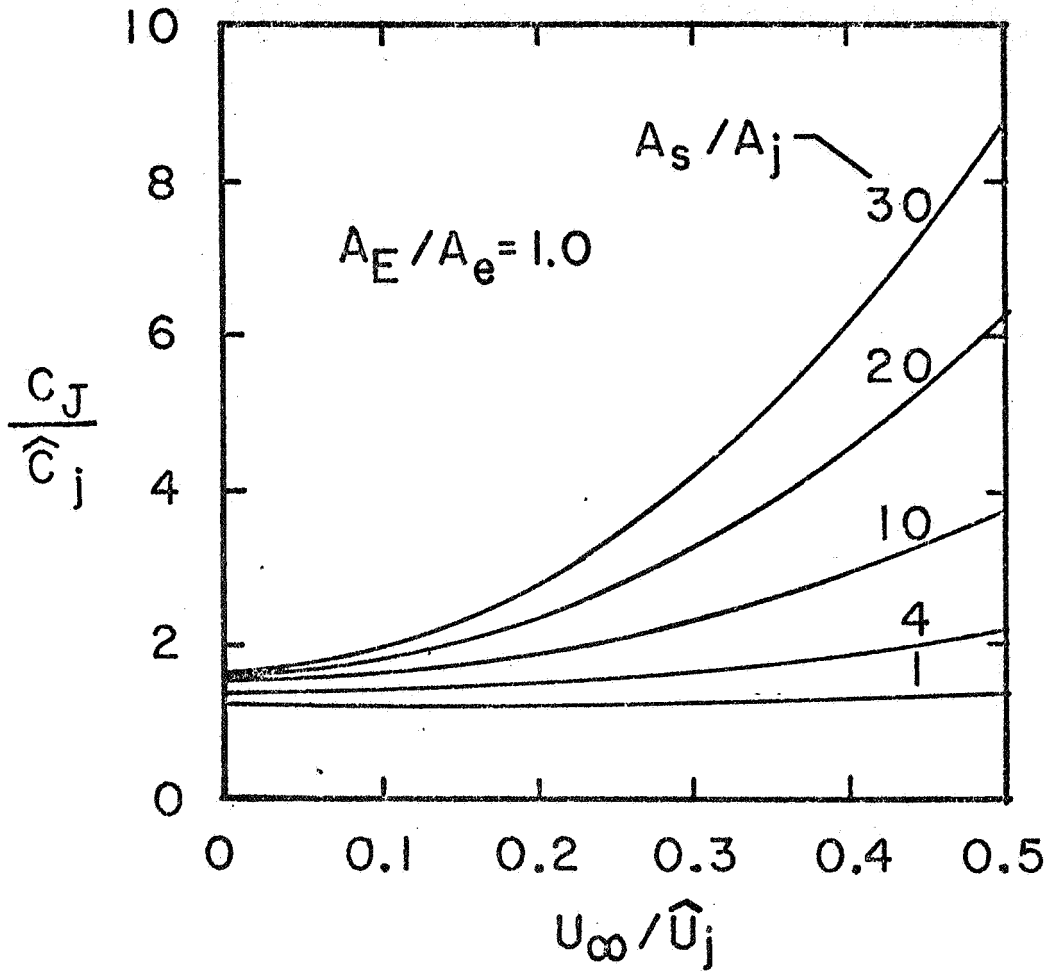

Figure 10.- Exit-momentum augmentation ratio as a function of the forward-speed ratio and injection-area ratio.

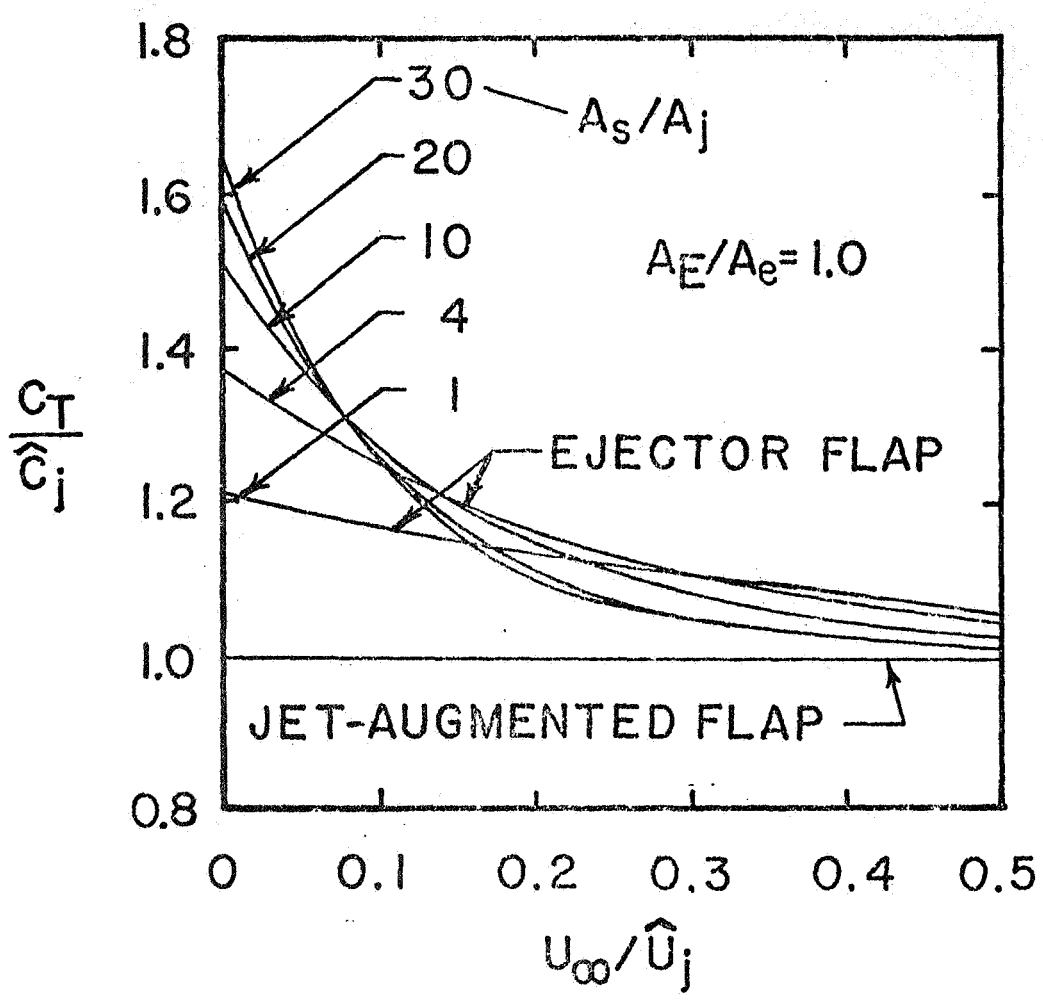

Figure 11.- Thrust-augmentation ratio as a function of the forward-speed ratio and injection-area ratio.

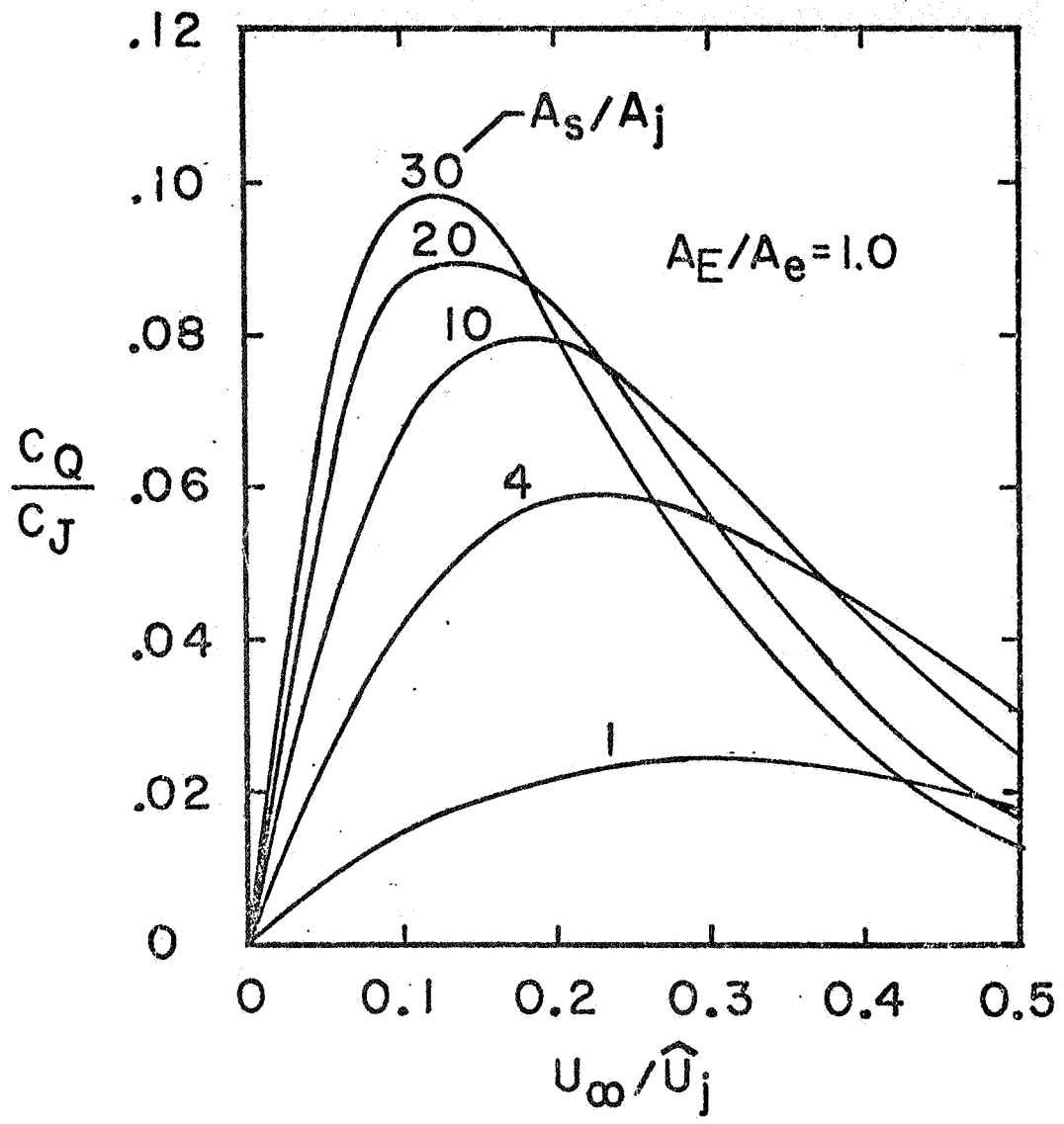

Figure 12.- Ratio of net suction coefficient to jet-momentum coefficient as a function of the forward-speed ratio and the injection-area ratio.

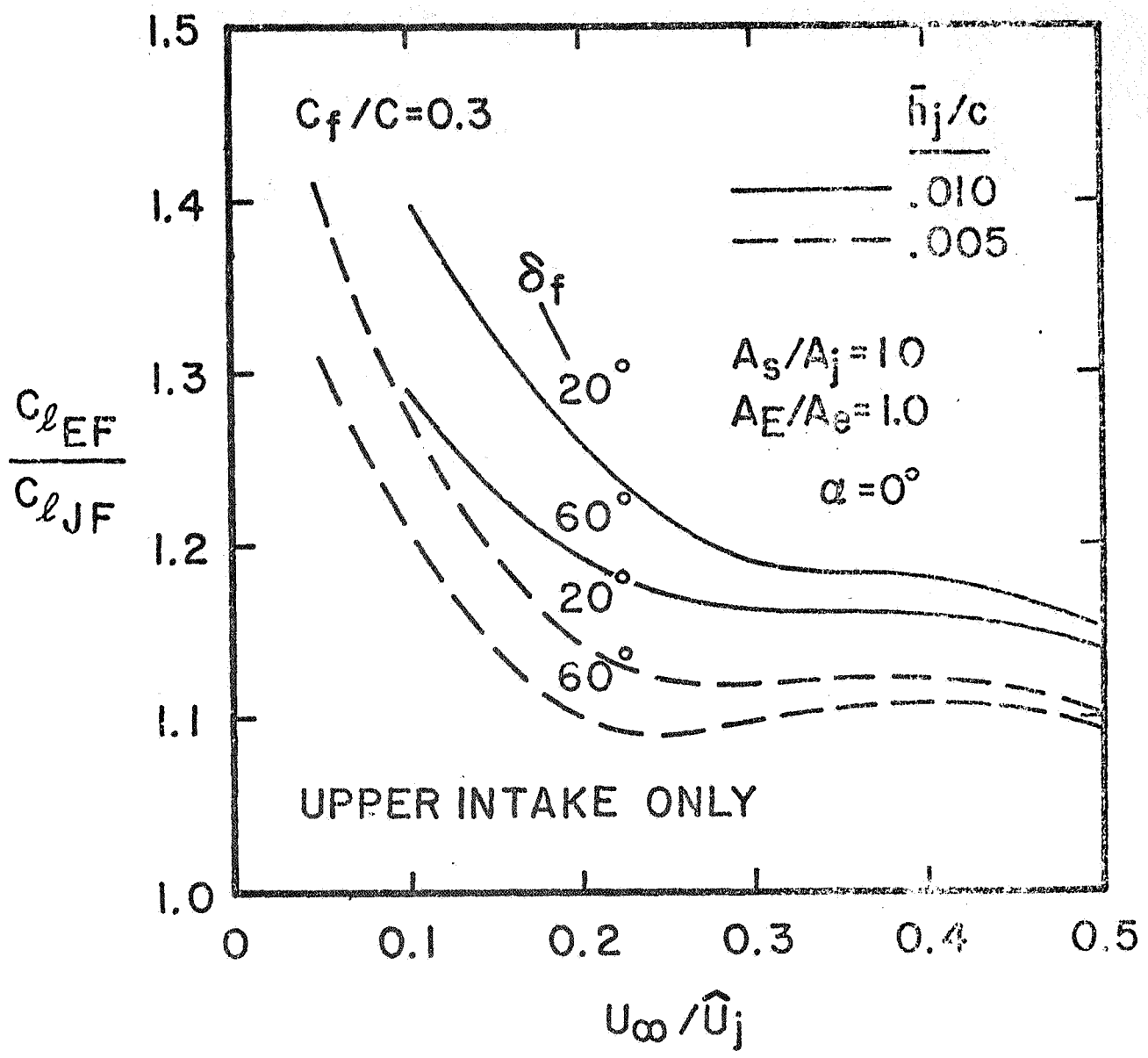

Figure 13.- Relative lift performance of ejector-flapped and jet-augmented-flapped wings.

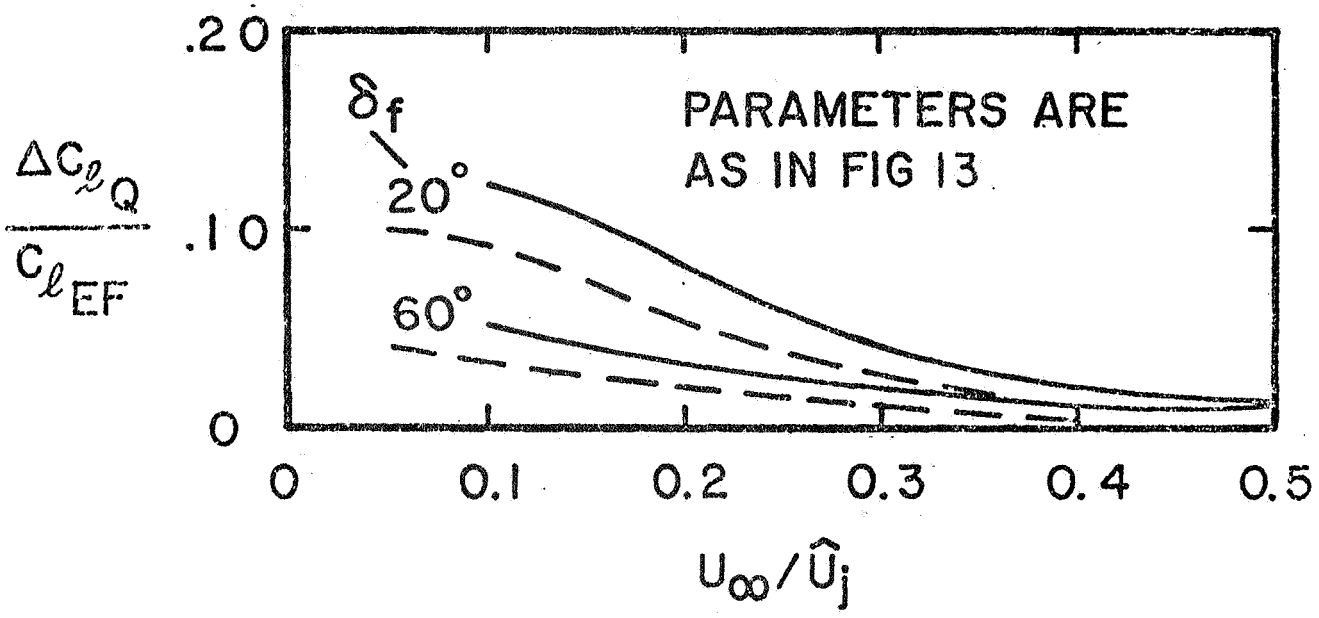

Figure 14.- Suction contribution to the lift of ejector-flapped wings.

ON THE RATIONAL DESIGN OF COMPRESSIBLE FLOW EJECTORS

P. J. Ortwerth

Chemical Laser Branch, Air Force Weapons Laboratory
Kirtland Air Force Base, New Mexico

SUMMARY

A fluid mechanics review of modern ejectors has identified the following parameters that must be considered when designing ejectors for a chemical laser pressure recovery system. The first parameter is called the secondary flow admittance, or inversely the flow impedance, defined as the ratio of secondary mass flow and secondary total pressure. The laser diffuser critical pressure recovery defines the ejector input impedance. Internally the ejector suction characteristics define an ejector impedance. The first design condition to be met is the secondary flow impedance matching condition. The second important characteristic is the secondary flow Mach number. The secondary flow Mach number is found to have an important influence on ejector performance for low mass ratio and should be optimized for the design operating point. The last critical parameter is the ejector throat area. The ejector area insures that impedance is matched correctly and the desired performance obtained. The throat area depends very strongly on the distortion produced by the dynamics of the mixing layer of primary and secondary flow. If the application permits, multiple driver nozzles can be used to minimize distortion which results in the maximum performance of the pressure recovery system.

1. INTRODUCTION

In the application of CW chemical lasers to military systems the ejector plays a critical role. The optimization of the ejector is important in reducing the weight and volume of the system. The ejector is normally the largest component of the laser device and consumes several times as much propellant as the laser cavity. An integrated laser diffuser ejector schematic is shown in figure 1 for comparing size and defining components. Research in ejector fluid mechanics has been largely experimental and a large body of relevant data is now available (refs. 1-4). These data must be exploited fully in order to reduce the time and expense of building future large systems. It is the purpose of this paper to explain the characteristics of the ejector from an elementary fluid mechanics approach. A modern ejector is defined as one in which the secondary Mach number is chosen to optimize performance, as opposed to previous designs where it is assumed that $M_s = 0.2$. It is desirable to avoid relying on purely empirical correlation of the data since such attempts have been known to fail in the past when scales and the primary and secondary flow properties have varied significantly.

II. REVIEW OF SELECTED EJECTOR PROPERTIES

As a prelude to developing the method and theory of ejector design we shall review selected ejector experimental data which are important for understanding the fluid mechanics of good ejectors.

Existence of a Critical Point

The data in figure 2 shows how the inlet pressure in the ejector varies with the back pressure. Two regions exist: the supercritical region at low back pressure in which the inlet pressure is constant independent of back pressure, and the subcritical region in which back pressure determines inlet pressure. The point separating these two regions is called the critical point. While chemical laser diffuser ejectors systems have operated in the subcritical ejector range, it is undesirable for the impedance to depend on back pressure. Highest efficiency of the diffuser ejector system is obtained when the diffuser and ejector operate at their respective critical points. For assured safe operation it is desirable to design both the diffuser and ejector at slightly supercritical conditions. A good design methodology must be able to predict the critical point for all operating conditions of the laser.

Supercritical Pressure Distribution

Let us examine the effect of back pressure on the axial pressure distribution in the ejector. The data in figure 3 shows a constant pressure distribution independent of back pressure in the mixing section. Downstream after the throat station, the pressure distribution is determined by back pressure in exactly the same way as back pressure affects supersonic diffusers. The critical point is reached when the shock structure has moved to the throat of the ejector. It is exactly these features which make the determination of the critical point a priori possible by applying standard flow conservation analysis.

Throat Flow Distortion and Mixing

The one-dimensional analysis of ejectors requires the flow be completely mixed at the throat. However, pitot-pressure profiles in the throat of an ejector are very distorted as shown in figure 4. Clearly, a longer mixing section would be required to completely mix the flow. A longer mixing section is definitely not desired, however, since that would only add to the weight and volume of the ejector. In fact the profiles in figure 4 correspond to the operating conditions of figure 3 in which critical operation was achieved at satisfactory performance level for many applications. A very important feature of these profiles is that the mixing zone has reached the wall as evidenced by the positive slope of the pitot profiles from the wall. This feature is important to achieve critical operation since the low momentum secondary flow cannot undergo compression unless shear forces are present to balance

the pressure gradient. Ideal calculations discussed later show the completely mixed flow would occupy an area 73% as large as the real area and performance would be 30% higher. We conclude that distortion is responsible for a significant correction to real ejector throat area requirements and, therefore, performance.

Existence of Ejector Flow Impedance and Impedance Matching with Diffusers

While most ejector characteristics are best presented in nondimensional coordinates the existence of flow impedance is readily recognized in dimensional coordinates. The data (ref. 2) for secondary flow rate versus secondary pressure commonly called the suction characteristics clearly show that for a wide range of conditions the secondary mass flow is dependent on secondary total pressure only (fig. 5). In fig. 5, the significant primary mass flow and nozzle diameter variations shown in the legend do not affect the linear relationship of secondary mass flow with secondary total pressure. The common practice of normalizing this curve by primary mass flow and pressure is fictitious and misleading. We can then define an ejector admittance.

$$A = \frac{\mathring{W}_s}{Pos} \tag{1}$$

This relation states that the secondary volume flow rate is constant over all conditions tested. This amazing fact correlates with the only other fixed parameter in the tests which is the mixing length. The absolute entrainment rate is also only pressure dependent when the other shear layer conditions are fixed. Thus, based on the properties of entrainment, constant volume flow rate is to be expected and is observed. This feature is one of the chief virtues of an ejector that make it a true pumping system. For completeness, figure 6 is included for the accepted critical diffuser impedance characteristics as determined from experimental data.

Impedance Dependence on Mixing Length[1] (Minimum impedance and critical mixing length)

A very important phenomena is observed when the position of the primary driver nozzle is moved relative to the ejector throat inlet. As shown in figure 7 the secondary total pressure depends on the nozzle location under condition of fixed secondary flow rate. This means flow impedance will also depend on mixer geometry. There is a critical zone, between seven and eight nozzle diameters upstream of the throat, where impedance is a minimum. An explanation of this phenomena can be constructed based on the mixing dynamics of the primary and secondary flows. The reasoning is based on the observed pitot-pressure profile of figure 4 which was obtained when the nozzle was located in the critical mixing zone. As stated above, we identify the

---

[1]The impedance depends on mixer contraction cone angle (refs. 1, 3, and 4) but will not be discussed here.

critical zone with the condition that the shear layer has just entrained the last secondary flow streamline.

For shorter distances unmixed secondary flow must pass through the restrictive throat area requiring an increased secondary total pressure. While the longer mixing lengths, the potential core is mixed out and the shear layer greatly expands. The expanded mixing zone also has to be compressed to fit through the throat area.

The exit pressure maximizes at the same mixing length. One reason for this is that the drag of the mixing section is a minimum at this condition.

Critical Point Performance Dependent on Secondary Flow

The last feature we wish to review is the dependence of the ejector critical point performance secondary flow rate in figure 8. The data illustrates the fact that lowest exit pressure is achieved when the secondary flow is zero. Pressure increases monotonically with increasing secondary flow and is entirely consistent with a conservation analysis of the ejector performance.

This curve reveals design point operation requires less primary mass flow than start conditions. Recalling that secondary flow entrainment does not depend on primary pressure means that the ejector can be turned down as the laser starts without fear of unstarting the laser.

III. DESIGN METHOD

Several theoretical tools are necessary to cope with the variety of issues just discussed. Every design will start with a requirement to pump a secondary mass flow and total pressure delivered by the laser to the final exhaust pressure level. A wide variety of laser gas and primary gas properties are encountered.

The selection of a primary nozzle propellant will not be considered in this paper but clearly is important in a real application. Laser gas properties can also vary and, importantly, the gases may be cooled. The overall length may be a constraint and multiple ejectors side by side might be in order. All these issues and more do not directly relate to the fluid mechanics methodology. In the next section we will develop the tools for the following method:

1. A method to compute an optimized performance map in which secondary Mach number and performance are computed versus mass ratio.

2. A method to compute the flow distortion at each optimized condition. Performance is adjusted for the distortion losses and the design point is selected.

3. The throat area is determined for the design point to match diffuser impedance. Off design performance is then computed to match other facility or system requirements using a fixed geometry performance calculation.

Optimization of the Ideal Ejector Design

The question usually asked by the system designer is, "What is the lowest mass ratio needed to pump from diffuser exit pressure to ambient?" Theoretically it is simpler to ask the question, "what's the highest pressure ratio available for a given mass ratio?" We consider secondary flow rate, total pressure, and total temperature to be fixed initial conditions. We consider the primary flow rate, Mach number, total temperature to be fixed. The question is, "what control is available to optimize performance?" Before we answer this question we should review the factors affecting performance.

The ejector is a pump with two important processes, both of which are inherently lossy. The first is an entrainment by tangential shear stress at constant pressure and the second is a compression of the mixed gases. The compressor is a normal shock followed with subsonic diffuser.

What we seek is to minimize the total pressure losses in the mixing and compression processes. At high mass ratio mixing losses will be inherently small and the dominant losses will be normal shock losses, and the reverse is true at low mass ratios. We shall not consider subsonic diffuser losses in this optimization process for the following reasons.

First, the normal shock compression losses are dominant. Second, in practice, the subsonic diffuser is usually conical in shape and designed for the optimum angle of subsonic diffusers. The performance of the subsonic diffuser then depends on the inlet flow blockage only, according to Sovran and Klomp (ref. 5). For flow after a normal shock, we would expect blockage to be constant, independent of upstream conditions and thus the C_p of the diffuser will also be considered constant.

For simplicity then we shall optimize the ejector for maximum pressure after the normal shock. From this brief inspection of the problem it is clear only one input parameter left unspecified can affect the losses in any meaningful way and this is the secondary velocity or Mach number. First, the secondary flow velocity directly determines the mixing losses and the mixed gas Mach number and, thus, the normal shock losses. Secondly, the secondary static pressure is dependent on secondary Mach number which has a strong effect on throat area. We proceed as follows:

Let the normalized optimization parameter be

$$\theta = \frac{Us}{Up} \tag{2}$$

Then the mixed gas velocity will be

$$U_2 = Up\left(\frac{\mu + \theta}{\mu + 1}\right) \tag{3}$$

where

$$\mu = \frac{\dot{W}p}{\dot{W}s} \tag{4}$$

is the ejector mass ratio. The mixed gas Mach number becomes

$$M_2^2 = \left(\frac{2}{\gamma - 1}\right)\left(\frac{U_2^2}{2H_2}\right)\left(1 - \frac{U_2^2}{2H_2}\right)^{-1} \tag{5}$$

The normal shock pressure ratio is thus dependent on the secondary static pressure and we write the function to be maximized in two parts:

$$\frac{P_3}{Pos} = \left(\frac{P_3}{P_2}\right)_{N.S.} \frac{P_2}{Pos} \tag{6}$$

where the normal shock pressure ratio

$$\left(\frac{P_3}{P_2}\right)_{N.S.} = \frac{2\gamma}{\gamma + 1} M_2^2 - \frac{\gamma - 1}{\gamma + 1} \tag{7}$$

and the secondary static pressure are dependent on θ.

$$\frac{P_2}{Pos} = \left(1 - \frac{Us^2}{2Hs}\right)^{\gamma s/\gamma s - 1} \tag{8}$$

Defining the following functions:

$$\theta_1 \equiv 1 + \frac{\theta}{\mu} \tag{9}$$

$$\theta_2 \equiv \theta_1{}^2 \tag{10}$$

and the following constants:

$$B \equiv \left(\frac{\mu}{1 + \mu}\right)^2 \frac{Up^2}{2H_2} \tag{11}$$

$$A = \left(\frac{\gamma + 1}{\gamma - 1}\right)^2 B \tag{12}$$

$$\theta_m^2 = \frac{2Hs}{Up^2} \tag{13}$$

we obtain

$$\frac{P_3}{Pos} = -\left(\frac{\gamma - 1}{\gamma + 1}\right)\left(\frac{A\theta_2 - 1}{B\theta_2 - 1}\right)\left(1 - \frac{\theta^2}{\theta_m^2}\right)^{\gamma s/\gamma s-1} \tag{14}$$

To obtain the condition for the maximum performance we differentiate with respect to θ and set the derivative equal to zero.

$$\frac{d\left(\frac{P_3}{Pos}\right)}{d\theta} = F(\theta) = \frac{\frac{2A}{\mu}\theta_1}{A\theta_2 - 1} - \frac{\frac{2B}{\mu}\theta_1}{B\theta_2 - 1} - \frac{\gamma_s - 1}{\gamma_s}\frac{2}{\theta} \tag{15}$$

This equation is solved numerically using a Newton-Raphson technique.

The variation of optimum secondary Mach number with mass ratio is shown in figure 9, from reference 6. At low mass ratio the secondary mass ratio increases to Mach 1 while at high mass ratio the results tend toward the classical rule of thumb secondary Mach number of 0.2. The importance of this parameter is shown in figure 10 also from reference 7, where a 50% increase in performance is obtained by doubling the secondary flow Mach number from the classical Ms = 0.2.

Calculation of the Admittance of the Ejector (Single Primary Nozzle)

In the previous discussion we found the best conditions for minimizing the ideal ejector losses. The ejector design will work only if the internal admittance of the ejector is matched to the requirements of the diffuser. The admittance is controlled by two factors the second throat area and the mixing section contraction and length. It is most important to be able to calculate the second throat area and we will proceed to formulate the solution to that problem. The mixer design requires the calculation of the absolute entrainment rate and is beyond the scope of the present paper.

The calculation of the area of the second throat for a single primary nozzle driver is based on the identification in the review section that admittance is optimized when the mixing zone just reaches the wall. In this case the flow consists of two regions: first, the potential core and, second, the shear layer. This condition is shown in figure 11. To calculate the area of the shear layer for the condition that all the secondary flow is entrained, we make the following simplifying assumptions for the profile, first that the turbulent Prandtl and Schmidt numbers are unity and second that the velocity profile can be approximated by a cosine law. We then proceed as follows:

Shear layer profiles are:

Velocity

$$\frac{U - Us}{Up - Us} = \frac{1}{2}\left[1 + \cos\left(\frac{\pi Y}{h}\right)\right] \tag{16}$$

where

$$Y = (r - r_i) \tag{17}$$

and

$$h = (r_o - r_i) \tag{18}$$

Total enthalpy

$$\frac{H - Hs}{Hp - Hs} = \frac{U - Us}{Up - Us} \tag{19}$$

Primary fluid mass fraction

$$Yp = \frac{U - Us}{Up - Us} \tag{20}$$

Secondary mass fraction

$$Ys = 1 - Yp \tag{21}$$

The conservation equations for the flows through the mixer are:

Continuity

$$\mathring{W}_2 = 2\pi \int_o^{r_o} \rho u r dr - \mathring{W}p + \mathring{W}s \tag{22}$$

Thrust balance

$$F_2 = P_s \pi r_o^2 + 2\pi \int_o^{r_o} \rho u^2 r dr \tag{23}$$

and

$$F_2 = F_p + F_s - P_s(\pi r_s^2 - \rho r_o^2) \tag{24}$$

The static pressure P_s is computed from the admittance and optimum secondary Mach number. The stream thrust of the primary and secondary flows are computed from the one dimensional formula

$$F = PA(1 + \gamma M^2 \eta_F) \tag{25}$$

Energy balance

$$\mathring{W}_2 H_2 = 2\pi \int_o^{r_o} \rho u H r dr \tag{26}$$

and

$$\mathring{W}_2 H_2 = \mathring{W}_p H_p + \mathring{W}_s H_s \tag{27}$$

The energy equation is not needed for the solution since only two unknowns exist r_i and r_o. The energy equation is a useful check sum of the calculation.

Normalizing the equations facilitate solution letting

$$\tilde{r} = \frac{r}{r_p}, \quad \tilde{\rho} = \frac{\rho}{\rho_p}, \quad \tilde{U} = \frac{U}{U_p}, \quad \text{and} \quad \eta = \pi \frac{\tilde{Y}}{\tilde{h}} \tag{28}$$

We obtain a transformed continuity equation

$$\tilde{r}_i^2 + \frac{2\tilde{r}_i \tilde{h}}{\pi} I_1 + \frac{2\tilde{h}^2}{\pi^2} I_2 = 1 + \frac{1}{\mu} \tag{29}$$

and transformed momentum equation

$$\tilde{r}_i^2 + \frac{2\tilde{r}_i \tilde{h}}{\pi} I_3 + \frac{2\tilde{h}^2}{\pi^2} I_4 = 1 + \frac{\theta}{\mu} \tag{30}$$

where

$$I_1 = \int_o^\pi \tilde{\rho}\tilde{U} d\eta \tag{31}$$

$$I_2 = \int_o^\pi \tilde{\rho}\tilde{U}\eta d\eta \tag{32}$$

$$I_3 = \int_o^\pi \tilde{\rho}\tilde{U}^2 d\eta \tag{33}$$

$$I_4 = \int_o^\pi \tilde{\rho}\tilde{U}^2 \eta d\eta \tag{34}$$

The normalized continuity and thrust balance equation can be solved numerically by the Newton-Raphson method.

Fixed-Geometry Performance

We can calculate the ejector performance for any Ws by using the conservation equations since we know the ejector throat area and admittance.

Pressure after the shock is computed as follows. Through the shock duct the quantity

$$N \equiv \frac{\mathring{W}_2}{F_2}\left(\frac{RT_t}{\gamma}\right)^{1/2} = \frac{M\left(1 + \frac{\gamma - 1}{2} M^2\right)^{1/2}}{1 + \gamma M^2} \tag{35}$$

is conserved. We can solve this equation explicitly for Mach number after shock

$$M_3 = \left(\frac{K - \sqrt{K - 2N^2}}{1 - \gamma K}\right)^{1/2} \tag{36}$$

where

$$K = 1 - 2\gamma N^2 \tag{37}$$

we find pressure after shock from the formula

$$P_3 = \frac{F_2/A_2}{1 + \gamma M_3^2} \tag{38}$$

This somewhat tedious method of computation does not require matched primary nozzle exit pressure and secondary static pressure. It also correctly accounts for the larger area due to distortion. Thus, this analysis is aptly suited for fixed geometry off design calculations.

We can compute ejector-off design performance since the admittance allows us to calculate Pos for any Ws and all other parameters are known including θ which is also constant.

The Critical Mass Ratio

The condition $r_i = 0$ represents the last condition for which the ejector falls in the high performance classification. Throat distortion rapidly increases at lower mass ratios and the required throat area also increases rapidly. The condition is

$$\mu_{min} = \left(1 - \theta \frac{I_2}{I_4}\right)\left(\frac{I_2}{I_4} - 1\right)^{-1} \tag{39}$$

Comparison of Theoretical and Experimental Ejector Results

Design point characteristics of the single-driven nozzle tested at UTRC by Zumpano (ref. 1) are shown in table 1.

Overall agreement between the theoretical and experimental ejector designs is very good. Particularly important is the power of using the distorted profile for determining the actual ejector throat area. This throat area is critical to insuring the admittance is determined correctly and we can compute the off-design performance. The entire operating range of the ejector is shown in figure 12 and compared with the fixed-geometry calculation using constant admittance. Also shown is the ideal performance computed for the one-dimensional throat area. This performance deficit between the ideal performance and the real performance dramatically illustrates the improvement available by eliminating the flow distortion.

While it is probably obvious that these results are not universal, note that for every different choice of initial conditions the ejector design and performance will be different.

Summary of Single-Nozzle Designs

Before considering ejectors with multiple-drive nozzles let us summarize what we can do up to this point.

1. Calculate the second throat area for any design point that matches the secondary flow admittance with ejector admittance.

2. Find the ejector with the minimum mass ratio for the design pressure ratio.

3. Since area and admittance are known we can compute off-design performance down to the critical mass ratio.

Multiple-Injector Nozzles

We shall now discuss a heuristic method for determining the number of primary nozzles necessary to reduce the distortion of the flow. Reducing the distortion means we can invoke the condition,

$$A_t = A_{ideal} \text{ (at the design point)} \tag{40}$$

First let us reexamine the two profiles with minimum distortion. In the ideal case of uniform profiles no distortion exists. In the second case, distortion is minimized when the mixing zone just reaches the wall, as in figure 13(a).

A feature of note is the existence core with very high mass flux. This feature is crucial in minimizing the overall distortion.

Now let us consider the following series of overlapping mixing zones[2] obtained by using multiple nozzles. As the geometry of the mixing zones show,

[2]This particular example is for Air-Air mixing at a mass ratio of 3.6.

the first case tested in which the mixing zones do not destroy the core flow is the case for five nozzles (fig. 13(e)). Based on the geometry of mixing zone overlap in figure 13 we have a criteria:

> "The minimum number of primary nozzles required to achieve ideal area ratio is that number for which the mixing zones of adjacent nozzles just osculate the potential core."

That this criteria is borne out in practice is demonstrated by the data of figure 14 in which ejector performance is compared for 1, 4, and 7 nozzles. The performance of the single nozzle and the four nozzle drivers is practically the same while a significant increase in performance is observed for the 7-nozzle driver. A similar improvement was noted for the 5-nozzle driver over the single-nozzle driver of reference 1.

Nonconstant Admittance of Multiple-Driver Nozzles

Multiple-driver nozzles now enjoy the condition

$$A_{real} = A_{ideal} \text{ (design point)} \tag{41}$$

whereas single-driver nozzles are required to operate with

$$A_{real} > A_{ideal} \tag{42}$$

Unfortunately the condition of constant admittance cannot be fulfilled at all off-design conditions since the condition

$$A_{real} < A_{ideal} \text{ (off design)} \tag{43}$$

occurs in theory but in practice area is fixed in steel. Because of this, another adjustment in operation is observed. This effect is shown in figures 15 and 16 for the five nozzle primary driver steam ejector system of reference 4.

In figures 15 and 16 the curves labeled 1 show the behavior of the mass flow and area for the constant admittance condition. We can see the ideal area required increases as the ejector operates off the design secondary mass flow point. By applying the condition that

$$\frac{(Pos)_r A_{real}}{(Pos)_i A_{ideal}} = 1 \tag{44}$$

the curves labeled 2 can be constructed giving a variable admittance which does in fact reproduce the data point at Ws = 0.1 lbm. The way in which this behavior influences the performance data is shown in figure 17.

CONCLUSIONS

An elementary fluid mechanics analysis of chemical laser ejectors has been accomplished. This analysis has been successful in explaining the characteristics of ejectors with single- and multiple-driver nozzles. As a result a rational methodology has been developed which can be applied to design the optimum ejector for specific application requirements without recourse to unreliable empirical formulas.

REFERENCES

1. Kepler, C. E.; Zumpano, F. R.; Landerman, A. A.; Biancardi, F. R.; Brooks, C. S.; and Russell, S: Pressure Recovery/Scrubber Systems for Chemical Lasers. Naval Surface Weapons Center, White Oak, Silver Spring, MD, Technical Report R75-911976-82, March 1975.

2. Teper, R.: Chemical Laser Ejector Demonstration. Air Force Weapons Laboratory, Technical Report AFWL-TR-76-92, Dec. 1976.

3. Teper, R. I.; and Arbit, H. A., Chemical Laser Advanced Diffuser/Ejector. Final Report, US Army Missile R&D Command Redstone Arsenal, Alabama, Report No. RI/RD 78-102, Jan. 1978.

4. Biancardi, F. R.; Landerman, A. M.; Melikian, G.; Schulman, E. R.; and Zumpano, F. R.: Design and Development of a Compact Pressure Recovery/Scrubber System for Chemical Lasers. Naval Sea Systems Command, PMS 405, Arlington, VA, Technical Report R76-952406, Nov. 1976.

5. Sovran, G.; and Klomp, E. D.: Experimentally Determined Optimum Geometries for Rectangular Diffusers with Rectangular, Conical or Annular Cross Section, Fluid Mechanics of Internal Flow, ed. Sovran, G., Elsevier Publishing Company, Amsterdam, 1967.

6. Ortwerth, P. J.: On Ejector Optimization. Laser Digest-Spring 1976, Air Force Weapons Laboratory Technical Report AFWL TR 76-131, 1976.

TABLE 1.- COMPARISON OF DESIGN POINTS FOR SINGLE-DRIVER NOZZLE (AIR/AIR)

	Mp	$\alpha^{1/2}$	μ	θ	Ms	A_t/An	A^a	$(Pe/Pos)_{crit}$	$\mu_{crit}{}^b$
Experiment	4.46	15°	3.6	---	---	4.59	66.7	5.2[d]	1.5[b]
Theory	4.3[c]	0	3.6	0.21	0.42	4.60	67.7	5.2[d]	1.4
Theory	4.46	0	3.6	.21	.42	4.78	67.7	5.3[d]	1.4

[a] Normalized admittance (see fig. 8).

[b] Last experimental data point given and presumed to be near breakdown.

[c] Nozzle Mach number with same thrust as M = 4.6 nozzle with 15° divergence losses.

[d] Performance computed assumes subsonic diffuser Cp = 0.7.

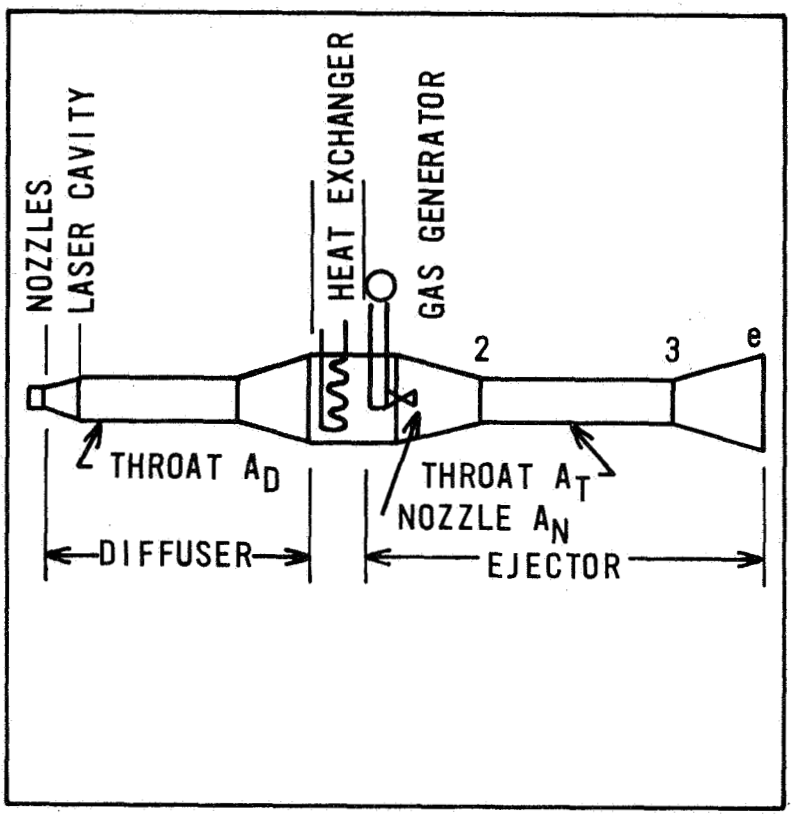

Figure 1.- Chemical laser pressure recovery system.

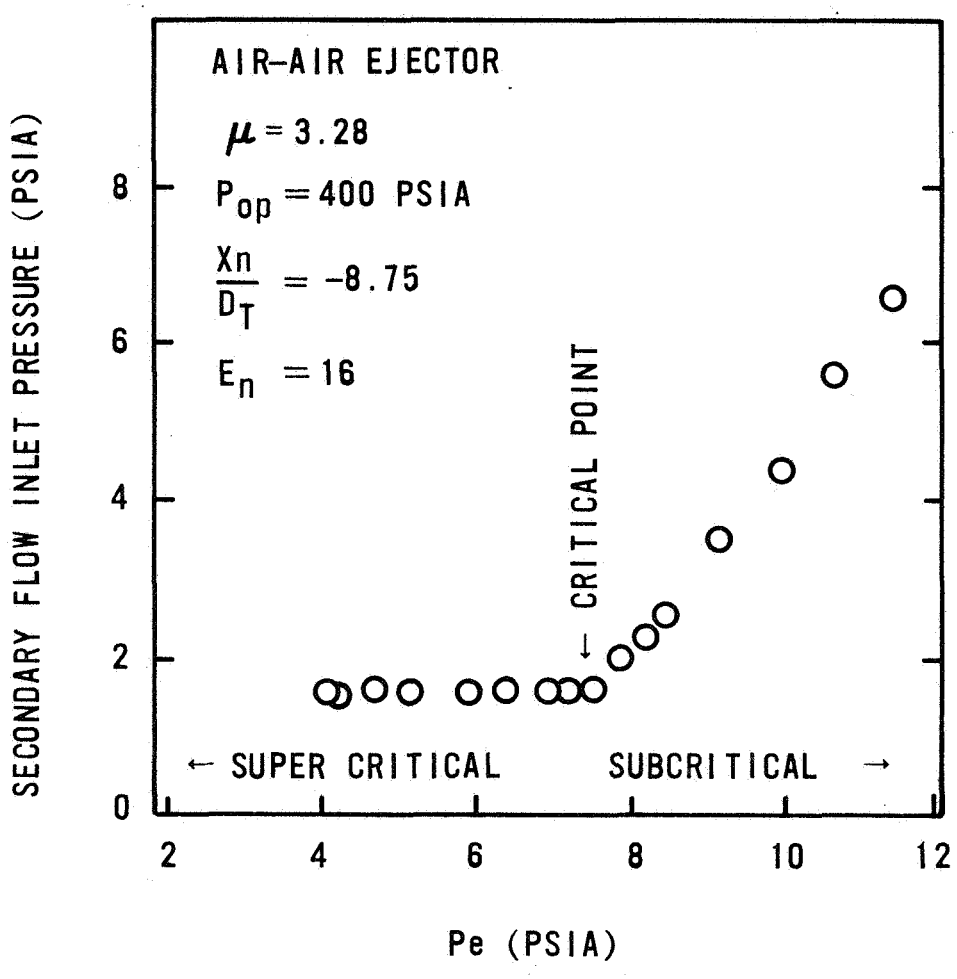

Figure 2.- Ejector operating conditions.

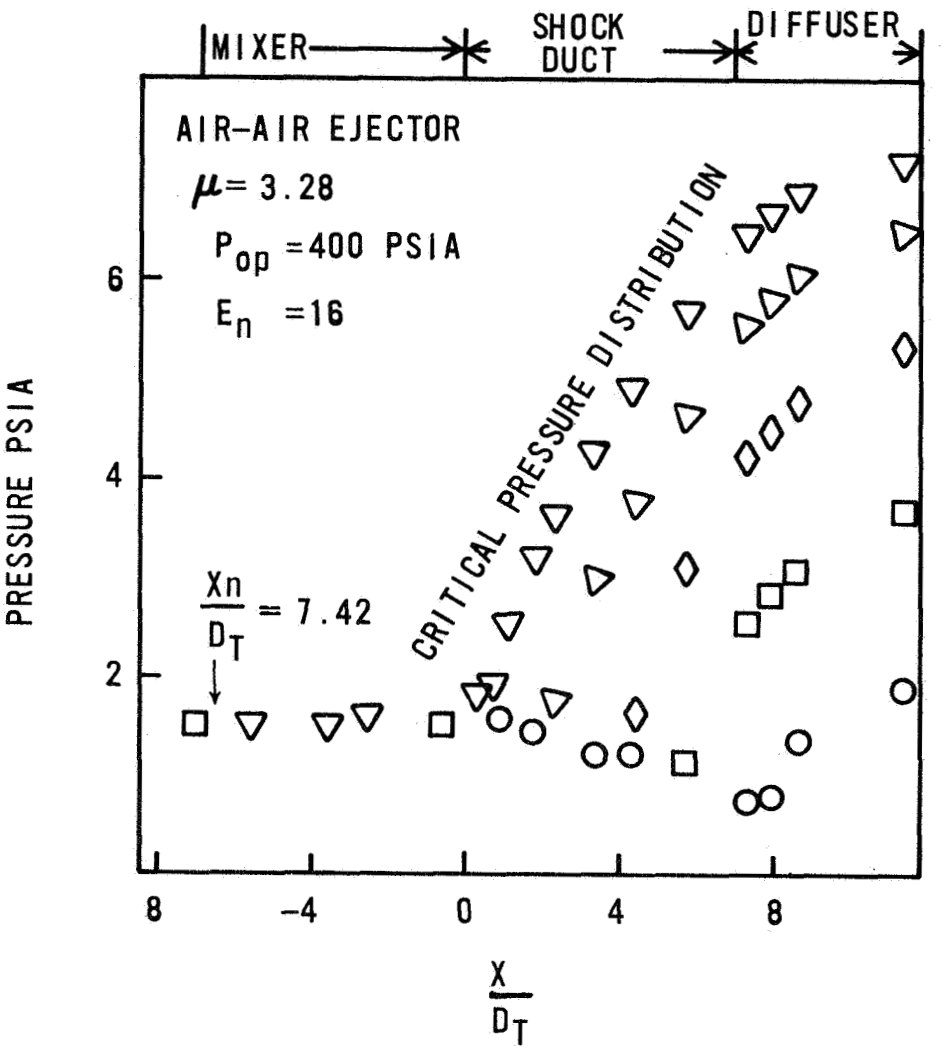

Figure 3.- Ejector axial pressure distributions.

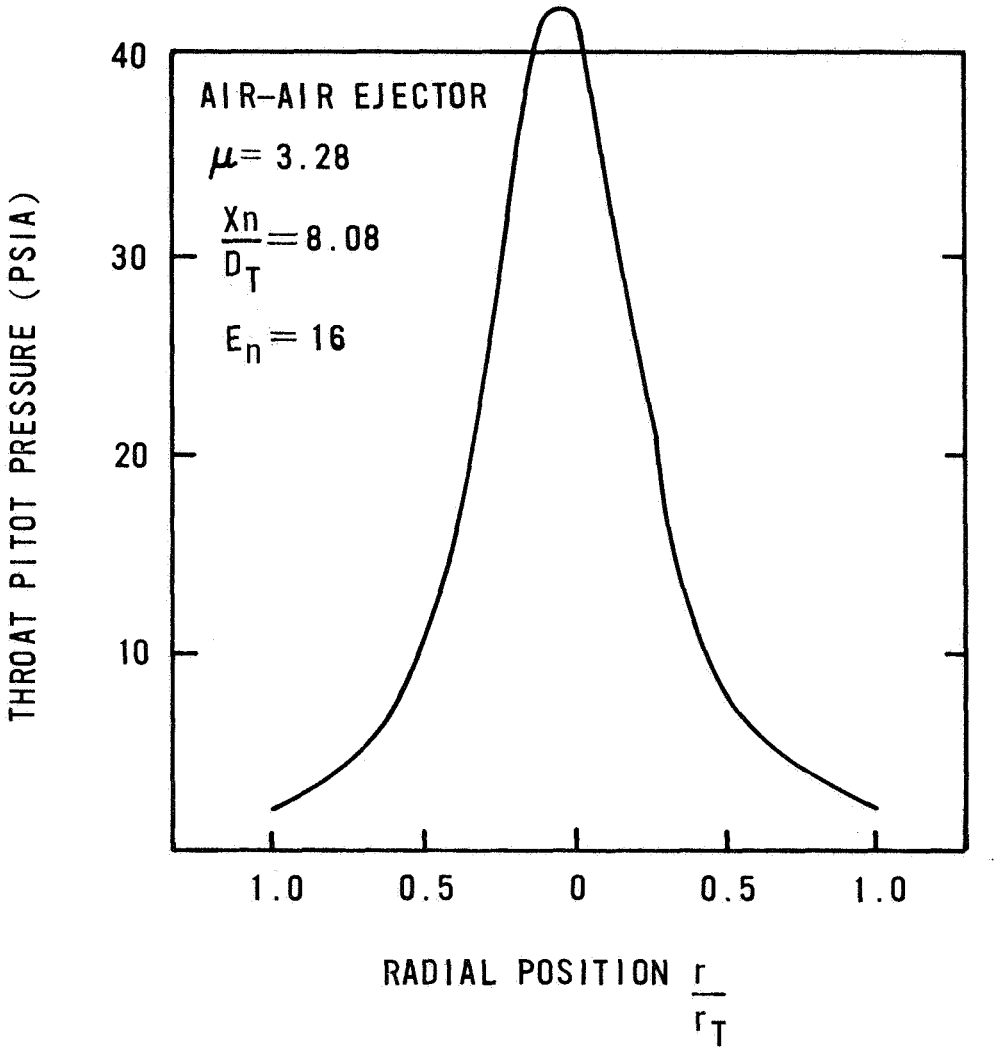

Figure 4.- Ejector throat pitot profile.

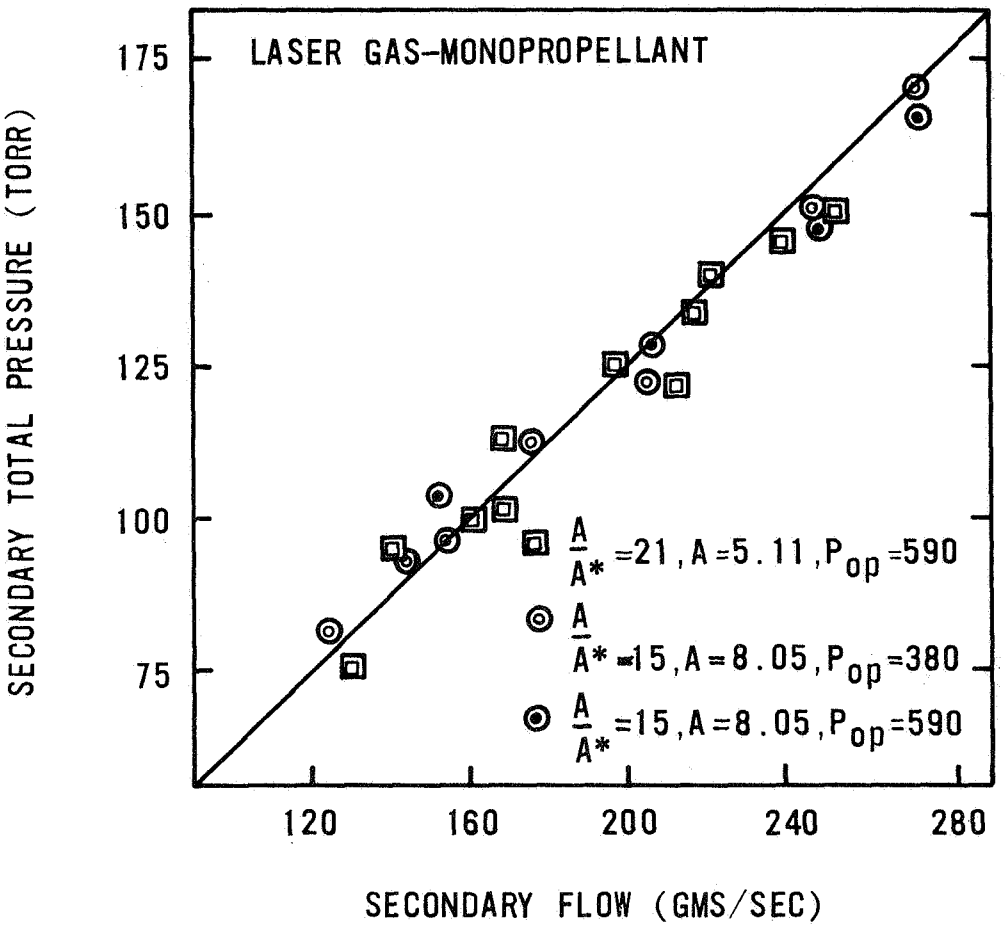

Figure 5.- Ejector suction characteristics.

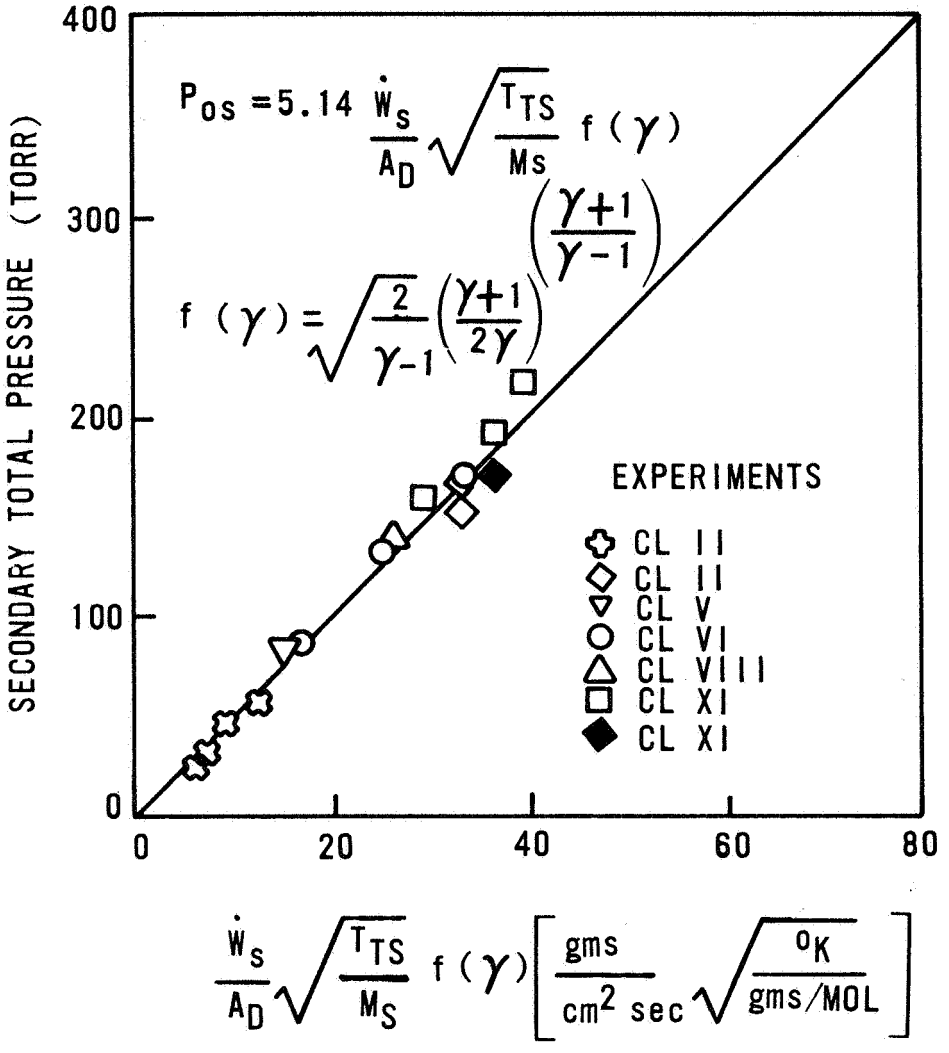

Figure 6.- Diffuser critical pressure recovery.

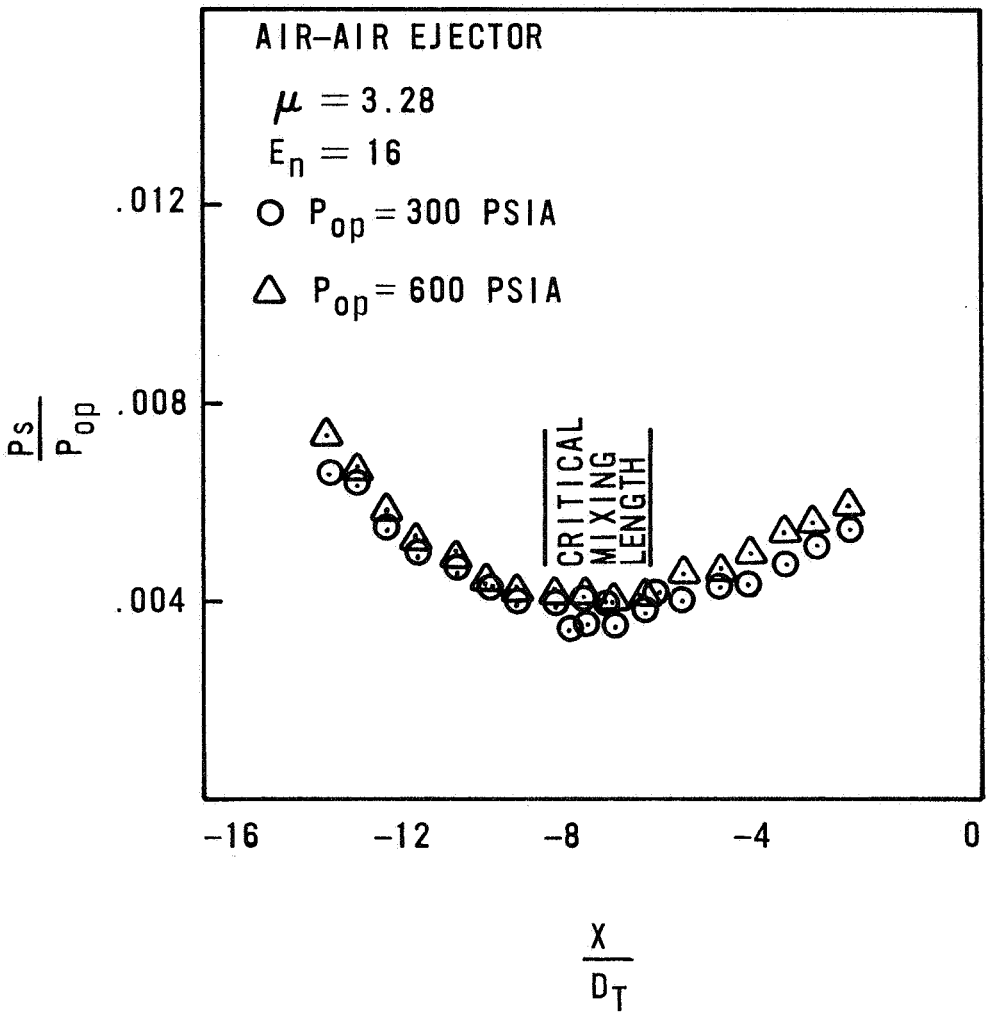

Figure 7.- Effect of mixing length on ejector suction characteristics.

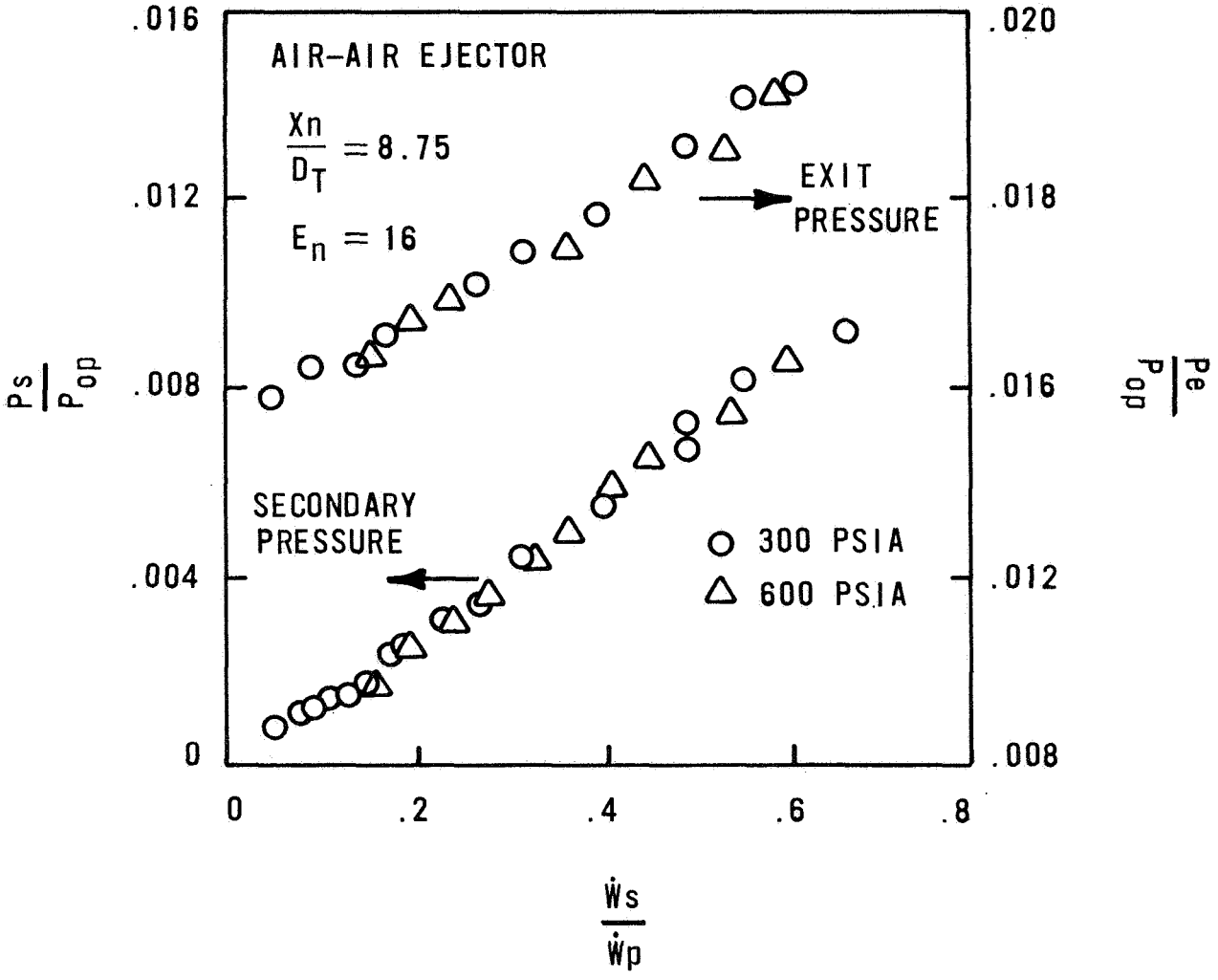

Figure 8.- Effect on secondary flow on ejector performance.

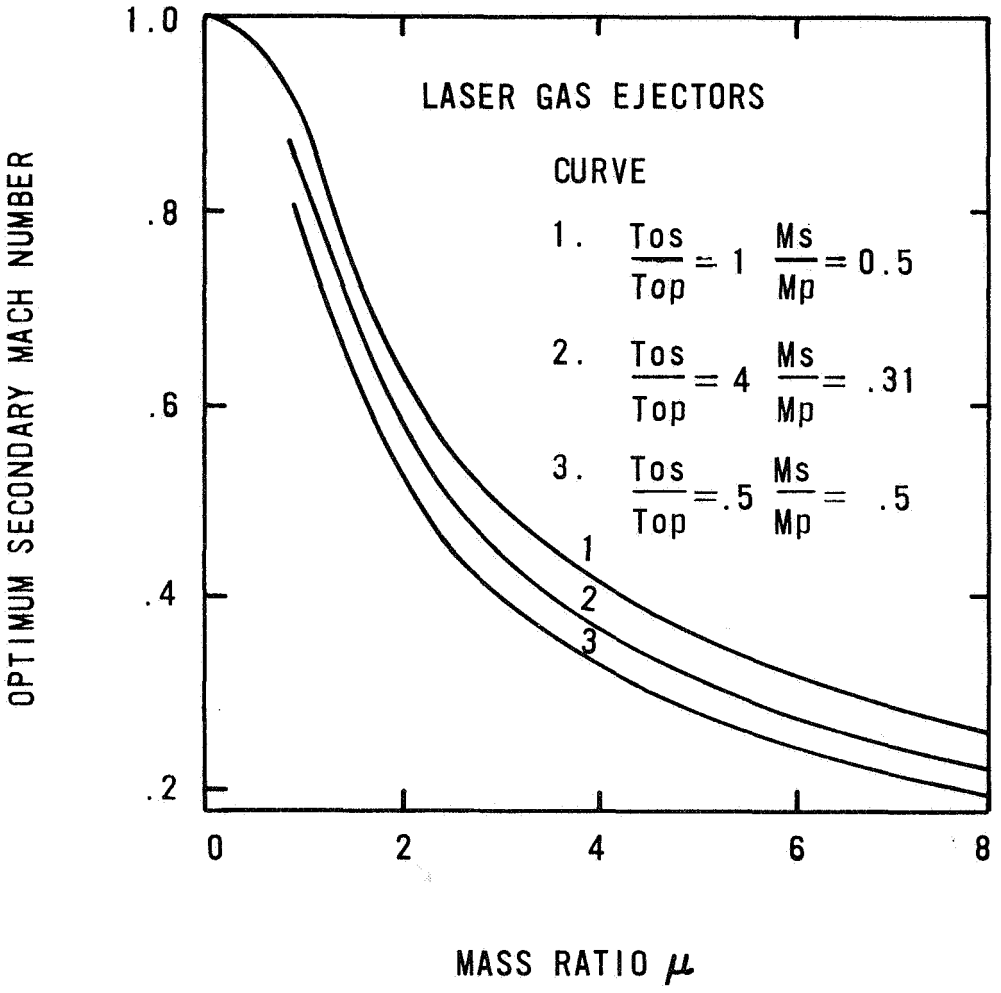

Figure 9.- Effect of mass ratio on optimum secondary Mach number.

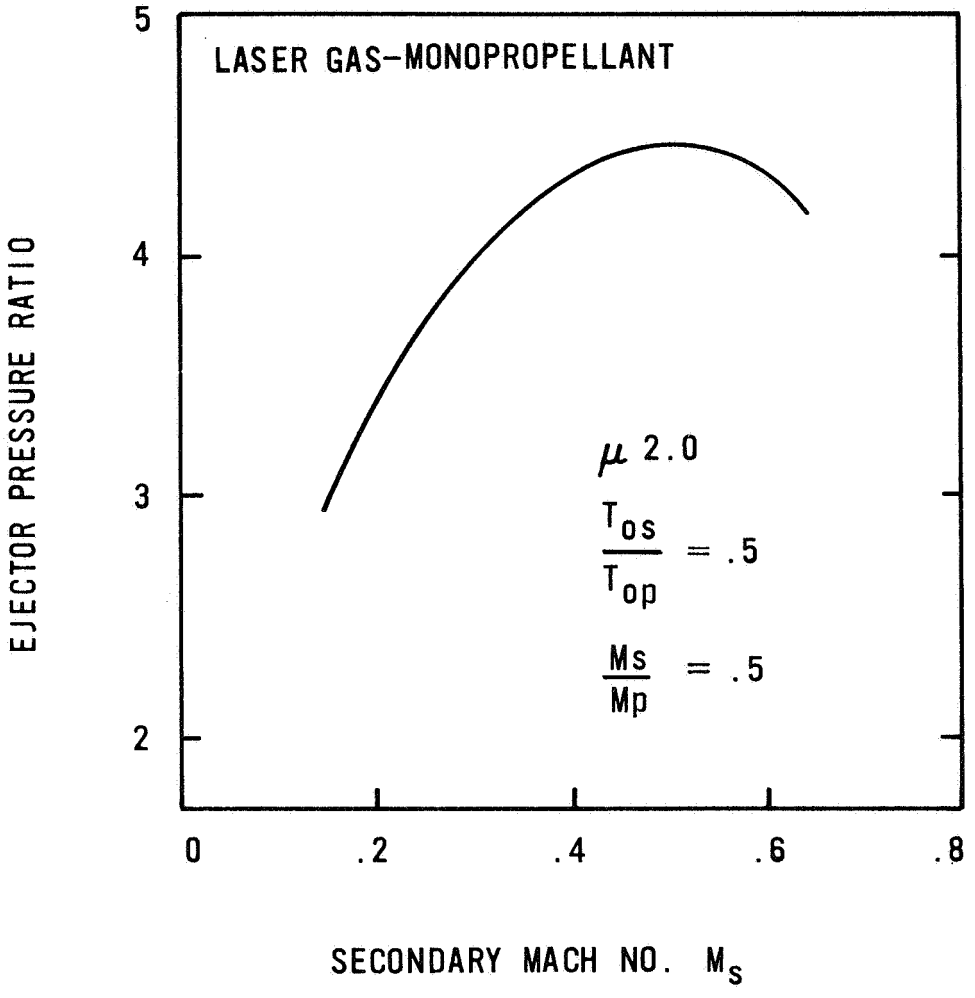

Figure 10.- Effect of optimization on ejector performance.

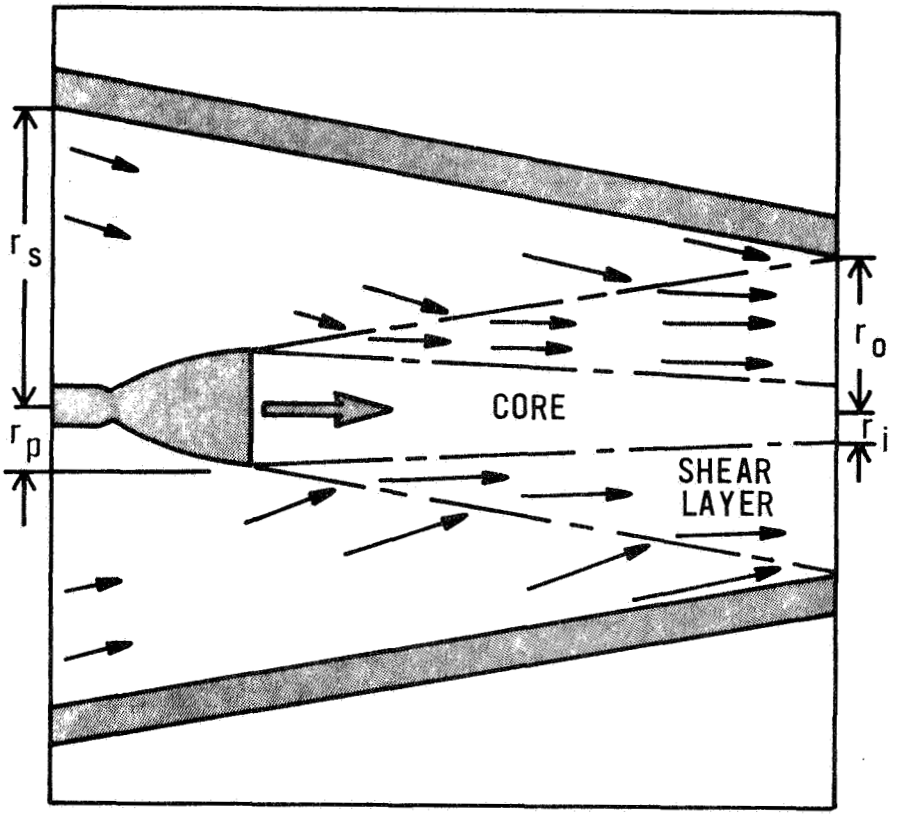

Figure 11.- Flow condition for computing throat area.

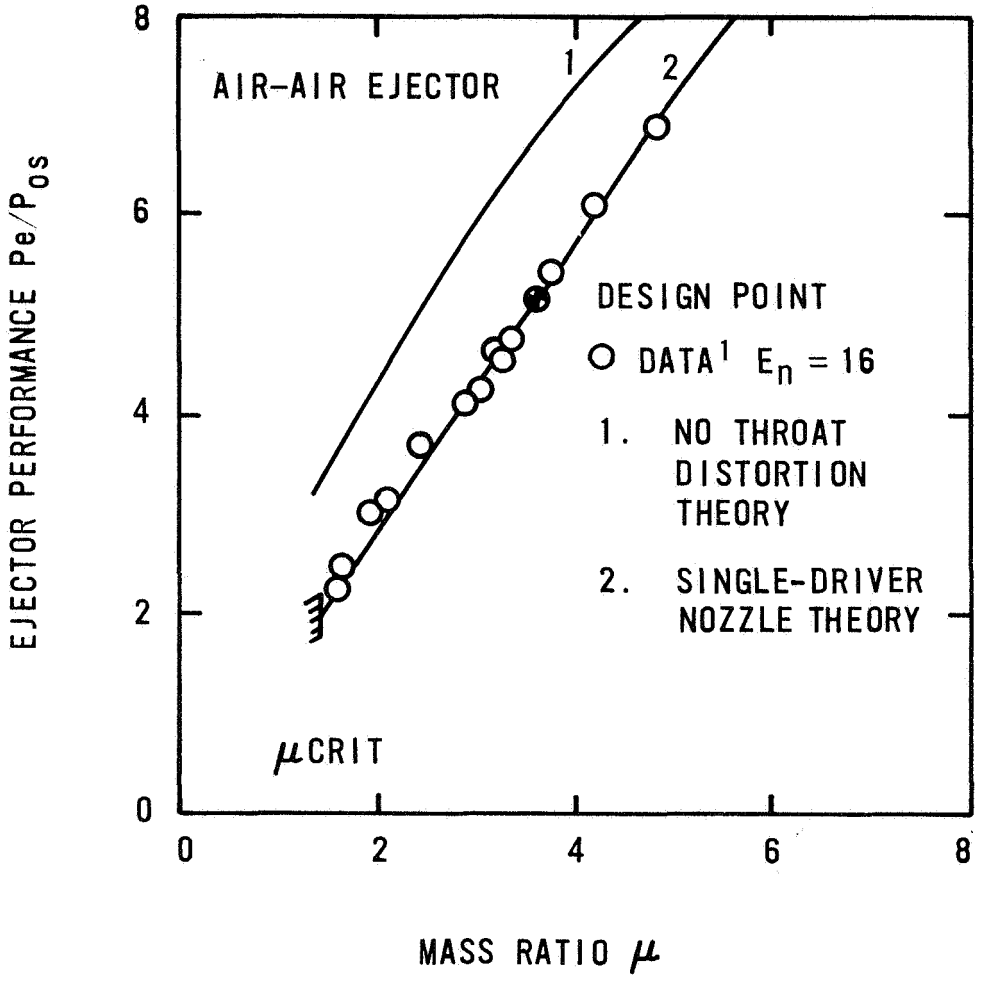

Figure 12.- Off-design ejector performance.

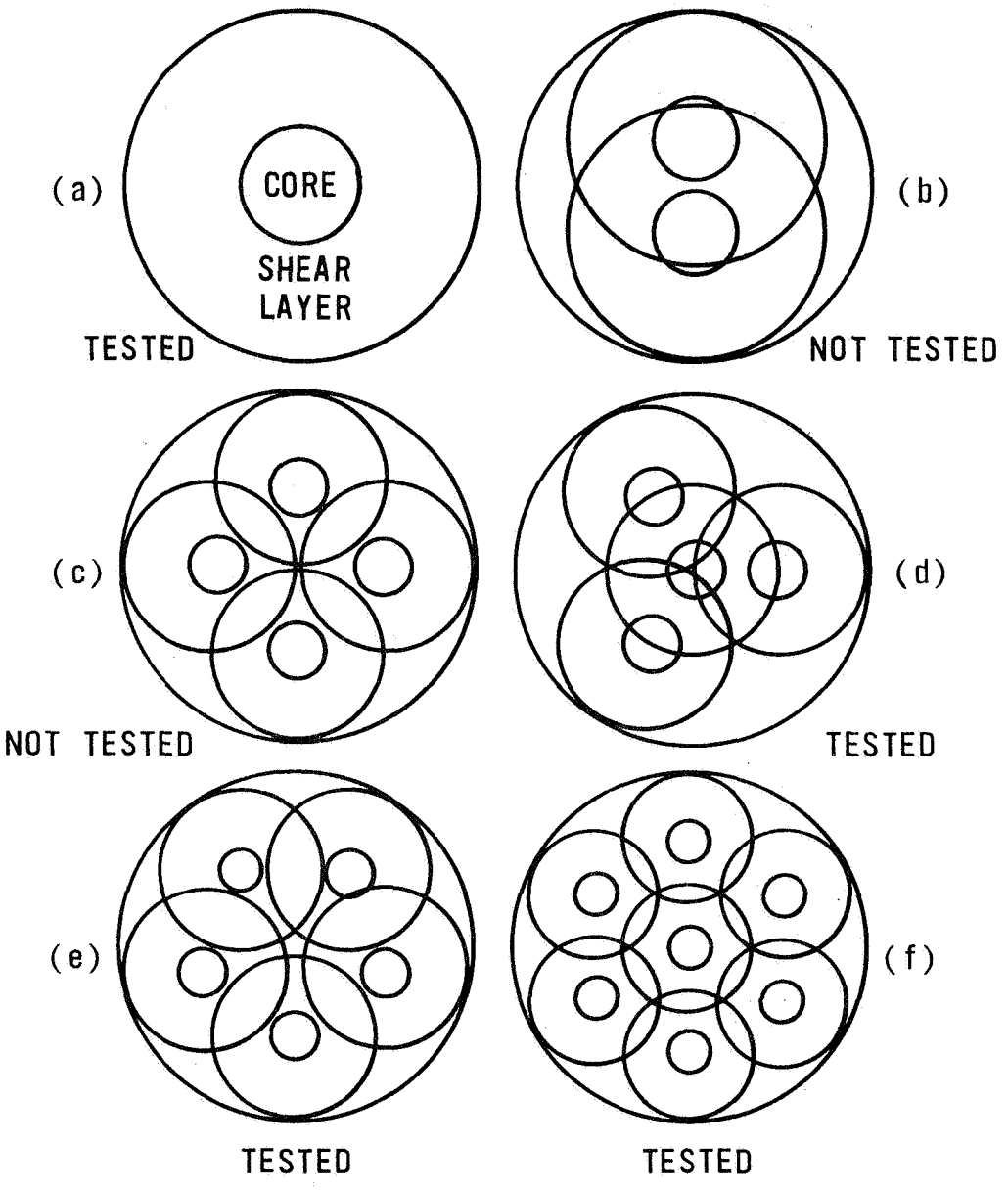

Figure 13.- Multiple-nozzle mixing zone interference.

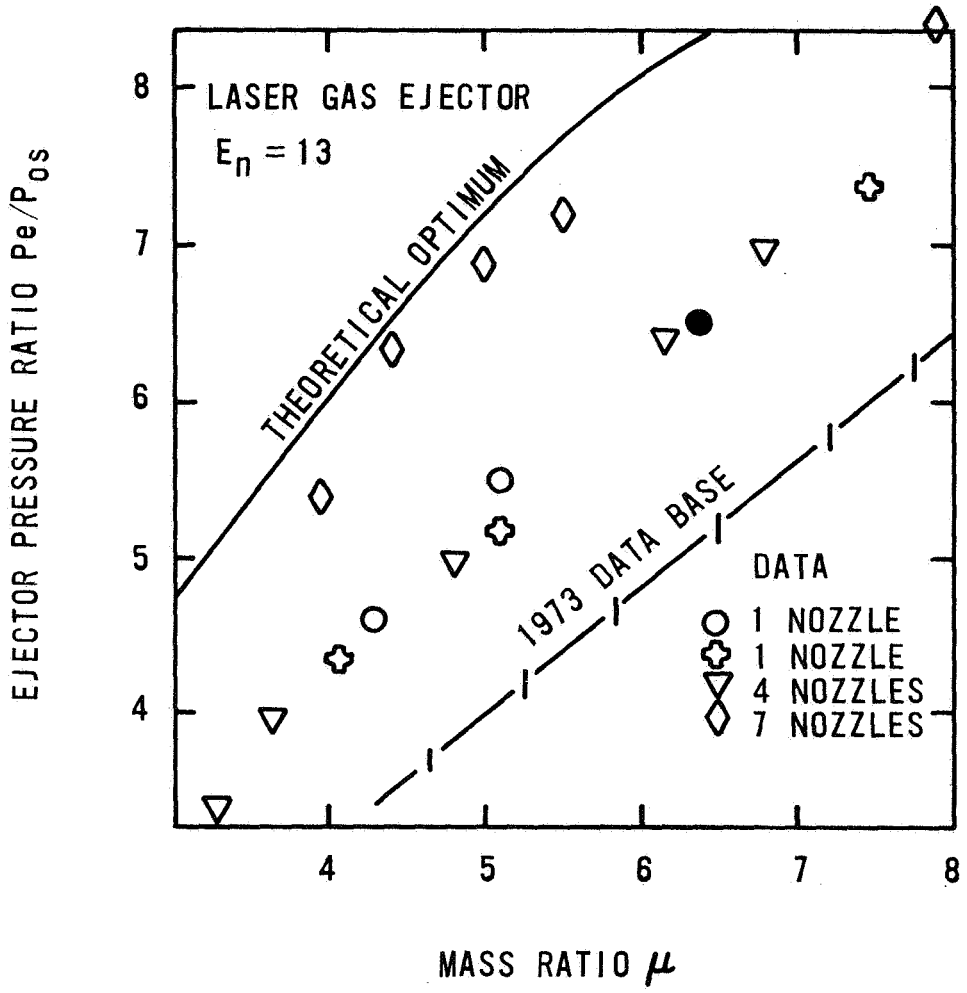

Figure 14.- Effect of number of driver nozzles on ejector performance.

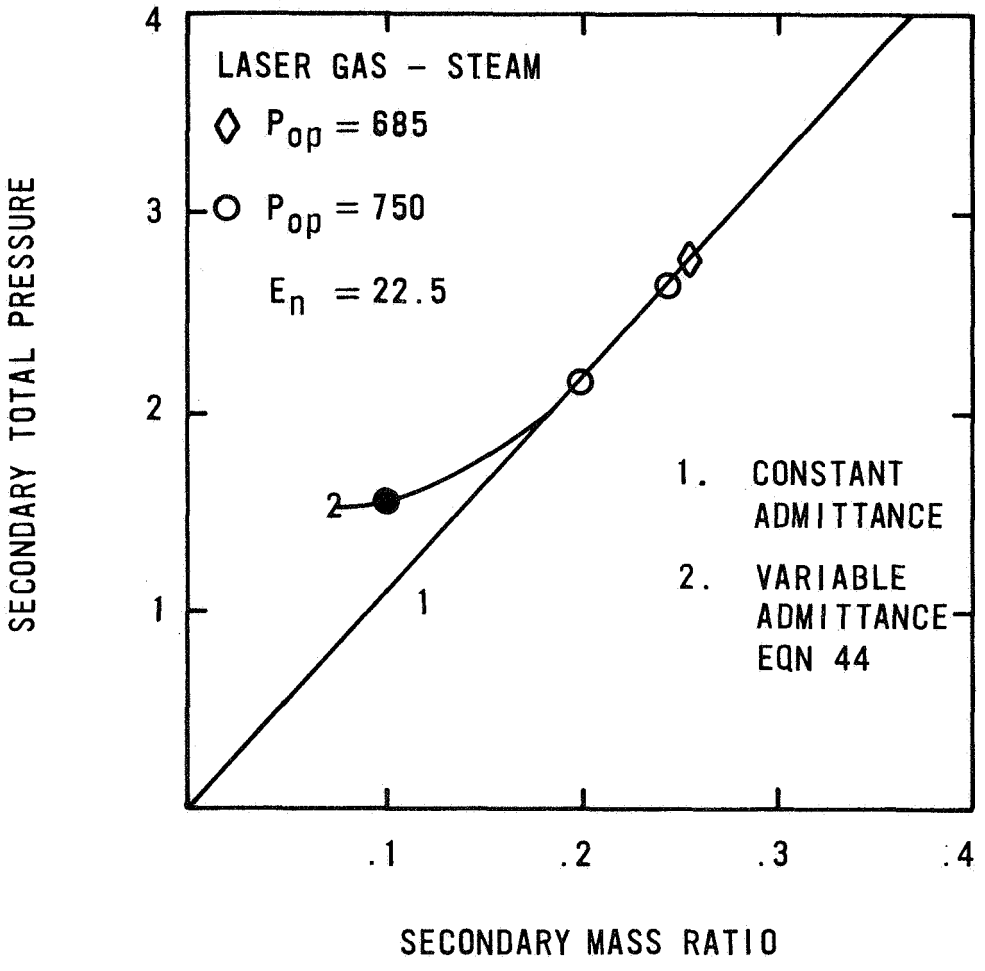

Figure 15.- Suction characteristics of multiple-driver nozzles.

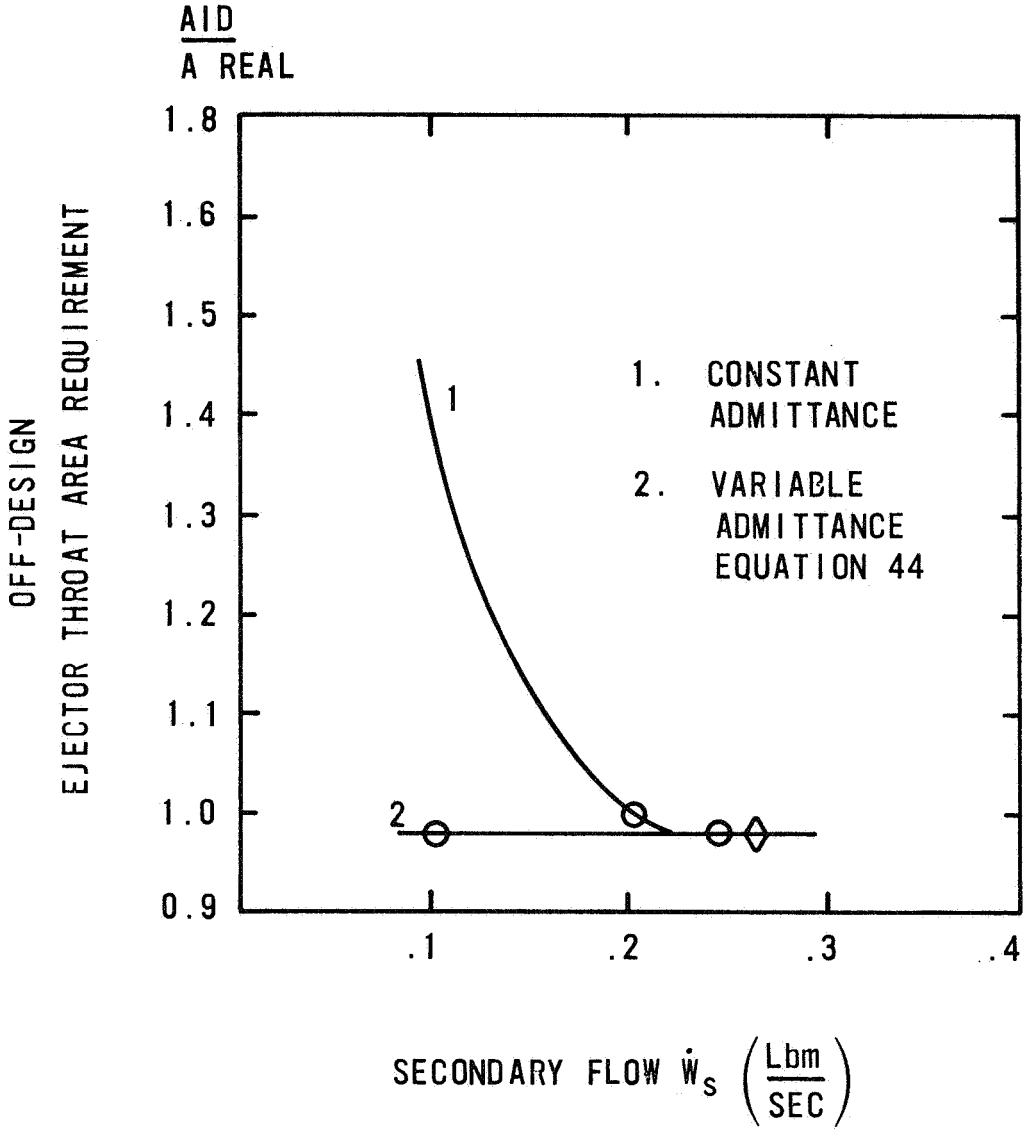

Figure 16.- Ejector area requirements.

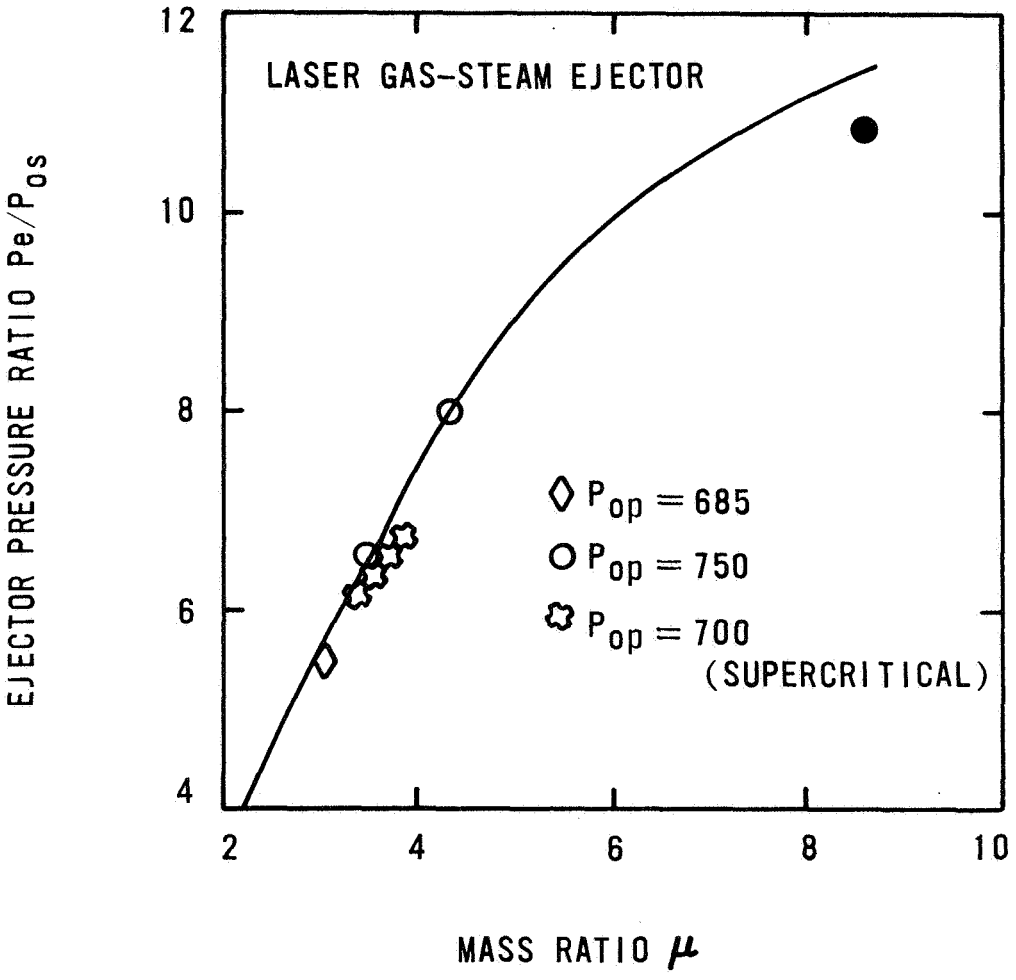

Figure 17.- Performance of multiple-driver nozzle ejector.

A COMPUTATIONAL MODEL FOR THREE-DIMENSIONAL INCOMPRESSIBLE WALL JETS WITH LARGE CROSS FLOW*

W.D. Murphy, V. Shankar, and N.D. Malmuth
Science Center
Rockwell International
Thousand Oaks, California 91360

SUMMARY

The flow field of three-dimensional incompressible wall jets prototypic of thrust augmenting ejectors with large cross flow is solved using a very efficient centered-Euler scheme in an orthogonal curvilinear coordinate system. The computational model treats initial conditions with arbitrary velocity profiles at the jet exit. An averaging approach is employed for the first few marching steps to overcome spurious numerical oscillations associated with arbitrary initial profiles. Laminar as well as turbulent wall jets are simulated. Turbulence is introduced using a two layer mixing length model appropriate to curved three-dimensional wall jets. Typical results quantifying jet spreading, jet growth, nominal separation and jet shrink effects due to cross flow are presented.

*This work was sponsored by the Naval Air Development Center under Contract N62269-77-C-0412. The monitor for this effort was Dr. Kenneth Green.

INTRODUCTION

Modern naval aircraft can reduce strike force vulnerability by the attainment of vertical lift-off capability. To achieve accelerations associated with typical payloads, a high augmentation ratio ϕ is required. Various propulsive lift concepts have been advanced toward obtaining this goal. In the XFV-12A, an ejector system composed of a centerbody and two Coanda wall jets is currently under development. A central feature of the flow fields produced by this device is three dimensionality. This has been particularly evident in subscale flow visualization on the Coanda surfaces. It is believed that these flow processes may be important toward ϕ maximization. One way of understanding this relationship is through theoretical modeling which can provide a means of reducing the high cost of powered lift testing. Unfortunately, existing methodology has been limited in the past to two-dimensional flows for the analysis of wall jets and complete ejector systems. Analytical methods and computational algorithms are therefore necessary to compute three-dimensional flows typical of reality.

To shed light on typical flow patterns encountered, due to the effect of taper and sweep on augmenter wings as well as upper-surface-blown configurations, a study, "Three-Dimensional Flow of a Wall Jet," was initiated by the Naval Air Development Center to investigate wall jet flows which exemplify typical features of more complex propulsive lift applications. The purpose of this study has been to apply modern computational methods to the treatment of wall jet flows with three dimensionality.

The formulation employs boundary-layer equations in an orthogonal curvilinear coordinate system. It can be shown from a systematic order of magnitude analysis that the boundary-layer equations also apply for wall jets, providing the distance from the jet exit is sufficiently large to establish complete mixing, the jet height is small compared to a characteristic radius of curvature, and the Reynolds number based on the exit height is large. A transformation is incorporated

to stretch the coordinate normal to the flow. At streamwise planes, the resulting nonlinear partial differential equations are treated as ordinary differential equations. These are solved using a very efficient two-point boundary value finite-difference method devised by Keller and Cebeci[1-3] known as "box method." The turbulence is introduced using a two-layer mixing length model appropriate to three-dimensional wall jets.

Equations in Curvilinear System

The governing equations for three-dimensional incompressible flows over a wall jet in a curvilinear orthogonal coordinate system shown in Figure 1 are given by the following equations:

Continuity

$$(\partial/\partial x)(h_2 u) + (\partial/\partial z)(h_1 w) + (\partial/\partial y)(h_1 h_2 v) = 0 \tag{1}$$

x-Momentum

$$\frac{u}{h_1}\frac{\partial u}{\partial x} + \frac{w}{h_2}\frac{\partial u}{\partial z} + v\frac{\partial u}{\partial y} - uwK_1 + w^2K_2 = -\frac{1}{\rho h_1}\frac{\partial p}{\partial x} + \frac{\partial}{\partial y}\left(\nu\frac{\partial u}{\partial y} - \overline{u'v'}\right) \tag{2}$$

z-Momentum

$$\frac{u}{h_1}\frac{\partial w}{\partial x} + \frac{w}{h_2}\frac{\partial w}{\partial z} + v\frac{\partial w}{\partial y} - uwK_2 + u^2K_1 = -\frac{1}{\rho h_2}\frac{\partial p}{\partial z} + \frac{\partial}{\partial y}\left(\nu\frac{\partial w}{\partial y} - \overline{w'v'}\right) \tag{3}$$

Here h_1 and h_2 are metric coefficients and are functions of x and z, and the parameters K_1 and K_2 are known as the geodesic curvatures of the curves z = const. and x = const., respectively.

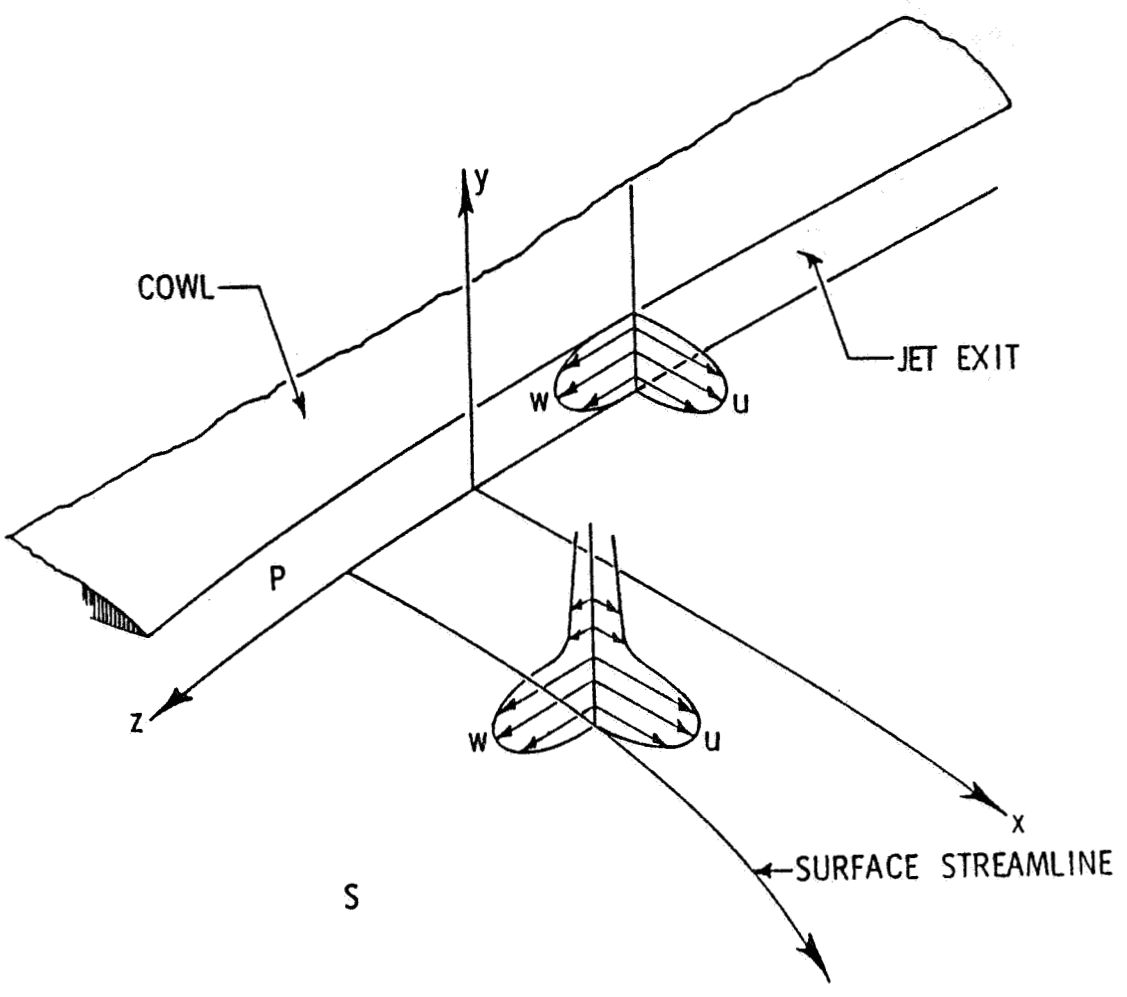

Figure 1.- Physical system and flow schematic.

The boundary conditions for Eqs. (1) through (3) for zero mass transfer are

$$y = 0 \qquad u,w,v = 0$$

$$y \to \infty \qquad u \to u_e(x,z) \qquad w \to w_e(x,z) \tag{4}$$

As indicated earlier, the previous equations are transformed by defining

$$x = x \qquad z = z \qquad \eta = (u_e/\nu s_1)^{\frac{1}{2}} y \tag{5}$$

and introducing a two-component vector potential given by

$$h_2 u = \frac{\partial \psi}{\partial y} \qquad h_1 w = \frac{\partial \phi}{\partial y} \qquad h_1 h_2 v = -\left(\frac{\partial \psi}{\partial x} + \frac{\partial \phi}{\partial z}\right) \tag{6}$$

In addition, the dimensionless variables f and g related to ψ and ϕ are defined by

$$\psi = (u_e \nu s_1)^{\frac{1}{2}} h_2 f(x,z,\eta) \tag{7a}$$

$$\phi = (u_e \nu s_1)^{\frac{1}{2}} h_1 (w_e/u_e) g(x,z,\eta) \tag{7b}$$

Here s_1, which denotes the arc length along the x coordinate, is defined by

$$s_1 = \int_0^x h_1 dx \tag{8}$$

The parameters K_1 and K_2 in Eq. (2) are defined by

$$K_1 = -\frac{1}{h_1 h_2}\frac{dh_1}{dz} \qquad \text{and} \qquad K_2 = -\frac{1}{h_1 h_2}\frac{dh_2}{dx}$$

With the concept of eddy viscosity and with the previous transformed variables, it can be shown that the system of Eqs. (1) through (4) can be written as

x-Momentum Equation

$$(bf'')' + P_1 ff'' + P_2[1 - (f')^2] + P_5[1 - f'g']$$

$$+ P_6 f''g + P_8[1 - (g')^2]$$

$$= xP_{10}\left[f'\frac{\partial f'}{\partial x} - f''\frac{\partial f}{\partial x} + P_7\left(g'\frac{\partial f}{\partial z} - f''\frac{\partial g}{\partial z}\right)\right] \tag{9}$$

z-Momentum Equation

$$(bg'') + P_1 fg'' + P_4(1 - f'g') + P_3[1 - (g')^2]$$

$$+ P_6 gg'' + P_9[1 - (f')^2]$$

$$= xP_{10}\left[f'\frac{\partial g'}{\partial x} - g''\frac{\partial f}{\partial x} + P_7\left(g'\frac{\partial g'}{\partial z} - g''\frac{\partial g}{\partial z}\right)\right] \tag{10}$$

$$\eta = 0 \qquad f = g = f' = g' = 0 \tag{11a}$$

$$\eta = \eta_\infty \qquad f' = g' = 1 \tag{11b}$$

Here the primes denote differentiation with respect to , and

$$b = 1+\epsilon^{+} \qquad \epsilon^{+} = \epsilon/\nu \qquad f' = u/u_e \qquad g' = w/w_e \tag{12a}$$

The coefficients P_1 to P_{10} are functions of u_e, w_e, h_1, h_2, K_1, and K_2 and are given by the following formulas:

$$P_1 = (M+1)/2 - s_1K_2 \qquad P_2 = M \qquad P_3 = R$$

$$P_4 = \left(\frac{u_e}{w_e}\right)Q - s_1K_2 \qquad P_5 = \frac{w_e}{u_e}\,(N - s_1K_1)$$

$$P_6 = R + \frac{w_e}{2u_e}\left(\frac{1}{h_1}\frac{\partial s_1}{\partial z} - N\right) - \left(\frac{w_e}{u_e}\right)s_1K_1$$

$$P_7 = \frac{h_1}{h_2}\frac{w_e}{u_e} \qquad P_8 = \left(\frac{w_e}{u_e}\right)^2 s_1K_2$$

$$P_9 = \left(\frac{u_e}{w_e}\right)s_1K_1 \qquad P_{10} = \frac{s_1}{xh_1} \tag{12b}$$

$$M = \frac{s_1}{u_eh_1}\frac{\partial u_e}{\partial x} \qquad N = \frac{s_1}{u_eh_2}\frac{\partial u_e}{\partial z}$$

$$Q = \frac{s_1}{u_eh_1}\frac{\partial w_e}{\partial x} \qquad R = \frac{s_1}{u_eh_2}\frac{\partial w_e}{\partial z}$$

In order to solve Eqs. (9) through (11), initial conditions are required at a starting plane. In the case of the boundary-layer problem,

the initial conditions at x = 0 and z = 0 planes are obtained by solving the limiting form of Eqs. (9) and (10). For a wall jet, initial velocity profiles are prescribed at some downstream x plane and along the z = 0 plane, attachment line equations are solved. The attachment line equations are obtained by differentiating the z-momentum equation with respect to z and setting

$$w = \frac{\partial p}{\partial z} = \frac{\partial u}{\partial z} = \frac{\partial v}{\partial z} = \frac{\partial^2 w}{\partial z^2} = 0$$

The resulting attachment line equations valid at the z = 0 plane are

$$(bf'')' + P_1 ff'' + P_2[1 - (f')^2] + P_3 gf'' = xP_{10}\left[f' \frac{\partial f'}{\partial x} - f'' \frac{\partial f}{\partial x}\right] \qquad (13)$$

$$(bg'')' + P_1 fg'' + P_4(1 - f'g') + P_3[1 - (g')^2]$$

$$+ P_3 gg'' = xP_{10}\left[f' \frac{\partial g'}{\partial x} - g'' \frac{\partial f}{\partial x}\right] \qquad (14)$$

Here, g' is defined as w_z/w_{e_z}

Eddy-Viscosity Model

Eqs. (2) and (3) contain Reynolds shear stress terms $-\overline{u'v'}$ and $-\overline{v'w'}$. In order to satisfy the closure assumptions for these shear stress terms, we use the eddy viscosity concept and define

$$-\overline{u'v'} = \varepsilon u_y = \bar{\varepsilon}\left[1 - \frac{C_1 u \kappa_2}{1 + \kappa_2 y} \frac{1}{u_y}\right] u_y$$

$$-\overline{w'v'} = \varepsilon w_y = \bar{\varepsilon}\left[1 - \frac{C_2 w \kappa_1}{1 + \kappa_1 y} \frac{1}{w_y}\right] w_y \qquad (15)$$

The second term inside the bracket in Eq. (15) is due to curvature where κ_1 and κ_2 denote the radius of curvature of z = const. and x = const. lines. The quantity $\bar{\varepsilon}$ is assumed to be same in both the x and z directions and is represented by a two-layer model. Referring to Fig. 2, the structure of these layers is as follows:

First Layer

$$\left.\begin{aligned} &\bar{\varepsilon} = (0.435\ y)^2 \sqrt{u_y^2 + w_y^2} \qquad 0 \leqslant y \leqslant y^* \\ &\text{Second Layer} \\ &\bar{\varepsilon} = (0.125\ y_1)^2 \sqrt{u_y^2 + w_y^2} \qquad y \geqslant y^* \end{aligned}\right\} \tag{16}$$

where at $y = y_1$,

$$\frac{\left|\sqrt{u_e^2 + w_e^2} - \sqrt{u^2 + w^2}\right|}{\sqrt{u_e^2 + w_e^2}} \cong 0.01$$

and y* is obtained by imposing continuity in $\bar{\varepsilon}$ at $y = y^*$. This yields $y^* = \frac{0.125}{0.435}\, y_1$. C_1 and C_2 appearing in Eq. (15) can be assigned values between one and three.

Finite Difference Equations

First, reduce the system (9)-(10) to the first order system

$$f' = u \tag{17}$$

$$u' = v \tag{18}$$

$$g' = w \tag{19}$$

$$w' = t \tag{20}$$

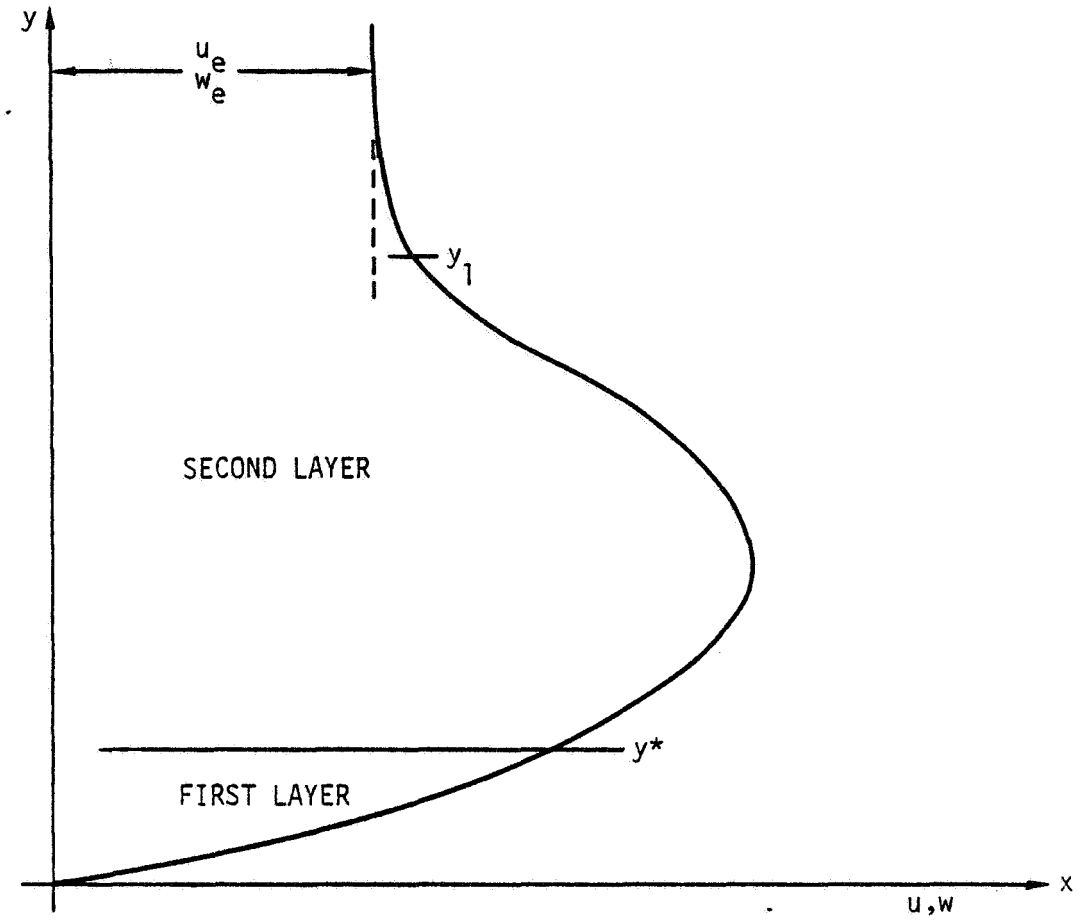

Figure 2.- Two-layer eddy viscosity model.

$$(bv)' + P_1 fv + P_2(1 - u^2) + P_5[1 - uw]$$

$$+ P_6 vg + P_8[1 - w^2] = xP_{10}\left[u\frac{\partial u}{\partial x} - v\frac{\partial f}{\partial x} + P_7\left(w\frac{\partial u}{\partial z} - v\frac{\partial g}{\partial z}\right)\right] \quad (21)$$

$$(bt)' + P_1 ft + P_4(1 - uw) + P_3(1 - w^2) + P_6 gt$$

$$+ P_9(1 - u^2) = xP_{10}\left[u\frac{\partial w}{\partial x} - t\frac{\partial f}{\partial x} + P_7\left(w\frac{\partial w}{\partial z} - t\frac{\partial g}{\partial z}\right)\right] \quad (22)$$

Let

$$x_0 = \text{constant} \qquad x_n = x_{n-1} + k_n \qquad n = 1,2,\ldots,N$$

$$z_0 = 0 \qquad z_i = z_{i-1} + r_i \qquad i = 1,2,\ldots,I$$

$$\eta_0 = 0 \qquad \eta_j = \eta_{j-1} + h_j \qquad j = 1,2,\ldots,J$$

Then, using the box method, we have

$$\frac{f_j^{n,i} - f_{n-1}^{n,i}}{h_j} = u_{j-\frac{1}{2}}^{n,i} \quad (23)$$

$$\frac{u_j^{n,i} - u_{j-1}^{n,i}}{h_j} = v_{j-\frac{1}{2}}^{n,i} \quad (24)$$

$$\frac{g_j^{n,i} - g_{j-1}^{n,i}}{h_j} = w_{j-\frac{1}{2}}^{n,i} \quad (25)$$

$$\frac{w_j^{n,i} - w_{j-1}^{n,i}}{h_j} = t_{j-\frac{1}{2}}^{n,i} \quad (26)$$

We use the notation

$$\overline{P} = P^{n-\frac{1}{2},i-\frac{1}{2}}_{j-\frac{1}{2}} \equiv P^{n-\frac{1}{2}}_{i-\frac{1}{2}}$$

and

$$\overline{v}_j = \frac{1}{4}\left(v_j^{n,i} + v_j^{n,i-1} + v_j^{n-1,i-1} + v_j^{n-1,i}\right)$$

$$\overline{u}_i = \frac{1}{2}\left(u^{n,i}_{j-\frac{1}{2}} + u^{n,i-1}_{j-\frac{1}{2}}\right)$$

$$\overline{u}_n = \frac{1}{2}\left(u^{n,i}_{j-\frac{1}{2}} + u^{n-1,i}_{j-\frac{1}{2}}\right)$$

Equation (21) becomes, with the box centered at $(x_{n-\frac{1}{2}}, z_{i-\frac{1}{2}}, \eta_{j-\frac{1}{2}})$

$$\begin{aligned}
&(\overline{b}_j\overline{v}_j - \overline{b}_{j-1}\overline{v}_{j-1})/h_j \\
&\quad = -\overline{P}_1(\overline{fv})_{j-\frac{1}{2}} - \overline{P}_2(1 - \overline{u}^2_{j-\frac{1}{2}}) - \overline{P}_5(1 - \overline{u}_{j-\frac{1}{2}}\overline{w}_{j-\frac{1}{2}}) \\
&\qquad - \overline{P}_6(\overline{vg})_{j-\frac{1}{2}} - \overline{P}_8(1 - \overline{w}^2_{j-\frac{1}{2}}) \\
&\qquad + x_{n-\frac{1}{2}}\overline{P}_{10}\left\{u_{j-\frac{1}{2}}\frac{(\overline{u}_n - \overline{u}_{n-1})}{k_n} - \overline{v}_{j-\frac{1}{2}}\frac{(\overline{f}_n - \overline{f}_{n-1})}{k_n}\right. \\
&\qquad \left. + \overline{P}_7\left[\overline{w}_{j-\frac{1}{2}}\frac{(\overline{u}_i - \overline{u}_{i-1})}{r_i} - \overline{v}_{j-\frac{1}{2}}\frac{(\overline{g}_i - \overline{g}_{i-1})}{r_i}\right]\right\}
\end{aligned} \tag{27}$$

Equation (22) and the attachment line equations (13)-(14) are discretized similarly. Details of the procedure are given in Ref. 4.

The solution procedures involves the following steps:

(1) Solve the attachment line equations (13)-(14) with boundary conditions (11) at $x = x_1$ and $z = 0$ assuming initial conditions on $x = x_0$.

(2) March in the z-direction along the plane $x = x_1$ and solve equations (17)-(22) with boundary conditions (11) for the unknowns (f,u,v,g,w,t).

(3) Repeat steps (1) and (2) for the next x-plane, $x = x_2$, and so on.

The most efficient way to solve the finite difference equations is to use a pseudo-Newton's relaxation scheme. These equations may be written as a system of nonlinear algebraic equations by writing

$$\underset{\sim}{\Phi}(\underset{\sim}{u}) = 0$$

where

$$\underset{\sim}{u} = (f_j^{n,i},\ u_j^{n,i},\ v_j^{n,i},\ g_j^{n,i},\ w_j^{n,i},\ t_j^{n,i})_{j=0}$$

Then, the relaxed Newton's method becomes

$$\frac{\partial \underset{\sim}{\Phi}^{(\nu-1)}}{\partial \underset{\sim}{u}} \delta \underset{\sim}{u}^{(\nu-1)} = - \underset{\sim}{\Phi}\left(\underset{\sim}{u}^{(\nu-1)}\right) \tag{28a}$$

$$\underset{\sim}{u}^{(\nu)} = \underset{\sim}{u}^{(\nu-1)} + \omega \delta \underset{\sim}{u}^{(\nu-1)} \tag{28b}$$

for $\nu = 1,2,\ldots$

The method is said to have converged when

$$\| \delta \underset{\sim}{u}^{(\nu-1)} \|_{\infty} \leqslant \varepsilon \text{ (a prescribed error tolerance)}$$

We call Eq. (28) a pseudo-Newton's method because we linearize the b terms in equations (21) and (28) by evaluating them at ν-2 before computing the Jacobian matrix, $\partial \underset{\sim}{\Phi} / \partial \underset{\sim}{u}$. Consequently, this algorithm will not be quite quadratically convergent. We, therefore, employ relaxation ($\omega \neq 1$) to accelerate it. Remarkably, underrelaxation ($\omega < 1$) works very well, while overrelaxation ($\omega > 1$) diverges. Values of w of 0.5, 0.6, 0.7, 0.9, and 0.9 all give good results with $\omega = 0.7$ slightly the overall best for some of our computational experiments.

An important feature of Keller's box method is that the Jacobian matrix can be put into block tridiagonal form and very efficient elimination schemes can be employed for solving equation (28a).

Minor Difficulties with the Numerical Algorithm

When starting at $x = x_0 \neq 0$ with supplied velocity profiles, unnatural oscillations developed in the solution. This difficulty was eliminated completely by employing the following "trick." The first 10 mesh points in the x-direction were set at $k_n = 10^{-4}$. For the first five planes in the x-direction and all points in the z-direction in these planes, an average value was used for past points, i.e.,

$$f_j^{n-1,i} = 0.5\left(f_j^{n-1,i} + f_j^{n-2,i}\right) \quad , \quad f_j^{n,i-1} = 0.5\left(f_j^{n,i-1} + f_j^{n,i-2}\right)$$

and

$$f_j^{n-1,i-1} = 0.5\left(f_j^{n-1,i-1} + f_j^{n-2,i-1}\right)$$

Beginning with the sixth x-plane, the averaging was eliminated (the standard algorithm was employed). At the eleventh x-plane a geometric mesh-stretching algorithm of the following form was used:

$$k_n = 1.2k_{n-1} \quad , \quad n = 11,12,13,...$$

No such stretching has been employed in the z-direction, but in the future it may also be required for rapidly changing profiles. It should be noted that our averaging algorithm was required in both the x and z directions to remove all oscillations.

A mesh refinement algorithm is used which adds or deletes points depending on the relative local variation in the truncation error of the difference equations. Roughly 80 grid points in the η-direction and 11 grid points in the z-direction are employed.

Results

Computations were performed on the Berkeley CDC 7600 machine. A typical calculation required about 6 minutes of CPU time. Fig. 3 indicates the external and initial velocity distributions which have been used as a basis for our calculations. The parameter θ was introduced as shown to vary the initial cross flow while keeping the total velocity constant as a rough simulation of a fixed supply of engine mass flow. The velocity profile was selected to have a characteristic fully developed character associated with turbulent wall jet flows. Future aspects of this effort will consider the "eating up" of the potential core which is assumed to occur upstream of the initial station of this analysis. The parameters C_2 and C_3 were chosen to provide slope and value continuity of the profile at $y = y_{max}$. For $y \geqslant y_{max}$ the profile has a half Gaussian character associated with a free jet. For $y \leqslant y_{max}$ the profile has a boundary-layer character. In the examples, the u and w initial profiles were assumed to be identical. Moreover, the θ distribution was selected to be

EXTERNAL VELOCITY

$$u_e = U_0 x^{-n} \cos\theta$$

$$w_e = U_0 x^{-n} \sin\theta$$

$$\theta = C z (z_{tip} - z) \frac{\pi}{2}$$

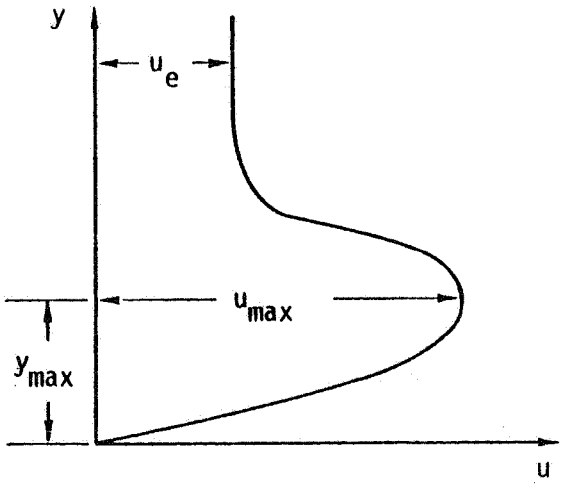

INITIAL PROFILE

$$\frac{u}{u_e} = \begin{cases} C_2 (e^{-y} - 1) + C_3 y & y \leq y_{max} \\ 1 + \left(\frac{u_{max}}{u_e} - 1\right) e^{-0.1(y - y_{max})^2} & y \geq y_{max} \end{cases}$$

$$\frac{w}{w_e} = \text{SAME AS } \frac{u}{u_e} \text{ PROFILE}$$

- SMALL CROSS FLOW IS ACHIEVED BY SETTING C IN θ VERY SMALL (10^{-15})

Figure 3.- Initial and boundary conditions.

qualitatively similar to that observed by rake surveys on the XFV-12A. The zero cross flow case was achieved by setting C to 10^{-15}.

Figure 4 demonstrates decay of the peak velocity with the standardized distributions of Fig. 3, with and without cross flow. It is evident from the figure that cross flow has a dramatic effect on enhancing the decay of the maximum velocity. In the calculations, the exponent n in the external velocities is assumed as ½, roughly in accord with a value obtained from a two-dimensional line sink simulating inflow originally proposed by G.I. Taylor.[5] In a more realistic model, these external velocity distributions should be corrected for three-dimensionality and elliptic interaction with the wall jet. A calculation of this type would be a more accurate representation than the present approach of planform and surface curvature effects. In this connection, we recognize that that means of simulating taper, sweepback, and spanwise pressure gradients in the present analysis is solely through cross flow adjustment.

The three-dimensional inviscid potential ϕ can be characterized by a surface sink distribution of the form (see Fig. 5)

$$\phi(x,y,z) = \frac{1}{4\pi} \iint_S \frac{\sigma(\xi,\zeta)d\xi d\zeta}{\sqrt{(x-\xi)^2 + y^2 + (z-\zeta)^2}} \tag{29}$$

where S the area of integration refers to the total jet area on and off the wing. The quantity σ is the sink strength obtained by matching with an "outer limit" of the second order solution for the velocity normal to the body appearing in the viscous inner wall jet solution. The quantity σ for two-dimensional boundary layers is analogous to the streamwise gradient of the displacement thickness $\delta'(x)$. To include lifting surface effects, a surface doublet or vortex distribution should be added to (29). The local vortex strength can also be determined by matching.

The inflow velocity related to the sink intensity σ in (29) is in turn a function of the entrainment. This quantity is also significant

$$u_e = u_o x^{-1/2} \cos\theta,\ w_e = u_o x^{-1/2} \sin\theta,\ \theta = \frac{\pi}{2} z(z_{tip} - z)$$

STANDARD INITIAL PROFILE ($z = z_1$)

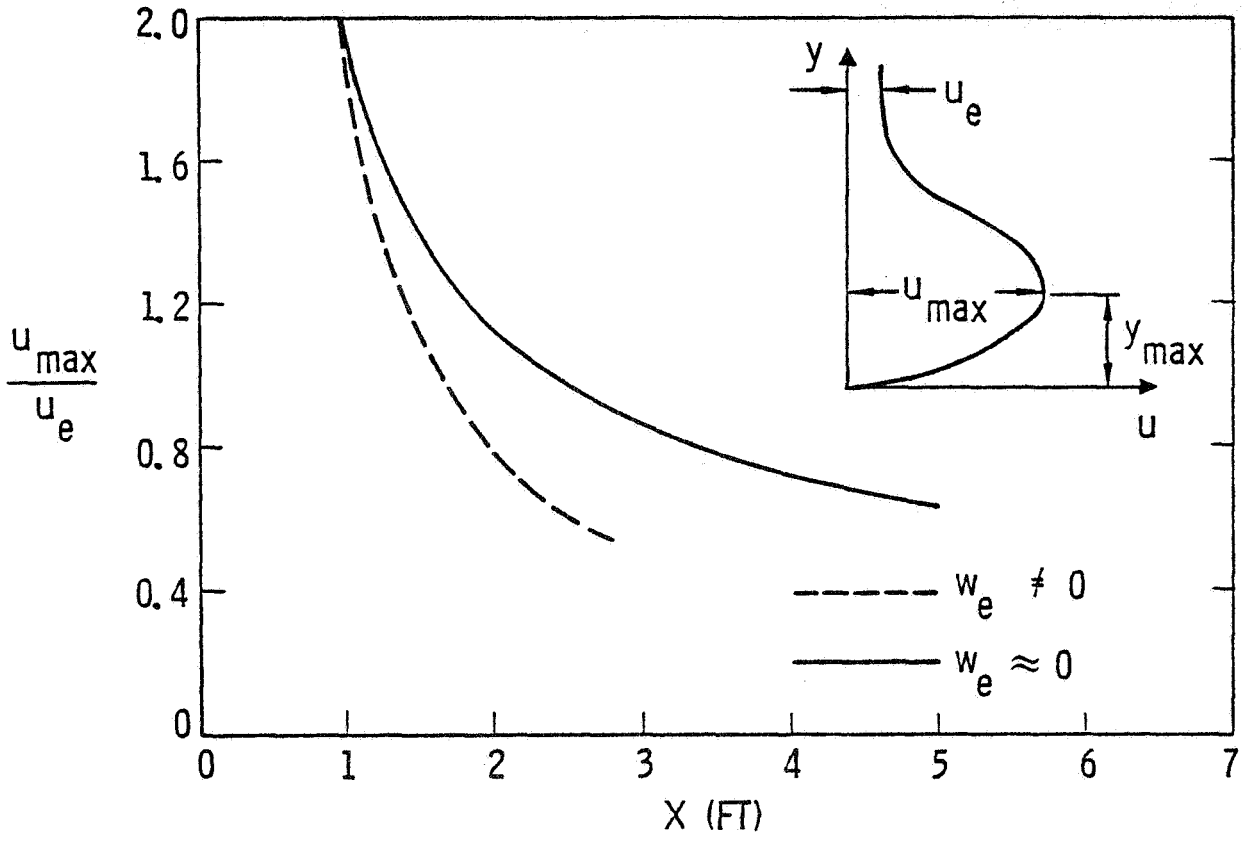

Figure 4.- Effect of cross flow on jet growth.

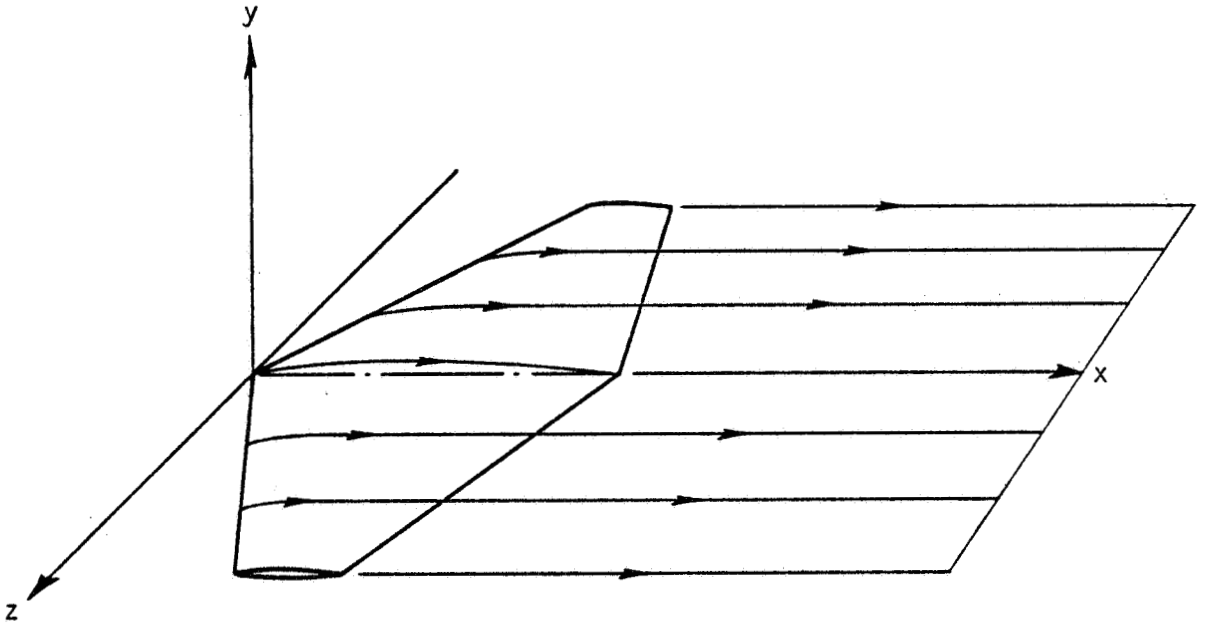

Figure 5.- Tapered thrust augmented wing (TAW).

from the standpoint of the tradeoff between skin friction, BLC, and rapid acceleration of the secondary in compact three-dimensional thrust augmenting ejectors such as those employed on the XFV-12A and upper surface blowing.

In Fig. 6, the comparison between cross flow and the absence of it gives the indicated entrainment variations with streamwise distance. In spite of the appreciable increase in decay of the maximum value of u shown in Fig. 4, and resultant shear stress in Fig. 7, only a slight difference in entrainment quantity and rate is shown in Fig. 6. The difference in maximum velocities which are similar for w, the spanwise component, are presumably related to the enhanced dissipation associated with cross flow and that implied by the eddy viscosity model. The lack of a corresponding decrease in entrainment rate may be due to nonlinear compensating effects built into the turbulence model and cannot be readily explained on an intuitive basis at this time. In this connection, other calculations will be performed for which the streamwise component of the initial velocity is held fixed rather than its overall magnitude on introduction of cross flow. It should be noted that the expression for entrainment Q given in Fig. 6 assumes that w at the tip $z = z_{tip} = 0$. If this is not the case, an additional term must be added to this relation.

Associated with the previous results, Fig. 8 shows the effect of cross flow on jet spreading rate related to y_{max}. As previously, only small differences are indicated for the cases considered. In Fig. 9, however, an important upstream movement of the separation line is indicated with the introduction in cross flow. This result is significant with respect to penalties associated with taper and sweep in three-dimensional ejector diffusors.

In Fig. 10, another important consequence of cross flow is examined in connection with the surface streamline pattern. In the figure, two cases are compared involving differing amounts of cross flow. Significant enhancement in downstream streamtube contraction is obvious with increase in cross flow. This contraction could presumably lead to end wall separation of the type observed on the XFV-12A.

$$u_e = u_o x^{-1/2} \cos\theta, \quad w_e = u_o x^{-1/2} \sin\theta, \quad \theta = C\frac{\pi}{2} z(z_{tip} - z)$$

$$Q = \int_0^{\infty} \int_0^{z_{tip}} u\,dy\,dz$$

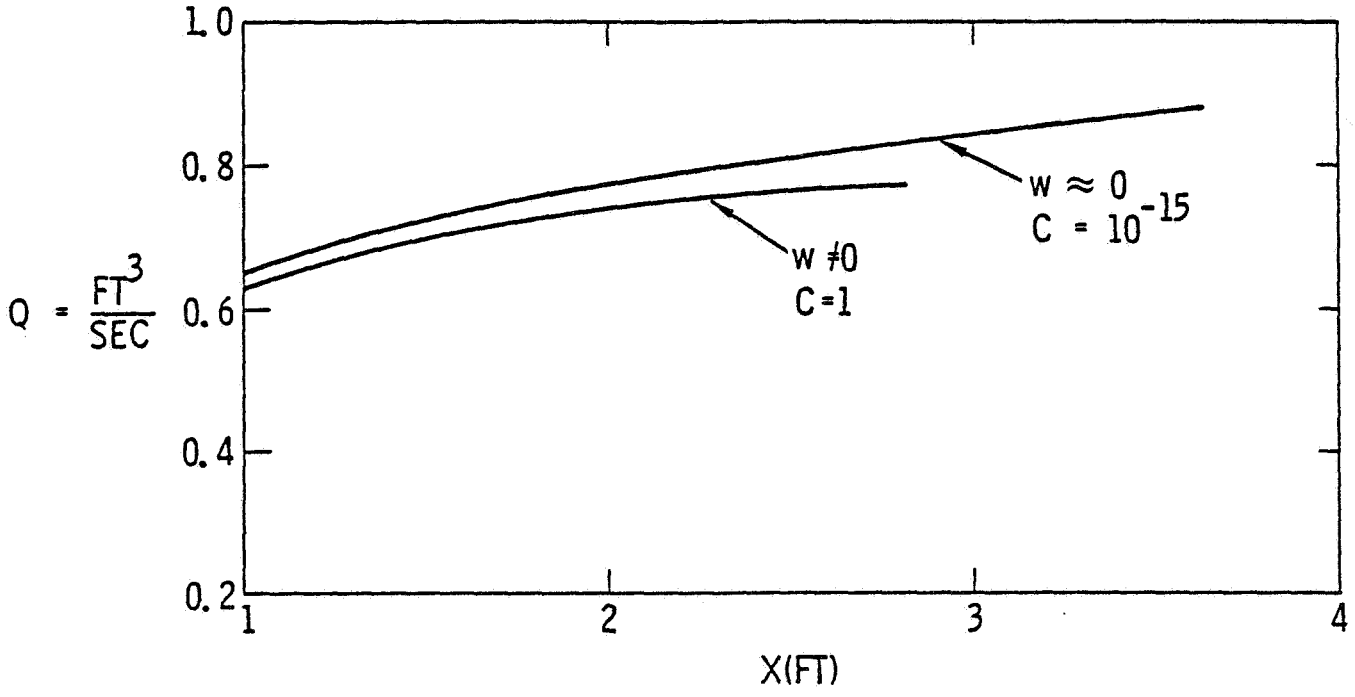

Figure 6.- Effect of cross flow on entrainment.

$$u_e = u_o x^{-1/2} \cos\theta, \quad w_e = u_o x^{-1/2} \sin\theta, \quad \theta = C\frac{\pi}{2} z (z_{tip} - z)$$

STANDARD INITIAL PROFILE ($z = z_1$)

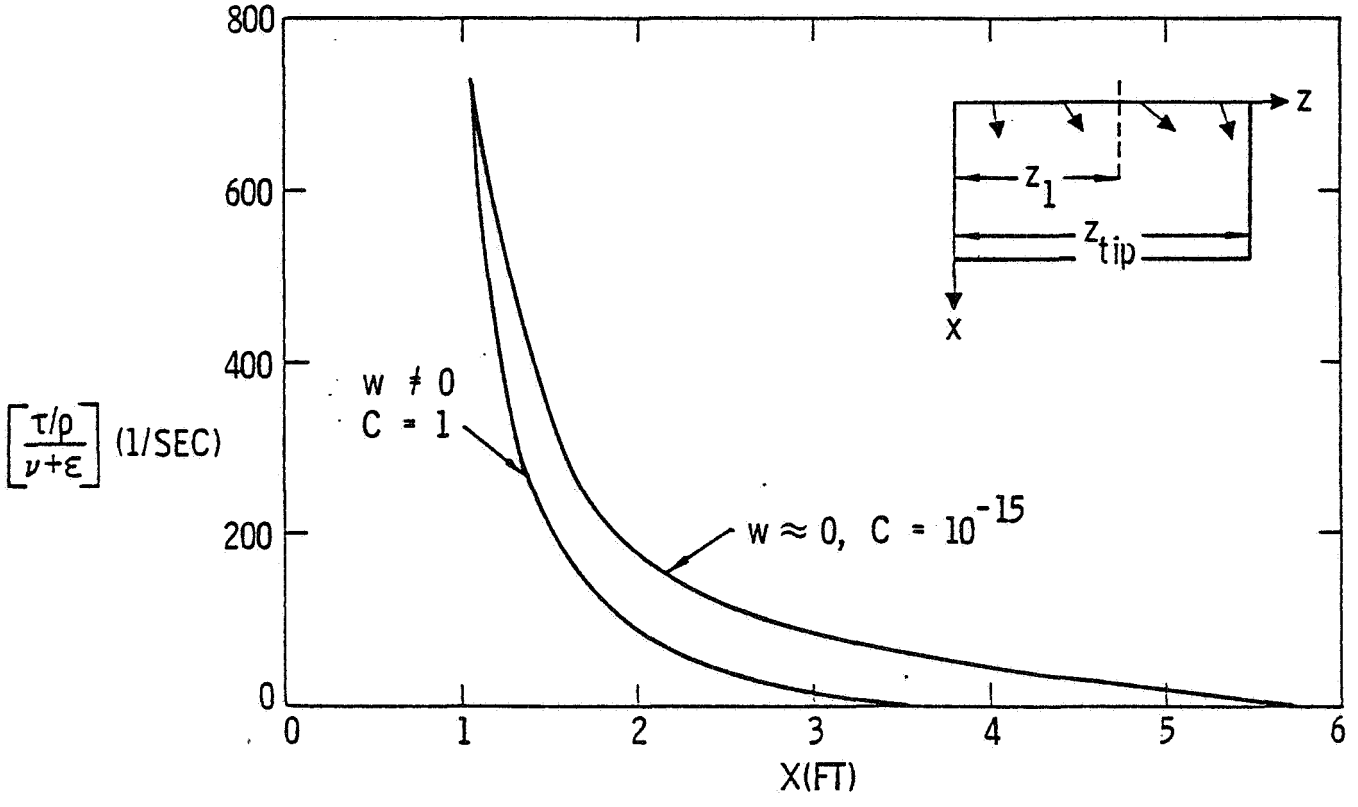

Figure 7.- Effect of cross flow on reduced shear stress.

$$u_e = u_0 x^{-1/2} \cos\theta, \quad w_e = u_0 x^{-1/2} \sin\theta, \quad \theta = C\frac{\pi}{2} z (z_{tip} - z)$$

STANDARD INITIAL PROFILE PLOTTED AT MIDSPAN

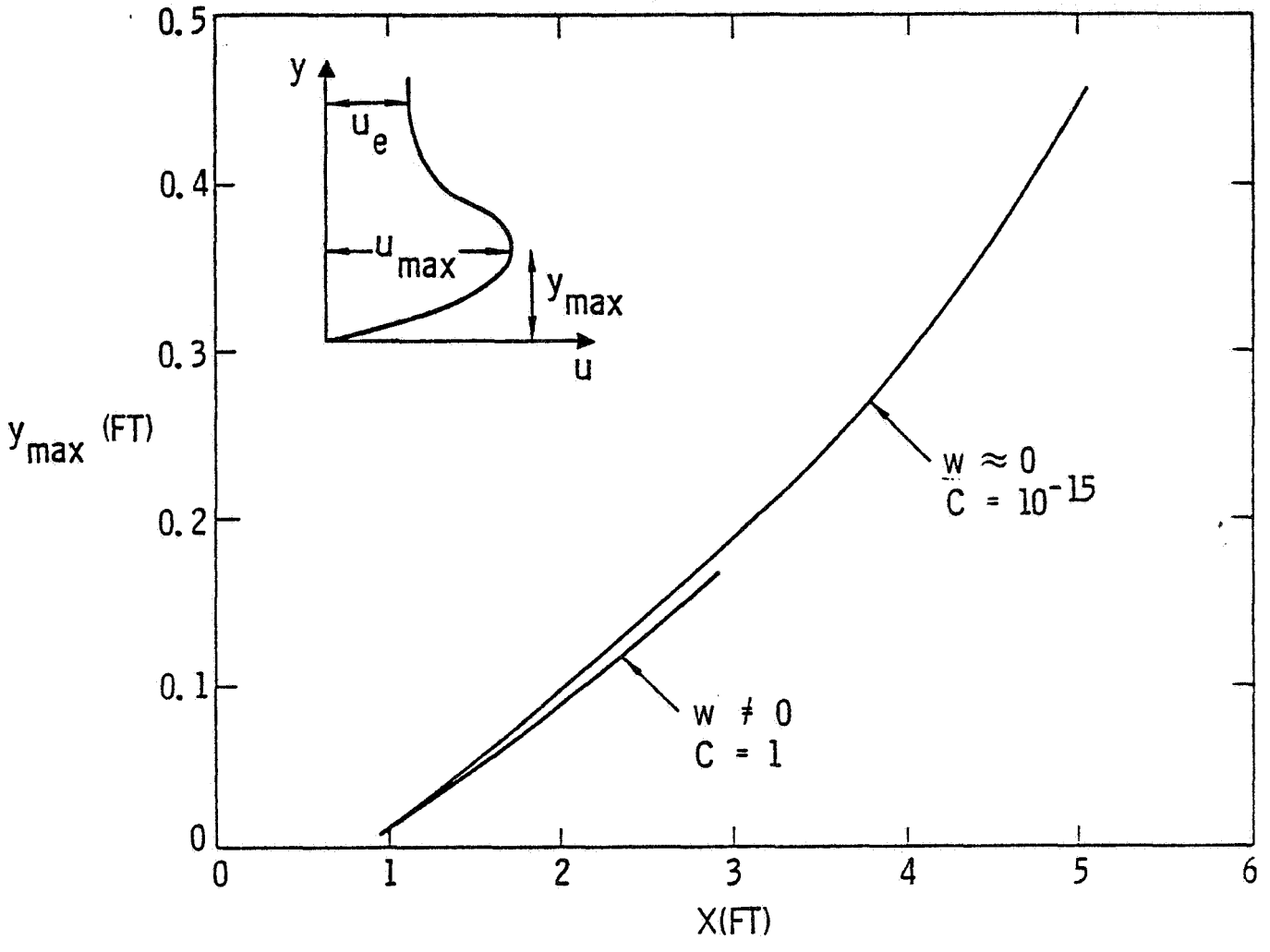

Figure 8.- Effect of cross flow on jet spreading.

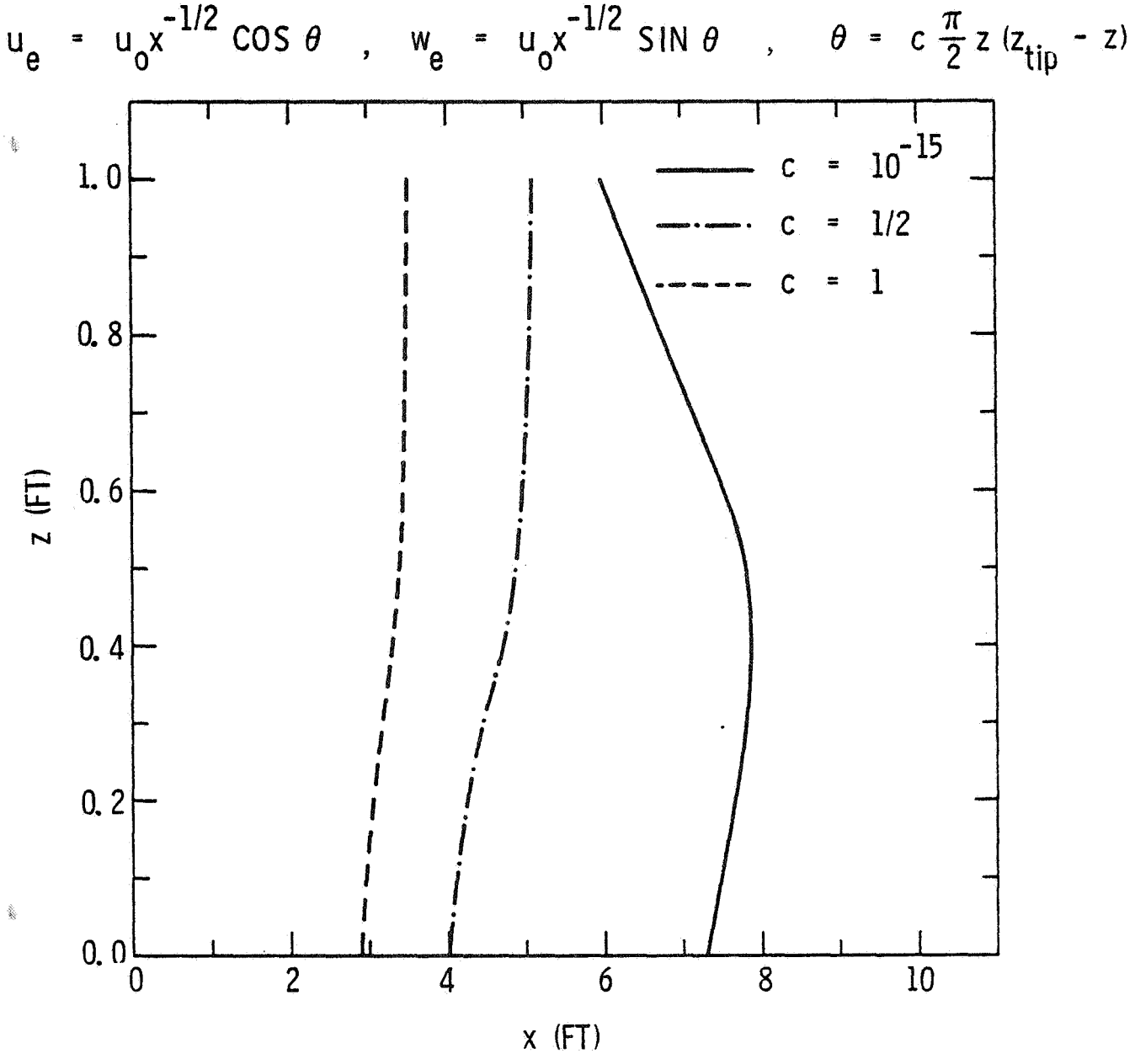

Figure 9.- Effect of cross flow on the locus of nominal separation.

$$u_e = u_o x^{-1/2} \cos\theta \quad , \quad w_e = u_o x^{-1/2} \sin\theta$$

$$\theta = \frac{c\pi}{2} z (z_{tip} - z)$$

$$\theta/2$$

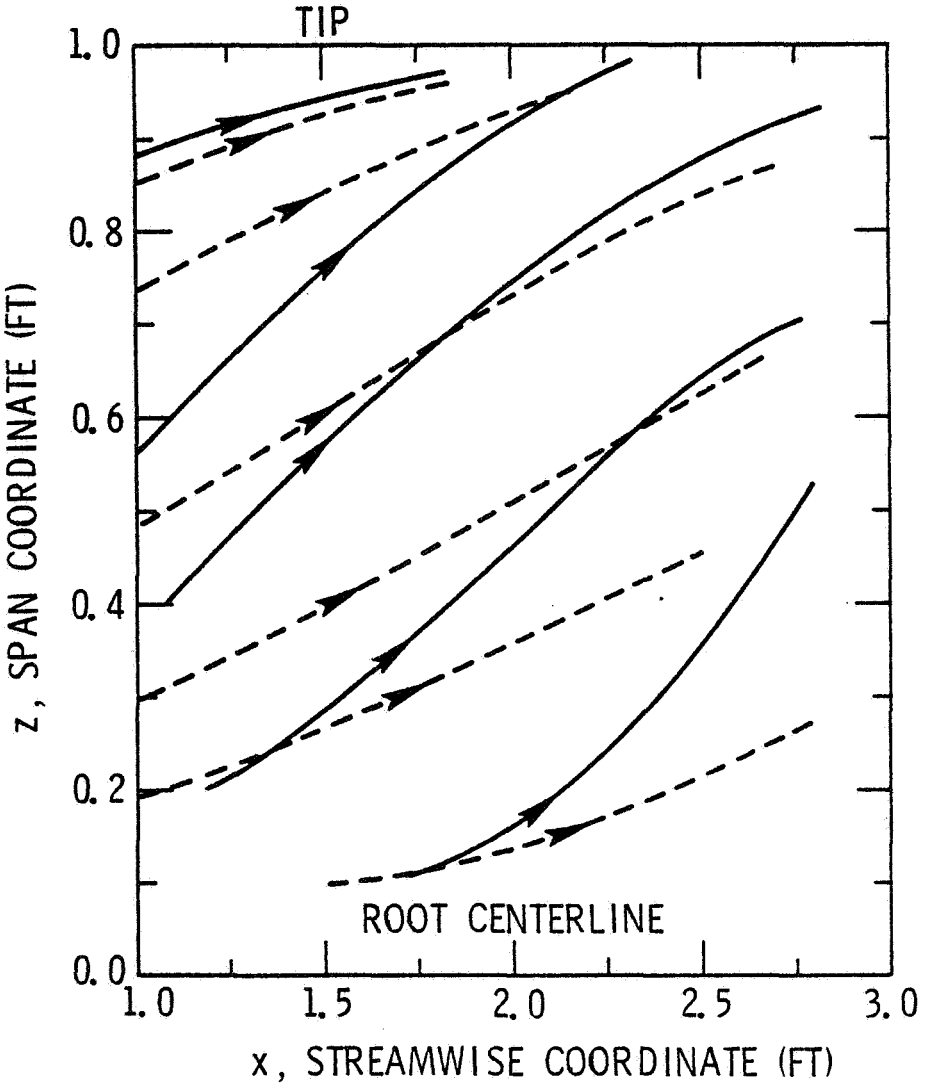

Figure 10.- Cross flow effect on jet "shrink" and "end-wall pullaway."

Conclusions

A class of cases were investigated roughly possessing initial flow angularity and adverse pressure gradients prototypic of those on the XFV-12A. Results obtained from the computational model indicate that if the initial total velocity is kept fixed then the introduction of the cross flow enhances the decay rate of the peak of the streamwise velocity component. In addition, the entrainment quantity and its rate decrease with increased cross flow. The implication of this phenomenon with respect to taper effect on boundary layer control (BLC) of the XFV-12A Coandas is not as significant as a "jet shrink" which has also been indicated in our approximate three-dimensional model. This contraction has been postulated as a mechanism promoting end-wall separation. To our knowledge, our model is the first to quantify such trends. Finally, the effect on the prescribed external adverse pressure gradient in the presence and absence of cross flow has also been examined. From the limited results, the spanwise separation line moves progressively further upstream with increasing cross flow.

References

1. Keller, H.B. and Cebeci, T., "Accurate Numerical Methods for Boundary Layers, I. Two-Dimensional Laminar Flows," Proceedings of the Second International Conference on Numerical Methods in Fluid Dynamics, Lecture Notes in Physics, Springer-Verlag, New York, Vol. 8, 1971.

2. Keller, H.B. and Cebeci, T., "Accurate Numerical Methods for Boundary Layers, II. Two-Dimensional Turbulent Flows," AIAA Journal, Vol. 10, September 1972, pp. 1197-1200.

3. Cebeci, T., "Calculation of Three Dimensional Boundary Layers, II. Three Dimensional Flows in Cartesian Coordinates," AIAA J., Vol. 13, No. 8, p. 1056, 1975.

4. Murphy, W.D., Shankar, V., and Malmuth, N.D., "Three Dimensional Wall Jets," Quarterly Progress Report No. 2, NADC Contract No. N62269-77-C-0412.

5. Taylor, G.I., J. of Aero. Sci., 25, 7, pp. 464-5 (1958).

COMPUTER AIDED DESIGN STUDY OF HYPERMIXING NOZZLES

L. A. Mefferd and P. M. Bevilaqua
Rockwell International
Columbus Aircraft Division

- Abstract -

A combination of computer analysis and scale model testing was employed to compare the entrainment of the jets from a variety of lobe and swirl nozzles. The spreading of each jet was predicted with a finite difference solution of Reynolds' equations for the three-dimensional flow field. A two-equation turbulence kinetic energy model was used for closure. Limited experimental testing was then performed to verify the predicted trends. It was concluded that the largest increase in the entrainment rate can be obtained by increasing the length of the nozzle lobes, and that an alternating lobe nozzle yields the greatest entrainment for a given lobe size.

Sponsored by the Naval Air Systems Command, Contract N00019-77-C-0527.

INTRODUCTION

The U. S. Navy is studying several types of V/STOL aircraft for use with smaller carriers, as a more economical means of maintaining sea control. One way of obtaining the additional thrust required to give an aircraft V/STOL capabilities is by diverting the engine exhaust flow through a thrust augmenting ejector, as shown in Figure 1. An ejector is a kind of jet pump which utilizes entrainment by a stream of primary fluid to accelerate a larger mass of air drawn from the atmosphere. According to the laws of momentum and energy conservation for flow through the ejector, greater thrust is obtained by transferring the kinetic energy of the primary jet to the entrained air. A more complete description of this process has been given by Bevilaqua.[1]

The mechanism of this energy transfer is the turbulent mixing of the two streams. Thus, increases in the thrust augmentation of short ejectors can be obtained by increasing the rate of turbulent mixing. Significant gains in augmentation have been achieved in this way, with hypermixing[2,3] and lobed nozzles shown in Figure 2. The alternating jet segments of the hypermixing nozzle function like a series of jet flaps at the trailing edge of the nozzle. Streamwise vorticity, corresponding to the tip vortices of each jet flapped section of the nozzle, are shed into the flow between alternating sections. These vortices serve to accelerate the turbulent mixing and thus increase entrainment.

The lobe nozzle divides the jet into many thin sheets spread across the ejector inlet. In addition, cutting back the exit of the nozzle elements to form a kind of wedge, as shown in Figure 2, produces a pair of counter-rotating vortices at the ends of each jet segment. The roll up process is similar to the interaction which occurs for a jet in a cross flow.[4] This combination of jet furcation and vortex production generates approximately the same increase in mixing and entrainment as the hypermixing nozzle.

The objective of this study was to develop a nozzle which combines the hypermixing and lobe mechanisms to achieve further increases in jet entrainment and ejector performance. A previously developed computer program,[5] incorporating a two-equation turbulence model, was used to predict and compare the evolution of jets from various nozzle designs. Experimental testing was then used to verify predicted trends and to determine the actual performance of a nozzle developed from the analytic results.

METHOD OF ANALYSIS

Governing Equations

In order to predict the complex jet flap fields which develop from the nozzles to be studied, it is necessary to determine the solution for a turbulent, three-dimensional velocity and pressure field. Considerable savings in computer storage and running time were achieved by utilizing a procedure developed by Patankar and Spalding[6] to reduce solution of the three-dimensional problem to the solution of a series of two-dimensional

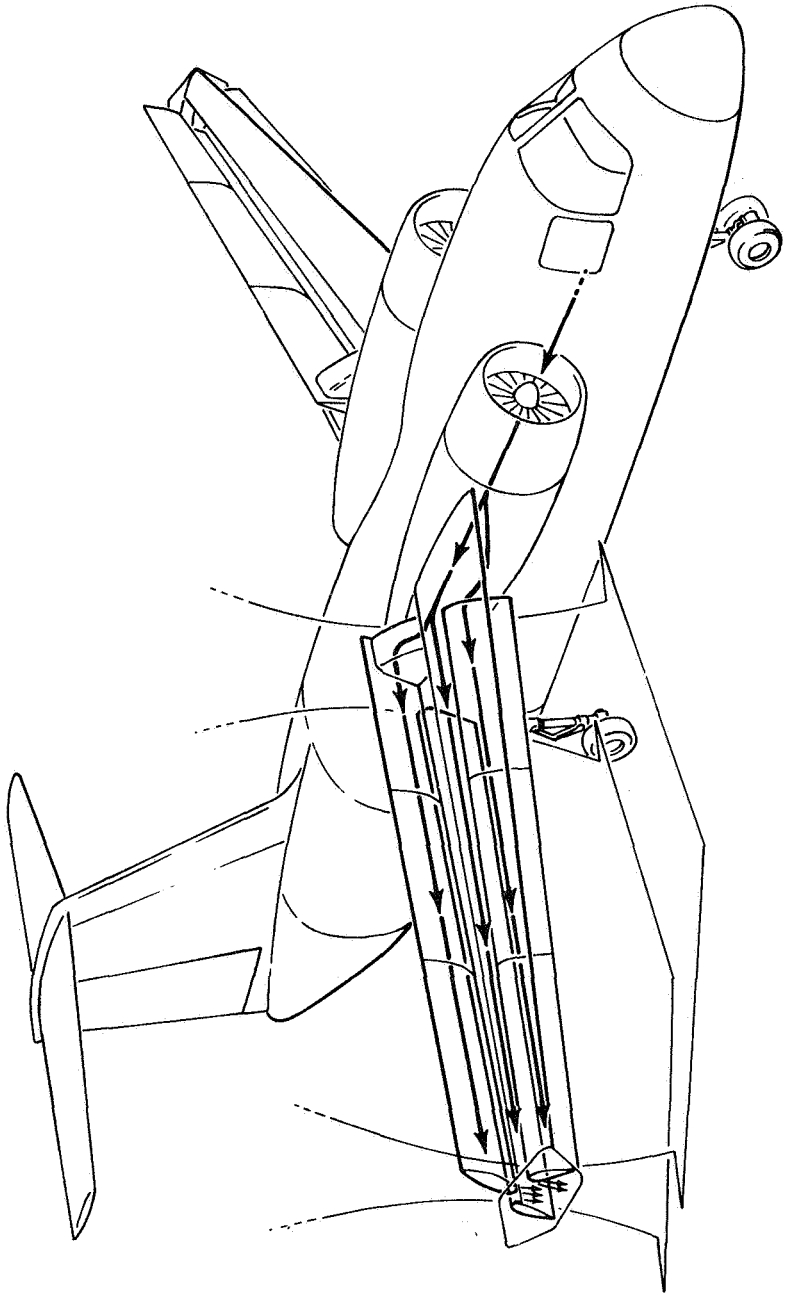

Figure 1. Ejector Wing V/STOL Aircraft.

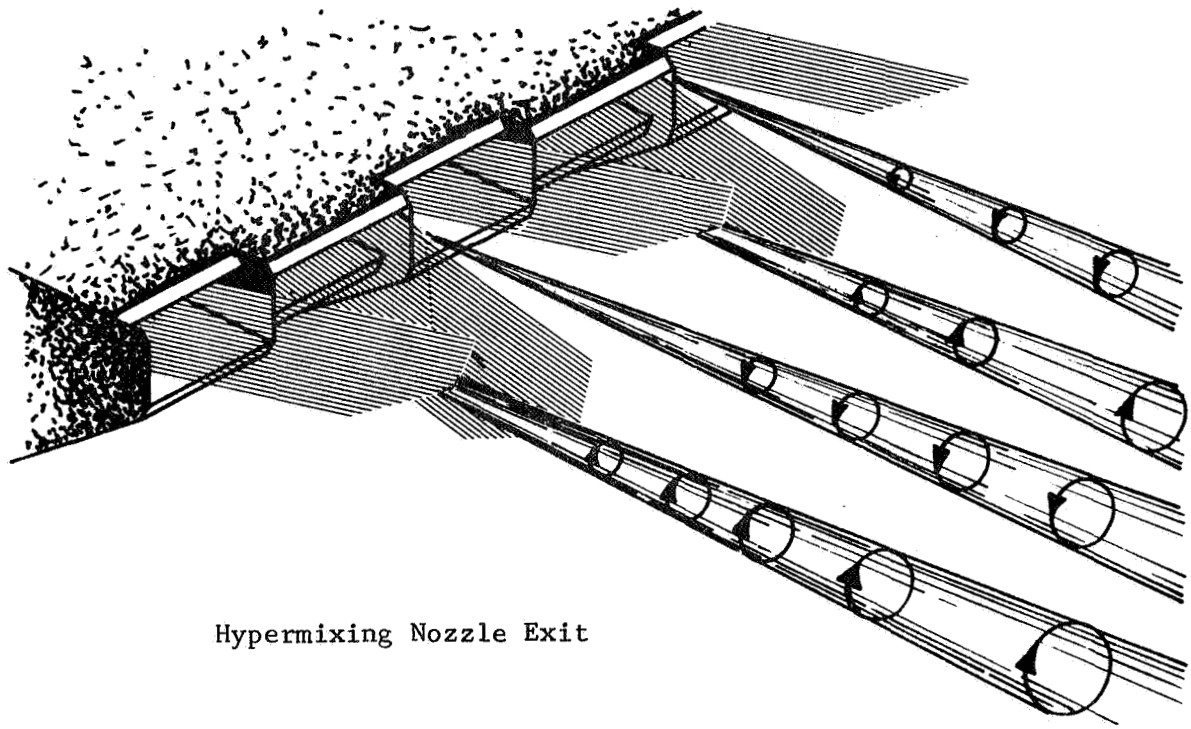

Hypermixing Nozzle Exit

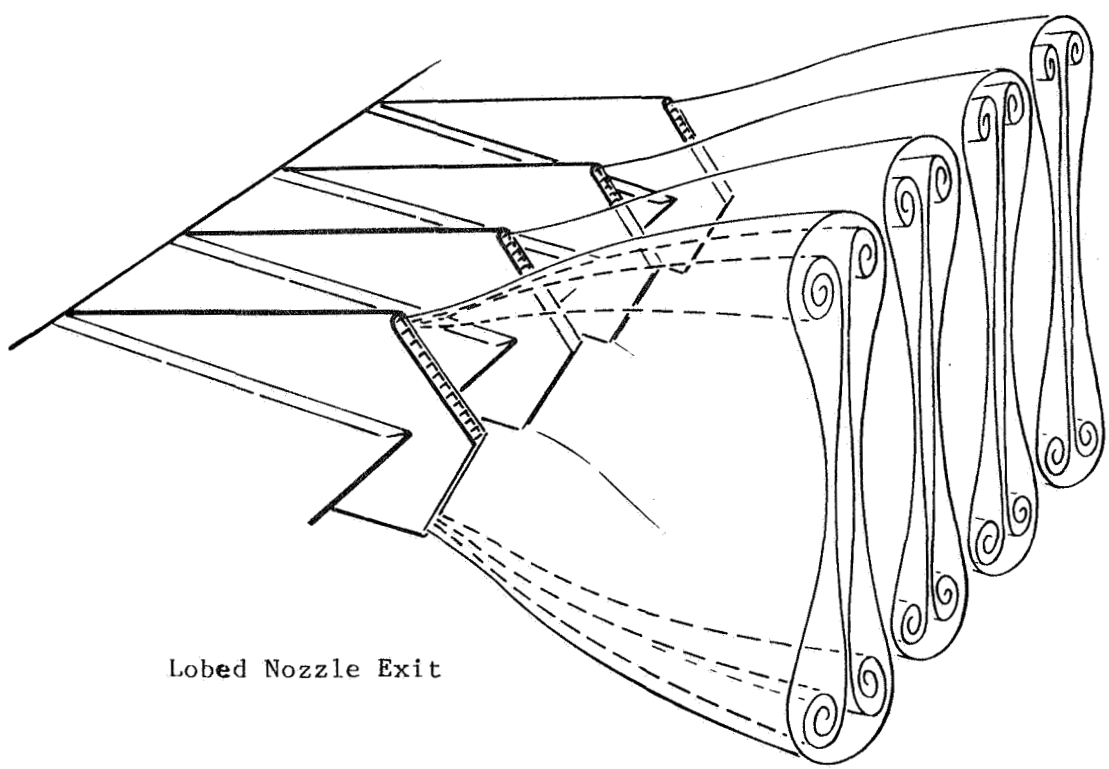

Lobed Nozzle Exit

Figure 2. Baseline Nozzles.

problems. Since there is a primary direction of flow (through the ejector), a thin shear layer approximation was applied. The gradients of the normal stress are thus neglected, and the streamwise velocity component is considered to be "driven" by a mean pressure $\overline{p}(x)$, which is decoupled from the perturbation pressures $p'(x,y,z)$ in the transverse planes. An additional assumption that the fluid density is constant was also made. These assumptions reduce the governing fully elliptic equations to a set which is parabolic in the streamwise direction, but elliptic in places across the flow. In Cartesian coordinates, the equations for the conservation of mass and momentum become

Continuity

$$\frac{\partial u}{\partial x} + \frac{\partial v}{\partial y} + \frac{\partial w}{\partial z} = 0 \tag{1}$$

Momentum

$$\rho u \frac{\partial u}{\partial x} + \rho v \frac{\partial u}{\partial y} + \rho w \frac{\partial u}{\partial z} = \frac{\partial \tau_{yx}}{\partial y} + \frac{\partial \tau_{zx}}{\partial z} - \frac{d\overline{p}}{dx} \tag{2}$$

$$\rho u \frac{\partial v}{\partial x} + \rho v \frac{\partial v}{\partial y} + \rho w \frac{\partial v}{\partial z} = \frac{\partial \tau_{yy}}{\partial y} + \frac{\partial \tau_{zy}}{\partial z} - \frac{\partial p'}{\partial y} \tag{3}$$

$$\rho u \frac{\partial w}{\partial x} + \rho v \frac{\partial w}{\partial y} + \rho w \frac{\partial w}{\partial z} = \frac{\partial \tau_{yz}}{\partial y} + \frac{\partial \tau_{zz}}{\partial z} - \frac{\partial p'}{\partial z} \tag{4}$$

Here, u, v, w are the time averaged velocity components and the τ_{ij} are the turbulent shear stresses.

The turbulent stresses are calculated using the two-equation turbulence model of Launder and Spalding.[7] An eddy viscosity assumption is used to relate the stresses to the velocity gradients. The expression in Cartesian tensor notation is:

$$\tau_{ij} = \mu_t \left(\frac{\partial u_i}{\partial x_j} + \frac{\partial u_j}{\partial x_i} \right) - \frac{2}{3} \rho k \delta_{ij} \tag{5}$$

where δ_{ij} is the Kronecher delta, and k is the kinetic energy of turbulence. For the parabolic flow considered here, the velocity gradients in the x-direction (i.e., $\partial u_i / \partial x_1$) will be neglected. The eddy viscosity μ_t is calculated from the turbulent kinetic energy and its rate of dissipation, ϵ. The expression for μ_t is

$$\mu_t = c_\mu \rho k^2 / \epsilon \tag{6}$$

in which c_μ is a constant of proportionality.

The equations for k and ϵ are

$$\rho u \frac{\partial k}{\partial x} + \rho v \frac{\partial k}{\partial y} + \rho w \frac{\partial k}{\partial z} = \frac{\partial}{\partial y}\left(\frac{\mu_t}{k}\frac{\partial k}{\partial y}\right) + \frac{\partial}{\partial z}\left(\frac{\mu_t}{k}\frac{\partial k}{\partial z}\right) + G - \rho\epsilon \tag{7}$$

$$\rho u \frac{\partial \epsilon}{\partial x} + \rho v \frac{\partial \epsilon}{\partial y} + \rho w \frac{\partial \epsilon}{\partial z}$$

$$= \frac{\partial}{\partial y}\left(\frac{\mu_t}{\sigma\epsilon}\frac{\partial \epsilon}{\partial y}\right) + \frac{\partial}{\partial z}\left(\frac{\mu_t}{\sigma\epsilon}\frac{\partial \epsilon}{\partial z}\right) + (c_1 G - c_2 \rho\epsilon)\left(\frac{\epsilon}{k}\right) \tag{8}$$

The quantity G is the rate of generation of k by the action of velocity gradients. Since, in the present situation, the only significant gradients are $\partial u/\partial y$ and $\partial u/\partial z$, the expression for G becomes

$$G = \mu_t \left[\left(\frac{\partial u}{\partial y}\right)^2 + \left(\frac{\partial u}{\partial z}\right)^2\right] \tag{9}$$

The turbulence model involves five empirical constants. According to the recommendation of Launder and Spalding,[7] the following values of the constants are used:

c_μ	c_1	c_2	σ_k	σ_ϵ
0.09	1.44	1.92	1.0	1.3

Thus, the turbulence constants were not adjusted for the present case.

These equations were put in finite difference form by integrating them over a control volume surrounding each grid point in the domain of solution. The resulting non-linear equations are linearized by using upstream values of the flow variables to evaluate the cross stream convection and diffusion coefficients. The equations are solved by the use of a tri-diagonal matrix algorithm. From known conditions at an upstream cross section, x, the flow field at the downstream cross section, $x + \Delta x$, is computed. This streamwise marching process is continued until the domain of interest has been covered. A more complete description of this program and an illustration of its use were given by Patankar and DeJoode.[5]

Boundary Conditions

The computational boundaries for representative nozzles are outlined with dashed lines in Figure 3. Although the jets are three-dimensional, the ejector shroud is two-dimensional, so that there is no change in the chordwise dimension, y, with respect to the spanwise dimension, z. Symmetry planes were used as computational boundaries in the spanwise direction, because most nozzle designs are periodic along the span. That is, there are no physical endwalls. The velocity normal to the symmetry planes is zero, and the normal gradients of other flow variables are also zero at these planes.

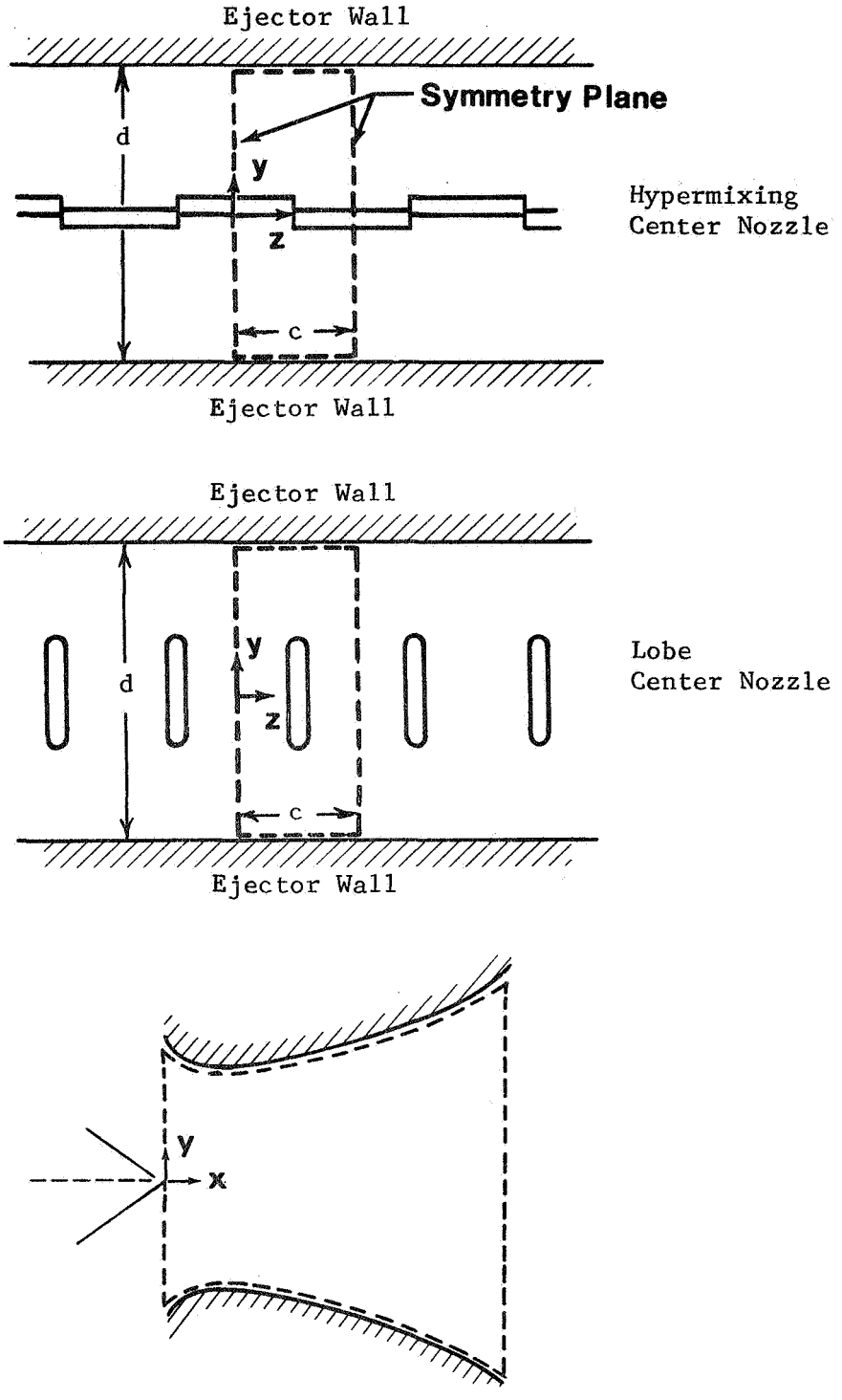

Figure 3. Computational Boundaries for Representative Nozzles.

The nozzles were compared by calculating their performance in an ejector representative of an average between the wing and canard on the XFV-12A ejector wing technology demonstrator aircraft.[8] The parameters used were an inlet area ratio of 13, diffuser length/throat width ratio of 2.0, diffuser area ratio of 1.8, and a flow split of 55% to the central nozzle. Although the performance of the nozzles depends to some extent on the ejector configuration, it was felt that conclusions regarding the relative performance of alternate nozzle concepts could be generalized for this type of ejector.

Initial Conditions

Solution of the ejector equations has thus been transformed to an initial value problem which is solved by streamwise integration. Initial values of all the flow variables must therefore be specified in order to start the calculation. Because there was no data available for the new nozzle concepts, experience with previously tested hypermixing and lobe nozzles was utilized to make reasonable assumptions for the initial conditions. The initial jet velocity of each nozzle was calculated by multiplying the isentropic velocity computed for the nozzle pressure ratio by an appropriate velocity coefficient, $C_V \equiv V_{actual}/V_{isentropic}$. The same value of this coefficient was used for every nozzle; that is, it was assumed that the internal viscous losses were the same for every nozzle. A value of $C_V = 0.925$ was chosen. The stagnation pressure, $P_S/P_{atm} = 2.1$, and temperature, $T_S = 550°R$, were chosen as typical of the primary jets of laboratory ejectors. Some deflection of the jet is utilized in each of the nozzles to promote vortex formation. The resultant tilt loss in the jet thrust was included by inclining the initial jet velocity vector at the appropriate deflection angle. Thus, the predictions of ejector performance balance the tilt loss in jet thrust against the associated increase of entrainment. Each of the nozzles had the same exit area and the same mass flow.

The wall jets were specified as being tangent to the surface of the inlet contraction, which made a 30° angle with the ejector axis. No corrections were made to the turbulence model or the momentum equations to account for the effect of wall curvature on these jets. The entrainment and thrust of the wall jets were therefore underpredicted, but since this treatment was the same in every case, the comparison of the central nozzles should not have been affected.

The initial turbulence intensity was not measured in any of the previous experiments. However, sensitivity studies performed by DeJoode and Patankar[5] showed that the development of the velocity profiles was relatively insensitive to probable variations in the initial turbulence level. This is because the hypermixing vortices dominate the turbulent processes. For the present analysis, the initial turbulence kinetic energy in the jet was specified to be 6% of the jet energy. In the secondary stream the turbulence energy was set equal to 0.01% of the stream energy. Similarly, the initial level of turbulence dissipation did not have a significant effect on the jet development. An initial value of $\epsilon = 0.13\ U_o^3/t$, where t is the initial nozzle gap, was chosen as being typical of the jets previously tested.

Evaluation of the Thrust Augmentation

The thrust augmentation ratio is defined to be the ratio of the ejector stream thrust to the isentropic thrust obtained by expanding the same mass of primary fluid to atmospheric pressure. The thrust of the ejector is evaluated by integrating the thrust of the mixed flow at the ejector exit. It is given by

$$T_e = \int_{A_3} \rho u^2 dy\, dz - (P_{atm} - P_3)A_3 \qquad (10)$$

in which u is the mainstream velocity, and P_3 and A_3 are the static pressure and area at the exit. The static pressure is assumed constant at the exit. It should be noted that even though the pressure force is negative, the reduced exhaust pressure results in a net thrust increase because the momentum flux is increased more than the pressure force is reduced.

NUMERICAL PREDICTIONS

In order to illustrate the predictions of the computer program and provide a baseline level of performance, the jets from representative hypermixing and lobed nozzles were examined. Development of the jets from these nozzles are shown in Figures 4 and 5. In each figure the axial velocity profiles at three streamwise stations corresponding to the ejector throat, a point midway through the diffuser, and the ejector exit are shown on the left. The convection velocities in the transverse planes at the first two stations are shown on the right. Note that the spanwise scale along the base of the axial velocity profiles has been elongated to show details. The location of the grid points is the same for the axial and transverse velocity profiles at each station. In the transverse planes, each velocity vector is centered on a grid point; the surface of the axial velocity profiles is defined by lines passing over these points. A sketch of the nozzle exit is shown at the bottom of the page. To simplify making comparisons, these same profiles will be shown for every nozzle.

In Figure 4 the hypermixing jet runs along the span on the centerline. There is a wall jet on each side of the hypermixing jet, and the relative magnitude of the secondary velocity is seen in the region between the primary jets. At the throat station, the displacement of adjoining segments of the hypermixing jets is apparent in the axial profiles, while the streamwise vortex can be seen in the transverse plane. The rotation of the vortex convects each jet segment around and behind the adjoining segment, as seen at the second station. This produces a characteristic double peak in the chordwise velocity profiles. Continued mixing acts to merge these peaks and broaden the profiles, as seen at the exit station. The thrust augmentation ratio, defined as the ratio of the exit momentum flux to the isentropic thrust of the primary jets, was predicted to be $\phi = 1.37$ for this nozzle. By comparison, the augmentation predicted for an ordinary slot nozzle is $\phi = 1.20$.

Axial Velocities

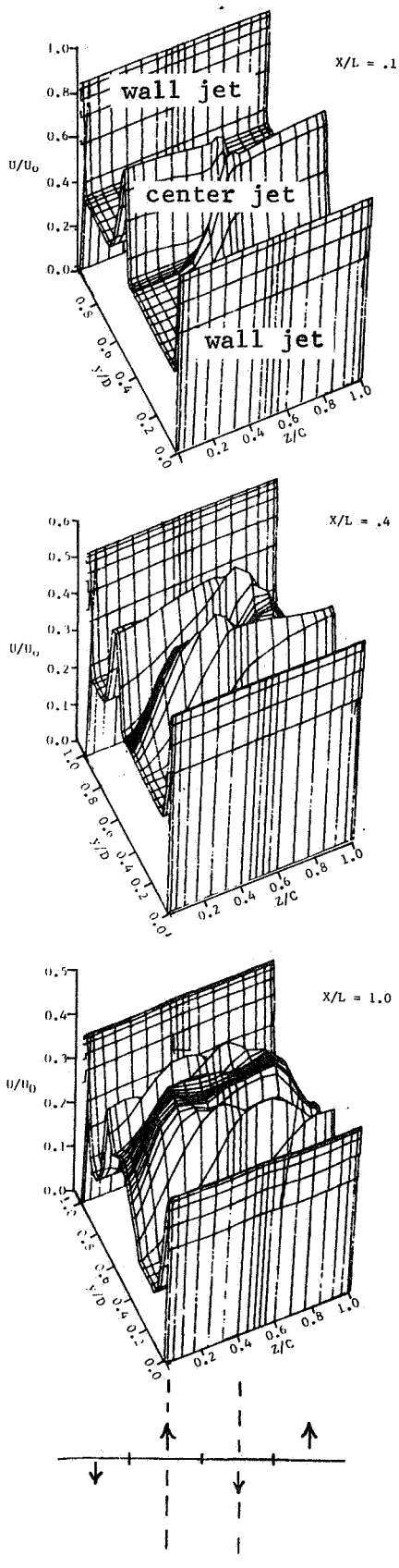

Convection Velocities

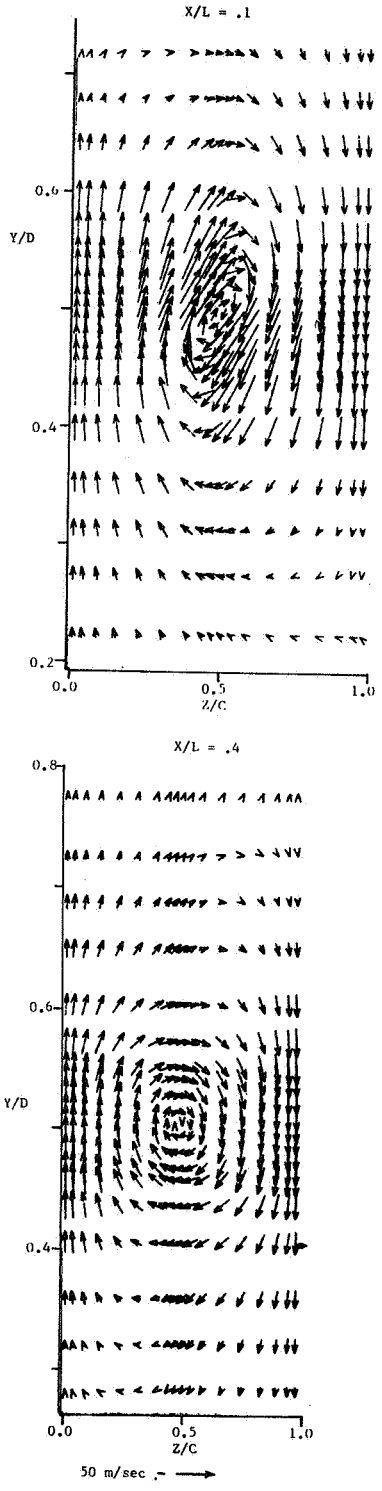

Figure 4. Baseline Hypermixing Nozzle, Ø = 1.37.

Development of the jet from the lobe nozzle is shown in Figure 5. The nozzle gap is the same as for the hypermixing jet and the length of each lobe is one-fourth of the ejector throat width. In the figure the left hand symmetry plane runs through the center of the segment so that only half of the jet is seen. The pair of counter-rotating vortices are at the ends of each segment. The mixing action of these vortices produces a local increase in the entrainment, and this causes the jet to develop the "dog bone" shaped cross section seen in the figure. The augmentation in this case is $\phi = 1.34$.

The jets from more than two dozen new nozzles were examined during the study. The basic nozzle consists of alternating crosswise and spanwise lobes. Only a few representative configurations will be discussed here. The nozzle shown in Figure 6 has a lobe positioned between the hypermixing vortices. In the figure the hypermixing vortex is at the center and the vortex pair eddies are on the sides. The velocities induced by the vortex pairs reinforce the hypermixing velocities on the diagonal running from lower left to upper right, but oppose them on the other diagonal. Comparison of the exit velocity profile with those of the baseline nozzles reveals that this interaction reduces the spreading of the hypermixing segment. However, the addition of the nozzle lobes increases the net entrainment and the thrust augmentation ratio is increased to $\phi = 1.41$.

For the nozzle shown in Figure 7, alternate sides of each lobe were deflected in opposite directions. Three streamwise vortices develop in this case. The central vortex is twice as strong as either tip vortex, since it is formed by combination of the two root vortices. The vortex pair eddies do not appear because there is no chordwise deflection of the jet. The rotation of the central vortex can be seen to drive the jets from adjacent lobes together at the symmetry planes. This limits the entrainment of these jets, leaving a large unmixed region between the merged jets. As a result, the augmentation ratio was reduced to $\phi = 1.26$ with this nozzle.

A composite nozzle in which the lobe vortex is centered over the hypermixing vortex is shown in Figure 8. The lobe vortex and the tip vortex on each side of it rotate in the same direction, so that they coalesce to form the single vortex seen in the figure. There is additional entrainment associated with this process, and the thrust augmentation ratio is increased over the previous nozzle. However, the lobe jet is rotated into the spanwise jet in this case also, and the augmentation ratio is only increased to $\phi = 1.31$.

In the last nozzle shown, the length of the lobe is equal to the ejector throat width. The development of the axial velocity profiles for one of the jets is shown in Figure 9. In this orientation the spreading of each jet is greater than if it were aligned with the ejector span, because the mean jet vorticity is stretched as it passes through the diffuser. Vortex stretching is the primary mechanism of turbulent energy dissipation[9] and entrainment is associated with this dissipation. It can be seen that adjacent jets have just merged with each other by the ejector exit. The augmentation ratio was increased to $\phi = 1.61$ with this configuration. A description of the predicted results for other nozzle configurations may be found in the contract report.[10]

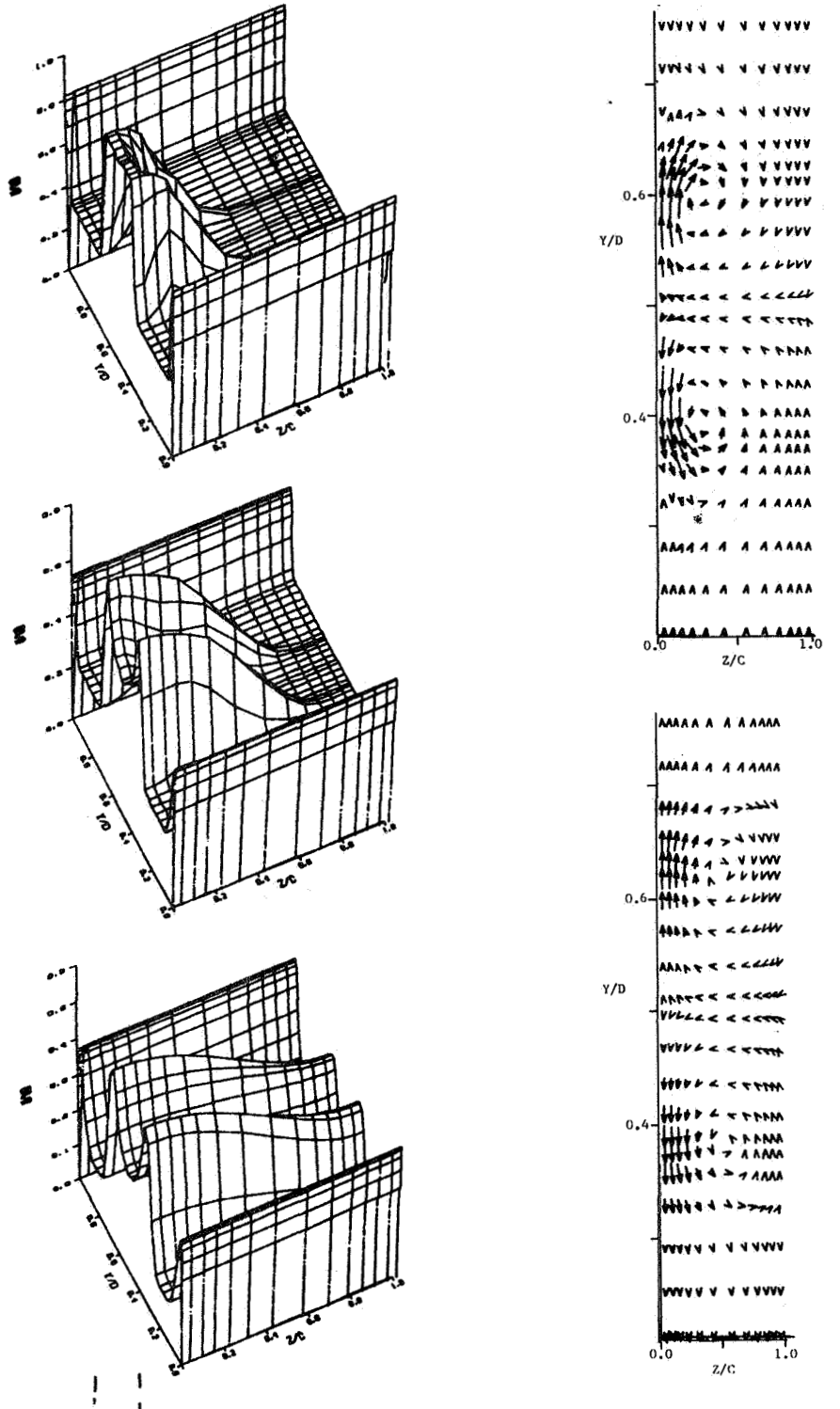

Figure 5. Baseline Lobe Nozzle, Ø = 1.34.

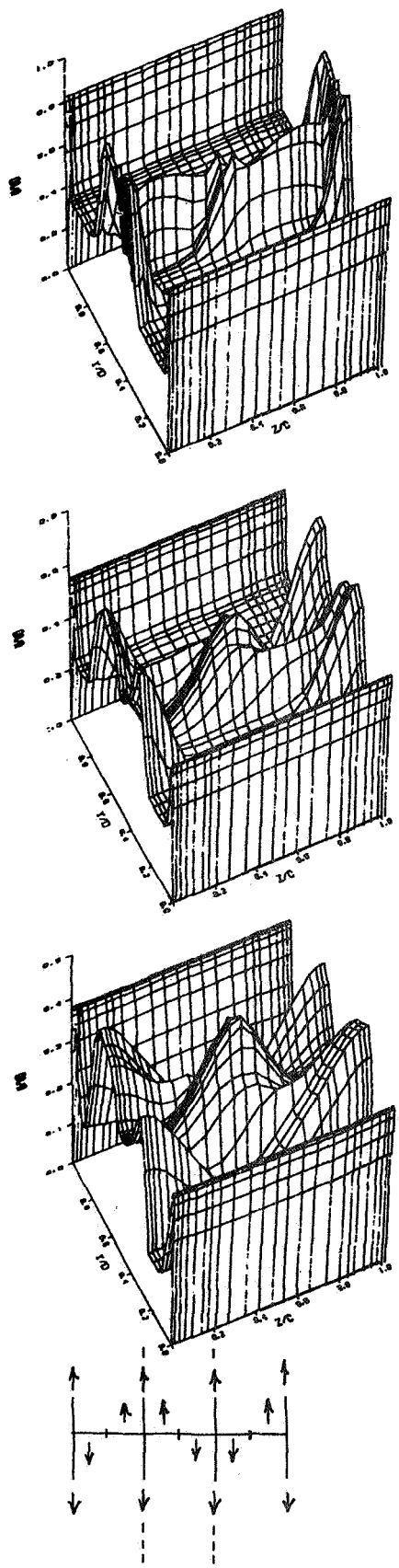

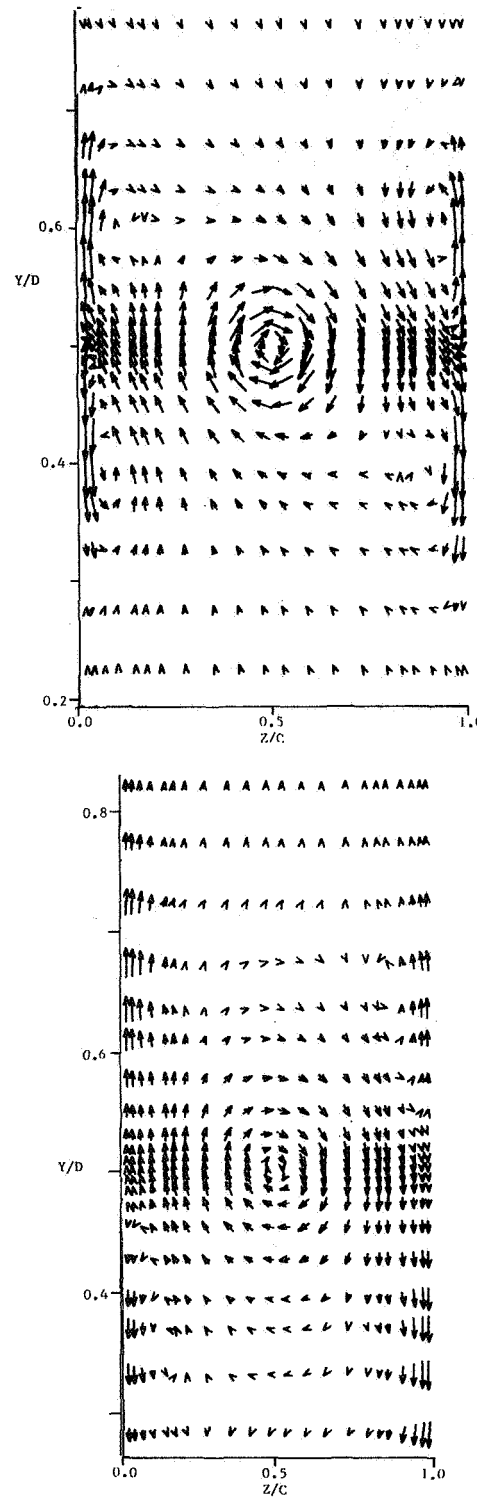

Figure 6. Vortex Centered Between Crosswise Lobes, Ø = 1.41.

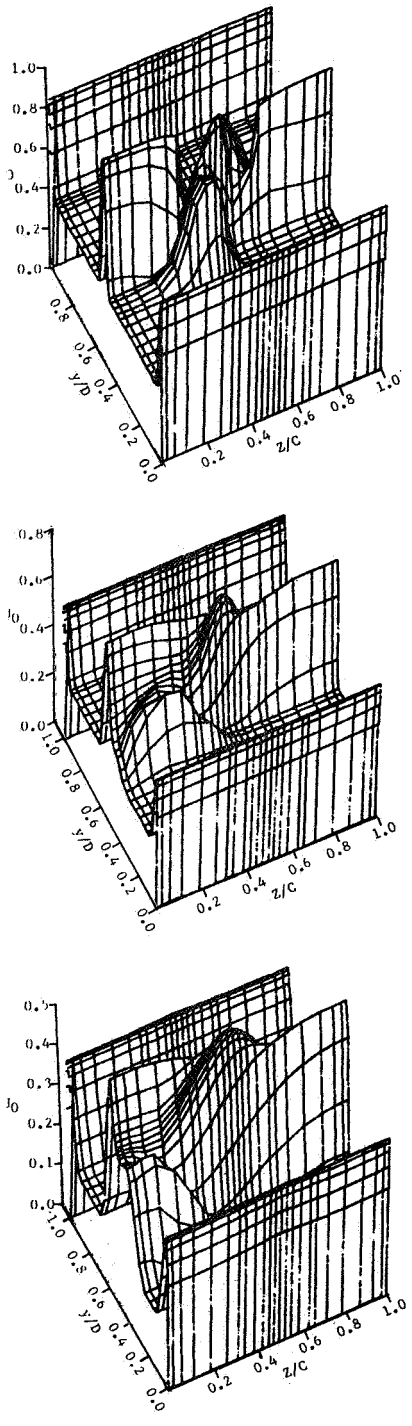

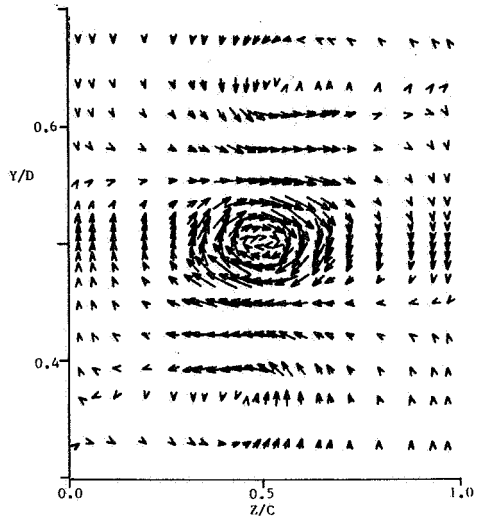

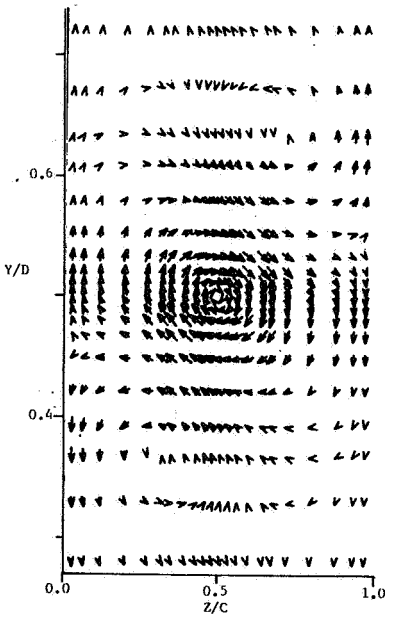

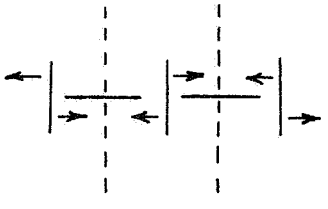

Figure 7. Vortex Centered on Lobes with No Wedge Angle, Ø = 1.26.

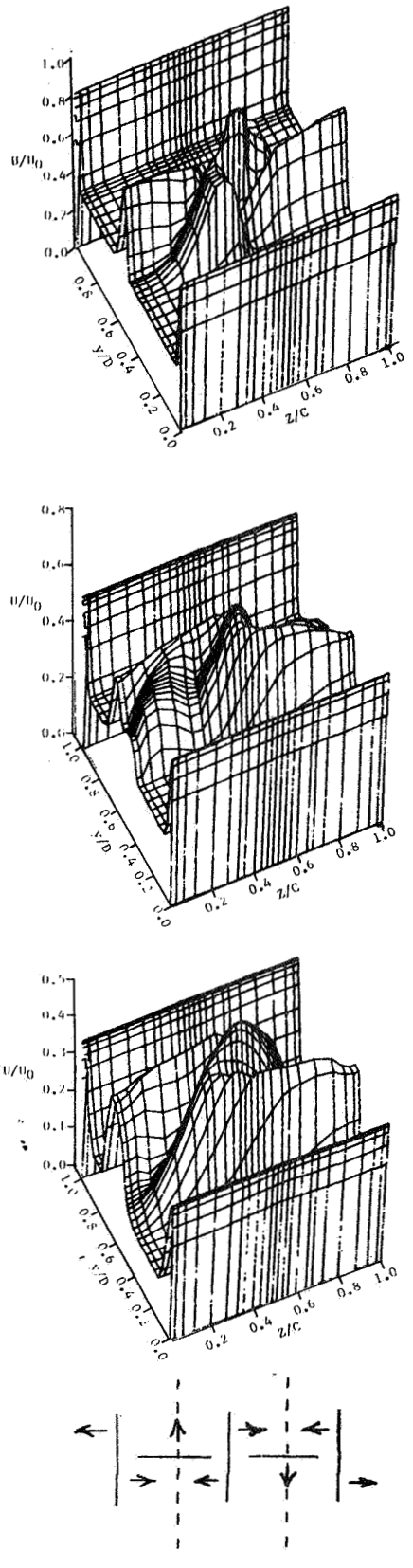

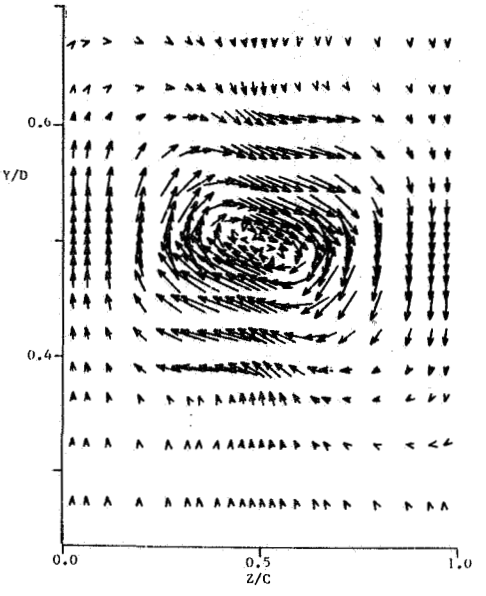

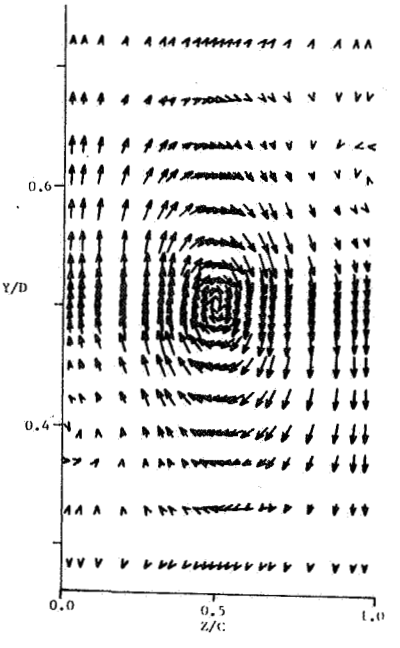

Figure 8. Crosswise Lobe Vortex Centered over Hypermixing Vortex, Ø = 1.31.

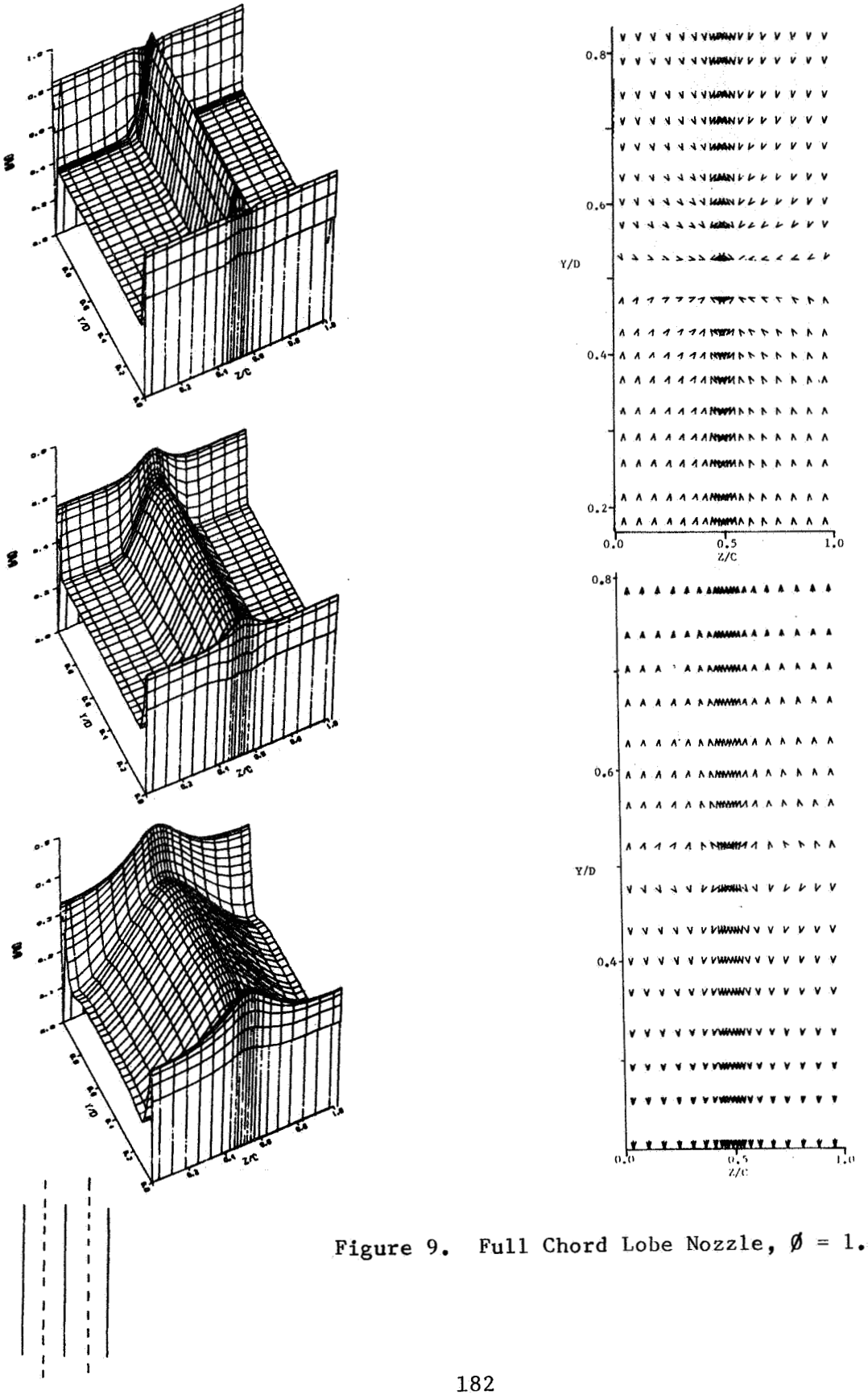

Figure 9. Full Chord Lobe Nozzle, Ø = 1.61.

EXPERIMENTAL RESULTS

Limited experimental testing was performed to verify the predictions that the addition of a vortex to a short lobe reduces the augmentation, but that the addition of a vortex between the lobes increases the augmentation. In the interest of economy, these tests were performed in an existing ejector model. The model was mounted on a cradle suspended on four cables attached to a fixed frame. The ejector thrust was measured with load cells installed between the cradle and frame. High pressure air was supplied to the primary nozzles through flexible hoses. The isentropic reference thrust was calculated from the measured primary flow and the nozzle exit pressure.

The effect of the lobe vortex was determined by direct comparison; the hypermixing lobe nozzle was constructed by cutting back opposite sides of the lobes on the reference nozzle. Each nozzle was installed in the ejector, and the thrust augmentation ratio was measured over a range of diffuser area ratios. As shown in Figure 10, the peak augmentation ratio was significantly reduced by the addition of the vortex. A hot wire anemometer was used to obtain midspan velocity profiles at a diffuser area ratio of 1.8, for both nozzles. The measured profiles matched the predicted profiles well, verifying the mechanism of the thrust loss. Thus, the prediction that the vortex reduced the augmentation by driving adjacent lobes together was confirmed.

In the second series of tests, the prediction that a vortex between the lobes increases the augmentation was verified. Since an existing hypermixing nozzle was the baseline in this case, another ejector was used for these tests. The measured thrust augmentation of $\phi = 1.54$ represents an improvement over the $\phi = 1.49$ attained with the hypermixing nozzle (Figure 11). The development of the profiles was the same as the numerical predictions. Thus, the analytic predictions were verified in this case also. The wide lobe nozzles were not tested because considerable development work has already been carried out in this case.[11]

CONCLUSIONS

There are two major conclusions of this study. First, the partially parabolic solution procedure can be used to predict the development of these highly three-dimensional jets. To our knowledge, this is the first time the method has been utilized in this way. We did not notice the sensitivity to initial turbulence properties sometimes noted as a deficiency of the method. The probable reason is that the large vortices dominate the turbulent processes. The second conclusion is that the hypermixing and lobe nozzles are not readily combined. Nevertheless, significant gains in augmentation can be achieved with nozzles developed by numerical analysis.

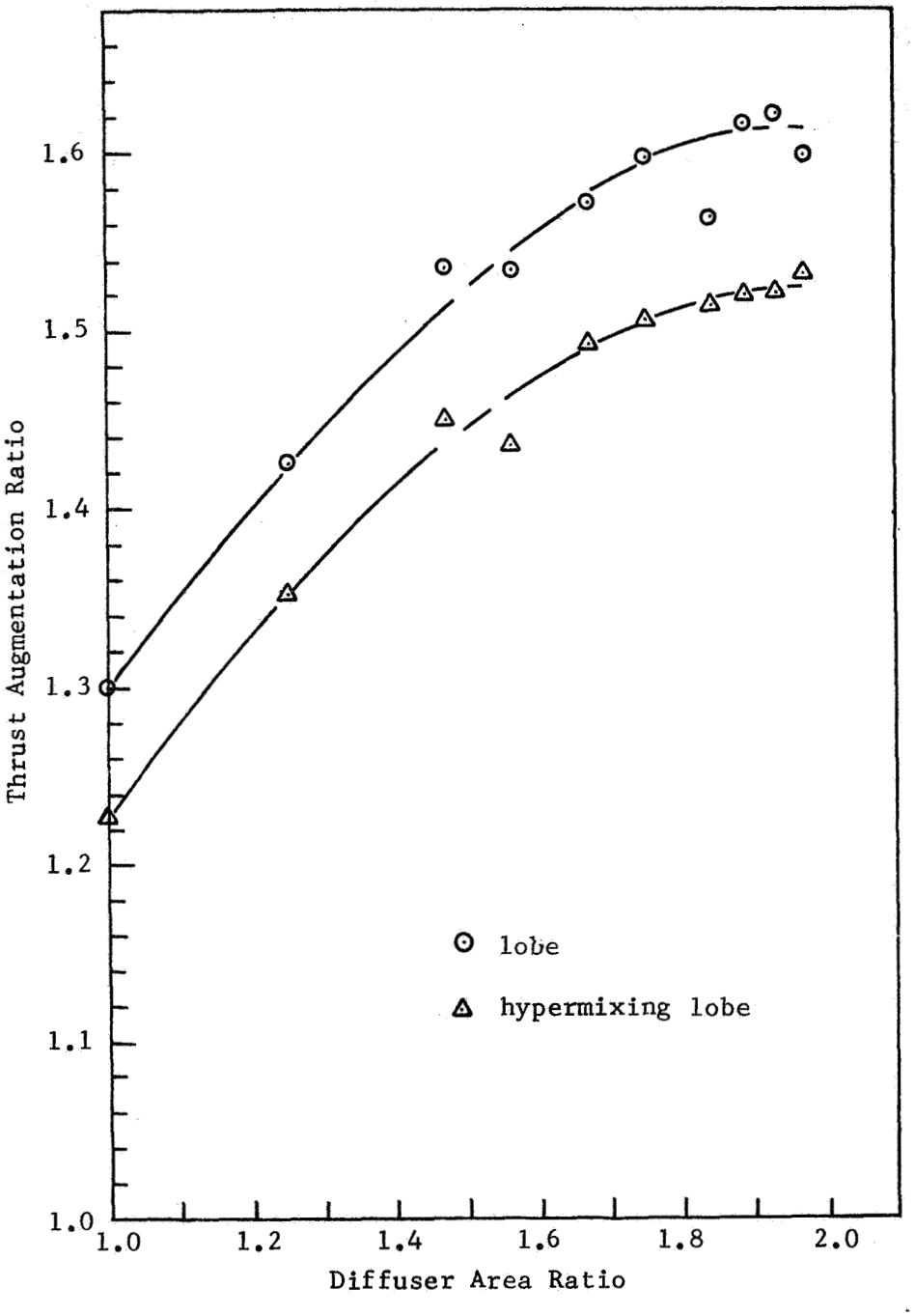

Figure 10. Effect of Hypermixing on Thrust Augmentation of Lobe Nozzles.

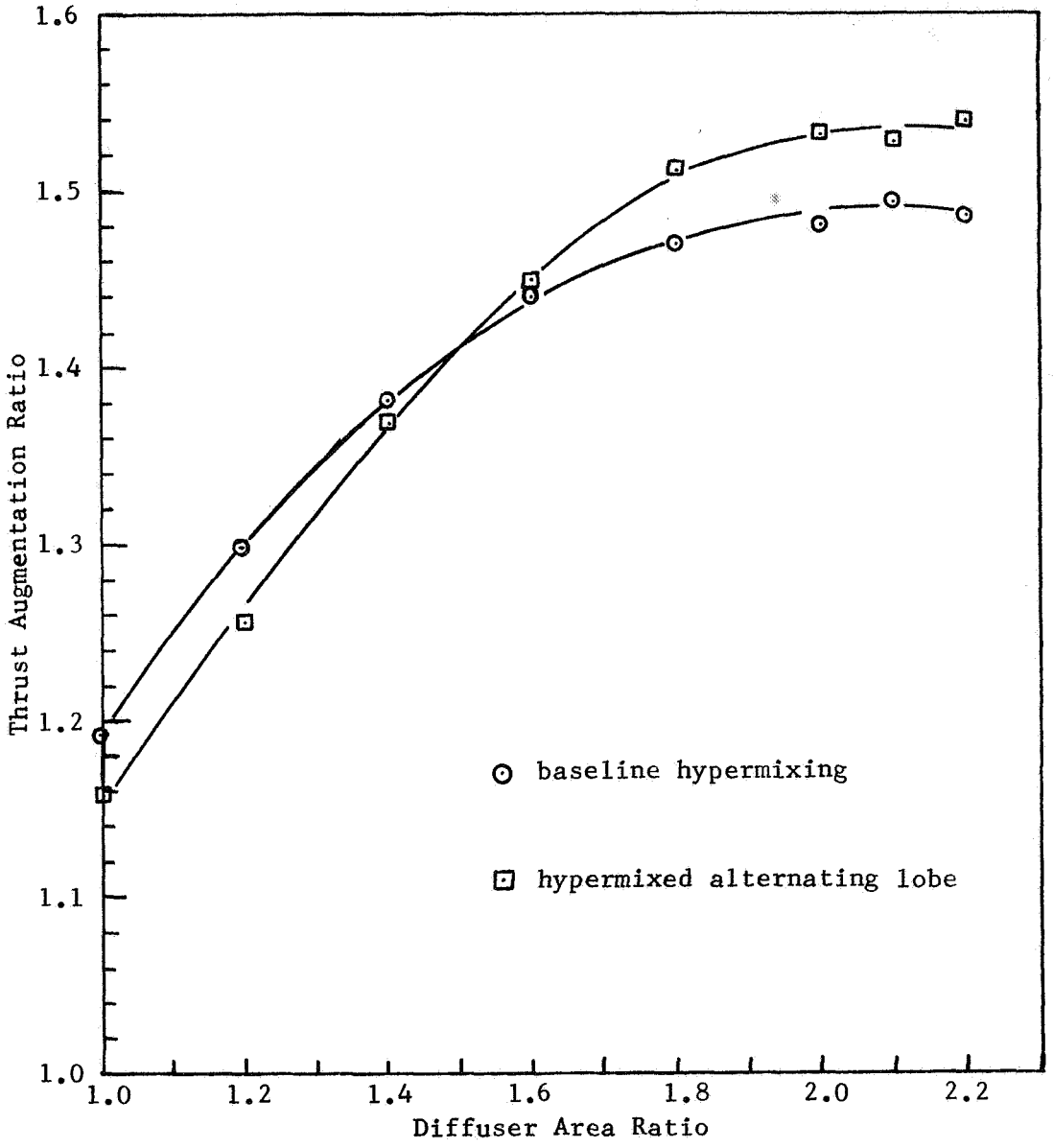

Figure 11. Comparison of Thrust Augmentation for Hypermixing Nozzle and Nozzle with Vortex Centered Between Lobes.

REFERENCES

1. Bevilaqua, P. M., "Lifting Surface Theory for Thrust-Augmenting Ejectors," AIAA Journal, Vol. 16, No. 5, May 1978, pp. 475-481.

2. Quinn, B. P., "Compact Ejector Thrust Augmentation," Journal of Aircraft, Vol. 10, No. 8, August 1973, pp. 481-486.

3. Bevilaqua, P. M., "Evaluation of Hypermixing for Thrust Augmenting Ejectors," Journal of Aircraft, Vol 11, No. 6, June 1974, pp. 348-354.

4. Fearn, R., and Weston, R. P., "Vorticity Associated with a Jet in a Cross Flow," AIAA Journal, Vol. 12, No. 12, December 1974, pp. 1666-1671.

5. DeJoode, A. D. and Patankar, S. V., "Prediction of Three Dimensional Turbulent Mixing in an Ejector," AIAA Journal, Vol. 16, No. 2, February 1978, pp. 145-150.

6. Patankar, S. V. and Spalding, D. B., "A Calculation Procedure for Heat, Mass and Momentum Transfer in Three Dimensional Parabolic Flows," International Journal of Heat and Mass Transfer, Vol. 15, October 1972, pp. 1487-1806.

7. Launder, B. E. and Spalding, D. B., "The Numerical Computation of Turbulent Flows," Computer Methods in Applied Mechanics and Engineering, Vol. 3, No. 2, March 1974, pp. 269-289.

8. Throndson, L. W., "Compound Ejector Thrust Augmenter Development" ASME Paper No. 73-GT-67.

9. Tennekes, H. and Lumley, J. L., "A First Course in Turbulence," MIT Press; Cambridge, Mass, 1972.

10. Mefferd, L. A. and Bevilaqua, P. M., "Computer-Aided Design Study of Hypermixing Nozzles," NASC Report NR78H-91, July 1978.

11. Viets, H., "Thrust Augmenting Ejectors," ARL, TR 75-0224, June 1975.

NONSTEADY-FLOW THRUST AUGMENTING EJECTORS

Joseph V. Foa
The George Washington University
Washington, D.C.

This note concerns those ejector augmenters in which the transfer of mechanical energy from the primary to the secondary flow takes place, at least in part, through the work of interface pressure forces. This mode of energy transfer, commonly referred to as "pressure exchange", is of interest in that the work of interface pressure forces is essentially nondissipative. It requires, however, that the interacting flows be nonsteady, because no work is done by pressure forces acting on a stationary interface.

The potential superiority of nonsteady-flow processes from the standpoint of energy transfer efficiency is also predicted by the energy equation,

$$\frac{1}{\rho}\frac{DH}{Dt} = \frac{1}{\rho}\frac{\partial p}{\partial t} + \vec{f}\cdot\vec{V} \quad \text{(for incompressible flow)}$$

or

$$\frac{Dh^\circ}{Dt} = T\frac{Ds}{Dt} + \frac{1}{\rho}\frac{\partial p}{\partial t} + \vec{f}\cdot\vec{V} \quad \text{(for compressible flow)}$$

where $\vec{f}$ is the resultant of body and surface viscous forces per unit mass, h° the specific stagnation enthalpy, H the total head, p the pressure, s the specific entropy, T the temperature, $\vec{V}$ the particle velocity, and ρ the density [1, 2,3]*. These equations show that, in the absence of body forces, the energy level of a particle in a flow can be changed reversibly only if the flow is nonsteady.

---

* Numbers in brackets designate References at the end of paper.

Of special interest in this connection are the results of a remarkable series of experiments conducted by Lockwood [4], where it was shown that the pulsating-flow ejector is capable of higher energy transfer efficiencies than its steady-flow counterpart, with greatly reduced interaction lengths (see Figs. 1 and 2). These results could, however, be misleading. The pulsating-flow ejector is clearly a promising arrangement when one deals with a primary that is pulsating to begin with -- e.g., with the exhaust of a pulsejet. But when the pulsation of the primary has to be obtained by "chopping up" an originally steady flow, the theory predicts -- and Lockwood's experiments have confirmed -- that the losses associated with the chopping up of the primary can be large enough to more than offset the thrust increment that is produced in the augmenter. Similar losses, in addition to analytical and control difficulties, are encountered in the design and operation of all flow induction devices based on the utilization of wave processes.

On the other hand, a steady flow can be transformed into a nonsteady one without chopping up or other losses, through the simple artifice of a change of frame of reference. A flow field that is not uniform throughout can be steady in, at most, only one coordinate system. An observer moving relative to this unique coordinate system will see the flow as nonsteady. We apply the designation "cryptosteady" to a process which is nonsteady but admits a frame of reference in which it is steady. The special merit of cryptosteady interactions is that they can be generated, controlled, and analyzed as steady-flow processes in that unique frame of reference

F_s in which they are steady, while retaining the efficiency advantages of nonsteady-flow processes in the frame of reference F_u in which they are utilized.

The simplest embodiments of this concept are those in which F_s rotates at constant angular velocity relative to F_u. In the "rotary jet" augmenter configuration (Fig. 3), the primary is discharged into the interaction space through skewed nozzles on the periphery of a free-spinning rotor, thereby driving the rotor and forming the helical rotating patterns that are referred to as "pseudoblades". The boundaries of the pseudoblades are the interfaces separating the primary from the secondary flow, and the pressure forces which the two flows exert on one another at these moving interfaces do work. Through this action, mechanical energy is extracted from the primary flow as in a turbine and is added to the secondary as through a fan or propeller. Since this "pressure exchange" component of the interaction is essentially nondissipative, the performance of the rotary jet can be expected to be better than that of the conventional steady-flow ejector. This fact had already been confirmed experimentally by Vennos at Rensselaer [5], by Avellone at Grumman [6], and by Hohenemser at McDonnell [7,8], prior to the start of the program of research that we have been carrying out on this subject at the George Washington University jointly with the U.S. Naval Academy for the past two years.

As for the theory, previous studies had been based primarily on two analytical models -- the two-dimensional and the thin-jet model. In the two-dimensional model [9] the penetration of the secondary flow into the spaces between the

pseudoblades is assumed to be completed before the two flows deflect each other to a common orientation in the rotor-fixed frame of reference (Fig. 4) and the depth of the interaction space is assumed to be small compared to its mean radius. This analytical model can be approximated in practice through the use of hooded nozzles (Fig. 5) or other design artifices. However, in the absence of such artifices the performance predictions of the two-dimensional theory must be viewed with caution. The other main approach available at the start of our current project was that of Homenemser's thin-jet strip theory [7], in which the primary is treated as a very thin jet successively interacting with infinitesimal layers of the secondary flow (Fig. 6). In each of these infinitesimal steps, as the two interacting flows deflect each other to a common orientation, the primary jet, which is finite, undergoes an infinitesimal deflection, and the secondary layer, which is infinitesimal, undergoes a finite deflection. The changes of angular momentum of the two flows in each step must be equal and opposite. The equation expressing this fact yields the distribution of deflections and velocities at the exit from the interaction space, and therefore also the thrust augmentation ratio.

A more realistic analytical model has recently been developed, whereby account is taken of that part of the interaction that takes place where the secondary flow enters the space between the pseudoblades. As Fig. 7 shows, different layers in both flows undergo different histories, different deflections, and different exchanges of mechanical energy.

A detailed study of the interaction according to this model has been carried out by Costopoulos (Ref. 10).

Fig. 8 shows a comparison of the performance predictions of the above-mentioned theories.

Fig. 9, also from Ref. 10, shows what happens when any appreciable mixing is allowed to take place during the deflection phase. The effect is in this case always an adverse one, as one would expect, since any energy that is transferred through mixing during the deflection phase is energy that could have been transferred more efficiently by pressure exchange.

In contrast, and contrary to previous results, Costopoulos (Ref. 12) has found that mixing after the mutual deflection phase is always beneficial if no account is taken of the drag and weight penalties that are associated with the required extension of the shroud. Actually, beyond a certain spin angle, the benefit that can be derived from mixing becomes too small to offset these penalties.

In a separate study (Ref. 11), a "black box" approach was used to show that the superiority of the rotary jet over the ejector can be explained as an effect of pressure exchange alone, quite apart from whatever benefit may be derived from the enhancement of mixing. The same paper also considered the effect if secondary-to-primary density ratio and showed that the effect of increasing this ratio may be beneficial or

adverse, depending on the magnitude of a parameter called "pressure exchange amplitude", which is a measure of the vigor of the collision. This study was continued in Ref. 12, with the interesting result that, whereas in the ejector the best density ratio is 1.0, in the rotary jet, beyond a relatively low spin angle, the effect of an increase of density ratio is always beneficial (Fig. 10).

References

1. Eck, B., "Technische Strömungslehre," Julius Springer, Berlin, 1957, p. 50.

2. Dean, R. C., Jr., "On the Necessity of Unsteady Flow in Fluid Machines," Journal of Basic Engineering, March 1959, pp. 24-28.

3. Foa, J. V., "Pressure Exchange," Applied Mechanics Surveys, Spartan Books, 1966, pp. 1177-1183.

4. Lockwood, R. M., "Energy Transfer from an Intermittent Jet to an Ambient Fluid," Hiller Aircraft Co., Summary Report No. ARD-238, June 30, 1959.

5. Foa, J. V., "The Bladeless Propeller," Proc. of Seventh Symposium on Naval Hydrodynamics, Rome, Italy, 1968, ONR, DR-148, pp. 1351-1372.

6. Avellone, G., "Theoretical and Experimental Investigation of the Direct Exchange of Mechanical Energy Between Two Fluids," Grumman Research Dept. Memorandum RM 365, June 1967.

7. Hohenemser, K. H., "Preliminary Analysis of a New Type of Thrust Augmenter," Proceedings of the 4th U.S. National Congress of Applied Mechanics, ASME, New York, 1962, pp. 1291-1299.

8. Hohenemser, K. H., "Flow Induction by Rotary Jets," Journal of Aircraft, Vol. 3, No. 1, Jan.-Feb. 1966, pp. 18-24.

9. Foa, J. V., "Cryptosteady Pressure Exchange," Rensselaer Polytechnic Institute Tech. Rept. TR-AE 6202, Troy, N.Y., March 1962.

10. Costopoulos, T., "A Wide-Jet Strip Analysis of Cryptosteady-Flow Thrust Augmenters-Parts 1 and 2," GWU Tech. Repts. TR-UTA-771 and 772, March 1977.

11. Foa, J. V., "Ejectors and Rotary Jets as Thrust Augmenters," article in Marine Propulsion, edited by J. Sladky, Jr., ASME Ocean Engineering Division, December 1976.

12. Costopoulos, T., "Constant-Area Flow Interactions in Cryptosteady-Flow Thrust Augmentors," GWU Tech. Repts. TR-UTA-773 and 774, April 1977.

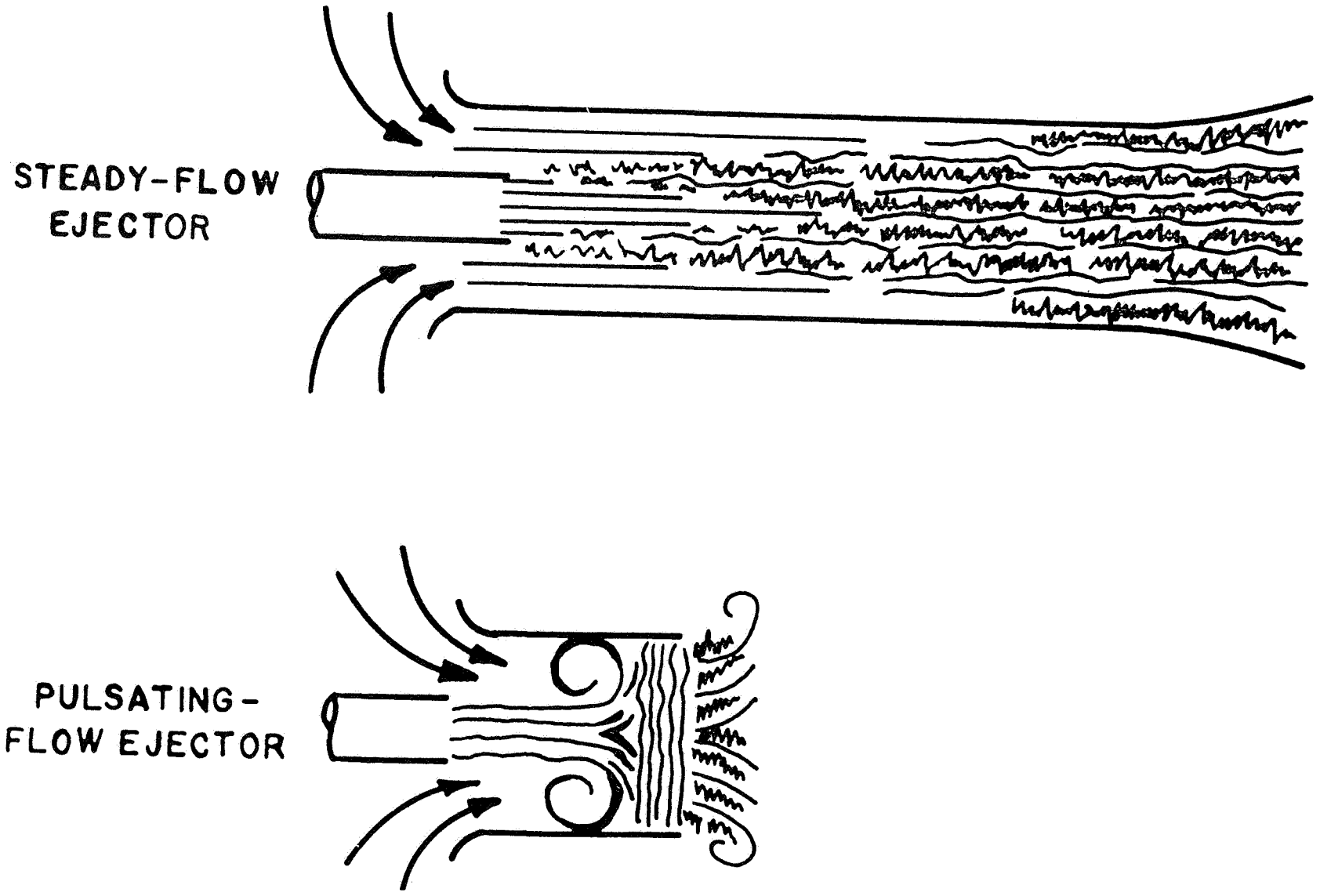

Figure 1.- Steady-flow and pulsating-flow ejectors (from ref. 4).

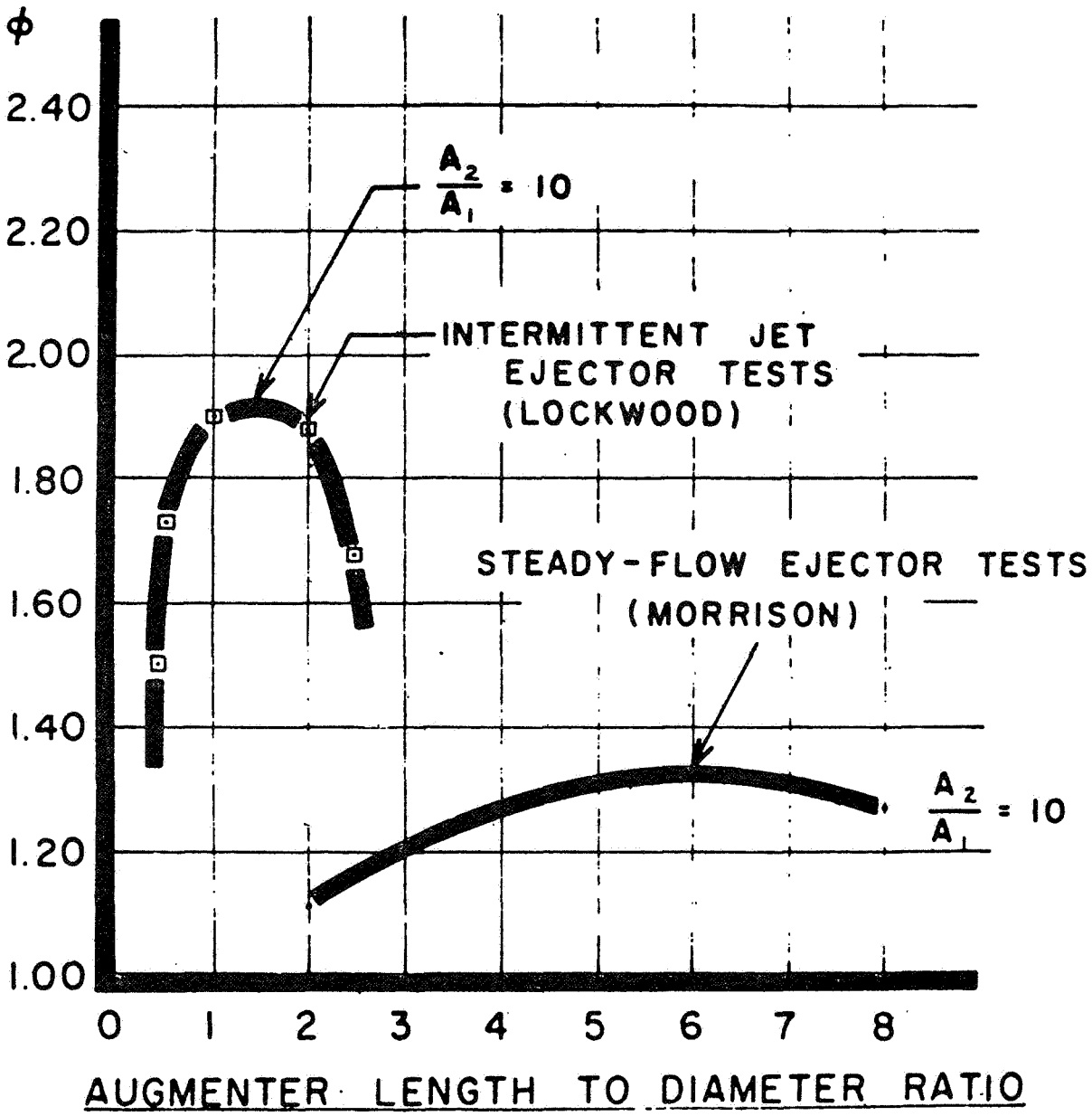

Figure 2.- Comparison of static thrust augmentation ratios of steady-flow and pulsating-flow ejectors (from ref. 4).

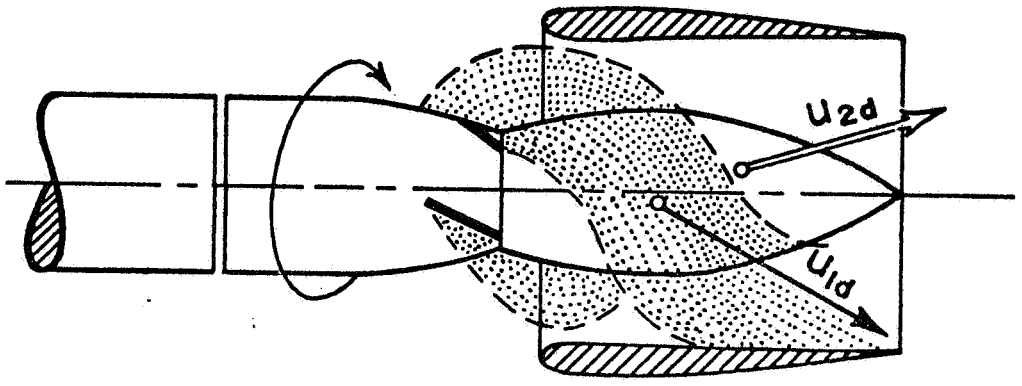

Figure 3.- Rotary-jet thrust augmenter.

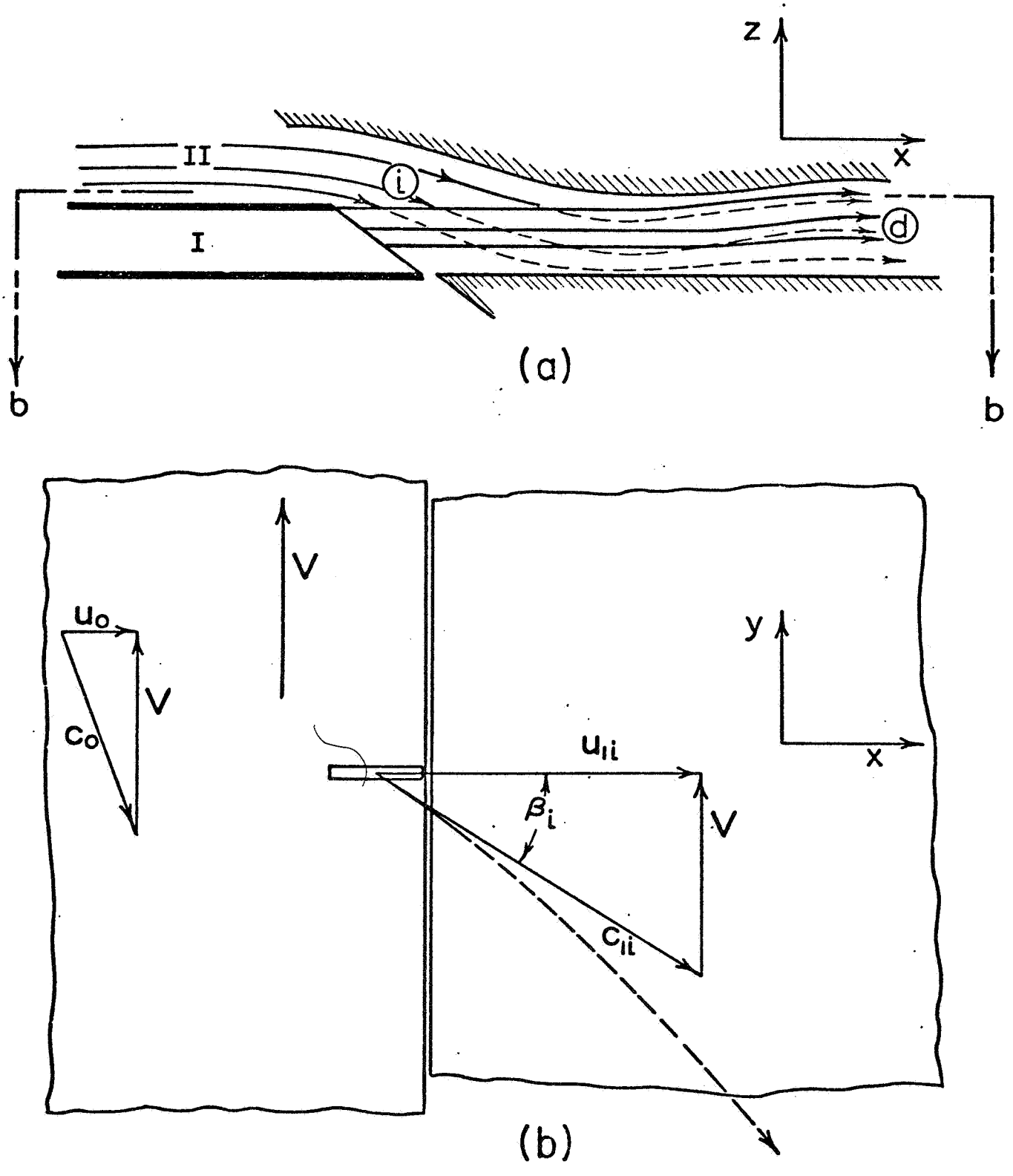

Figure 4.- Analytical model for two-dimensional theory.

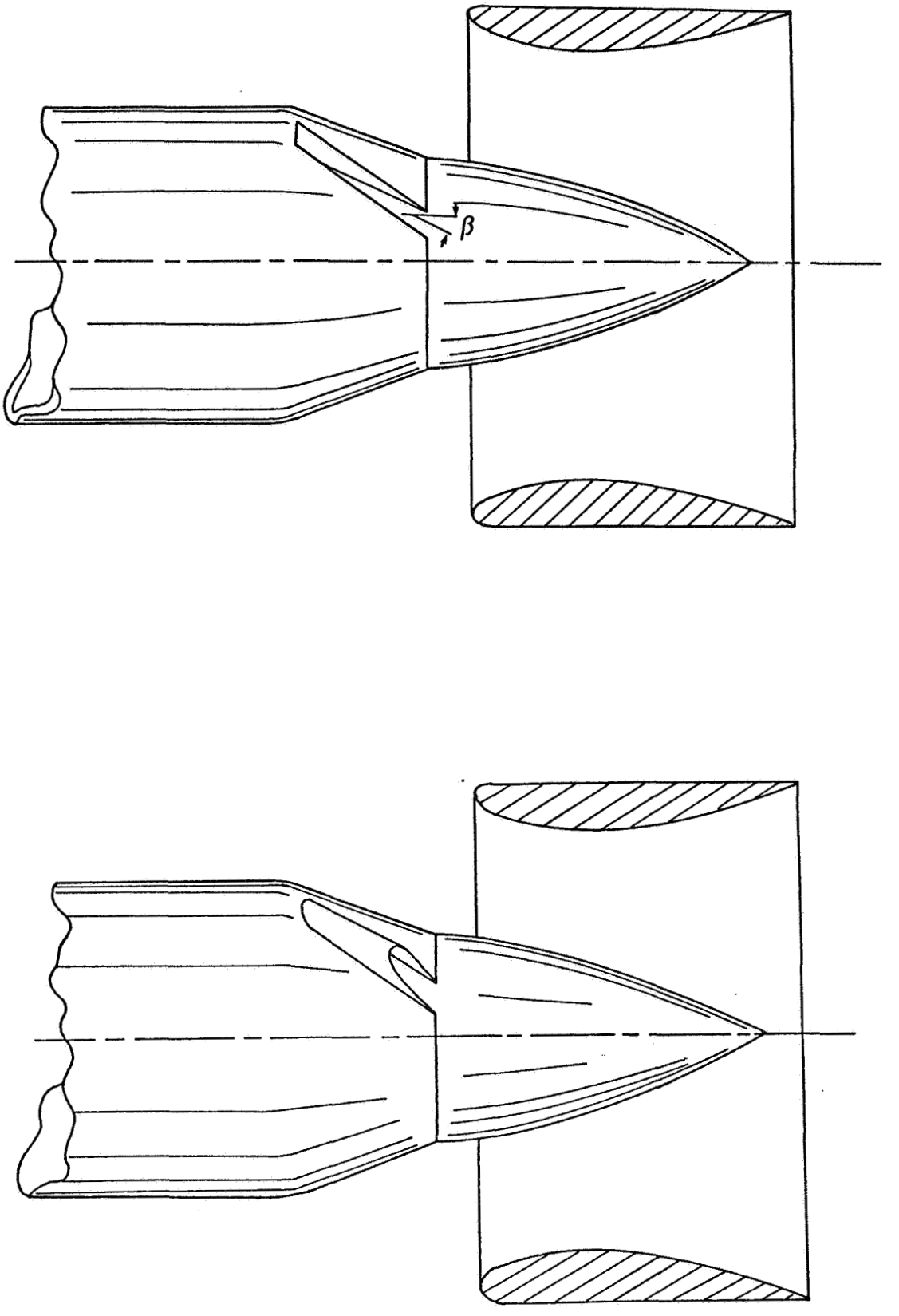

Figure 5.- Unhooded and hooded rotor nozzles.

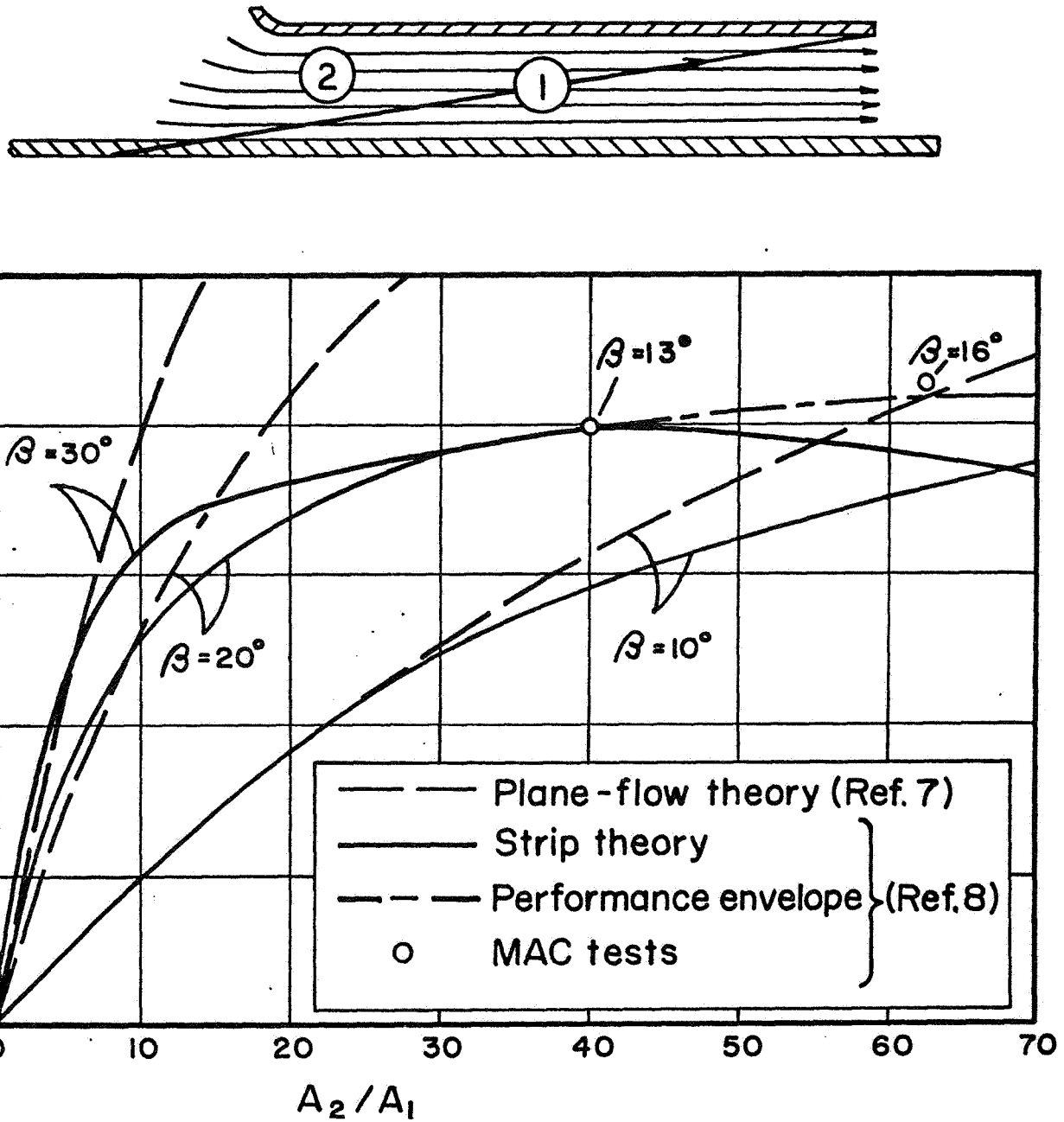

Figure 6.- Analytical model for thin-jet strip theory.

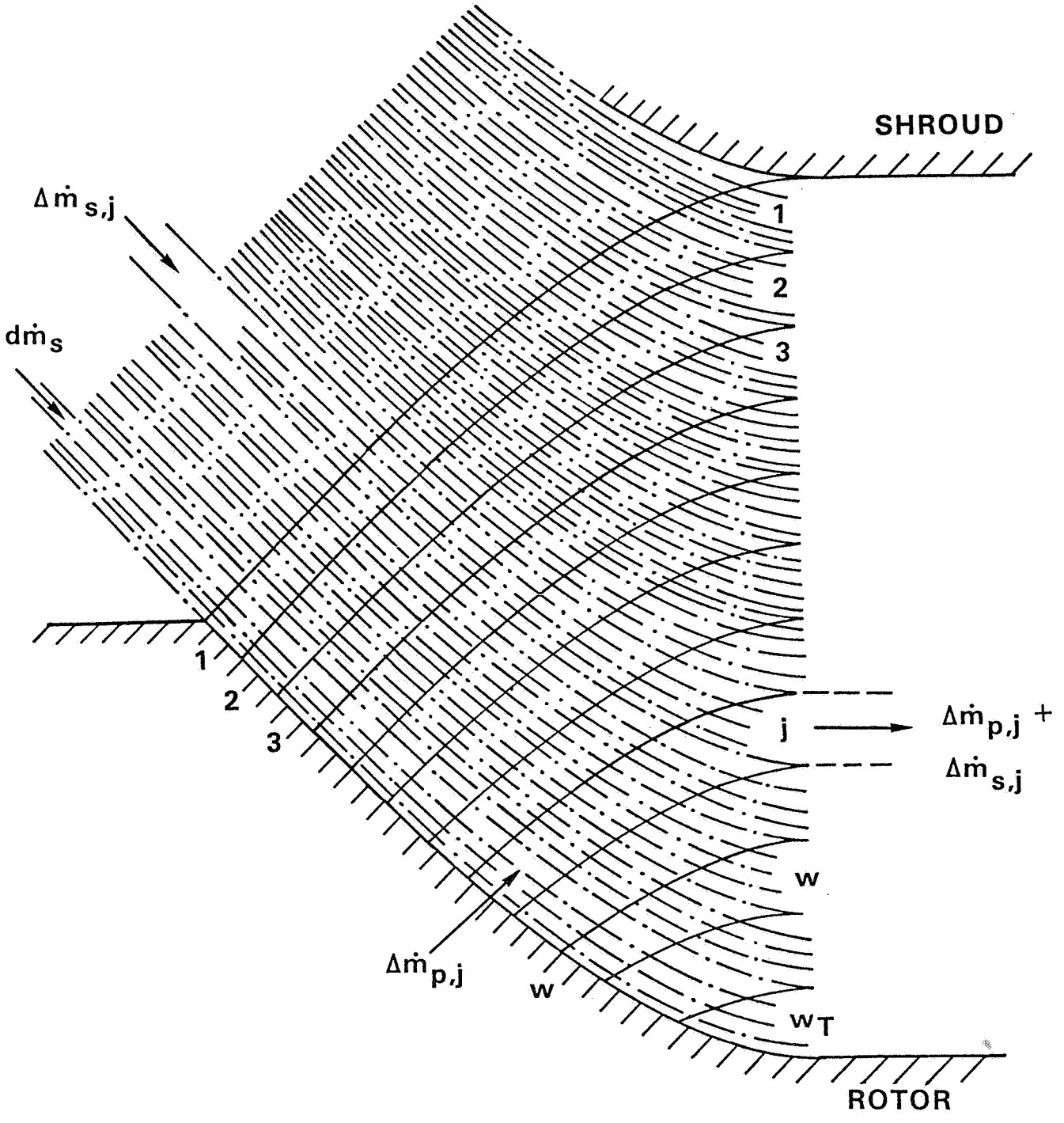

Figure 7.- Analytical model for wide-jet strip theory.

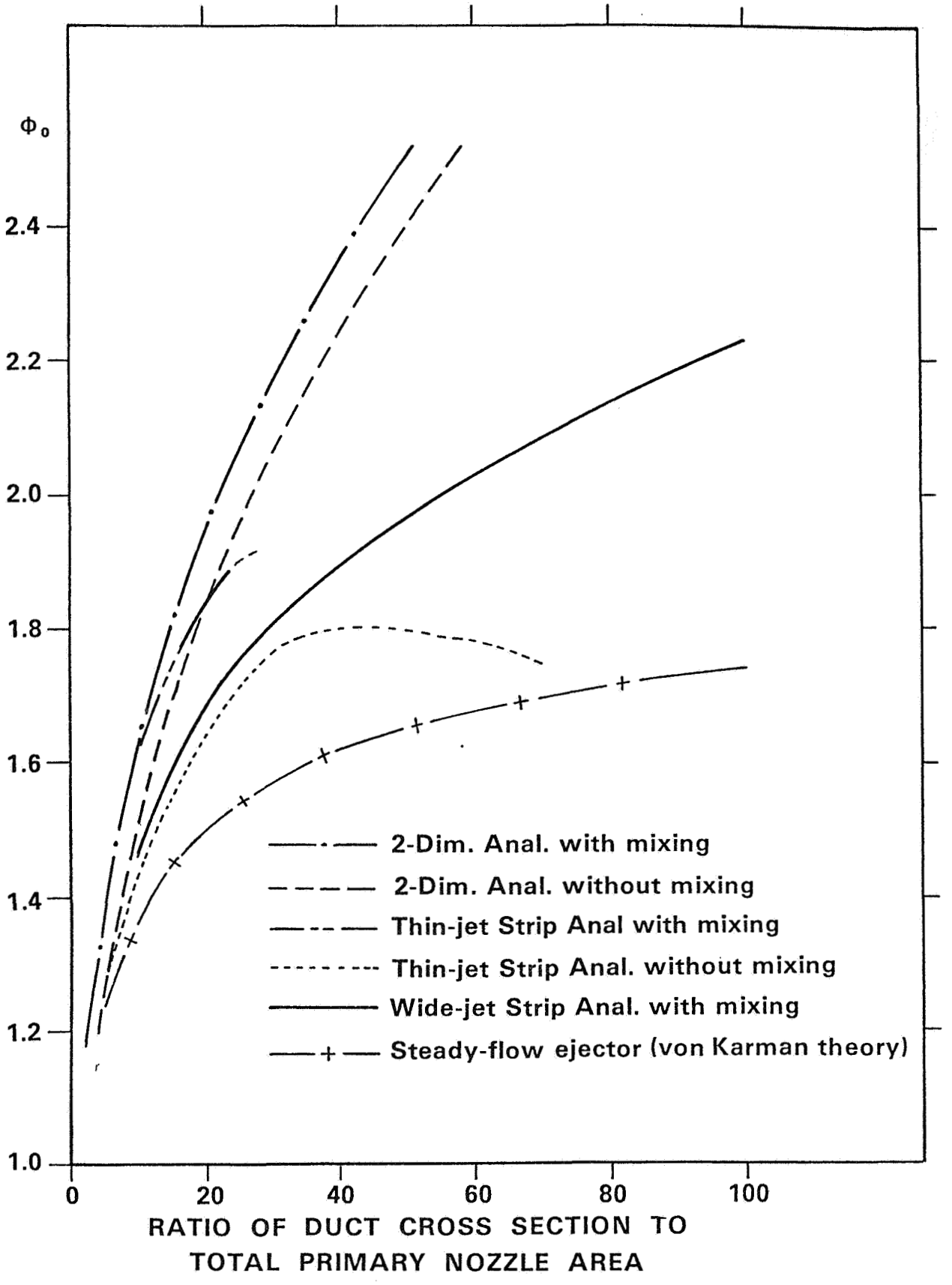

Figure 8.- Comparison of static thrust augmentation ratios predicted by various theories for constant-area interaction ducts and for a rotary-jet spin angle (inclination of primary nozzle axis to meridional plane) of 20°.

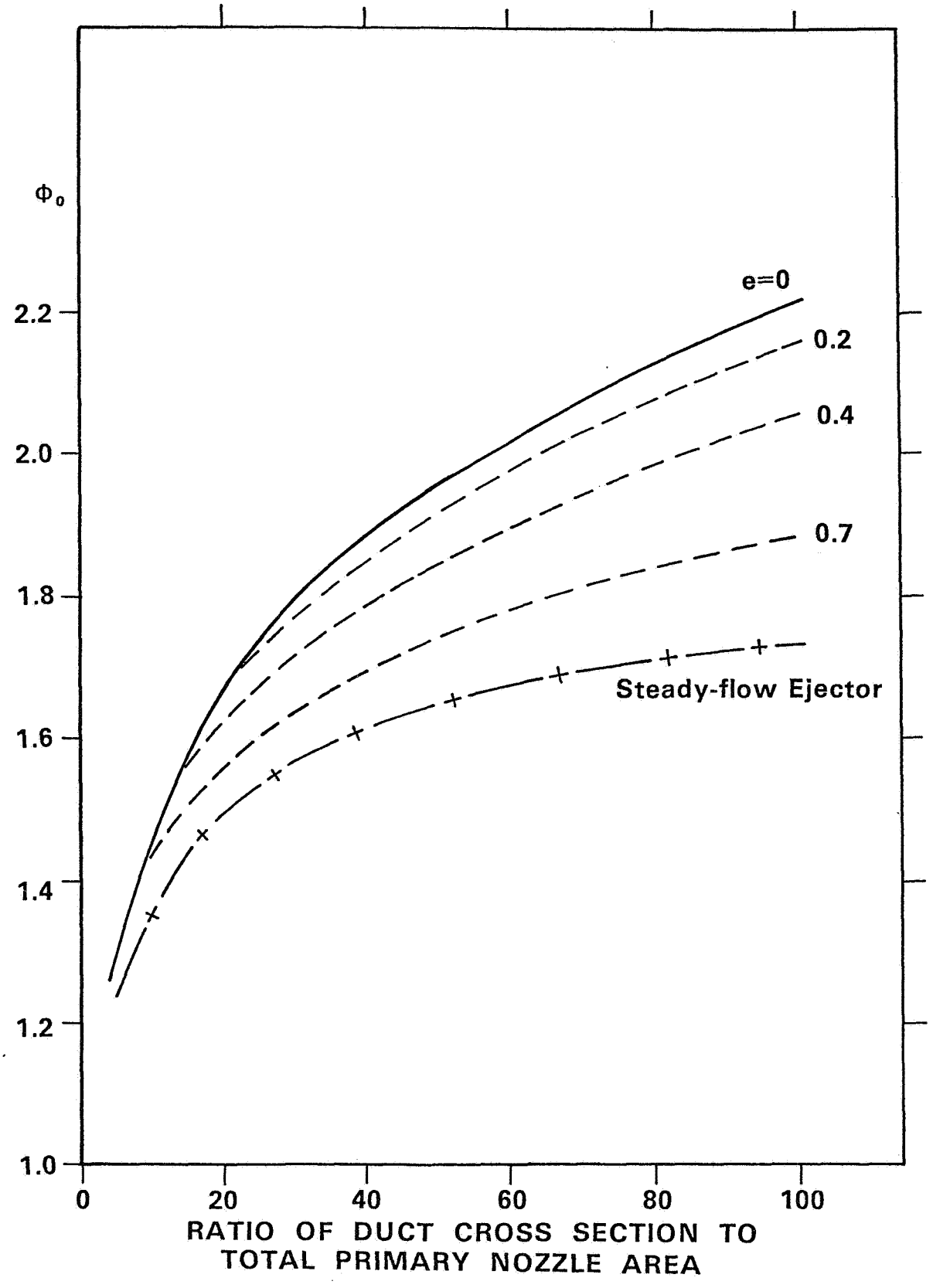

Figure 9.- Effect of mixing during pressure exchange. e = percentage of secondary flow entrained during pressure exchange. Rotary-jet spin angle = 20°.

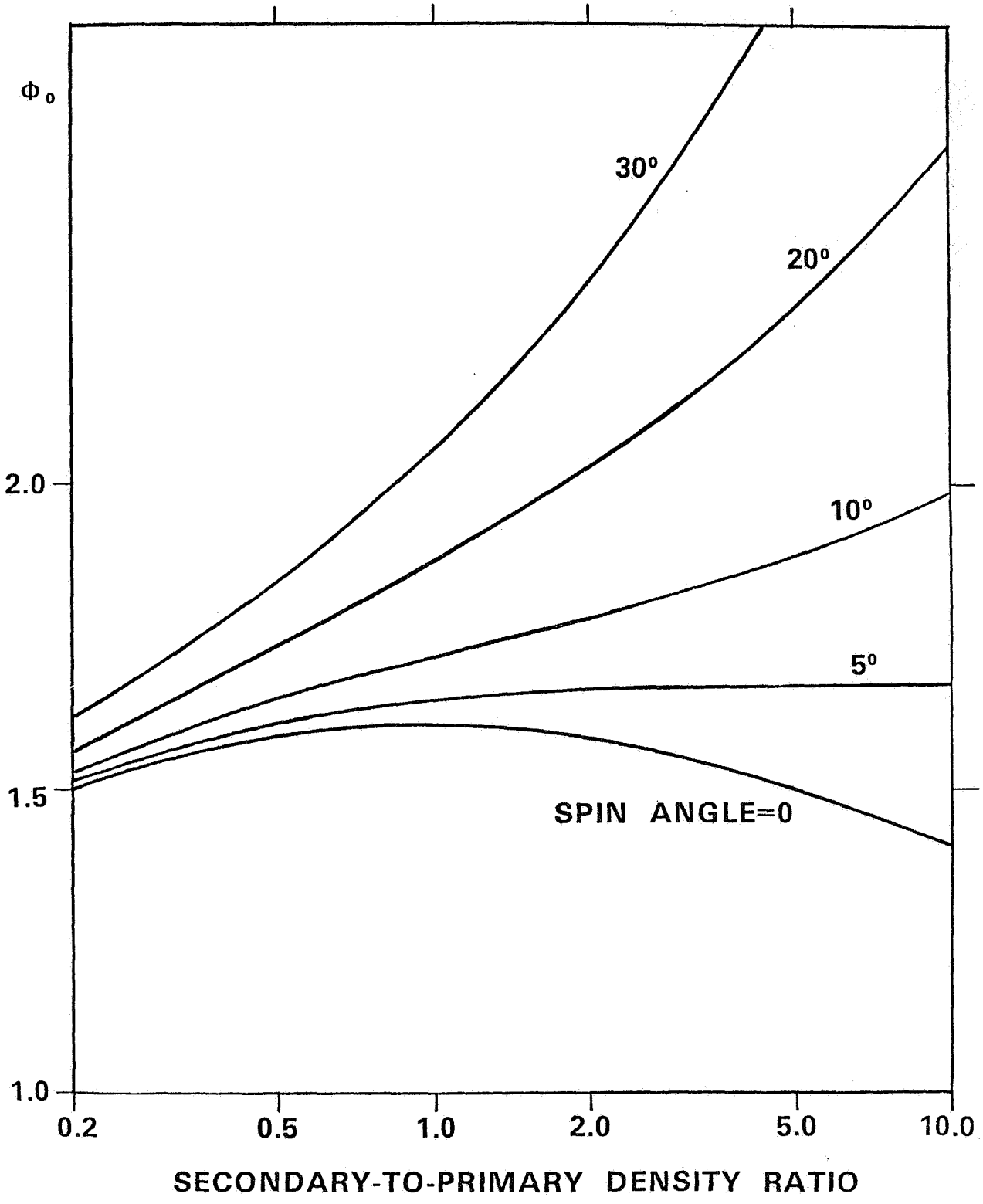

Figure 10.- Effect of secondary-to-primary density ratio on static thrust augmentation, for various spin angles. Constant-area interactions. Ratio of duct cross section to primary nozzle area = 30. Ratio of primary total pressure to ambient pressure = 1.5.

LINEARIZED UNSTEADY JET ANALYSIS

Hermann Viets** and Michael Piatt***
Wright State University
Dayton, Ohio 45435

1. Introduction

The introduction of a time dependency into a jet flow to change the rate at which it mixes with a coflowing stream or ambient condition has been investigated by several researchers[1-7]. The advantage of the unsteady flow is an increase in the mixing rate as compared to a "steady" jet. The disadvantage, in the case of a jet nozzle, is the fact that the nozzle efficiency suffers significantly[6].

Examples of the types of jets which may be treated by the present analysis are shown in Figures 2-4. The jet exit position of Figure 2 oscillates from side to side and produces a relatively constant magnitude streamwise wave. In Figure 3 the velocity vector at the jet exit oscillates in direction and produces a growing streamwise wave. The unsteadiness of Figure 4 consists of a sinusoidal change with time of the mass flow at the jet exit and thus produces a nominally constant amplitude wave pattern.

The mathematical complexity of time dependent flows is such that one usually is forced to resort to one of three possible attacks:

(a) A fully numerical solution of the governing equations

(b) A phenomenological model

(c) The use of limiting assumptions which simplify the governing equations.

A fully numerical solution is possible but requires the dedication of very

* Supported by AFOSR Grant No. 78-3525, Monitored by AFFDL/FXM.
Thanks are due to M.W. Ball for the construction of the experimental apparatus.
** Associate Professor
*** Graduate Student

significant amounts of time and effort. A recent interesting example of a phenomenological model is presented by Simmons, Platzer and Smith[8], who assume that the unsteady jet may be decomposed into a number of steady jets which exist during short intervals at the nozzle exit and produce short bursts along the steady jet trajectories.

Much of the unsteady flow work employing limiting assumptions is based in principle on the celebrated work of Lin[9], who analysed the boundary layer beneath a time dependent external flow. Lin's technique is limited to high frequencies and benefits from the fact that the particular problem allows the specification of an unsteady static pressure distribution within the boundary layer. The extension of Lin's analysis to the jet case is hampered by the fact that the time dependent pressure distribution is unknown and there is no comparable technique to Lin's use of the unsteady Bernoulli equation.

The application of Lin's technique to unsteady jets was carried out by McCormack, Cochran and Crane[4] for the case of a jet vibrated from side to side at high frequency (see Figure 2). However, the strict application of the Lin analysis leads to the conclusion that the convective term in the momentum equation is negligibly small. This result is not acceptable to McCormack, et al., since it is clear that the convective term is of importance as in the steady flow case. Thus, the authors present a phenomenological argument that the convective term must be included (in spite of the fact that the analysis excludes the term) and proceed to assume a linear form for it which then results in a linear equation. The analysis, therefore, is a mixture of types b and c above.

The present analysis follows the spirit of the linearized jet analyses due to Pai[10]. The linearization of the equations is achieved by an order of magnitude analysis which is rigorous and removes the need for a phenomenological argument. The requirement of high frequency is also removed and a technique described for including a time dependent pressure distribution which is produced

by the motion of the jet.

2. RELATIONSHIP BETWEEN UNSTEADY AND TIME AVERAGED FLOWS

The objective of this study is to determine the effect of the unsteady flow components on the time averaged flow. That is, what advantages does the unsteady flow hold in terms of steady state mass and momentum transfer? The answer should appear in a steady flow relation including time averaged effects of the unsteady components.

The two-dimensional boundary layer equations are

$$\frac{\delta u}{\delta t} + u\frac{\delta u}{\delta x} + v\frac{\delta u}{\delta y} = -\frac{1}{\rho}\frac{\delta p}{\delta x} + \frac{1}{R}\frac{\delta^2 u}{\delta y^2} \qquad (1)$$

$$\frac{\delta u}{\delta x} + \frac{\delta v}{\delta y} = 0 \qquad (2)$$

where each term is non-dimensionalized so R = Reynolds Number.

Consider the velocity profiles shown in Figure 1. The initial jet velocity is a function of time while the coflowing stream velocity is steady. The independent variables can then be separated into time averaged ($\bar{}$) and time dependent ( )′ quantities with U = coflowing stream velocity.

$$\begin{aligned} u(x, y, t) &= U + \bar{u}(x, y) + u'(x, y, t) \\ v(x, y, t) &= \bar{v}(x, y) + v'(x, y, t) \\ p(x, y, t) &= \bar{p}(x, y) + p'(x, y, t) \end{aligned} \qquad (3)$$

Substituting the expansions of the independent variables into the momentum equation and taking the time average of each term results in

$$(U+\bar{u})\frac{\delta \bar{u}}{\delta x} + \bar{v}\frac{\delta \bar{u}}{\delta y} = \frac{\delta \bar{p}}{\delta x} - \left[\overline{u'\frac{\delta u'}{\delta x}} + \overline{v'\frac{\delta u'}{\delta y}}\right] + \frac{1}{R}\frac{\delta^2 \bar{u}}{\delta y^2} \qquad (4)$$

It may be seen that the effect of the unsteady terms on the average velocity is the same as an additional (or artificial) pressure gradient. Thus, if the time dependent velocities are known, the bracketed term can be evaluated and the effect of the unsteadiness on the mean flow determined. The following

section will discuss the evaluation of the unsteady flow conditions.

3. DETERMINATION OF TIME DEPENDENT VELOCITIES

The objective is, therefore, to determine the unsteady velocity components u' and v', to evaluate the bracketed term in Eqn. 4 and thereby to find the average velocity distribution $U + \bar{u}, \bar{v}$. Approximate solutions for u' and v' can be found by the following order of magnitude analysis.

Consider the case where the steady state jet velocity deviates only slightly from the coflowing stream velocity and, as well, the unsteady velocity components are small compared to the coflowing stream velocity.

Mathematically -

$$\bar{u},\bar{v},u',v', \ll U \qquad (5)$$

Expanding the momentum equation (1) by the steady and unsteady velocity components (Eqn. (3)) results in

$$\frac{\delta u'}{\delta t} + (U+\bar{u}+u') \frac{\delta}{\delta x}(U+\bar{u}+u') + (\bar{U}+v') \frac{\delta}{\delta y}(U+\bar{u}+u')$$

$$= \frac{\delta}{\delta x}(\bar{p}+p') + \frac{1}{R} \frac{\delta^2}{\delta y^2}(U+\bar{u}+u') \qquad (6)$$

In view of the assumptions (5), all products of small variables in Eqn. (6) are neglected and only terms up to first order in the small variables are retained.

(Note also that U = constant)

$$\frac{\delta u'}{\delta t} + U \frac{\delta \bar{u}}{\delta x} + U \frac{\delta u'}{\delta x} = - \frac{\delta p}{\delta x} - \frac{\delta p'}{\delta x} + \frac{1}{R}\left(\frac{\delta^2 \bar{u}}{\delta y^2} + \frac{\delta^2 u'}{\delta y^2}\right) \qquad (7)$$

The steady and unsteady portions of Eqn. (7) may be separated by taking the time average of (7):

$$U \frac{\delta \bar{u}}{\delta x} = - \frac{\delta p}{\delta x} + \frac{1}{R} \frac{\delta^2 \bar{u}}{\delta y^2} \qquad (8)$$

and subtracting this from (7) to yield

$$\frac{\delta u'}{\delta t} + U\frac{\delta u'}{\delta x} = -\frac{\delta p'}{\delta x} + \frac{1}{R}\frac{\delta^2 u'}{\delta y^2} \qquad (9)$$

This, then, is the governing equation for the unsteady velocity distribution for the jet in Figure 1 with the small perturbation assumptions of equation (5). The initial condition may be seen from Figure 1 to be a top hat velocity profile whose magnitude is a function of time. The lateral boundary conditions are that

$$\lim_{y \to \pm\infty} u' = 0 \qquad (10)$$

The unsteady pressure gradient may, in general, be a function of position and time,

$$\frac{\delta p'}{\delta x} = f(x,y,t)\,, \qquad (11)$$

but is not known directly in the jet case. In a later section a technique is described which allows an approximation to the unsteady pressure distribution. For the present, the pressure will be neglected and thus the governing equation reduces to

$$\frac{\delta u'}{\delta t} + U\frac{\delta u'}{\delta x} = \frac{1}{R}\frac{\delta^2 u'}{\delta y^2} \qquad (12)$$

This equation is similar to that developed in Reference 4, but in this case it is not limited to high frequencies and requires no phenomenological arguments. The initial and boundary conditions are the same as those for Equation (9). The solution to the linear Equation (12) is

$$u' = \frac{\alpha U}{2}\, e^{i(wT - wX)} \left[\operatorname{erf}\left(\frac{1-y}{2\sqrt{X}}\right) + \operatorname{erf}\left(\frac{1+y}{2\sqrt{X}}\right)\right] \qquad (13)$$

where

$$T = t/R,\ X = x/RU,\ \alpha = \frac{u'}{U}\bigg|_{x=0}$$

and the error function is defined as

$$\operatorname{erf}\eta = \frac{2}{\sqrt{\pi}}\int_0^{\eta} e^{-\eta^2}\, d\eta \qquad (14)$$

The actual form of the exponential depends upon the initial condition on the jet. If the initial condition is that the unsteady flow varies about some mean as a cosine function, then the solution is -

$$u' = \frac{\alpha U}{2} \cos(wT - wX) \left[\operatorname{erf}\left(\frac{1-y}{2\sqrt{X}}\right) + \operatorname{erf}\left(\frac{1+y}{2\sqrt{X}}\right)\right] \qquad (15)$$

4. DETERMINATION OF THE STEADY ARTIFICIAL PRESSURE GRADIENT

The overall continuity Equation (2) can be expanded by the velocity definitions, Eqn. (3), and then split into steady and unsteady forms,

$$\frac{\delta \bar{u}}{\delta x} + \frac{\delta \bar{v}}{\delta y} = 0 \quad \text{and} \quad \frac{\delta u'}{\delta x} + \frac{\delta v'}{\delta y} = 0 \qquad (16)$$

from which it follows that

$$v' = -\int_0^y \frac{\delta u'}{\delta x}\, dy \qquad (17)$$

Then from Eqns. (15) and (17)

$$v' = -\frac{\alpha w}{2} \sin(wT - wX) \int_0^y \left[\operatorname{erf}\left(\frac{1-y}{2\sqrt{X}}\right) + \operatorname{erf}\left(\frac{1+y}{2\sqrt{X}}\right)\right] dy$$

$$\frac{\alpha \cos(wT - wX)}{4\sqrt{\pi}\, X^{3/2}} \int_0^y \left[\exp\left(-\left(\frac{1-y}{2\sqrt{X}}\right)^2\right)(1-y) \right.$$

$$\left. + \exp\left(-\left(\frac{1+y}{2\sqrt{X}}\right)^2\right)(1+y)\right] dy \qquad (18)$$

The resulting artificial pressure gradient term is

$$\left[\overline{u' \frac{\delta u'}{\delta x}} + \overline{v' \frac{\delta u'}{\delta y}} \right]$$

$$= F_1 F_3 \overline{\cos(wT - wX) \sin(wT - wX)}$$
$$+ F_1 F_4 \overline{\cos^2(wt - wX)}$$
$$+ F_6 F_9 \overline{\sin(wt - wX) \cos(wT - wX)}$$
$$+ F_7 F_9 \overline{\cos^2(wT - wX)} \qquad (19)$$

where the F_i terms are independent of time. The averaging of the trigonometric terms over one cycle results in

$$\overline{\cos^2(wT - wX)} = \tfrac{1}{2}$$
$$\overline{\sin(wT - wX) \cos(wT - wX)} = 0 \qquad (20)$$

so-

$$\left[\overline{u' \frac{\delta u'}{\delta x}} + \overline{v' \frac{\delta u'}{\delta y}} \right] = \frac{1}{2} F_1 F_4 + \frac{1}{2} F_7 F_9 \qquad (21)$$

where

$$F_1 = \frac{\alpha U}{2}\left[\operatorname{erf}\left(\frac{1-y}{2\sqrt{X}}\right) + \operatorname{erf}\left(\frac{1+y}{2\sqrt{X}}\right)\right]$$

$$F_4 = \frac{-\alpha}{4\sqrt{\pi}}\, X^{3/2}\left\{\exp\left[-\left(\frac{1-y}{2\sqrt{X}}\right)^2\right](1-y) + \exp\left[-\left(\frac{1+y}{2\sqrt{X}}\right)^2\right](1+y)\right\}$$

$$F_7 = \frac{\alpha}{2\sqrt{\pi}}\, X^{1/2}\left\{\exp\left[-\left(\frac{1-y}{2\sqrt{X}}\right)^2\right] + \exp\left[-\left(\frac{1+y}{2\sqrt{X}}\right)^2\right]\right\}$$

$$F_9 = -U F_7 \qquad (22)$$

With the artificial pressure gradient known, the steady state velocity distribution may be found numerically from Eqn. (4). The numerical results, however, are not yet available.

It should be noted that the final solution of Eqn. (4) cannot be a function of magnitude of the jet frequency since none of the terms in Eqn. (22) depend on frequency. The importance of this fact will become apparent in the next section.

5. EXPERIMENTAL OBSERVATIONS

The jet flow illustrated in Figure 3 has been investigated experimentally, as shown schematically in Figure 5, to determine the unsteady inputs into the time averaged jet behavior. The data are taken by a two channel hot wire anemometer probe, linearized, averaged, and read out on a set of digital voltmeters. The average is found by an electronic filter designed for this experiment by McCormack[11]. The jet nozzle is fluidically controlled, as shown in Figure 6, and is based on a design by Viets[5].

A set of time averaged velocity profiles showing the typical development of the jet in the streamwise direction is shown in Figure 7. The double

peaked profiles are caused by the time dependent flow inclination at the nozzle exit and disappear as the mixing progresses downstream. Although these profiles are for a jet streaming into an ambient condition, upcoming experiments will address the coflowing stream situation.

The most important data from the point of view of the present analysis is shown in Figure 8; the comparison of steady half width growth rates for the same jet at various oscillation frequencies. The half width is defined here as the distance from the jet centerline to the position on the profile where the velocity is half the maximum velocity found on the profile. It may be seen that there is an appreciable effect of frequency on the jet half width growth, with the minimum growth at a frequency of zero, i.e. the steady two dimensional jet.

If one examines the time averaged term which reflects the effect of unsteadiness on the mean velocity distribution, Equation (21), it can be seen that this term is not a function of frequency. This is true since none of its components [Eqn. (22)] depend on frequency. There are three strong possibilities for this discrepancy.

a. The analysis is linear while the jet is non-linear. ———
   This effect will be investigated in upcoming tests which will feature an experiment satisfying the linearizing assumptions.

b. The analysis is applicable but the eddy viscosity is not the same as the steady state (a very likely situation) and is, in particular, a function of frequency. ———
   This point may be clarified by comparison of the analysis to the experiments in a.

c. The time dependent pressure distribution in Equation (9) is not zero as was assumed earlier in the analysis but is really a function of frequency. ———
   This possibility is examined in the following section.

6. EFFECT OF A TIME DEPENDENT PRESSURE VARIATION

The basis for an unsteady pressure distribution is the interaction between the unsteady jet and the coflowing stream. If one considers the simplest case of a jet which does not mix with the ambient fluid, then the jet surface appears as a traveling sinusoidal wave to the coflowing stream. The inclusion of mixing modifies the shape of this wave but near the jet exit the shape is still very nearly sinusoidal.

The simplest model for the pressure variation produced by a wave pattern is that produced by the inviscid flow over a wavy wall, shown in Figure 9. A linearized treatment of this problem is given by Liepmann and Roshko[12] and results in the pressure distribution

$$P = P_\infty \left(1 - B \epsilon \alpha \sin \alpha x\right) \qquad (23)$$

where B depends upon the freestream conditions, P_∞ is the freestream pressure and the other variables are defined in Figure 9. It may be seen that the pressure variation is in phase with the wall shape.

The real jet case is, of course, a viscous problem (as is the real wavy wall case). Thus, the pressure dependence is not as straight-foreward as indicated above. This has been demonstrated experimentally by Kendall[13], who studied a mechanical wave traveling relative to a free stream. Kendall's results indicate a phase shift between the wall shape and the pressure distribution. The magnitude of the phase shift depends upon the ratio of the wave speed to the coflowing stream velocity. For a wave speed approximately equal to the coflowing stream velocity, the phase shift is approximately 10° downstream.

With the velocity varying as a cosine function as in Eqn. (15), the static pressure should vary as a sine function. In addition there must be a phase shift and the boundary conditions require that the pressure approach

the limit of the free stream pressure as the distance from the jet increases. The pressure dependence satisfying these conditions as well as the requirement that the pressure be proportional to the square of the velocity difference between the coflowing stream and wave speed is

$$P' = -\frac{C_p \rho (U - c)^2}{2} e^{-\sqrt{R}|y|} \sin\left[w(T - T_0) - wX\right] \qquad (24)$$

where C_p may be obtained from Kendall[13]. Including this term in the governing differential Equation (9) gives rise to another term in the solution for u' in order to balance the $\frac{dp}{dx}$ term.

Then

$$u' = u'_{p'=0} - \frac{C_p \rho (U - C)^2}{U/w} e^{-\sqrt{R}|y|} \cos\left[w(T - T_0) - wX\right] \qquad (25)$$

The main point here is that u' now is a function of frequency and therefore the bracketed term in Eqn. (4) is also a function of frequency. Thus the inclusion of the time dependent pressure allows the prediction of an average velocity $\bar{u}$ which depends upon frequency. The numerical results for this case are not yet available.

7. CONCLUSION

The foregoing analysis shows that the unsteady flowfield generated by a time dependent jet can be treated by a linearized attack which is not limited by frequency constraints and evolves through a rigorous simplification of the equations of motion. The numerical integration of the full non-linear equations to produce the time averaged solution is currently underway.

8. REFERENCES

1. Binder, G. and Favre-Marinet, M. "Mixing Improvement in Pulsating Turbulent Jets," ASME Symposium on Fluid Mechanics of Mixing, June 20-22, 1973.

2. Curtet, R.M. and Girad, J.P., "Visualization of a Pulsating Jet," ASME Symposium on Fluid Mechanics of Mixing, June 20-22, 1973.

3. Crow, S.C. and Champagne, F.H., "Orderly Structure in Jet Turbulence," J. of Fluid Mechanics, Vol. 48, Part 3, 1971, pp. 547-591.

4. McCormack, P.D.; Cochran, D. and Crane, L., "Periodic Vorticity and Its Effect on Jet Mixing," Physics of Fluids, Vol. 9, No. 8, August 1966, p. 1555.

5. Viets, H., "Flip-Flop Jet Nozzle," AIAA Journal, Vol. 13, No. 10., October 1975, pp. 1375-1379.

6. Viets, H.; Blaster, D. and Toms, H.L., "Time Dependent Fuel Injectors," AIAA Paper No. 75-1305, 11th Propulsion Conference, 1975.

7. Platzer, M.F.; Deal, L.J. and Johnson, W.S., "Experimental Investigation of Oscillatory Jet Flow Effects, Unsteady Aerodynamics, Vol. 1, R. B. Kinney, Ed., U. of Arizona, March 1975.

8. Simmons, J.M.; Platzer, M.F. and Smith, T.C., "Velocity Measurements in an Oscillating Plane Jet Issuing into a Moving Air Stream," J. Fluid Mechanics, Vol. 84, part 1, 1978, pp. 33-53.

9. Lin, C.C., "Motion in the Boundary Layer with a Rapidly Oscillating External Flow," in the Proceedings of the Ninth International Congress on Applied Mechanics, Vol. 4, p. 155, Elsevier, Inc., Amsterdam, 1957.

10. Pai, S.I. and Hsieh, T.Y., "Linearized Theory of Three Dimensional Jet Mixing With and Without Walls," J. Basic Engineering, Vol. 92, March 1970, pp. 93-100.

11. McCormack, W.S., Personal Communication, Wright State University, 1978.

12. Liepmann, H.W. and Roshko, A., Elements of Gas Dynamics, Wiley, 1957.

13. Kendall, J. M., "The Turbulent Boundary Layer Over A Wall With Progressive Surface Waves," J. Fluid Mechanics, Vol. 41, Part 2, 1970, pp. 259-281.

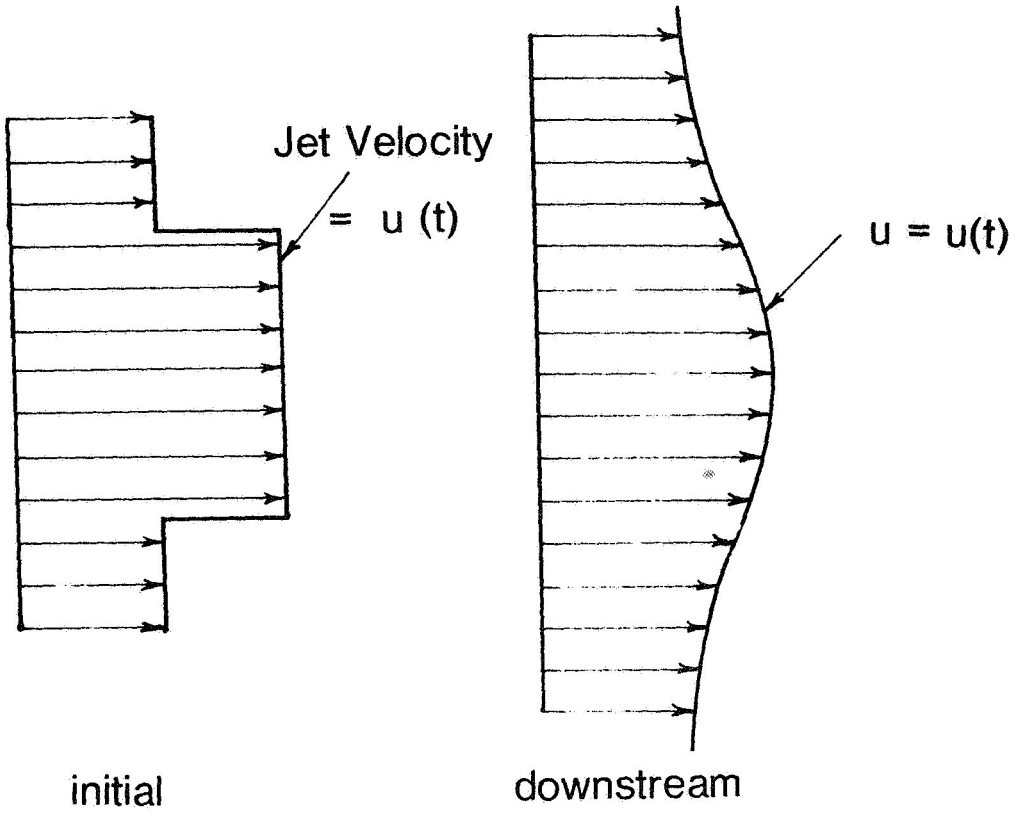

Figure 1. Initial and downstream velocity profiles.

Figure 2. Schematic of the vibrated jet studied by McCormack, Cochran and Crane[4].

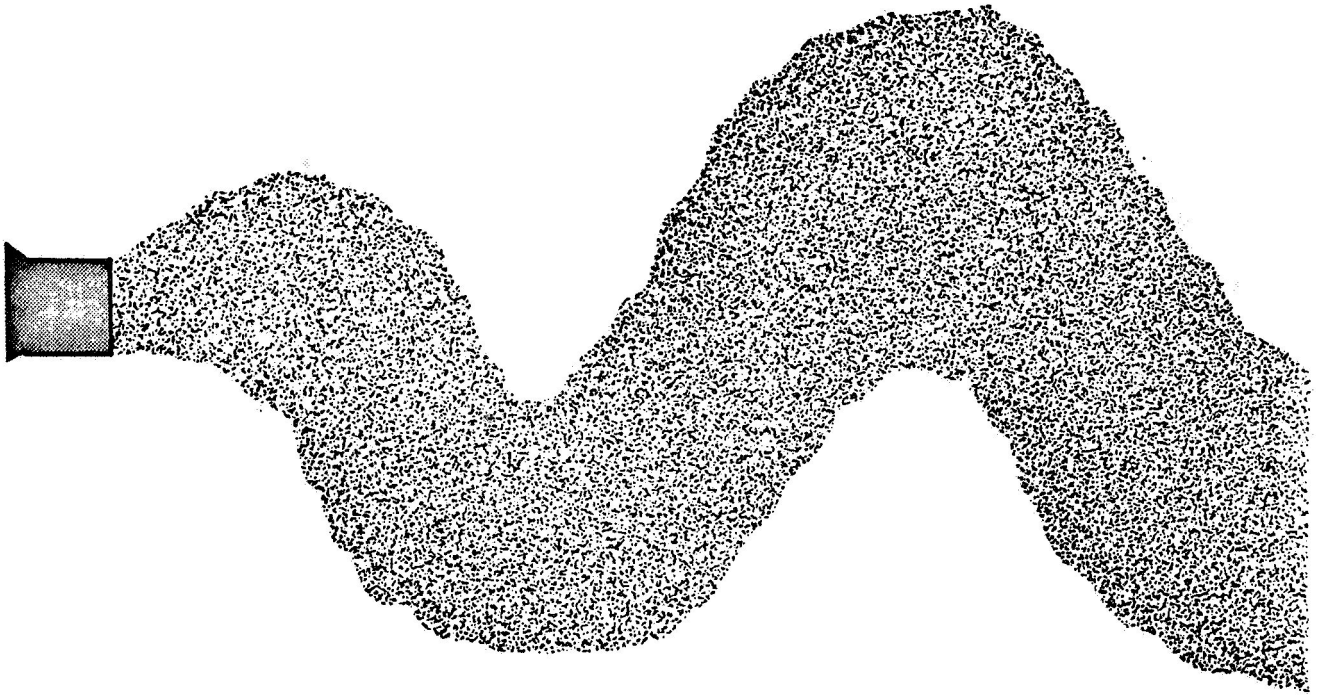

Figure 3. Flapping jet with angular time variation at the exit studied by Viets et al.[5-6] and Platzer et al.[7-8]

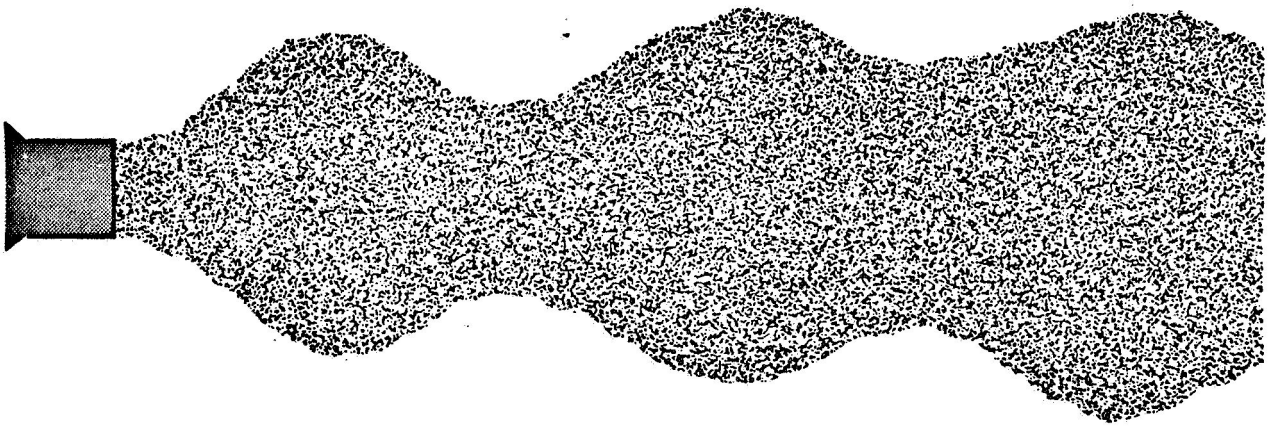

Figure 4. Jet with time dependent mass flow studied by Binder and Favre-marinet[1] and Curtet and Girad[2].

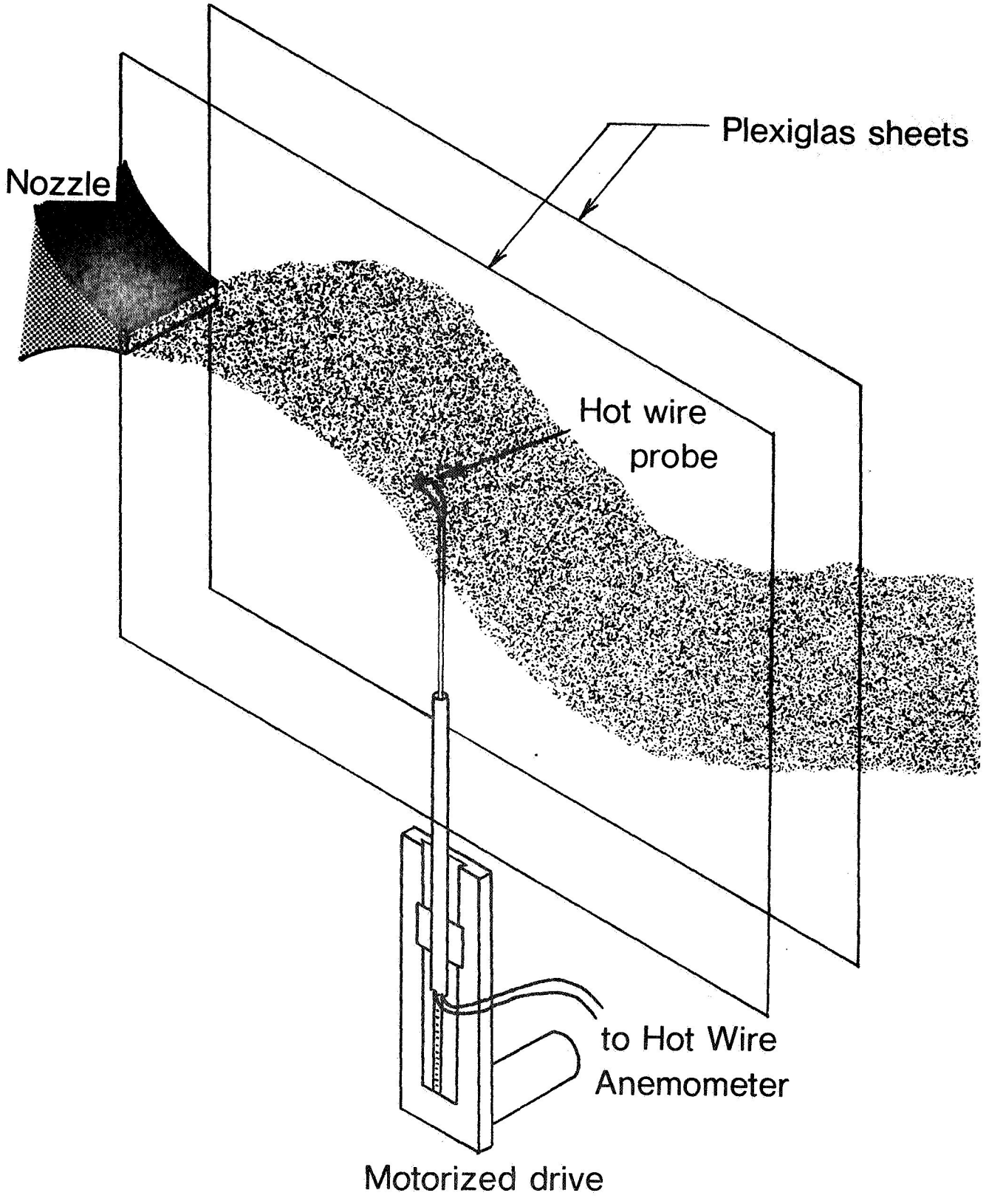

Figure 5. Experimental Setup.

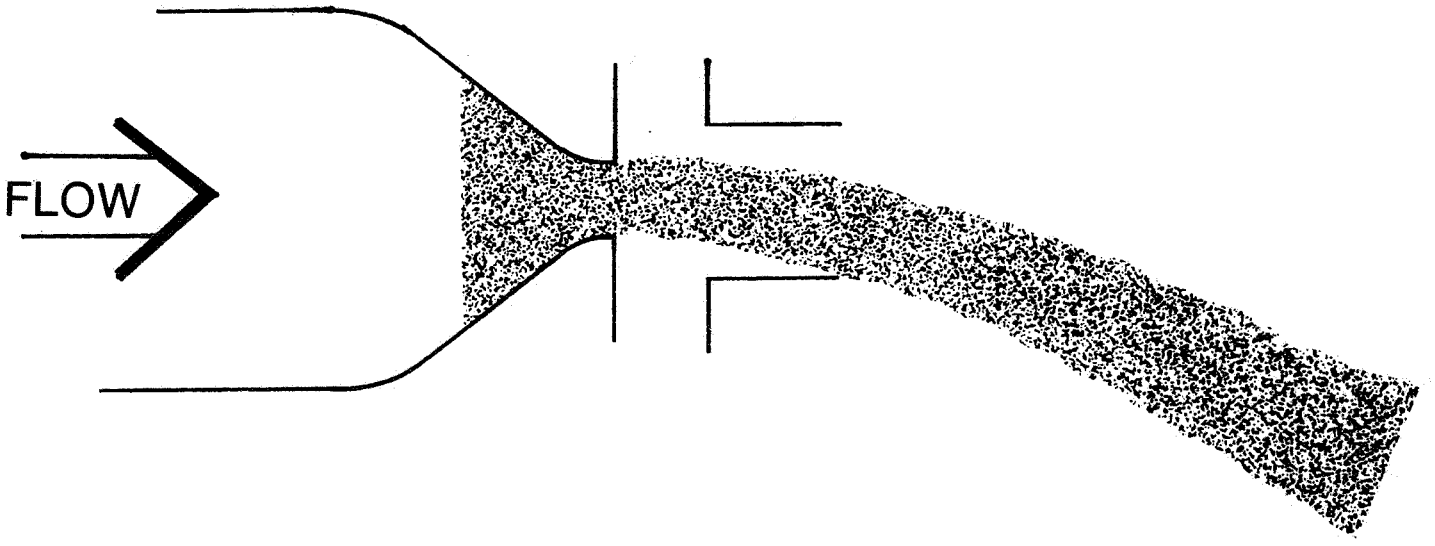

Figure 6. Fluidically Controlled Jet Nozzle Design.

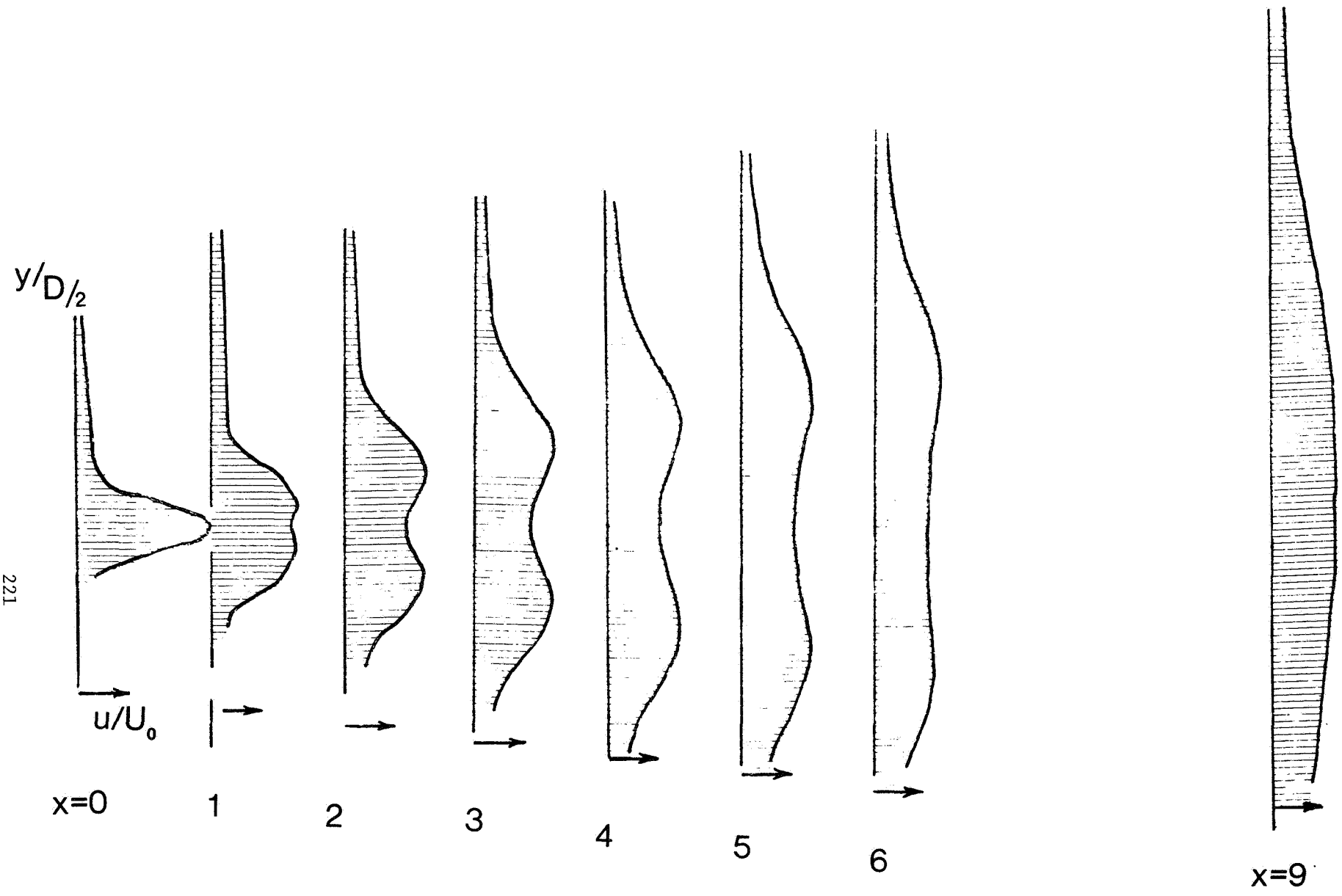

Figure 7. Development of the flapping jet in the streamwise direction.

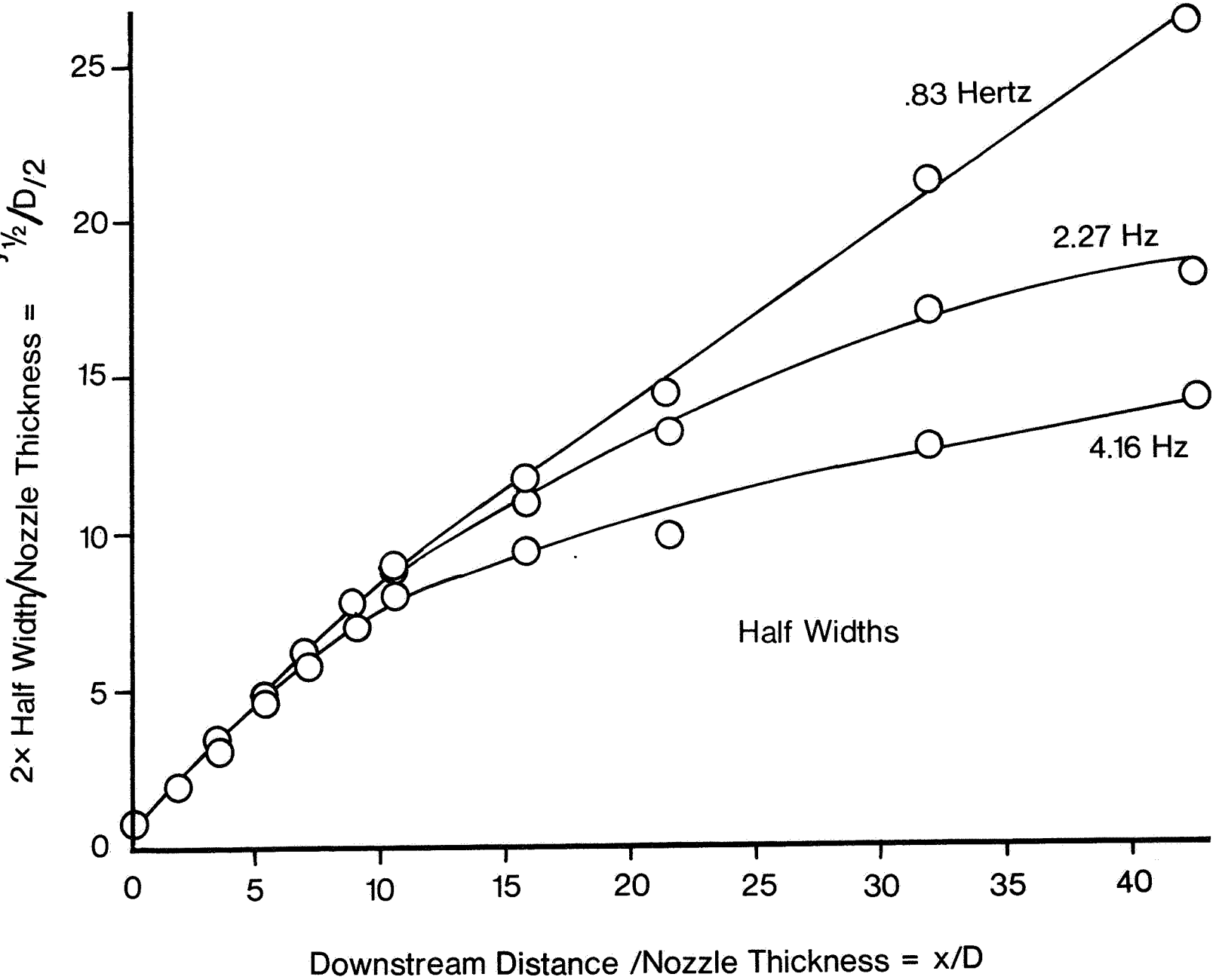

Figure 8. Half width growth dependent upon oscillation frequency.

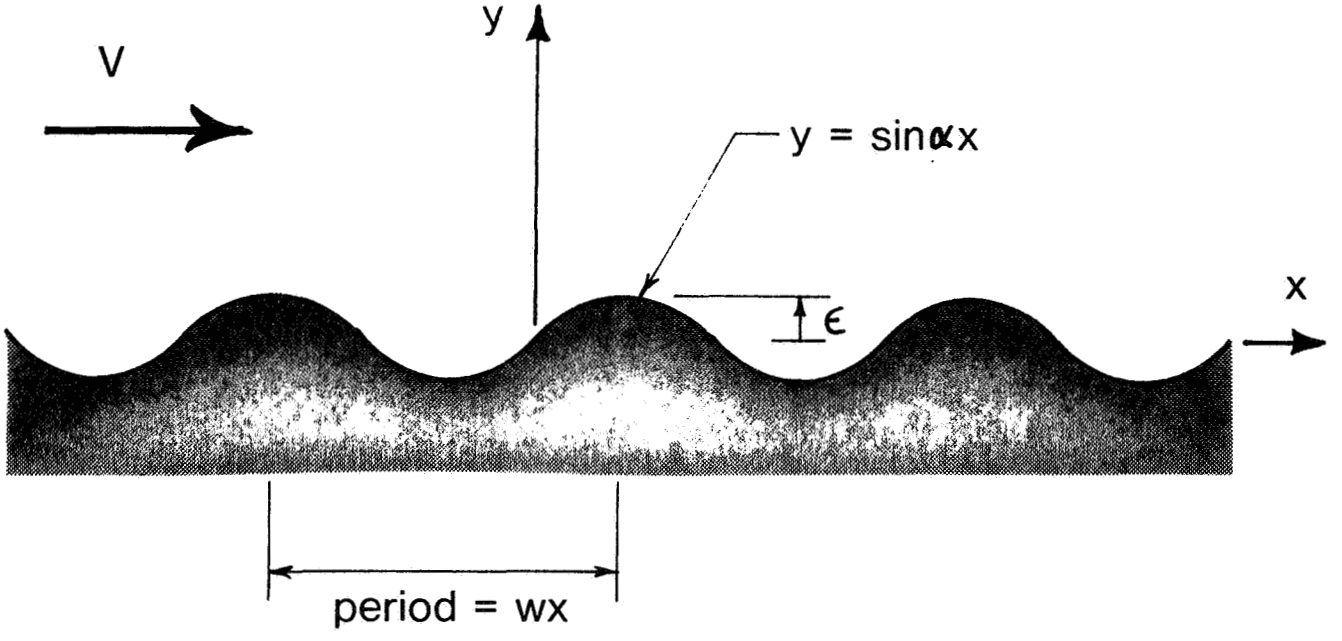

Figure 9. Flow over a wavy wall.

INTEGRATION OF EJECTORS INTO HIGH-SPEED AIRCRAFT

Tirumalesa Duvvuri

Duvvuri Research Associates
Chula Vista, California

The subject I will talk about is of interest in the sense that most of the studies and analyses that are done on the ejectors are for static case and do not attend to the forebody effects. Because most of the ejectors are mounted on something, we might call the analysis that we have essentially isolated ejector analysis.

Now everything that we normally see in these analyses is what we might call rectilinear mixing; in other words, we assume that the two flows, the primary and the secondary, are more or less parallel. But even a very small pressure differential could create a curvature in the flow, and then the rectilinear mixing has to be modified to account for the curvature. For example, this would modify the eddy viscosity, and in cases where you have coanda jet, the flow will be completely asymmetric. There is no asymmetric in the flow at all inside the ejector. In addition to this, when the forebody is put in there, the flow that enters the ejector is not a very simple flow. So we have the question, what happens? We spend money developing a beautiful ejector producing 2.5 to 3 augmentation. Then we put it on a machine that we would like to fly and find it doesn't work. The problem that I am talking about is essentially the integration of ejectors into aircraft (fig. 1).

In general terms, what I am saying is valid whether you're considering subsonic, transonic, supersonic, or whatever sonic you're considering because you always have the same problems except that there may be differences in the actual flow field. For the purpose of illustration, I have just shown here two cases: one for the transonic and one for the supersonic case. As far as the forebody is concerned, it could be either a fuselage, a wing, a nacelle, or anything. It doesn't matter. I have just shown a type of airfoil situation there.

Before we look into the flow field that is shown there, let us first cancel the transonic case. In the transonic situation the flow that enters into the ejector is that flow which is downstream of the shock boundary-layer interaction region. If there is no shock wave, in other words, we have a smooth supersonic flow, then we still have a boundary layer that enters into the ejector. Depending on the width and the thickness of the boundary layer the flow that enters into the ejector will have a very nonuniform flow. Even if you consider a situation where you don't have a boundary layer, you still have the pressure field due to the forebody which is not uniform necessarily in front of the ejector. Also, if you consider the upper and lower sides, the pressure distribution is not necessarily the same all the time, so you have asymmetry. All these factors are

very important in finding out whether the ejector will do what we want it to do, as far as the inlet portion of the ejector is concerned.

With the exit portion we have to consider the question of matching between the flow inside and outside — the external flow coming over the ejector flap and that which is coming from inside where they are mixing. So this is the other aspect that is very important in analyzing the integration of the ejector into the aircraft. Below I show a situation where we have a supersonic flow. Of course, under these conditions you have a bow shock, then subsonic region, then a sonic and a supersonic flow. This can shock down into the ejector. All these things are going to make a lot of difference. If the flow inside is supersonic, it will have to match that external flow through Prandtl-Meyer expansion. All these things are very important in terms of the actual usages of an ejector, whether it be in flight or hover, in transition, or a few minutes after takeoff while it's going up — wherever there's a flow over the forebody.

What we are really saying is that the whole problem should be looked into as a single problem. Of course, one can divide up the analysis of each of these items separately. For example, one can develop a mixing analysis for the flow inside, just as I have seen several very nice analyses today. Or you might just develop an external aerodynamics analysis to present what the flow would look like outside. But then these have to be matched together in order to get the actual flow field and see whether the ejector will do the job we want it to do. Naturally we'll also be interested in finding out whether we could design an ejector for a given type of pressure distribution in the exit plane, which means that we should be able to modify the shape of the ejector flaps or the forebody, whatever it be.

This is a problem that we think is very important, and in my review for all the available literature, I haven't come across anything that has been done to this end. Consequently, we have developed a methodology on how to do the various aspects. I'm going to talk about those, and of course we are interested in finding someone who might be interesting in supporting it. The way we say it can be done is, for example, I was talking about boundary-layer mixing; this is the type of thing that has primary and secondary flows, so when I say parallel, I don't mean exactly parallel — there could be slight differences in angle. But whenever there are pressure differentials between the lower and upper, or anywhere, there is going to be a correction ΔP which is simply related to the curvature of the flow. So the curvature is very important. What I'm going to show is the work we have done in this connection as a starting point. The work is connected with taking into account the effect of curvature on the mixing inside a given duct, and that's what I'm going to show in the next few figures. After I will show how we have developed a methodology to match the external and internal flows for a simple case of a kind of average velocity assumed on these two slides — two different velocities, naturally. Then we'll examine the methodology for predicting the flow field over a system like this (fig. 2).

Now here we are considering a situation where we have a differential between the secondary and the primary, and this leads naturally to correcting

the flow. The mixing region will be curved, and the flow within the duct will be entirely nonsymmetric. It is quite possible that the jet boundary will reach the wall either on the lower or upper side first, and this makes a difference as to what kind of pressure profile you're going to have within the duct. Also, depending on the length of the duct, the pressure profile at the exit then is going to be different. Here this is just nomenclature to show: η_{ui} simply means the inner jet boundary, etc. Now our analysis modifies the eddy viscosity to account for the curvature, and with that we have some results which I will show.

Figure 3 shows essentially the various types of nonuniformity that you can find within an ejector, depending on what type of curvature you have in the initial flow region. For example, the upper jet boundary may reach the wall earlier or later. The main jet itself may extend beyond the point where the lower and upper boundaries reach the walls. Each of these makes a different type of nonuniformity. Even if you have a pipe-type of flow where everything is turbulent, you still have a nonuniform profile.

In figure 4(a) we have taken a duct inclined to a primary at 45°, and we have considered a centerline jet of 100 ft/sec, about 40 ft/sec on the top, and 20 ft/sec on the bottom. This produces a certain curvature. You can see that the lower jet already reaches the wall much before the upper jet boundary reaches the wall. The center line is also curved, but it naturally uncurves itself as soon as it reaches the lower boundary. You can see that there is already a nonuniformity. For example, the secondary flow that is coming from outside and this is all the mixed turbulent flow.

Figure 4(b) shows the velocity distribution at the three places. We have a hundred ft per second centerline velocity decaying naturally as you go along the duct. You can see that the centerline velocity and the velocity in the lower boundary become almost equal. But the upper velocity does not — it still takes a lot of time. For example, in this case, at 8 ft we still haven't reached equilibrium or a completely mixed flow yet.

Figure 4(c) shows the pressure distribution. This is a pressure which is initially constant in the jet-core region, and the pressure increases as we go down along the duct and this line. Both the pressures on either side are like that; you see the difference is very small. You can see also that even that small difference (less than a pound or half a pound) could still produce a curvature that has very large effect on the flow field within the duct. Figure 4(d) shows what happens to the velocity profile within the duct. To start with, you have the natural top hat, but an asymmetric top hat, because the velocities are not the same on both sides. They gradually mix so that the inviscid core is gradually annihilated. Finally, it reaches the area where the mixing is taking place. Hereafter there is a situation where one side has reached the wall and the other side has not reached the wall. This shows the velocity profile in the duct.

Essentially what these figures show is that even a small amount of pressure differential across the primary could lead to very important effects

within the duct with many nonuniformities. Any analysis of ejectors should take this fact into account, and the question of matching becomes more urgent because it cannot match and simply say the pressure is ambient outside. Then you'll have a very long ejector — 100 ft longer or 200 ft longer — before you reach complete matching of pressures from either side.

Figure 5 shows the other aspect of which I was talking. Namely, how do you know what flow or what velocity should be there in the inlet portion, in order to arrive at a matched pressure at the exit plane? Of course, we developed the methodology, and it depends on what we call parametric differentiation. It started with the usual differential equations of all the flow. Each of the variables is a function for the geometries of the pressures of the initial velocities, and so on. You can differentiate each of the flow equations and come up with a set of equations which are functions of the parametric planes. Here I am showing, for example, a simple situation where you assume that the flow velocity on one side is U_{1g} and on the other side is U_{2g} ("g" for guess). You get a pressure from that, then you integrate the basic and parametric differential equations. You can use several analyses or parametric methods, and you come down to the exit plane and ask whether the pressure difference on the lower side is less than a given value. If it is less, see what happens on the upper side. But also, if it's the correct thing, no problem. Otherwise, you have to correct the initial guess that U_{1g} is corrected by the factor ΔU_{1g} which comes out of this solution. As we proceed along the ΔU that we calculated at the end and that can be substituted, you get a new value of the U_{1g} and U_{2g}. You go ahead and iterate until you get a convergent solution. This is the second aspect of how to match these two things. Of course, I have done it for a single velocity on either side, but this could be done for a velocity distribution. You can assume that U_{1g} is like an average velocity and you have a certain distribution over that place. You can still do the same thing.

The third aspect that I will talk about is shown in figure 6 — the external aerodynamics. Here we are considering a simple forebody. You can have any type of forebody — you can have a nacelle if you want. You can still do the same type of work. What we're simply showing, for example, is the stagnation streamline of the forebody. There are two stagnation streamlines off the ejector flaps in the two-dimensional case. It simply shows the amount of in-flow that is ingested into the ejector from the top and the bottom. Then you have a certain jet that is coming out of the exit plane. This jet naturally is also going to produce some lift, as you have seen in the paper by Bevelaqua, considering this particular aspect. I won't go into any great detail except to say that in the analysis for ϕ the velocity potential, ψ is the stream function and, as you know, the circulation is related to the $\Delta\phi$ jump. If you take two points on a particular line on this jet, they don't have the same potential. There will be a potential jump between those two points.

This methodology is valid for high subsonic and also small supersonic flows that have no shocks. But if you have shocks, then the analysis that I have to talk about here must be modified. The center will have to come

up with some other method, like transonic analysis, that is available right now, many numerical analyses using relaxation methods. But this is valid for subsonic incompressible flow up to high subsonic speeds, and you don't have to make any changes in the methodology — it remains the same. It becomes very simple for incompressible flow, and the methodology is very similar to Spence's work. What you essentially do from this physical plane is go into a complex potential plane where the airfoil and the augmentor flaps and the jet become a cut on the ξ axis. You see this, of course, is the jump because of the amount of flow ingested into the ejector. This distribution is essentially the amount that has been ingested at different points around the boundary. From there we can transform this to another situation where it becomes just a simple cut on the ζ axis, real axis. We can make another transformation so that the whole flow field, essentially the upper portion of the semi-infinite plane, with the airfoil and the jet being reduced to a small piece D' to D' on the axis.

There are different methods. For example, this morning you heard of a method of how to account for the flap which was a one-sided flap in the paper by Mr. Woolard. Those methods all assume that the ejector is very thin almost like one singular line. This method that we have developed here, however, is valid even if you get a very thick jet. The boundary condition matching happens right at each of the upper trailing edges and lower trailing edges of the ejector flaps. Pressure matching has to be done there. Also, for example, if one wants to design something; say that I give you this kind of pressure distribution, why don't you give me what the ejector should look like, what the forebody should look like. That can be done. You can impose the pressure distribution that is required in one of these planes. The pressure distribution is translated into the velocity which you impose and that way you can do this work. Of course this leads to integral differential equations that have to be solved and this is where we are right now. We have reached the stage where all the equations will double up then, and it is a question of implementing the equations, writing the difference equations, and so on.

One point I want to make very clear is what happens to B' to C'. Let me get that number, what is it? Which is the boundary? What are the flow velocities there, etc. Now this is essentially where this matching analysis comes: the matching procedure. You start at a certain distribution of U_{1g} or U_{2g} on either side, then carry out the matching procedure to find out what this means in terms of the pressure differential at the end. If it's wrong, then you proceed. The important point essentially is that once you assume a certain thing, go ahead and compute the whole flow field, and match it to the ejector exit plane. Then whatever is happening here becomes part of the solution.

In summary, we feel that it is very important to do this analysis and take the integration of ejectors into whatever forebody you are having, from the beginning. At the same time you should have isolated ejector analysis, experiments, and things like that to get them up to beautiful augmentations. Thank you very much.

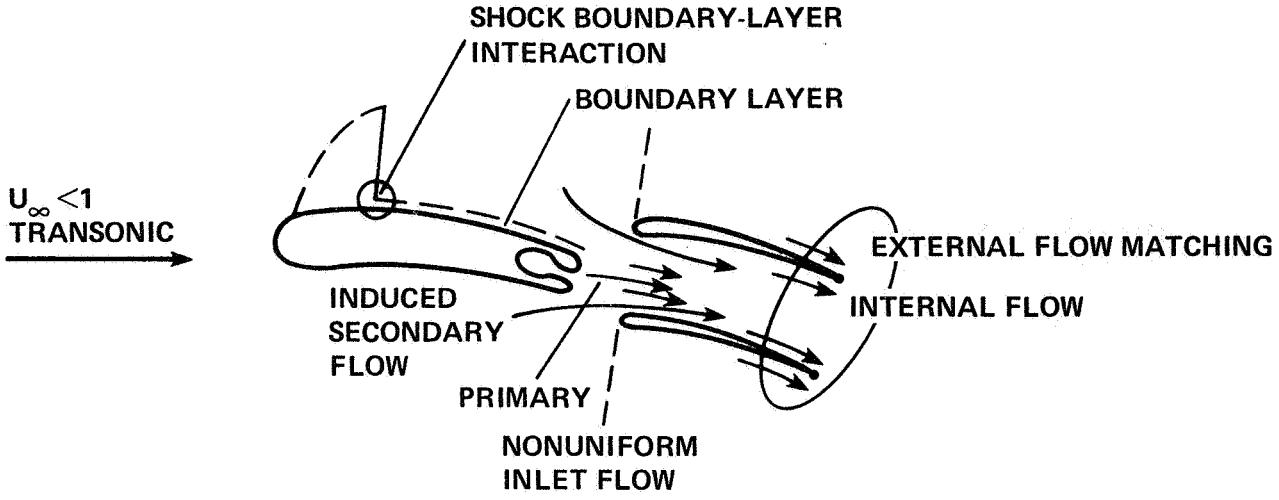

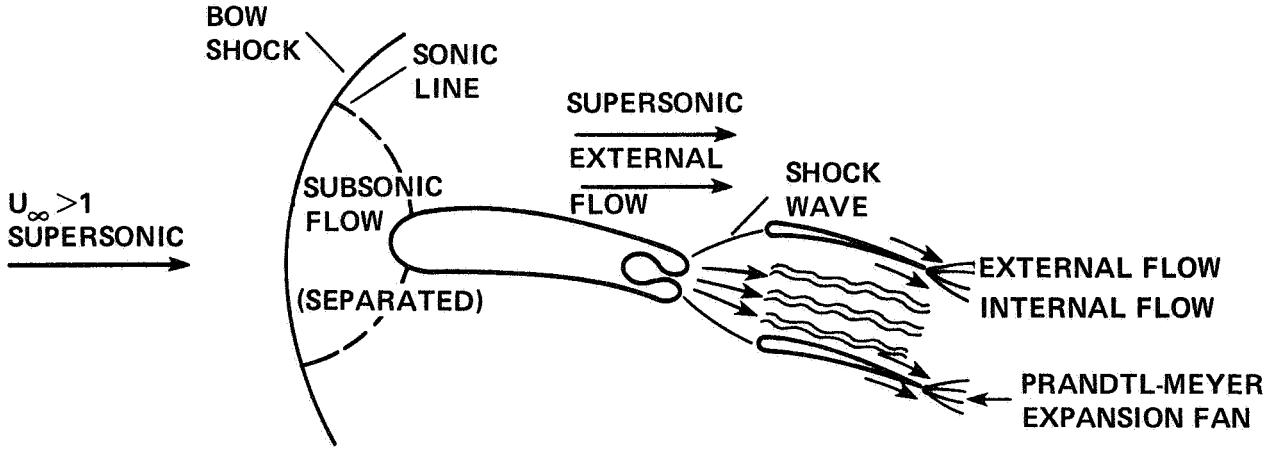

IDEALIZED MIXING

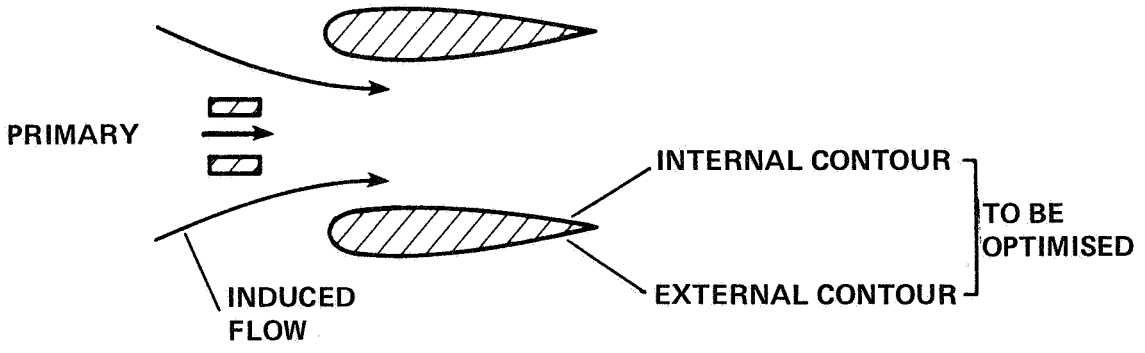

Figure 1.- Schematic of ejector integration problem.

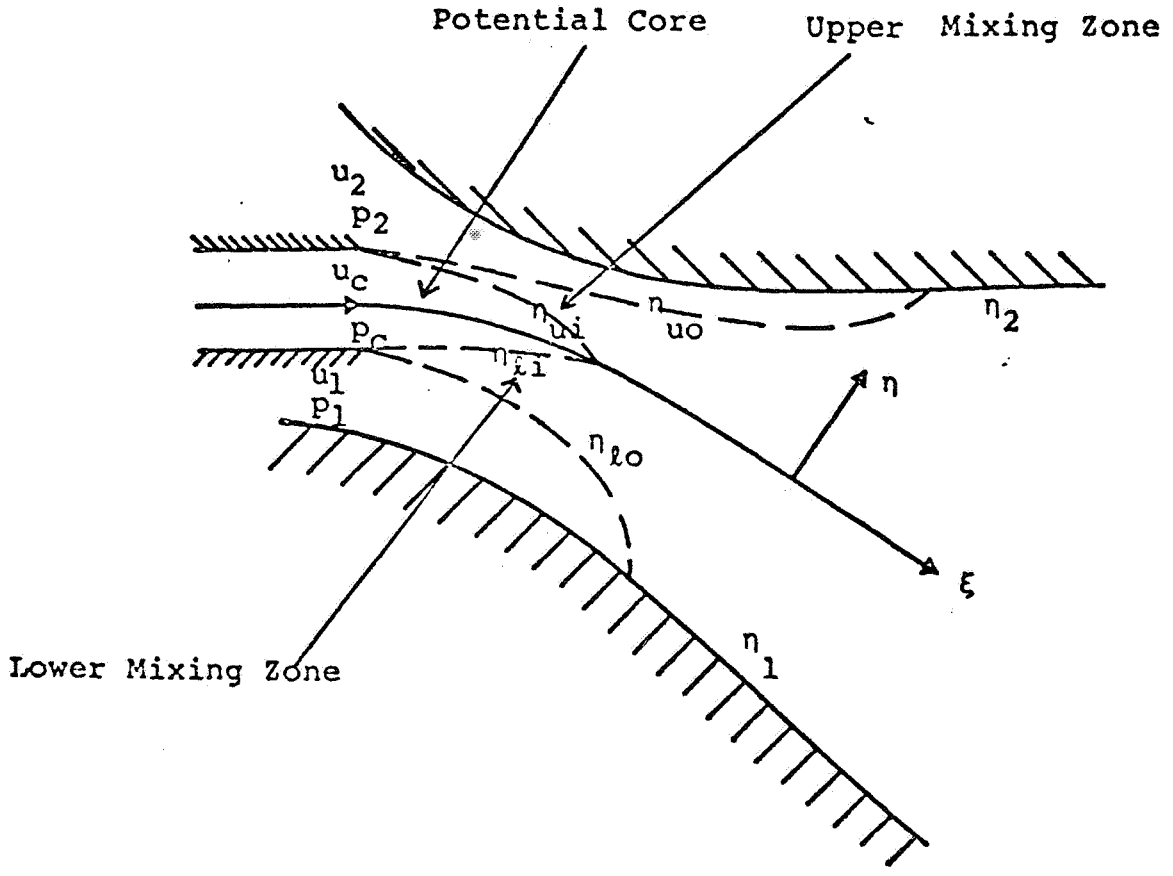

Figure 2.- Schematic of the flow field of ducted jet mixing for nonsymmetric secondary flow.

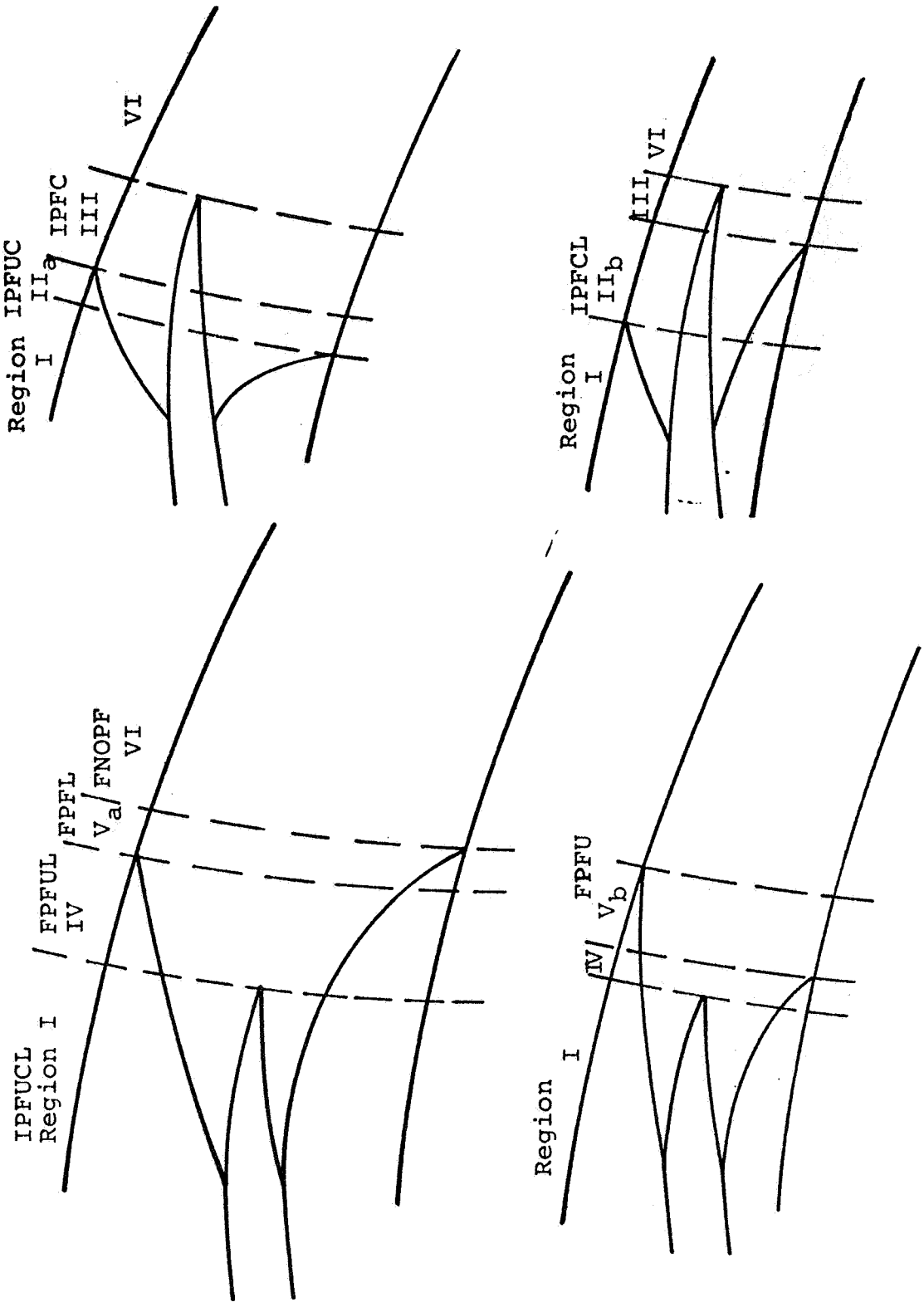

Figure 3.- The various flow regions.

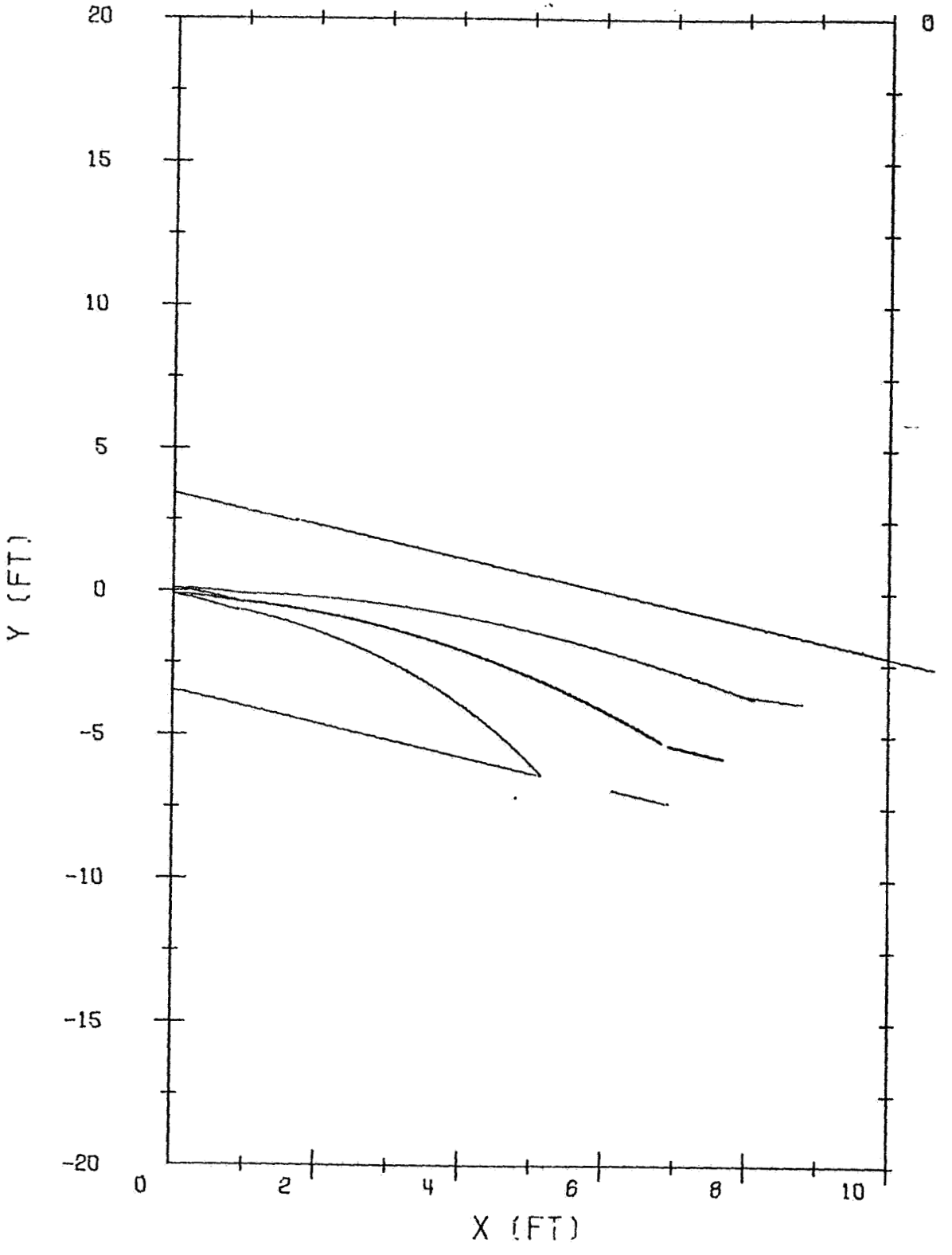

(a) Jet mixing zone boundaries, jet centerline and mixing duct walls.

Figure 4.- Flow-field characteristics inside the duct. Inclined ducted jet mixing; table V, case 11.

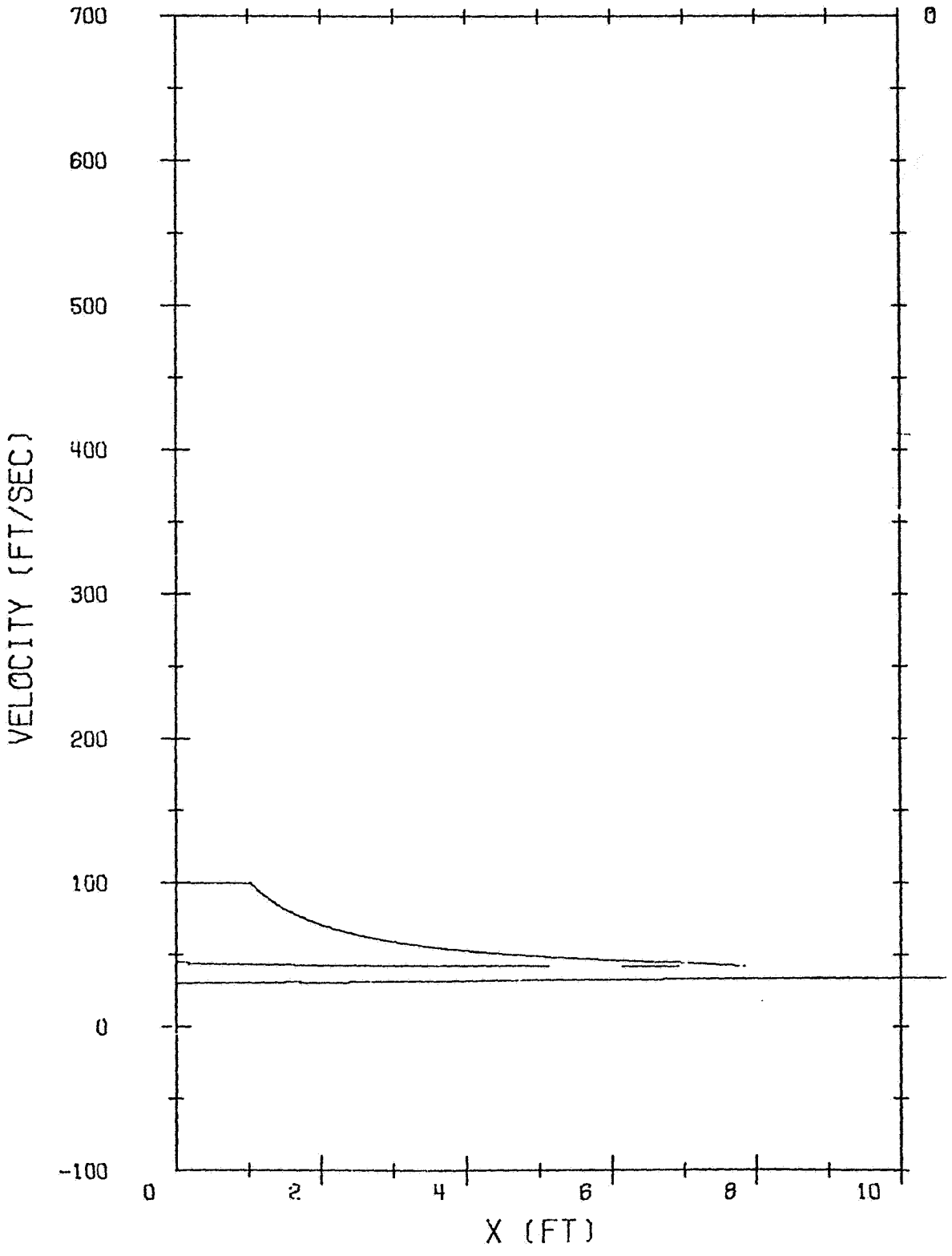

(b) Velocity distribution along the jet centerline and along the upper and lower duct walls.

Figure 4.- Continued.

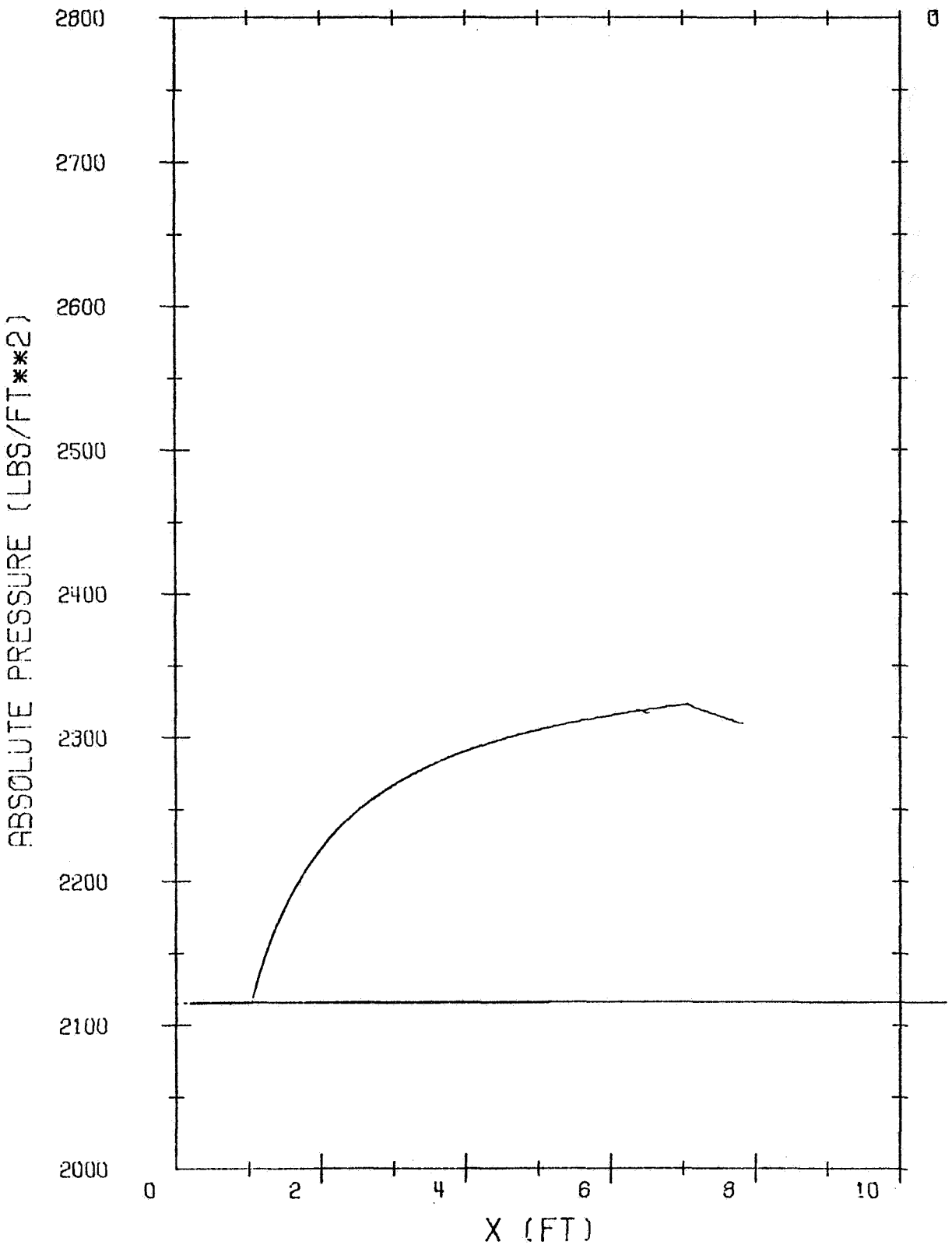

(c) Pressure distribution along the jet centerline and along the upper and lower duct walls.

Figure 4.- Continued.

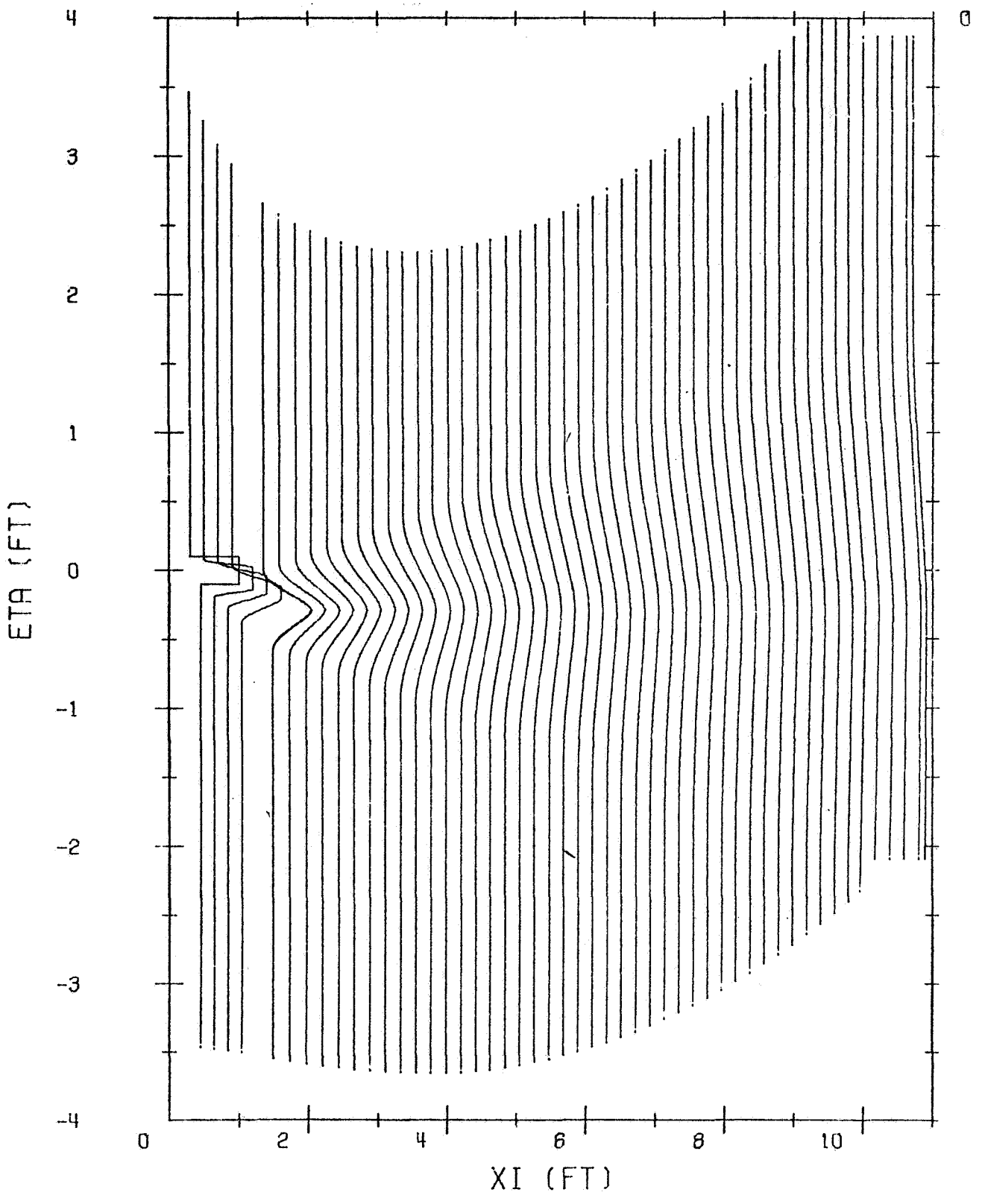

(d) Velocity profile across the mixing duct for increasing distance along the jet centerline ξ.

Figure 4.- Concluded.

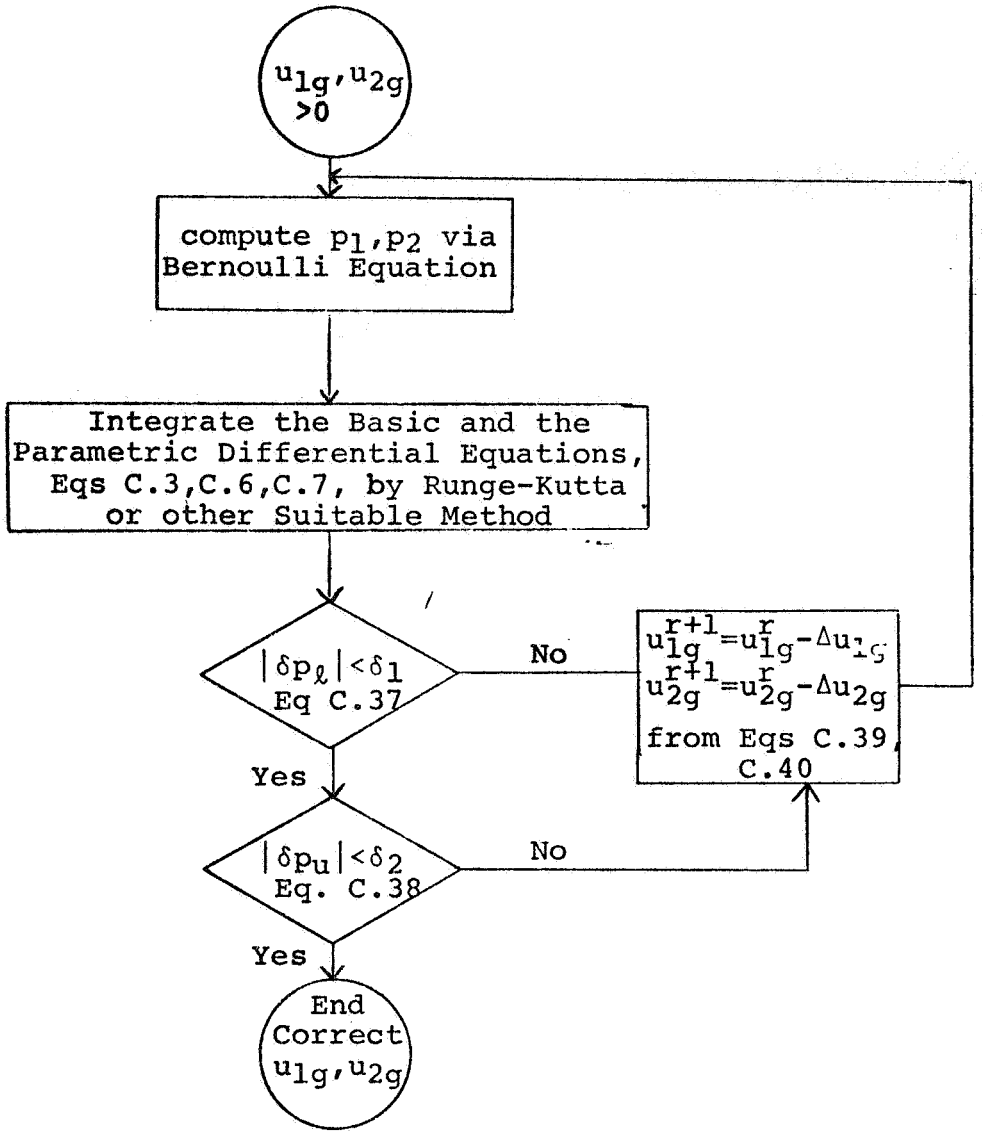

Figure 5.- Flow chart for the iterative solution to determine correct entrainment velocities of secondary flow at the mixing duct entrance.

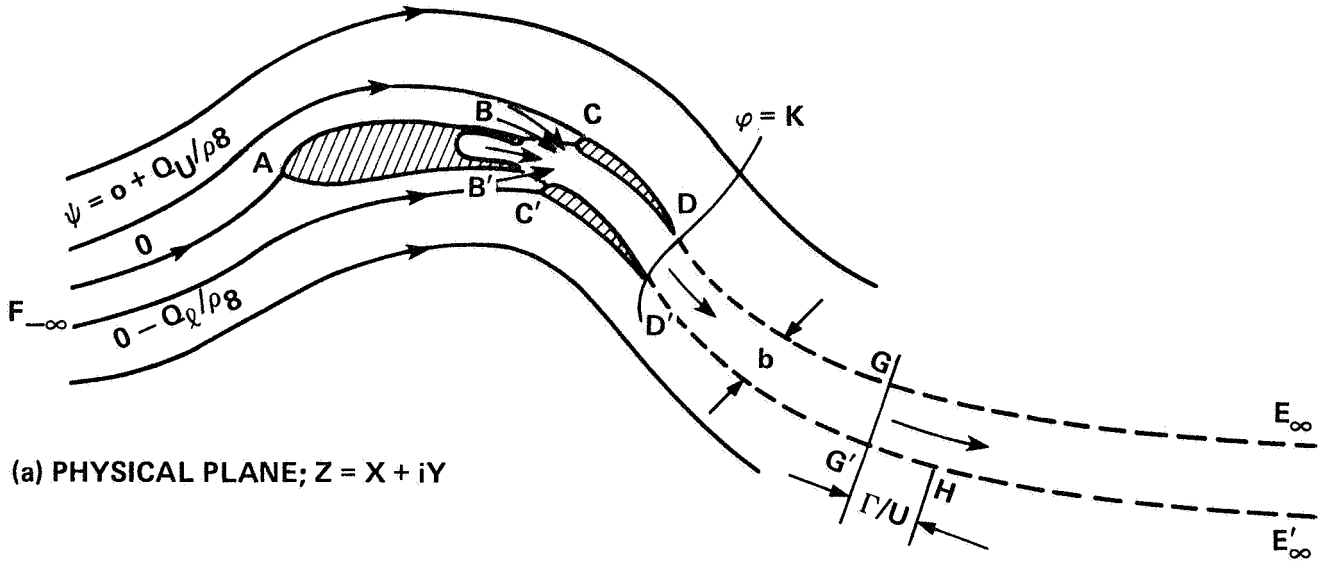

(a) PHYSICAL PLANE; $Z = X + iY$

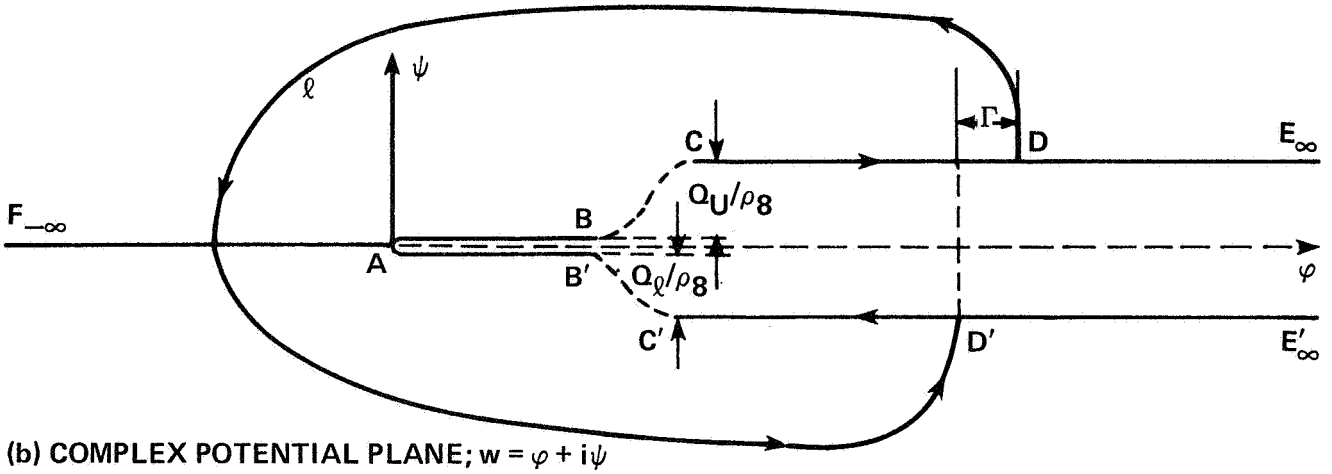

(b) COMPLEX POTENTIAL PLANE; $w = \varphi + i\psi$

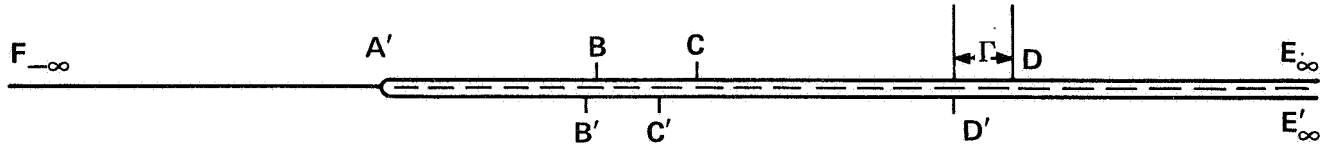

(c) COMPLEX POTENTIAL PLANE; $w_s = \varphi_s + i\psi_s$

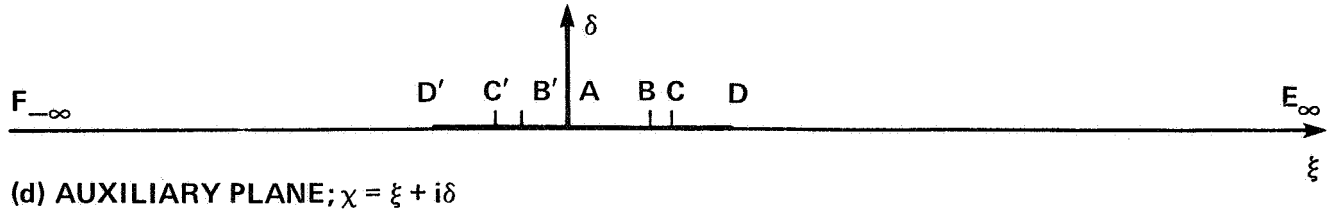

(d) AUXILIARY PLANE; $\chi = \xi + i\delta$

Figure 6.- The problem in Z, w, w_s and χ planes; nomenclature.

SOME TESTS ON A SMALL-SCALE RECTANGULAR THROAT EJECTOR

W. N. Dean, Jr.* and M. E. Franke

Air Force Institute of Technology
Wright-Patterson AFB, OH 45433

ABSTRACT

A small-scale rectangular throat ejector with plane slot nozzles and a fixed throat area was tested to determine the effects of diffuser sidewall length, diffuser area ratio, and sidewall nozzle position on thrust and mass augmentation. The thrust augmentation ratio varied from approximately 0.9 to 1.1. Although the ejector did not have good thrust augmentation performance, the effects of the parameters studied are believed to indicate probable trends in thrust augmenting ejectors.

INTRODUCTION

In recent years much effort has been devoted to V/STOL research and development. Many of these programs have been concerned with the use of ejectors to achieve the thrust augmentation required for V/STOL type operations (refs. 1-6). To achieve high thrust augmentation with an ejector rapid mixing is important. This has led to studies of ways to improve mixing and the development of hypermixing nozzles (refs. 1 and 2). The effects of other design parameters on mixing and ejector performance are also still of interest; for example, the effects of diffuser area ratio, angle, and length, effects of fluid injection along the diffuser sidewalls, and effects of the position of plane sidewall, slot nozzles (private communication from P. M. Bevilaqua, 1977). The tests described herein were undertaken to provide some additional information and trends on the effects of the above indicated parameters on ejector performance.

The definitions of the augmentation ratios used in this study are as follows:

$$\text{thrust augmentation ratio } \phi = \frac{\text{measured ejector thrust}}{\text{reference thrust}}$$

where the reference thrust is defined as the thrust that would be obtained by the isentropic expansion of the primary mass flow from the primary nozzle reservoir pressure to ambient conditions.

$$\text{mass augmentation ratio} = \frac{\text{secondary mass flow rate}}{\text{primary mass flow rate}}$$

---

*2d Lt., USAF; presently, Air Force Flight Test Center, Edwards AFB, CA.

TEST APPARATUS AND PROCEDURE

Ejector

A two-dimensional sketch of the ejector is shown in figure 1. The diffuser throat had a width of 1.8 in. and a span of 5 in. The primary nozzles consisted of a central plane slot nozzle positioned at the center of the inlet and plane slot nozzles located along the sidewalls. The nozzles were sized so that the central nozzle (slot width of 0.09 in.) delivered approximately one-half of the primary flow. The two sidewall nozzles (slot width of 0.04 in. each) delivered the remaining amount of primary flow, except for a very small flow through endwall nozzles positioned at the throat that were used to reduce diffuser stall. Also, fillets were made to fit into the corners of the diffuser to help reduce stall. The sidewall nozzles were designed to enhance jet wall attachment to the diffuser sidewalls and thus possibly reduce flow separation and diffuser stall. The sidewall nozzles were located in cylinders that could be rotated independently of the interchangeable diffuser sidewalls.

Several ejector parameters were varied during the tests. Variables included the sidewall nozzle position (20° to 90°), diffuser sidewall length (1.3, 3.25, and 6.5 in.) and sidewall angle (0° to 25°).

Air Supply and Flow and Pressure Measurements

The primary airflow was supplied by two air compressors each capable of delivering approximately 1/2 lbm/sec at 40 psig. The pressure and flow rate to the ejector were adjusted during tests with a main valve and a bleed valve. The primary airflow rate was measured with a flange-type orifice meter with a 1.375-in. diam orifice in a 3-in. line. The upstream pressure, pressure drop, and temperature were measured with a pressure gage, mercury manometer, and a copper-constantan thermocouple, respectively.

The total pressure in the sidewall cylinders was measured with a pressure gage and checked with a total pressure probe at the sidewall slot nozzle exit. Preliminary tests showed a difference of no more than 1 psig between the two cylinders under operating conditions. The tests were run at a total pressure of approximately 20 psig in the sidewall cylinders.

The total mass flow rate at the diffuser exit was approximated from total and static pressure measurements at 3-18 equally spaced positions across the width at center span. The flow rates obtained were optimistic, since the effects of the endwalls were ignored. Preliminary tests showed, however, that the velocity was relative constant across the diffuser exit, except when diffuser stall occurred in which case large variations in velocity existed across the exit plane.

Thrust Measurement

Thrust was measured with the ejector suspended from two flexible air supply hoses as shown in figure 2. With the ejector free to swing, the thrust was obtained from two strain gages mounted on a flexure piece. The strain gages were bridged to compensate for temperature and were zeroed electronically prior to each run and checked for drift after each run. The system was preloaded to prevent movement during operation.

RESULTS

Thrust Augmentation

The effects of sidewall nozzle position (angle) θ on thrust augmentation ratio ϕ for different diffuser sidewall angles ψ and three different diffuser sidewall lengths (L/W = 0.7, 1.8, and 3.6) are shown in figures 3-5. The maximum value of the thrust augmentation ratio was approximately 1.1. Although the ejector did not give high thrust augmentation, the results are believed to be useful and also to indicate possible trends in higher performance augmenting ejectors.

The results (figs. 3-5) show that ϕ generally increased with increasing values of θ up to approximately 40° and generally decreased for values of θ above 60°. Thus, the sidewall nozzle was most effective between 40° and 60°. The effect of the absence of sidewall jets on ϕ is also shown in figures 3 and 4 for ψ = 5° and 15°. Without sidewall jets, ϕ was considerably lower. It was also found that ϕ generally increased as ψ increased up to approximately 10° to 15°, then decreased at higher values of ψ where diffuser stall occurred in many cases. Diffuser stall conditions are noted in the figures. The trends with ψ are similar to those found by Foley (ref. 4).

The diffuser area ratio A_e/A_t (exit area to throat area) depends on ψ and the diffuser sidewall length L. Values of A_e/A_t are given in figures 3-5 for values of ψ and L. The effect of A_e/A_t on ϕ is shown in figure 6. Maximum ϕ occurred for A_e/A_t between 1.5 and 2, which is in general agreement with results given by Salter (ref. 3).

The effect of diffuser length L on ϕ is shown in figures 7-9 in terms of L/W for three different diffuser area ratios. Bevilaqua (ref. 6) infers that ϕ generally increases with length, since this allows increased mixing of primary and secondary airstreams. The results given in figures 7-9, in most cases, indicate an increase in ϕ with increase in L/W.

Mass Augmentation

The mass augmentation ratio was found to vary from 2 to 4, that is, the secondary airflow rate was generally 2 to 4 times the primary airflow rate. Mass augmentation ratio appeared to increase slightly with increases in θ

and with increases in diffuser area ratio. The results, however, are inconclusive because of the small number of static and total pressure measurements made at the diffuser exit. A more complete survey is needed to accurately measure the exit mass flow rate.

CONCLUSIONS

The results obtained in this study generally agree with those of previous studies regarding the effects of diffuser area ratio, sidewall angle, and length, in spite of the low augmenting performance of the ejector. This low performance is possibly due, in part, to the inlet design. The sidewall slot nozzle position in the range of 40-60° provided the highest augmentation ratio. The sidewall nozzles were not particularly effective for thrust augmentation when positioned closer to the throat or when directed toward the central primary nozzle at the higher angle positions.

REFERENCES

1. Fancher, R. B.: Low-Area Ratio, Thrust-Augmenting Ejectors. J. Aircraft, vol. 9, no. 3, 1972, pp. 243-248.

2. Bevilaqua, P. M.: Evaluation of Hypermixing for Thrust Augmenting Ejectors. J. Aircraft, vol. 11, no. 6, 1974, pp. 348-354.

3. Salter, G. R.: Method of Analysis of V/STOL Aircraft Ejectors. J. Aircraft, vol. 12, no. 12, 1975, pp. 974-978.

4. Foley, W. H.: An Investigation of 3-Dimensional Effects on Augmentors. Rockwell International Report prepared for the Naval Air Development Center, NADC-76153-30, 1977.

5. Viets, H.: Thrust Augmenting Ejector Analogy. J. Aircraft, vol. 14, no. 4, 1977, pp. 409-411.

6. Bevilaqua, P. M.: Lifting Surface Theory for Thrust-Augmenting Ejectors. AIAA J., vol. 16, no. 5, 1978, pp. 475-481.

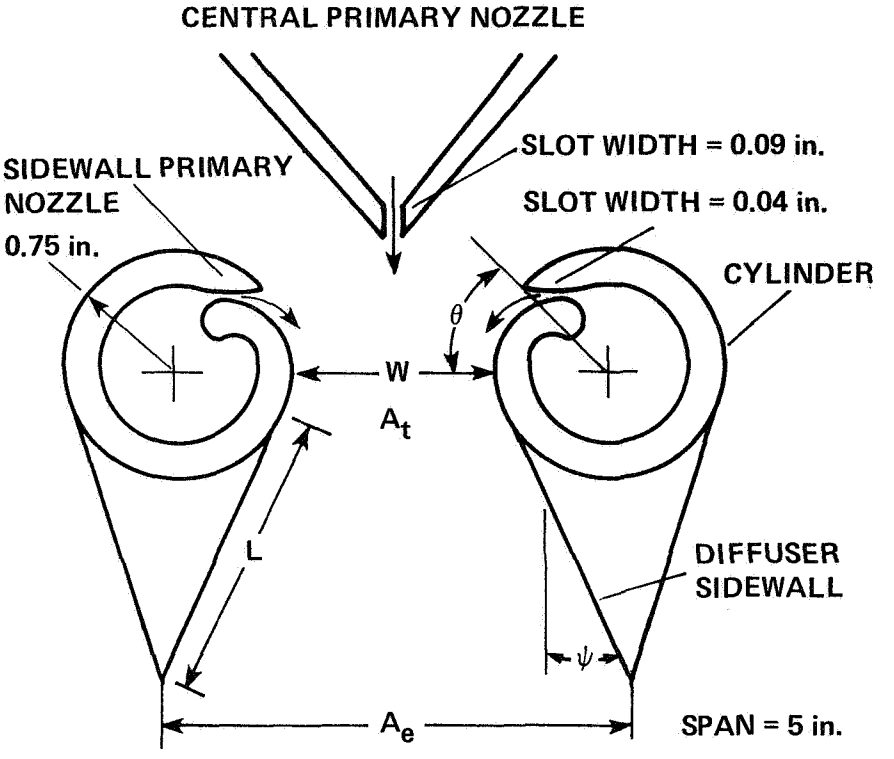

θ – SIDEWALL NOZZLE POSITION (VARIABLE: 20° TO 90°)

ψ – DIFFUSER SIDEWALL ANGLE (VARIABLE 0° TO 25°)

L – DIFFUSER SIDEWALL LENGTH (VARIABLE 1.3 in., 3.25 in., and 6.5 in.)

W – THROAT WIDTH = 1.8 in.

A_t – THROAT AREA = 9 $in.^2$

A_e – DIFFUSER EXIT AREA (VARIABLE: DEPENDS ON L AND ψ)

$\frac{A_e}{A_t}$ – DIFFUSER AREA RATIO

Figure 1.- Two-dimensional sketch of ejector.

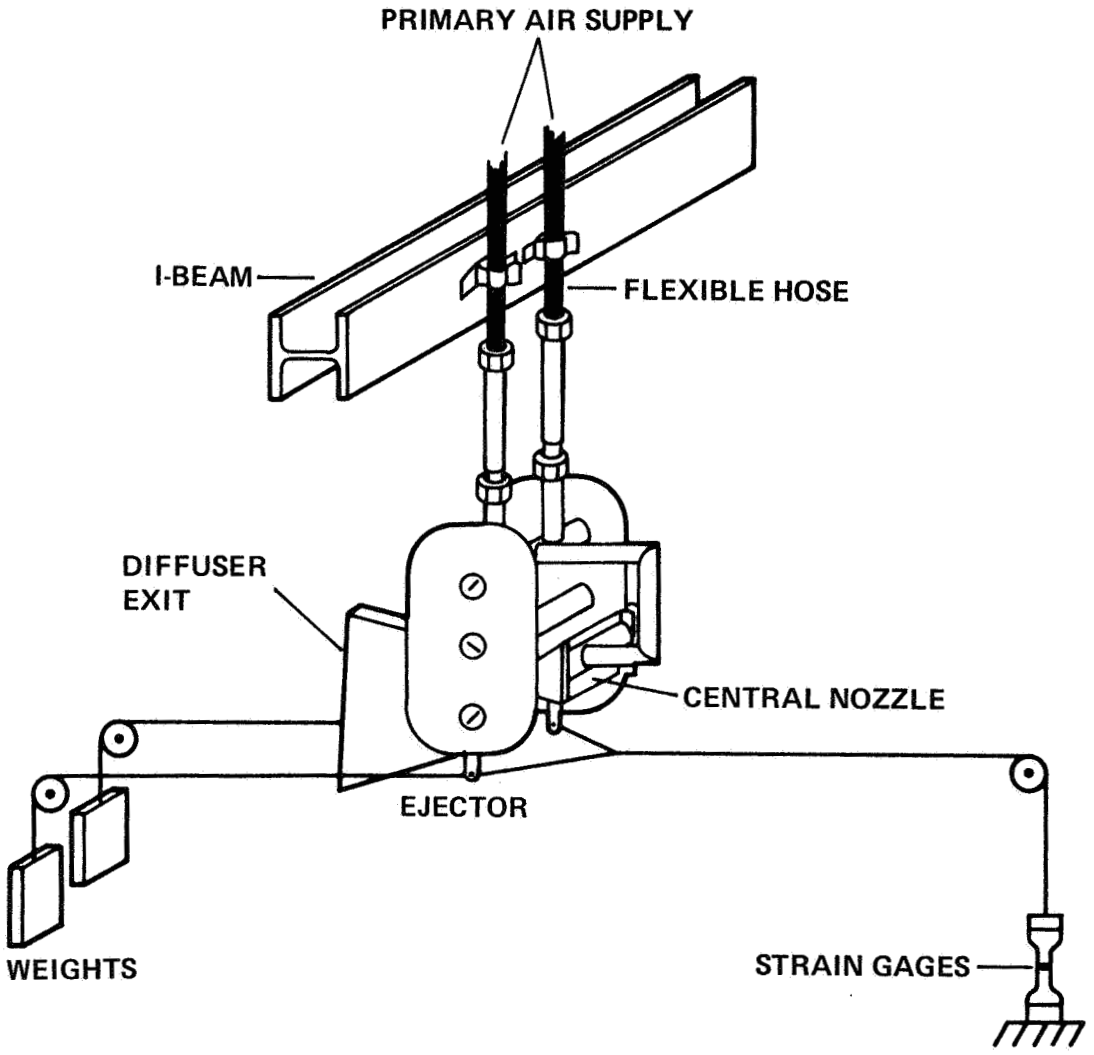

Figure 2.- Thrust measuring system.

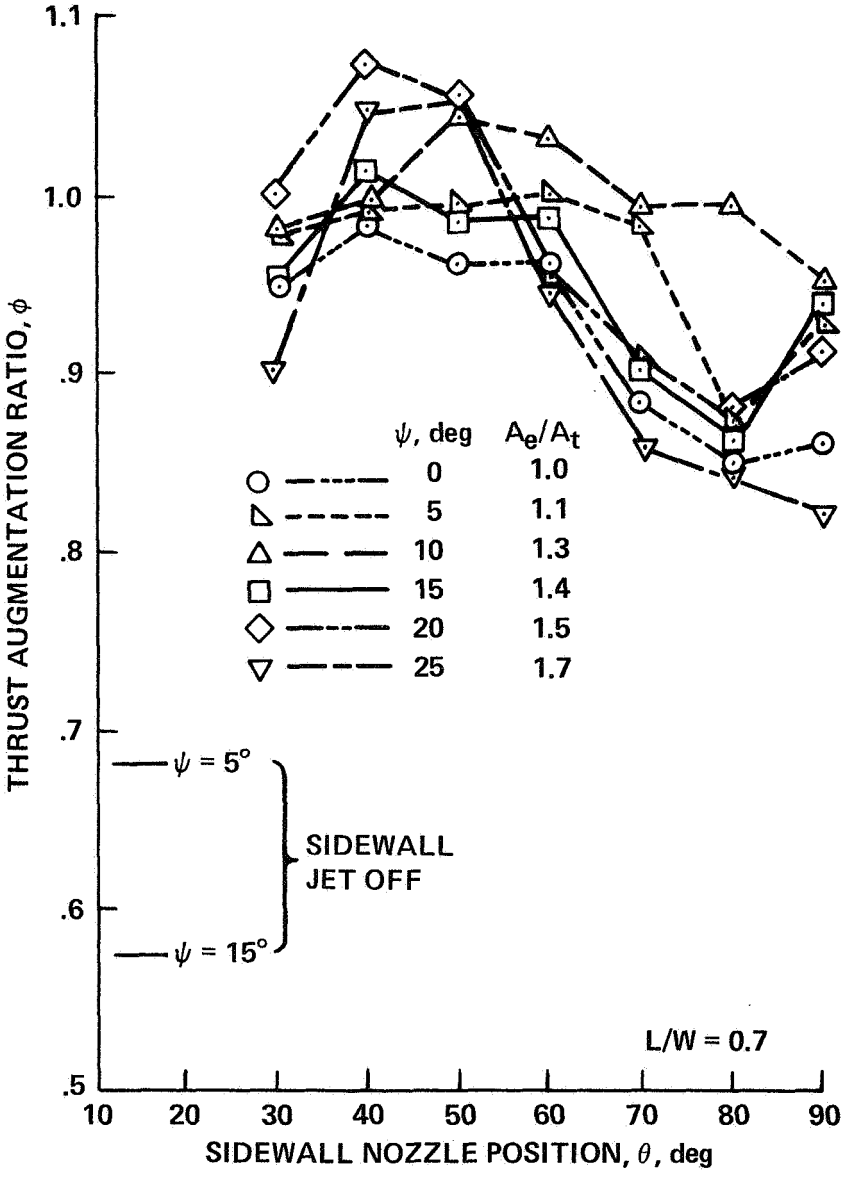

Figure 3.- Effect of sidewall nozzle position on thrust augmentation ratio for L/W = 0.7 and various diffuser area ratios.

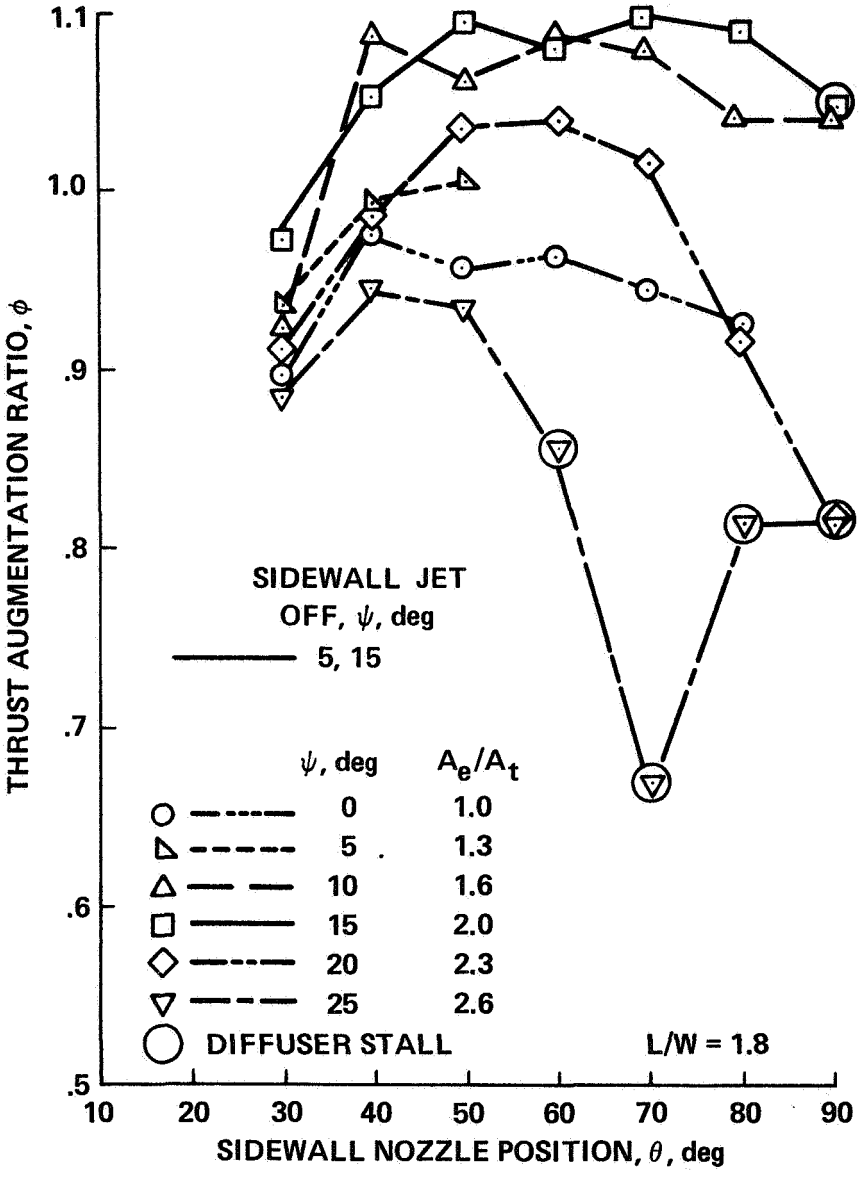

Figure 4.- Effect of sidewall nozzle position on thrust augmentation ratio for L/W = 1.8 and various diffuser area ratios.

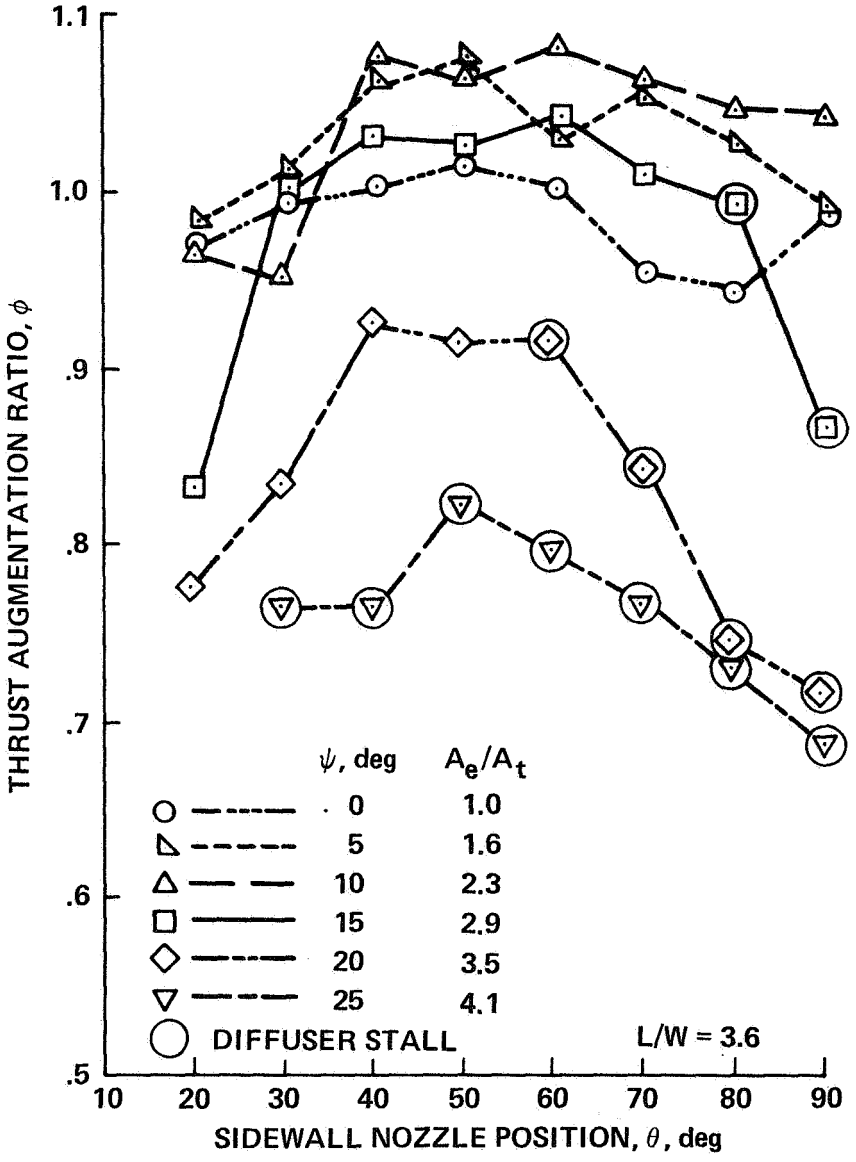

Figure 5.- Effect of sidewall nozzle position on thrust augmentation ratio for L/W = 3.6 and various diffuser area ratios.

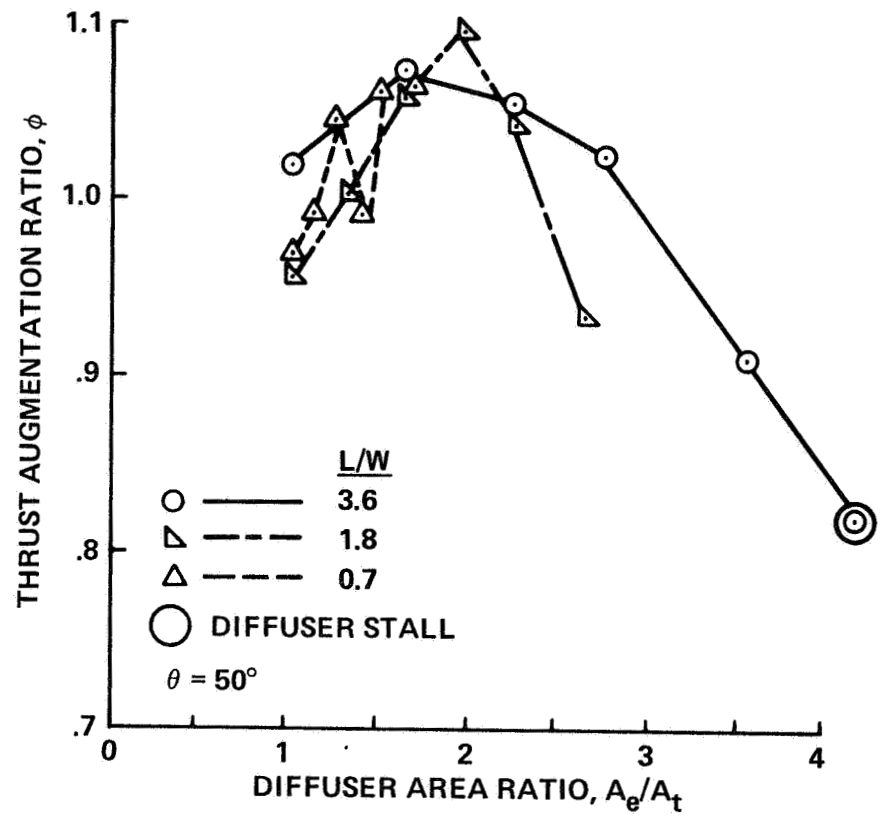

Figure 6.- Effect of diffuser area ratio on thrust augmentation ratio for constant sidewall nozzle position θ.

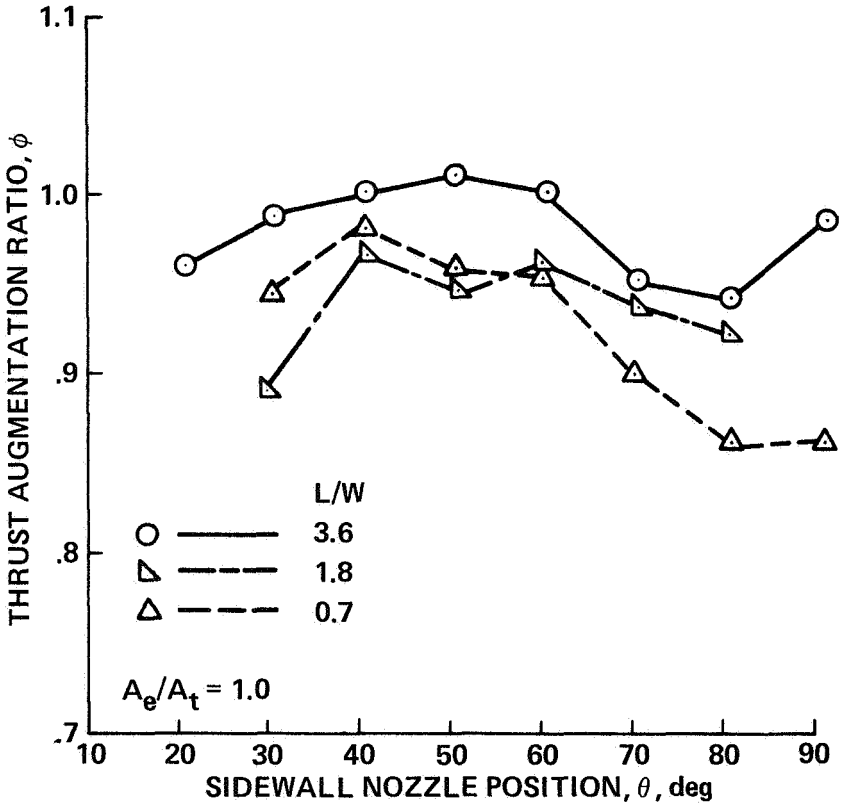

Figure 7.- Effect of diffuser sidewall length on thrust augmentation ratio for diffuser area ratio = 1.0.

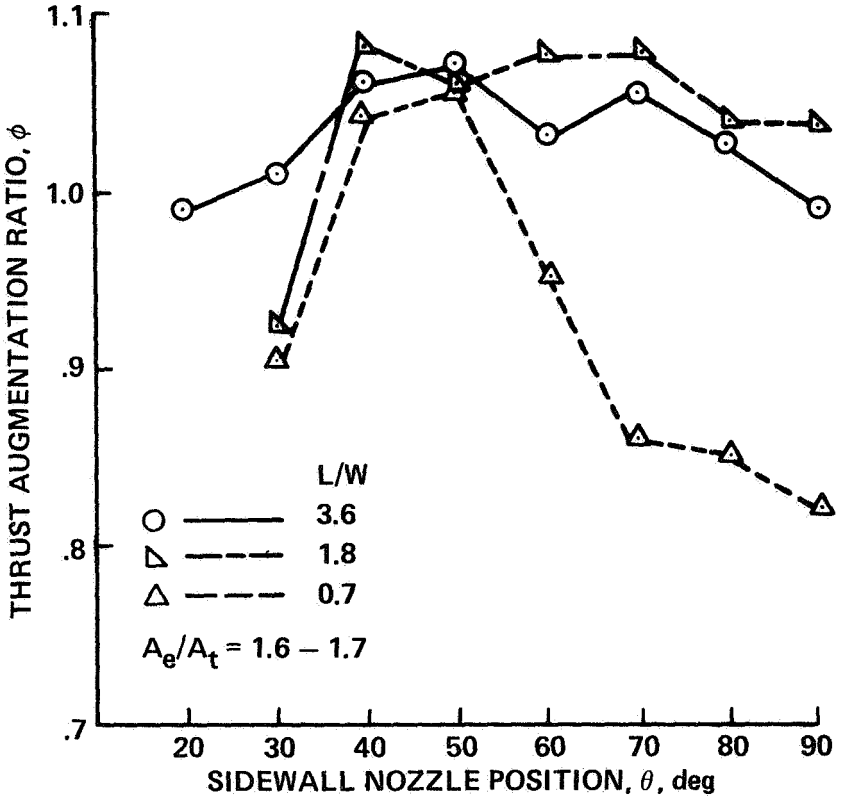

Figure 8.- Effect of diffuser sidewall length on thrust augmentation ratio for diffuser area ratio = 1.6 to 1.7.

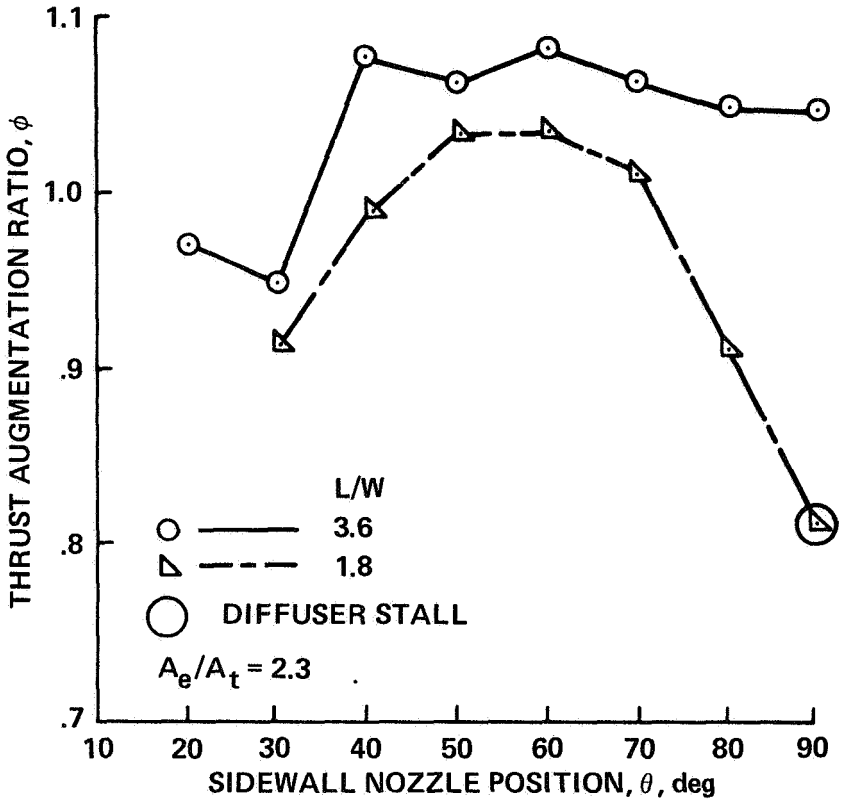

Figure 9.- Effect of diffuser sidewall length on thrust augmentation ratio for diffuser area ratio = 2.3.

AUGMENTING EJECTOR ENDWALL EFFECTS

J. L. Porter and R. A. Squyers

Vought Corporation
Advanced Technology Center, Inc.
P.O. Box 6144, Dallas, Texas 75222

SUMMARY

Rectangular inlet ejectors which had multiple hypermixing nozzles for their primary jets were investigated for the effects of endwall blowing on thrust augmentation performance. The ejector configurations tested had both straight-wall and active boundary-layer control type diffusers. Endwall flows were energized and controlled by simple blowing jets, suitably located in the ejector. Both the endwall and BLC diffuser blowing rates were varied to determine optimum performance. High area ratio diffusers with insufficient endwall blowing showed endwall separation and rapid degradation of thrust performance. Optimized values of diffuser BLC and endwall nozzle blowing rates in an ejector augmenter are shown to achieve high levels of augmentation performance for maximum compactness.

SYMBOLS

A area

AR diffuser area ratio, $\frac{A_3}{A_2}$

ARL Aerospace Research Laboratory

ASME American Society of Mechanical Engineers

ATC antiseparation tailored contour

BLC boundary-layer control

C_L centerline

F thrust

h ejector span

L total ejector length

L_M constant area mixing length

L_D axial diffuser length

$\dot{m}$ mass flow, lb/sec

P pressure

W width

ϕ thrust augmentation ratio

Subscripts:

0 total, stagnation, condition

1 primary nozzle property

2,M mixing area exit plane

3,D diffuser exit plane

BLC boundary-layer control, diffuser wall

EW endwall property

isen isentropic

max maximum

S blowing slot condition

Superscripts:

' value for ideal expansion to ambient static pressure

INTRODUCTION

Proposed use of augmenting ejectors for V/STOL aircraft has placed emphasis on two-dimensional ejector designs in order to comply with constraints imposed by aircraft wing and body physical restrictions. In general, such restrictions also limit the ejector diffusion, and consequently augmentation possible, either by length or area ratio constraints. Achieving maximum augmentation and compactness for ejector configurations thus frequently means achieving maximum diffusion in the shortest length. Active boundary-layer control (BLC) has been shown to be one method of accomplishing this goal (refs. 1 and 2). Experiments at Vought Corporation Advanced Technology Center, Inc. have shown that for so-called "two-dimensional" ejector-diffuser configurations three-dimensional effects are significant. Thus, boundary-layer control must be used not only on the diffusing walls, but also must be applied to the endwalls whose flow must traverse the same static pressure gradient (ref. 3).

The objectives of this study were to investigate the effects of finite span ejector endwalls on the performance of rectangular inlet ejectors. Tests were performed on configurations with hypermixing primary nozzles for diffusers with straight (no BLC) walls and contoured (BLC) walls. Performance for varying amounts of endwall boundary-layer control was investigated.

EXPERIMENTAL APPARATUS

Experimental Setup

Testing for endwall effects was conducted in the suspended test bed of the ejector/augmenter facility which was located in the Vought High Speed Wind Tunnel Complex. A schematic of the basic ejector test bed is shown in figure 1. The location of the ejector endwall blowing jets is shown in the figure. Pressurized air supplied by storage tanks to the ejector test bed was measured using ASME calibrated orifice plate flowmeters. Endwall nozzle and endwall blowing corner jets used a common flowmeter and were measured separately from other system flows. The ejector test bed, shown in a front view in figure 2, has a constant area mixing region width of 10 in. and an aspect ratio of 6.0.

Instrumentation

Measurements of ejector endwall blowing parameters and internal flow qualities were obtained for evaluation and analysis. Hypermixing nozzle primary plenum pressures, blowing slot plenum pressures, and endwall jet nozzle plenum pressures were measured by calibrated gage pressure transducers. Ejector test bed total thrust was monitored through a six-component strain gage balance for determination of system thrust augmentation performance. Diffuser wall surface pressure distributions were sensed by flush mounted static pressure taps. Visualization of endwall flows was accomplished with streamwise flow tufts. Interaction of endwall and diffuser flows was determined by a multiprobe total pressure rake which traversed the internal flows.

Ejector/Diffuser Configurations

Planviews of the ejector/diffuser configurations investigated for endwall effects in the ejector test bed are shown in figure 3. Two straight-wall diffusers tested were the Air Force Aerospace Research Laboratories (ARL) Configuration "F" and an equivalent baseline model. Both had only endwall blowing for control of diffuser flows. The results from two compact BLC diffusers included both endwall and diffuser wall blowing slot flows for the optimization of thrust augmentation. All four configurations were tested at various diffuser area ratios for optimization of performance.

RESULTS AND DISCUSSION

The thrust augmentation ratio, ϕ, is defined as the total ejector thrust, F, divided by the thrust generated by an isentropic expansion of the primary mass from the driving pressure to the ambient total pressure. The general form for the ejectors being studied is

$$\phi = \frac{F}{F_{isen}} = F\left(\dot{m}_1 V_1' + \dot{m}_{BLC} V_{BLC}' + \dot{m}_{EW} V_{EW}'\right)^{-1}$$

where $\dot{m}_1$, $\dot{m}_{BLC}$, $\dot{m}_{EW}$ are the mass flow rates from the hypermixing, boundary-layer control and endwall nozzles, respectively. The quantities V_1, V_{BLC}, V_{EW} are the corresponding velocities achieved after isentropic expansions to ambient pressure from the measured total pressures P_{01}, P_{0BLC} and P_{0EW}.

Because the maximization of thrust augmentation was the primary goal, in some instances data were not obtained for the limiting cases of zero endwall blowing mass flow, $\dot{m}_{EW}$. Rather, low values of $\dot{m}_{EW}$, for which diffuser separation and rapid falloff of thrust occurred, were defined and then variations were investigated to determine the optimum values. Data were obtained for ejectors with straight-wall diffusers and for ejectors with specially contoured diffuser walls.

Straight-Wall Diffusers

Two straight-wall diffuser configurations were tested: (a) an Air Force Aerospace Research Laboratory (ARL) design with a 45-in. diffuser length, and (b) a shorter, 11.75-in. diffuser length, designed to provide baseline comparisons with the specially contoured ATC diffusers. As shown in figure 1, various area ratios and equivalent half-angles were available through a mechanical/flexible wall design.

Results (ref. 4) for the ARL diffuser are shown in figure 4 for a range of area ratios up to 2.5 and a range of primary jet pressures. As may be seen, with a long diffuser length a high value of augmentation can be achieved, $\phi_{max} = 2.10$.

The maximum area ratio achievable without flow separation was 1.5 for the shorter baseline straight-wall diffuser. At area ratios greater than 1.5, no amount of endwall blowing would prevent diffuser wall separation on this configuration. Figures 5 and 6 show the effects of $\dot{m}_{EW}$ variations on the thrust augmentation of the baseline straight-wall ejector/diffuser configuration. As shown in these figures, the maximum thrust augmentation for both area ratios, 1.25 and 1.50, was achieved at approximately the same endwall blowing rate, $\dot{m}_{ew} \approx 0.15$ lb/sec. Data have shown that increasing the diffuser area ratio results in a lower mixing plane static pressure, a higher entrained secondary flow velocity and consequently a proportional change in the endwall boundary-layer momentum loss entering the diffuser. Because of the small change in straight-wall diffuser area ratio this apparent boundary-layer phenomena

impact on endwall blowing requirements was not readily quantified. Thus, while the adverse pressure gradient through the 1.5 area ratio diffuser is larger, the total energization as indicated by the $\dot{m}_{ew}$ required was approximately the same as for the lower area ratio configuration, at the optimum condition.

Specially Contoured (ATC) Diffusers

The specially contoured diffusers were designed to achieve rapid diffusion in a short length through the use of boundary-layer energization on the diffusing walls as well as the endwalls. Figure 7 shows the effects of variations in the endwall blowing rate for a short, area ratio of 2.10, diffuser at two values of the diffuser wall BLC blowing rates, $\dot{m}_{BLC}$. As shown in the figure, although considerable data scatter occurred, peak performance was obtained for both values of $\dot{m}_{BLC}$ at endwall blowing rate between 0.17 and 0.18 lb/sec. This value is close to the optimum value of 0.15 lb/sec found for the straight-wall diffusers of equivalent length. The increase is required by the more rapid diffusion of the specially contoured wall and the 30% increase in diffuser area ratio (2.1 vs 1.5). The tendency of the thinner endwall boundary layer, found at higher entrained velocities, to counteract the effect of adverse pressure gradient on the required blowing rate is apparently overcome at an area ratio between 1.5 and 2.1.

In the data of figure 8 the optimum value of endwall blowing rate was held fixed while the boundary-layer control on the diffusing wall was varied. Peak performance of $\phi = 1.88$ was obtained at $\dot{m}_{BLC}$ slightly over 0.55 lb/sec; however, values as low as $\phi = 1.80$ were obtained for approximately the same $\dot{m}_{BLC}$. This difference appears to be due to a slight hysteresis effect wherein data taken as $\dot{m}_{BLC}$ increases have slightly lower augmentation values due to incomplete boundary-layer energization. Once a value of $\dot{m}_{BLC}$ high enough to completely energize the boundary layer has been achieved, a somewhat lower value is sufficient to maintain energization. The lower value of $\dot{m}_{BLC}$ results in a lower value of the corresponding ideal thrust and hence a higher augmentation ratio.

Diffuser-Endwall Corner Effects

During the course of the experimental study, flow tuft visualization indicated that when diffuser separation occurred, it was generally initiated in the corners formed by the intersection of diffuser walls and endwalls. Consequently, corner "buttons" were added to the configuration, as shown in figure 9, to provide additional boundary-layer control in this area. The button flow was derived from the same source as the endwall blowing flow, at the same total pressure. While visual observations indicated that the button flow was effective in preventing corner separation, comparison of optimum peak augmentation values indicated that the optimum endwall/corner blowing configuration had not been obtained. Figures 10 and 11 show these peak augmentation values for two discrete values of $\dot{m}_{EW}$, which for figure 10 includes the button flow, as functions of the diffuser BLC flow, $\dot{m}_{BLC}$. While the total blowing flow rate for the maximum augmentation is approximately constant at

$\dot{m}_{BLC} + \dot{m}_{EW} = 0.76$ lb/sec, the configuration without buttons has the better maximum performance. Stated differently, increasing the diffuser wall BLC flow, which was at a higher total pressure than that for the endwall/button flow, was more effective in energizing the corner boundary layer than was increasing the endwall/button flow by the same amount. From these results it thus appears that while corner flow BLC is important, additional investigations are required to determine the optimum geometry and flow conditions for the corner jets.

Comparison of Straight- and Contoured-Wall Ejector/Diffuser Results

A summary comparison of the best performance obtained for all combinations of area ratio, mixing plus diffuser length, and endwall and diffuser wall blowing, is shown in figure 12. As may be seen in this figure, significant gains in ejector/diffuser compactness were achieved for the specially contoured wall diffusers with optimized BLC, over the straight-wall diffusers with only endwall BLC.

CONCLUSIONS

Two-dimensional (rectangular) ejector diffuser configurations experience significant three-dimensional flow effects on their endwalls. Providing boundary-layer control for the endwalls can significantly improve the performance of straight-wall diffusers. However, maximum gains in compactness for a given level of thrust augmentation can be achieved through the use of specially contoured, rapid-diffusion diffuser walls with both diffuser wall and endwall boundary-layer control. For the straight-wall diffusers, an optimum endwall blowing rate, $\dot{m}_{EW}$, exists. For the contoured-wall diffusers, an optimum combination of $\dot{m}_{EW}$ and the diffuser wall blowing rate, $\dot{m}_{BLC}$, exists.

RECOMMENDATIONS

The significance of boundary-layer control, or the absence thereof, becomes even greater as experimental devices are pushed to full scale development. Use of ejector/diffuser configurations with actual engine exhaust supplying the primary driving flow frequently results in higher pressure and temperature conditions than were achieved experimentally. Mechanization of designs to comply with wing/fuselage structural constraints may also alter experimentally obtained optima. Recommendations to enable experimental data to be achieved on flightworthy configurations therefore take the following form:

- Optimum endwall and diffuser wall boundary-layer control (BLC) conditions should be investigated for scaling effects.

- Optimum BLC conditions should be determined for pressures and temperatures corresponding to current jet engine exhaust flow.

- Configurations corresponding to actual flight hardware should be investigated to determine optimum flow parameters.

REFERENCES

1. Squyers, R. A.: Feasibility Tests on Mating an Antiseparation Tailored Contour With a Large Area Ratio Thrust Augmenter. ATC Report No. B-94300/4TR-27, 1974.

2. O'Donnell, R. M.; and Squyers, R. A.: V/STOL Ejector Short Diffuser Study. NADC-77165-30, Naval Air Development Center, 1976.

3. Seiler, M. R.: An Investigation of Corner Separation Within a Thrust Augmenter Having Coanda Jets. NADC-76153-30, Naval Air Development Center, 1977.

4. Haight, C. H.; and O'Donnell, R. M.: Experimental Mating of Trapped Vortex Diffusers with Large Area Ratio Thrust Augmentors. ARL TR 74-0115, Air Force Systems Command, 1974.

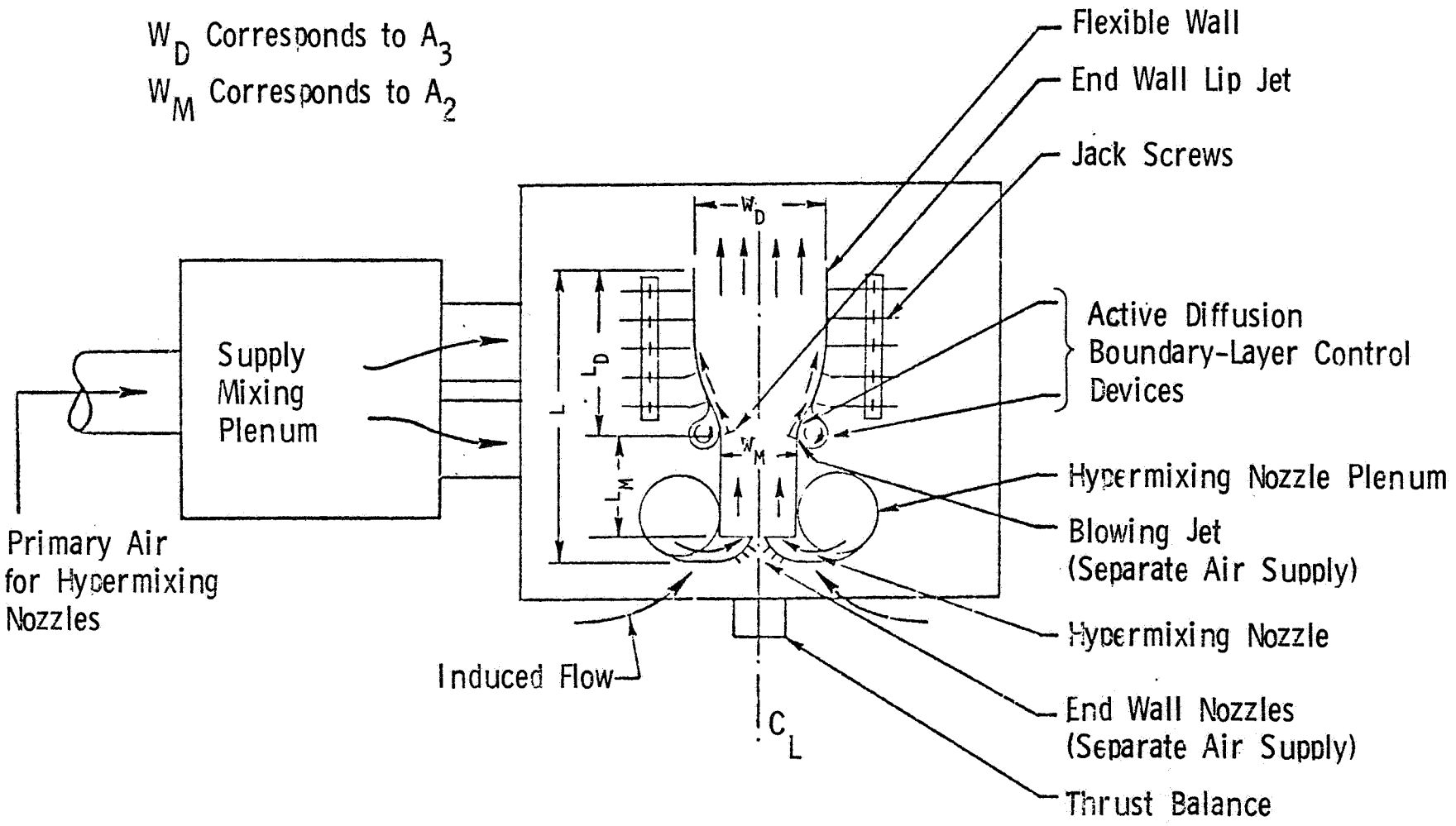

Figure 1.- Schematic of ejector/diffuser test bed.

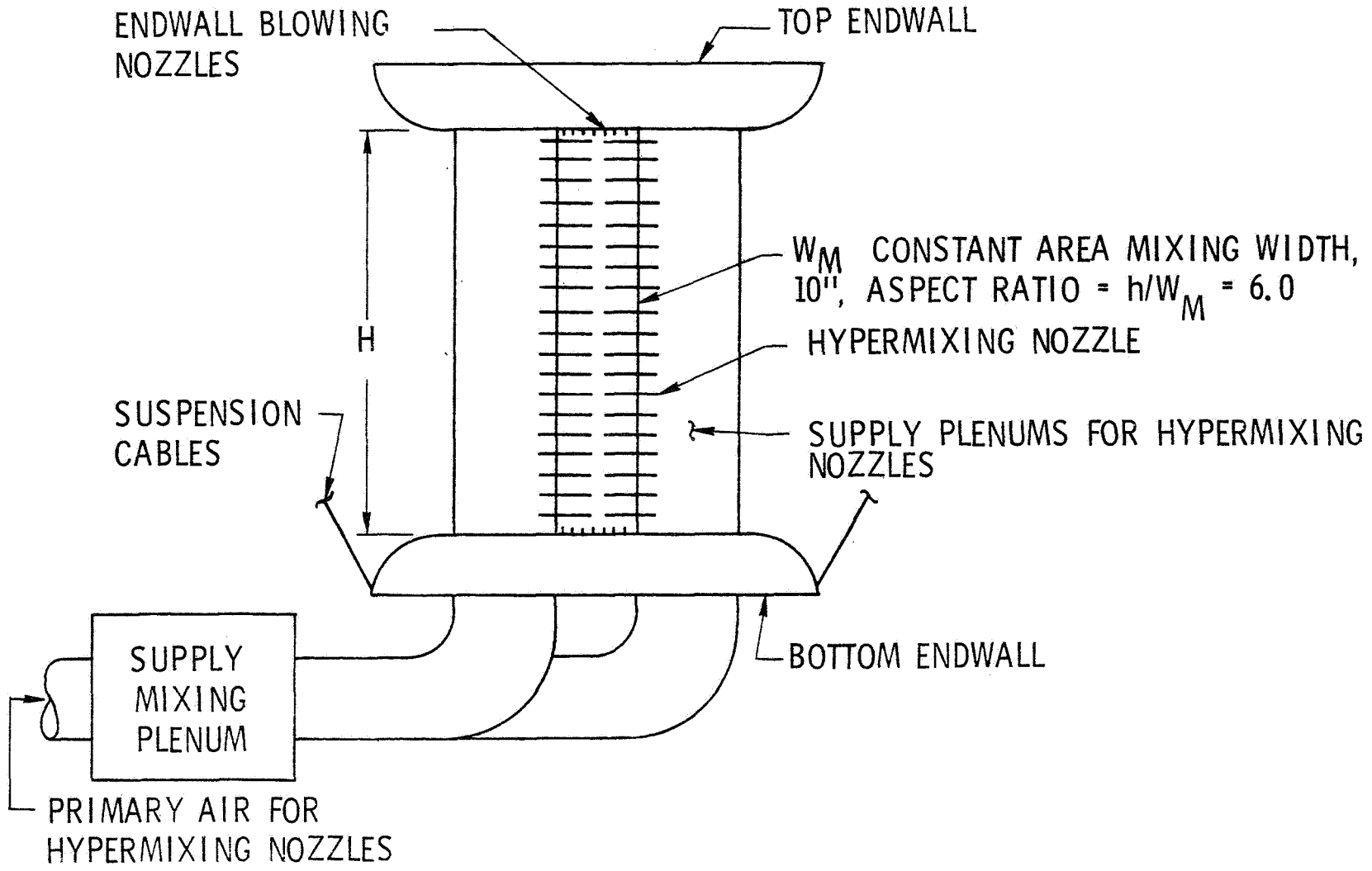

Figure 2.- Front view of ejector test bed (looking downstream).

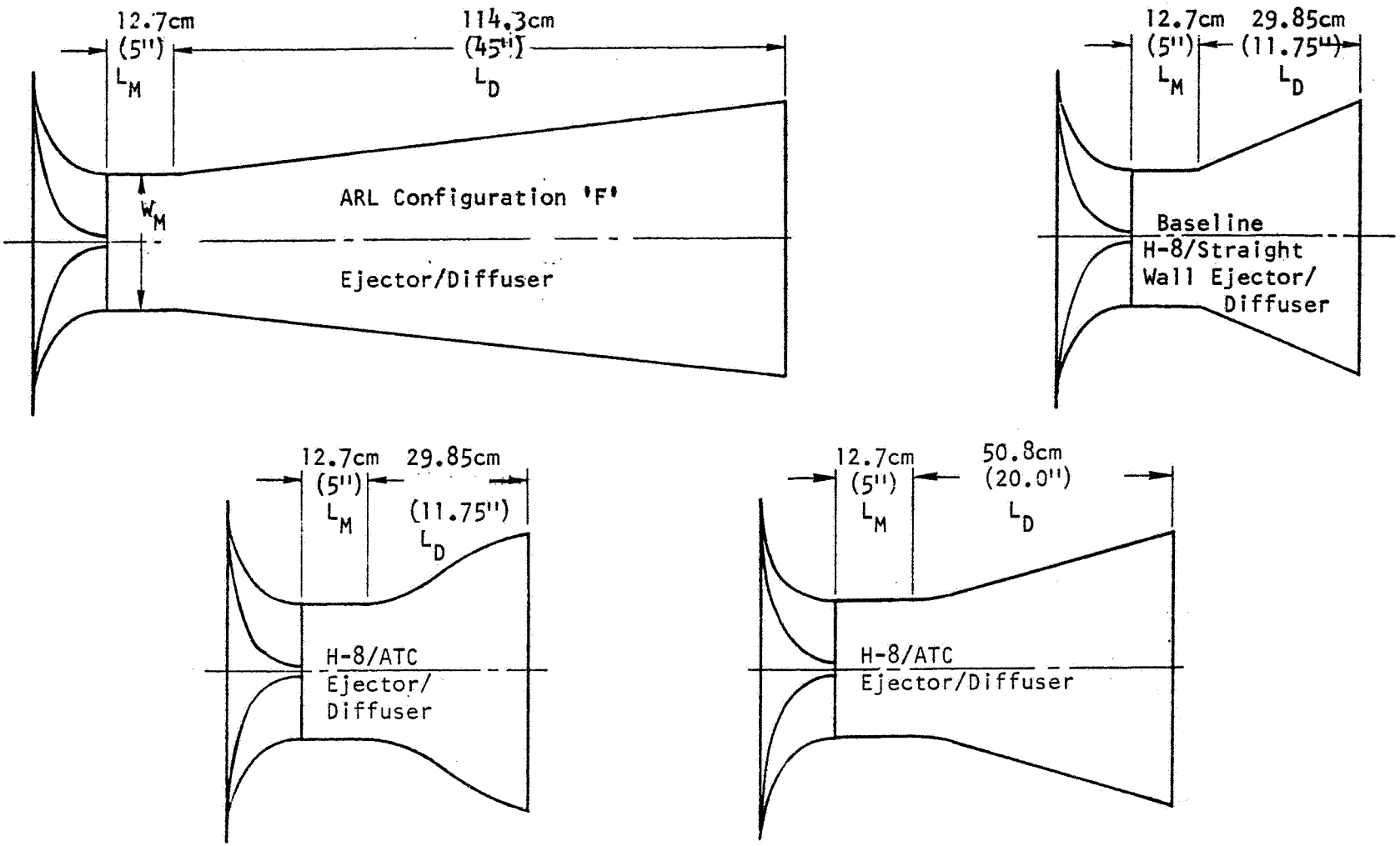

Figure 3.- Planviews of ejector/diffuser test configurations.

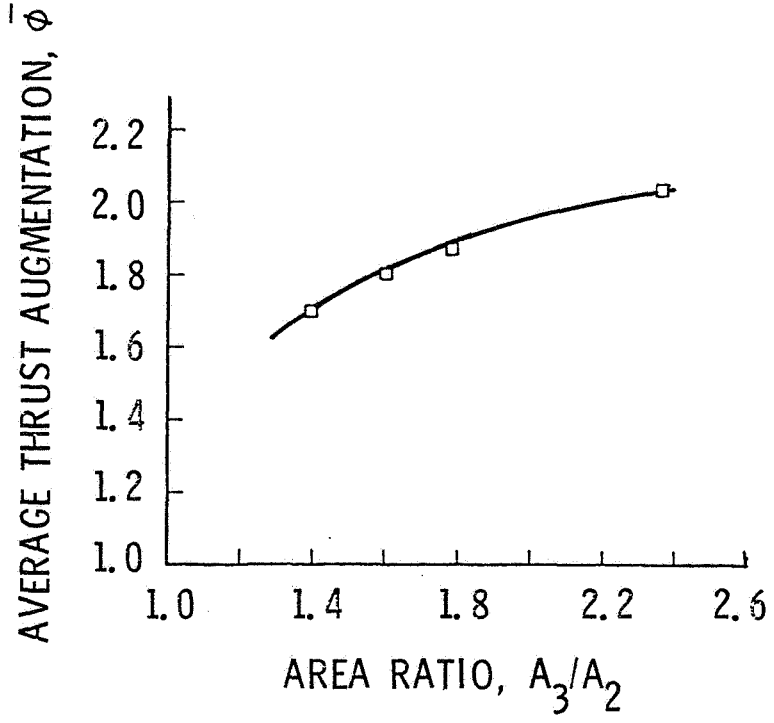

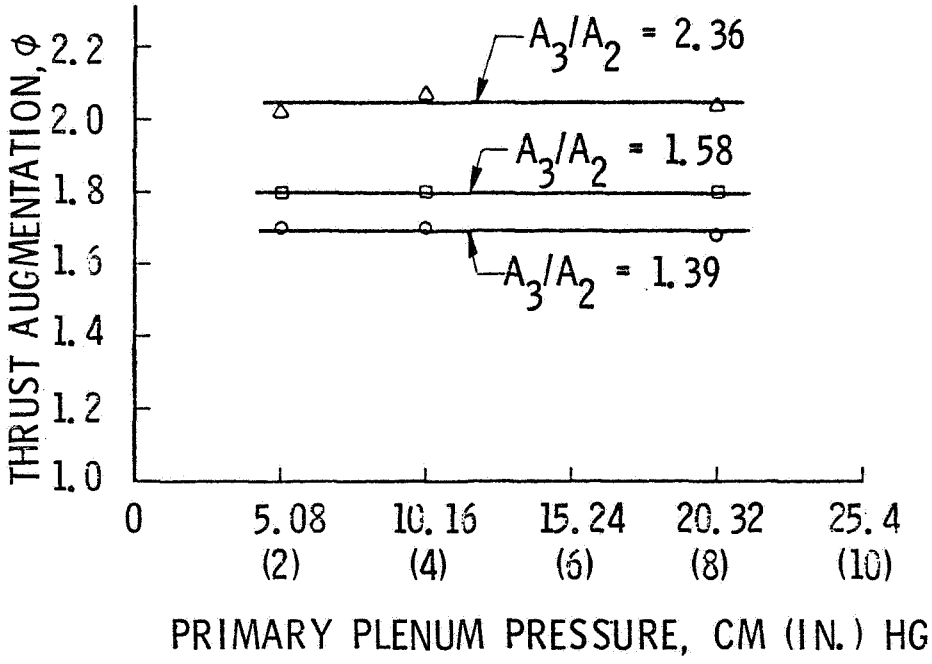

Figure 4.- Variation of thrust augmentation ratio with diffuser area ratio and pressure, for configuration "F", ARL/H-8 nozzles, from reference 4.

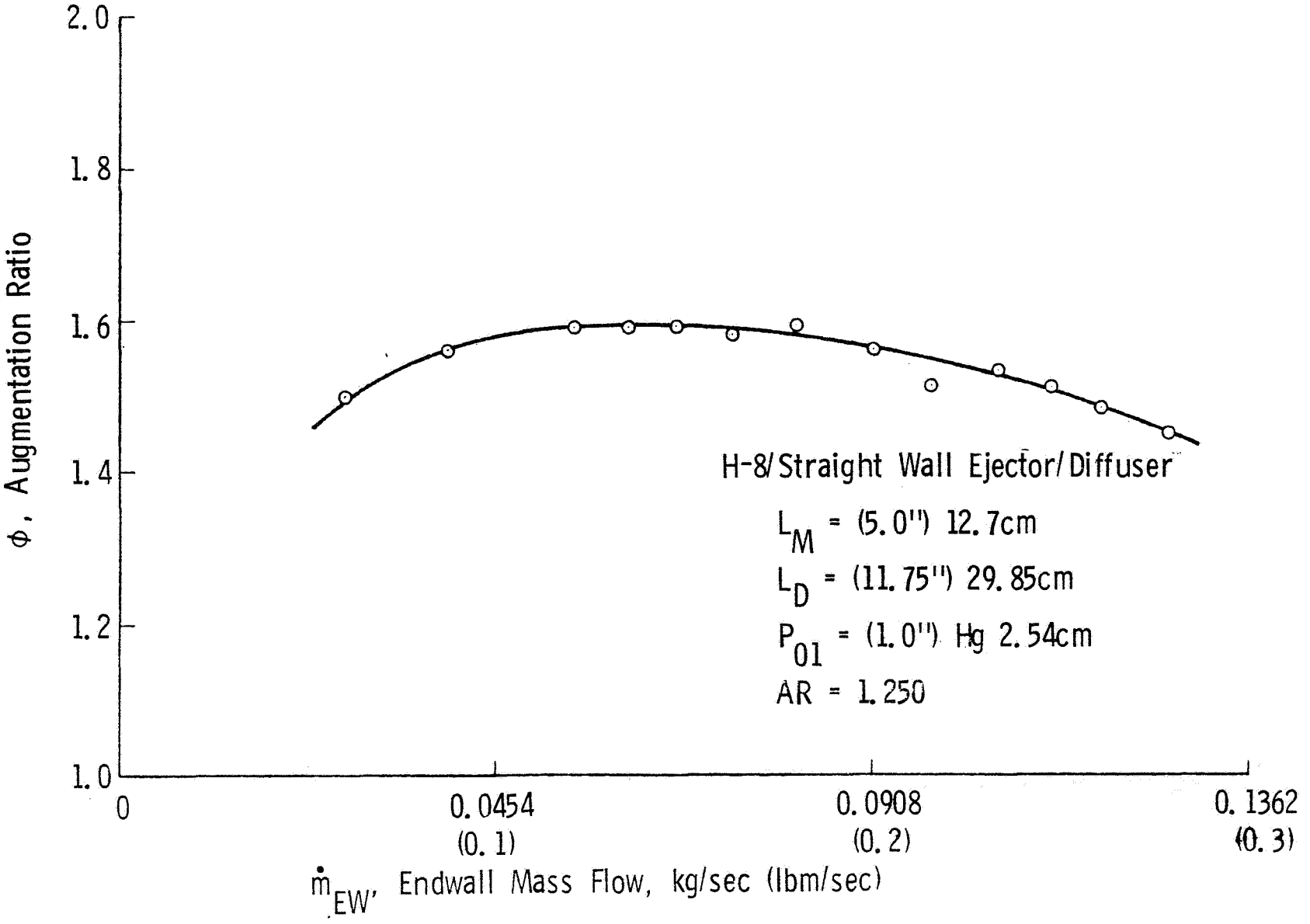

Figure 5.- Variations with endwall blowing for baseline straight-wall diffuser, $A_3/A_2 = 1.25$.

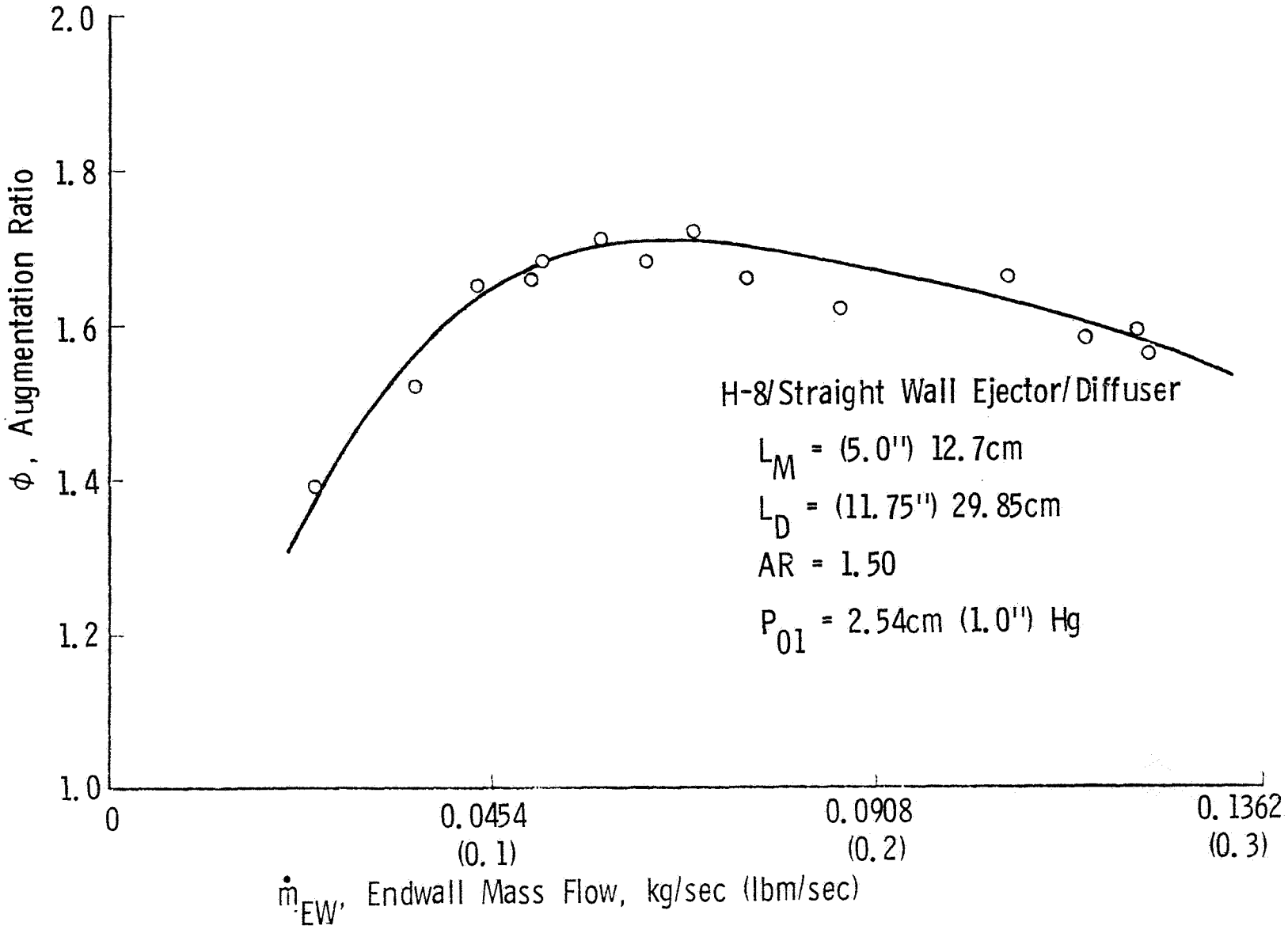

Figure 6.- Variations with endwall blowing for baseline straight-wall diffuser, A_3/A_2 = 1.50.

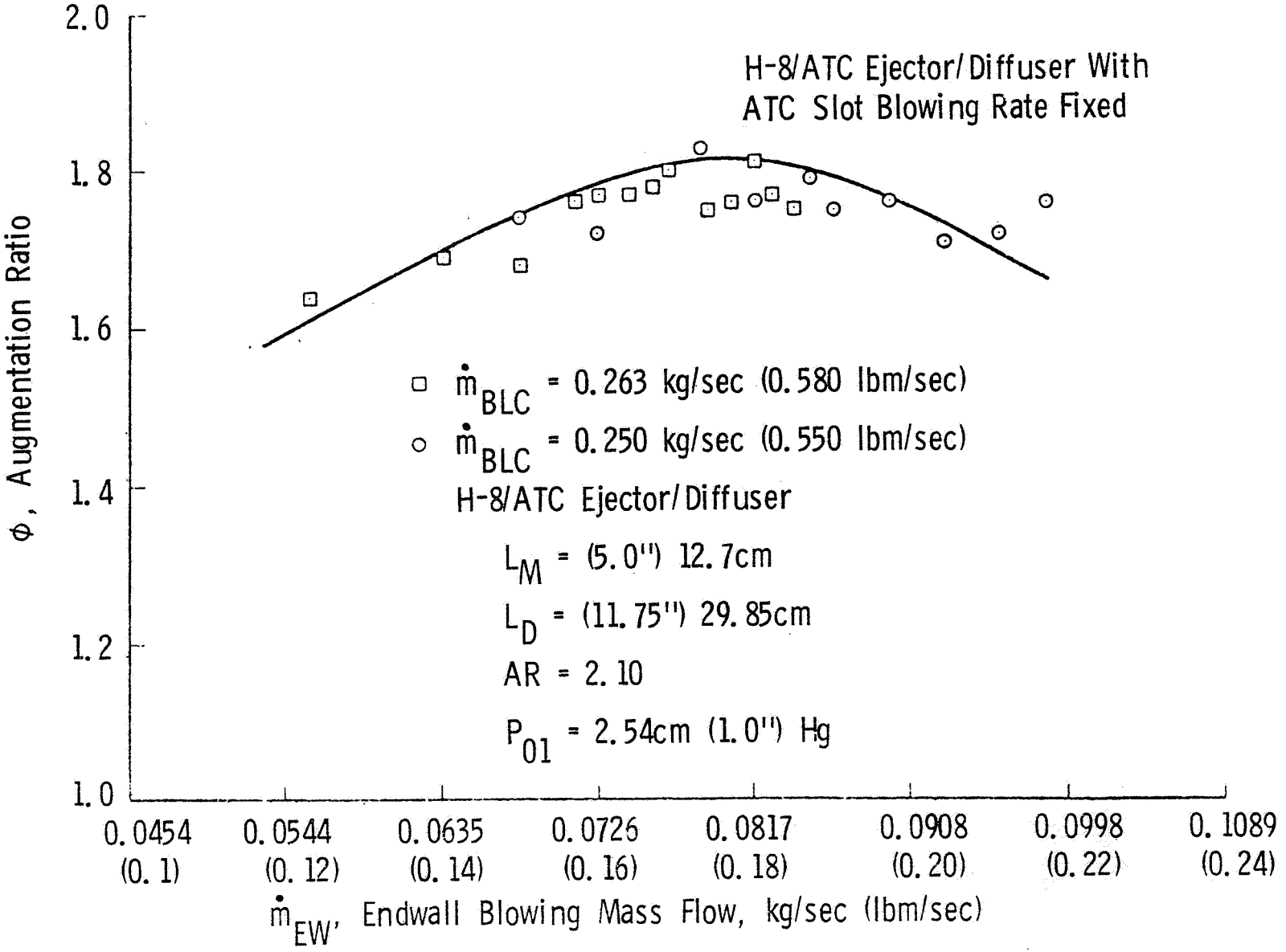

Figure 7.- Optimization of endwall blowing for a specially contoured (ATC) diffuser.

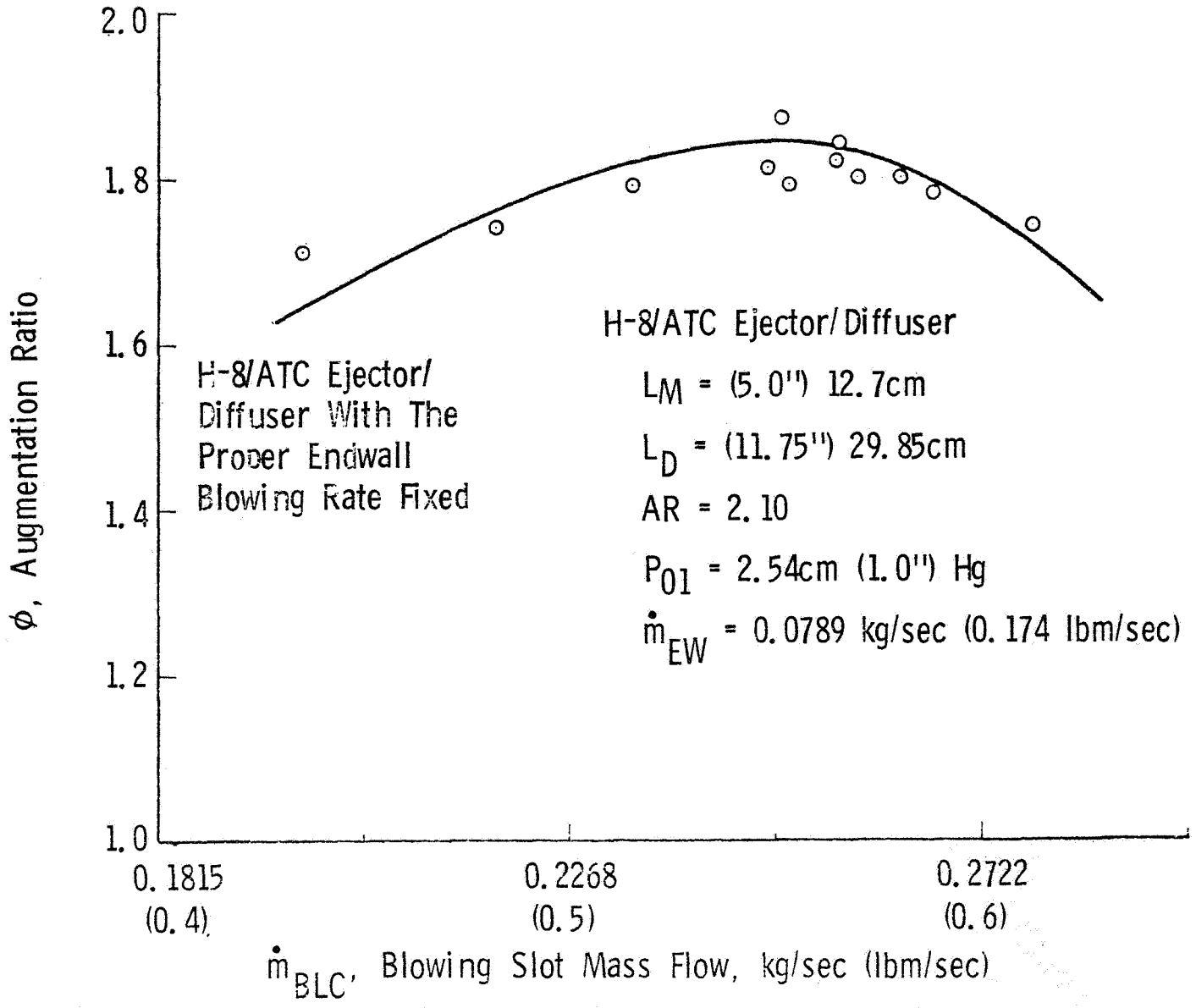

Figure 8.- Optimization of diffuser wall blowing for a specially contoured (ATC) diffuser.

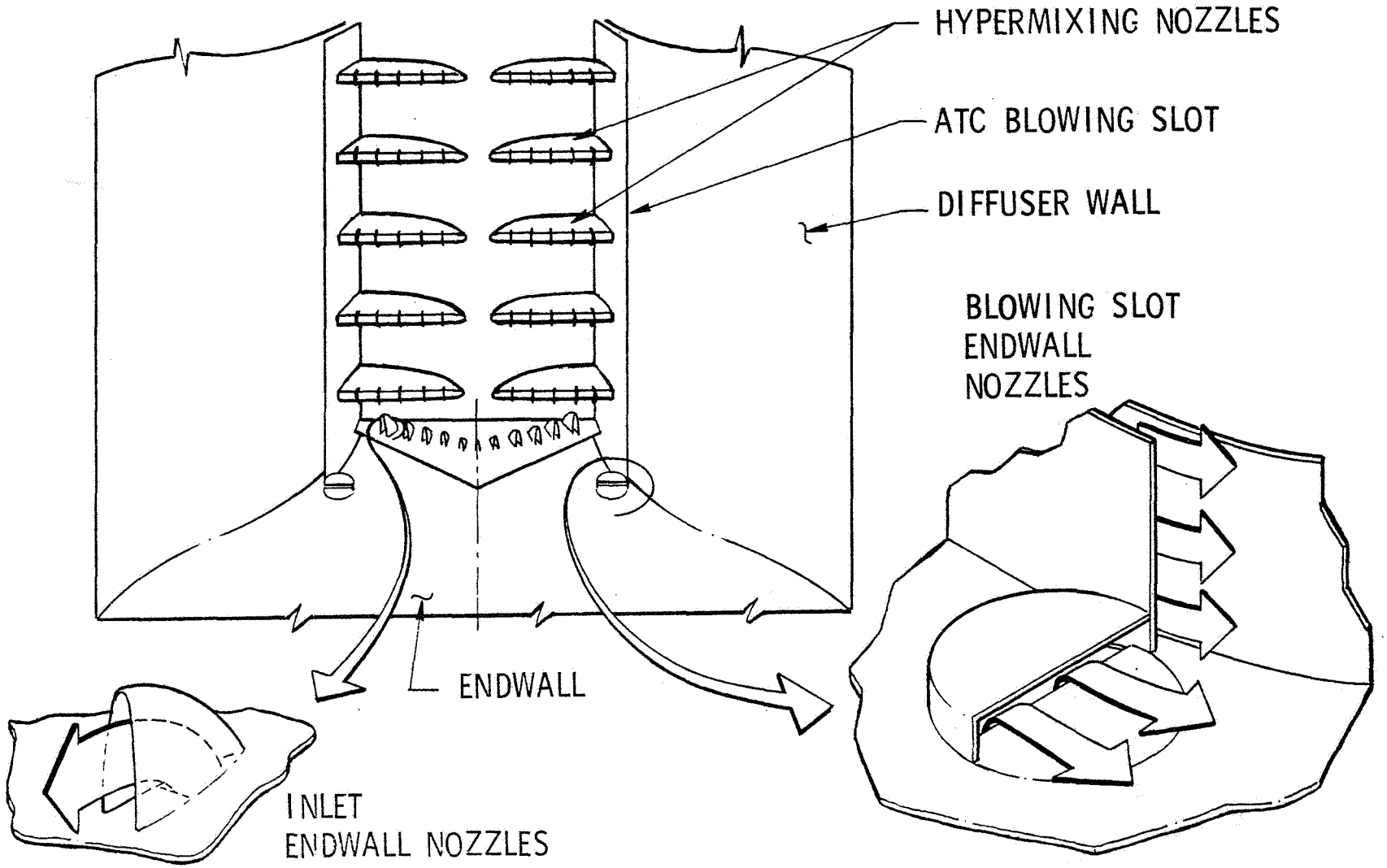

Figure 9.- View of ejector test configuration showing special endwall blowing nozzles (looking upstream).

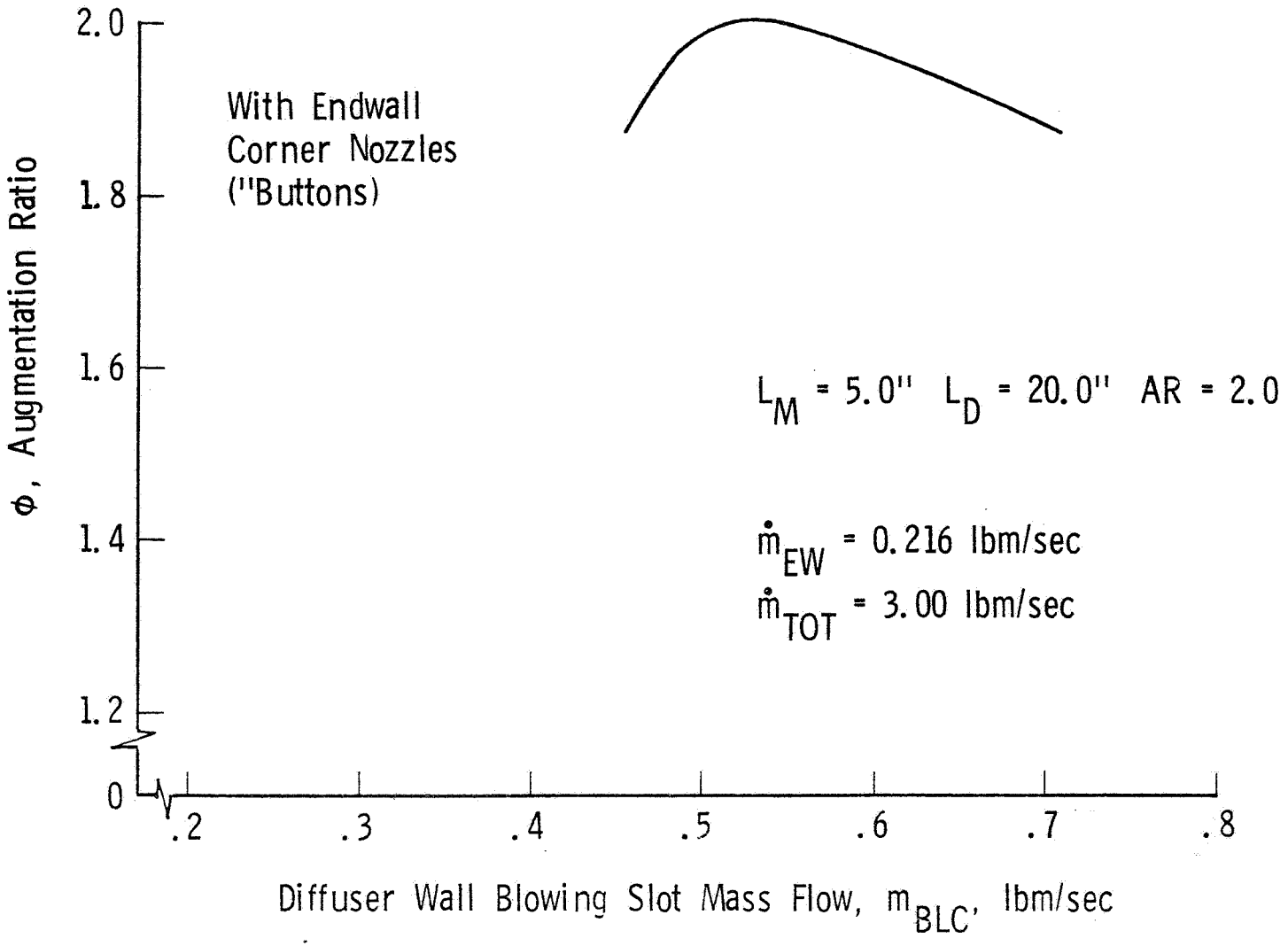

Figure 10.- Variation of peak augmentation ratio with diffuser wall slot mass flow, for no corner blowing.

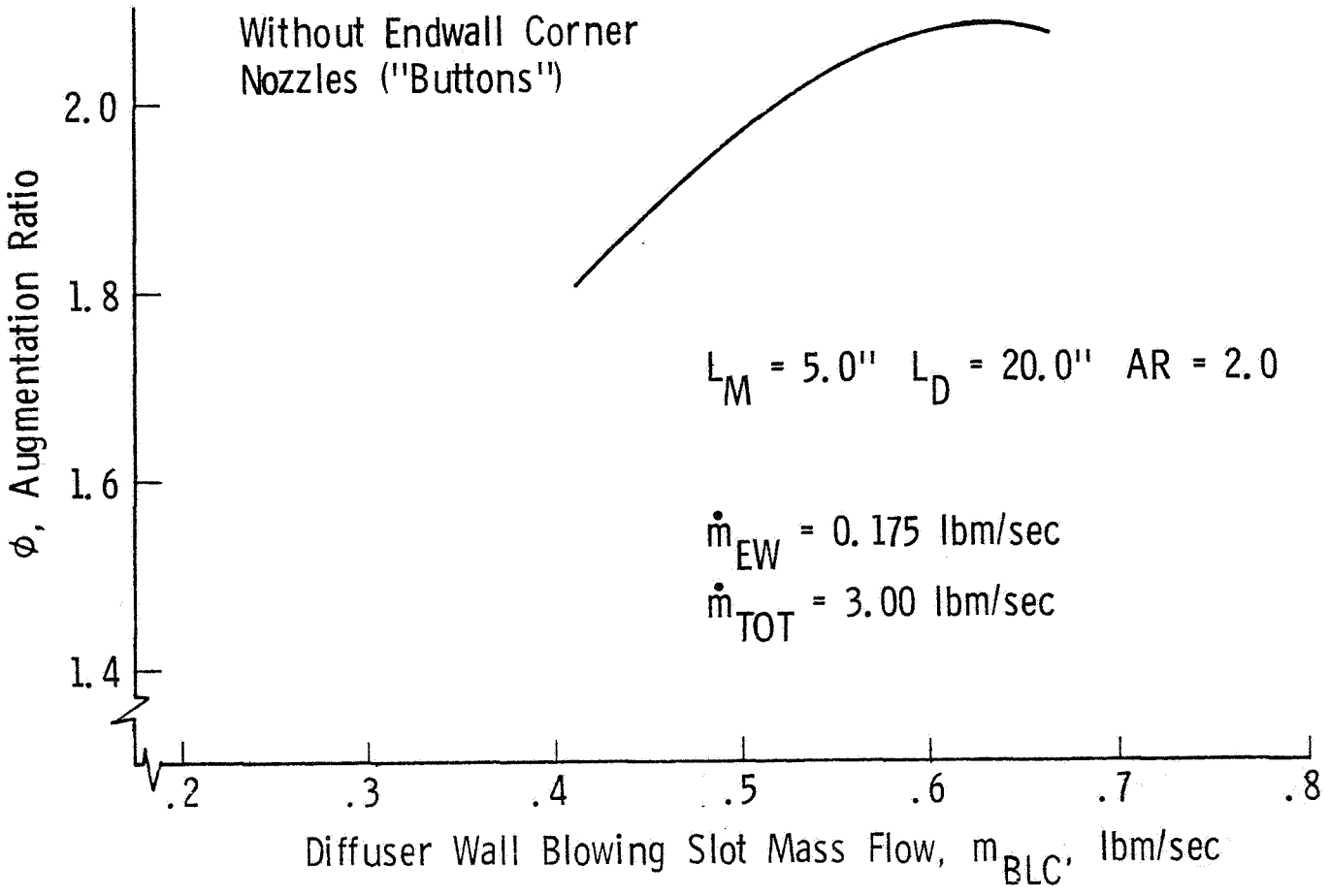

Figure 11.- Variation of peak augmentation ratio with diffuser wall slot mass flow, for no corner blowing.

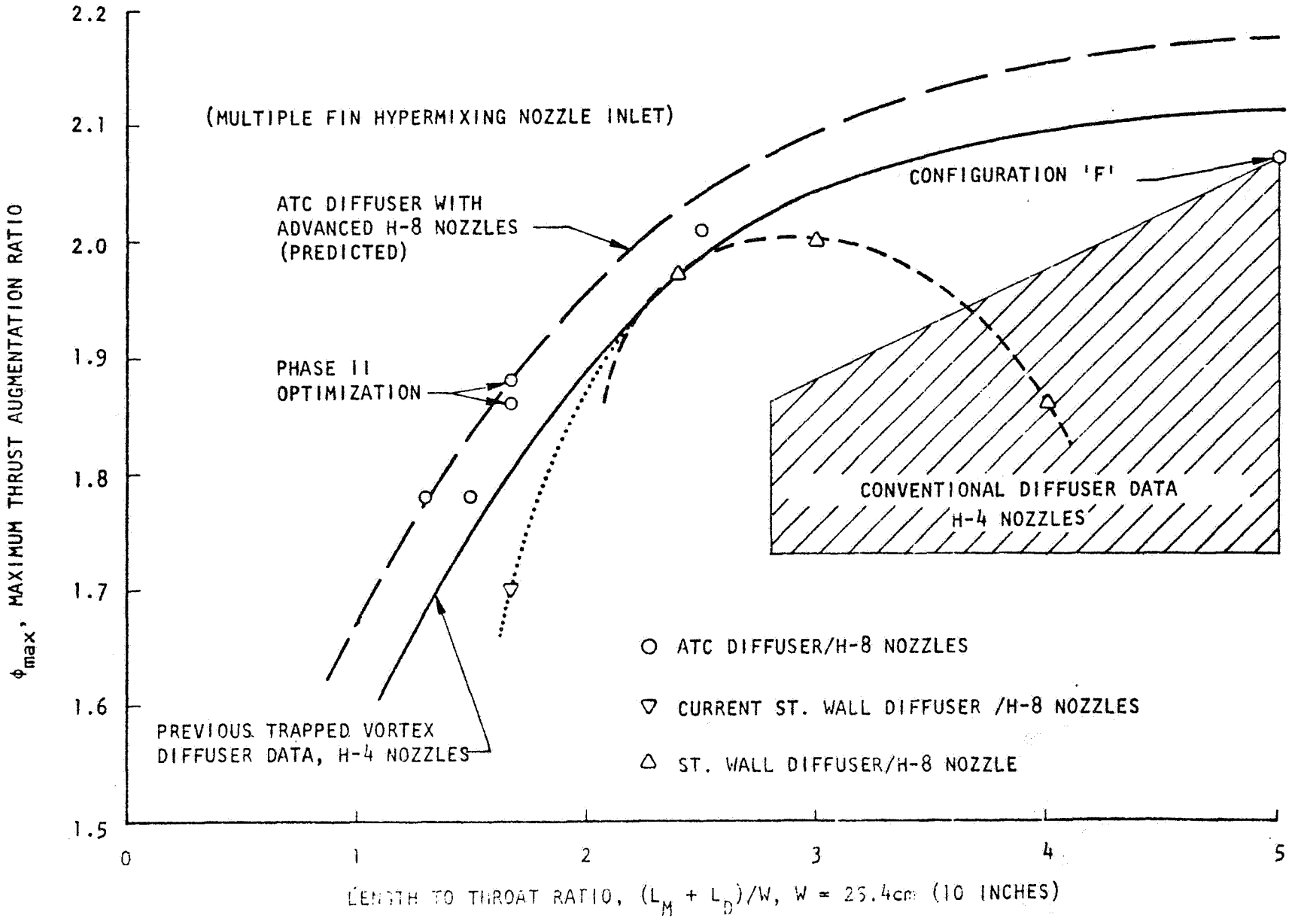

Figure 12.- Comparison of maximum augmentation ratios for ATC and conventional diffusers.

AN INVESTIGATION OF CORNER SEPARATION WITHIN A THRUST AUGMENTER HAVING COANDA JETS*

M. R. Seiler

Rockwell International
Columbus Aircraft Division

- Abstract -

An investigation was conducted to determine the way separation develops in the corners of thrust augmenter wings having Coanda jets. Hot film surface sensors and pressure transducers were used, and the results indicated that separation on the test augmenter began at a corner very close to the augmenter exit and then rapidly proceeded upstream. Measurements of the pressure fields in the corner region indicated that a modified form of the Stratford criterion could be used to predict the onset of separation. Testing was conducted over a range of nozzle pressure ratios, aspect ratios, diffuser angles and designs of the boundary layer and Coanda nozzles.

*Research supported by the Naval Air Development Center, Contract N62269-76-C-0402, Final Report No. NADC 76153-30

I. Introduction

Thrust augmenters have been used in aircraft applications for a number of years. One of the first applications was to use them to draw cooling air over a jet engine nozzle.[1] Modest increases in thrust were also observed. During the early 1960's thrust augmenters were used to provide lift for the XV-4A research VTOL aircraft. More recently[2] they have been used in the design concept of thrust augmenter wings (TAW) for direct lift in the Navy XFV-12A. Experimentally it has been observed that flow separation within the augmenter diffuser is often the limiting factor. The purpose of this study was to conduct a suitable testing program and analysis of an unswept, untapered (rectangular), model augmenter so that a preliminary separation criterion could be established.

II. Approach

The type of augmenter under consideration is one having a centerjet and two Coanda jets, as shown in Figure 1. The Coanda jets originate upstream of the throat and provide a wall jet through the diffuser section. Without these Coanda jets, diffuser half-angles are limited to $\delta_D \approx .1$ radian to prevent separation. Small, boundary layer control (BLC) blowers were also mounted through the endwall and could be rotated manually to direct flow parallel to the diffuser flap. The end elements of the cross-slot centerbody also direct some flow onto the endwalls to accomplish a BLC function. Figure 2 shows a photograph of the test augmenter looking into the exit.

Flow to each of the major augmenter components was measured by a separate venturi and nozzle pressures were recorded by a total pressure probe at the nozzle exit. Nozzle pressure ratios were varied between 1.5 and 2.5. The entire 50 cm (20") span augmenter was mounted on a horizontal cradle suspended by four tie-rods attached to a rigid frame. Two 500-pound load cells measured the thrust. The tares of the flexible hoses, which deliver the primary air, were recorded versus supply pressure and removed from the measured thrust. A 4500 hp Ingersoll-Rand compressor was used as the continuous air supply.

Experience has shown that flow separation generally occurs at or near a corner formed by the diffuser and the endwall.[3] There are two possible modes through which separation might develop (Figure 3). In the first mode separation would initiate at the augmenter exit and, because of the adverse pressure gradient within the diffuser, rapidly progress upstream. A second possible mode would be for separation to begin in the corner on the highly stressed Coanda surface and then proceed downstream until the entire diffuser corner was involved.

The type of BLC being used may have an effect on the separation mode and the angle at which separation occurs. The aspect ratio (AR = span/throat

width) also effects the separation angle.[4] Finally, a reasonable data base should include testing over a wide nozzle pressure range.

The objective of the study was then to accomplish the following tasks:

a) To determine which of the two possible corner separation modes actually occur in an operating augmenter with Coanda jets.

b) To measure the pressure and velocity fields in the vicinity of the separation point for a range of nozzle pressure ratios (P_R) and BLC conditions at and near separated flow conditions.

c) To alter the augmenter AR and repeat task b, above.

d) To alter the Coanda design to provide comparative data on Coandas of smaller R/t. This provides a more highly stressed Coanda surface. In addition, the internal Coanda nozzle configurations were altered to examine the possible effects of exit velocity profile on separation.

e) To analyze the data to derive a separation criteria.

III. Results

For all tests the throat width, flap length, centerbody and BLC were as shown in Figure 1. Three different Coanda configurations, shown in Figure 4, were used. The first, called a reference profile, maintained a Coanda radius to nozzle gap ratio of 26.5. The ratio of augmenter throat area to total nozzle area was $A_2/A_0 = 20.5$. This reference Coanda was used in the study of separation mode and to provide a baseline augmentation ratio versus diffusion ratio, A_3/A_2.

Separation Mode

The augmenter was instrumented as shown in Figure 5. Two flush-mounted Thermo-Systems, Inc., Model 1237 hot film sensors were mounted on one flap surface at the endwall corner .032 cm and 5.01 cm upstream from the flap trailing edge. Two Statham ±2 psi differential pressure transducers were connected to surface pressure taps similarly located on the opposite flap. The hot film sensors were connected to a model 1050-2C Thermo-Systems, Inc., dual channel constant temperature anemometer whose output, together with that of the two transducers, was connected to a multi-channel Consolidated Electronics Corporation oscillograph.

The response time of the hot-film sensor ($\approx 5 \times 10^{-6}$ sec) was an order of magnitude faster than any mean flow changes likely to occur within the augmenter. Using the A.C. anemometer output, the diffuser angle, θ_D, was gradually increased to a point where a slight buffeting could be

detected audibly (incipient separation). As shown in Figure 6 the turbulence level increased suddenly at the downstream sensor. Next the augmenter δ_D was rapidly raised beyond the point of attached flow and the two signals were displayed on the oscilliscope. Turbulence levels on the upstream sensor increased markedly within .0023 to .0027 seconds after the downstream sensor showed a similar increase. These tests, done at a nozzle pressure ratio of 2.0, show that the separation was initiating downstream. Similar results were obtained at a pressure ratio of 1.5.

Augmentation Ratio

The augmentation ratio is defined:

$$\emptyset = \frac{\text{measured load-stand thrust}}{\text{ideal thrust from all primary jets and BLC}}$$

where the ideal thrust uses the measured venturi mass flow and the isentropic nozzle velocity (expanded to atmospheric pressure). Using the reference profile Coandas, the results of Figure 7 were obtained with aspect ratio = 4.1. Notice that separation occurs at a half angle of .21 radian without BLC and at .35 radian with BLC. When the aspect ratio is changed to 2.5, Figure 8 shows that the overall $\emptyset$ levels are similar but separation occurs at a slightly lower diffuser angle. A_2/A_0 was 20.5. BLC blowers were manually adjusted to blow parallel to the flaps.

Subsequent tests at $A_2/A_0 = 17$ were made on the top-hat profile and the vortex profile Coandas of Figure 4. The top-hat was designed to achieve a uniform velocity profile at the nozzle but R/t was reduced to 9.3. The vortex profile Coanda was intended to produce a nozzle velocity that was greatest on the inner radius.

Figure 9 shows results of augmentation ratio versus A_3/A_2 for the top-hat profile. Although the initial slope, $\emptyset$ vs A_3/A_2, is similar to the reference profile, flow separation in the diffuser corner limits the performance to lower values of $\emptyset$.

Similar behavior was also noted on the vortex profile Coanda (Figure 10). At nozzle pressure ratios of 2.5, corners became more difficult to attach on both of these Coanda shapes.

Pressure Measurements

A series of 13 flush-mounted static taps were added in one corner of the diffuser near the exit, as shown in Figure 11. These taps were connected to a water manometer and recorded during operation at all diffuser angles. Also recorded was the throat secondary static pressure. Figure 12 shows the location of the probe.

Figures 13 and 14 show the static pressure profiles in the diffuser corner for the reference profile Coanda. These measurements were taken at the diffuser angle for incipient separation, which also corresponds to the angle for maximum $\emptyset$. Figure 13 gives results without BLC for an aspect ratio of 4.1. Figure 14 is for full BLC; that is, the BLC nozzle pressure was set equal to the Coanda and centerjet pressures. Also shown in the figures are the calculated term xdp/dx_{exit}, which is derived from the gradient of the pressure readings. The trend is toward a steeper gradient at the diffuser exit as the BLC is applied. Nominal A_2/A_0 was 20.5.

Figures 15 and 16 show results for the top-hat and vortex profile Coandas at an aspect ratio of 4.1. A_2/A_0 was 17. Notice that the static pressures are more negative than for the reference profile and the gradient is more steep. This is related to the increased Coanda nozzle gap and the reduced A_2/A_0.

IV. Separation Criteria

One of the more successful airfoil separation criteria and the one considered herein is that of Stratford[5] where the criteria is expressed as a non-dimensional number N_{ST},

$$N_{ST} = \frac{C_p \, (x dC_p/dx)^{1/2}}{(R_N \times 10^{-6})^{1/10}} \tag{1}$$

where C_p is the pressure coefficient, defined by

$$C_p = \frac{P(x) - P(0)}{q(0)} \tag{2}$$

C_p is based upon the difference between local wall static pressure P(x) and that pressure occurring at the start of the interaction region, P(0), at x = 0. q(0) is the dynamic pressure $1/2\rho U_{max}^2$, where U_{max} is the maximum velocity at x = 0. R_N is the Reynolds number based upon U_{max} and x. Stratford's method involves an approximate solution of the equations of motion, and matching the solutions at the junction of the "inner" and "outer" boundary layer. A subsonic airfoil will not separate if $N_{ST} < .37$.

Although Stratford used P(0) as the wall pressure at x = 0, there are experimental difficulties in determining its value accurately on a Coanda radius at choked pressures. Furthermore, because of the highly curved flow near the Coanda, the value of P(0) at the wall is also difficult to predict analytically. For these reasons, P(0) was chosen for the ejector diffuser to be the value of the static pressure in the uniform secondary stream (see Figures 12 and 17).

q(0) is merely a normalizing factor for the other pressure terms. Rather than take $q(0) = 1/2\rho U_{max}^2$ at the throat, it seemed correct in the high Mach number flow to use q(0) as the maximum gage total pressure. Experience has shown that all static pressures (gage) in an augmenter can be normalized by nozzle gage total pressure. In a corner near the throat, the maximum value of q is either:

(1) The gage total pressure set on the BLC blower, or

(2) The gage total pressure of the Coanda flow.

The greater of the above two quantities was used to set q(0). With no BLC turned on, the Coanda flow sets q(0). With full BLC, the BLC nozzle pressure determines q(0). Since R_N must use the maximum velocity U_{max}, the isentropic flow equations were used to determine the relationship between U_{max} and q(0) (see Figure 18).

$$U_{max} = \left(2RT \frac{\gamma}{\gamma-1} \left(1 - P_R^{-\frac{\gamma-1}{\gamma}}\right)\right)^{1/2} \quad \text{meters/sec} \tag{3}$$

$R = 287$ Joules/°K-kg
$\gamma = 1.4$
T = temperature, °K (nominally 290°K)
$P_R = (q(0) + P_\infty)/P_\infty$
P_∞ = barometric pressure (nominally 99 Kilopascals)

Table I presents a summary of the Stratford number calculations for the augmenters constructed under the present study. There are three BLC conditions--full, minimum and no BLC for aspect ratios of 4.1 and 2.5 using the reference Coandas. Also included are the top-hat and vortex profile Coanda results. The table gives the nominal pressure ratio and the flap angle where the measurements and calculations were made.

It is instructive to consider the difference in the three augmenters and to try to visualize what mechanism is setting $N_{ST} \approx .02$ as a common upper limit. Figure 19 shows a plot of the term $P_\infty - P(0) \approx P(x) - P(0)$ and the term xdP/dx versus diffuser angle for the three augmenters. The conditions are full BLC and PR ≈ 2.0. Notice that the vortex and top-hat profiles produce larger values of xdP/dx than does the reference profile. This, as mentioned earlier, is related to the larger nozzle gap and decreased A_2/A_0. The throat static gage pressure, or its negative, $P_\infty - P(0)$, is also greater for the vortex and top-hat at small diffuser angles. This is due to the reduced overall A_2/A_0. Finally near .175 to .2 radian, the reference profile produces the largest values of xdP/dx and $P_\infty - P(0)$. The reference profile also produces the greatest Ø.

A lesson to be learned from Figure 19 is that a high Ø augmenter should produce a large drop in throat static pressure (as is well known) but simultaneously must not produce a large value of xdP/dx at the exit.

This implies that small primary nozzles should be used to achieve well-mixed flows and nearly ambient static pressures at the exit. In other words, the exit static pressure should be nearly recovered to ambient. These facts are entirely consistent with the experience of many workers in the area of thrust augmentation.

Figure 20 shows the calculated values of N_{ST} for these augmenters under the same operating conditions; i.e., full BLC and PR = 2.0. The Stratford number rises to a maximum as flap angle is increased and does provide a useful separation criteria.

These plots indicate that we have not mistakenly selected a criteria this is insensitive to flap angle. The flow will be stable and attached provided

$$N_{ST} \leq .0196$$

For flap angles that produce separation, the Stratford number has no meaning; that is, the criteria is to be used only in the range of flap angles where $d N_{ST}/d\delta$ is positive.

It should be noted that some care in selecting BLC orientation is needed if these experiments are to be repeated. As stated earlier the BLC tubes were rotated manually to direct flow parallel to the flap. If this is not done, the unusual exit pressure profiles of Figure 21 will be obtained. Case 1 is caused by directing the BLC flow into the flap. It likely represents a helical flow pattern in the corner. Case 2 is similar with the opposite flap attached. Case 3 is the profile most like those of this study, with BLC blowing parallel to the flap. Case 4 is a separated flap.

V. Conclusions

1. Corner separation of the test thrust augmenting wing-type augmenter initiates at or near the augmenter diffuser exit and then rapidly progresses upstream until the whole corner from the vicinity of the augmenter throat to the exit is involved.

2. A modified form of the Stratford airfoil stall criterion successfully correlates the onset of augmenter separation in the test augmenter where the independent test variables were nozzle pressure ratio, augmenter aspect ratio, boundary layer control blower pressure ratio and Coanda configuration. The modification consists of a change in reference pressure, P(0), and in definition of q.

3. Circular Coandas with small R/t cause separation to occur at lower diffuser angles.

References

1. Greathouse, W. K., "Preliminary Investigation of Pumping and Thrust Characteristics of Full-size Cooling Air Ejectors at Several Exhaust-Gas Temperatures," NACA RM E54A18, 1954.

2. Throndson, L. W., "Compound Ejector Thrust Augmentation Development," ASME 73-GT-67, 1973.

3. "Three-Dimensional Effects on Augmenters," Rockwell International Report NR76H-36, 1976.

4. Stewart, V. R., "A Study of Scale Effects on Thrust Augmenting Ejectors," Rockwell International Report NR76H-2, 1976.

5. Stratford, D. S., "The Predictions of Separation of the Turbulent Boundary Layer," J. Fluid Mechanics, p. 1, January 1959.

TABLE I.

SUMMARY OF STRATFORD NUMBER CALCULATIONS

Case	Nom. Pressure Ratio	Flap Angle, Radians	P(x) Pascals (Gage)	P(o) Kilo-pascals (Gage)	Q(o) Kilo-pascals	$[xdP/dx]_{exit}$ Kilopascals	$R_N \times 10^{-6}$	N_{ST}*	Remarks
Reference Profile	1.5	0.33	−200	− 6.0	51.0	2.32	2.99	0.0217	Q(0) set by BLC
1. R/t = 26.5	2.0	0.33	−400	−11.5	102.0	4.60	3.81	0.0202	nozzle pressure
Full BLC, AR = 4.1	2.5	0.33	−650	−15.0	147.0	6.95	4.25	0.0184	which is identical to all other nozzles.
Reference Profile	1.5	0.33	−200	− 5.0	47.4	2.32	2.92	0.0201	Q(0) set by BLC
2. R/t = 26.5	2.0	0.33	−450	− 9.7	91.5	4.65	3.68	0.0200	nozzle pressure.
Min. BLC, AR = 4.1	2.5	0.33	−600	−14.0	136.0	6.50	4.17	0.0187	
Reference Profile	1.5	0.21	−150	− 4.2	35.2	1.86	2.58	0.0241	Q(0) set by Coanda
3. R/t = 26.5	2.0	0.21	−375	− 8.1	70.5	3.95	3.28	0.0230	flow at throat.
No BLC, AR = 4.1	2.5	0.21	−550	−11.5	101.0	5.60	3.56	0.0225	
Reference Profile	1.5	0.30	−150	− 5.1	51.0	2.89	2.99	0.0207	Q(0) set by BLC noz-
4. R/t = 26.5	2.0	0.30	−300	− 9.4	102.0	5.12	3.81	0.0175	zle pressure which
Full BLC, AR = 2.5	2.5	0.30	−375	−13.2	147.0	6.85	4.25	0.0163	is identical to all other nozzles.
Reference Profile	1.5	0.30	−125	− 4.85	48.0	3.02	2.92	0.0222	Q(0) set by BLC
5. R/t = 26.5	2.0	0.30	−250	− 9.0	88.0	5.33	3.63	0.0215	nozzle pressure.
Min. BLC, AR = 2.5	2.5	0.30	−375	−12.7	135.0	7.0	4.17	0.0180	
Reference Profile	1.5	0.175	−125	− 3.66	38.0	2.19	2.65	0.0203	Q(0) set by Coanda
6. R/t = 26.5	2.0	0.175	−200	− 6.92	76.0	4.4	3.22	0.0189	flow at throat.
No BLC, AR = 2.5	2.5	0.175	−250	− 9.2	109.0	6.05	3.56	0.0170	
Top Hat Profile	1.5	0.175	−250	− 4.73	51.0	2.44	2.99	0.0172	Q(0) set by BLC noz-
7. R/t = 9.3	2.0	0.175	−450	− 8.7	98.0	6.5	3.77	0.0190	zle pressure which
Full BLC, AR = 4.1	2.5	0.14	−700	−12.3	145.0	9.75	4.24	0.0180	is identical to all other nozzles.
Vortex Profile	1.5	0.175	−225	− 4.93	51.0	3.48	2.99	0.0216	Q(0) set by BLC noz-
8. R/t = 9.3	2.06	0.175	−520	− 9.25	108.0	7.0	3.90	0.0180	zle pressure which
Full BLC, AR = 4.1	2.5	0.14	−575	−11.2	145.0	8.85	4.24	0.0157	is identical to all other nozzles.

$$*N_{ST} = \frac{P(x) - P(0)}{Q(0)} \left[\frac{xdP/dx}{Q(0)}\right]^{1/2} (R_N \times 10^{-6})^{-0.1}$$

Average N_{ST} = 0.0196

Standard Deviation = 0.002 (11%).

CAD 8989

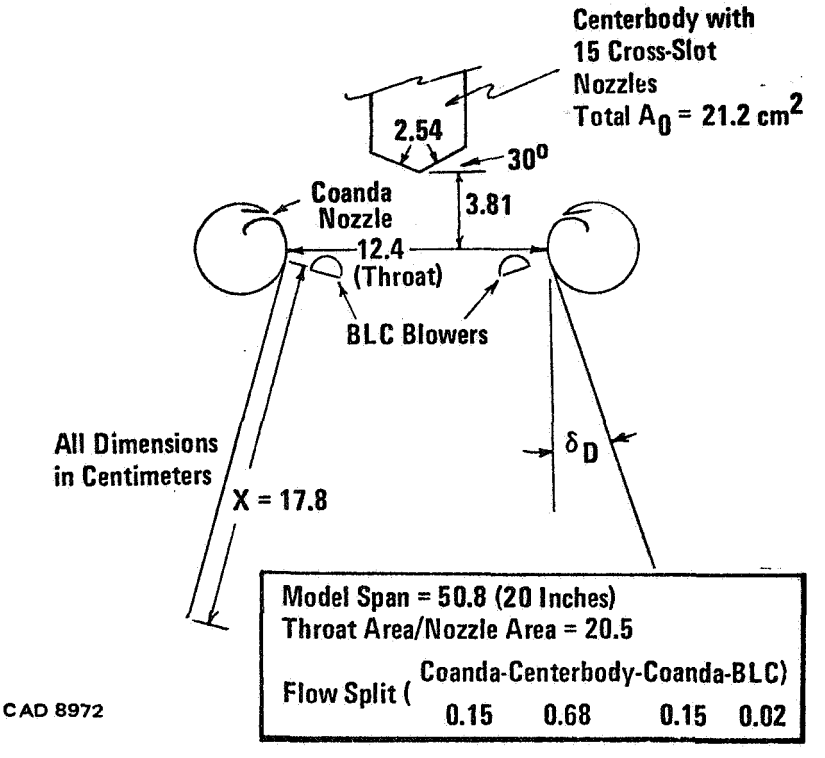

Figure 1. Sectional view of test augmenter.

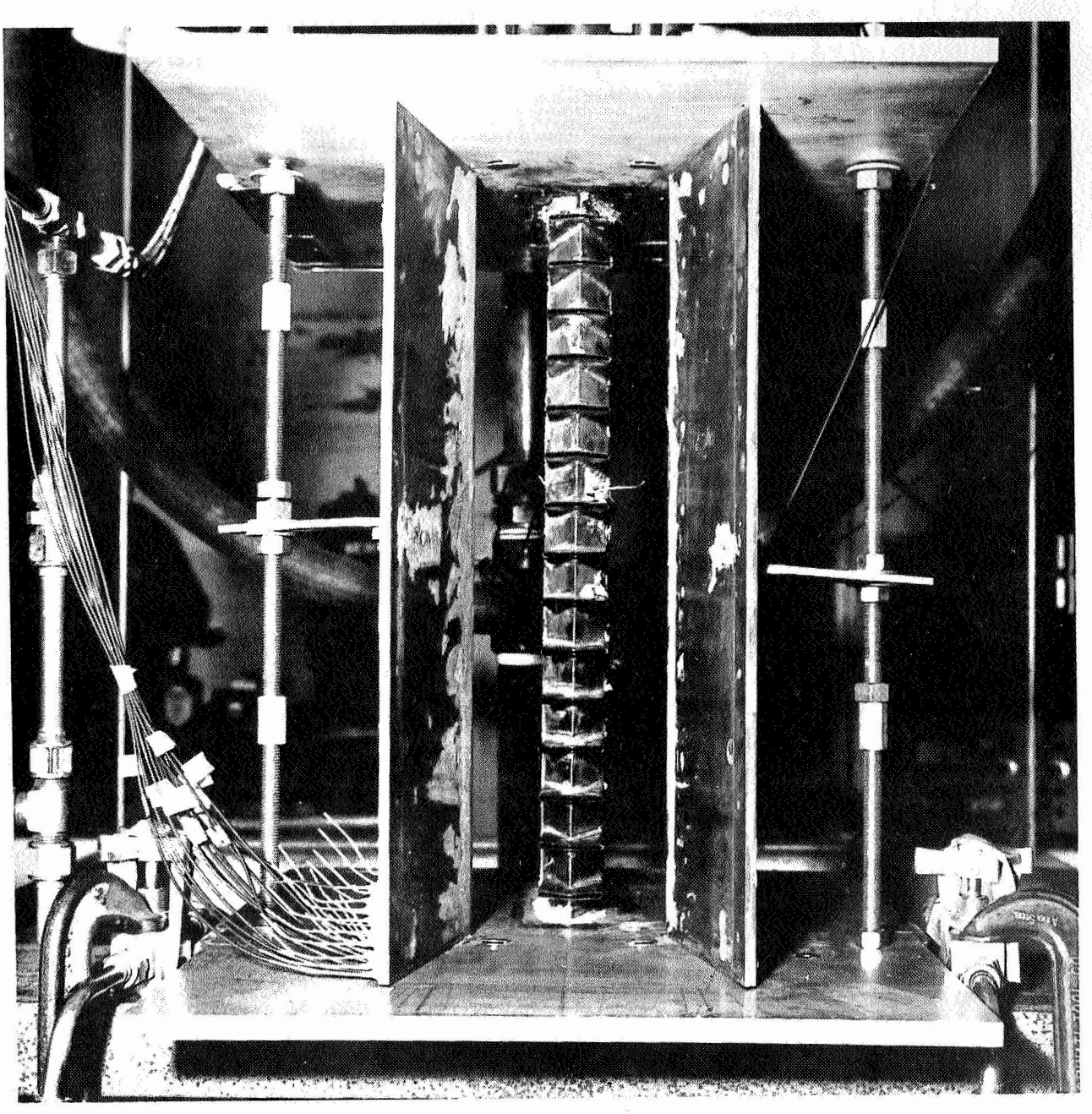

Figure 2. Test augmenter.

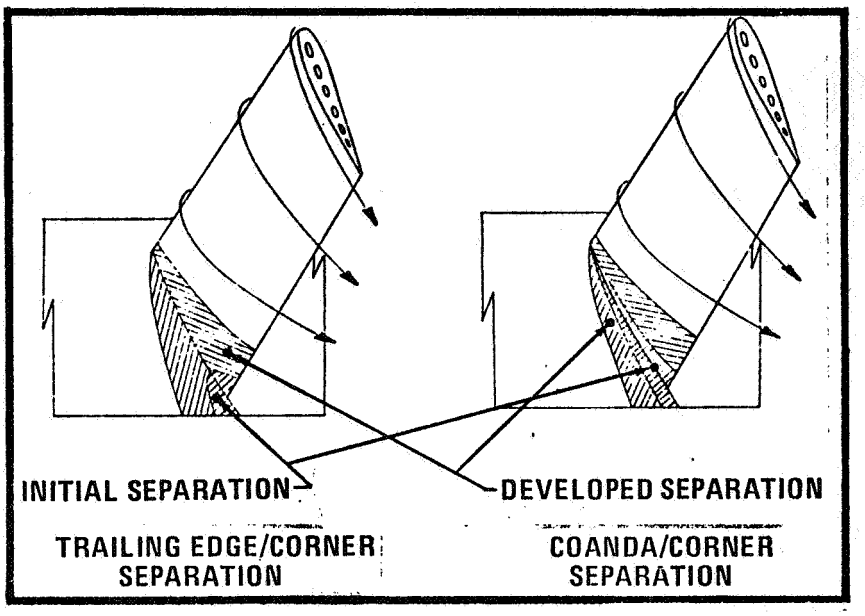

Figure 3.- Possible modes of Corner separation.

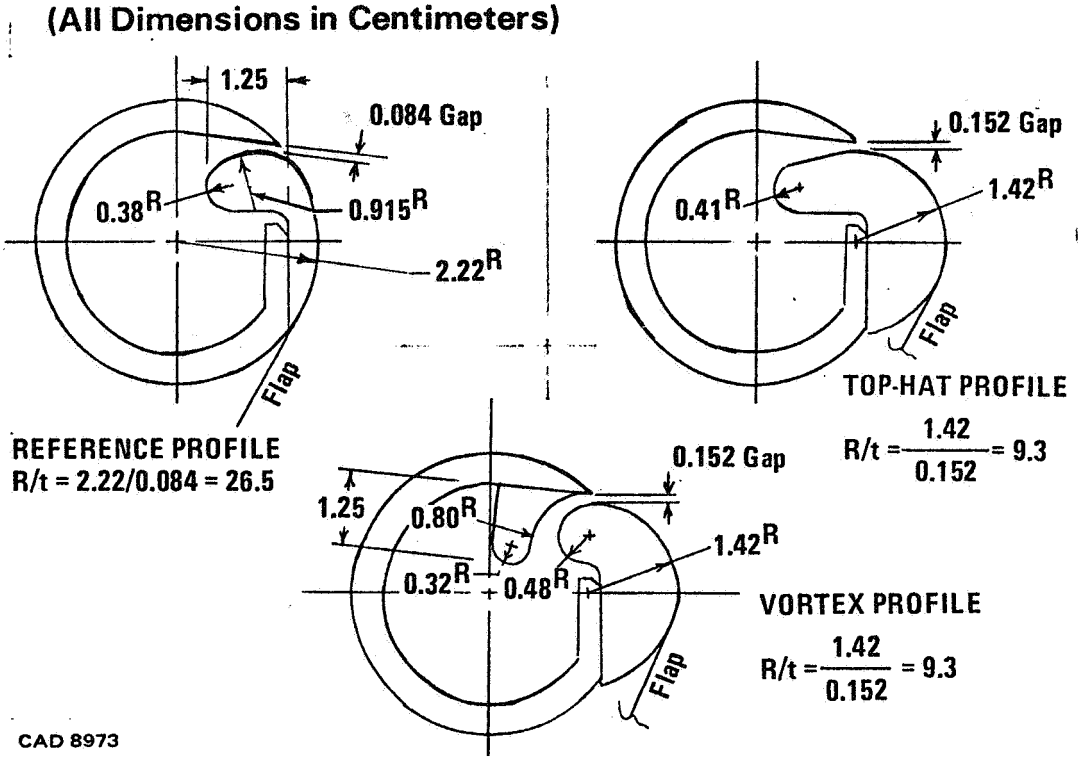

Figure 4. Coanda nozzles tested in present study.

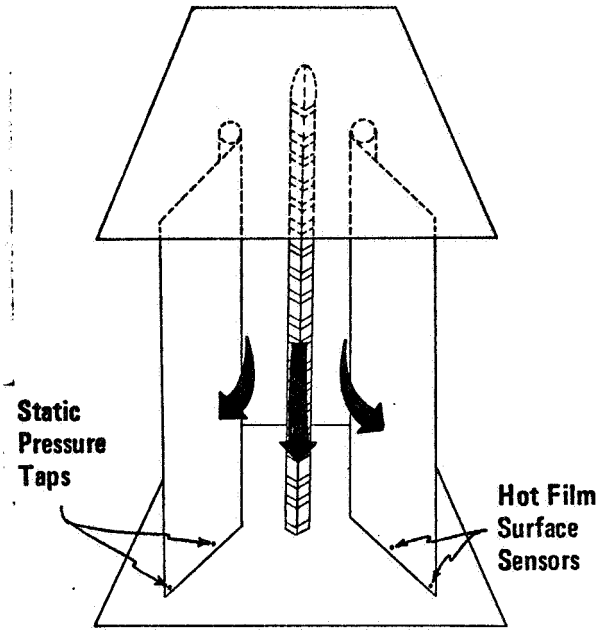

CAD 8976

Figure 5. Instrumentation for separation mode determination.

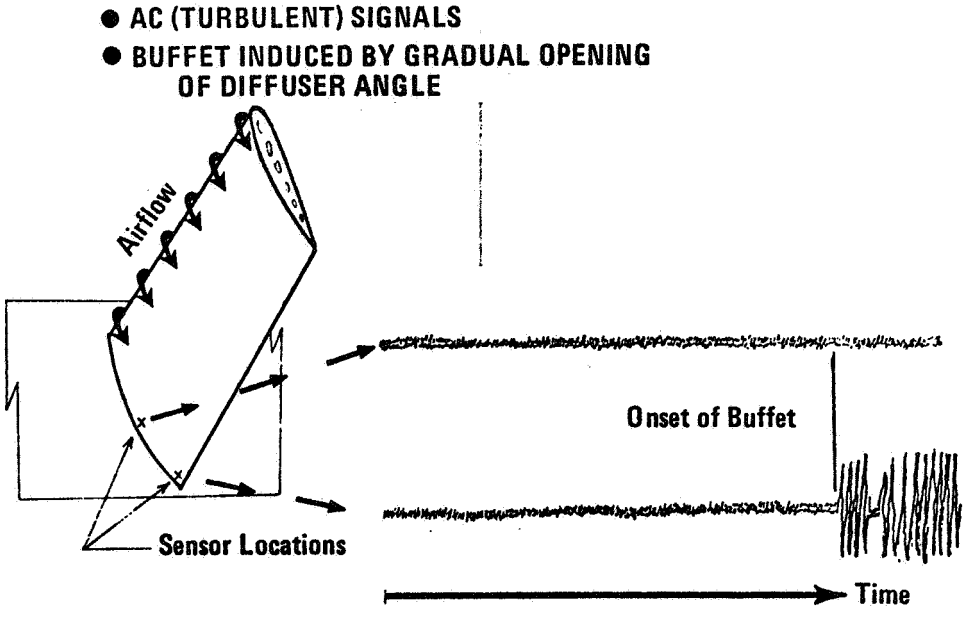

CAD 8977

Figure 6. Buffet response of hot film sensors: $P_R = 2.0$.

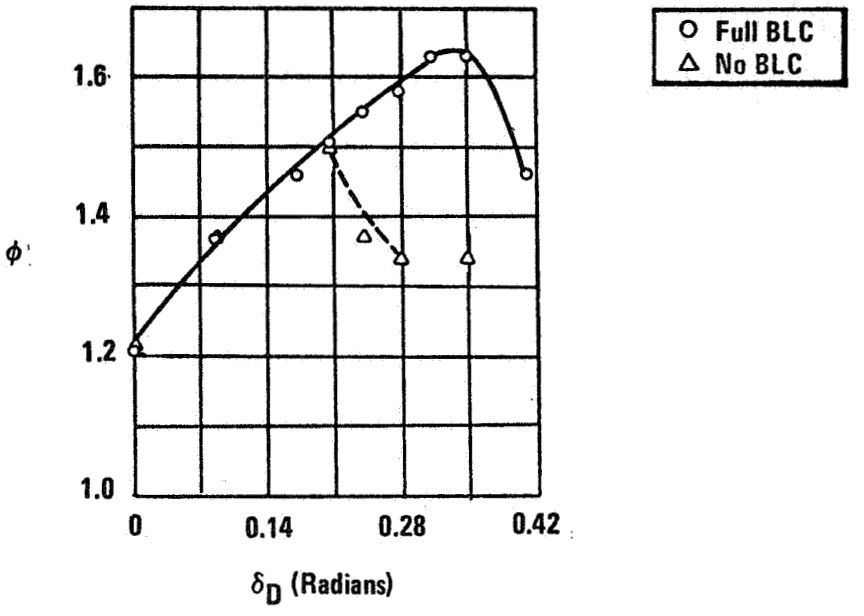

Figure 7. Augmentation ratio vs diffuser angle: AR = 4.1.

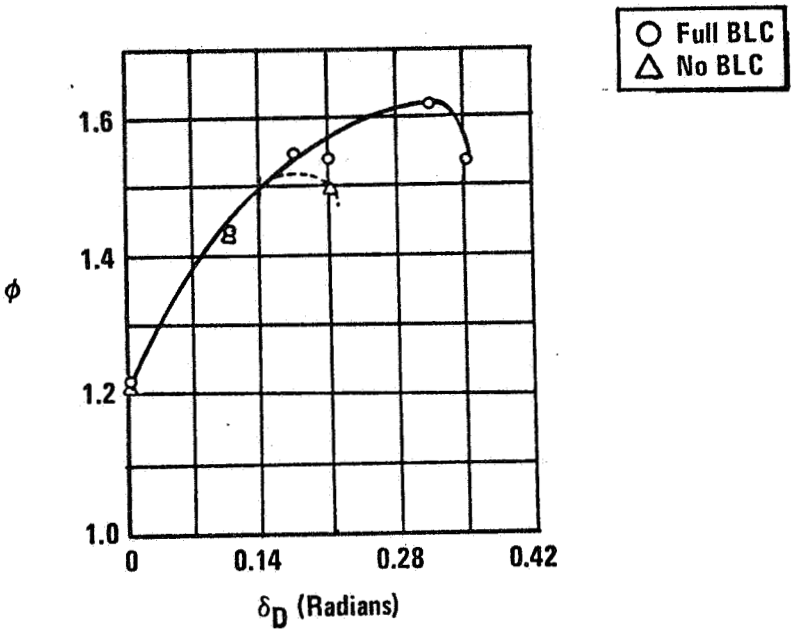

CAD 8975

Figure 8. Augmentation ratio vs diffuser angle: AR = 2.5.

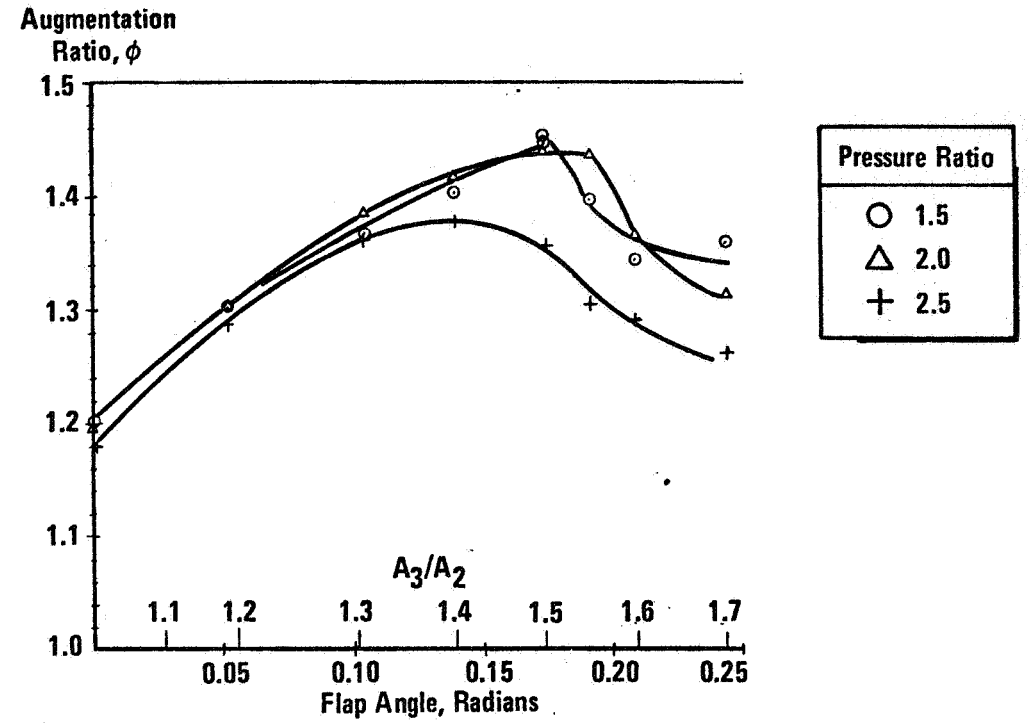

Figure 9. Augmentation ratio vs diffuser angle, top-hat profile.

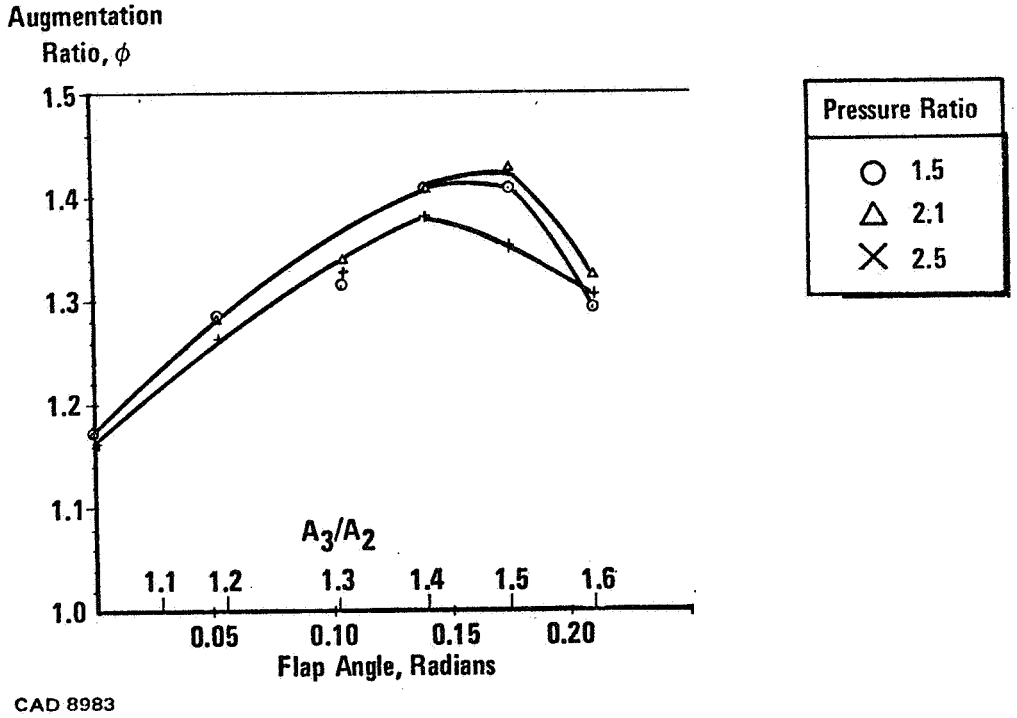

Figure 10. Augmentation ratio vs diffuser angle, vortex profile.

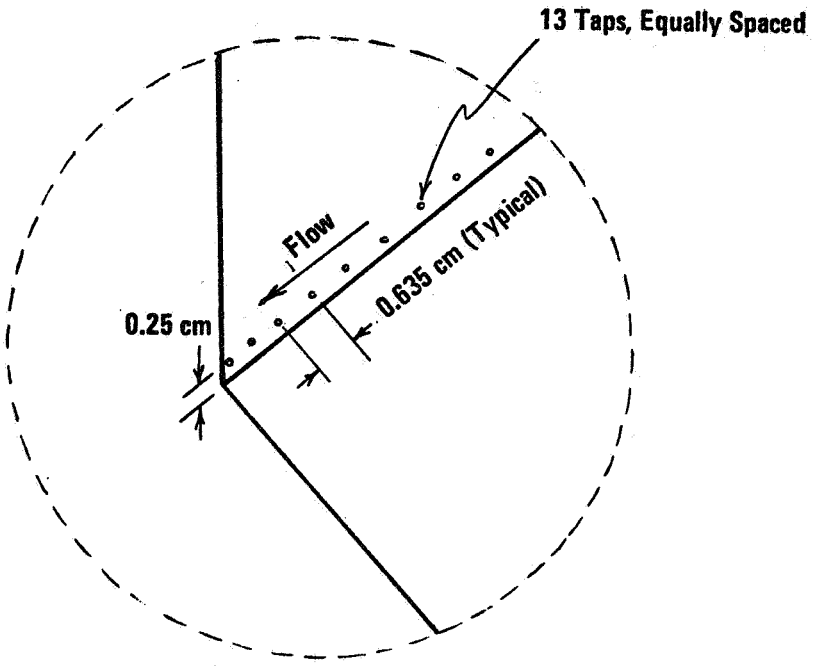

Figure 11. Location of corner static pressure taps.

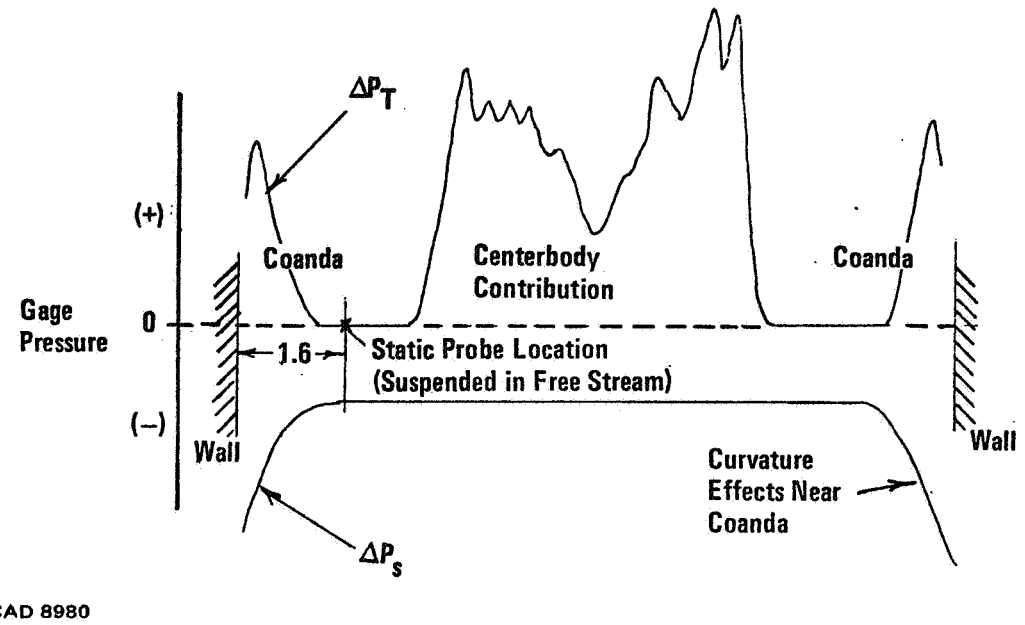

Figure 12. Typical total, ΔP_T, and static ΔP_S distribution across the augmenter throat.

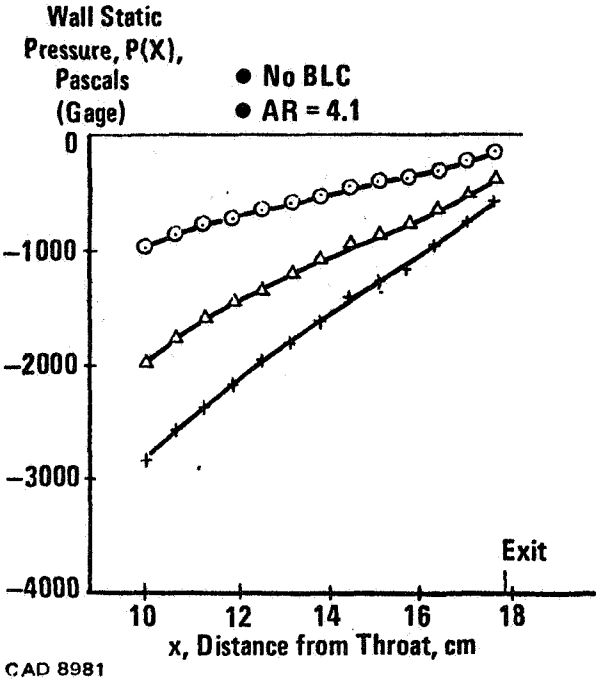

Symbol	Pressure Ratio	Flap Angle Radians	[xdP/dx] exit Pascals
o	1.5	0.21	1860
Δ	2.0	0.21	3950
+	2.5	0.21	5600

Figure 13. Corner static pressure readings for reference profile Coandas, R/t = 26.5, no BLC.

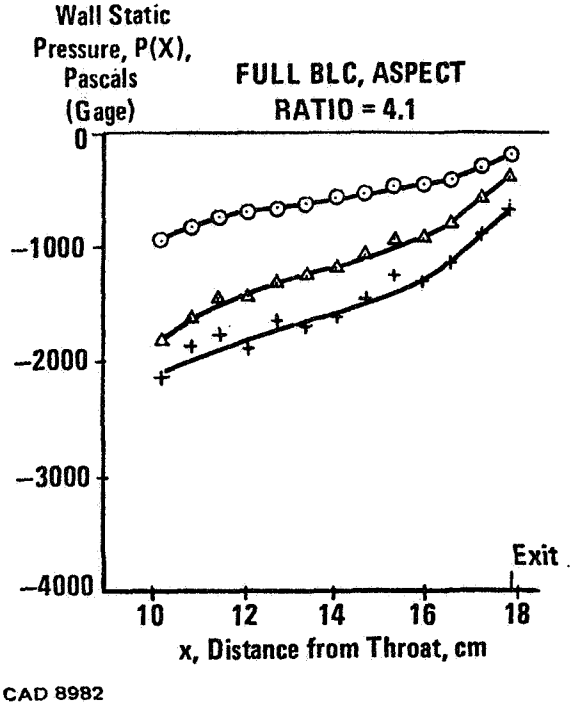

Symbol	Pressure Ratio	Flap Angle Radians	[xdP/dx] exit Pascals
o	1.5	0.33	2320
Δ	2.0	0.33	4600
+	2.5	0.33	6950

Figure 14. Corner static pressure readings for reference profile Coandas, R/t = 26.5, full BLC.

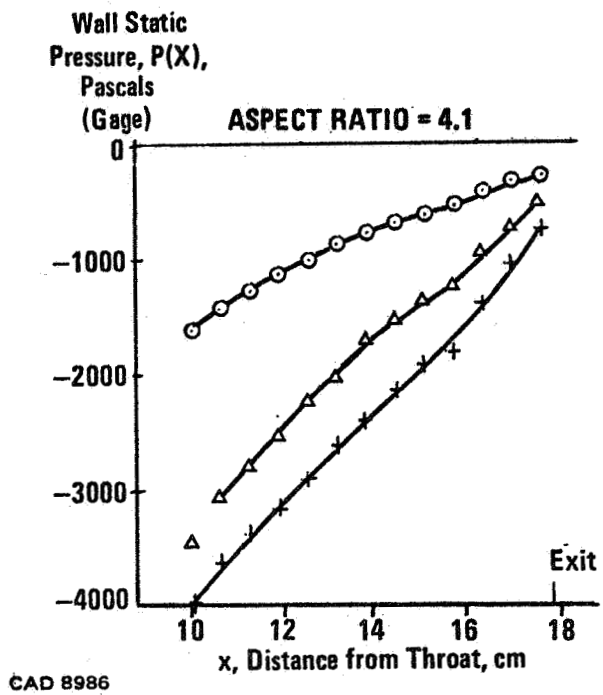

Symbol	Pressure Ratio	Flap Angle Radians	[xdP/dx] exit Pascals
o	1.5	0.175	2440
Δ	2.0	0.175	6500
+	2.5	0.140	9750

Figure 15. Corner static pressure readings for top-hat profile, R/t = 9.3, full BLC.

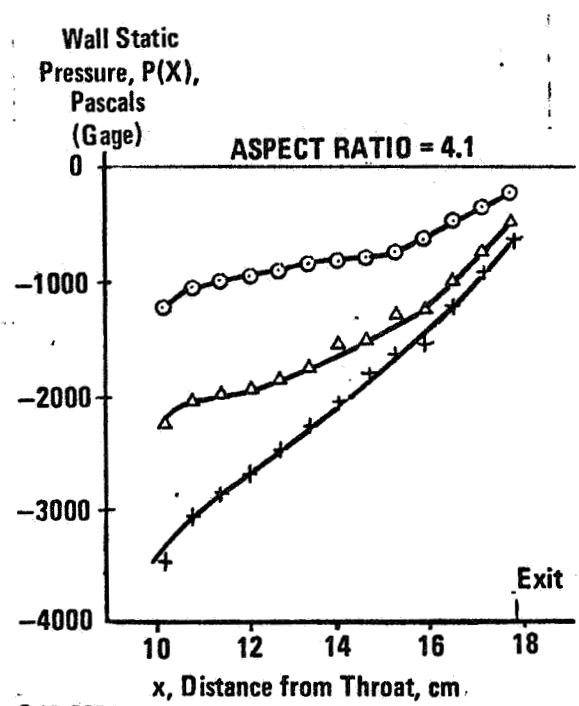

Symbol	Pressure Ratio	Flap Angle Radians	[xdP/dx] exit Pascals
o	1.5	0.175	3480
Δ	2.1	0.175	7000
+	2.5	0.140	8850

Figure 16. Corner static pressure readings for vortex profile, R/t = 9.3, full BLC.

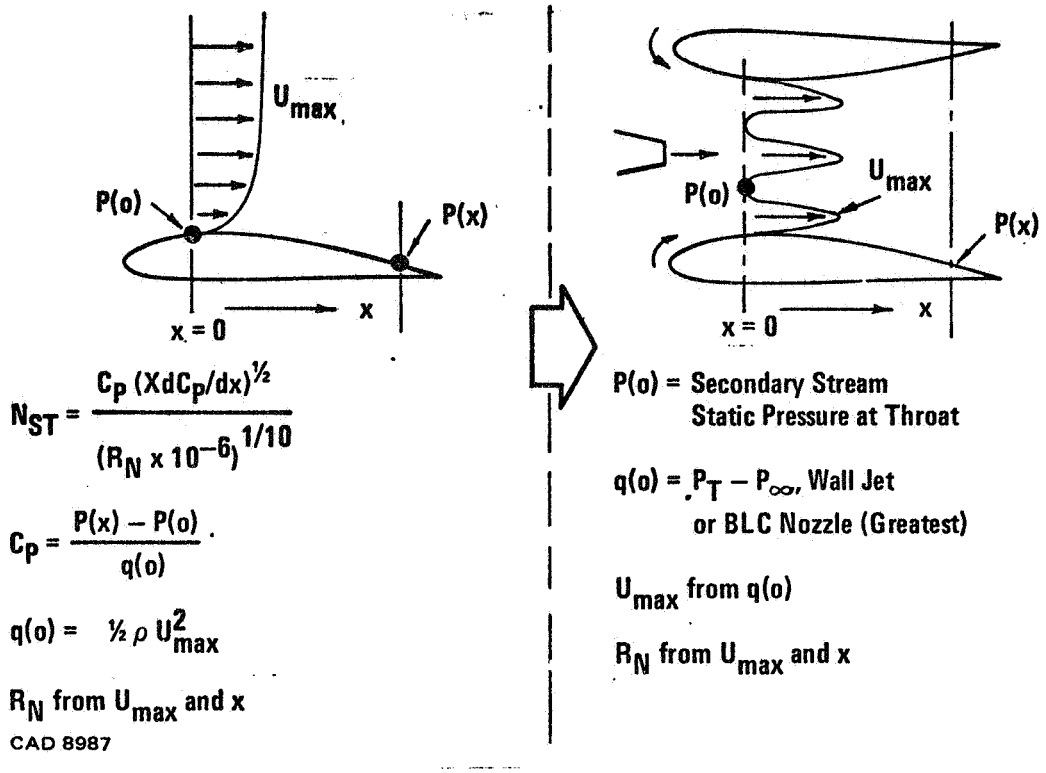

Figure 17. Stratford and modified Stratford.

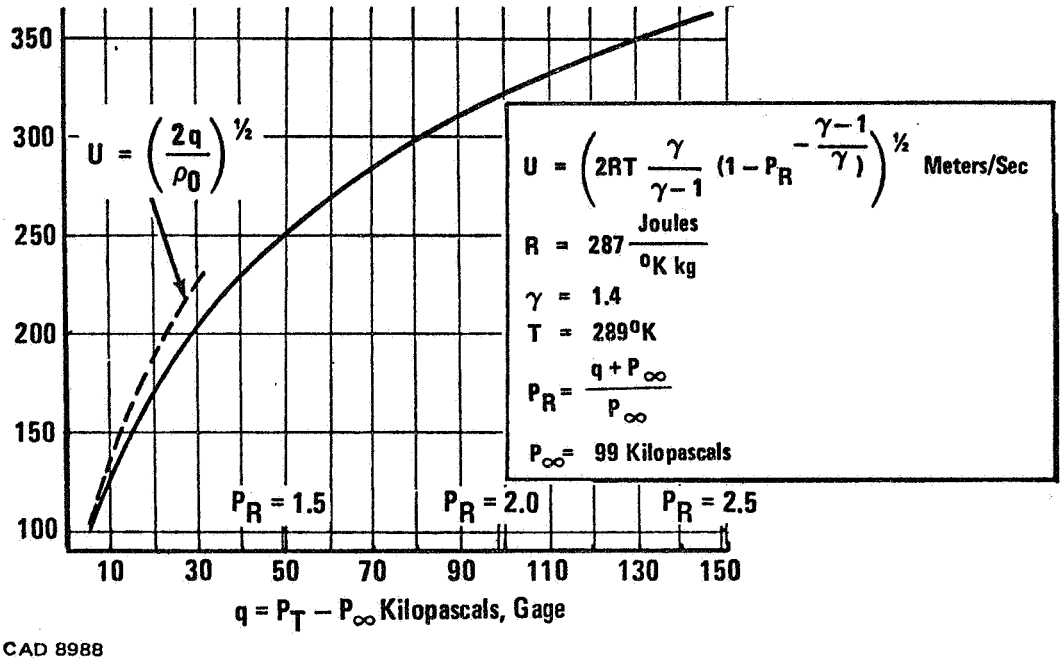

Figure 18. Velocity vs q.

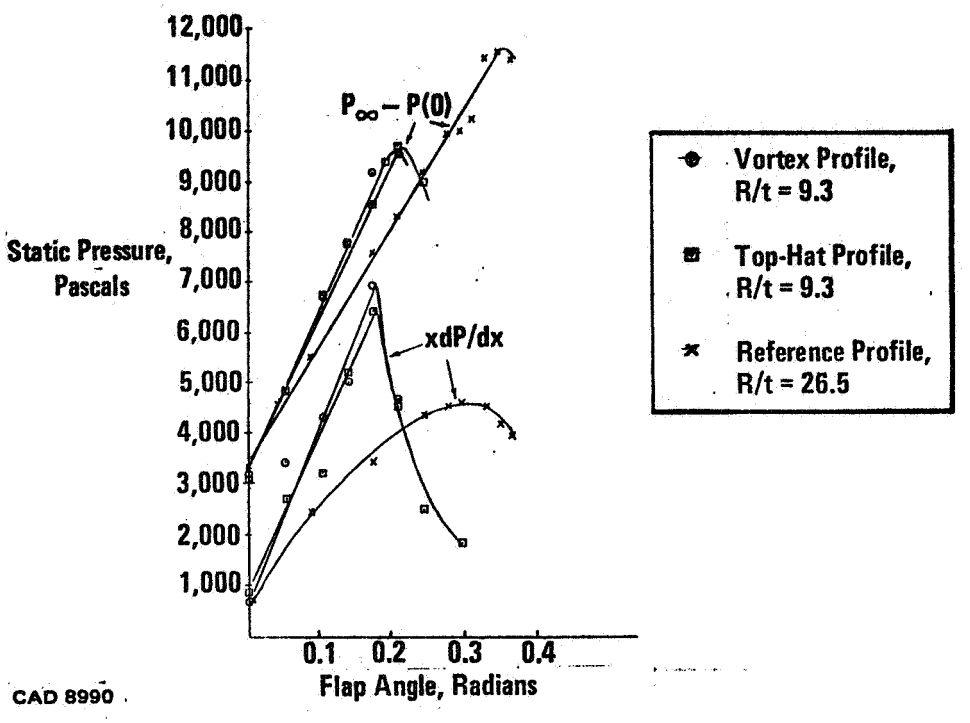

Figure 19. Variation of static pressure components with flap angle.

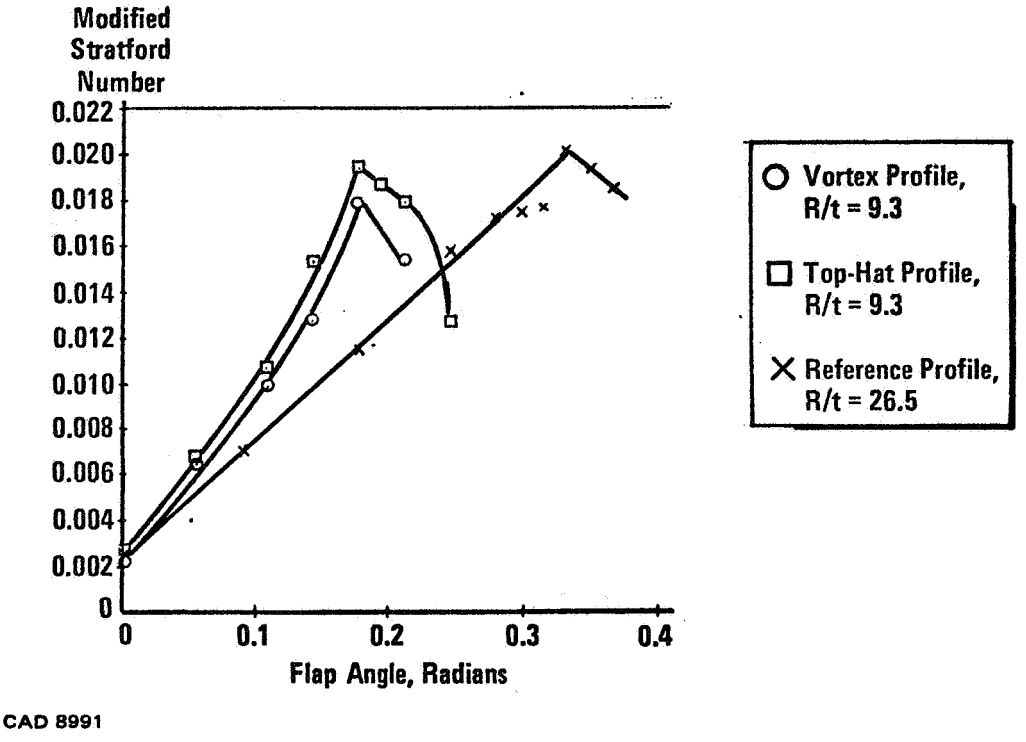

Figure 20. Variation of Stratford number with flap angle.

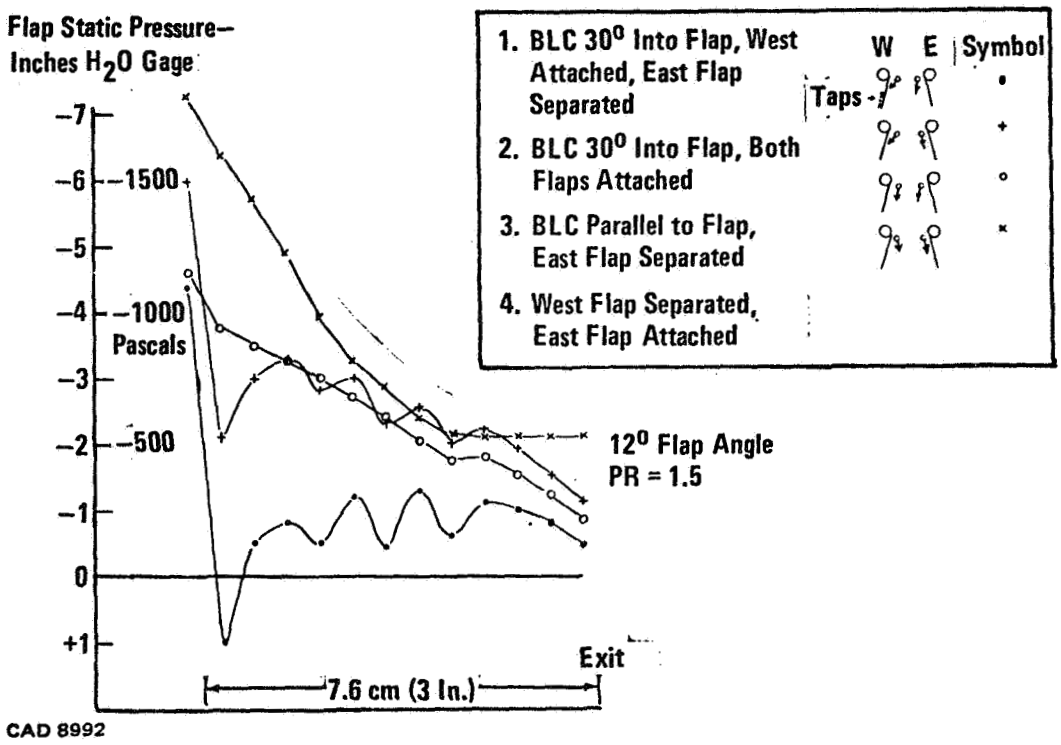

Figure 21. Effects of BLC nozzle orientation on flap statics.

LARGE-SCALE TURBULENT STRUCTURES IN JETS AND IN FLOWS OVER CAVITIES AND THEIR RELATIONSHIP TO ENTRAINMENT AND MIXING

V. Sarohia and P. F. Massier

Jet Propulsion Laboratory
California Institute of Technology

Introduction

Results of an experimental study are presented elucidating the presence of large-scale turbulent structures both in free jets and in axisymmetric flows over cavities. The purpose was to determine their role in entrainment, in mixing, in their growth, and in the production of noise. Although the flow configuration in the experiments was not that which exists in a thrust augmentor, the results nevertheless are of importance in understanding the various mixing and entrainment processes associated with the performance of such a device.

Recent realization of the presence of large-scale structures [1-5] in turbulent shear flows has generated an interst in advancing the understanding of their role in entrainment, mixing, production of noise and of the Reynolds stresses. In the present investigation the large-scale structures in jet flows were observed by simultaneous flow visualization and measurements of physical flow quantities to determine their development and their interaction with each other. Near field pressure signals as sensed by microphones were analyzed and matched with motion picture frames in an attempt to establish any link between the dynamics of these large-scale structures and the production of jet noise.

The experimental results on cavity shear layers were obtained under oscillating and non-oscillating flow conditions, i.e., with and without the presence of strong organized large-scale structures in the shear flow. Oscillations in flows over an axisymmetric cavity are caused by strong feedback from the downstream cavity corner [6-7]. They are accompanied by large-scale structures in

the shear layer and can be altered by changing the cavity geometry or by changing the freestream flow conditions.

Results of Jet Flow Measurements

Subsonic jet flows were generated by expanding air at room temperature through a convergent nozzle which had an exit diameter of 4.2 cm. The jet discharged into an anechoic chamber. The Mach number M_e ranged between 0.1 and 0.9. The flow in the plenum chamber could also be modulated between 100 and 2000 Hz by first passing the flow through a pneumatic transducer, thereby exciting the jet flow. The rms velocity fluctuations at the center of the nozzle exit plane could be varied from 2% to as high as 8% of the mean jet velocity. These periodic flow fluctuations produced organized large-scale vortex structures in the jet shear layer. The interaction of these large-scale structures as they convected downstream and their role in the production of jet noise was investigated using the instrumentation system shown in Figure 1. Both still and high-speed Schlieren motion picutres up to 7000 frames/sec were taken. The duration of the flash used for the movies was 0.3 μs. The jet flow was made visible by mixing a small amount of CO_2 gas with the airflow in the plenum chamber. A series of microphones were placed in the near field and their output was synchronized with the high-speed motion picture frames so that near field pressure fluctuations could be analyzed simultaneously with the movies on a frame-by-frame basis.

A spark shadowgraph showing the large-scale sctructures in a non-excited jet flow at a nozzle exit Mach number M_e, of 0.69, and at a Reynolds number based on nozzle exit dia. $Re_D = 0.4 \times 10^6$ is shown in Figure 2. This shadowgraph

clearly indicates the presence of large-scale structures as far as 5 to 7 jet dia. downstream of the nozzle exit. On close scrutinity of Figure 2 one can infer that the spacing between the structures approximately doubles as they propagate downstream. Because the merging of the large-scale structures occured many times at a relatively fast rate within a few jet diameters, it was not possible to relate the convection of these large-scale structures and their merging with each other to the near-field pressure signal. The process of merging of these structures was slowed down by exciting the jet flow, thereby introducing large-scale structures whose behavior could be studied visually and hence, merging identified.

A set of a sequential Schlieren motion-picture frames showing the behavior of artificially introduced large-scale structures is shown in Figure 3. The time duration between the frames was approximately 140 μs. The lower part of the mixing layer in frame 2 of Figure 3 shows a vortex structure which can be seen subsequently in frames 3, 4 and 5. In these frames the vortices that were shed earlier can also be seen. In frame 5, there are two vortices side by side which merged with each other sometime before frame 6 was taken. The merged structure then propagated downstream as can be seen in frames 7 and 8. From these high-speed motion picture observations, it was concluded that the time taken for the merging process of two artifically generated vortex structures to occur was about 10% of their life span in the jet flow. Under similar mean flow conditions in the nozzle an increase of 15 to 20% in the radial growth of the jet was observed when the jet was excited as compared to a jet that was not excited.

Figure 4 shows successive Schlieren motion picture frames along with a near-field pressure trace of microphone C, the location of which is shown above

frame No. 1. Note the similarity of the behavior of the organized large-scale structures in Figure 4 as compared to those discussed in Figure 3. Observe that as a vortex structure passed below microphone C in frame 4 of Figure 4 there was no significant change in the near-field pressure signal. In frame 7, however, two adjacent organized structures interacted with each other, and instantaneously there was a rapid change in the pressure signal. This pressure pulse was then traced at later times by the other microphones located farther downstream in the near-field. From these measurements it was concluded that the near-field pressure signal of a jet is largely dependent on the dynamics of the interaction of large-scale structures in the jet. A more in-depth discussion on the relationship of large-scale structures and their generation of near-field pressure signals is given in Reference 8.

The influence of jet flow excitation on the distribution of the mean velocity along the jet centerline is shown in Figure 5. It is interesting to note the differences in these velocity distributions for cases in which the rms velocity fluctuations were random in nature with a magnitude of 2% as compared to periodic velocity fluctuations of nearly the same value at 2.3%. It can be seen in Figure 5 that the length of the potential core was reduced by almost half for the excited (pulsated) case as compared to the non-pulsated condition. One can infer from these results that the presence of large-scale structures produced by exciting the jet flow are greatly responsible for the rapid spread of the jet with greatly increased entrainment and mixing of the flow. Furthermore, increased excitation reduces the length of the potential core even more and also substantially reduces the mean velocity at the centerline at any given X/D beyond the potential core.

Flows Over External Axisymmetric Cavities

The experiments on flows over axisymmetric cavities were performed using a model which had an outside diameter d, of 2.0 in. as indicated in Figure 6. The model had an ellipsoidal nose with provision for variation of depth d, in steps together with a continuously adjustable width b. Either laminar or turbulent boundary layers could be obtained at the upstream edge of the cavity.

Flow over the cavity was visualized by injecting CO_2 gas at the base inside the cavity. Figure 7 shows a typical shadowgraph with width b = 0.4 in. and depth d = 0.5 in. Organized large-scale structures are observable over the cavity. For a Reynolds number, $Re_{\Theta_0} = 1.60 \times 10^3$ (where Θ_0 is the momentum thickness at the upstream corner), and a depth $d/\Theta = 37.5$, the growth of the cavity shear layer is shown in Figure 8. Results are given both for a non-oscillating (with organized large-scale structures in the cavity shear layer) and for an oscillating shear layer over the cavity. The momentum thickness Θ, was determined by integrating the profiles of the mean velocity as determined by constant-temperature hot-wire anemometry. That is,

$$\Theta = \int_{-\infty}^{\infty} \frac{U}{U_\infty}\left(1 - \frac{U}{U_\infty}\right)dy \qquad (1)$$

In Eq. (1) y is the transverse coordinate, U is the local mean velocity and U_∞ is the freestream velocity. It is quite clear from Figure 8 that the growth rate $d\Theta/dx$, which indicates the entrainment rate, was approximately 0.021 for the non-oscillating shear layer. In the presence of organized large-scale structures for an oscillating flow over the cavity the value of $d\Theta/dx$ increased to as much as 0.046. This high entrainment rate of the shear layer seems to

result from the presence of the organized large-scale structures shown in Figure 7.

Conclusions

From the experimental results of large-scale structures in jets and in flows over cavities, it can be concluded that the presence of these structures is greatly responsible for the growth of the shear layer, and for the entrainment. Furthermore, the near-field pressure signal in excited jet flows is caused primarily by the merging of adjacent large-scale structures. It is believed that both the entrained fluid as well as its eventual mixing with the jet flow can be controlled by introducing pulsation in the jet flow at a frequency for which the flow is most unstable.

REFERENCES

1. Bradshaw, P., Ferris, D. H., and Johnson, R. F., "Turbulence in the Noise-Producing Region of a Circular Jet," Journal of Fluid Mechanics, Vol. 19, 1964, pp. 591-624.

2. Crow, S. C., and Champagne, F. H., "Orderly Structure in Jet Turbulence," Journal of Fluid Mechanics, Vol. 48, Part 3, 1971, pp. 547-591.

3. Brown, G. L., and Roshko, A., "On Density Effects and Large Scale Structures in Turbulent Mixing Layers," Journal of Fluid Mechanics, Vol. 64, 1974, pp. 775-816.

4. Browand, F. K., and Weidman, P. D., "Large Scales in the Developing Mixing Layer," Journal of Fluid Mechanics, Vol. 76, 1976, pp. 127-144.

5. Winant, C. D., and Browand, F. K., "Vortex Pairing: The Mechanism of Turbulent Mixing-Layer Growth at Moderate Reynolds Numbers," Journal of Fluid Mechanics, Vol. 63, Part 2, 1974, pp. 237-255.

6. Sarohia, V., "Experimental and Analytical Investigation of Oscillations in Flows over Cavities," Ph.D. Thesis, Dept. of Aeronautics, California Institute of Technology, March 1975.

7. Sarohia, V., "Experimental Investigation on Oscillations in Flows over Shallow Cavities," AIAA Journal, Vol. 15., July 1977, pp. 984-991.

8. Sarohia, V., and Massier, P. F., "Experimental Results of Large-Scale Structures in Jet Flows and Their Relation to Jet Noise Production," AIAA Journal, Vol. 16, August 1978, pp. 831-835.

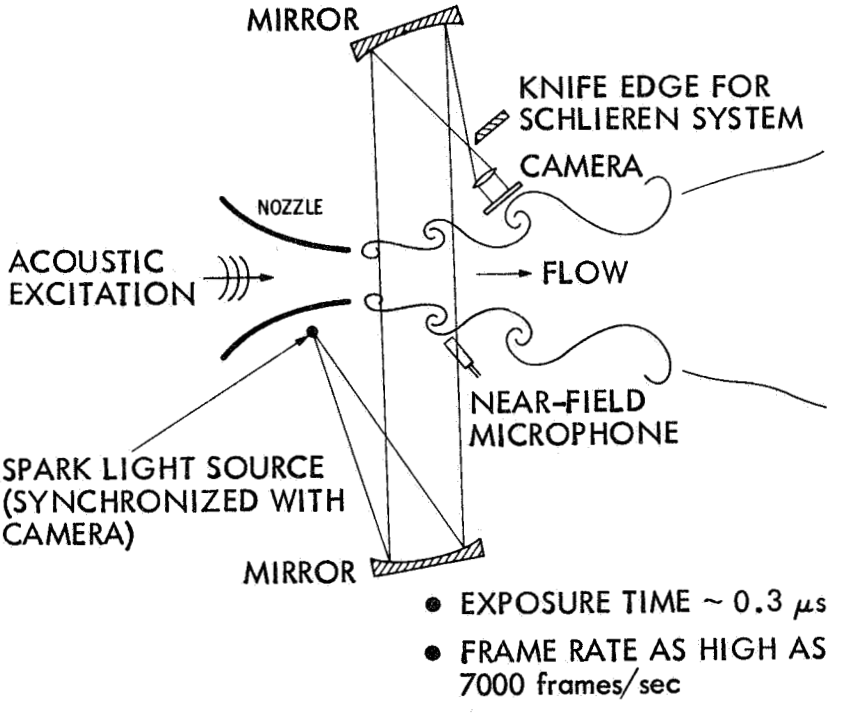

Figure 1. Schematic diagram indicating the experimental setup.

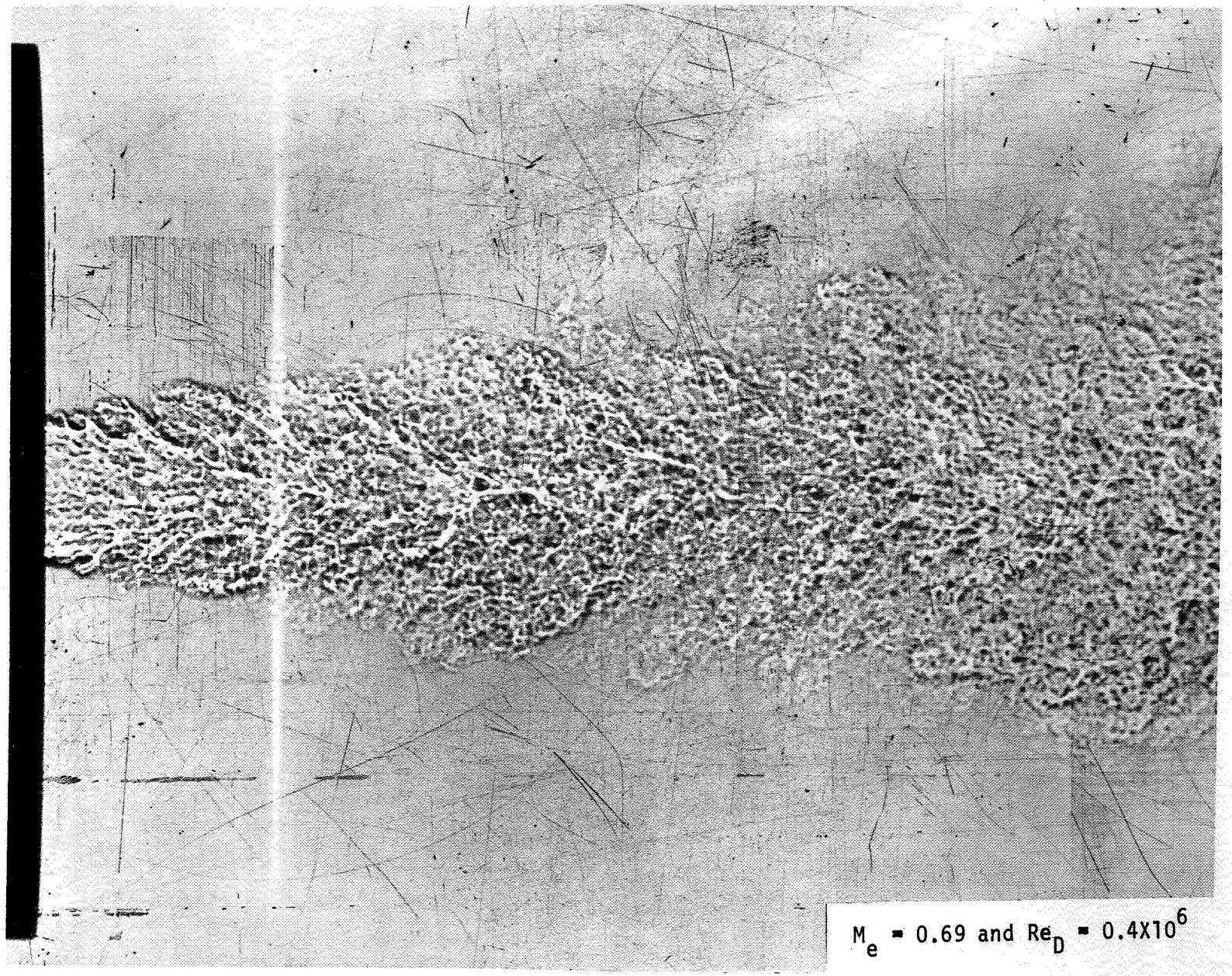

Figure 2. Shadowgraph showing large-scale turbulent structures.

$$M_{exit} \simeq 0.44$$

$$S \equiv fD/U_{exit} \simeq 0.14$$

DURATION IN BETWEEN FRAMES $\simeq 120\mu$/sec

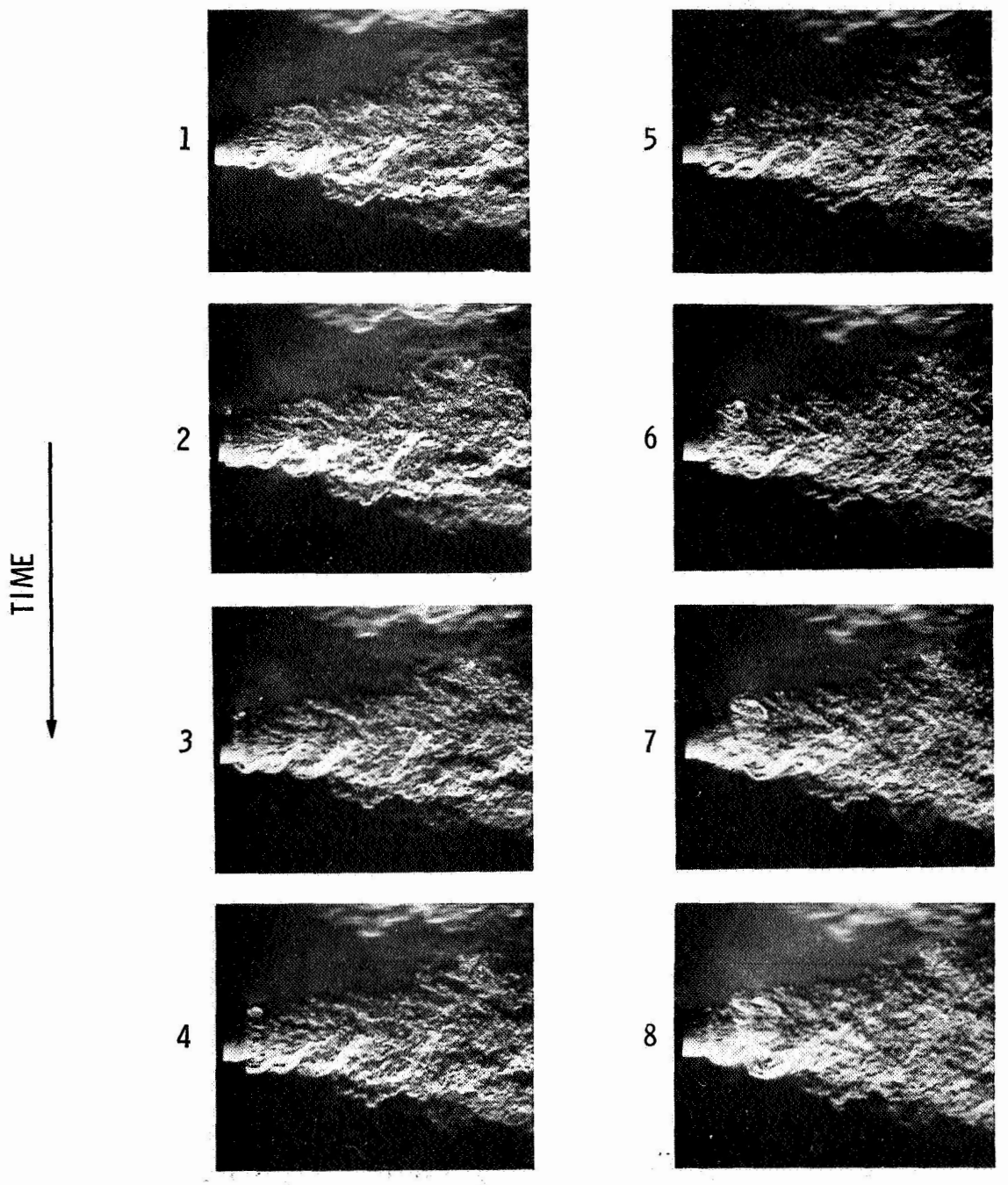

Figure 3. Large-scale coherent structures in excited jet flow.

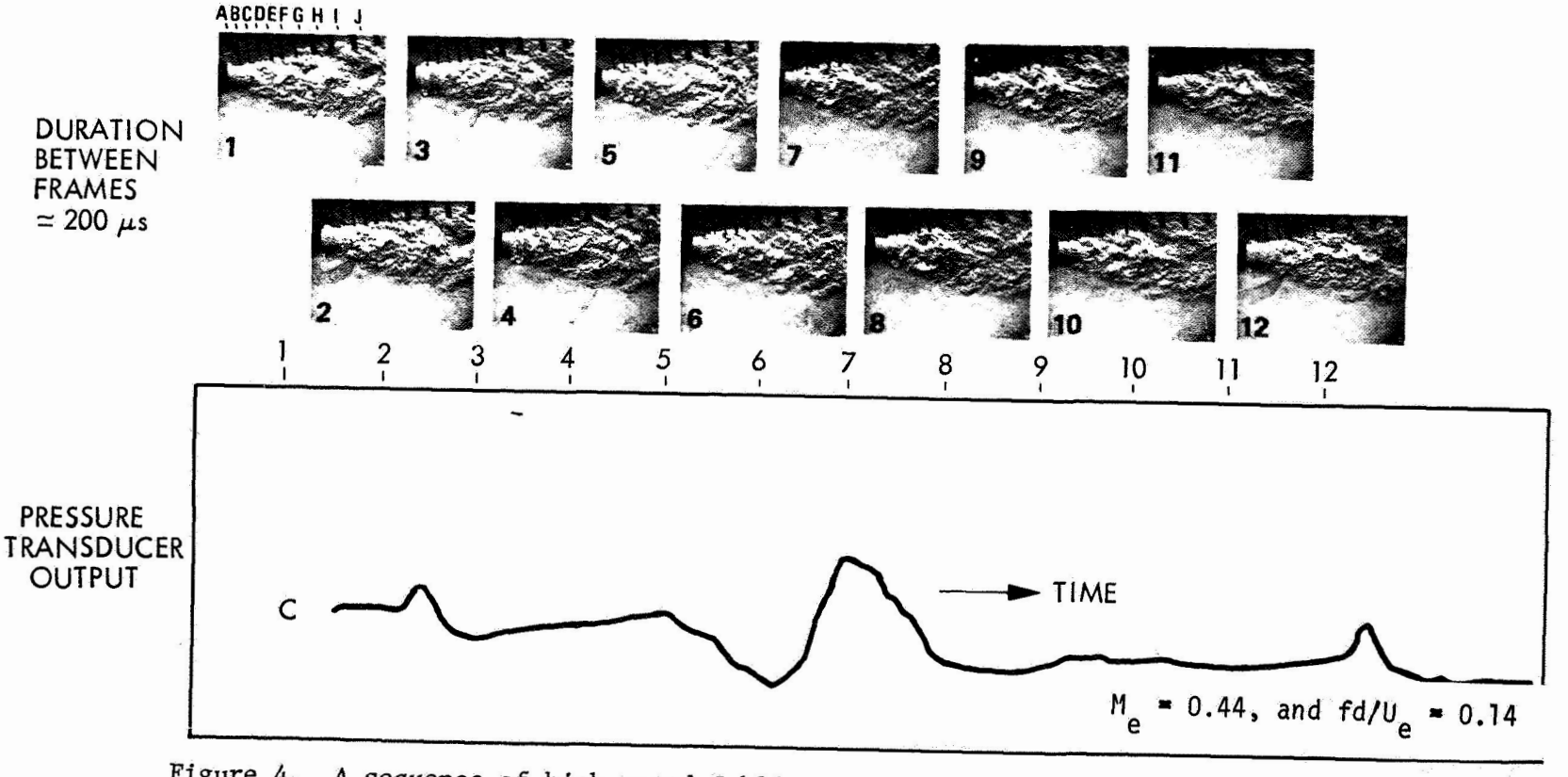

Figure 4. A sequence of high-speed Schlieren motion pictures of an excited jet along with a near-field pressure signal.

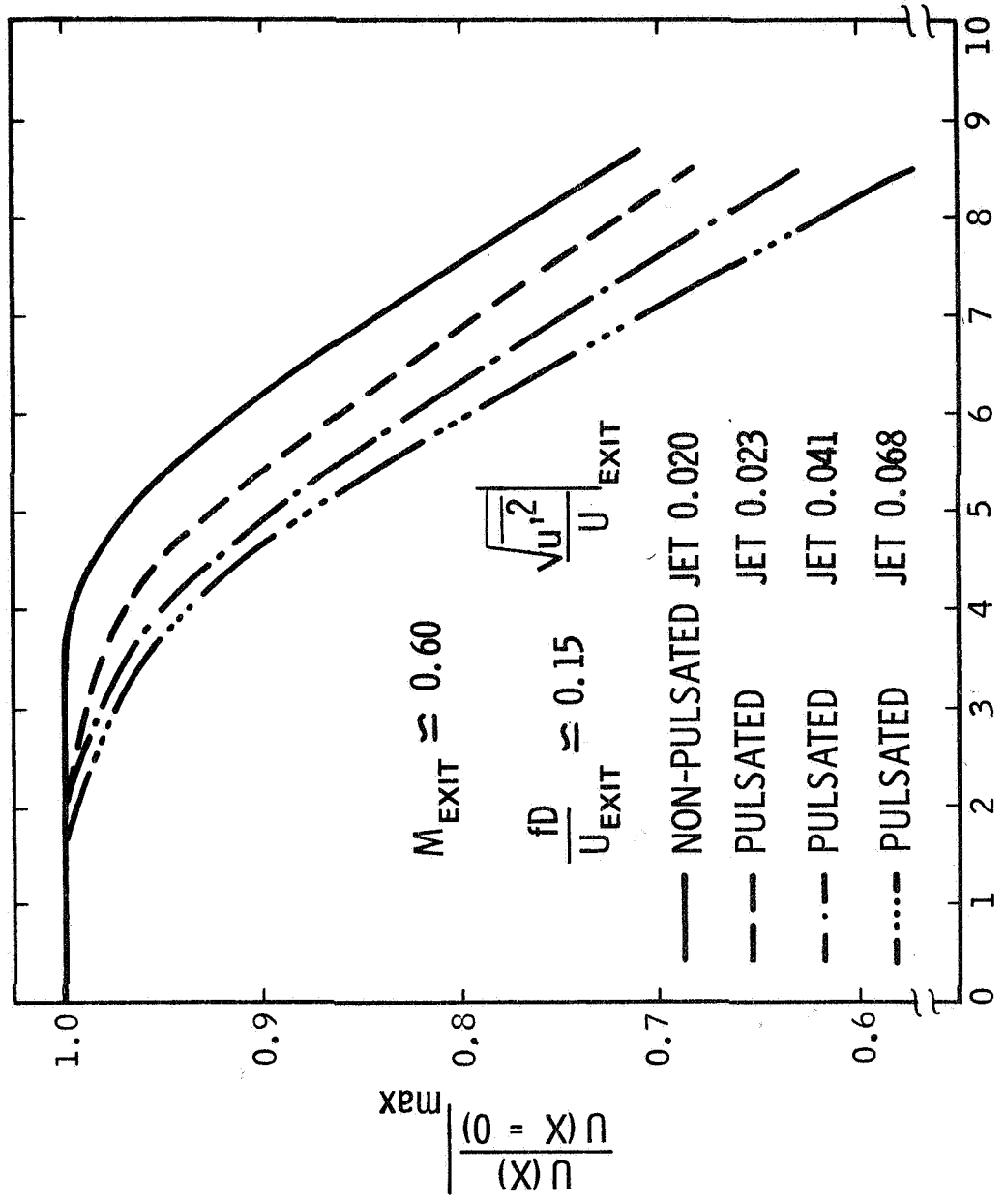

Figure 5. Influence of large-scale coherent structures on jet mixing.

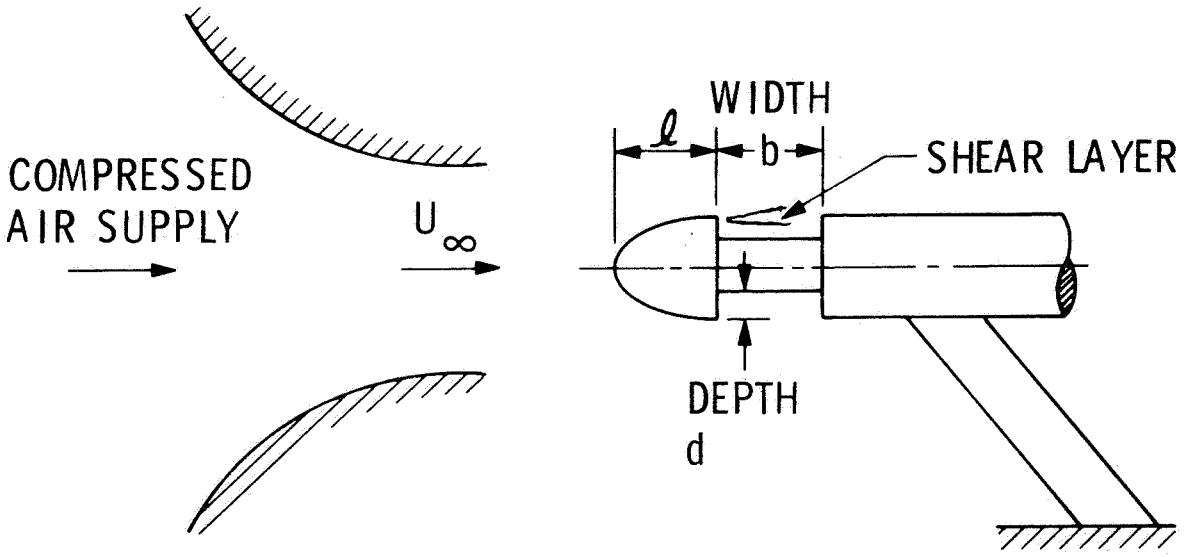

Figure 6. Sketch of axisymmetric cavity model.

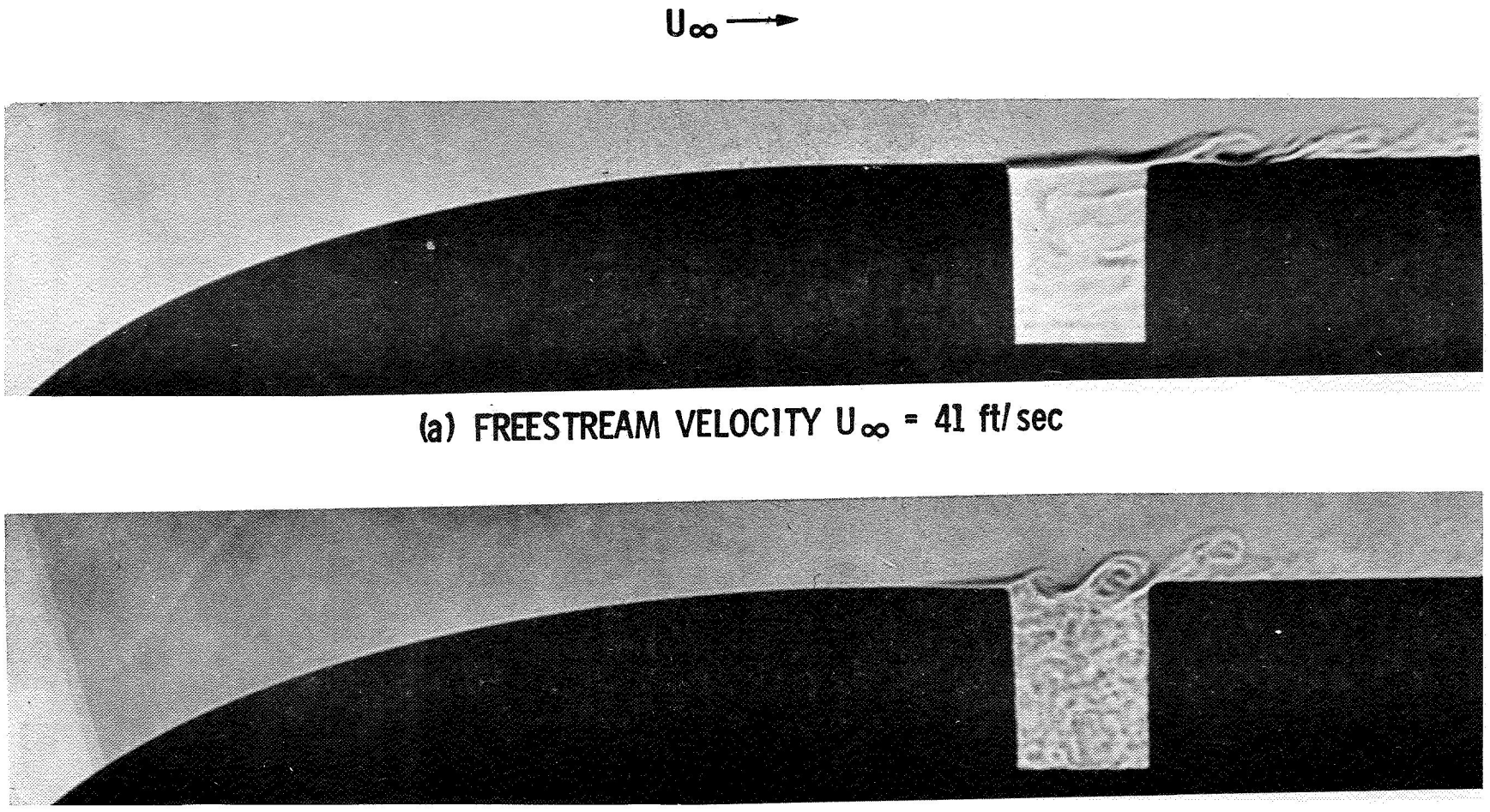

Figure 7. Flow over a cavity.

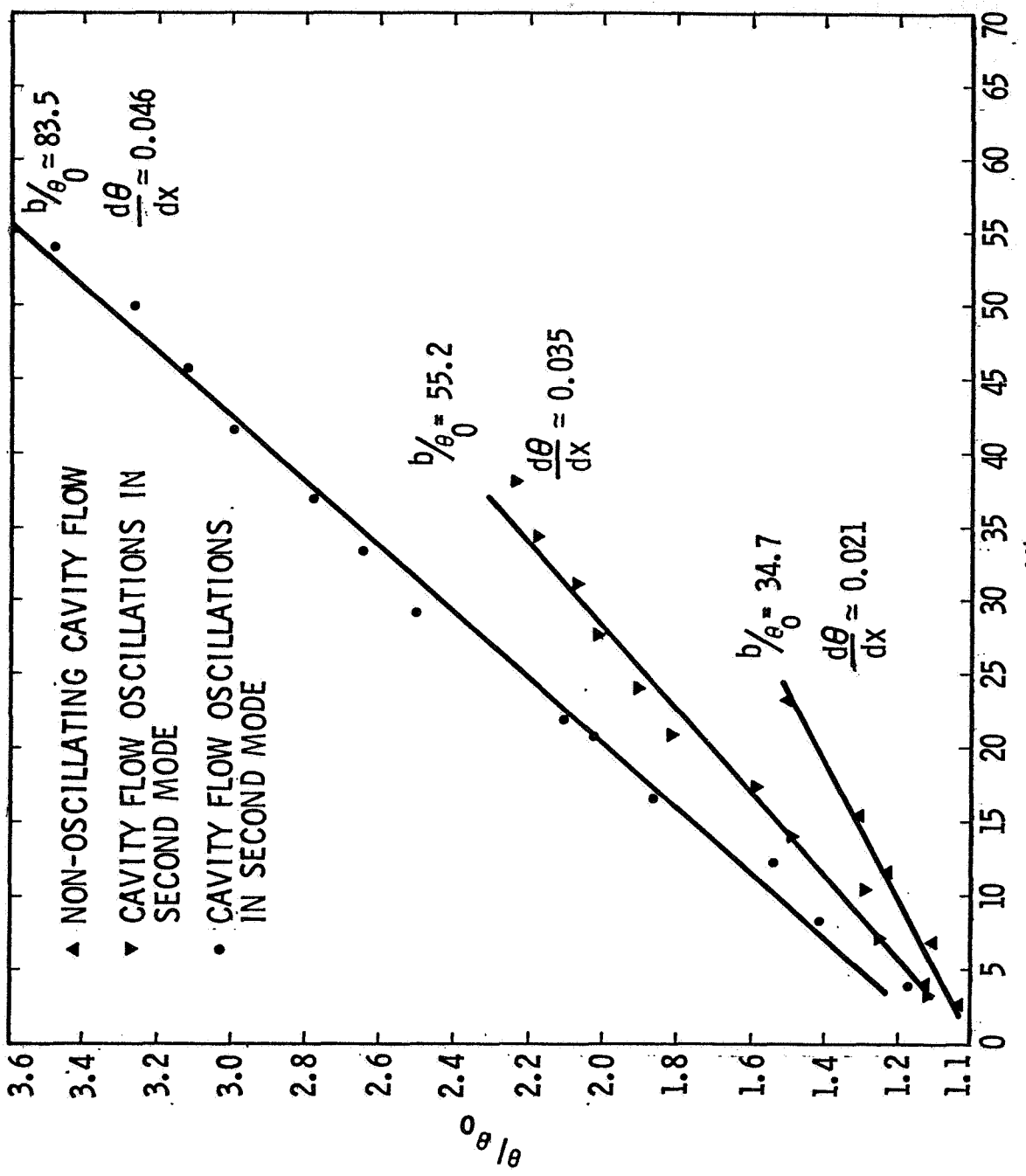

Figure 8. Effect of cavity width on shear layer growth.

ENTRAINMENT CHARACTERISTICS OF UNSTEADY SUBSONIC JETS

M. F. Platzer
U. S. Naval Postgraduate School, Monterey, California

and

J. M. Simmons and K. Bremhorst
University of Queensland, Brisbane, Australia

A revised version of this paper was published in the AIAA Journal, Vol. 16, No. 3, pp. 282-284, March 1978. Permission to include in the workshop proceedings has been granted by AIAA.

INTRODUCTION

The entrainment mechanism in turbulent jets has been a subject of considerable basic and applied interest for many years. Recently, this problem has received increased attention because of the need to develop compact, yet highly efficient thrust augmenting ejectors for VSTOL applications[1]. Several new techniques have been introduced or proposed to increase the jet entrainment e.g., hypermixing[2], swirling[3], acoustic interaction[4] and unsteady jet techniques[5]. It is the objective of this paper to present recent results on the entrainment characteristics of two types of unsteady jet flows, i.e., oscillating jets with time-varying jet deflection and pulsating jets with time-varying mass flow.

The use of oscillating jets for enhanced flow entrainment was first advocated by Viets[5] who also developed a rather ingenious fluidic jet actuation device. Other oscillating jet studies have been reported[6,7,8,9] but they do not contain entrainment measurements.

The favourable effect of pulsating jets on flow entrainment seems to have been first recognized during the development of the pulse jet engine[10,11,12]. Lockwood[10] also noted the generation of ring vortices due to pulsating flow, an effect later verified more clearly by Curtet and Girard[13]. Further pulsating jet studies are those of Johnson and Yang[14], Didelle et al.,[15,16], Binder and Favre-Marinet[17], Crow and Champagne[18] and, very recently Bremhorst and Harch[19].

The following section is a report of three different experiments which were conducted to assess the effectiveness of jet unsteadiness in enhancing flow entrainment.

EXPERIMENTS

Definition of the edge of a turbulent jet raises subtleties which are discussed by Crow and Champagne[18] in terms of the turbulent (or inner rotational) region and the induced potential flow (or potential tails). In the experiments mean volumetric flow rates $Q(x)$ in the turbulent region of unsteady subsonic jets were determined at a number of distances x from the nozzle by integration of mean jet velocity distributions. A constant temperature hot-wire anemometer was used in all cases and the mean of its linearized output was assumed to be proportional to the mean velocity in the direction of the center line of the nozzle. Errors arising from estimation of the edge of the turbulent region and from the influence of high ratios of rms to mean velocities near the edge of the jet are regarded as tolerable in this investigation.

Various measures of entrainment are defined in the literature. Here, entrainment is defined as $(Q(x) - Q_R)/Q_R$ where Q_R is a reference flow rate and is properly taken as the mean volumetric flow rate Q_E at the nozzle exit in two of the experiments. In the third experiment Q_R is taken, for lack of precise nozzle flow rate information, as the volumetric flow rate Q_1 at a station near the nozzle in a steady jet. This still enables comparisons and is discussed later in more detail. Clearly, the entrainment differs by unity from the dimensionless local flow rates $Q(x)/Q_R$ which are presented in this paper.

Fluidically Oscillated Three-Dimensional Jet

The fluidic nozzle illustrated in figure 1 was used by the first and second authors to exhaust a jet of air with oscillating angle into still air.

The nozzle was based on a design by Viets[5]. Flow from a plenum chamber and a contraction emerges from a 6.2 x 49.0 mm rectangular section into a rapid diffusion section where it is bistable because of the proximity of the walls. The flow is illustrated at the moment it attaches to the lower wall A. This sets up an entrainment process and generates compression and rarefaction waves in the feedback tube connecting control parts A' and B'. Continuous jet oscillation results at a frequency which depends on the length of the feedback tube.

In both the oscillating and the steady tests the nozzle was operated at a pressure ratio of 1.13 to produce a mean mass flow rate of 0.0188 kg/s as measured with an upstream orifice plate. The jet oscillated through about 7 degrees either side of the nozzle center line and with a fundamental frequency of 52 Hz. However, higher harmonics were appreciable because of the flip-flop mode of operation. Viets[5] showed that velocity fluctuations at the half-width position of the mean velocity profile have almost a square wave shape.

The values of volumetric flow rate $Q(x)$ used in figure 2 were obtained by integration of the mean velocity distribution across the jet cross-sections. The limits of integration were stations at which the mean velocity was between 5 and 10 percent of the maximum value in a distribution. This necessitated mild extrapolation of the distribution furthest downstream so that the value of $Q(x)$ there has a possible error of about 10 percent.

For the two cases of oscillating and fixed jet angle, $Q(x)$ is normalized by the mean volumetric flow rate Q_E at the nozzle exit. Mass flow rate upstream of the nozzle (measured with an orifice plate) was used to determine Q_E. The hydraulic diameter of the nozzle (4 x area/perimeter) is used as the length scale because of the essentially three-dimensional

nature of the flow. The change in slope of the curve of $Q(x)/Q_E$ for the steady jet is attributed to the transition from a high aspect ratio three-dimensional flow to a more axisymmetric mean flow.

Mechanically Oscillated Two-Dimensional Jet

Recent two-dimensional studies of flow past an airfoil at zero incidence and with an oscillating trailing edge jet flap have been extended by the first and second authors to measurements of entrainment. Details of the mechanically oscillated nozzle have been reported previously[9,20]. In these tests the nozzle was oscillated through 5.2 degrees either side of the airfoil chordline and at frequencies of 4 and 20 Hz. The free stream velocity was 29.2 m/s and the nozzle exit velocity of 137 m/s was estimated, using the results of Bradbury and Riley[21], from measurements of the velocity profile close to the nozzle with the jet held parallel to the free-stream.

The instantaneous velocity profiles measured in a previous study[20] were averaged over a cycle of nozzle oscillation to obtain mean velocity profiles and hence mean volumetric flow rates. Because nozzle velocity was not measured directly the measurements in figure 3 for the oscillating and the steady cases are both normalized by the volumetric flow rate in the steady jet across the measuring section nearest the nozzle (i.e. 35 nozzle widths downstream). The use of a small nozzle width (0.38 mm) and measuring stations many nozzle widths downstream is a legacy of the preceding studies of jet flaps and leads to an uncertainty in $Q(x)/Q_1$ which increases to about 10 percent at the downstream limit. Nevertheless, the measured insensitivity of $Q(x)/Q_1$ over the range of x to the frequency of oscillation is significant. It must be stressed that the jet flowed into a moving airstream.

Axisymmetric Jet with Pulsed Core

Bremhorst and Harch[19] recently studied a fully pulsed axisymmetric air jet exhausting into still air and their measurements of $Q(x)/Q_E$ are reproduced in figure 2. They used a mechanical valve connected to a plenum chamber by a smooth transition piece. The valve allowed flow for one third of its period of cyclic operation. The first and third authors used the same valve to study an axisymmetric air jet flowing into still air but with pulsation restricted to the inner core by the fitting of a two-stream coaxial nozzle downstream of the valve (figure 1). The nozzle consisted of a central reducer with 6.9 mm exit diameter to which air was supplied solely from the pulsating valve, and an annular section of 25.4 mm diameter which was fed through a regulating valve with air taken from upstream of the plenum chamber.

The total jet flow rate was measured with a flow meter well upstream of the plenum chamber. The inner coaxial jet flow rate for the pulsed core was metered separately upstream of the plenum chamber. The mean exit velocities for the steady annular portion of the jet and the pulsed core were 18.3 and 12.6 m/s respectively.

The results in figure 2 were obtained by planimeter integration of the radius times local mean velocity versus radius profiles. These profiles were faired to zero in order to exclude the potential tails as was done by Crow and Champagne[18]. The total volumetric flow rate across a downstream section was then normalized by the mean volumetric flow rate at the nozzle exit. Measurements by Crow and Champagne[18] for a steady axisymmetric jet are presented for comparison.

DISCUSSION

The results in figure 2 show the powerful effect of full jet pulsation on entrainment. Also, the entrainment is seen to increase with frequency, but measurements are available for only two frequencies. Pulsation of only the jet core still provides significant entrainment benefits over the steady jet (figure 2) and this method can be regarded as an entrainment control device which enables the setting of the desired entrainment level for a jet of given flow rate. The fluidically oscillated jet shows equally significant entrainment increases (up to 55 percent increase in $Q(x)/Q_E$ at the most downstream station) when compared in figure 2 with the steady jet. Similar results with the same fluidic nozzle operated at a higher pressure ratio (1.33) were obtained by Veltman[22] with a cruder measuring technique (pitot-static tube). Finally, in figure 3 the volumetric flow rate measurements for the sinusoidally oscillated jet flap show negligible variation from the corresponding steady jet measurements. This indicates that any significant influence of jet oscillation on the entrainment processes must, if it exists, be confined to the as yet uninvestigated vicinity of the nozzle.

These results indicate that entrainment depends on the type and amount of jet unsteadiness. Apparently the mere introduction of jet unsteadiness by small sinusoidal flow angle variations is insufficient to enhance entrainment but it should be noted that the results in figure 3 were obtained at measuring stations which are all many nozzle widths downstream of the jet nozzle. Thus, no fully conclusive statement can be made at this time about the entrainment close to the nozzle. However, the measuring stations for the sinusoidally oscillated jet were all within less than one half of

the jet wave length. Therefore, the sinusoidally oscillated jet was operated at a much smaller reduced frequency than the other two jets. In effect, it approached quasi-steady conditions which may well explain its low entrainment. Indeed, in two previous papers[20,23] it was shown that quasi-steady concepts are quite successful in explaining the major flow features.

The high entrainment of the fluidically oscillated jet would appear to be caused by the high-frequency content of this square wave type of oscillation but more detailed measurements are clearly needed, in particular for the fluidically oscillated and the pulsed jets. Such studies are presently in progress. Furthermore, practical ejector application requires the proper trade-off between entrainment and primary nozzle thrust efficiency. While some information is available on the thrust efficiency[5,22] of the fluidic nozzle there seems to be none available for pulsating nozzles.

REFERENCES

1. Schum, E. F., "Techniques for Increasing Jet Entrainment Rates in Ejector Augmenters," *Proceedings of the Workshop on Prediction Methods for Jet V/STOL Propulsion Aerodynamics*, Naval Air Systems Command, July 1975, pp. 639-652. (available from DDC as AD-A024023).

2. Quinn, B., "Compact Ejector Thrust Augmentation," *J. Aircraft*, Vol. 10, Aug 1973, pp. 481-486.

3. Chigier, N. A. and Chervinsky, A., "Experimental and Theoretical Study of Turbulent Swirling Jets Issuing from a Round Orifice," *Israel J. Technology*, Vol. 4, Feb 1966, pp. 44-54.

4. Hill, W. and Greene, P., "Self-Excited Superturbulence: The Whistler Nozzle," Grumman Research Department Rep. No. RE-488, Oct 1974, (available from DDC as AD-A001021).

5. Viets, H., "Flip-Flop Jet Nozzle," *AIAA Journal*, Vol. 13, Oct 1975, pp. 1375-1379.

6. Trenka, A. R. and Erickson, J. C., Jr., "The Determination of Unsteady Aerodynamics of a Two-Dimensional Jet-Flap Wing," CAL AC-2260-S-1, Cornell Aeronautical Laboratory, Buffalo, NY, April 1970.

7. Kretz, M., "Commande Asservie des Forces Aerodynamiques Instationnaires," De 07-44E5, Giravions Dorland, Suresnes, France, 1973.

8. Simmons, J. M. and Platzer, M. F., "Experimental Investigation of Incompressible Flow Past Airfoils with Oscillating Jet Flaps," *J. Aircraft*, Vol. 8, Aug 1971, pp. 587-592.

9. Simmons, J. M., "Measured Pressure Distribution on an Airfoil with Oscillating Jet Flap," *AIAA Journal*, Vol. 14, Sept 1976, pp. 1297-1302.

10. Lockwood, R. M., "Pulse Reactor Lift-Propulsion System Development Program," Hillier Aircraft Company, Rep. No. ARD-308, March 1963.

11. Foa, J. V., *"Intermittent Jets,"* High-speed Aerodynamics and Jet Propulsions, Vol. XII, Sect. F, Princeton University Press, 1958.

12. Bertin, J., "Dilution Pulsatoire sur Reacteur, *C. R. Acad. Sci. Paris,* Vol. 240, 1955, pp. 1855-1857.

13. Curtet, R. M. and Girad, J. P., Visualization of a Pulsating Jet," *Proc. of ASME Symposium on Fluid Mechanics of Mixing,* Atlanta, GA., June 1973, pp. 173-180.

14. Johnson, W. S. and Yang, T., "A Mathematical Model for the Prediction of the Induced Flow in a Pulsejet Ejector with Experimental Verification," *ASME Winter Annual Meeting and Energy Systems Exposition,* New York, Paper 68-WA/FE-33, Dec 1968.

15. Didelle, H., Binder, G., Craya, A. and Laty, R., "L'augmentation de la poussée d'une trompe à jet inducteur pulsant: Project, installation et mise au point de la soufflerie, de la trompe et du banc de mesure de poussée," Laboratoires de Mécanique des Fluids, Univ. Grenoble, Oct 1971.

16. Didelle, H., Binder, G., Craya, A. and Laty, R., "L'augmentation de la pousée d'une trompe à jet inducteur pulsant: Résultats des essais," Laboratoires de Mécanique des Fluides, Univ. Grenoble, June 1972.

17. Binder, G. and Favre-Marinet, M., "Mixing Improvement in Pulsating Turbulent Jets," *Proc. ASME Symposium on Fluid Mechanics of Mixing,"* Atlanta, GA., June 1973, pp. 167-172.

18. Crow, S. C. and Champagne, F. H., "Orderly Structure in Jet Turbulence," *J. Fluid Mech.,* Vol. 48, Aug, 1971, pp. 547-591.

19. Bremhorst K. and Harch, W. H., "Near Field Velocity Measurements in a Fully Pulsed Subsonic Air Jet," *Symposium on Turbulent Shear Flows*, Pennsylvania State University, April 1977.

20. Simmons, J. M., Platzer, M. F. and Smith, T. C., "Velocity Measurements in an Oscillating Plane Jet Issuing into a Moving Airstream," *J. Fluid Mech.*, vol. 84, part 1, pp. 33-53, 1978.

21. Bradbury, L. J. S., and Riley, J., "The Spread of a Turbulent Plane Jet Issuing into a Parallel Moving Airstream," *J. Fluid Mech.*, Vol. 27, Feb 1967, pp. 381-393.

22. Veltman, R. J., "An Experimental Investigation of the Efficiency and Entrainment Rates of a Fluidically Oscillated Jet," Master's Thesis, U. S. Naval Postgraduate School, June 1976.

23. Simmons, J. M. and Platzer, M. F., "A Quasi-steady Theory for Incompressible Flow Past Airfoils with Oscillating Jet Flaps," AIAA Journal, Vol. 16, No. 3, pp. 237-241, March 1978.

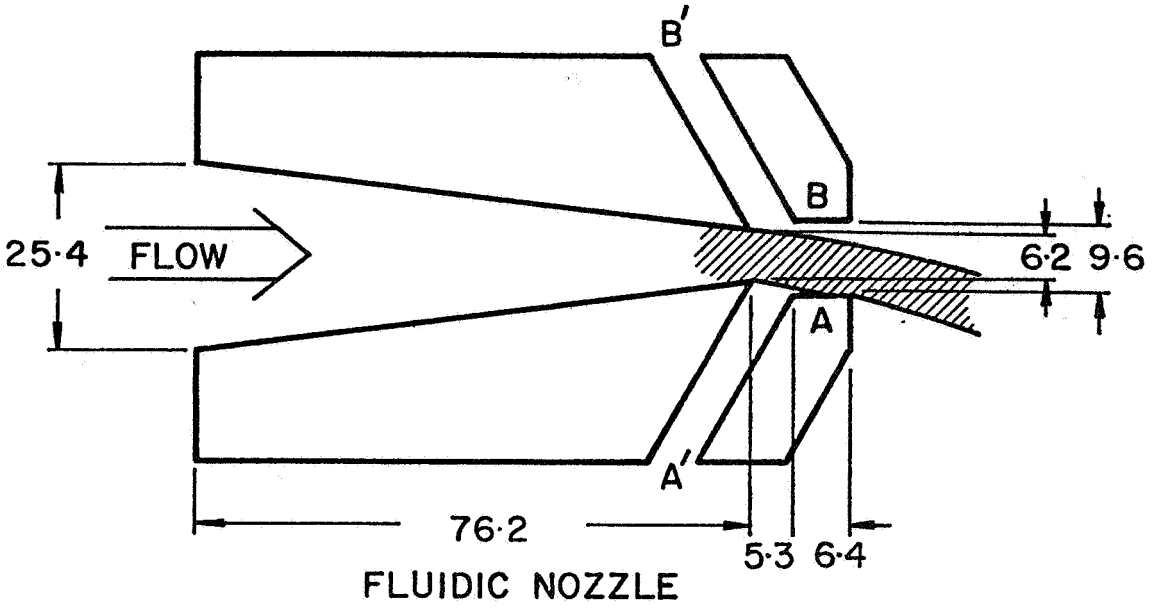

FLUIDIC NOZZLE

dimensions in mm

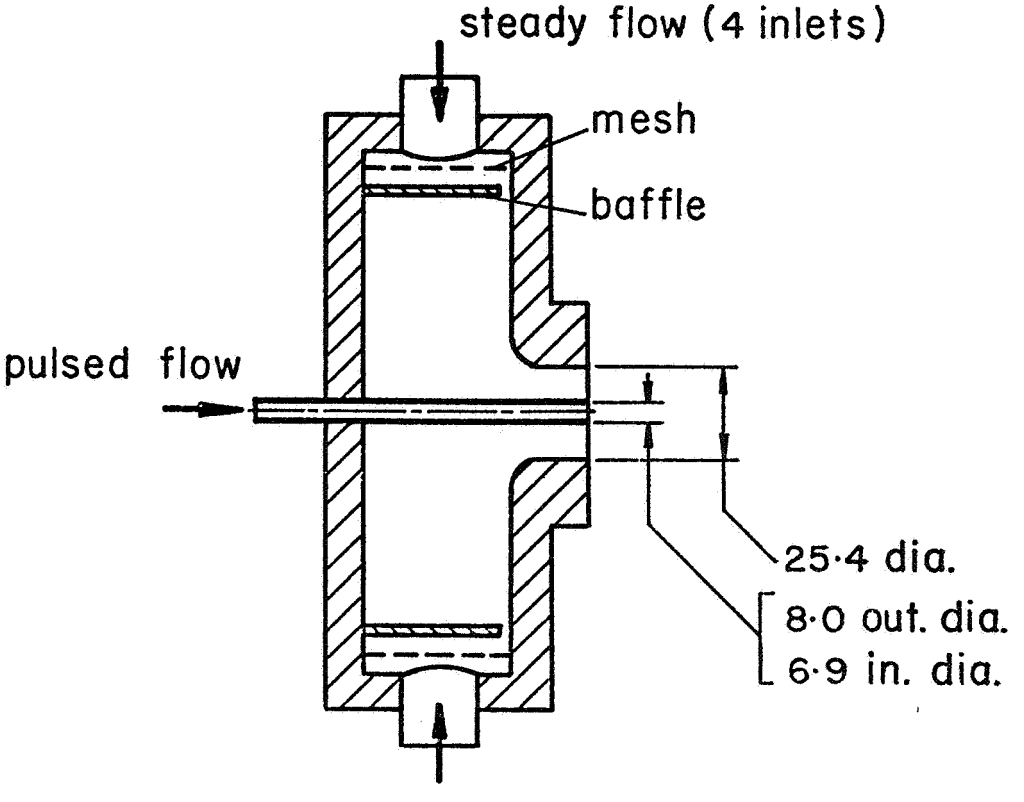

PULSED CORE NOZZLE

Figure 1. Schematic of fluidic and pulsed core nozzles.

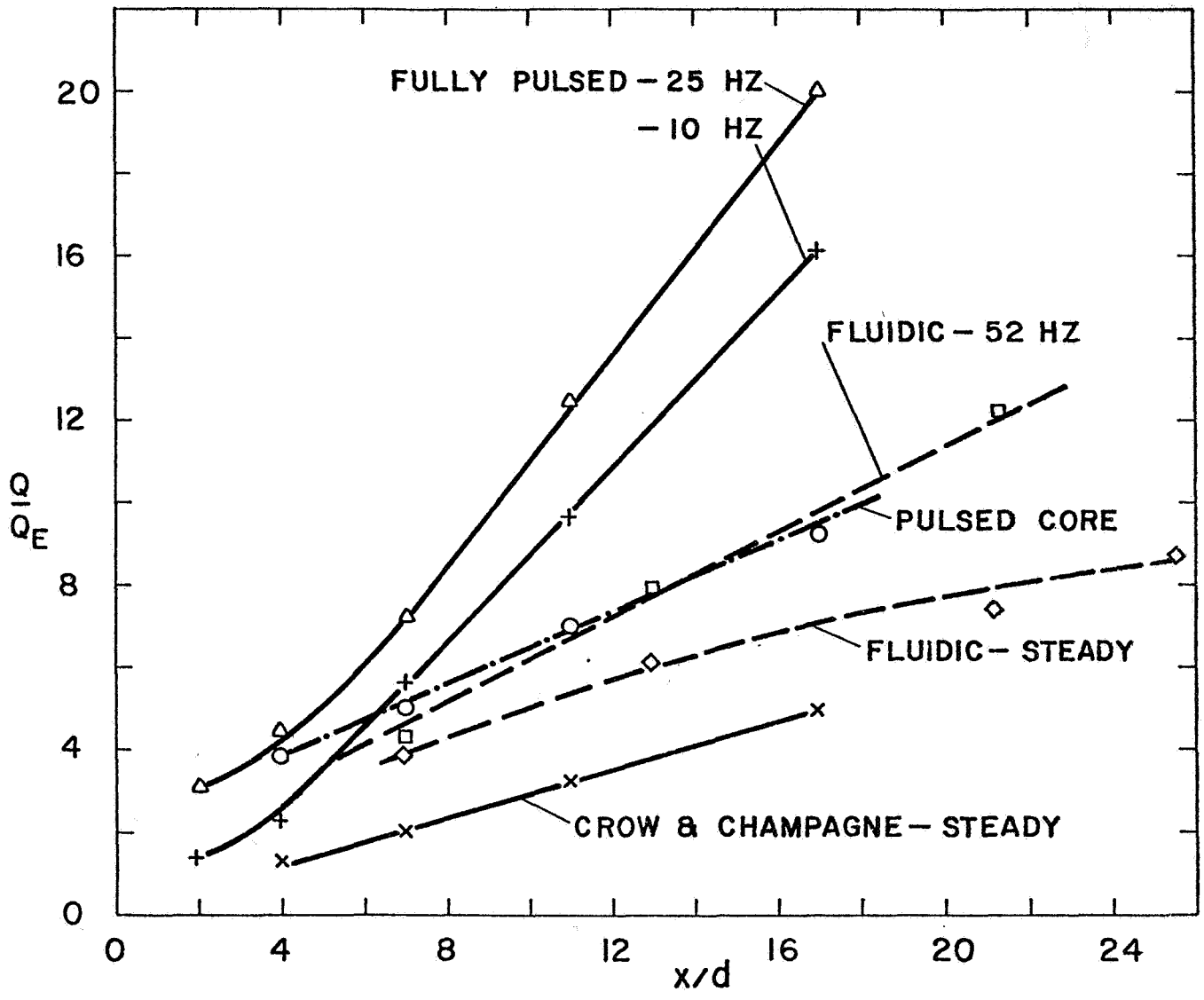

Figure 2. Mean volumetric flow rates Q(x) versus streamwise distance x for fluidic, fully pulsed and pulsed core nozzles. Q_E is mean nozzle exit flow. d is hydraulic diameter of fluidic nozzle or diameter of axisymmetric nozzles.

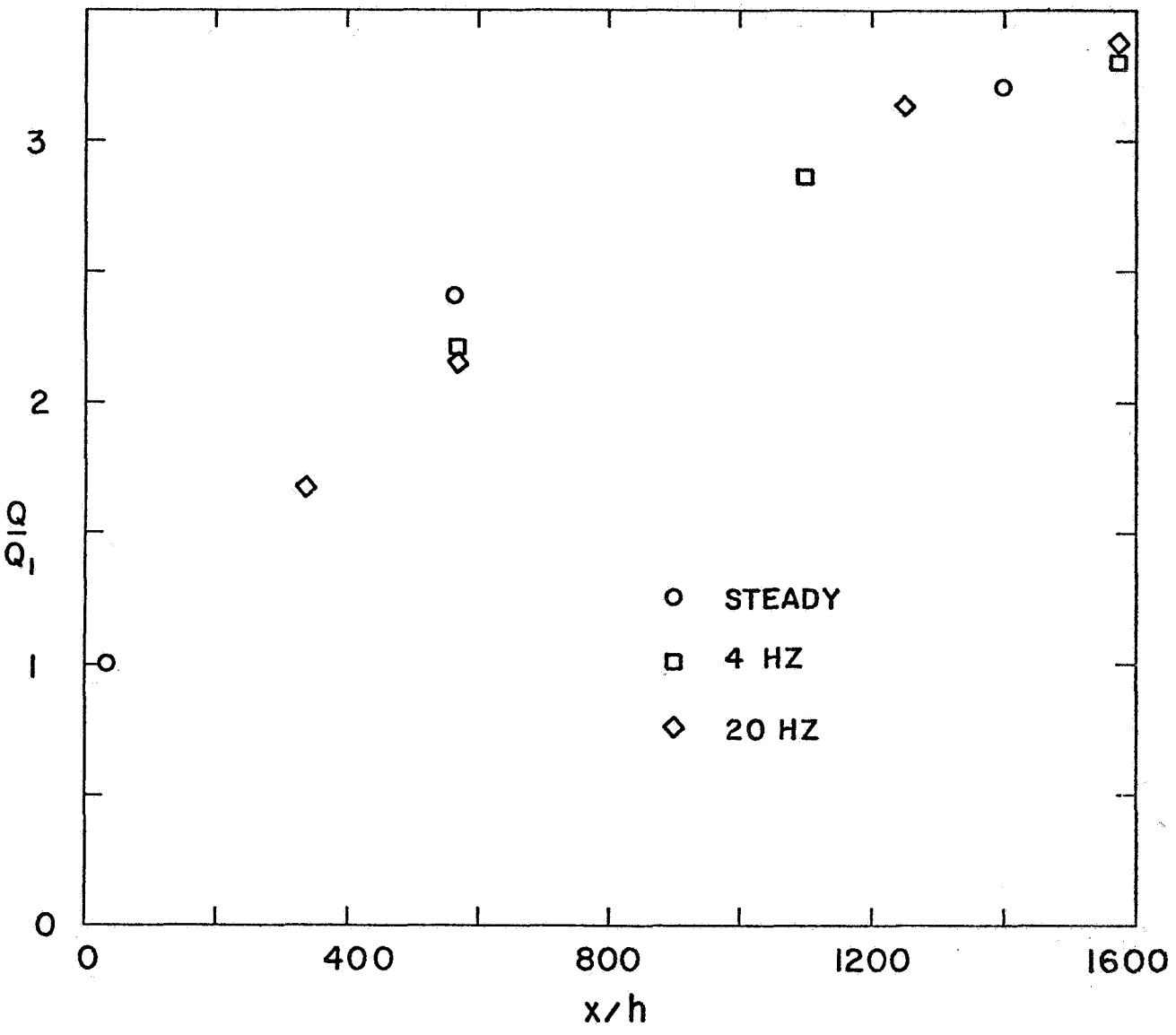

Figure 3. Mean volumetric flow rates Q(x) versus streamwise distance x for mechanically oscillated two-dimensional jet. Q_1 is flow in steady jet at x/h = 35 . h is nozzle width.

A SIMPLE APPARATUS FOR THE EXPERIMENTAL STUDY OF NON-STEADY FLOW THRUST-AUGMENTER EJECTOR CONFIGURATIONS

J. M. Khare* and J. A. C. Kentfield+
Department of Mechanical Engineering
Faculty of Engineering
University of Calgary
Calgary, Canada

ABSTRACT

Some advantages of non-steady flow ejectors as thrust augmenters are reviewed briefly. It appears that the main benfits to be derived from non-steady flow ejectors stem from the relatively small primary-to-secondary (cross-sectional) area ratios, and short "mixing" lengths, required, for prescribed thrust augmentation ratios, compared with those of steady flow ejectors. The fundamental benefit of a non-steady as compared with a steady flow ejector results from the nature of the process by which energy is transferred from the primary to secondary streams. In a non-steady flow ejector a component of pressure-exchange is involved in addition to the conventional mixing processes of steady flow ejectors. It is shown that the combined pressure-exchange flow-mixing mechanism presents substantial analytical difficulties even for so called one-dimensional systems in which the primary stream intensity, but not direction, is modulated. This suggests the need for an adaptable test rig to investigate experimentally the performance of non-steady flow ejectors.

A flexible, and easily modified, test rig is described which allows a one-dimensional non-steady flow stream to be generated, economically from a steady flow source of compressed air. This non-steady flow is used as the primary stream in a non-steady flow ejector constituting part of the test equipment. Standard piezo-electric pressure transducers etc. allow local pressures to be studied, as functions of time, in both the primary and secondary ("mixed") flow portions of the apparatus. Provision is also made for measuring the primary and secondary mass flows and the thrust generated. Sample results obtained with the equipment are presented.

---

*Graduate Student +Associate Professor

NOMENCLATURE

a	acoustic velocity
D	internal diameter of primary flow channel
L	length of primary flow channel
$\dot{m}$	mass flow
m'	dimensionless Riemann variable $[\equiv \frac{a}{a_{ref}} - (\frac{\gamma-1}{2}) \frac{u}{a_{ref}}]$
n'	dimensionless Riemann variable $[\equiv \frac{a}{a_{ref}} + (\frac{\gamma-1}{2}) \frac{u}{a_{ref}}]$
p	static pressure
P	stagnation pressure
p'	normalised pressure $[\equiv \frac{p}{p_{ref}}]$
t	time
t'	normalised time $[\equiv \frac{t\, a_{ref}}{L}]$
u	fluid (particle) velocity
u'	normalised velocity $[\equiv \frac{u}{a_{ref}}]$
x	distance along primary channel from rotary valve
x'	normalised distance $[\equiv \frac{x}{L}]$
z	gap between primary and secondary channels
z'	normalised gap $[\equiv \frac{z}{D}]$
β	mass flow ratio $[\equiv \frac{\dot{m}_S}{\dot{m}_P}]$
θ	pressure parameter: $(p_D - P_S)/(P_P - P_S)$
Φ	augmentation ratio: (thrust with augmenter)/(thrust due to primary mass flow when expanded isentropically from receiver-to-surroundings pressure)
Φ_A	augmentation ratio: (thrust with augmenter)/(thrust due to primary stream with augmenter present)

Φ_B augmentation ratio: (thrust with augmenter)/(thrust due to primary stream with augmenter removed)

Subscripts

D exit of secondary flow channel

P primary stream

S secondary stream

ref reference conditions

INTRODUCTION

The renewed interest, in recent years, in the use of ejectors as thrust augmenters appears to have arisen because of remarkable progress in the field of ejector design which allows (static) thrust augmentation ratios (Φ) in the region of 2:1 to be achieved in practice (1,2,3,4). One of the problems of modern, improved, high augmentation ratio ejectors is the large area ratio required. A primary-to-secondary area ratio of approximately 24:1 is necessary in order to achieve a (static) thrust augmentation ratio of about 2:1 (1,2,3,4).

The possibility appears to exist of utilising unsteady-flow ejectors of relatively modest area ratio to achieve Φ values in the region of 2:1. On the basis of available experimental data, for one type of non-steady flow ejector, a primary-to-secondary area ratio of only about 6:1 will be necessary to achieve a Φ value approaching 2:1 (5). When consideration is given to the fact that, for the device in question, flow passes through the primary nozzle for only about 50% of the ejecter running time, it can be seen that it should be possible to reduce the secondary duct cross-sectional area, for a prescribed value of Φ, to about half that necessary for a comparable steady flow system.

The inherent advantage of non-steady flow ejectors appears to stem from the nature of the primary-to-secondary stream energy transfer process which, for most types of non-steady flow ejectors, seems to involve a component of pressure-exchange. Pressure-exchange is an energy transfer process, independent of mixing, in which the primary and secondary flows

interact via an interface normal, or substantially normal, to the (local) flow direction. Quantitative prediction of the flow field in the secondary zone becomes particularly difficult when the pressure-exchange mechanism is combined intimately with mixing. This situation appears to prevail in most non-steady flow ejectors and suggests the desirability of an experimental approach to performance investigation.

TYPES OF NON-STEADY FLOW EJECTOR

There are at least three classes of ejector in which organised non-steady flow is an essential feature of the device. Each type is illustrated diagrammatically in Fig. 1. In every case the primary stream is the source of the flow non-steadiness.

Crypto-Steady Ejector

Perhaps the best known form of thrust augmenter involving non-steady flow (at least flow which is non-steady relative to a stationary observer) is the crypto-steady device due to Foa (6,7,8). In this system, illustrated in Fig. 1(a), "pseudo-blades" formed from fluid issuing from orifices in a self-driven, freely spinning, hub constitute the primary stream of the ejector. This type of machine, which is axi-symmetric, relies upon the "pseudo-blades" pumping the secondary flow somewhat along the lines of a turbo-machine with, of course, the important difference that the blades are non-rigid and are not attached to the hub. In part, at least, energy is transferred from the primary to the secondary stream by pressure-exchange. Presumably both the primary and secondary streams leave the apparatus at least partially mixed. An inherent advantage of the Foa device, relative to some other types of non-steady flow ejector, is that the expansion of the primary flow can be executed efficiently.

Oscillating Jet Ejector

A form of non-steady flow device which is not constrained to be axi-symmetric is an ejector in which the primary flow oscillates laterally in the secondary flow zone: a device of this type is shown in Fig. 1(b). Preferably, from an operational view point, the primary stream is caused to oscillate by fluidic means thereby eliminating the need for mechanical moving parts. Again a pressure-exchange mechanism can be seen to come into

play in the transfer of energy between the primary and secondary flow. It appears that a major problem of the oscillating jet system is irreversibility in the fluidic primary nozzle (9).

One-Dimensional Non-Steady Flow Ejector

Perhaps the most simple form of non-steady flow ejector is that in which the intensity of the primary stream is modulated as a function of time. An ejector of this type is shown in Fig. 1(c). It was an ejector of this kind, subjected it seems to but little prior development, which was shown, by Lockwood (5) to be capable of producing a basic augmentation ratio, ϕ_B, of 1.95:1 with a primary-to-ejector-thrust area ratio of only 2.2:1. Lockwood used a flow converter which converted a steady flow into four, separate, non-steady streams one of which constituted the primary stream of the ejector. The thrust augmentation ratio ϕ was substantially lower than ϕ_B due to losses in the conversion device. However the best converter performance coefficient obtained was 0.91 (5). The converter performance coefficient was defined by Lockwood to be the time-averaged non-steady flow thrust (without the augmenter) divided by the thrust which would be obtained by expanding the same primary mass flow, isentropically, to the surroundings pressure. The value of ϕ_A lay between the values of ϕ_B and ϕ: the presence of the augmenter obviously affected the primary flow.

It would seem, therefore, that provided an efficient means can be found to generate the non-steady primary stream, an ejector of the type shown in Fig. 1(c) can be very effective. In the case of an application as a thrust augmenter for a pulse-jet, for example, the ejector primary stream (i.e. outflow from the pulse-jet) is modulated in intensity automatically and this problem vanishes. For applications in which the primary stream originates from a steady flow source a spinning primary jet, on the lines of that of Foa's ejector (6), entering sequentially a cluster of secondary flow channels, Fig. 2, may be acceptable for some thrust augmenter applications. The rigorous phase control of such a system may serve to minimise noise and vibration both of which tend to be problems with non-steady flow equipment.

The merits of one-dimensional (dynamic) pressure-exchange processes

are, when isolated from the complexities associated with significant mixing, well understood and are amenable to analysis by the method-of-characteristics as applied to non-steady flows (6,10). In fact when a machine is designed to utilise dynamic pressure-exchange processes exclusively it is possible to achieve isentropic efficiencies of expansion and compression comparable, at least for some operating conditions, with those of turbines and compressors (10,11,12). The dynamic pressure-exchanger counterpart of an ejector is a machine termed an equaliser. However this device appears to be relatively unattractive as a large-scale thrust augmenter because of the size, and complexity, of the major moving component (11,12).

A special test rig was constructed in order to assist in obtaining an understanding of devices of the type shown in Fig. 1(c) in which internal events represent a combination of pressure-exchange and flow mixing.

TEST RIG

A prime consideration during the conceptual stage of planning the test rig for testing one-dimensional type ejectors was that the device should make efficient use of the primary flow available. This prevented the application of a multi-channel flow converter as used by Lockwood (5) and it is believed, although it is not stated explicity, also by Johnson and Yang (13). Another important factor was that the time-averaged thrust generated should be measurable, by simple means, with instrumentation etc. connected to the apparatus. It was, therefore, decided to use a suspended-plate type thrust meter. The thrust meter essentially turned through a right angle all flow impinging on the plate normal to the working face. A justification for the use of this type of thrust measuring device will be found elsewhere (14).

Other considerations were that it should be possible to measure the (average) primary and secondary mass flow rates, the pressures and temperatures of both the primary and secondary flows (i.e. reservoir conditions) and pressures, as a function of time, within the primary and secondary flow channels. It was felt that the provision of a heated air supply for the primary stream would have been desirable but to equip the apparatus with this facility would have complicated the system substantially.

Accordingly no provision was made to control the temperature of the primary, or secondary, stream. The apparatus is shown in diagrammatic form in Fig. 3.

Figure 4 shows details of the slotted, drum-type rotary valve used for creating the pulsing primary flow. The valve was driven by a variable speed electric motor (Fig. 3). The transition section, connecting the rotary valve stator to the primary tube, and the primary tube itself are shown in Fig. 5. Further details of the apparatus are available (15).

ANALYSIS OF PRIMARY-TUBE FLOW

One of the first tasks undertaken with the rig was to compare actual with theoretical pressure $\sim$ time traces in the primary tube. In this way it should be possible to detect any major shortcomings of the simple rotary valve mechanism as these should show up as major discrepancies between the theoretical (predicted) and actual (measured) pressure or time records.

Figure 6 shows a wave diagram (method-of-characteristics) constructed, ignoring wall friction, for the flow within the primary tube. Two operational cycles are depicted, the first cycle (duration $\Delta t'_{\text{cycle 1}}$) was based on uniform initial conditions, with the air at rest, within the primary tube at $t' = 0$. The second cycle was constructed with its initial conditions based on the final conditions of the first cycle. The second cycle should, therefore, be much more representative of the cyclic operation of the apparatus. Figures 7 and 8 show theoretical and experimental pressure traces in the primary tube at $x = 2"$ and $x = 10"$ respectively. For the case of the theoretical prediction (solid line) the pressure trace is shown for cycles 1 and 2. For the experimental case (dotted line) the comparison is made with the second cycle since this is more representative of cyclic operation, the conditions for which the experimental measurements were made. Figures 7 and 8 implied that the operation of the rotary valve appeared to be quite satisfactory. Figures 6, 7 and 8 correspond to a nominal design-speed operation of the rotary valve at 1800 rev/min. The design speed of the rotary valve was based on a cycle duration of $\Delta t'_{\text{cycle 2}}$.

The ratio of the primary-flow settling-tank pressure to the surroundings pressure was 1.5:1. This value was invoked in the construction of the wave diagram (Fig. 6) and was maintained constant for all the tests carried out with the apparatus.

SAMPLE RESULTS FROM EJECTOR TESTS

For preliminary tests of the complete ejector system three, simple, augmenter ducts were made, each of uniform diameter, provided with a bellmouth at the upstream end. The augmenter ducts were each 20 inches long, equal to the length of the primary tube, and were not provided with diffusers. The internal cross-sectional area of each augmenter tube divided by the internal cross-sectional area of the primary tube were as follows:

Augmenter Duct # 1	:	3.35
Augmenter Duct # 2	:	5.35
Augmenter Duct # 3	:	9.40

The initial tests were generally of an exploratory nature and were not intended to produce optimised performance characteristics. The first operational parameter investigated was the influence on performance of valve speed. This investigation was carried out using Augmenter Duct #1. The influence of valve speed on the thrust produced is shown in Fig. 9. From this diagram it can be seen that the thrust of the system increases steadily as the valve speed is increased from 50% to 150% of the nominal design-speed of 1800 rev/min. Exactly the opposite influence of valve speed is apparent in Fig. 10 which shows the ratio, β, of the secondary (induced) mass flow to the primary mass flow. It is apparent from Fig. 11 that the pressure parameter θ, representing the non-dimensional pressure-gain, is a maximum at the design valve-speed. The sensitivity of θ to a variation of valve speed is quite strong.

The results of a simple investigation to establish the optimum axial gap, z, between the open end of the primary tube and the face of the bellmouth of the augmenter duct are presented in Fig. 12. The diagram shows that β is relatively insensitive to changes in z'; the optimum value of z' is about 1.3. The finding that β is maximised with a positive value of z' is, qualitatively at least, in agreement with the findings of Lockwood (5).

It remains to offer an explanation of the performance characteristics displayed in Fig. 9 and 10.

The Influence of Valve Speed on the Primary Mass Flow

Figure 13 presents simplified wave (left hand side) and state (right hand side) diagrams constructed to show that the effective primary tube exit velocity can be expected to increase as the valve speed increases. The wave and state diagrams at the top of the figure depict conditions in the primary tube when the valve is operating at its design speed. The outflow velocity is represented by point 3, in the u ~ a chart, for 50% of the cycle duration with a low velocity inflow, state point 1, for the remainder of the cycle.

The lower pair of diagrams in Fig. 13 shows what happens when the valve is operated at twice the design speed. The outflow velocity for 50% of the cycle duration is given by state point D (a velocity much greater than that corresponding to state point 3 in the upper diagram) and for the remainder of the cycle the inflow velocity, noted in the upper diagram, is reduced to zero (state point B). The consequence of doubling the valve speed is, therefore, to increase very substantially the average flow velocity, and hence the mass flow, through the primary tube.

The foregoing characteristics offer an explanation of the increase of thrust with increasing valve speed apparent in Fig. 9 and, at the same time, account, in part, for the trend observed in Fig. 10.

CONCLUSIONS

Three classes of non-steady ejectors were surveyed briefly and it was found that the one-dimensional type, sometimes also known as a pulse-jet ejector, offered considerable promise in that it appears to permit a reduction in the secondary, or augmenter, duct cross-sectional area to about half that of a steady flow ejector of equal augmentation ratio.

It was further concluded that because of uncertainties associated with the analysis of the flow field in pulse-jet ejectors an experimental technique was preferred to a wholly theoretical one for investigative performance analysis. An apparatus designed specifically for studying the performance of pulse-jet ejectors was described and sample test results

were presented. It was found that these results were, in general, in accordance with theoretically based expectations.

ACKNOWLEDGEMENT

The authors wish to acknowledge the support of the National Research Council of Canada for the work reported here. The assistance given was in the form of an Operating Grant made available to the second author.

REFERENCES

1. Quinn, B., "Compact Ejector Thrust Augmentation", Journal of Aircraft, Vol. 10, No. 8, August 1973, pp. 481-486.

2. Bevilaqua, P.M., "Evaluation of Hypermixing for Thrust Augmenting Ejectors", Journal of Aircraft, Vol. 11, No. 6, June 1974, pp. 348-354.

3. Campbell, D.R. and Quinn, B., "Test Results of a VTOL Propulsion Concept Utilizing a Turbofan Powered Augmentor", Journal of Aircraft, Vol. 11, No. 8, August 1974, pp. 467-471.

4. Bevilaqua, P.M., "Analytic Description of Hypermixing and Test of an Improved Nozzle", Journal of Aircraft, Vol. 13, No. 1, January 1976, pp. 43-48.

5. Lockwood, R.M., "Interim Summary Report Covering the Period 1 April 1962 to June 1962 on Investigation of the Process of Energy Transfer from an Intermittent Jet to Secondary Fluid in an Ejector-Type Thrust Augmenter", Hiller Aircraft Corp. Report No. ARD-305, June 30, 1962.

6. Foa, J.V., "Elements of Flight Propulsion", Chapter 10, John Wiley and Sons, 1960.

7. Hohenemser, K.H., "Flow Induction by Rotary Jets", J. Aircraft, Vol. 3, No. 1, 1966, pp. 18-24.

8. Hohenemser, K.H. and Porter, J.L., "Contribution to the Theory of Rotary Jet Flow Induction", J. Aircraft, Vol. 3, No. 4, 1966, pp. 339-46.

9. Viets, H., "Oscillating Jet Nozzles for V/STOL Application", AIAA Paper No. 74-1189, October 1974.

10. Azoury, P.H., "An Introduction to the Dynamic Pressure Exchanger", I. Mech. E. Proc. 1965-66, Vol. 180, Part 1, No. 18.

11. Kentfield, J.A.C., "The Performance of Pressure Exchanger Dividers and Equalizers", A.S.M.E. Journal of Basic Engineering, Series D, Vol. 91, No. 3, 1969.

12. Ruf, W., "Berechnungen und Versuche an Druckwellen-Maschinen unter besonderer Berücksichtigung des Druckteilers und Injektors", Juris Druck (publisher) Zürich, 1967 (Doctoral Thesis, Eidgenossischen Technischen Hochschule, Zürich).

13. Johnson, W.S. and Yang, T., "A Mathematical Model for the Prediction of the Induced Flow in a Pulsejet Ejector with Experimental Verification", ASME Paper No. 68-WA/FE-33, 1968.

14. Marzouk, E.S., "A Theoretical and Experimental Investigation of Pulsed Pressure-Gain Combustion", Ph.D. dissertation, University of Calgary, Calgary, Alberta, Canada, 1974.

15. Khare, J.M., "An Analytical and Experimental Investigation of an Unsteady Flow Ejector", M.Sc. dissertation, University of Calgary, Calgary, Alberta, Canada, 1973.

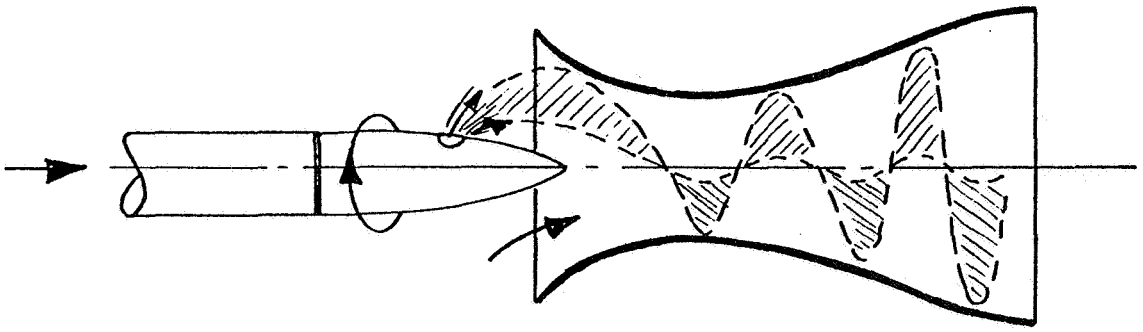

(a) Crypto-Steady, or Spin-Jet, Ejector (Foa).

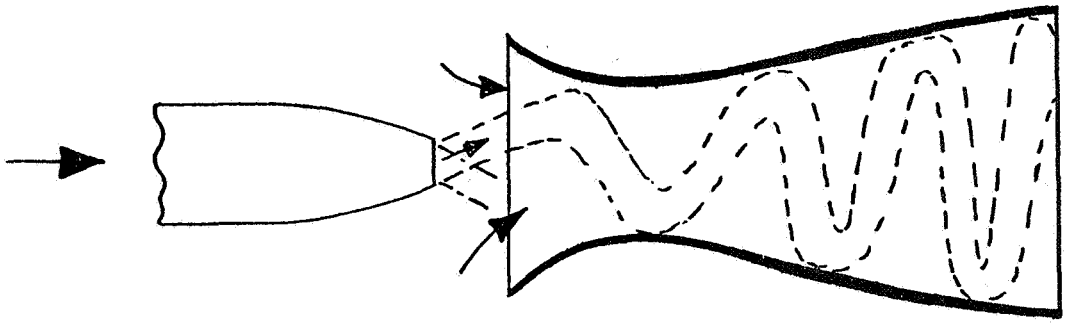

(b) Ejector with Oscillating Primary Jet.

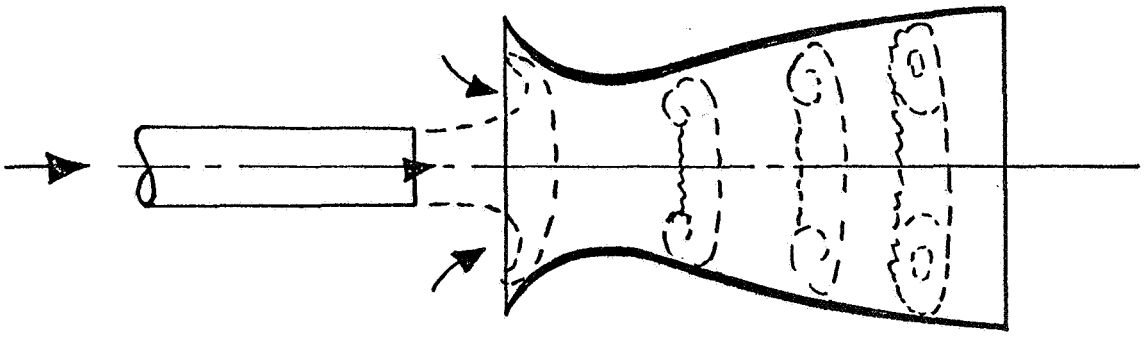

(c) One-Dimensional, or Pulse-Jet, Ejector.

Fig. 1 Types of Non-Steady-Flow Thrust-Augmentation Ejectors.

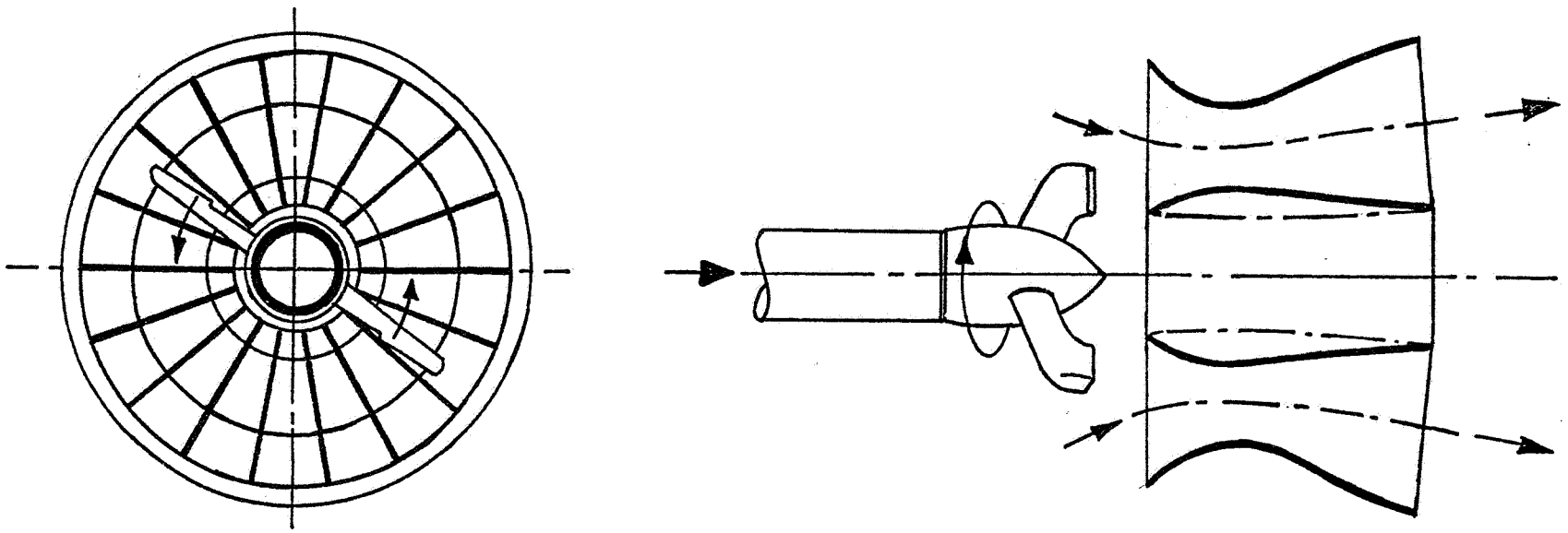

Fig. 2 Clustered One-Dimensional Non-Steady Flow Ejectors Supplied with Primary Fluid Issuing from Nozzles Mounted on a Freely Rotating Hub.

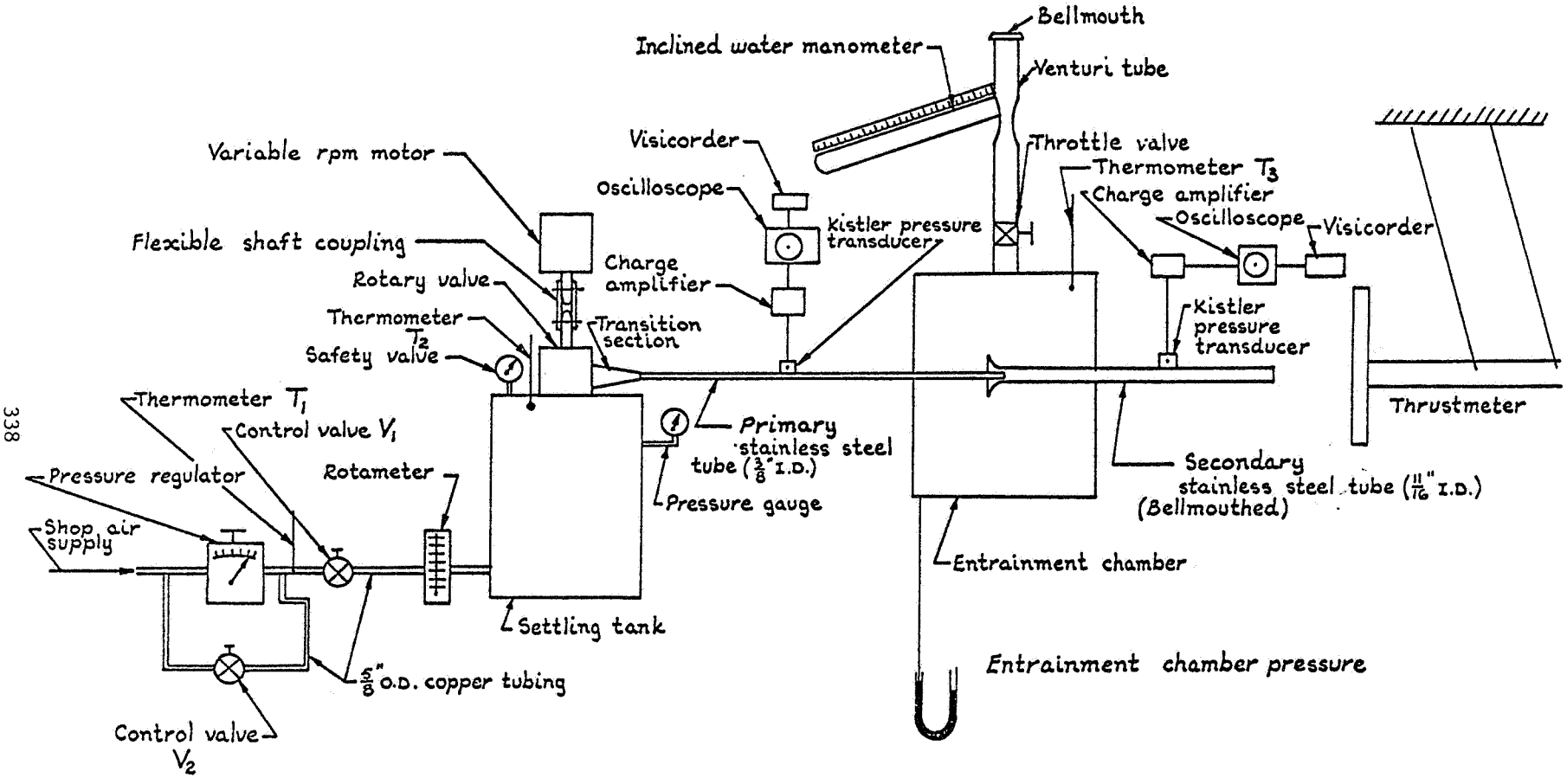

Fig. 3 General Schematic Arrangement of the Experimental Apparatus.

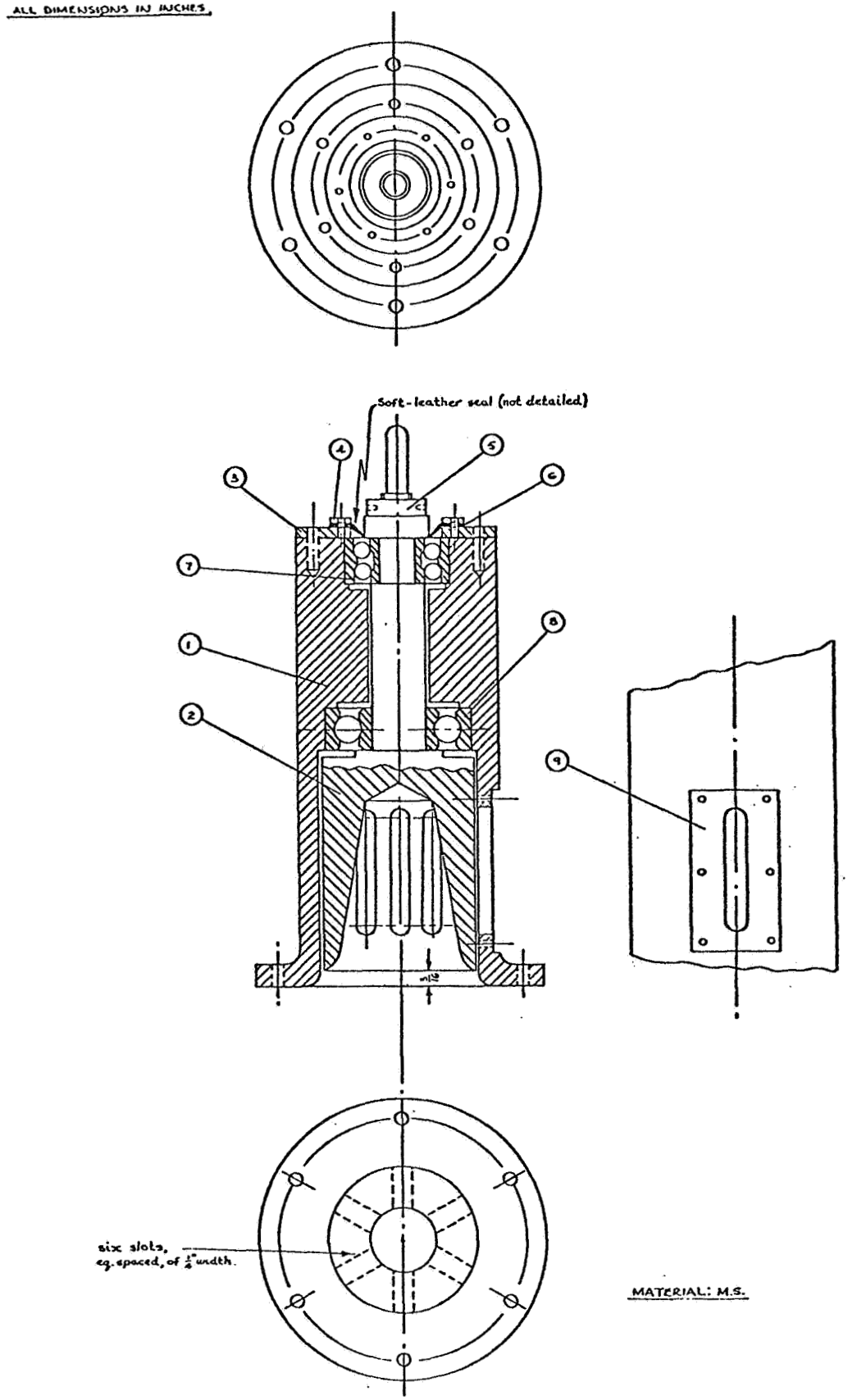

Fig. 4 Rotary Valve Details.

ALL DIMENSIONS IN INCHES

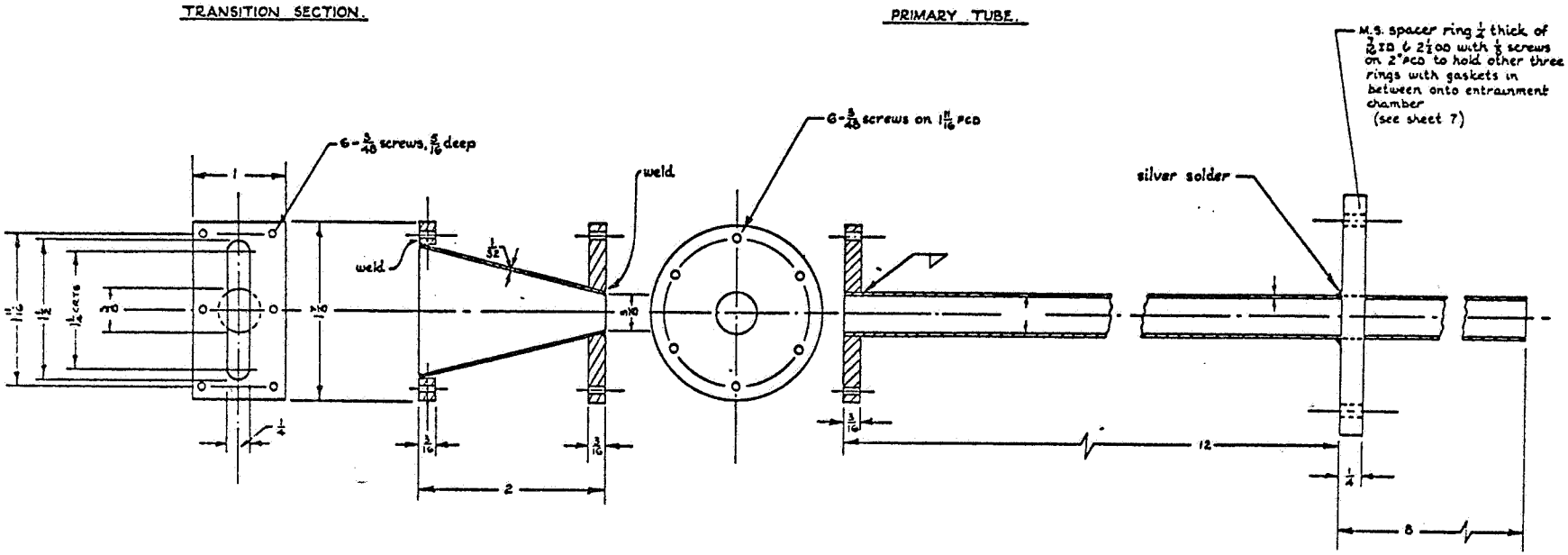

NOTE:

1. Transition section is to be fastened to rotary valve stator.
2. The other (R Hand end) of transition section is to be coupled to the primary tube.

MATERIAL: STAINLESS STEEL.

Fig. 5 Details of the Transition Section and the Primary Tube.

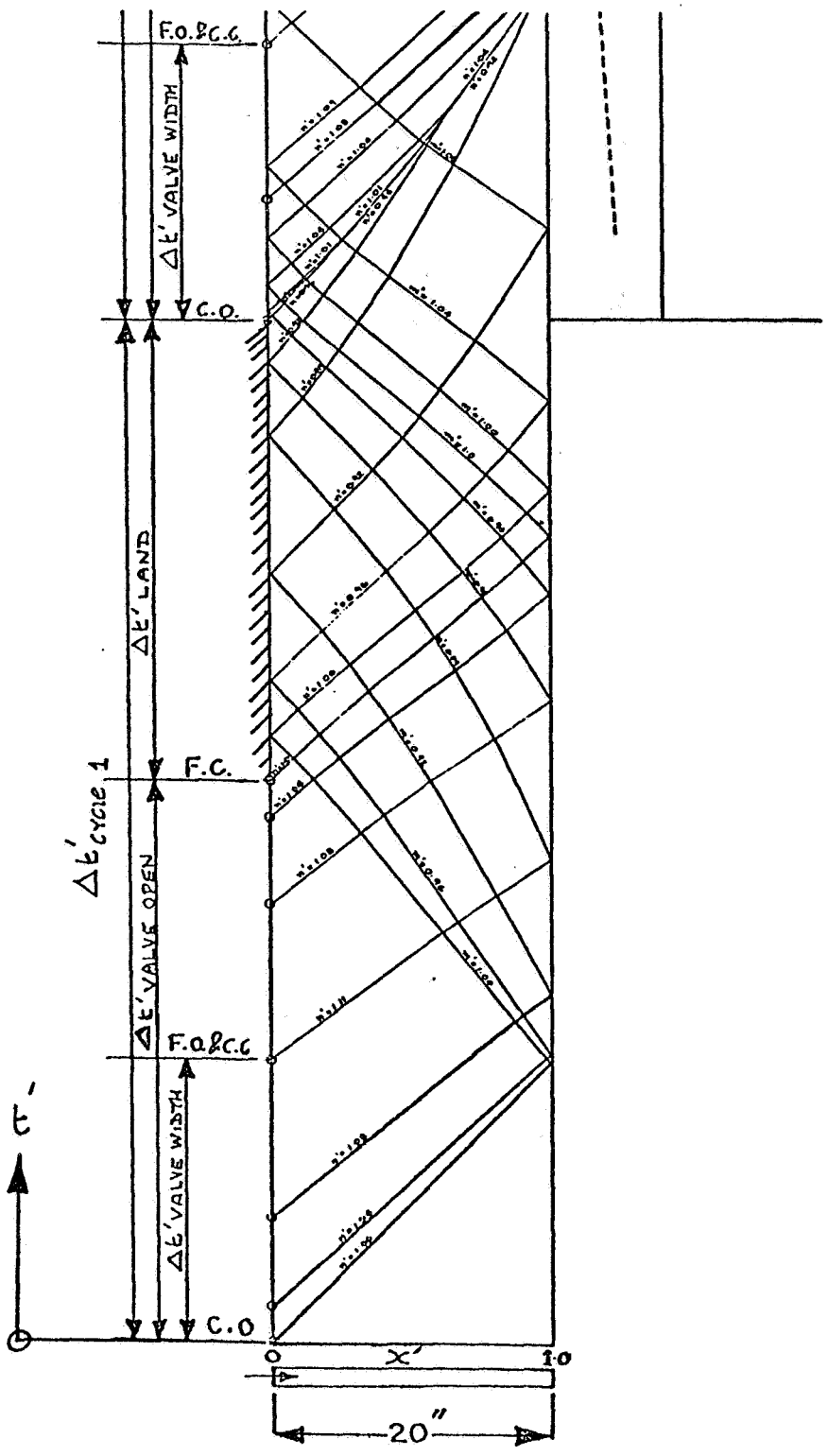

Fig. 6 Predicted Flow Field, for the First (Start-Up) Cycle of Operation, in Primary Tube on x' ∿ t' Plane. Rotary Valve at Left Hand End of Primary Tube.
a_{ref} = 1120 ft/s (340 m/s)

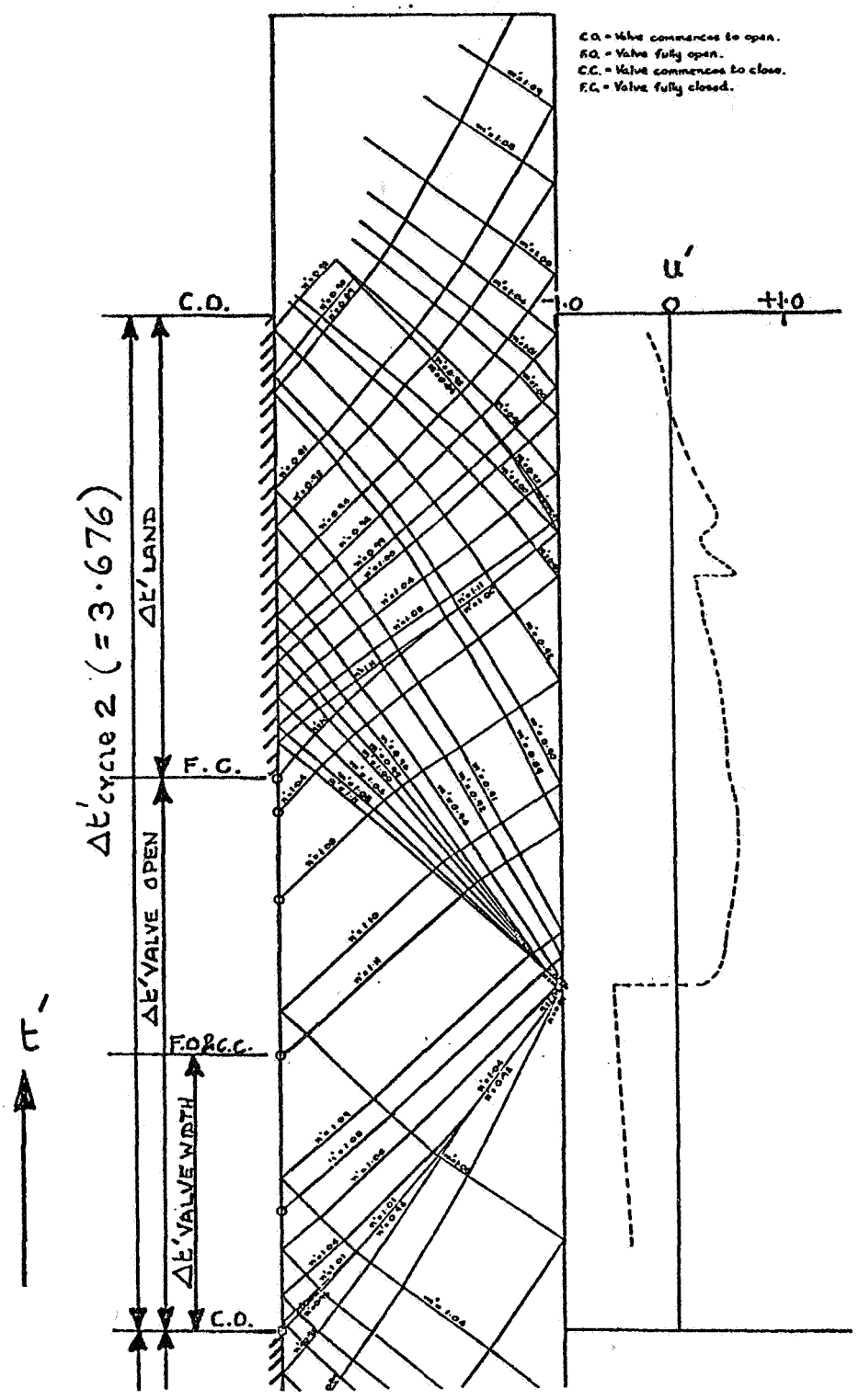

Fig. 6 (continued) x' ∿ t' Diagram for the Second Cycle of Operation. The Normalised Velocity Profile at the Outlet End of the Primary Tube is also Shown.

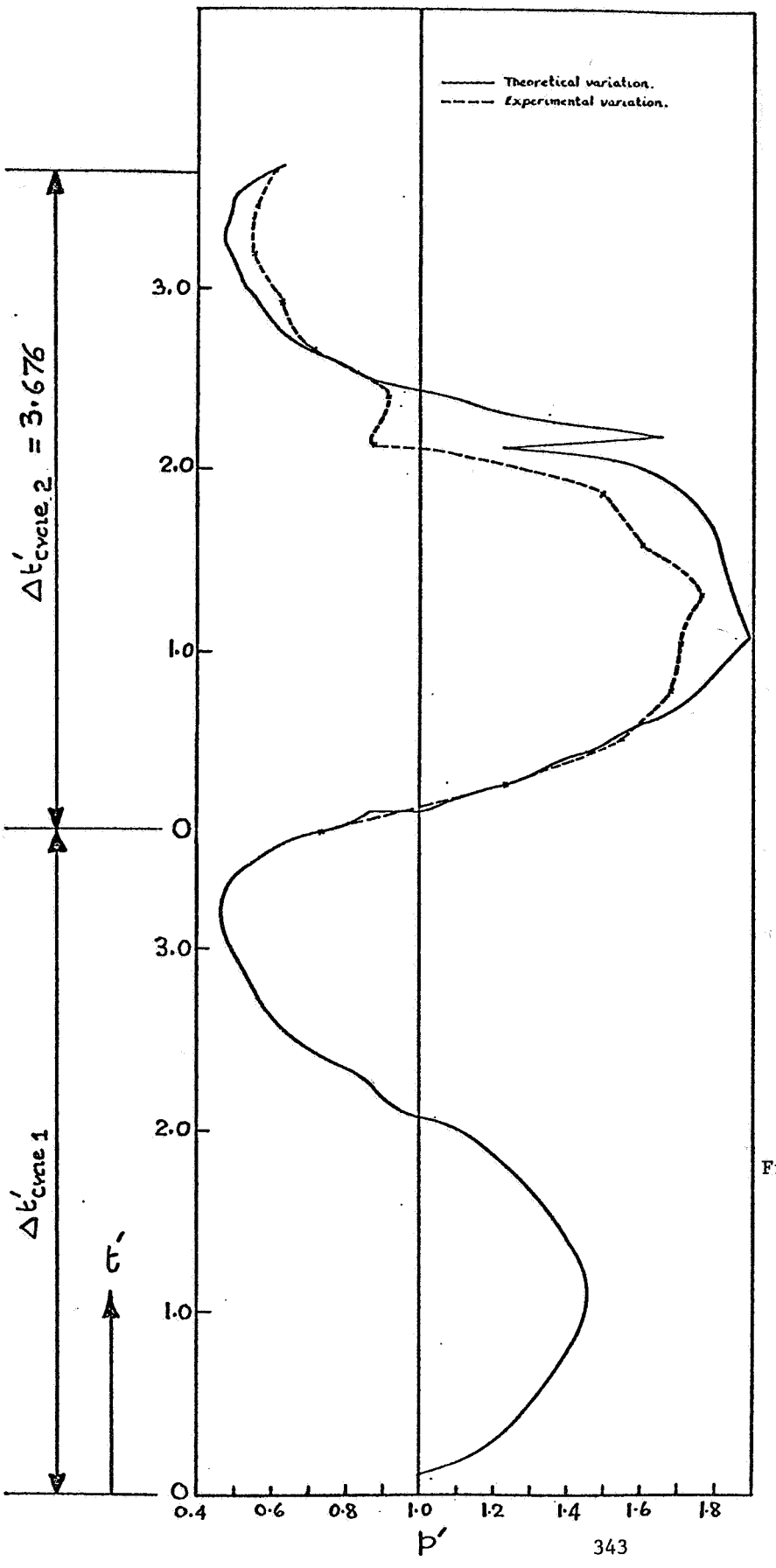

Fig. 7 Experimental and Theoretical Pressure-Time Plot (p' ~ t') at the 2 inch Location in the Primary Tube; Optimum Valve Speed

(p_{ref} = Surroundings pressure = Static pressure at exit of primary tube.)

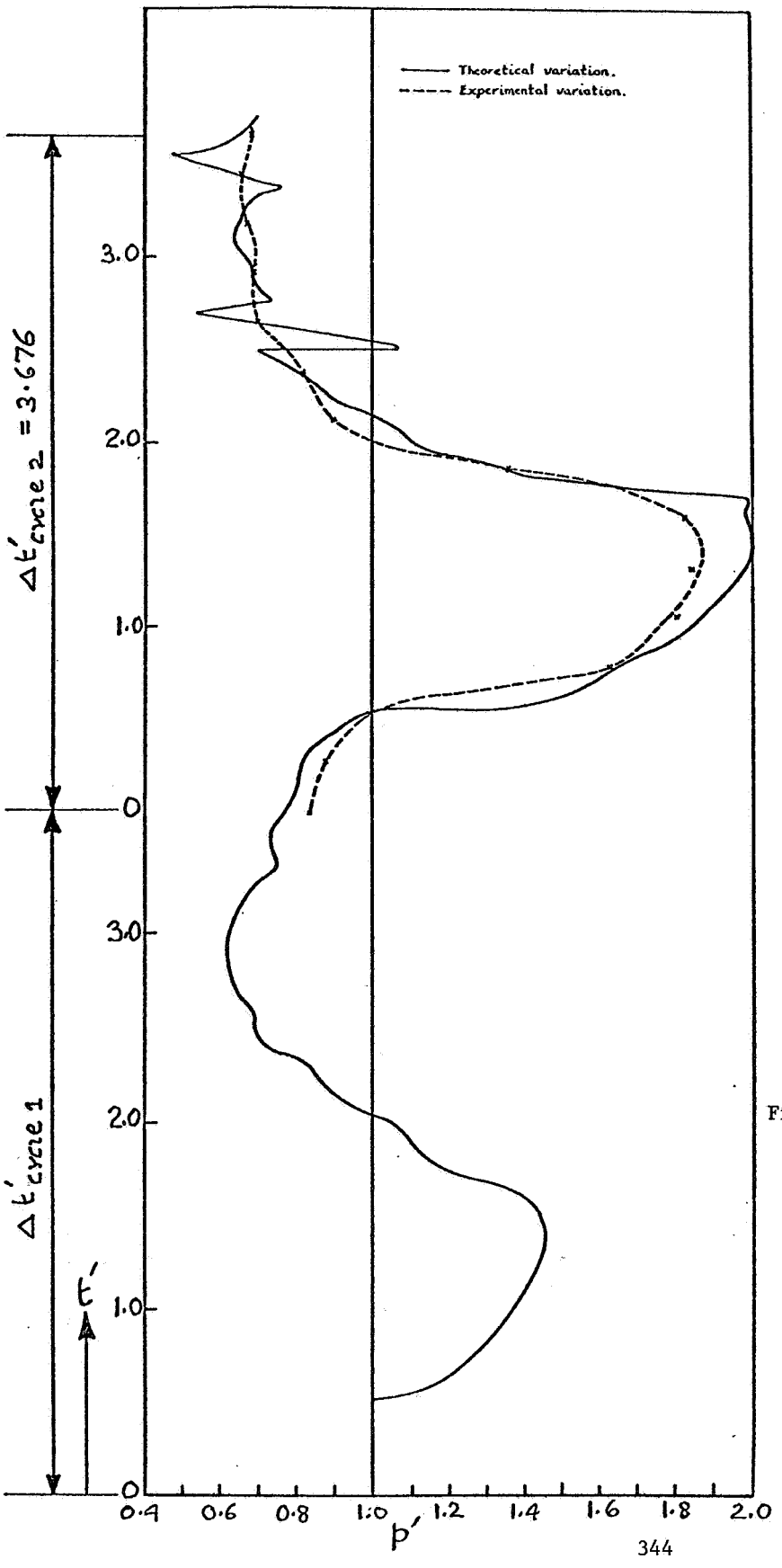

Fig. 8 Experimental and Theoretical Pressure-Time Plot (p' ~ t') at the 10 inch Location in the Primary Tube; Optimum Valve Speed

(p_{ref} = Surroundings pressure = Static pressure at exit of primary tube.)

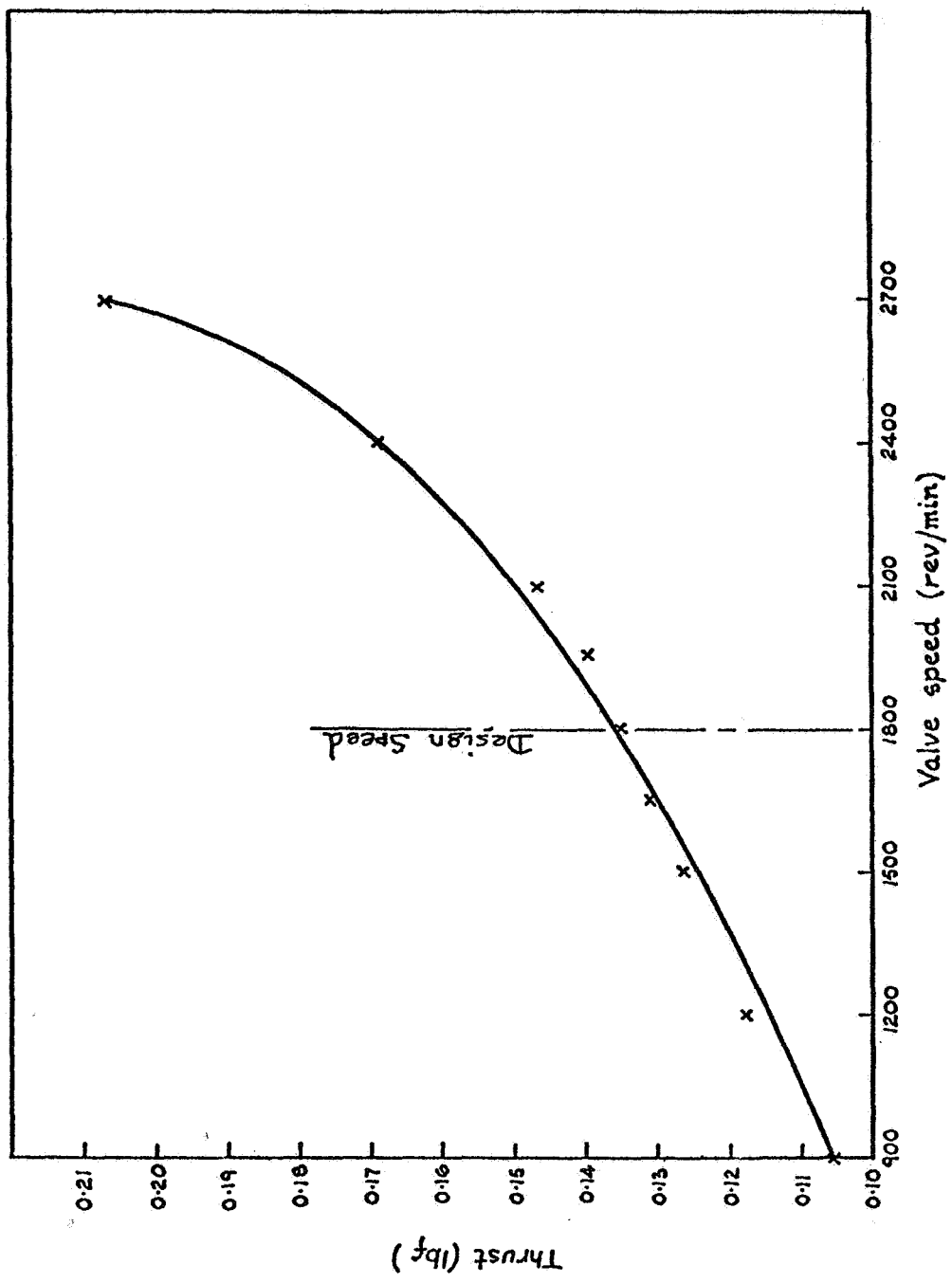

Fig. 9 Average Thrust - Valve Speed Plot for Augmenter Duct #1.

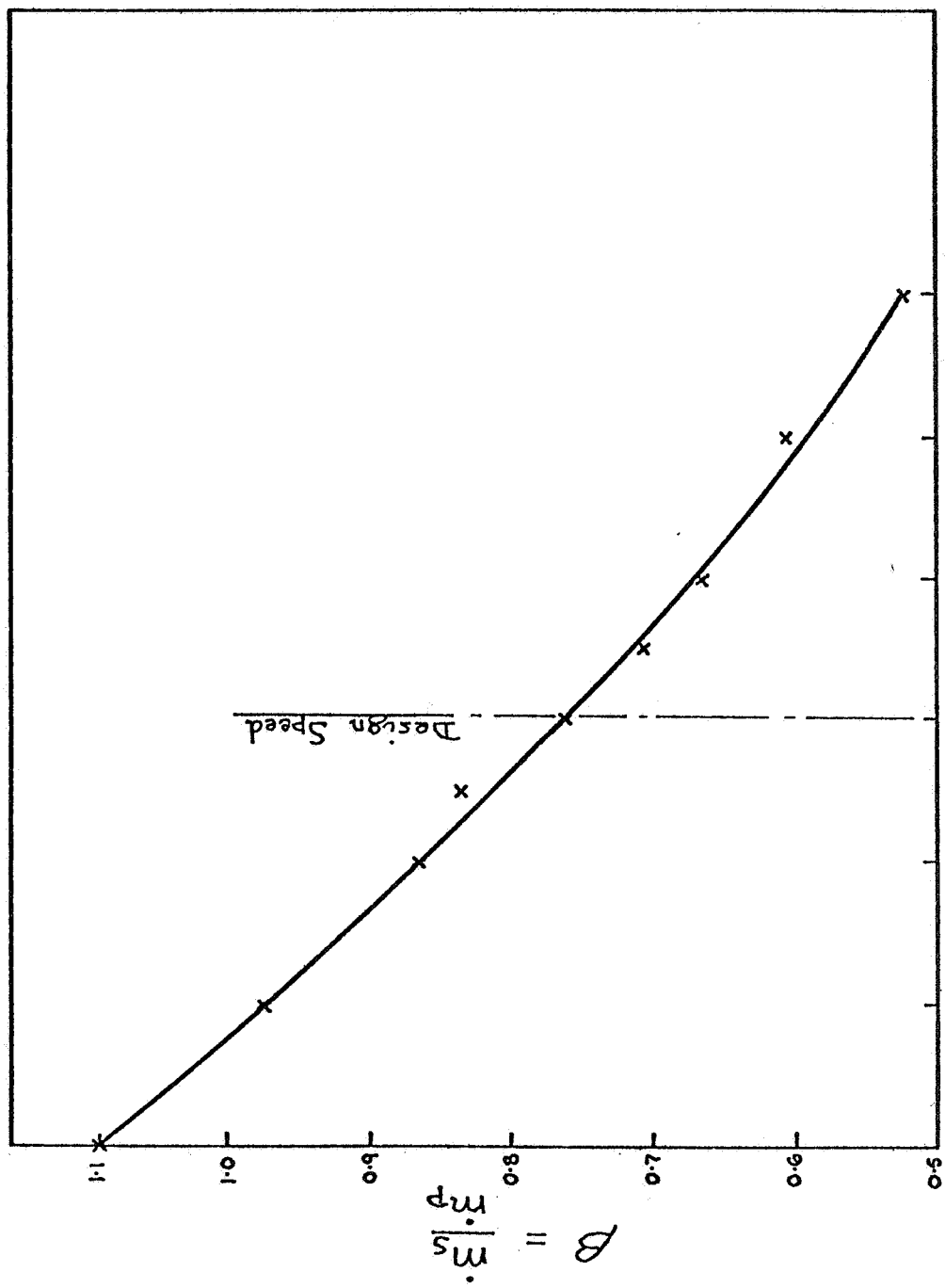

Fig. 10 Mass Flow Ratio - Valve Speed Plot for Augmenter Duct #1.

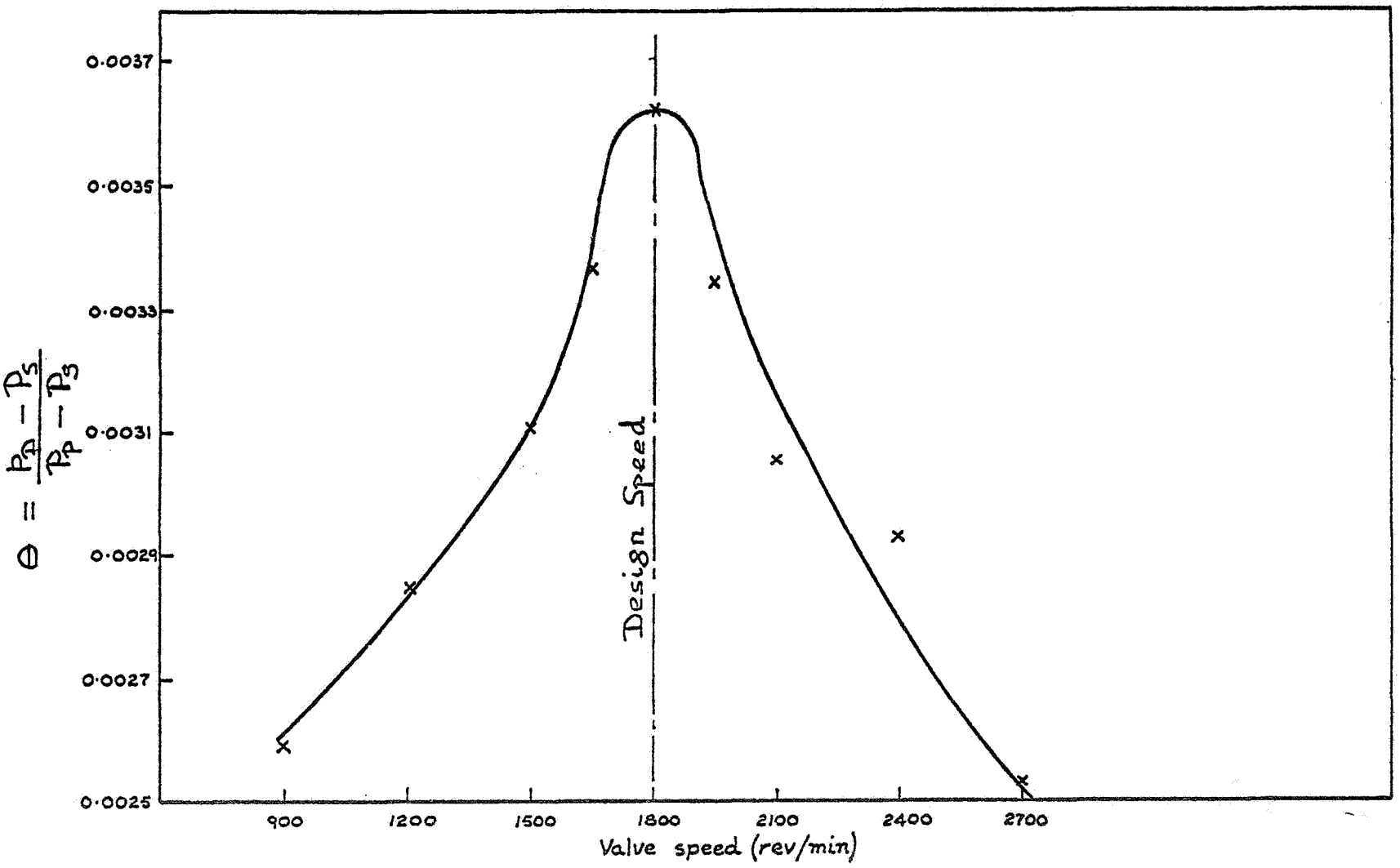

Fig. 11 Pressure Parameter - Valve Speed Plot for Augmenter Duct #1.

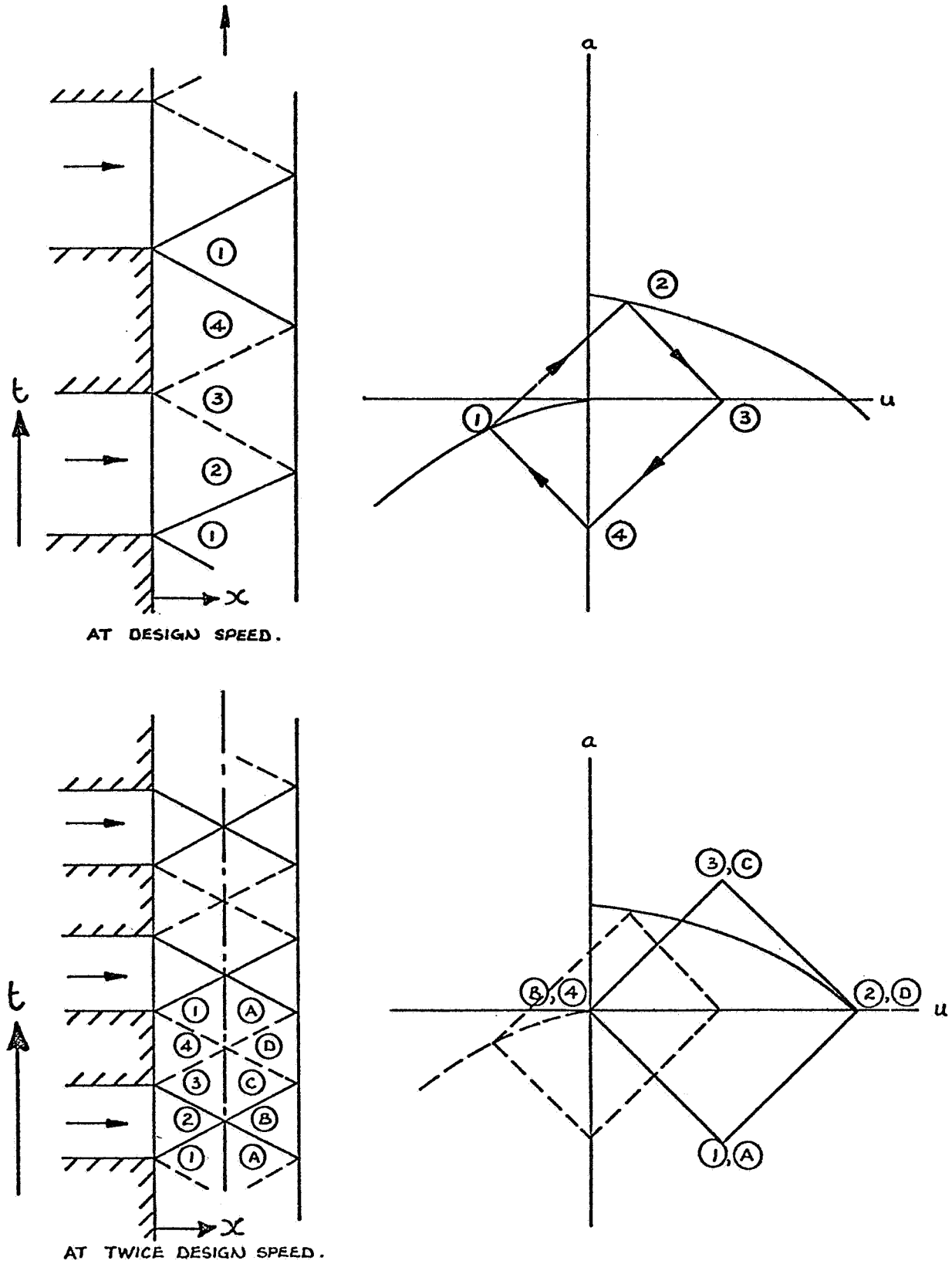

Fig. 13 Increase of Primary Tube Flow Velocity With Increase of Valve Speed.

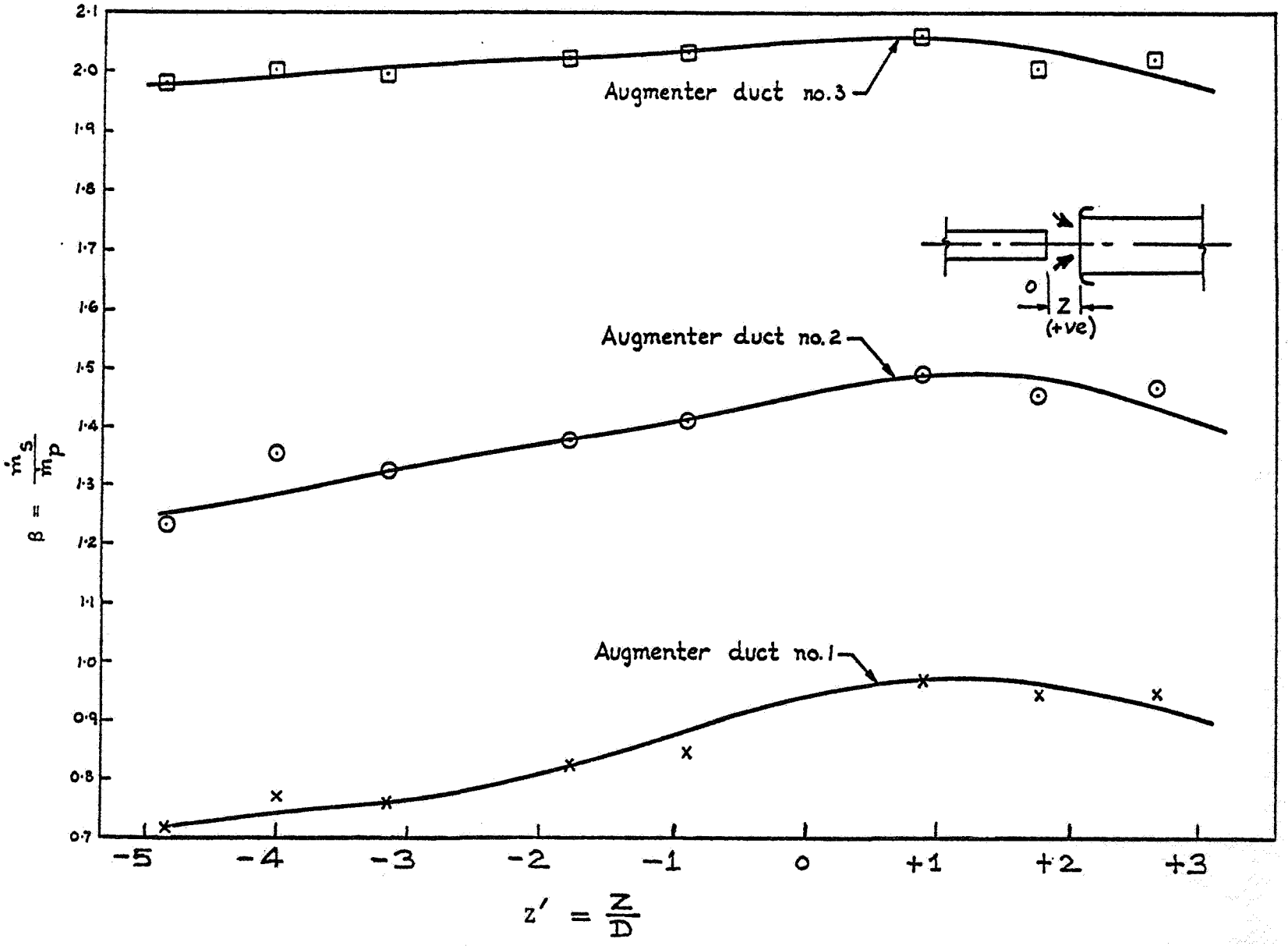

Fig. 12 Mass Ratio β versus Z′ for Augmenter Ducts #1, 2 and 3: Optimum Valve Speed.

PRESSURE AND VELOCITY MEASUREMENTS IN A THREE-DIMENSIONAL WALL JET*

G. D. Catalano,† J. B. Morton,‡ and R. R. Humpris§

PROBLEM

One of the present designs being investigated for increasing the lifting capabilities of aircraft is termed Upper Surface Blowing. The exhaust gases of the jet engine are directed along the upper surface of the wing and, becoming attached, are turned by the wing's upper surface and trailing-edge flaps. It has been found that a significant increase in lift is realized but the loading that the structure must endure is greatly increased. Hence there exists a need for more information about the flow field for this three-dimensional wall jet.

SCOPE

Several reports (refs. 1, 2) have dealt with the experimental investigation of the near field region of a three-dimensional wall jet (fig. 1). The first report dealt with the one point statistical properties of the flow exiting the nozzle without any confining surfaces present. The vortex shedding model of a turbulent jet was clearly reinforced by the appearance of peaks in the velocity spectra in the potential core region of the flow.

The effects on the flow field of the axisymmetric jet of placing a flat wall surface, referred to as the plate, and a wall surface with large curvature, the flap, adjacent to the lip of the nozzle were the subject of the second report. It was found that the curved wall surface served to break up the potential core region of the jet much more rapidly than was the case for either the unconfined flow or the flow over the flat wall.

In the third paper, emphasis was placed on obtaining space-time correlations in the different turbulent flow fields from which isocorrelation

---

Presented at the AIAA 17th Aerospace Sciences Meeting, January 15-17, 1979, New Orleans, Louisiana.

*Work Supported in part by NASA Grant No. NGR 47-005-219-3 and NSF Grant No. 7522488.

†Aerospace Engineer, Air Force Flight Dynamics Laboratory/FXM, Wright-Patterson Air Force Base, Ohio 45433.

‡Associate Professor, Mechanical and Aeronautical Engineering Department, University of Virginia.

§Senior Scientist, Nuclear Engineering Department, University of Virginia.

contour maps were constructed. The isocorrelation contours for the turbulent flow fields demonstrate the existence of large-scale structures. The shape of the contours was significantly different for each of the three flow configurations in both the longitudinal and horizontal cross-sectional views. The contours depended on whether or not a confining surface was present and whether the wall was flat or curved.

The present paper has two main emphases. First, the effects on the flow fields of varying the ratio of the velocity at the exit plane of the nozzle to the outer tunnel flow are reported. Second, pressure-velocity correlations are taken and some trends are discussed. Emphasis is placed on comparing the coherence between the fluctuating pressure and velocity fields at various locations in the different flow configurations.

The same three flow fields investigated in the second and third reports (ref. 2 and 3) are studied here. The arrangement of the confining surfaces, the flap and the first plate are shown in figure 2(a) and a schematic of the whole facility is shown in figure 2(b).

A two-color laser Doppler velocimeter in conjunction with a phase locked-loop processor is used to make the velocity measurements. The two strongest frequencies of an argon ion laser in the "all lines" mode of operation are selected for use. The two-color LDV system allows the velocity at two different points in the flow fields to be determined with displacement between the probes possible in all three directions. This system is described in more detail in reference 1.

To determine the static and wall surface pressures, the system developed by Schroeder (ref. 4) and Herling (ref. 5) is used. The essential items include a 1/2 in. condenser-type microphone and a tape recorder. When cross-correlations are made between the fluctuating pressure and velocity fields, both signals are filtered (10 Hz to 100 Hz) before being processed to achieve a good signal-to-noise ratio. Figures 3 through 8 show the effects of confining surfaces on the various statistical properties.

SUMMARY

The value of the velocity ratio, λ_j, was found to have a significant influence on the mean velocity field. For the case of the flow over the flap, an increasing value of λ_j decreased the effectiveness of the curved wall surface in diminishing the x-directed momentum. Evidence existed that as λ_j approached infinity, the flow would not remain attached. The parameter λ_j influenced the width of the mean velocity profiles as well, especially in the case of the flow over the flap. An increase in λ_j caused a resultant decrease in the mixing width, y_m.

Pressure velocity correlations using both the static pressure probe and the surface ports yielded strong evidence that as the flow progresses downstream and the flow becomes a fully developed turbulent flow, the relationship between the pressure and velocity field diminishes. For the

first several diameters downstream from the exit plane when the pressure and velocity spectra peak at approximately 300 Hz, the coherence between the two fluctuating fields is the strongest.

The material presented in this paper is new and has been excerpted from the author's dissertation. In fact, the information concerning the effects of the value of the velocity ratio has important implications as far as proper testing procedures for a USB design.

The question that immediately comes to mind is the value of testing without the presence of a coflowing secondary stream. In fact, the jet may not stay attached to the airfoil's upper surface.

DATA DESCRIPTION

Documentation of the effects of the value of the velocity ratio, λ_j, on the width and decay of the centerline velocity for the three respective mean flow fields is presented.

Turbulent intensity is the ratio of the rms turbulent velocity fluctuations to a reference mean velocity. In this investigation, turbulence level is nondimensionalized by excess centerline mean velocity at the exit plane of the nozzle. The turbulent intensities are corrected for ambiguity noise using the method of Morton (ref. 6) and shown for various downstream positions.

The longitudinal integral time scale is defined as follows:

$$T_1 = \int_0^{t^*} \overline{u(t)u(t + t')dt'}$$

where t^* is the time at which the integral first reaches the value of zero (ref. 7).

Additional information concerning the turbulence structure of the various flow fields can be gained from measurements of the pressure fluctuations at both the wall and in the turbulent jet and correlating those signals with fluctuating turbulent velocities in the potential core and in the shearing region.

Pressures are measured either at surface ports located on the flap or plate or by a pressure probe in the flow. In either case, the following space-time correlation are measured:

$$R_{pa}(\vec{x},\vec{\xi},t,\tau) = \frac{P(x,t)u(\vec{x} + \vec{\xi},t + \tau)}{[p(\vec{x},t)^2]^{1/2}[u(\vec{x} + \vec{\xi},t + \tau)^2]^{1/2}}$$

where $\vec{\xi}$ is the position of the velocity "probe," measured relative to the pressure probe and p is the static pressure measured at the wall or in the flow field.

The primary focus of this segment of the experimental investigation is to determine the relationship between the pressure and the velocity fields. To show the dependence between the two fields, the coherence is plotted for various pressure and velocity monitoring locations. Coherence, which can be considered a correlation coefficient which varies with frequency, is defined as follows:

$$\delta_{12}^2 = \frac{|G_{12}|^2}{G_{11}G_{22}}$$

where G_{11}, G_{12} are the Fourier Transforms of the individual autocorrelation functions and G_{12} is the Fourier Transform of the cross-correlation function.

REFERENCES

1. Catalano, G. D.; Morton, J. B.; and Humphris, R. R.: Experimental Investigation of an Axisymmetric Jet in a Coflowing Airstream. AIAA J., vol. 14, no. 9, 1976, pp. 1157-1158.

2. Catalano, G. D.; Morton, J. B.; and Humphris, R. R.: An Experimental Investigation of a Three Dimensional Wall Jet. AIAA J., vol. 15, no. 8, 1977, pp. 1146-1151.

3. Morton, J. B.; Catalano, G. D.; and Humphris, R. R.: Some Two-Point Statistical Properties of a Three-Dimensional Wall Jet. AIAA J., vol. 16, no. 7, July 1978.

4. Schroeder, J. C.: Development of Experimental Techniques for Investigation of Unsteady Pressures Behind a Cold Model Jet. Master's Thesis, Univ. of Virginia, 1976.

5. Herling, W. W.: The Development of an Experimental Facility for the Investigation of Scaling Effects. Master's Thesis, Univ. of Virginia, 1976.

6. Morton, J. B.: Experimental Measurements of Ambiguity Noise in a Laser Anemometer. J. Phys. E, vol. 6, no. 4, 1973.

7. Monin, A. S.; and Yaglom, A. M.: Statistical Fluid Mechanics. Vol. 1. MIT Press, 1971.

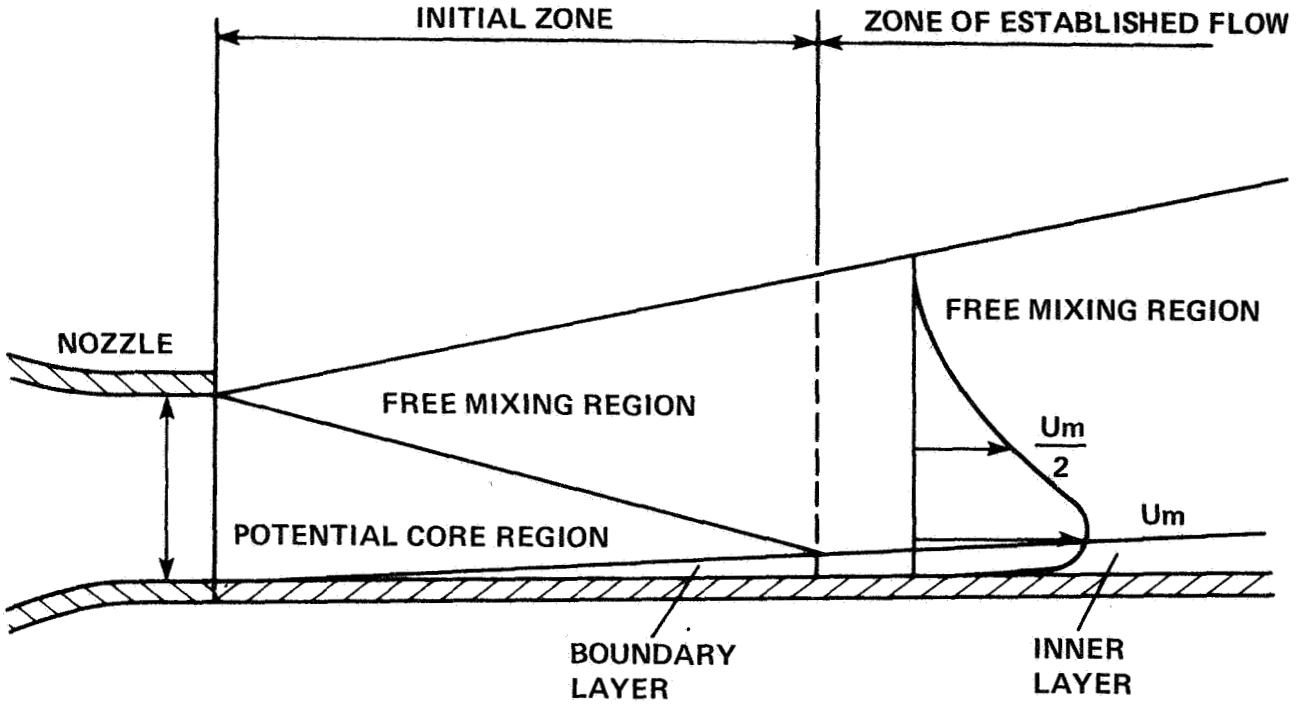

Figure 1.- Schematic of a wall jet.

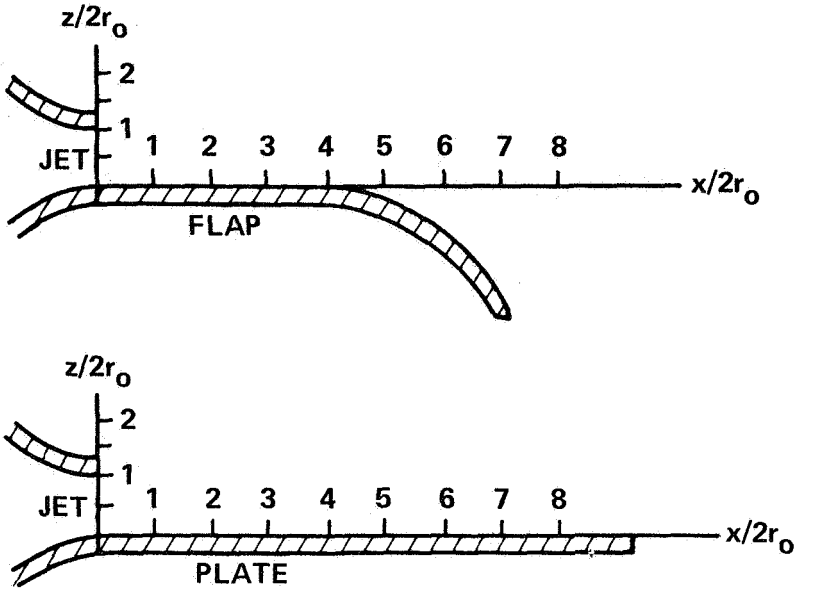

(a) Flow configurations.

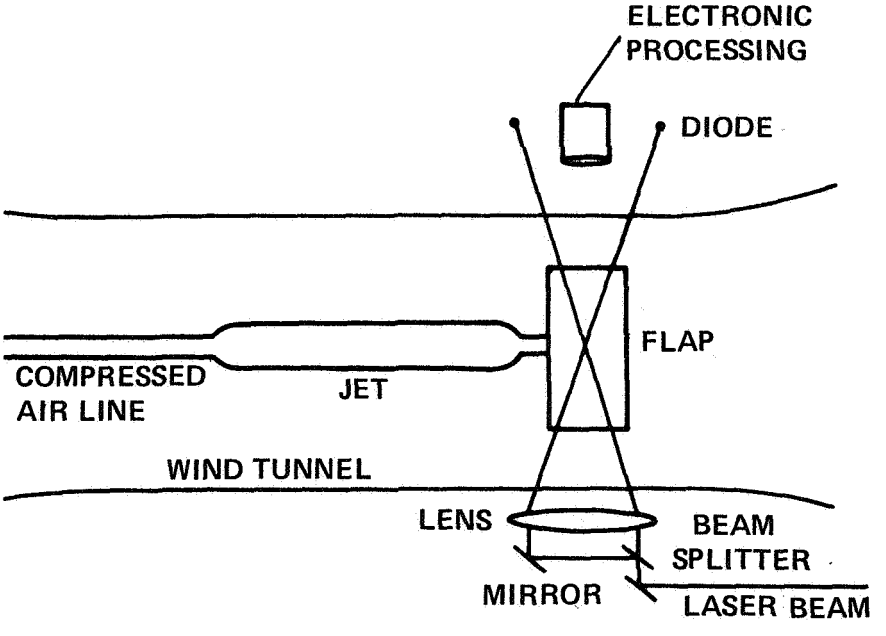

(b) Schematic of laboratory setup.

Figure 2.- Text configurations.

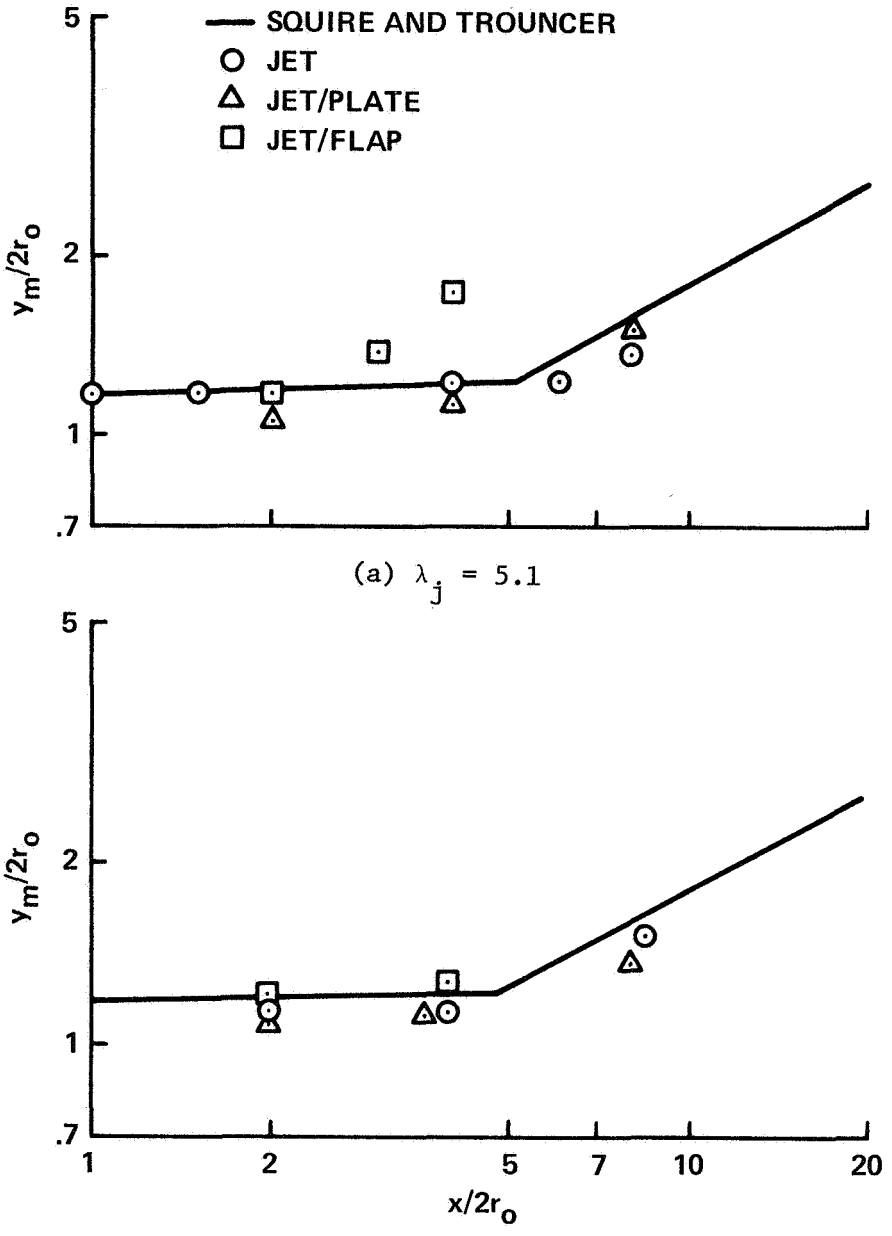

(a) $\lambda_j = 5.1$

(b) $\lambda_j = 10.88$

Figure 3.- Growth of mixing width.

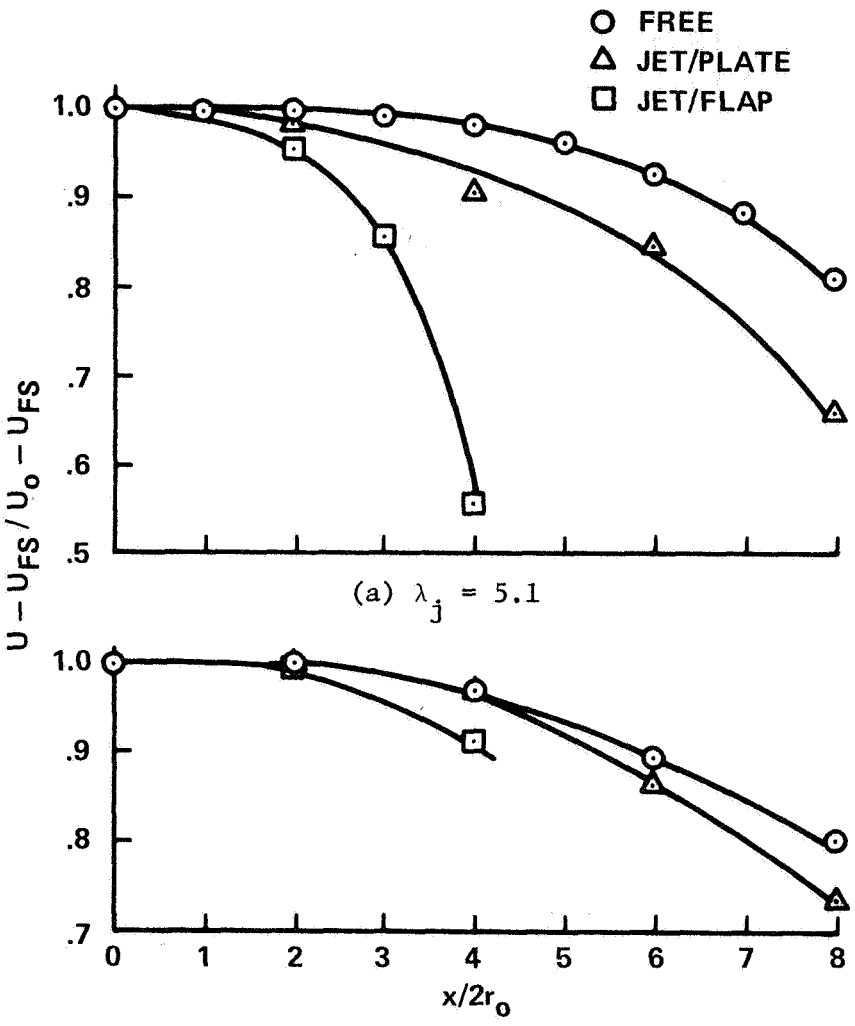

(b) λ_j = 10.88

Figure 4.- Decay of centerline mean velocity, $z/2r_o$ = 0.5.

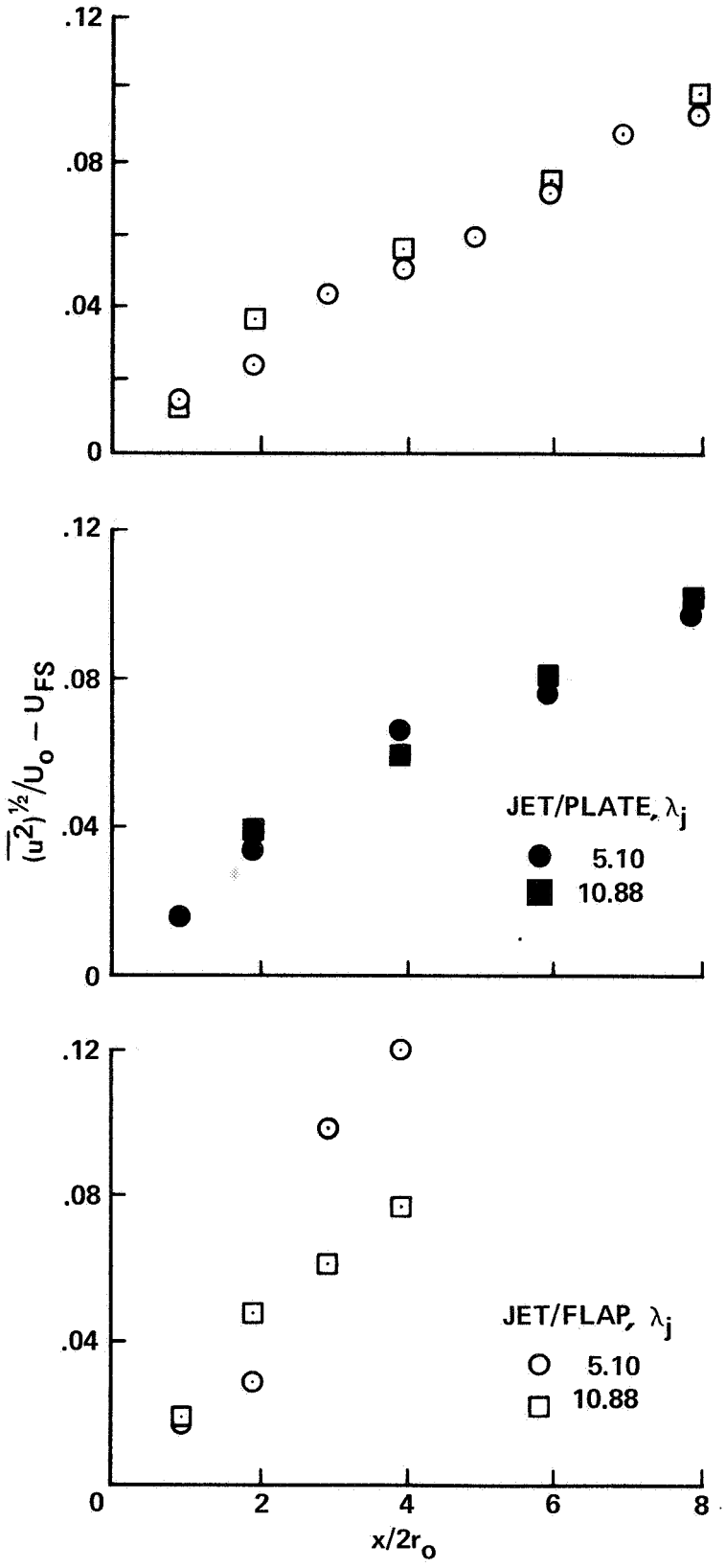

Figure 5.- Growth of turbulent intensity, $(\overline{u^2})^{1/2}$, at centerline.

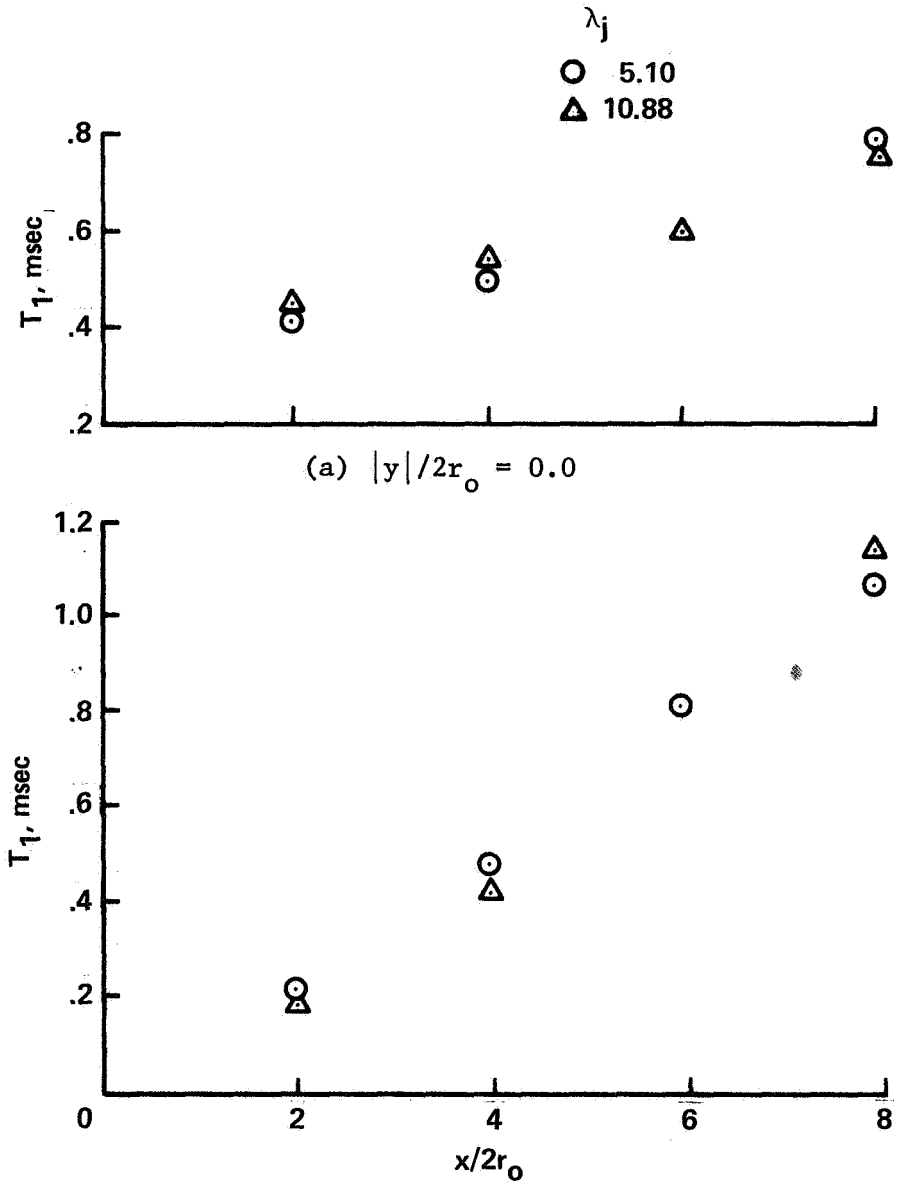

Figure 6.- Development of integral time scale for jet, $z/2r_o$ = 0.5.

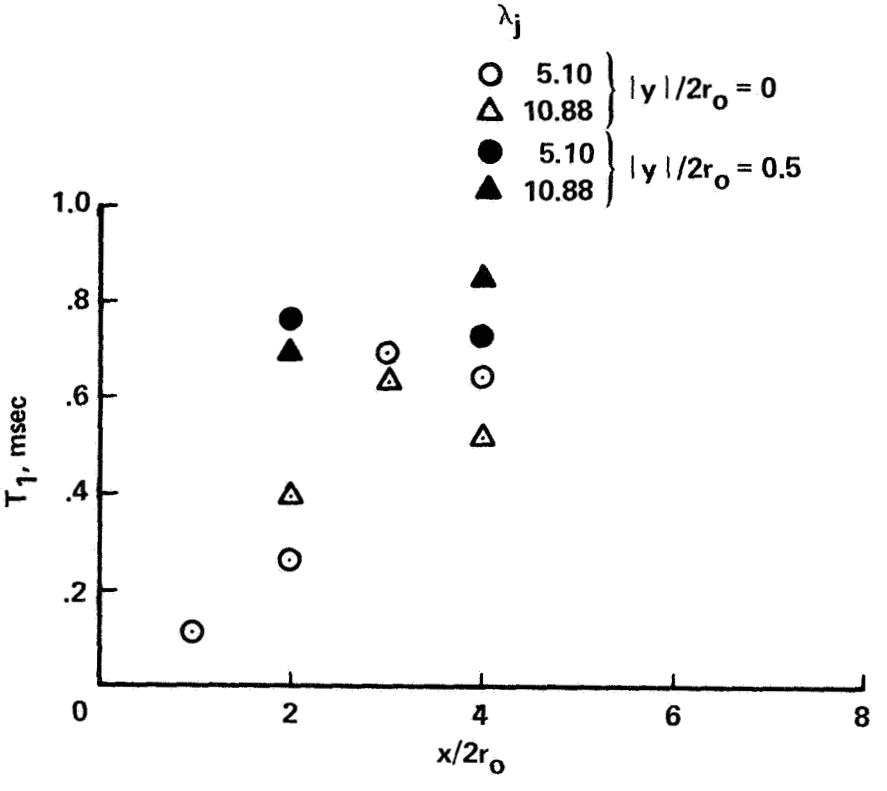

Figure 7.- Development of integral time scale for jet/flap, $z/2r_o = 0.5$.

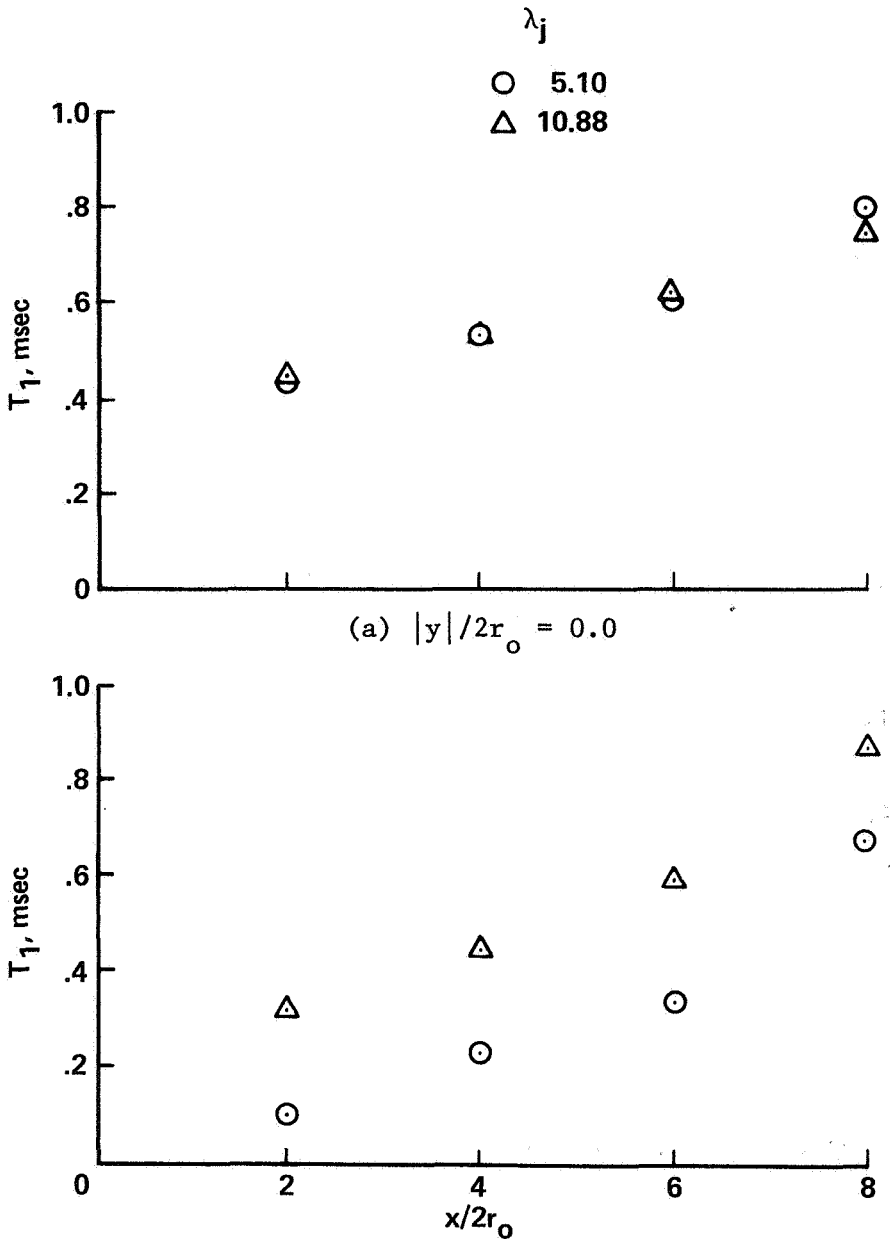

Figure 8.- Development of integral scale for jet/plane, $z/2r_o$ = 0.5.

CONSIDERATION OF SOME CRITICAL EJECTOR PROBLEMS

by

Morton Alperin and Jiunn-Jenq Wu

JUNE 1978

FLIGHT DYNAMICS RESEARCH CORPORATION
15809 Stagg Street, Van Nuys, California 91406

CONSIDERATION OF SOME CRITICAL EJECTOR PROBLEMS

M. Alperin and J.J. Wu
Flight Dynamics Research Corporation

INTRODUCTION

Recent research and development related to ejector thrust augmentation for V/STOL applications has been directed towards either a) methods for the achievement of improved mixing, or, b) attempts to minimize ejector size by the design of wide angle diffusers.

While FDRC has been concerned with these areas and has devoted a major portion of its effort to diffuser as well as simple and effective primary nozzle design, there has also been considerable effort to investigate other aspects of ejector design and application, including,

1. Three dimensional effects
2. Cross flow effects
3. Ejector as a propulsion device (underwater, subsonic, supersonic).

It has been shown that in a practical ejector, even one as small as the jet diffuser ejector, the mixing process, using a segmented slot nozzle, can provide sufficient mixing to permit performance equivalent to complete mixing, provided the effective diffuser area ratio is increased to compensate for the incomplete mixing. This increase of the effective diffuser area ratio is accomplished by a jet-diffuser.

The design of an efficient jet-diffuser, however, must consider the three-dimensionality of the flow field and provide a flow uniformity around the entire periphery of the ejector exit.

The influence of cross flow due to translation normal to the thrust vector has been investigated in the FDRC wind tunnel. The results indicate a very large increment of thrust (or lift) resulting from the ejector induced flow over the external fairings.

Work on the propulsive ejector, although of great interest, will not be discussed here.

LIST OF SYMBOLS

A_2	Area of ejector throat
a_∞	Area of primary jet after lossless expansion to ambient pressure
a_1	Area of primary jet after expansion to p_1, with loss corresponding to η_N
C_{di}	Inlet drag coefficient = $(P_{oe} - P_{o1})/[(\rho/2)U_1^2]$
C_F	Coefficient of skin friction based on A_2 and $\overline{U}_2$
C_f	Coefficient of skin friction based on two-dimensional wetted surface
C_{fdj}	Coefficient of skin friction for diffuser jet (jet-diffuser ejector)
ℓ_T	Mixing duct + diffuser length
$\dot{m}$	Mass flow rate
P_o	Stagnation pressure (gage) ($P_{op} = P_{od}$)
U	Velocity
U'	Perturbation velocity
$\overline{U}$	Average velocity
V	Jet velocity
s_∞	Area of diffuser jet after lossless expansion to ambient pressure
X	Section width of a two-dimensional ejector
$\tilde{X}$	Effective section width of a two-dimensional ejector
α	Inlet area ratio = X_2/a_1
δ	Diffuser area ratio = X_3/X_2
δ^*	Effective diffuser area ratio (solid diffuser ejector) = $\tilde{X}_3/X_2$
η_{dj}	Efficiency of jet diffuser
η_N	Primary nozzle thrust efficiency = $V_{p\infty}/[(V_{p\infty})_{lossless}]$
λ	Non-dimensional velocity = U/V_{pl}
ρ	Mass density
ϕ	Thrust augmentation

SUBSCRIPTS

c	Core flow
d	Diffuser jet
e	Intake of induced flow
p	Primary jet, or intake of primary flow
∞	Free stream
1,2,3,4,J	Section index, see Figure 1

MIXING

The integration of ejectors with modern airframe designs, particularly for high speed aircraft, demands the development of small ejectors. As ejector size becomes smaller, the adequacy of mixing within the ejector duct becomes questionable. In a solid diffuser ejector, the flow returns to ambient pressure at or before the end of the solid surfaces. Thus mixing must be sufficiently complete within the ejector duct, to avoid performance penalties. The influence of incomplete mixing upon ejector performance is therefore an important area for investigation.

In a jet diffuser ejector, the flow does not return to ambient pressure for a considerable distance downstream of the solid surfaces of the diffuser. Thus the region available for effective mixing is considerably larger than that represented by solid surfaces, but the length of the extension of the flow pattern, beyond the solid surfaces, depends upon the adequacy of the design.

Three-dimensional effects in a jet-diffuser ejector of finite aspect ratio have been shown to limit the extent of the jet diffuser, but recent work in this area (to be discussed later) has improved this three-dimensional limitation.

Returning to the question of "How much mixing is adequate?", we have shown that, under the assumption that with incomplete mixing the velocity distribution at the diffuser exit can be described by the relationship

$$U_3 = \bar{U}_3 + U_3' \qquad (1)$$

where $|U_3'/\bar{U}_3| << 1.0$, (Figure 1).

Other parameters, and loss coefficients utilized in the analysis, are also illustrated on Figure 1.

Then with the assumption of incomplete mixing, the thrust augmentation ϕ of a stationary solid diffuser ejector in an incompressible fluid can be expressed as

$$\phi = \frac{\text{Ejector Thrust}}{\text{Reference Jet Thrust}} \tag{2}$$

$$= \eta_N \frac{\rho \int U_3^2 d\tilde{X}_3}{\text{Primary Jet Thrust at Ambient Pressure}} \tag{3}$$

$$= \eta_N (\dot{m}_c/\dot{m}_p) \left\{ \frac{\bar{U}_3 [1 + \overline{U_3'^2}/\bar{U}_3^2]}{V_{p\infty}} \right\} \tag{4}$$

$$= \eta_N \, (\dot{m}_c/\dot{m}_p)^2 \left\{ \frac{1 + \overline{U_3'^2}/\bar{U}_3^2}{\tilde{X}_3/X_2} \right\} \frac{1}{\alpha \sqrt{1 - (1 + C_{di})\lambda_1^2}} \tag{5}$$

$$= \eta_N \, [1+(\alpha-1)\lambda_1] \sqrt{\frac{1}{[1-(1+C_{di})\lambda_1^2]} \left\{ \frac{1-\lambda_1^2}{\alpha^2} \left[1 + \frac{2(\alpha-1)}{1+\lambda_1} \right] - C_{di}\lambda_1^2 - C_F \left[\frac{1+(\alpha-1)\lambda_1}{\alpha} \right]^2 \right\}} \tag{6}$$

where

$$\lambda_1 = U_1/V_{p1} = \frac{-B + \sqrt{B^2 - AC}}{A} \tag{7}$$

and

$$A = (\alpha - 1)^2 + D^2 + \alpha^2 D^2 \left[C_{di} + \left(\frac{\alpha - 1}{\alpha} \right)^2 C_F \right] \tag{8}$$

$$B = (\alpha - 1) \left[D^2 (1 + C_F) + 1 \right] \tag{9}$$

$$C = 1 - D^2 \left[(2\alpha - 1) - C_F \right] \tag{10}$$

$$D = \frac{\tilde{X}_3/X_2}{1 + (\overline{U_3'^2}/\bar{U}_3^2)} \tag{11}$$

$$\alpha = X_2/a_1 \tag{12}$$

$$C_F = 2C_f \times [(\text{Mixing Duct} + \text{Diffuser Length})/\text{Throat Width } (X_2)] \tag{13}$$

Reference Jet Thrust = Thrust of lossless free jet having mass flow and power equal to those of ejector's primary jet.

It is well known that in a non-separating uniform flow analysis, the thrust augmentation increases with increasing values of X_3/X_2.

As a result of the above analysis, it is shown that the parameter $[\tilde{X}_3/X_2]/[1 + (\overline{U_3'^2}/\bar{U}_3^2)]$ can replace the diffuser area ratio (X_3/X_2) and $[\bar{U}_3/V_{pl}][1 + (\overline{U_3'^2}/\bar{U}_3^2)]$ replaces U_3/V_{pl}. With these substitutions, the thrust augmentation for the non-uniform case is identical to the thrust augmentation for the uniform flow analysis. Therefore, if the mixing is incomplete $(\overline{U_3'^2}/\bar{U}_3^2) > 0$, the parameter $[\tilde{X}_3/X_2]/[1 + (\overline{U_3'^2}/\bar{U}_3^2)]$ can be increased by increasing $\tilde{X}_3$. In other words, an increase in the effective diffuser area ratio can compensate for the lack of complete mixing. Detailed analyses are presented in a forthcoming report on work sponsored by ONR (Reference 1).

One simple method for evaluation of the non-uniformity parameter $\overline{U_3'^2}/\bar{U}_3^2$ consists of the use of ejector tests where no separation exists in the diffuser. Then $\delta^* = \delta$ and the parameter $\delta^*/[1 + (\overline{U_3'^2}/\bar{U}_3^2)]$ and C_F can be determined from Equations 5 and 6 with the knowledge of ϕ, α, λ_1, η_N, and C_{di}, for a stationary ejector, since $\dot{m}_c/\dot{m}_p = 1 + (\alpha - 1)\lambda_1$. Since $\delta^* = \delta$, for non-separating ejectors, the non-uniformity parameter can be evaluated from the identity

$$\overline{U_3'^2}/\bar{U}_3^2 = \left[\frac{1 + \overline{U_3'^2}/\bar{U}_3^2}{\delta^*}\right]\cdot\delta - 1$$

where

δ = geometric diffuser area ratio X_3/X_2

δ^* = effective diffuser area ratio $\tilde{X}_3/X_2$

However, λ_1 $(= U_1/V_{pl})$ is a quantity which is difficult to measure accurately, but can be determined from Equation 6 if C_f, and thus C_F, are assumed.

Using Quinn's data (Reference 2), and his estimates of the loss coefficients, it was determined that for all the ARL ejectors reported in Reference 2, there is a maximum value of C_f which satisfies the physical restriction that

$$(\delta/\delta^*)[1 + (\overline{U_3'^2}/\bar{U}_3^2)] \geq 1$$

This value of C_f ia about 0.0057. (After correcting for the aspect ratio effect, the coefficient of skin friction based on the wetted surface area becomes 0.0049, which is the typical value for a flat plate turbulent boundary layer over a wide range of Reynolds Number near 10^6). Using the value of $C_f = 0.0057$, the quantitiy $(\delta/\delta^*)[1 + (\overline{u_3'^2}/\bar{U}_3^2)]$ of the ARL ejectors are calculated and summarized on the upper chart of Figure 2. The average value of $(\delta/\delta^*)[1 + (\overline{u_3'^2}/\bar{U}_3^2)]$ for Configuration F is about 1.05. This value appears to be adequate for the low diffuser area ratio range of all other Configurations under consideration. Therefore, for non-separating ARL ejectors, $(\delta = \delta^*)$, the non-uniformity parameter, $\overline{u_3'^2}/\bar{U}_3^2$, is about 0.05.

Using this value, the theory and experiments agree very closely, as illustrated on Figure 2. However, the assumption that $\delta^* = \delta$ breaks down for Configuration D near $\delta = 1.4$, which indicates that flow separation occurred at diffuser area ratios larger than 1.4 and that $\delta^* < \delta$.

These considerations indicate that for fixed values of the loss coefficients, an increase of the effective diffuser area ratio can compensate for the degradation due to incomplete mixing. Attempts to improve the mixing of primary and induced flows frequently involve an increase in other losses and therefore do not result in improved performance. For example, as shown by Equation 6, a decrease in nozzle efficiency (η_N) or an increase in C_{di} or C_F (or ejector length) always results in smaller thrust augmentation as might be expected. An increase of δ^* however, can result in improved performance as indicated by Bevilaqua (Reference 3) for the Hypermixing Nozzle.

In the light of the above discussion and Bevilaqua, it is apparent that the Hypermixing Nozzle, developed in the Air Force Aerospace Research Laboratories, achieved its performance improvement at large values of the diffuser area ratio as a result of improved diffuser performance as well as a result of improved mixing. This is made apparent by the fact, reported in Reference 3, that the performance improvement was achieved at large diffuser area ratios.

At smaller diffuser area ratios (where the diffuser was efficient), hyper-mixing resulted in a performance degradation, due to increased inlet drag and decreased nozzle efficiency.

It must therefore be concluded that the search for improvement in mixing must be directed towards those methods which decrease the loss parameters, and that the development of a high performance, short, wide angle diffuser is of greater significance than the recent emphasis on improved mixing.

The jet-diffuser ejector is an example of an ejector designed with major emphasis on the diffusion process, and its large performance/size ratio indicates the practicality of the above remarks.

JET-DIFFUSION CONCEPT

The concept of jet-diffusion is basically an extension of the concepts of boundary layer control by the use of blowing jets and of the jet flap to provide additional diffusion beyond that of the solid surfaces. Blowing jets have been used to delay separation in large area ratio solid diffusers with some degree of success. By blowing a jet having a higher stagnation pressure than the ambient pressure in the diffuser, separation can be delayed to the point where the effective diffuser area ratio is almost as large as the geometric area ratio of the solid surface.

Using energized fluid for the avoidance of separation is a costly process, since the momentum of the boundary layer control fluid must be considered in the evaluation of ejector performance. Thus, unless extreme care is exercised in the design of the blowing jet system, the net effect can be more detrimental than that of the use of a smaller diffuser area ratio without boundary layer control.

Jet diffusion has the advantage over conventional blowing jet systems in that it has the potential for providing a diffuser area ratio larger than the geometric area ratio of the solid surfaces in addition to its capability for avoiding separation despite extremely large divergence angles of the solid surfaces.

A typical jet diffuser ejector developed under the U.S. Navy/Marine Corps STAMP (Small Tactical Aerial Mobility Platform) Program and tested at the Naval Air Propulsion Center is illustrated on Figure 3. This ejector was the result of an intensive development program aimed at its eventual use as the lifting, thrusting and controlling element of an apterous vehicle and details of its development program and its performance are described in Reference 4. It is of particular interest to note that, as shown on Figure 3, the ends of the ejector are flat, with a semi-circular end plate protruding beyond the solid diffuser

surfaces at the ends of the ejector as a means of providing two-dimensional flow in the diffuser. This protruding end plate, although somewhat undesirable from the viewpoint of ejector integration and drag characteristics was essential for the avoidance of some performance degradation associated with the use of flat ends within the diffuser.

Attempts to utilize diverging end bells resulted in local flow separation and performance penalties not acceptable under the STAMP Program and the design illustrated on Figure 3 was utilized as a quick-fix alternative, the advantage of which is best illustrated by perusal of the data presented on Figures 4 and 5.

To illustrate the characteristics of the flow within the region of jet diffusion, the pressure distribution in that region is plotted on Figure 4 with a large end plate extending from the end of the solid diffuser to a distance of 27.4 cm, 0.9 of the exit dimension. Obviously, the recovery of kinetic energy attributable to the jet diffuser is directly related to the pressure recovery in the region illustrated by the isobars. Removal or reduction in size of the end plate would seriously collapse the isobar pattern and cause a pressure increase throughout the ejector, with an accompanying reduction in secondary/primary flow ratio and thrust augmentation.

The influence of end plate size on the thrust augmentation of the ejector, with a diffuser area ratio of 3, is plotted on Figure 5. The semi-circular end plate (labelled STAMP) is shown to produce a thrust augmentation factor of 2.12 with the illustrated ejector and end plate configuration. Increasing the end plate to a 27.4 cm x 61 cm shape similar to that used in Figure 4 resulted in an increase of 3% or a thrust augmentation of 2.18. Decreasing the end plate size resulted in a more serious performance degradation, equivalent to a reduction of 14% in the thrust augmentation, to a value of 1.82. Thus it appears that the three-dimensional effects resulting from the requirement for finite ejector aspect ratio contribute significantly to the degradation of performance and that some effort to avoid the peripheral discontinuity of flow properties is required.

THREE-DIMENSIONAL EFFECTS

In an ideal jet-diffuser ejector, the mixing process can proceed for a considerable distance downstream of the end of the solid surfaces, since the core flow pressure remains below ambient. The extent of this region of sub-ambient pressure is limited, in a real three-dimensional ejector if the uniformity of the peripheral distribution of the diffuser jet properties are interrupted, as in the case of the STAMP ejector which had flat ends.

Recent work under NADC sponsorship (Reference 5) resulted in a method for diffuser design, using potential flow theory, which provided better continuity of the peripheral distribution of flow properties in the diffuser and eliminated the requirement for protruding end plates. The method utilized a three-dimensional closed (ring) vortex distribution of constant circulation whose shape could be adjusted to vary the maximum pressure gradient and/or length of the diffuser. The influence of various ring vortex shape parameters upon maximum pressure gradient distribution, diffuser length, and other practical limitations has been determined and a selection based upon these parameters was made.

The ejector designed by this method is illustrated on Figure 6, (designated as Model 0232) and as shown, the end plates required by the flat end design of the STAMP ejector have been eliminated.

The performance of this ejector whose diffuser is designed by the methods of potential flow is described in comparison to the performance of the STAMP ejector, in the following section.

GROUND EFFECTS

The influence of ground plane proximity to the ejector's exit plane on thrust augmentation is of importance for V/STOL applications of ejector thrusters. Since it appears likely that the influence of the ground plane is related to its influence upon the flow pattern within and around the ejector, and the effectiveness of the diffuser in particular, some limited investigations were conducted. This test set-up utilized a large 2.74 m x 3.05 m flat plate which could be moved with respect to the ejector, to vary its distance from the exit plane of the ejector.

The thrust augmentation of the STAMP and Model 0232 ejectors were measured over a range of distances from 0.5 to more than 5 meters between ejector exit plane and ground plane.

As indicated on Figure 7, the thrust augmentation of Model 0232 decreased less than 2% over most of the range of distances until the ejector was within 0.75 m from the ground plane. As the distance decreased to values smaller than 0.75 m, the mean thrust dropped rapidly. Preliminary observation of the Model 0232 ejector when the ground plane is at 0.56 m from its exit indicates that the flow within the ejector duct and near the diffuser exit is free from abnormality while violent unstable flow is developed on and near the ground plane.

The thrust augmentation of the STAMP ejector decreased by about 4% over most of the range of distances, compared to about 2% for Model 0232, as indicated on Figure 7. The decrease in thrust augmentation with distances smaller than 0.75 m was more pronounced for the equivalent STAMP Ejector with semi-circular end plates than for the Model 0232 ejector, as shown on Figure 7. This indicates that the Model 0232 is a more stable ejector than the STAMP ejector. This effect may depend upon the ejector's stagnation pressure and upon its geometric arrangement; more detailed tests are required for further understanding of this subject.

CROSS FLOW

V/STOL ejector applications require that the ejector provide a lift force varying from the all-up gross weight of the aircraft at take-off decreasing to zero at cruise.

When the ejector is producing thrust in a direction normal to the flight direction, there is no thrust decrement due to ram drag. The translational motion normal to the thrust vector may result in some drag and moment, due to the external influence of the jet on the aircraft surface pressure distribution. However, the momentum increment resulting from the ejector process is unaffected by the motion normal to the thrust, except for the indirect influence of inlet or diffuser flow distortion resulting from the cross flow.

Careful design of ejector external fairings can result in large additional thrust (or lift) forces on these fairings, attributable to the ejector. For example, tests on the STAMP ejector, reported in Reference 4, and shown on Figure 8, indicated large increases in thrust resulting from motion normal to the thrust. Thrust augmentation in excess of 2.6 were achieved at speeds of 60 ft/sec, with a small fairing.

As indicated, the phenomenon is related to the stagnation pressure of the ejector jets, and tests were performed at relatively low pressure. Increasing stagnation pressure delays the stall (as indicated) and further effort is required to determine the continuity of the trend indicated.

REFERENCES

1. Alperin, M., and Wu, J.J., "Underwater Jet-Diffuser Ejector Propulsion, Real Fluid Effects", Flight Dynamics Research Corporation, August 1978.

2. Quinn, B., "Recent Developments in Large Area Ratio Thrust Augmentors", AIAA Paper No. 72-1174, 1972.

3. Bevilaqua, P.M., "Evaluation of Hypermixing for Thrust Augmenting Ejectors", Journal of Aircraft, June 1974.

4. Alperin, M., Wu, J.J., and Smith, Ch.A., "The Alperin Jet-Diffuser Ejector (AJDE) Development, Testing and Performance Verification Report", Feb. 1976, Flight Dynamics Research Corporation, NWC Report No. 5853.

5. Alperin, M., and Wu, J.J., "End Wall and Corner Flow Improvements of the Rectangular Alperin Jet Diffuser Ejector", Flight Dynamics Research Corporation, NADC-77050-30, May 1978.

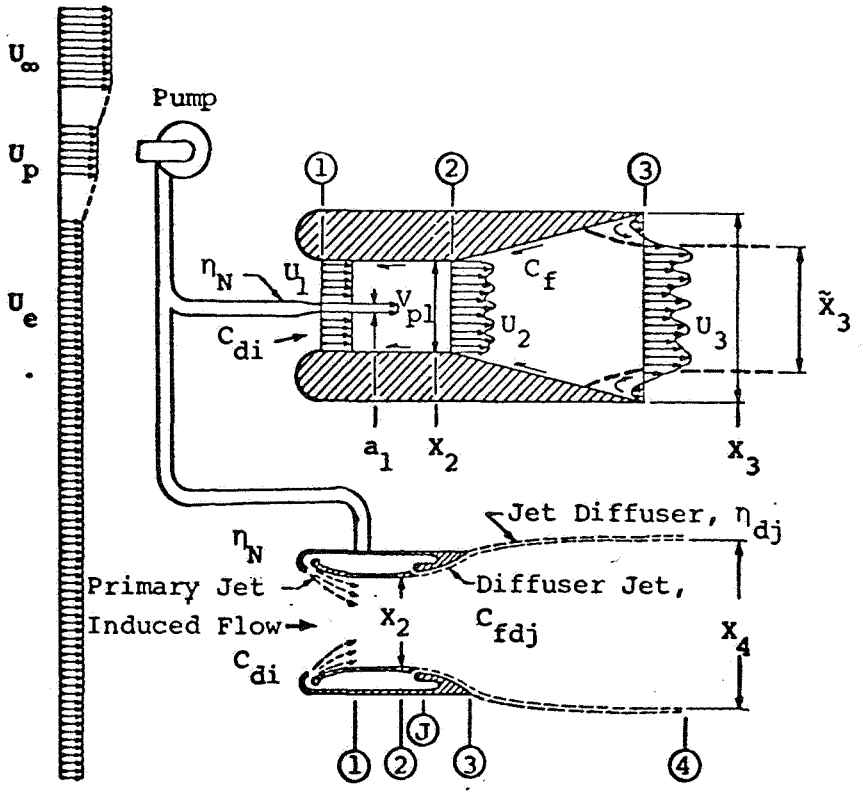

Solid Diffuser Ejector:

η_N = Primary Nozzle Thrust Efficiency

C_{di} = Inlet Drag Coefficient

C_f = Coefficient of Skin Friction

$$\frac{\tilde{X}_3/X_2}{1 + (\overline{U_3'^2}/\bar{U}_3^2)}$$ (Generalized Diffuser Area Ratio)

Jet-Diffuser Ejector:

η_N = Primary Nozzle Thrust Efficiency

C_{di} = Inlet Drag Coefficient

C_{fdj} = Coefficient of Skin Friction (Diffuser Jet)

η_{dj} = Efficiency of Jet Diffuser

$$= \frac{X_4/X_{4,ideal}}{1 + (\overline{U_4'^2}/\bar{U}_4^2)}$$

$\dot{m}_d/\dot{m}_p$ = Diffuser Jet/Primary Jet Mass Flow Ratio

Figure 1.- Basic parameters.

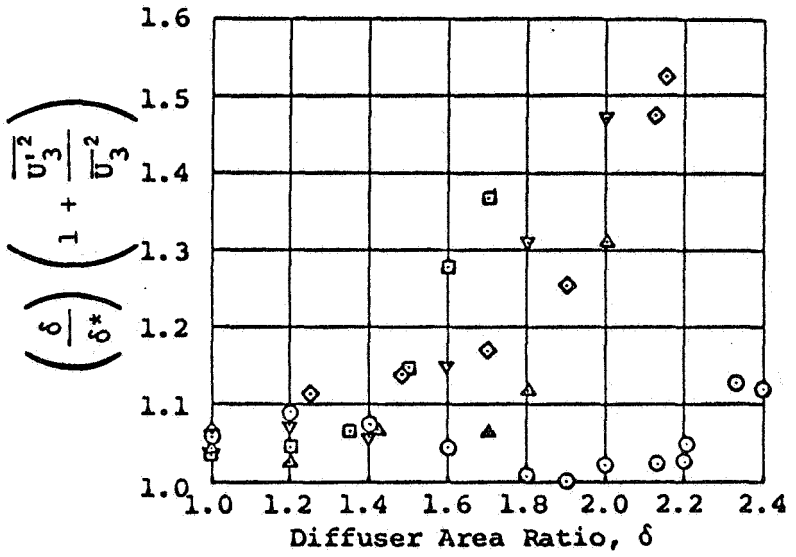

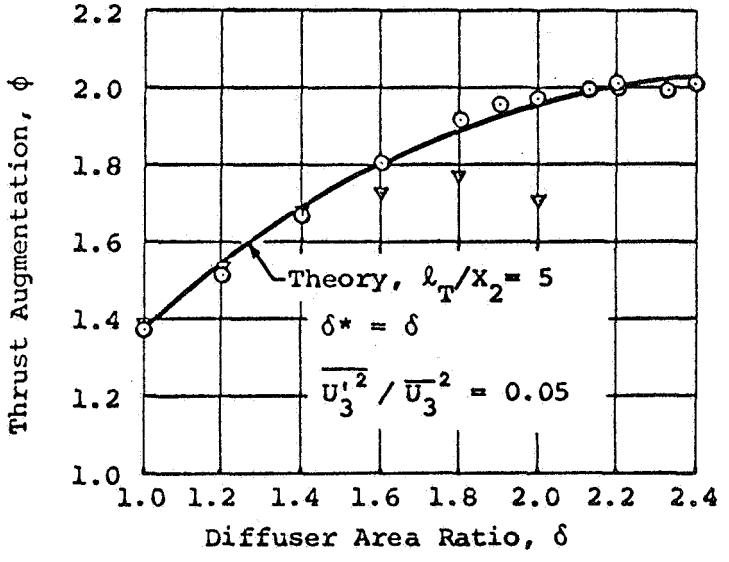

α = 25.3; η_N = 0.96; C_{di} = 0.025

C_f = 0.0057 (assumed)

Configuration	Symbol	ℓ_T/X_2
A	△	4.525
B	⊡	2.825
C	◇	2.8
D	▽	5
F	⊙	5

Figure 2.- Comparison of theory to ARL ejector experiments.

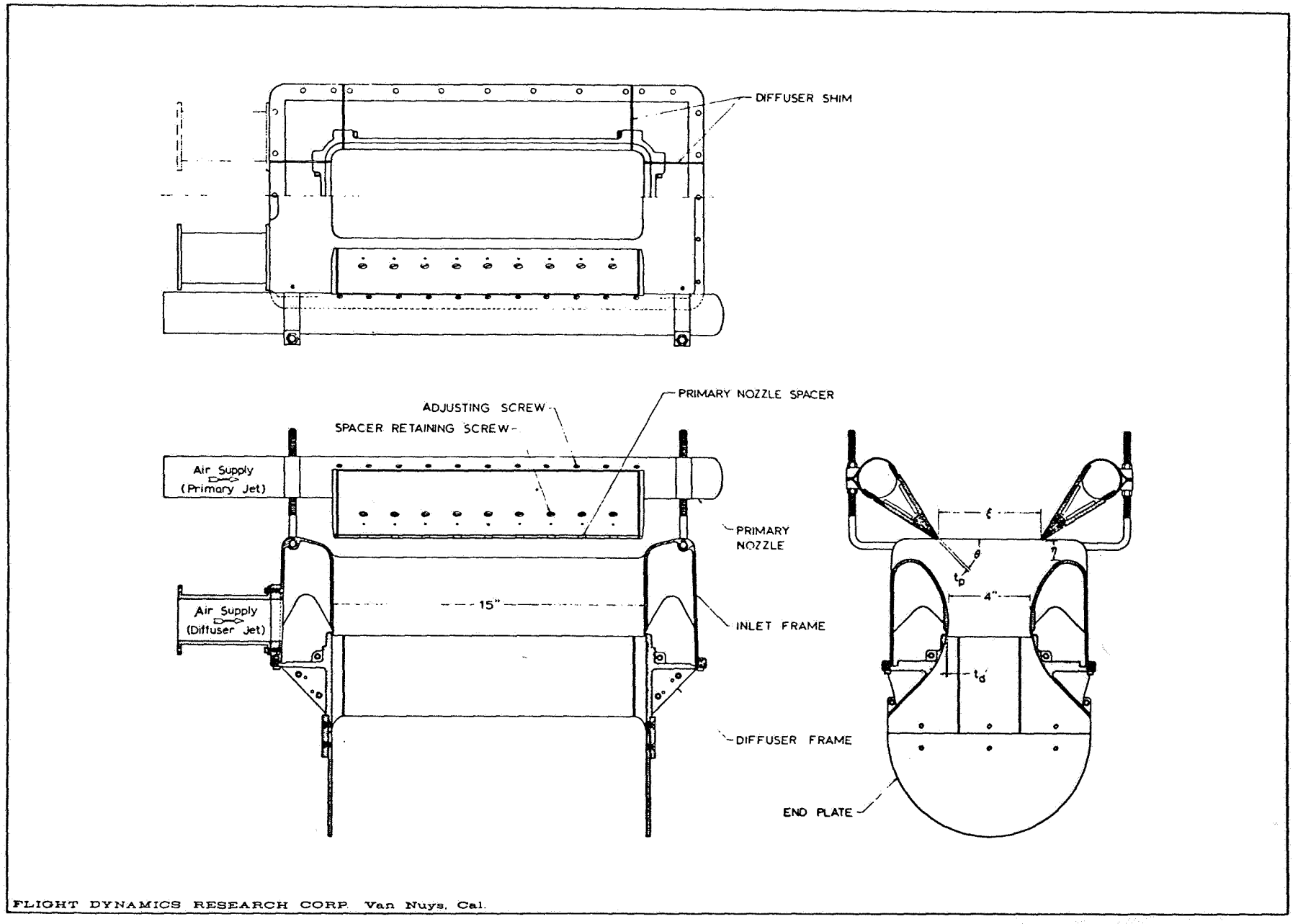

Figure 3.- Alperin jet-diffuser ejector, model 0542, 1976.

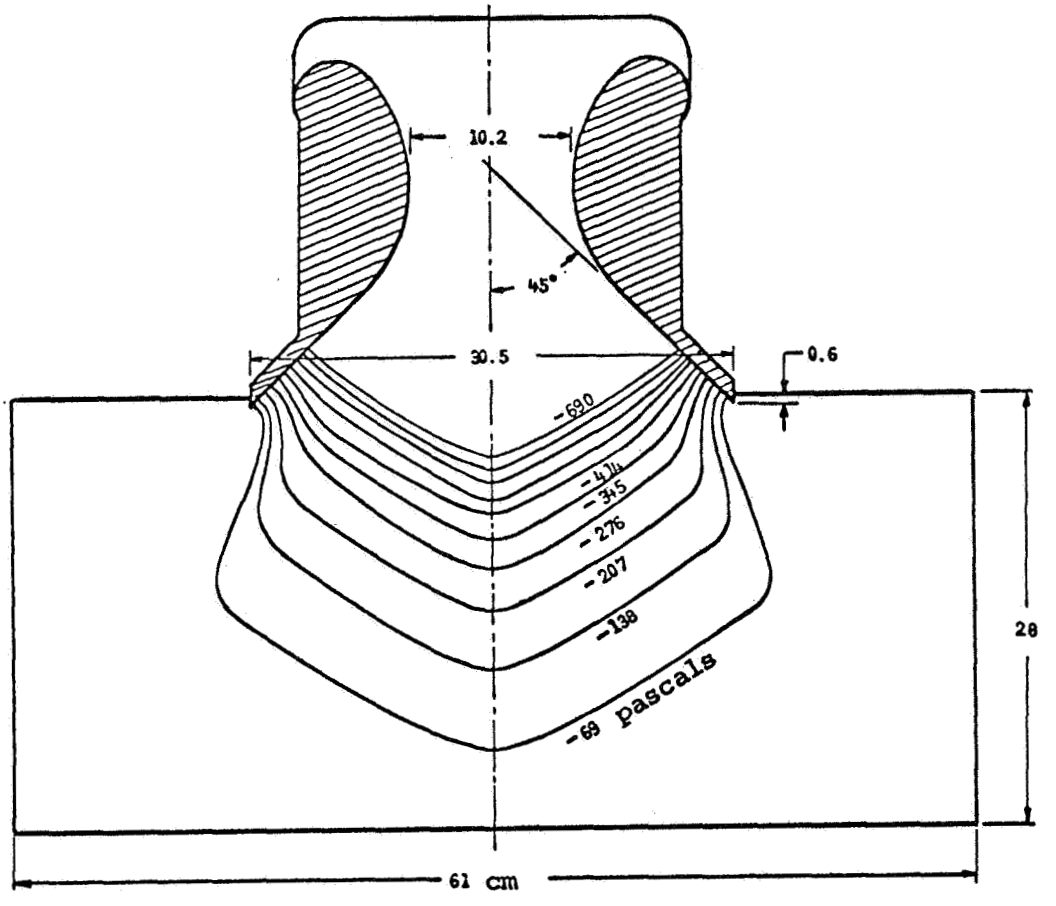

Figure 4.- Isobars on end plate of stamp AJDE ejector; P_o = 24.3 kilopascals, $A_2/(s_\infty + a_\infty)$ = 21.6, s_∞/a_∞ = 0.62.

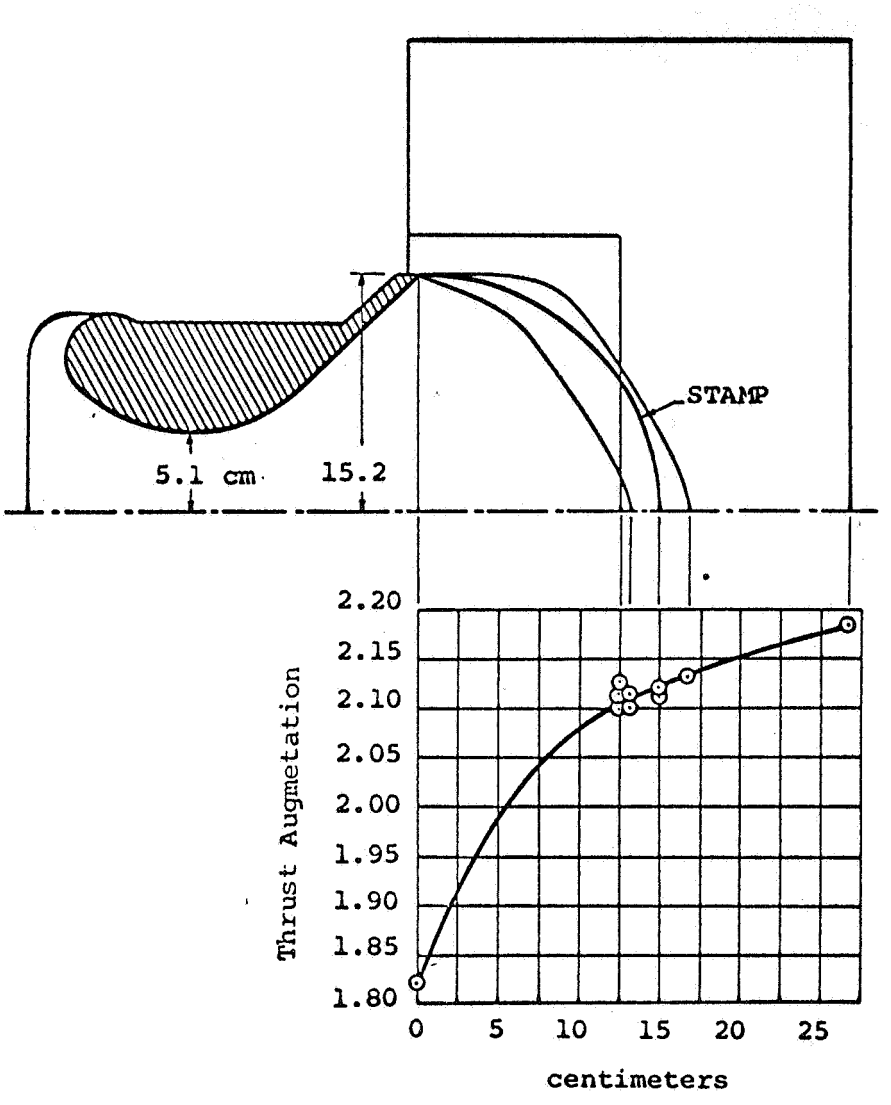

Figure 5.- End plate configuration and performance; P_o = 24.3 kilopascals, $A_2/(s_\infty + a_\infty)$ = 21.6, s_∞/a_∞ = 0.62.

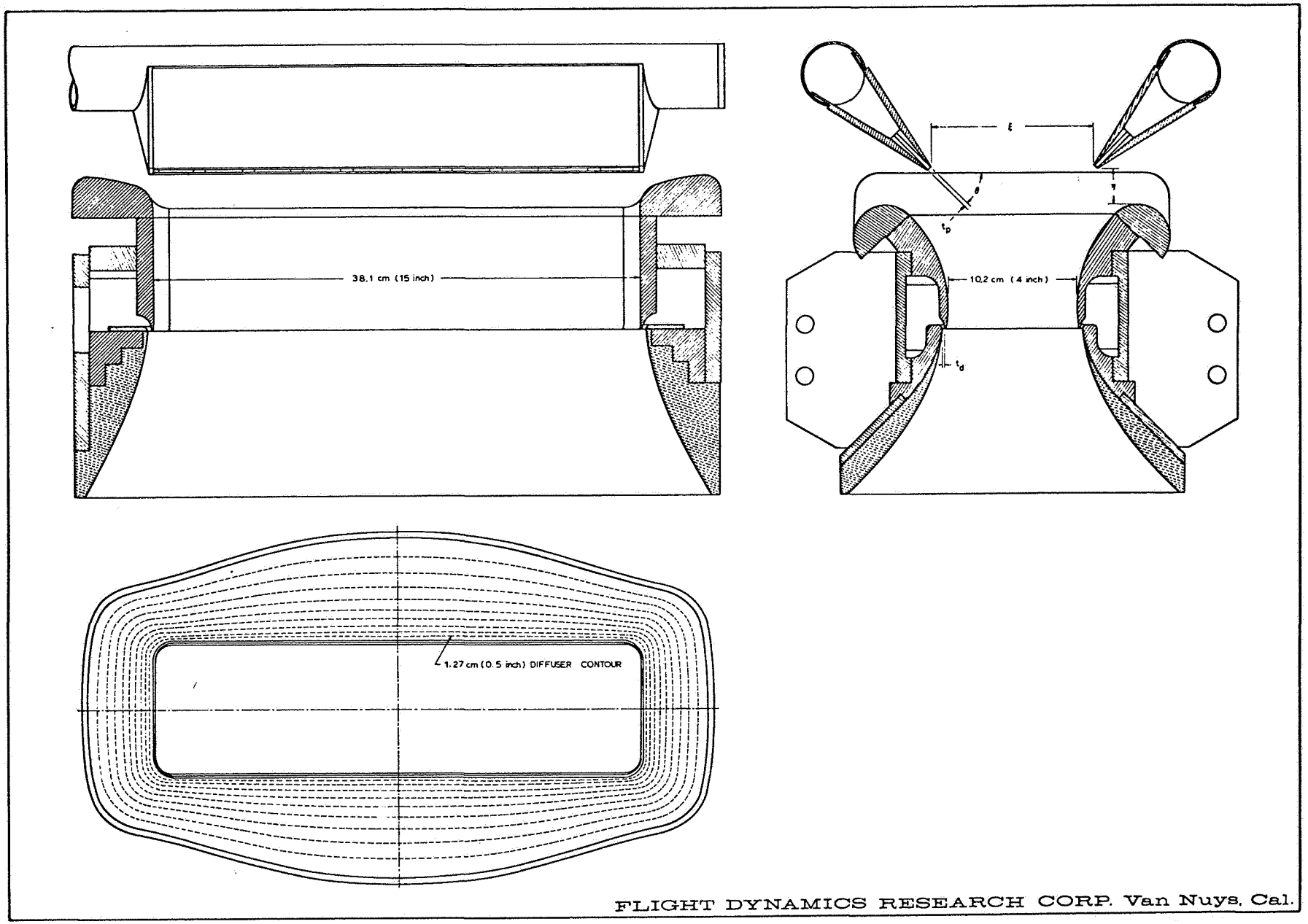

Figure 6.- Alperin jet-diffuser ejector, model 0232, 1978.

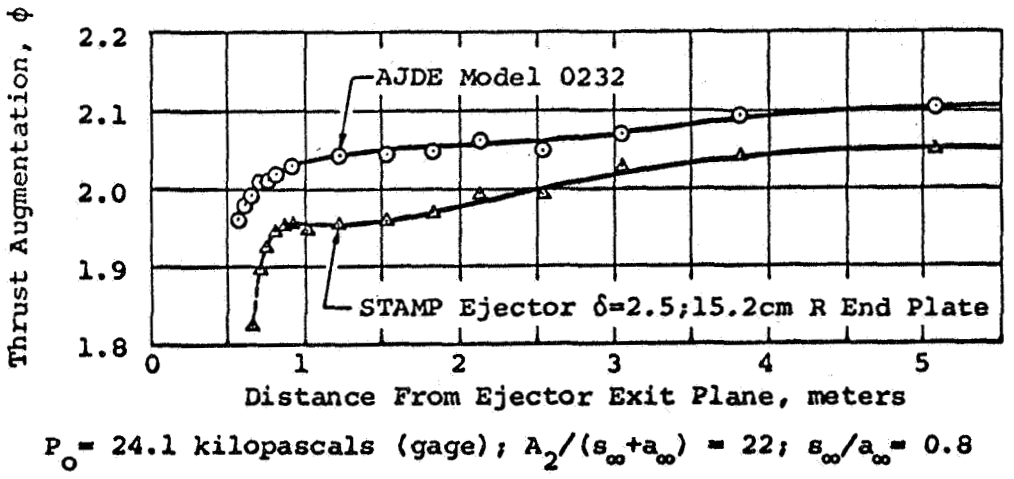

Figure 7.- Influence of ground plane on ejector performance.

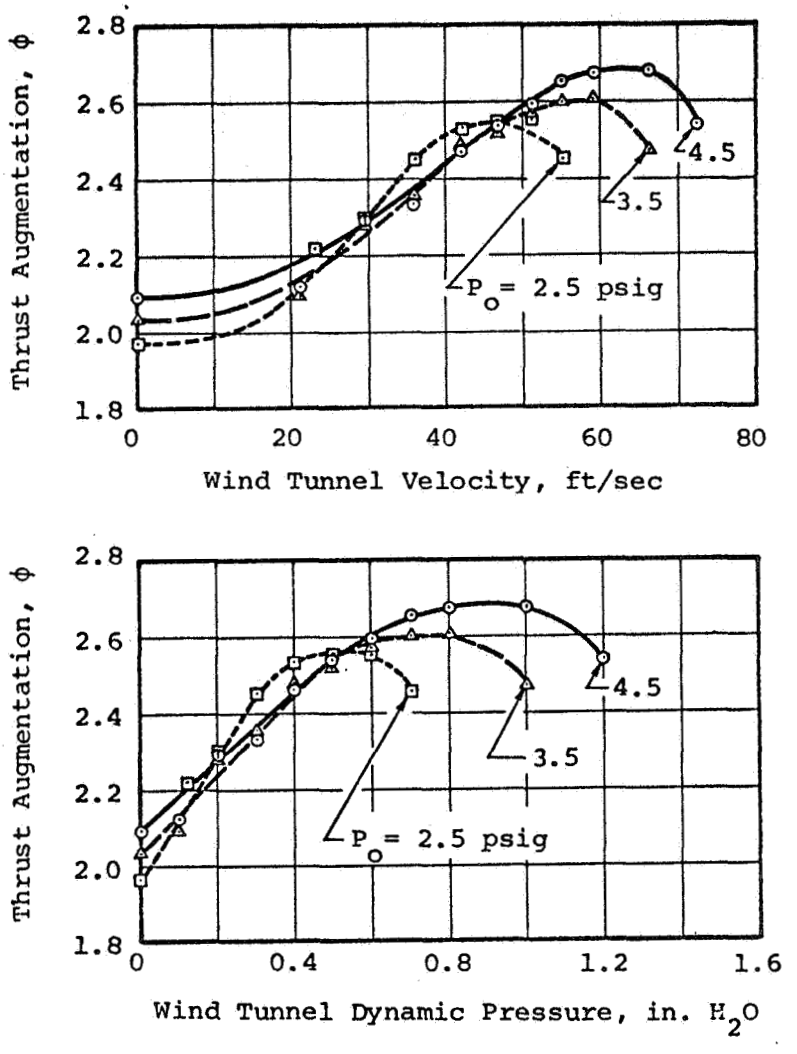

Figure 8.- Influence of translational motion and plenum pressure on AJDE performance.

COANNULAR SUPERSONIC EJECTOR NOZZLES

by

Allan R. Bishop

Lewis Research Center

The nozzles discussed in this papaer are associated with the transonic and supersonic propulsion work that is performed by the Aerodynamics Analysis Section at Lewis Research Center. There are two aspects of these nozzles which are different from most of the other nozzles discussed at this workshop: most of the flow field within the nozzle is supersonic, except for the initial secondary flow region; and the secondary mass flow is typically about five percent of the primary or core flow.

The original analysis for two stream ejectors was developed and programmed by Anderson, References 1 and 2. Two types of ejector nozzles were discussed in those references; a contoured shroud with no centerbody, and a cylindrical or contoured shroud with a conical plug centerbody. Schematics of these nozzles are shown in Figure 1. In the nozzle in 1a, the flow expansion is controlled by the shape of the shroud contour. In the nozzle in 1b, where the shroud is cylindrical, the expansion is controlled by the shape of the centerbody plug. The core flow is assumed to be inviscid and is treated with the method of characteristics. The secondary flow is treated one-dimensionally so that both the subsonic and supersonic portions can be analyzed in a rapid manner.

The analysis has two features to improve the accuracy of the performance calculations. A special calculation is made to get as realistic a sonic line as possible for this geometry, using an analysis developed by Brown, Reference 3. In addition, the mixing between the secondary and core flows is treated to account for entrainment of the secondary flow into core. Both of these phenomena directly affect the pressure distribution on the shroud and therefore the thrust that the nozzle produces. Figure 2 shows

the importance of using a realistic sonic line and a mixing analysis. At the top is the nozzle efficiency, in the middle is the stream thrust, and at the bottom the ratio of secondary total pressure to core total pressure. All are plotted as a function of the ratio secondary to core corrected weight flow. The curves are the results from the analysis with various combinations of sonic lines and mixing. The symbols are data from an experiment at Lewis Research Center (Reference 4). The curve that is closest to the data is the analysis that includes both a realistic sonic line and mixing. The curve furthest from the data uses a uniform sonic line and no mixing.

There are two secondary flow regimes. For low secondary mass flow ratio, less than four percent of the core flow, the secondary stream is entirely mixed with the core, and the core flow impinges on the shroud and is recompressed. For secondary mass flow ratios greater than four percent the secondary flow accelerates and becomes supersonic, but maintains its identity as a separate layer along the shroud. These two regimes are illustrated in Figure 3.

The analysis assumes that at some point in the nozzle the entire flow is supersonic. The flow field is therefore independent of the exit pressure. Since the secondary total pressure ratio and mass flow ratio are not independent, the secondary mass flow ratio is taken as known and iterative calculations are made on the secondary total pressure ratio until a consistent value is obtained.

Recently, a number of ejector nozzles with two separate core streams have been proposed, particularly in connection with variable cycle engine designs. They consist of a core flow surrounded by a fan flow which is itself surrounded by a secondary cooling flow along the shroud surface. Figure 4 shows schematics of two typical designs, with 4a having a conical splitter between the core and fan flow and 4b having an isentropic splitter. Both have conical plug centerbodies.

In the updated analysis the fan and secondary flow interaction are treated as before. The core flow is assumed to be supersonic so that the method of characteristics can be used. The boundary between the fan and the core flows is determined by matching the static pressure across the interface. Typically, at the end of the splitter plate neither the static pressure nor the flow angle of the two streams will match, so that a shock wave will propagate into one or both streams. These shocks are not treated explicitly but as a compression wave in the method of characteristics. The effects of mixing of the fan and core streams is not included in the analysis.

Figure 5 is a visualization of the flow field in a typical three stream nozzle. The secondary flow occupies the gap near the shroud. The secondary mass flow ratio is four precent. In this plot a symbol is plotted at each grid point in the characteristic net, which highlights the expansion and compression regions. Note the end of the splitter, where a compression occurs in the fan flow and an expansion in the core flow due to a mismatch in the static pressure at this point.

Figure 6 is a similar plot for a three stream nozzle with an isentropic splitter. The matching of core and fan flows at the end of the splitter is much better, at least for this set of conditions.

There are several additions that could be made to the program to improve the accuracy of the calculations. Particularly important is a subroutine to generate better initial flow profiles for the sharply angled throat regions in these geometries. There is currently no simple way of producing the sonic line for an annular converging nozzle. Treating the shock waves more exactly and bridging some local subsonic bubbles would also enhance the capabilities of the program.

References

1. Anderson, Bernhard H.: Assessment of an Analytical Procedure for Predicting Supersonic Ejector Nozzle Performance. NASA TN D-7601, 1974.

2. Anderson, Bernhard H.: Computer Program for Calculating the Flow Field of Supersonic Ejector Nozzles. NASA TN D-7602, 1974.

3. Brown, Eugene F.: Compressible Flow Through Convergent Conical Nozzles with Emphasis on the Transonic Region. Ph.D. Thesis, University of Illinois, 1968.

4. Shrewsbury, George D., and Jones, John R.: Static Performance of an Auxiliary Inlet Ejector Nozzle for Supersonic Cruise Aircraft. NASA TMX-1653, 1968.

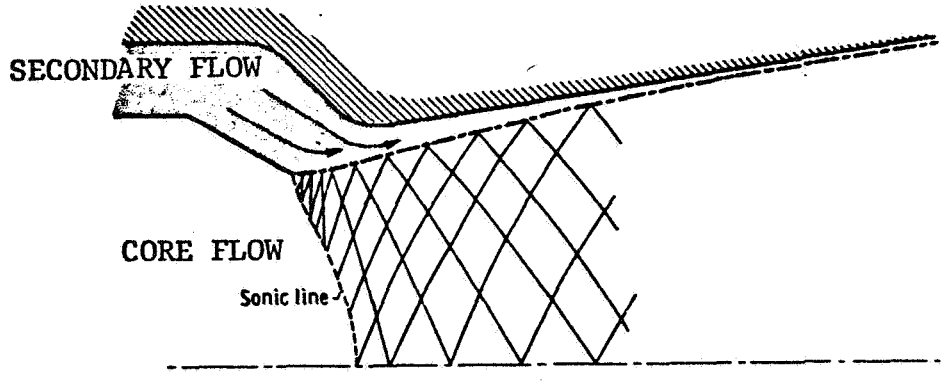

(a) Contoured shroud two-stream ejector.

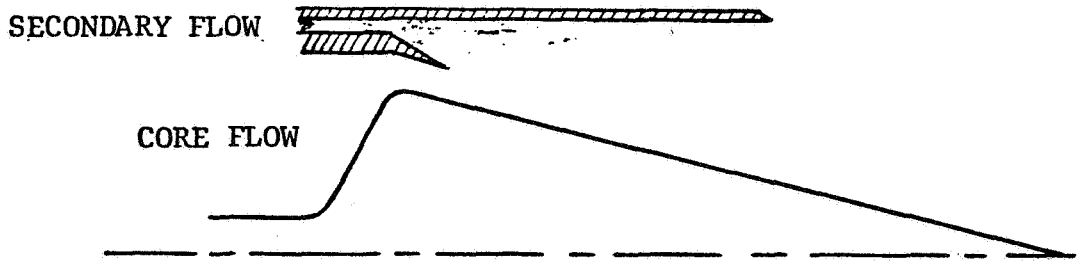

(b) Conical plug two-stream ejector.

Figure 1.- Schematic of typical two-stream ejector nozzles.

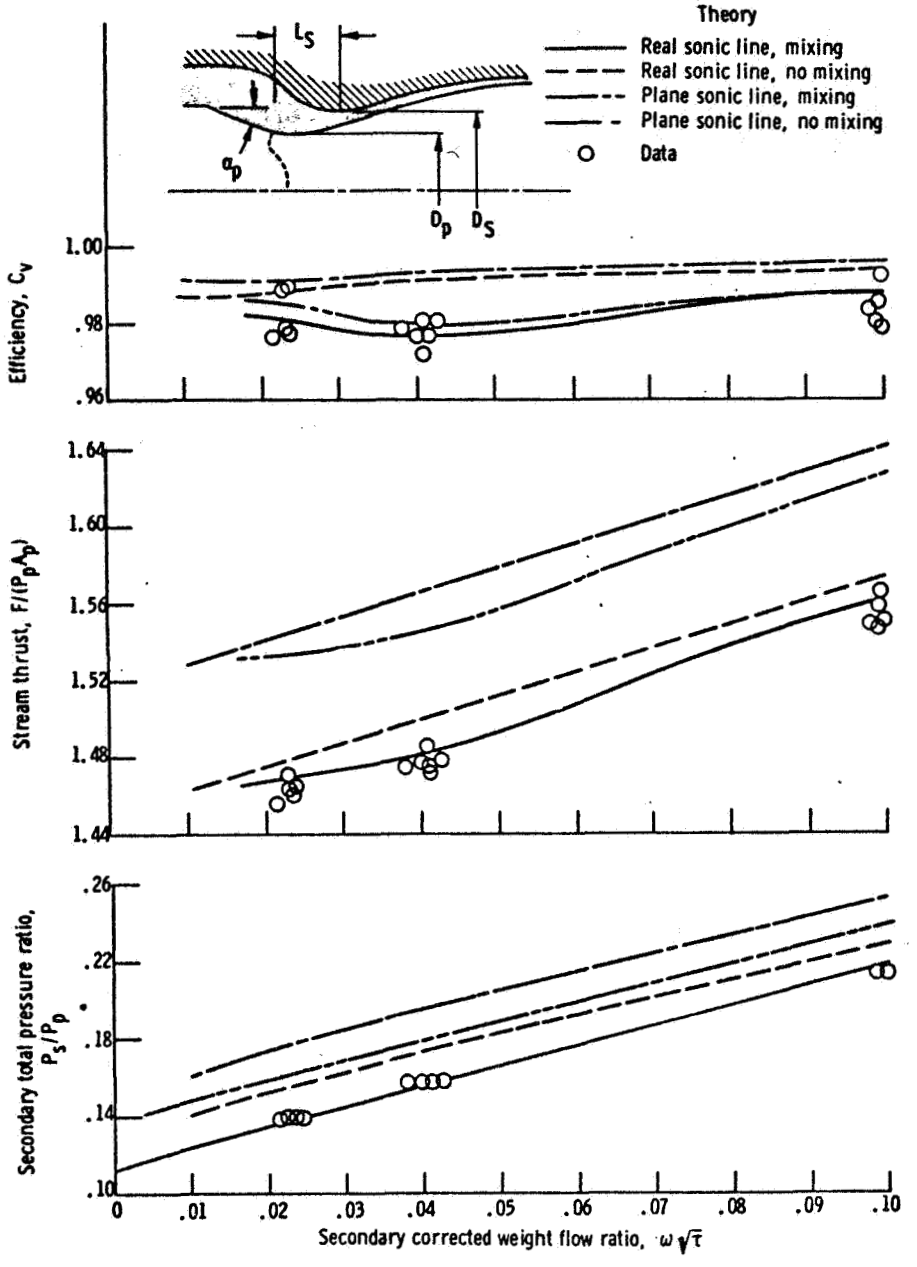

Figure 2.- Influence of sonic line and mixing process on performance of a convergent-divergent contoured flap ejector. Shroud shoulder diameter ratio, D_S/D_O, 1.37; spacing ratio, L_S/D_p, 0.5; primary nozzle lip angle, α_p, 27°; Reynolds number, Re, 3.3×10^6; ratio of primary total pressure to free-stream static pressure, P_p/p_O, 27.

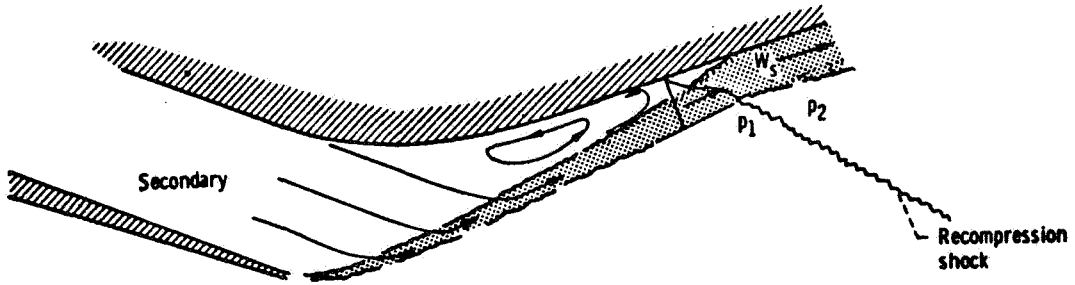

(a) Low secondary flow.

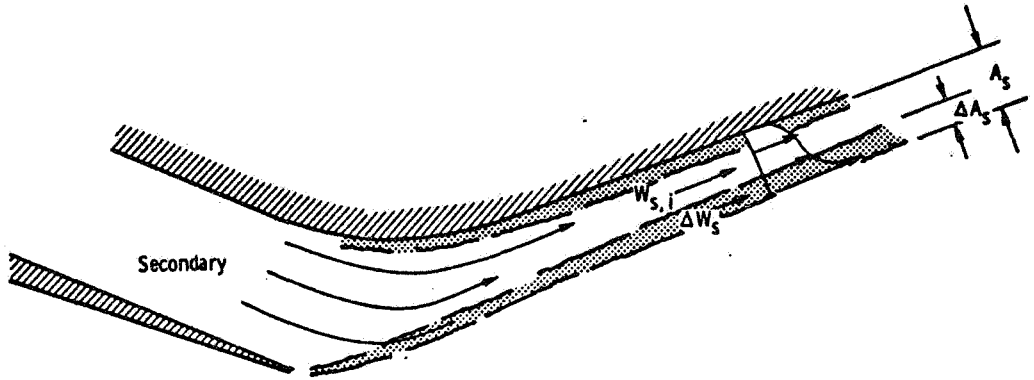

(b) High secondary flow.

Figure 3.- Schematic of typical secondary flow regimes.

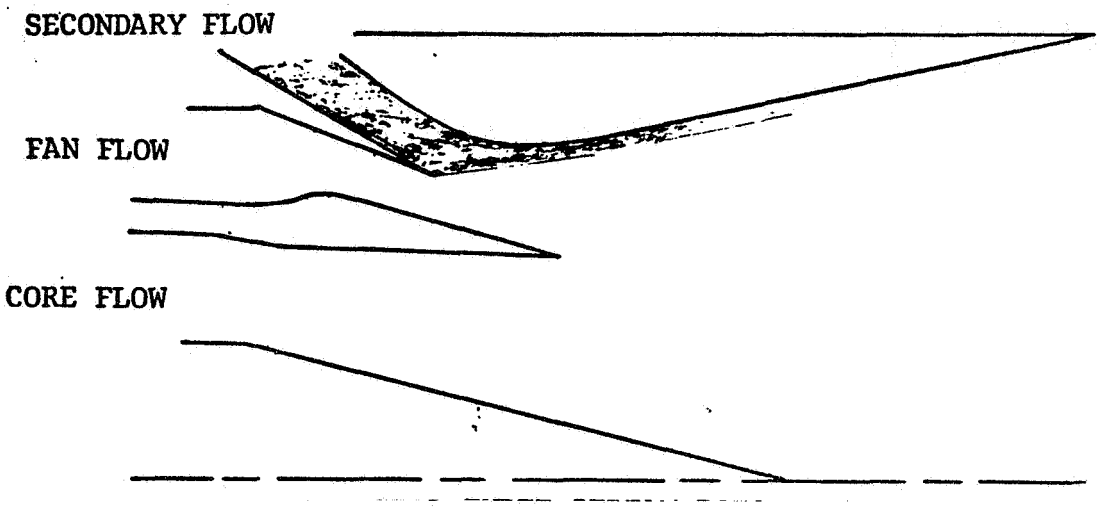

(a) Conical splitter three-stream ejector.

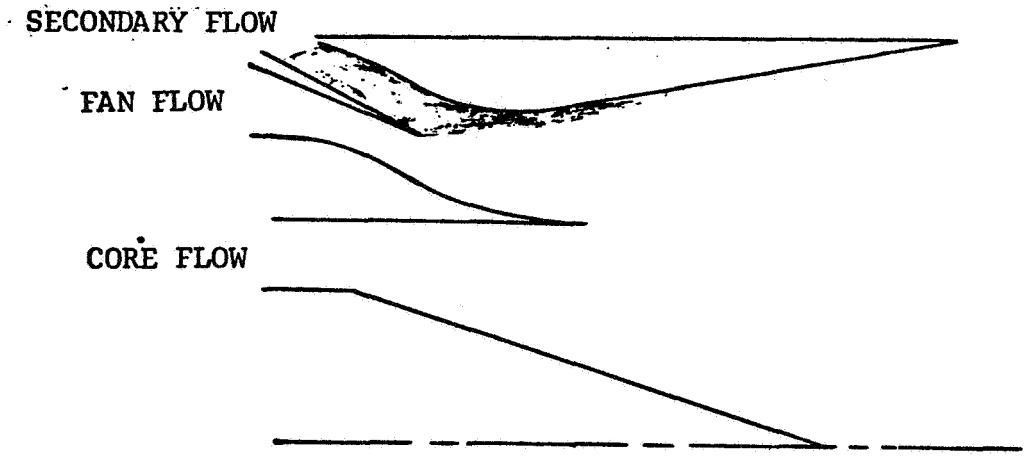

(b) Isentropic splitter three-stream ejector.

Figure 4.- Schematic of typical three-stream ejector nozzle.

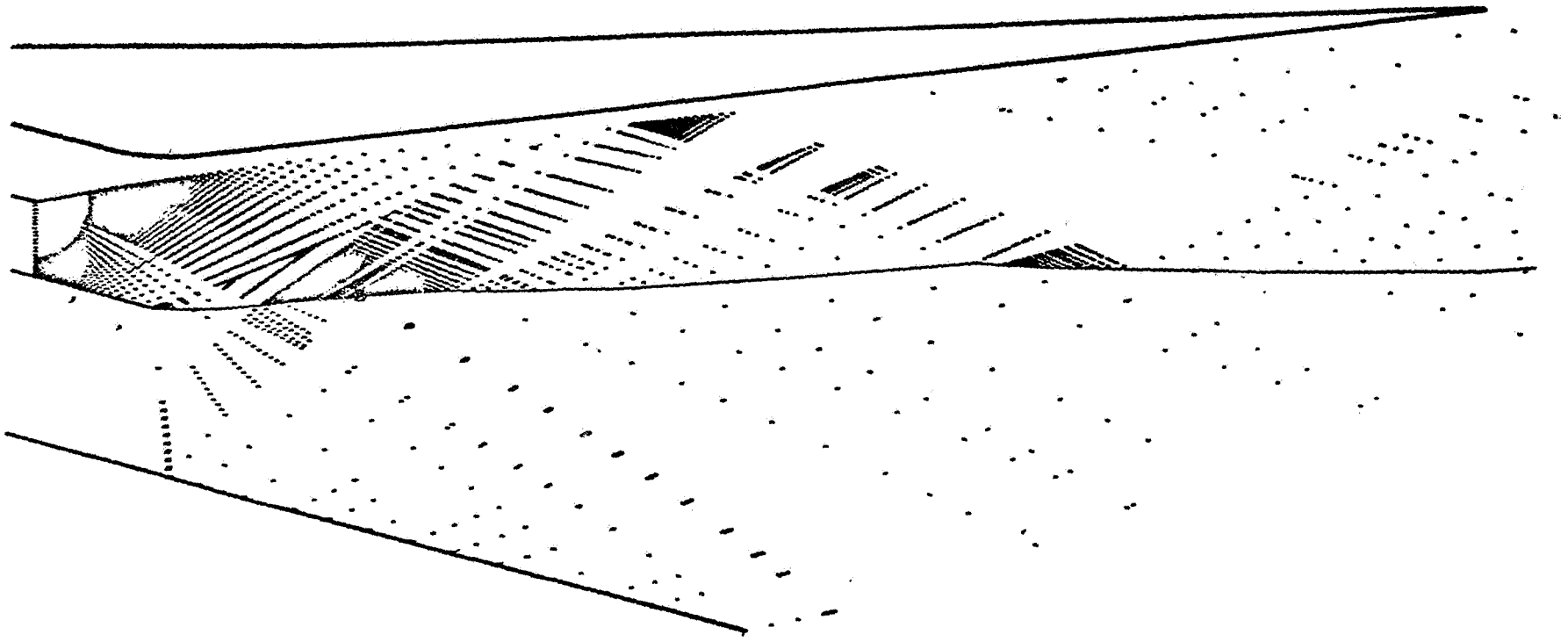

Figure 5.- Flow visualization for three-stream ejector nozzle with conical splitter.

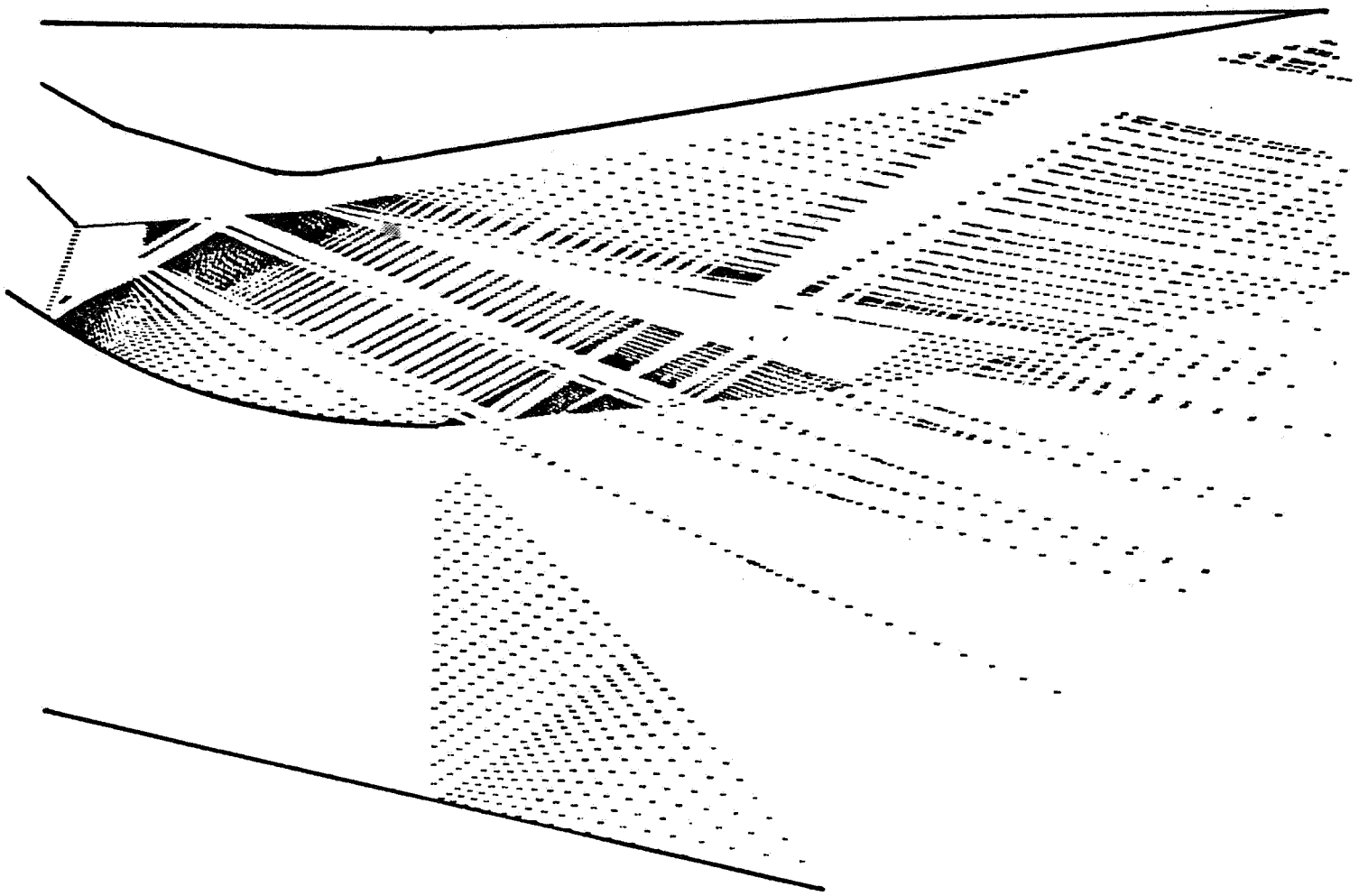

Figure 6.- Flow visualization for three-stream ejector nozzle with isentropic splitter.

INTERFACE CONCERNS OF EJECTOR INTEGRATION IN V/STOL AIRCRAFT

Randall B. Lowry

Aeromechanics Division
Air Force Flight Dynamics Laboratory
Wright-Patterson Air Force Base, Dayton, Ohio

The development of ejector technology has historically been concerned with achieving higher augmentation ratios through improved nozzle development, better mixing and overall ejector design. Most efforts have been successful with augmentation ratios in excess of 2.0 being achieved in the laboratory. However, the two experimental military aircraft, the XV-4A in the 1961-1964 time period and the XFV-12 in the 1971-1978 time period, have been developed using ejector systems for vertical thrust; both have been rated at best only marginally successful. In spite of the modest design augmentation ratios, 1.41 for the XV-4A and 1.55 for the XFV-12, neither aircraft achieved these levels. The reasons for not achieving the design level of augmentation and the lack of success of these aircraft can largely be attributed to the interface of the ejector with the aircraft, ejector characteristics, and the additional requirements (other than vertical thrust production) imposed on the ejector. The compromises required to interface the ejector into the V/STOL aircraft result in systems losses, weight increases, volume requirements and additional complexity. These interface areas include the engine/ejector, ducting system, force vector control, flight control, ground effects and VTOL translation/transition characteristics.

ENGINE/EJECTOR INTERFACE

In ejector-equipped aircraft, the engine(s) must perform the dual function of providing primary gas to the ejector system and of providing thrust for conventional flight. When operating in the ejector-powered mode, the engine exhaust gases are directed into the ejector system through a diverter valve scheme. The XV-4A incorporated a two-door block and turn diverter and the XFV-12 a sliding sleeve arrangement. The compromises associated with installation of the diverter valve include (fig. 1): exhaust gas pressure losses in the order of 3%, exhaust gas leakage losses in the order of 1%, weight increase in the order of 200 lb (generally aft of the C.G.). The XFV-12 diverter valve weighs approximately 400 lb. Depending on the diverter valve scheme, a possible increase in engine tail pipe length and to date no diverter valve has been flown that is compatible with afterburner operation. Another engine/ejector interface is the engine tailpipe area/ejector primary nozzle area matching. In the ejector mode, for proper engine operation, the engine must feel an exhaust area equivalent to the trim design tail pipe area. In the case of the XFV-12, F401 engine, this is approximately 8.3 ft^2. The ejector system must be designed and the nozzles sized for this equivalent area. Figure 2 shows that too little equivalent area can back pressure the engine and reduce thrust; too much

area, depending upon the engine control system, can reduce stall margin. The ejector system must be designed to allow matching of the engine operating line or complications such as reduced thrust or reduced stall margin may result.

DUCTING SYSTEM

The propulsion system is connected to the ejector through a ducting system. The ducting system is comprised of duct runs, expansion bellows, integral turning vanes, attachments for mounting and insulation. In addition to being a potential source of problems ranging from intolerable internal airframe temperatures to catastrophic loss of augmentation, the ducting system compromises the vehicle through increased weight and large volume requirements, and reduces primary nozzle thrust through system pressure losses. In general, the ducting design parameters (i.e., temperature, pressure and flow Mach number) are conducive to relatively large cross-section ducts of thin gage material. Figure 3 shows some typical duct characteristics. These in turn present areas for potential problems in manufacturing such as duct joining, mismatch and welding difficulties leading to stress concentrations and hot spots which can result in duct ruptures as shown in figure 4. In addition, maintenance problems can be encountered in handling and inspection. Typical ducting systems can add 200 to 300 lb to the vehicle weight (the XFV-12 ducting system weighs approximately 900 lb) and exact a thrust loss, before augmentation, of approximately 8%. Example pressure losses are shown in figure 5. The duct pressure losses in the XFV-12 were initially estimated to be approximately 12% and the XV-4A at 10%. A rule of thumb converts 2% pressure losses into 1% thrust loss.

FORCE VECTOR CONTROL

When operating in the vertical mode, a VTOL aircraft requires some method of providing a horizontal thrust component for translation acceleration to wingborne flight. In the XV-4A, the ejector nozzles were canted 12° aft and acceleration was accomplished by assuming a nosedown attitude. Due to the limited augmentation of the XV-4A this resulted in a bouncing leapfrog translation until sufficient speed was obtained to eliminate all hot gas reingestion and to develop sufficient augmentation to maintain altitude. In the XFV-12, the horizontal thrust component is generated by rotation of the augmentor flaps to an aft position. These schemes are shown in figure 6. If sufficient augmentation can be achieved, such a scheme is more desirable and comes with relatively little penalty except complexity since the augmentor flaps are stowed in a rotated position for conventional flight. However, if accomplished by doors or louvers, the system can be back pressured resulting in loss of thrust and, if not efficient, can add to ram drag.

FLIGHT CONTROL

A VTOL vehicle must incorporate supplemental control power to hover and low-speed flight where aerodynamic controls are ineffectual. The XV-4A utilized continuous flow exhaust gas for pitch and yaw and compressor bleed air (on demand) for roll control. The pitch/yaw system required 450-lb engine thrust and at a 5% bleed rate the roll system extracted the equivalent of 216 lb of thrust (108 lb per valve). In addition to the extra weight and volume, the reaction control system extracted a total of 666 lb of thrust before augmentation (a 10% thrust loss). The XFV-12 utilizes a total force management system in which the ejector provides functions of pitch, roll, yaw, height control and force vector control. These control functions are shown in figure 7. Such a force management system imposed on the ejector requires that a certain amount of lift be retained (unusable) for control purposes, for example, with full-up height control the system must allow for further open modulation (additional lift) if a lateral or pitch control moment is demanded. Also, such a system usually suffers from a marginal lateral control capability during transition speeds before aerodynamic control is effective. Figure 8 depicts the relationship. With the ejector rotated aft and a lateral control moment demanded, the resultant effective lateral control force is equal to the delta force times the cosine of the rotational angle. In addition an unbalanced horizontal force equal to the delta force times the sine of the rotational angle induces a yaw moment; that is, as rotational angle is increased lateral control is reduced in effectiveness and is coupled with yaw. This type control system requires that either mechanical or electronic control mixing and aerodynamic/reaction control blending for smooth transition. This adds both weight and complexity to the vehicle.

GROUND EFFECTS

The ground effects generated by a VTOL aircraft have been proven to be very configuration oriented. Ground effects are characterized in four forms: hot gas reingestion into the engine, suckdown or positive lift, temperature effects and ground erosion. Ejectors generally have good velocity and temperature profiles. The mixed exhaust gas temperature at the ejector exit approaches 300° F and the velocity is approximately 600 ft/sec. This advantage gives good erosion characteristics and little temperature effect on the vehicle or surrounding equipment. However, due to the large mass of airflow through the ejector (fig. 9), five to six times the primary engine exhaust and the flow field around the vehicle, hot gas reingestion and suckdown/positive lift effects are pronounced. Reingestion of hot gases can cause two detrimental effects. Operation of the engine in a uniform elevated temperature environment causes a loss of thrust equal to about 1% for 5° F temperature rise. Both the XV-4A and the XFV-12 experienced compressor inlet temperature increases of 25° F after short periods of operation in ground effect. The second detrimental effect of reingestion occurs when the engine ingests a spike of high temperature air causing compressor stall. This is a

function of temperature rate of change and not necessarily only high temperature; a 20°F temperature increase in 0.1 sec gives a 200° F/sec spike and can cause compressor stall. Compressor stall can be catastrophic if it results in engine flameout. Insofar as suckdown/positive lift is concerned, the vehicle/ejector configuration is the determiner. The XFV-12 claims positive ground effect, but testing is required to verify this claim. The XV-4A suffered from suckdown while in a three-point landing attitude; but upon raising the nose to 12° (hover attitude due to the canted ejector nozzles) the vehicle experienced positive ground effect as shown in figure 10. In any case, ground effects are clearly a design consideration for an ejector V/STOL aircraft and can attribute greatly to lift losses. In some cases, special provisions to increase the engine stall margin, such as upstaging the inlet guide vanes or increasing the turbine nozzle area have been necessary. This results in additional thrust losses before augmentation.

VTOL TRANSITION/TRANSLATION CHARACTERISTICS

For the VTOL aircraft, the transition from vertical-powered to wingborne flight (and vice versa) is the most demanding and critical phase of flight. Below about 60 knots airspeed, the power-induced effects upon the vehicle are predominant and are particularly so on the ejector vehicle because of the large amount of secondary airflow taken through the ejector system. The vehicle design configuration is clearly a driving factor on the transition characteristics. A configuration such as the XFV-12 (four poster arrangement) should exhibit good stability characteristics relative to induced pitching and rolling moments; but the single-ejector configuration such as the XV-4A develops severe low-speed pitch and roll characteristics due to the ejector-induced mass flow. Figure 11 depicts the upset moments that are induced by forward translation, sideslip or a combination of the two. These large mass flow effects were very pronounced on the XV-4A and on the XV-5A, fan-in-wing vehicle, which also induced large mass flows. To obtain adequate pitch control for transition, both vehicles required special longitudinal control design. The XV-4A required installation of a down spring to offset the high elevator hinge moments, a 30° elevator droop mechanism and boundary layer blowing on the elevator to prevent separation. With these controls the angle of attack was limited to 10° to prevent pitchup. The XV-5A required the complete horizontal tail to be positioned at an 11° leading-edge-up incidence angle and a nose-mounted pitch fan when operating in the transition regime. The moments generated in sideslip required that the XV-4A be limited to 5° and that the XV-5A limited to winds of 6 knots while in the vertical mode of operation. In addition, the large mass of air being turned through the ejector system causes high ram drag which limits forward speed while operating in the vertical transition mode. This characteristic can require special transition techniques. For example, to achieve wingborne flight speed above stall, it was necessary for the XV-4A to accomplish sequential diversion of the engine exhaust from the ejector to the thrusting mode. The XV-4A transition shown in figure 12 is undesirable from an operational standpoint. The ejector vehicle configuration should be designed to provide for a smooth continuous transition and conversion, however

the requirements of transition and conversion add weight and complexity to the ejector V/STOL aircraft.

SUMMARY

A number of areas have been identified which have in the past contributed to weight, complexity, and thrust losses in the ejector-powered V/STOL vehicle. A summary of the area is shown in figure 13. Most of these interfaces taken singly do not represent a severe compromise to the vehicle; however, the bottom line is that the sum of compromises and the subsequent effects on performance, flight operations and maintenance have rendered the ejector V/STOL aircraft unattractive. In addition to some of the unique ejector/aircraft integration problems, the vehicle by virtue of having a V/STOL capability is compromised in other areas such as inlets for low speed (blow-in doors, sliding inlets, auxiliary inlets, rounded lips) and high speed compatibility, zero-zero/bad attitude ejection capability, additional controls and displays, stability augmentation, and weapons compatibility. To be successful and acceptable, the advantages must outweigh the disadvantages and simplicity with minimum penalties must be the rule. Figure 14 lists the advantages and disadvantages of the V/STOL ejector-aircraft. It is clear that more emphasis must be placed on the ejector/aircraft interface for the concept to be successful.

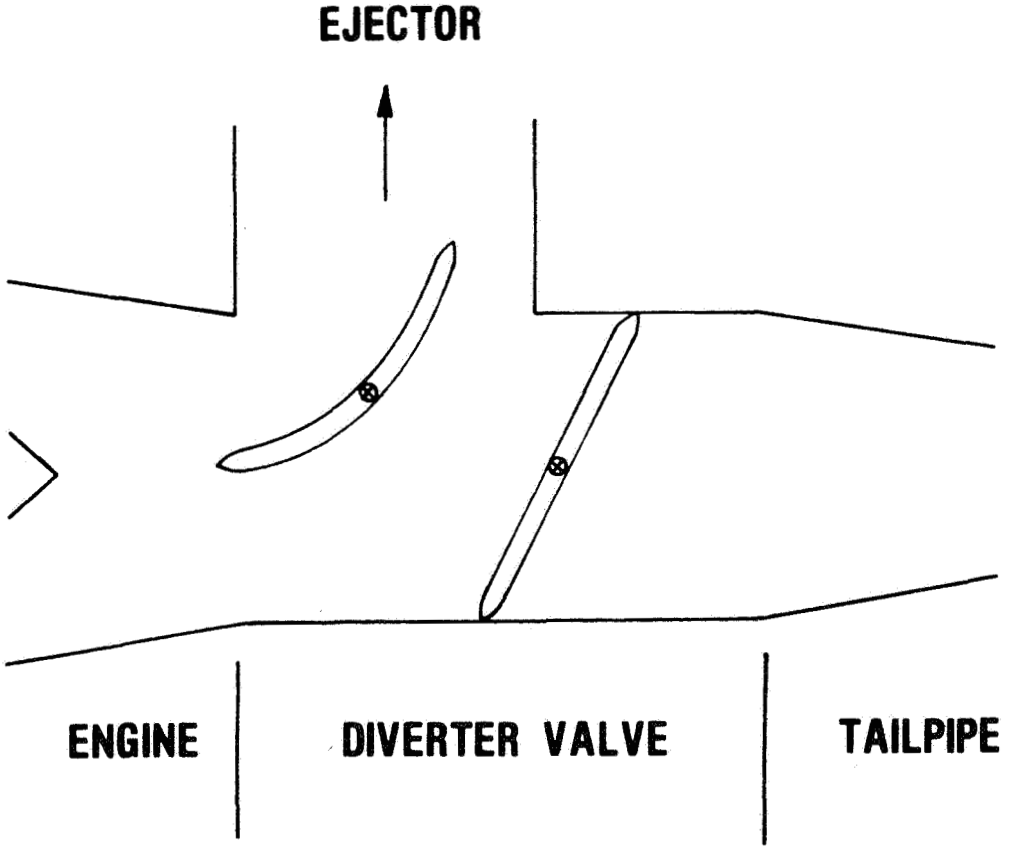

PRESSURE LOSS ~ 3%
LEAKAGE LOSS ~ 1%
WEIGHT ~ 200 LB
INCREASE IN TAILPIPE LENGTH

Figure 1.- Diverter valve.

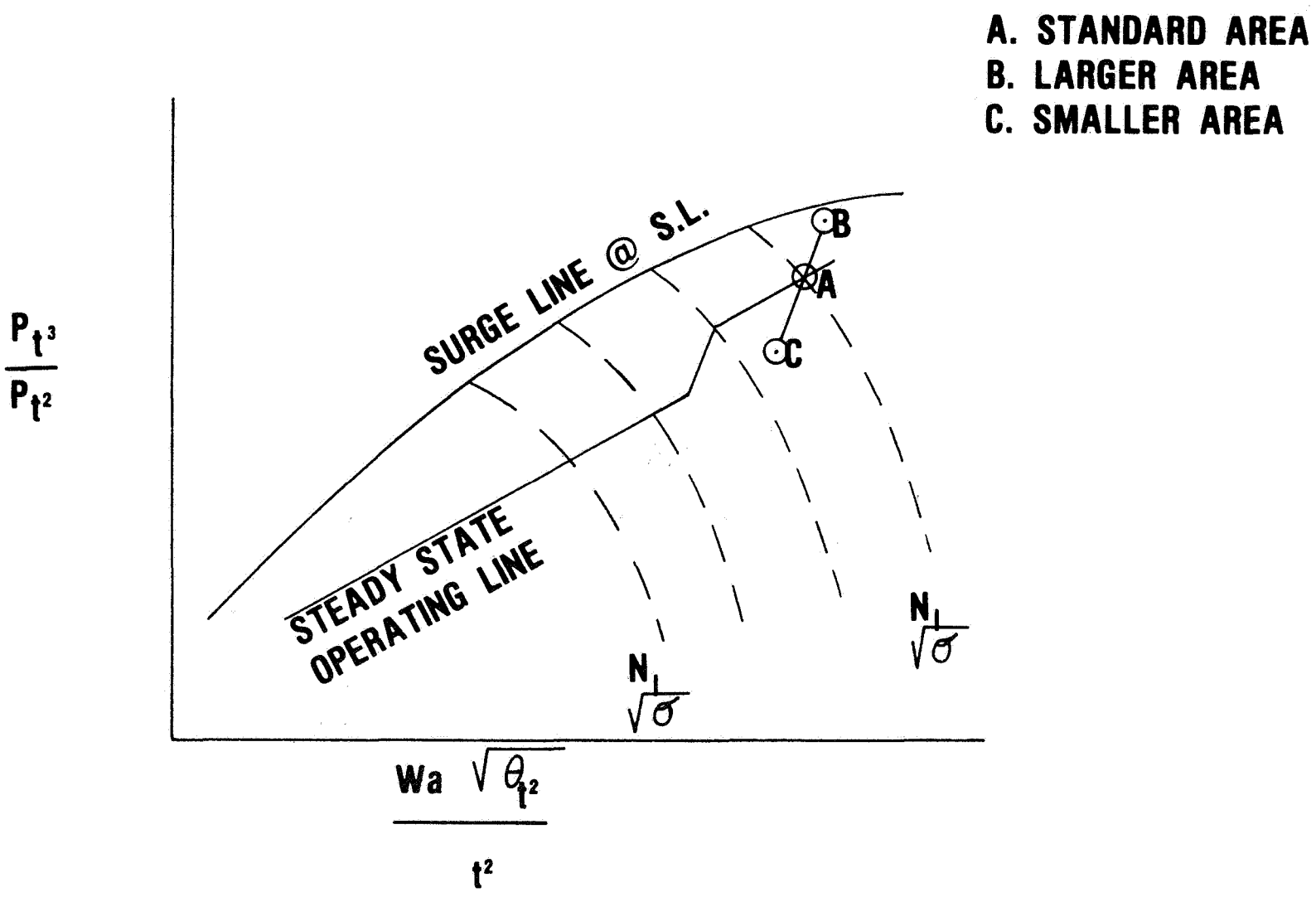

Figure 2.- Area matching.

XV-4B

	MANIFOLD	COLLECTOR	REACTION CONTROL	DIVERTER
TEMPERATURE	540°F	540°F	540°F	1000°F
PRESSURE	102 PSI	153 PSI (PROOF)	153 PSI (PROOF)	30.8 PSI (PROOF)
MATERIAL	INCONEL X-750	SS 321/347	INCONEL X-750	INCONEL 718
THICKNESS	.016	.016	.016	.025

404

Figure 3.- Ducting characteristics.

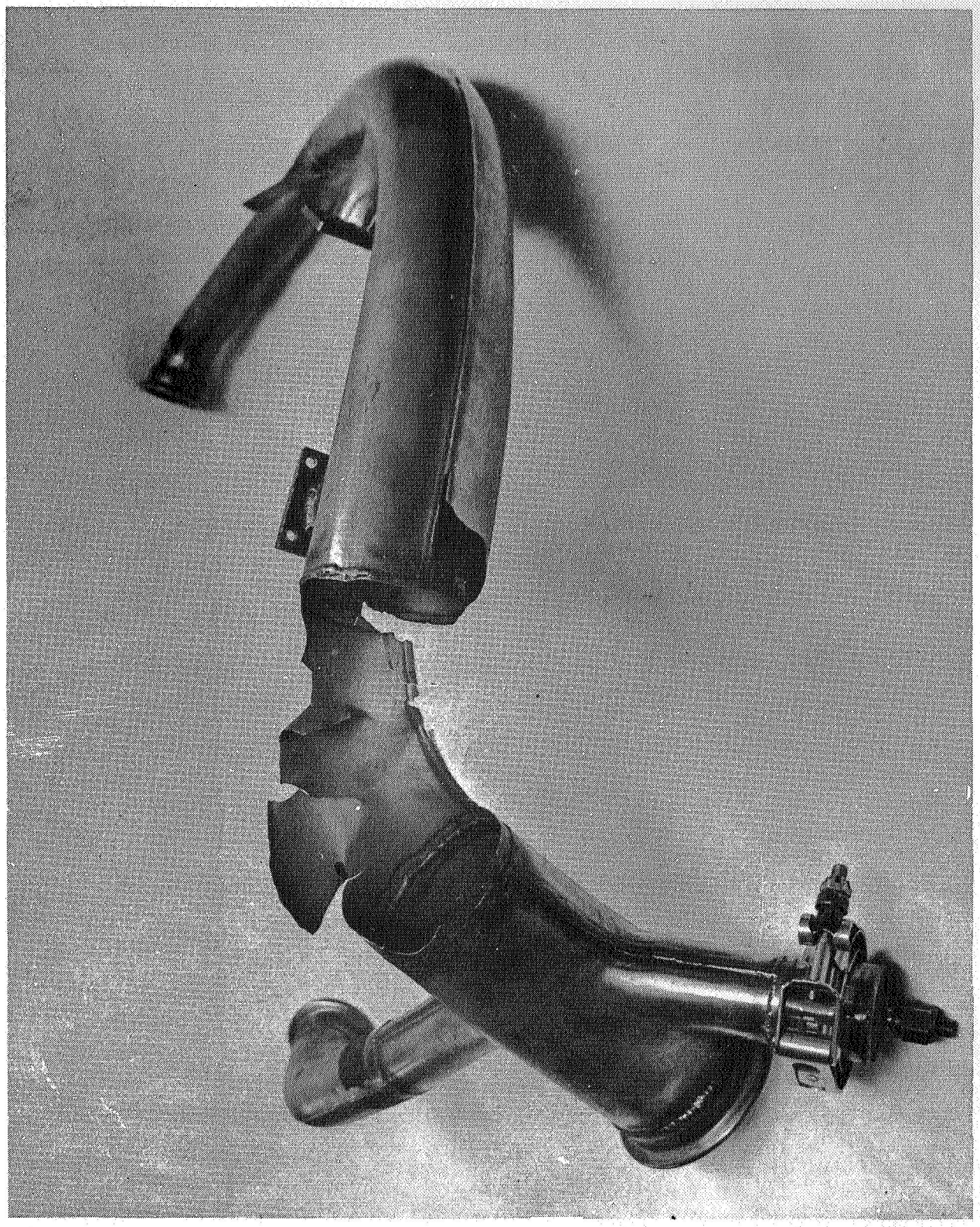

Figure 4.- Example of rupture due to hot spot.

A DUCT RUNS
B EXPANSION BELLOWS
C TURNING VANES
D ATTACHMENTS
E INSULATION

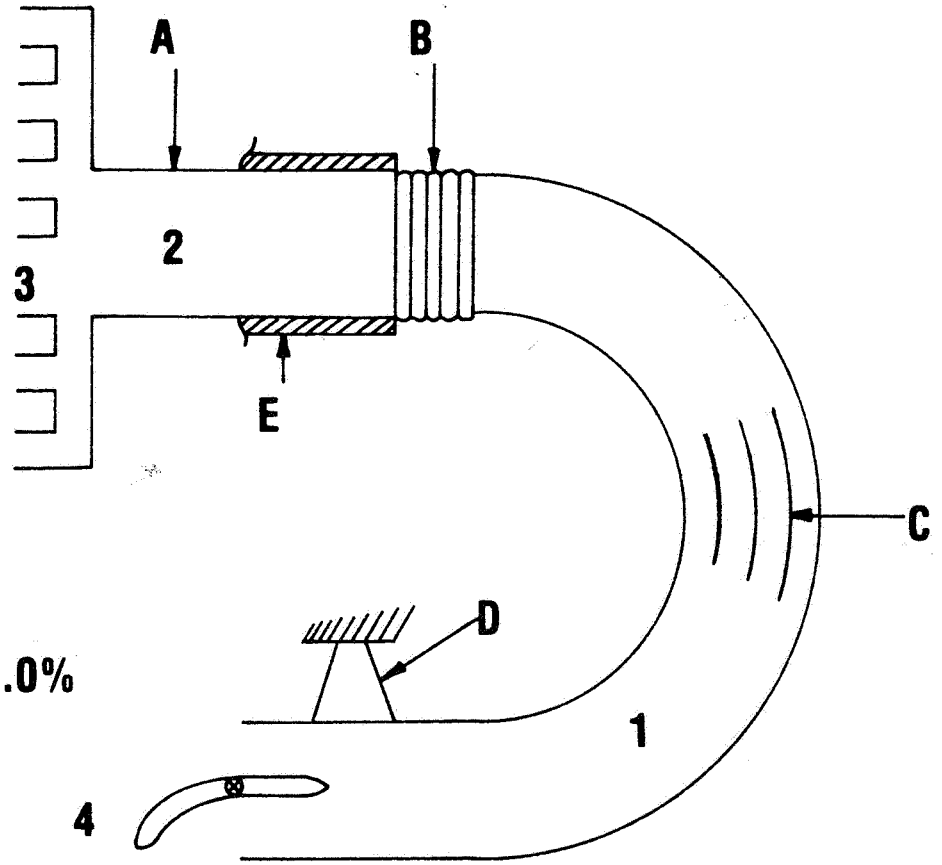

1 180° BEND ~ 1.5%
2 MANIFOLD INLET ~ 4.0%
3 NOZZLE DUCT ~ 1.5%
4 ENGINE TAILPIPE DIFFUSER ~ 1.0%

Figure 5.- Ducting system.

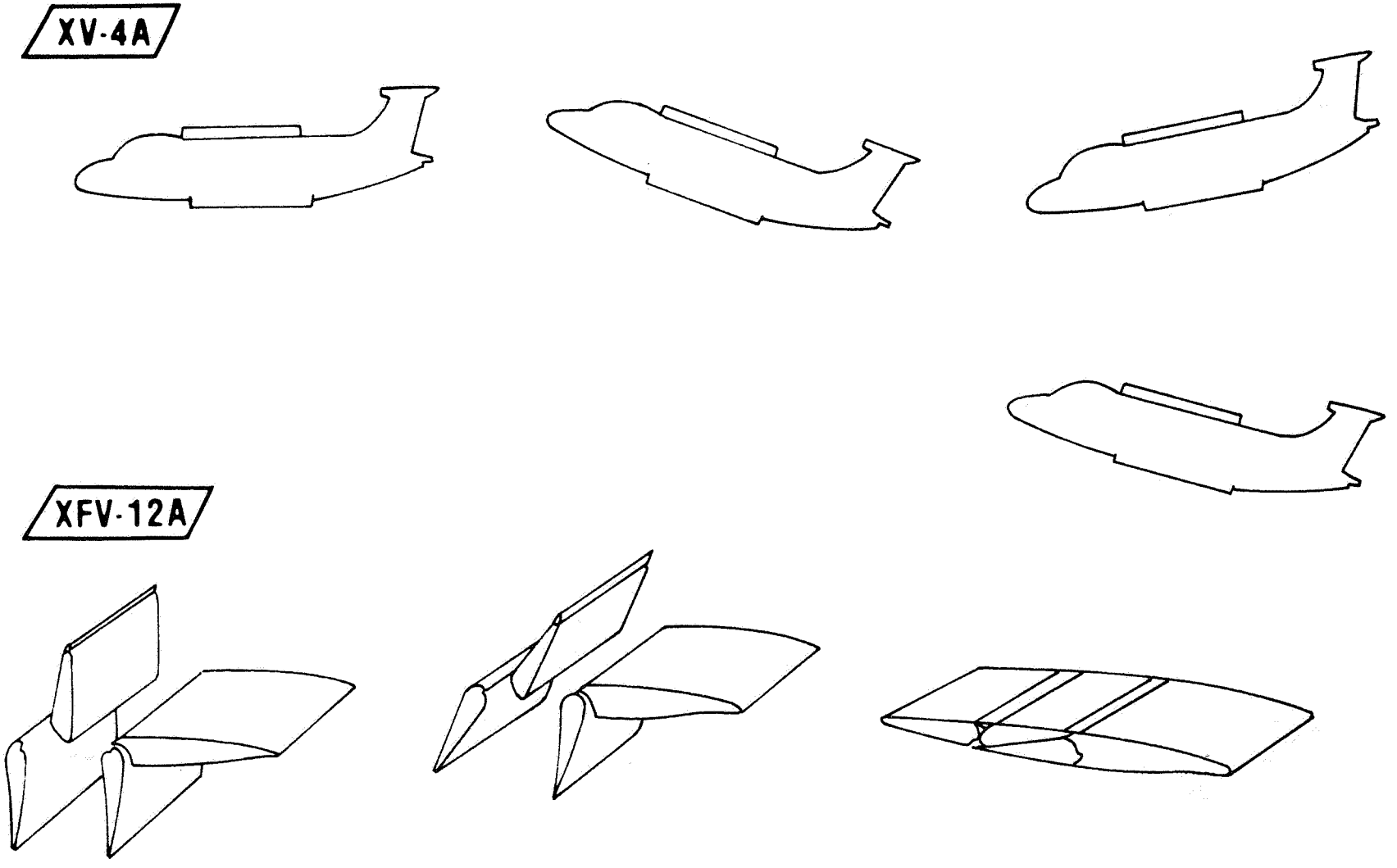

Figure 6.- Force vector control.

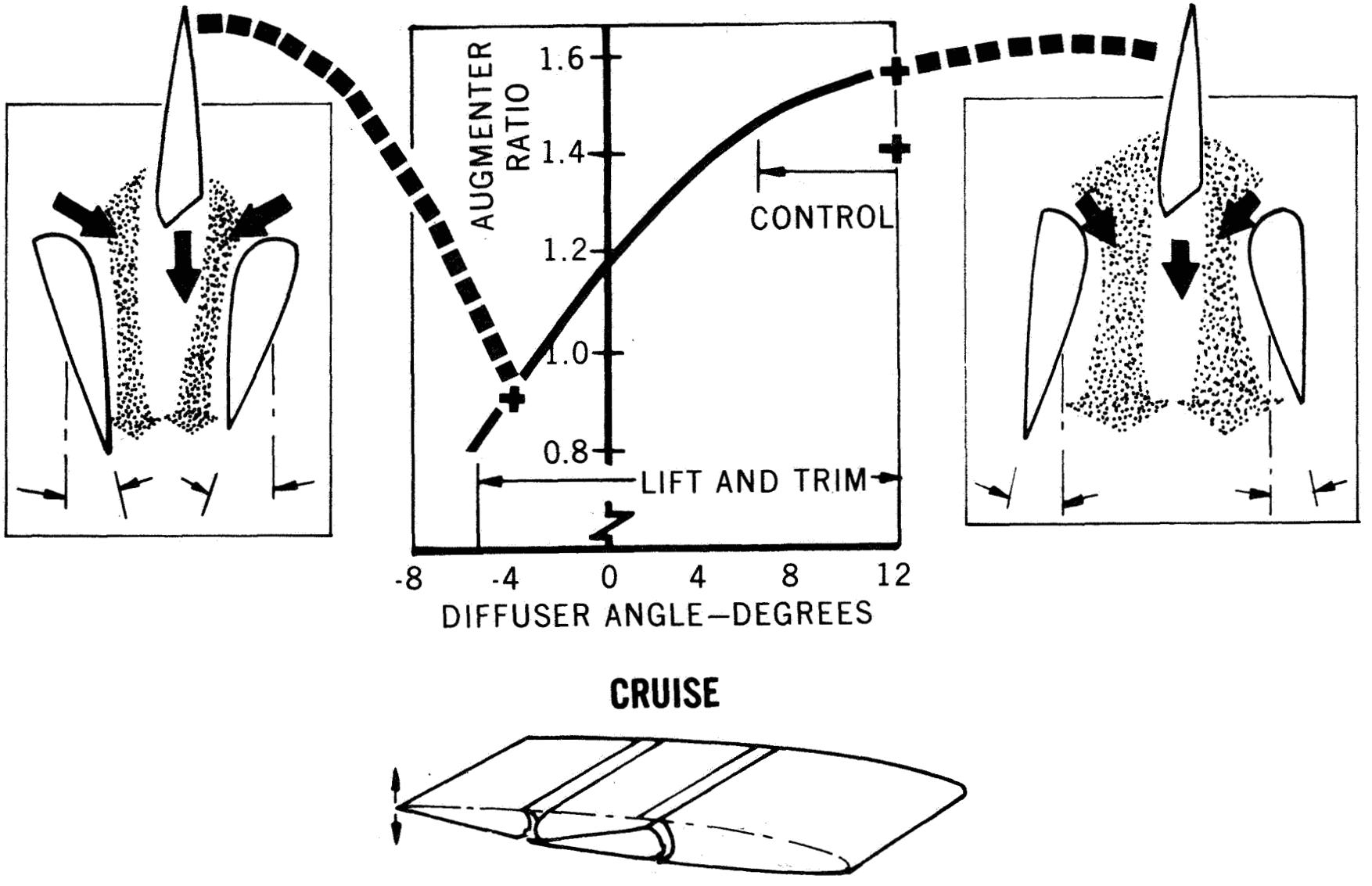

Figure 7.- V/STOL technology Rockwell TAW.

Figure 8.- Flight-control effectiveness.

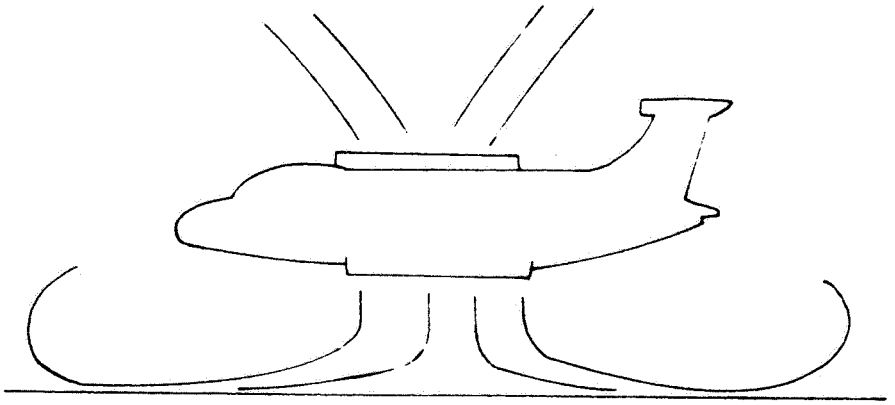

Figure 9.- Ground effects.

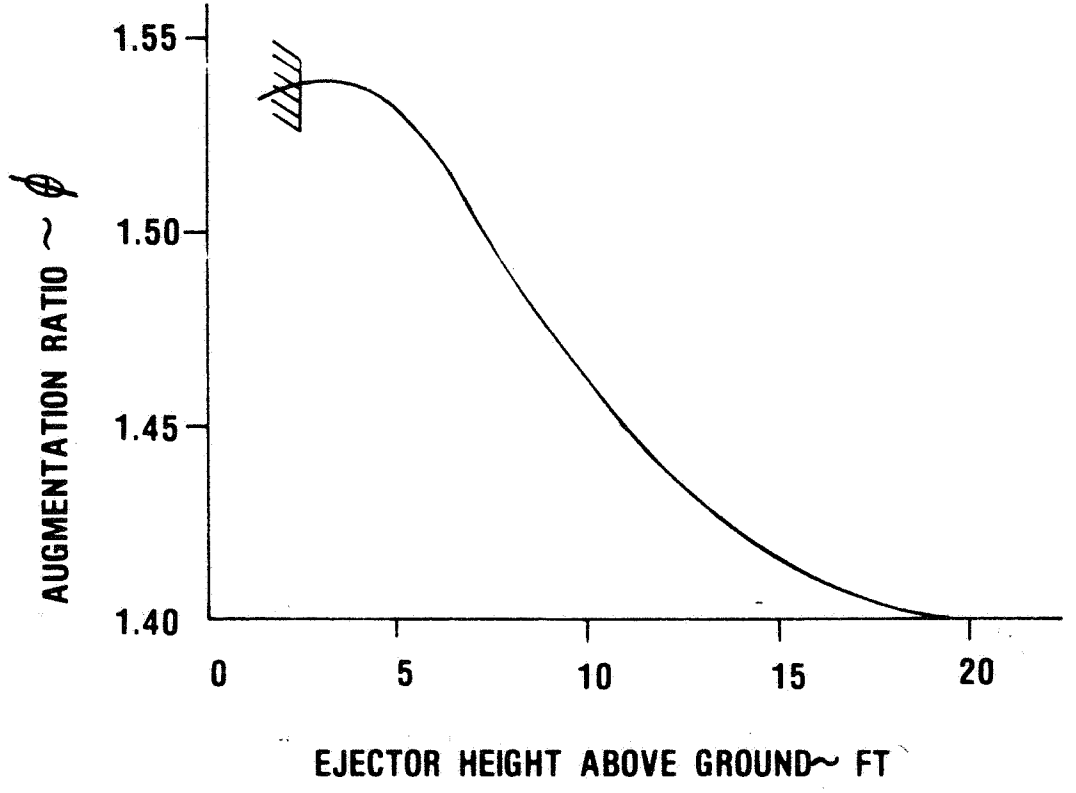

Figure 10.- XV-4A positive ground effect.

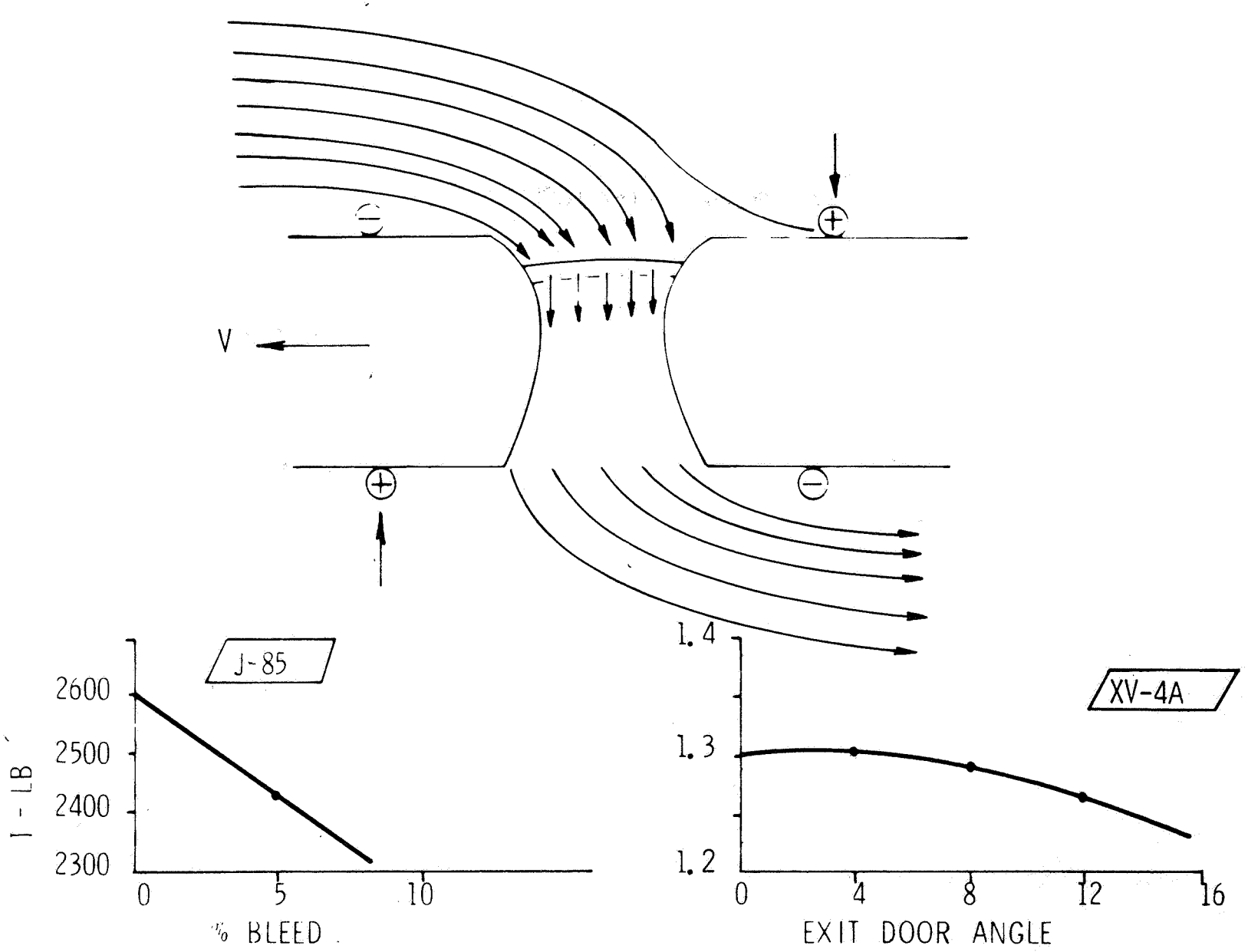

Figure 11.- Control considerations.

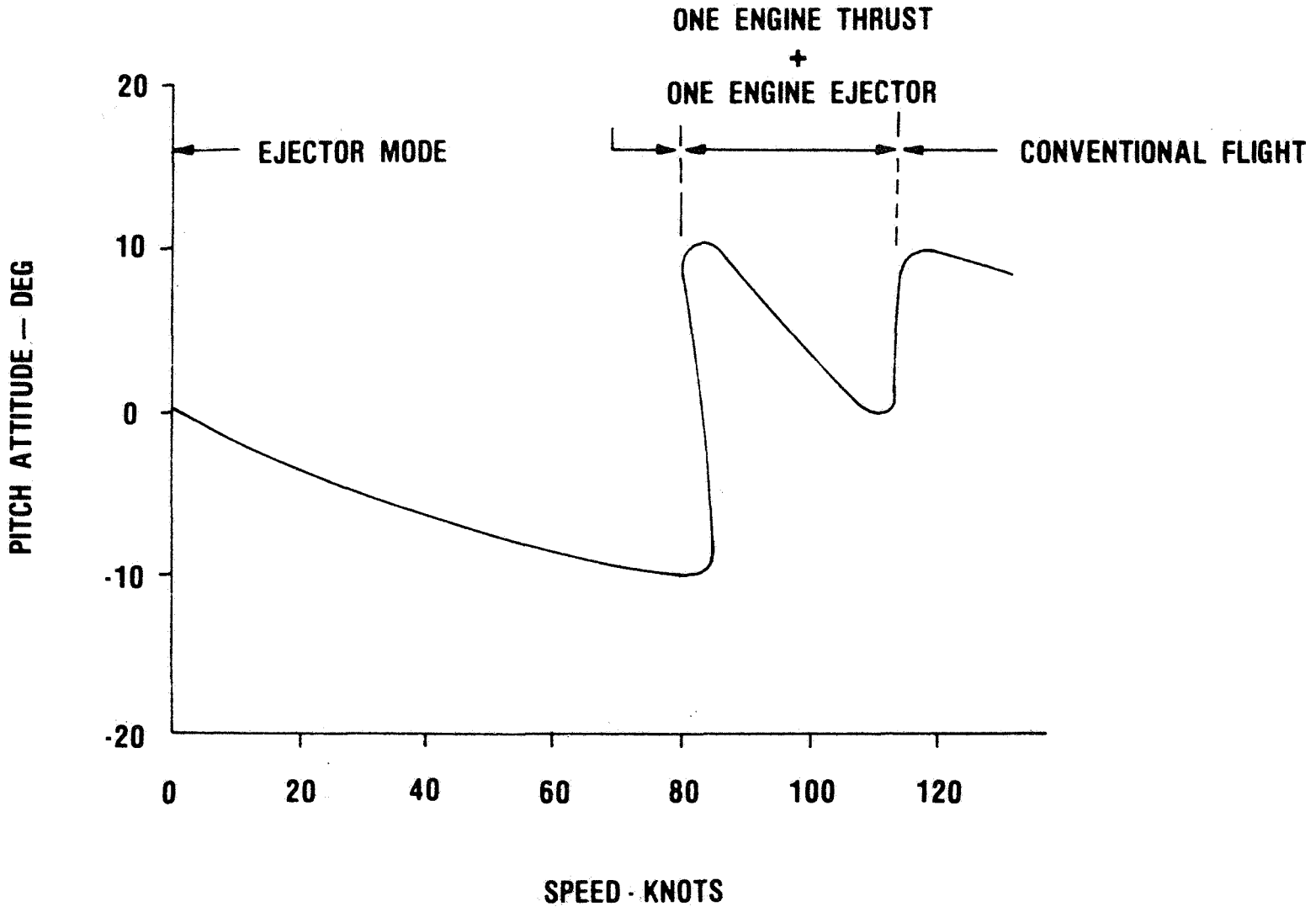

Figure 12.- Transition sequence (XV-4A).

INTERFACE AREA	WEIGHT	VOLUME	COMPLEXITY	THRUST LOSS
ENGINE INLET	X		X	
DIVERTER VALVE	X	X	X	X
TAILPIPE/NOZZLE TRIM				X
DUCTING SYSTEM	X	X	X	X
FORCE VECTOR CONTROL	X		X	
FLIGHT CONTROL	X	X	X	X
REINGESTION				X
SUCKDOWN				X
TRANSLATION			X	

Figure 13.- Summary.

ADVANTAGES

LOW-TO-MEDIUM DOWNWASH VELOCITY
LOW-TO-MEDIUM DOWNWASH TEMPERATURE
SINGLE PROPULSION SYSTEM FOR HOVER AND CRUISE
GOOD HOVER/CRUISE THRUST MATCH
INHERENT STOL CAPABILITY

DISADVANTAGES

LARGE VOLUME INSTALLATION REQUIRED
INTERNAL HOT GAS DUCTING REQUIRED
HIGH VTOL DRAG AND MOMENTUM MOMENTS
CONTROL CONSIDERATIONS COMPROMISE THRUST AUGMENTATION
COMPROMISES EXTERNAL/INTERNAL STORES CARRIAGE

Figure 14.- V/STOL ejector configurations.

REACTION CONTROL SYSTEM AUGMENTATION FOR V/STOL AIRCRAFT

H. G. Streiff and R. E. Donham

Lockheed California Company
Burbank, California

INTRODUCTION

V/STOL control during hover and low-speed flight is provided directly or indirectly by the propulsion system. The control requirements during these flight conditions have a large influence on and, in fact, generally dictate the propulsion system size. Means of obtaining control from the propulsion system are varied and are generally dictated by configuration design and control required by emergency conditions. Reaction controls produced by bleeding air from the engine compressor, and ducting that air to extremities of the aircraft is one of those means. Advantages and problems associated with augmentation of reaction controls are the subject of this paper.

ADVANTAGES OF REACTION CONTROL AUGMENTATION

Generally, when evaluating the relative merits of ejector thrust augmentation and the net gain obtained from incorporating such advice into a particular design, the losses associated with transferring the air from the gas generator to the ejector must be included. These losses can be of the order of 15% or more. In addition, in order to minimize these losses, the ducting of the air while keeping flow losses to these levels requires the using up of large fuselage and wing volumes. In arguing the case for augmenting reaction controls, these losses need not be initially considered because the ducting and transfer losses exist whether or not the air provided to the reaction control nozzles is augmented. With the exception of the incremental increase in configuration nozzle weight caused by adding the ejector and, of course, assuming the ejector does not significantly alter the aerodynamic performance or flying qualities of the configuration, the gains achieved through augmentation of the reaction controls are real gains.

Several advantages of augmenting reaction control are presented in figure 1. The first two listed advantages appear identical, but differ in design philosophy and propulsion system selection. The first item alludes to the ability to achieve the maximum amount of control power from the amount of bleed available from a given gas generator. For example, consider an aircraft such as the AV-8 where the flying qualities are constrained by the amount of control available and the performance varies in accordance to the amount of bleed demanded by the control system. Installation of a compact ejector into a redesigned wing tip, out board of the outrigger landing gear, would significantly increase the maximum roll control available and decrease the amount of bleed required for normal roll control inputs.

The second item applies to the design of a new configuration where the propulsion system is sized according to the amount of compressor bleed required to provide adequate control for acceptable flying qualities. In this case, designing the engine to provide the control power required for minimum bleed reduces the size of the gas generator as well as the engine specific fuel consumption. The reduced propulsion system weight and SFC has a payoff in cruise performance as well as the V/STOL flight modes.

The advantages can be put in perspective by considering the impact of compressor bleed on the design of a V/STOL aircraft. Figure 2 presents the weights, inertia, and control requirements for a typical medium size four engine, four fan V/STOL transport. If reaction control is considered for the roll axis only, the amount of control force required for the one engine inoperative condition is 4,000 lb. The amount of engine bleed required to provide that amount of force and the effect of providing that bleed on engine SFC and weight is summarized in figure 3 for both augmented and unaugmented reaction controls. A relatively modest augmentation of 1.4 was assumed for the example calculations in order to show that significant improvements can be attained without having to achieve extremely large values of augmentation. It is realistic to assume that augmentation in excess of 1.4 is achievable, however a value of 1.4 produces a reduction in VTO gross weight or an increase in VTO payload of approximately 2,700 lb for a 40,000 lb aircraft.

PROBLEM AREAS

Figure 4 summarizes the problem areas that require careful consideration before the amount of compressor bleed augmentation achievable can be ascertained. The vast majority of all ejector test work accomplished to date has been performed at ambient temperatures and very low (less than 2.5) pressure ratios. The pressure ratios of compressor bleed air are of the order of 7.0 to 10.0 and the temperatures can be as high as 1200° F. Test data is required for these large pressures and temperatures. Almost all ejector test programs have been conducted under static conditions. Test data is required for ejectors operating at speed and in crossflows. In designing an ejector for augmenting reaction controls, it is desirable to get the largest amount of force out of the smallest possible ejector. The effect and limitations of large mixing sections velocities (near sonic) on ejector performance is not currently known and is important in determining the optimum ejector size. The packaging of the ejector into a convenient operational installation without adversely affecting the ejector performance or the external aerodynamics of the cruise configuration must be given careful consideration. Lastly, the operation of the ejector under failure conditions must be evaluated to insure compliance with the level 2 and 3 control requirements.

STATE OF THE ART IN EJECTOR DESIGN

The remainder of the paper presents the current status of compact ejector technology and the expected performance of known efficient designs for reaction control applications.

Figure 5 presents the ejector definitions used in the report. In all cases in this report, augmentation is defined as the gross measured force produced by the ejector divided by the amount of thrust that can be produced by an isentropic expansion of the measured primary mass flow. Figure 6 presents the thrust augmentation that can be obtained from an ideal ejector. In a practical case however, the ideal thrust can be significantly reduced by the losses listed in figure 7. Assuming flow separation in the ejector can be minimized, either through BLC jets or generous turning radii, and applying reasonable loss coefficients to each of the listed losses, the curves of figure 6 are reduced to the augmentation values presented in figure 8. Augmentation values of these magnitudes have, in fact, been experimentally achieved by several investigators. Compact ejector designs that have achieved augmentation ratios on the order of 2.0 are presented in figure 9. The one problem with these results is that they have been attained at static conditions, ambient temperatures, and pressure ratios less than 2.5. Figure 9 also contains the results obtained from tests of an axisymmetric ejector at ambient temperature and pressure ratio 10.0. These tests have achieved augmentation ratios as high as 1.45, however, the apparatus had a relatively long mixing and diffuser length and would be very difficult to package.

Results of augmentation ratio as a function of pressure ratio for an axisymmetric ejector are presented in figure 10. These data indicate that if the ratio of mixing section area (A_m) to primary (A_p) is low, there is a large decrease in augmentation as pressure ratio is increased. As A_m/A_p is increased, the augmentation becomes constant with pressure ratio. This indicates that with the proper ejector sizing the pressure ratio effect can be minimized. Figure 11 is a compilation of test results obtained for many single- and multiple-nozzle ejector designs. In this figure, it is seen that the axisymmetric results of the preceding figures fit in the single source band quite nicely while the compact ejector results of figure 9 fit into the multiple-source band. Since an axisymmetric ejector can be designed to remain relatively constant with pressure ratio, it is reasonable to assume that the multiple-source configurations can also be designed to give good performance at high pressure ratios.

A theoretical prediction of the effect of temperature on thrust augmentation is shown in figure 12. These results do not agree with the experimental results of Quinn.[1] In this work, Quinn measured the mass entrainment in an

---

[1]Quinn, Brian: Ejector Performance at High Temperatures and Pressures. J. Aircraft, vol. 13, no. 12, Dec. 1976.

axisymmetric ejector at high temperature and pressure ratios. He found very little change in entrainment with temperature and concludes that "theoretical analyses argue only from thermodynamics and ignore the dynamic role played by the heart of the ejector process, turbulent mixing. Present theories fail to identify which effect of heating the primary stream, higher impact losses or increased mixing, will dominate the performance of compact ejectors." Compact ejectors with enhanced mixing have not been tested at temperatures of the magnitude of compressor bleed air. It appears that a controversy exists as to just how significant temperature is to thrust augmentation and will only be resolved from a comprehensive test program of an efficient compact ejector.

With the exception of significantly increased friction losses caused by the sonic velocities, the gross effects of choking the flow in the mixing section of an ejector are not currently known. Intuitively, it is assumed that choking should be avoided and the mixing section velocity should be Mach 0.7 or less. With this as a constraint and the primary thrust known, the curves of figure 8 can be reworked to provide lines of constant mixing section velocity as a function of gross thrust, mixing section area, and diffusion ratio. These data are shown in figure 13. From these curves, it is seen that the mixing section for an ejector with a thrust augmentation of 1.4 (gross thrust of 4000 lb) would have to have a mixing area on the order of 600 $in.^2$ for a mixed velocity of $M \leq 0.7$.

Figure 14 shows the thrust augmentation received from several ejector configurations tested at WPAFB-ARL. This data shows that extremely good augmentation can be obtained using the ARL hypermixing nozzles in a compact ejector. The configuration C ejector geometry with aspect ratio 8 hypermixing nozzles was selected for the design of a V/STOL reaction control augmentor. A typical configuration that is capable of providing the required 4000 lb force for roll control of the figure 2 V/STOL aircraft is shown as a wing tip configuration in figure 15.

CONCLUSIONS

From the preceding discussion the following conclusions have been made:

- Significant benefits are to be gained in the following through augmentation of reaction control
  - Reduced cruise SFC
  - Increased payload capability or reduced VTO G.W.
  - Increased engine life because of reduced bleed requirements
  - Maximum control force obtainable from specified available bleed

- Small increase in thrust augmentation produces a relatively large improvement in VTO G.W.
- Augmentation limitations encountered at large PR and TR do not appear insurmountable but require systematic evaluation
- A practical compact ejector of the ARL hypermixing nozzle type can be incorporated into a wing tip and will have minor influence on the aircraft's overall aerodynamic characteristics

- MAXIMUM CONTROL POWER FROM AVAILABLE BLEED
- SATISFACTORY CONTROL POWER FOR MINIMUM BLEED AIR
- MINIMIZE CRUISE SFC'S WHILE PROVIDING ADEQUATE BLEED
- MINIMIZE ENGINE WEIGHT REQUIRED BY VTOL, STOL, AND CRUISE FLIGHT CONDITIONS
- VTO GROSS WEIGHT ENHANCEMENT BY ENGINE WEIGHT REDUCTION AND CRUISE SFC IMPROVEMENT
- REDUCE ENGINE ABUSE AND PROLONG ENGINE LIFE
- FAIL SAFE/OPERABLE CONTROL

Figure 1.- Advantages of augmented reaction controls.

INERTIA

I_X = 57,000 SLUG FT^2
I_Y = 73,000 SLUG FT^2
I_Z = 116,000 SLUG FT^2
WT = 40,000 LB

CONTROL REQUIREMENT FROM MIL SPEC 83300

N_Z 1.05 (1.03)
35 KT. WIND (CRITICAL WINDS)
ADVERSE C.G.
SIMULTANEOUS CONTROL:
.5 (.3) RAD/SEC^2 ROLL
.25 (.2) RAD/SEC^2 PITCH
.2 (.15) RAD/SEC^2 YAW

NOTE: ( ) = LEVEL 2

CONSIDERING REACTION CONTROL USED FOR ROLL AXIS ONLY

CRITICAL CONDITION IS ONE ENGINE INOPERATIVE, LEVEL 2 REQUIREMENTS

CRITICAL CONDITION REQUIRES ROLL CONTROL FORCE OF 4000 LB

Figure 2.- Control required for a typical ASW V/STOL transport.

	% BLEED	% CRUISE SFC	% ENGINE WEIGHT
UNAUGMENTED	22.0	11.0	20.0
1.4 AUGMENTATION	15.7	7.0	12.5

	ENG WT (4 ENG)	ΔWT	Δ% SFC	ΔGR. WT
UNAUGMENTED	5424			
1.4 AUGMENTATION	5017	–407	4	2700*

* 3.7 LBS AIRCRAFT WEIGHT PER 1 LB ENGINE WEIGHT
300 LBS AIRCRAFT WEIGHT PER 1% SFC

Figure 3.- Reaction control roll axis only effect of augmentation on G. W. typical ASW V/STOL transport.

- EJECTOR PERFORMANCE AT HIGH PRESSURE RATIOS
- HIGH TEMPERATURE CHARACTERISTICS
- CROSSFLOW PERFORMANCE
- SONIC OR NEAR SONIC FLOW IN EJECTOR MIXING SECTION
- PACKAGING INTO A PRACTICAL OPERATIONAL INSTALLATION
- SATISFACTORY FAILURE MODES AND EFFECTS CHARACTERISTIC

Figure 4.- Areas requiring detailed evaluation.

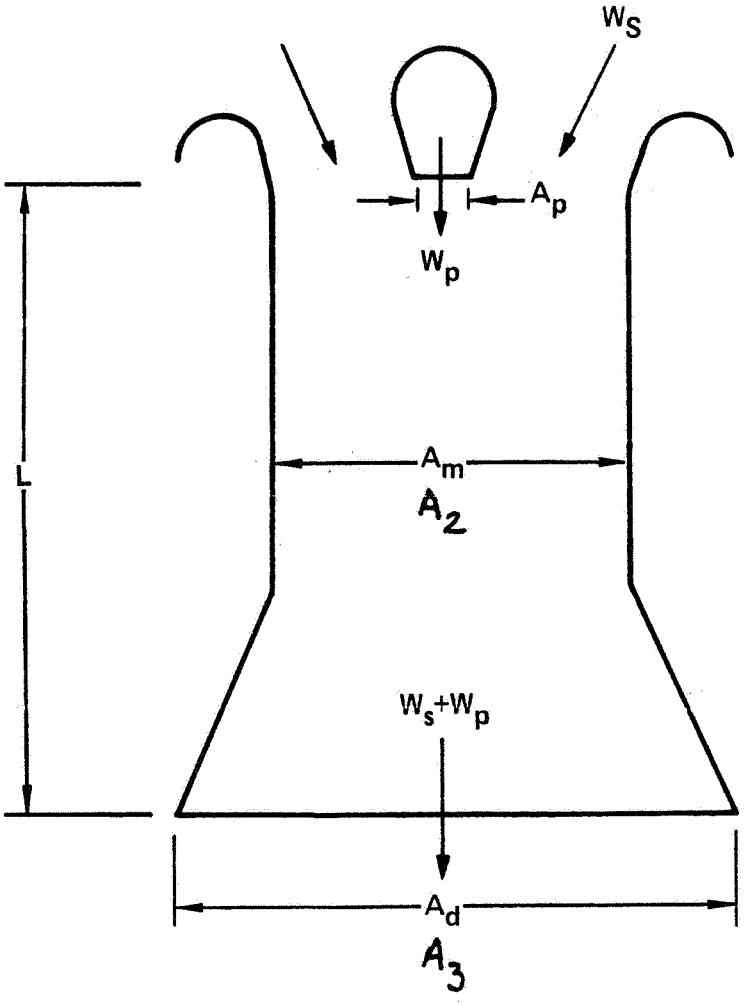

GEOMETRIC VARIABLES:

- MIXING SECTION AREA RATIO A_m/A_P
- DIFFUSER AREA RATIO $(A_m/A_d)^{-1}$
- LENGTH RATIO L/dm

AUGMENTATION RATIO

$$\phi = \frac{F_{GROSS}}{F_{ISENTROPIC\ PRIMARY}}$$

Figure 5.- Ejector definition.

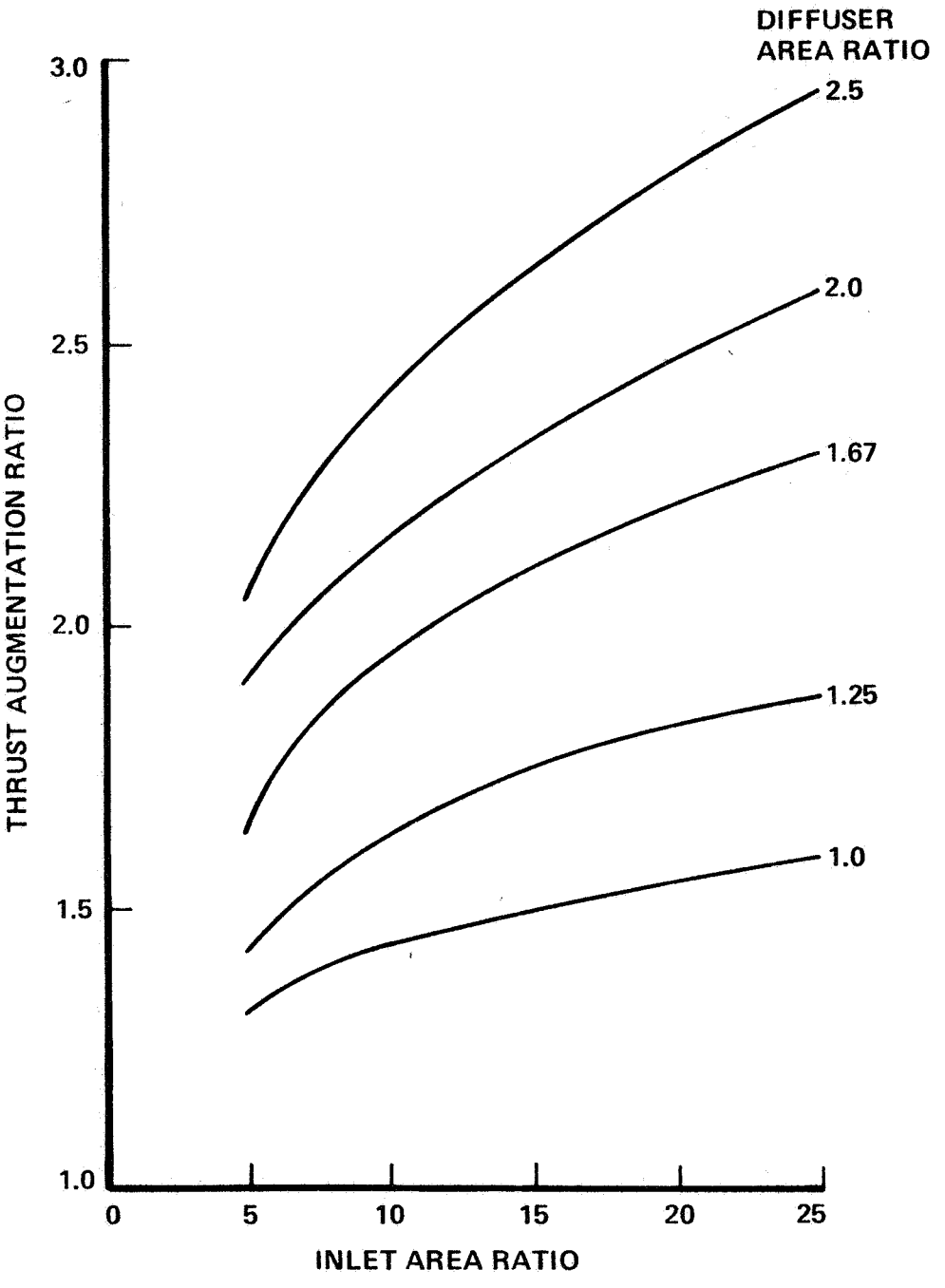

Figure 6.- Thrust augmentation of an ideal ejector.

- INLET TOTAL PRESSURE LOSS
- WALL FRICTION LOSS
- DIFFUSER LOSS
- MIXING LOSS

Figure 7.- Ejector performance losses.

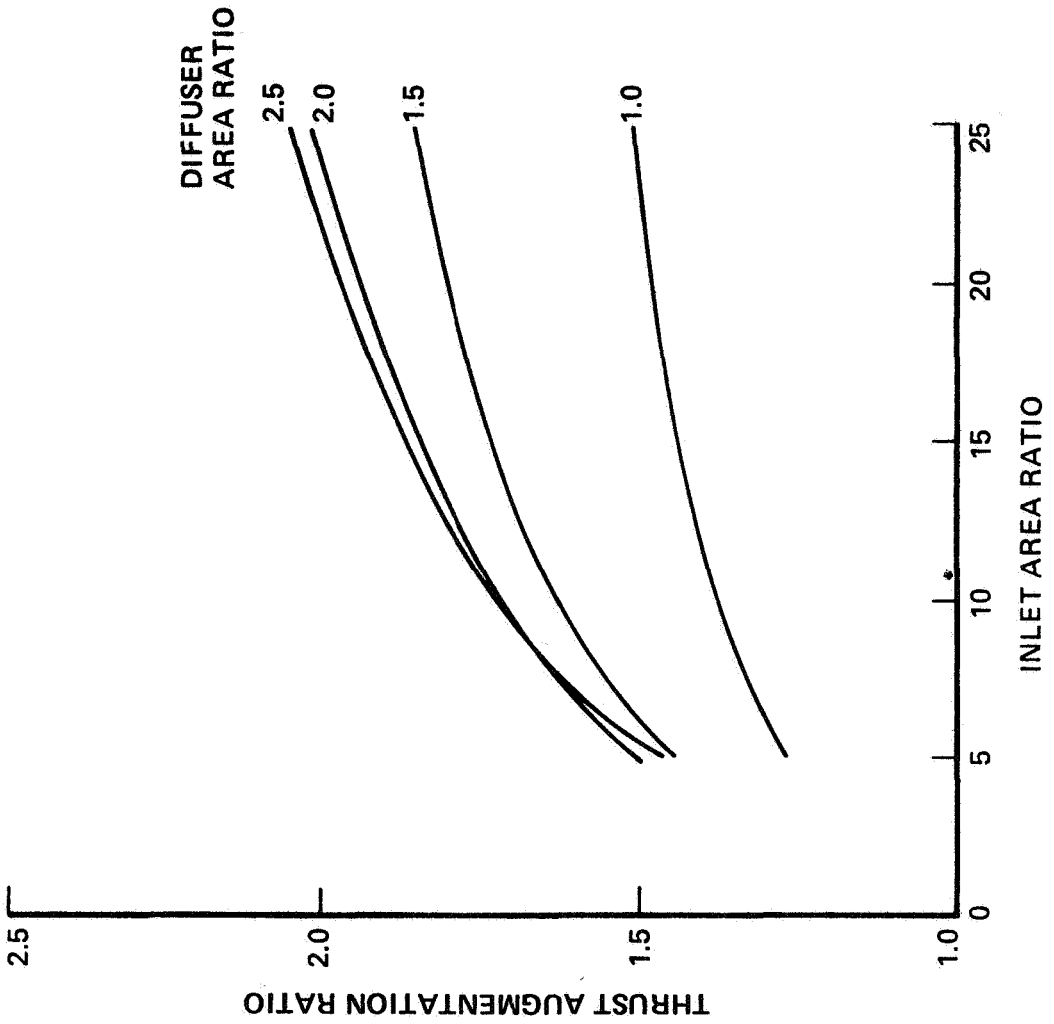

Figure 8.- Thrust augmentation with losses.

HIGH PERFORMANCE COMPACT EJECTORS

ARL HYPERMIXING NOZZLES STRAIGHT DIFFUSER	2.0
LTV TAILORED CONTOUR EJECTOR	1.87
ALPERIN JET DIFFUSER EJECTOR	2.09

ALL TESTED AT RELATIVELY LOW PR (PR < 2.5) AND AMBIENT TEMPERATURES

NSRDC AXISYMETRIC EJECTOR TESTS

MIXER ALONE	1.25
SINGLE VENTED DIFFUSER	1.35
STAGED VENTED DIFFUSER	1.45

TESTED TO PR OF 10 AT AMBIENT TEMPERATURE

Figure 9.- Summary of ejector performance.

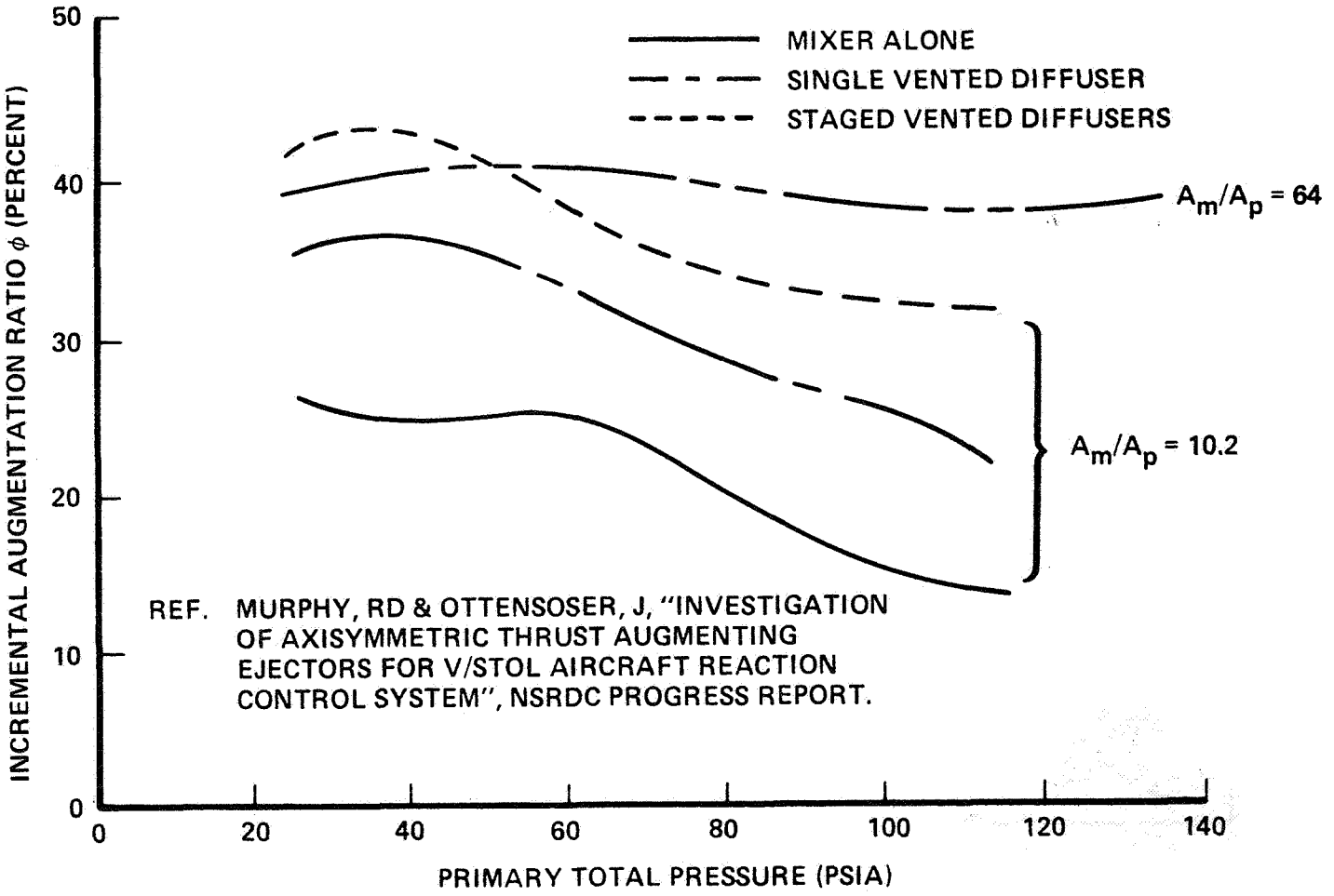

Figure 10.- Effect of primary pressure ratio on thrust augmentation.

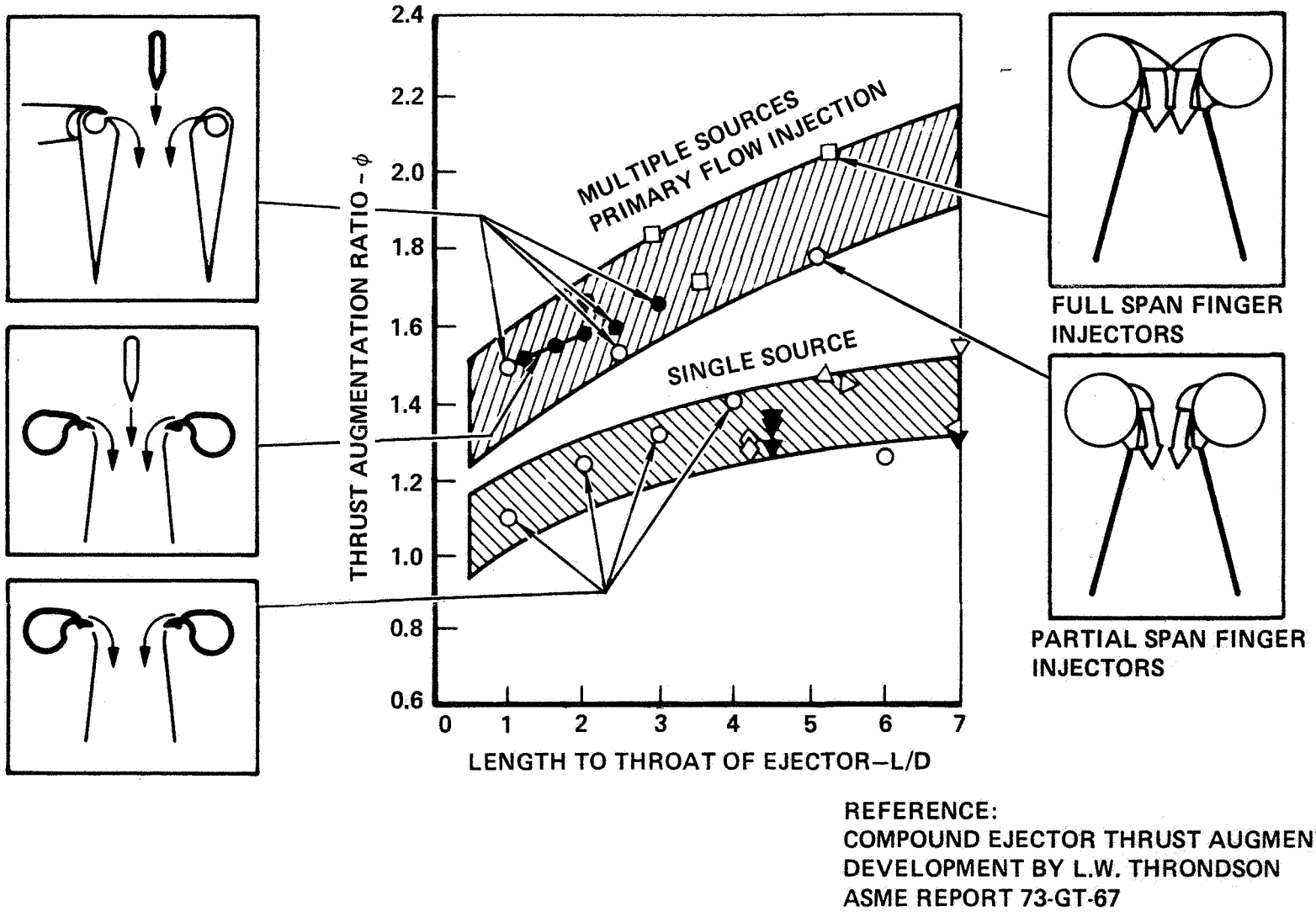

Figure 11.- Summary of ejector thrust augmentation experimentally achieved.

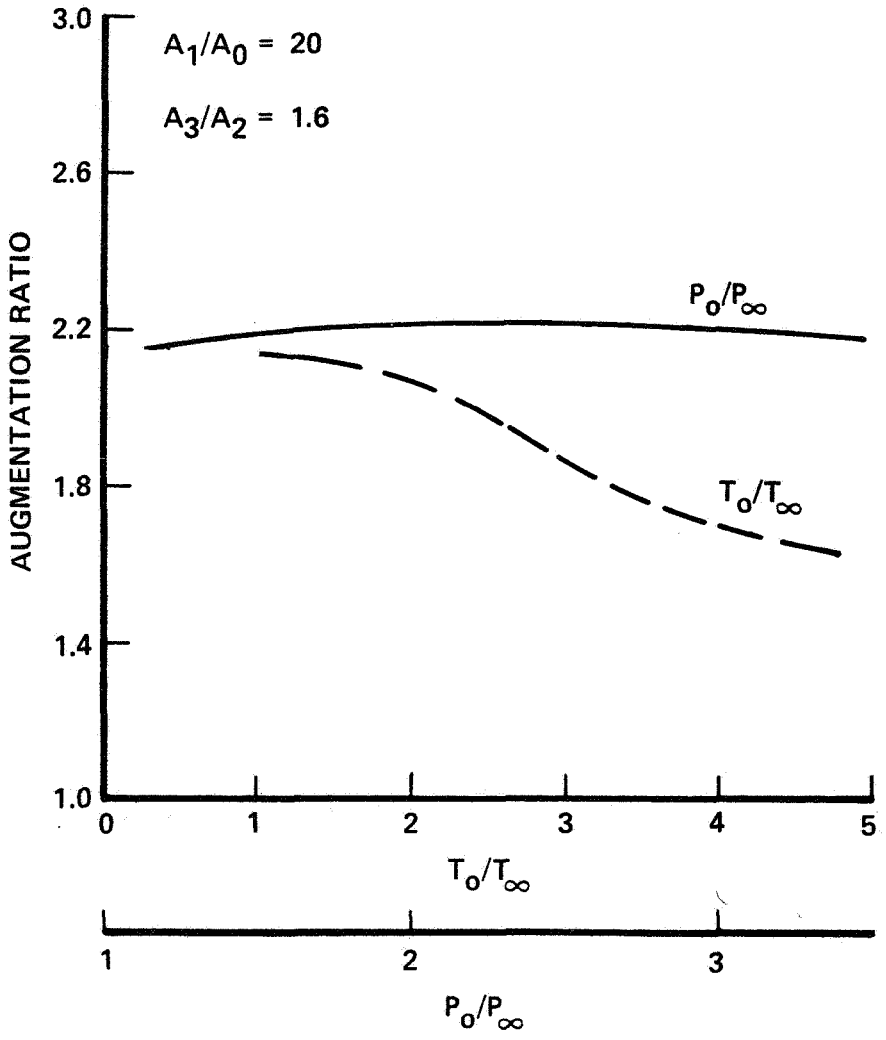

Figure 12.- Primary temperature and pressure ratio (theory).

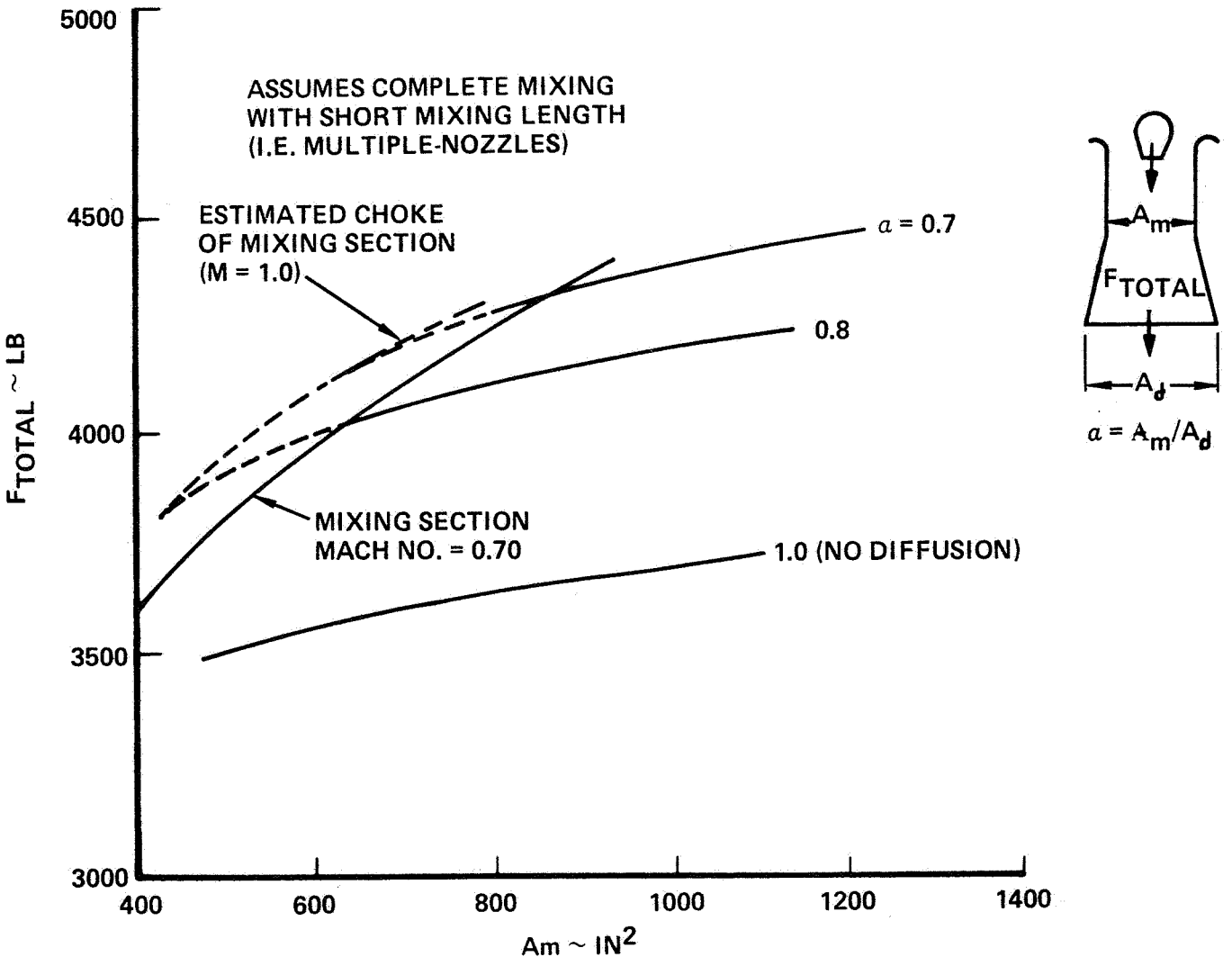

Figure 13.- Preliminary estimated augmentor performance.

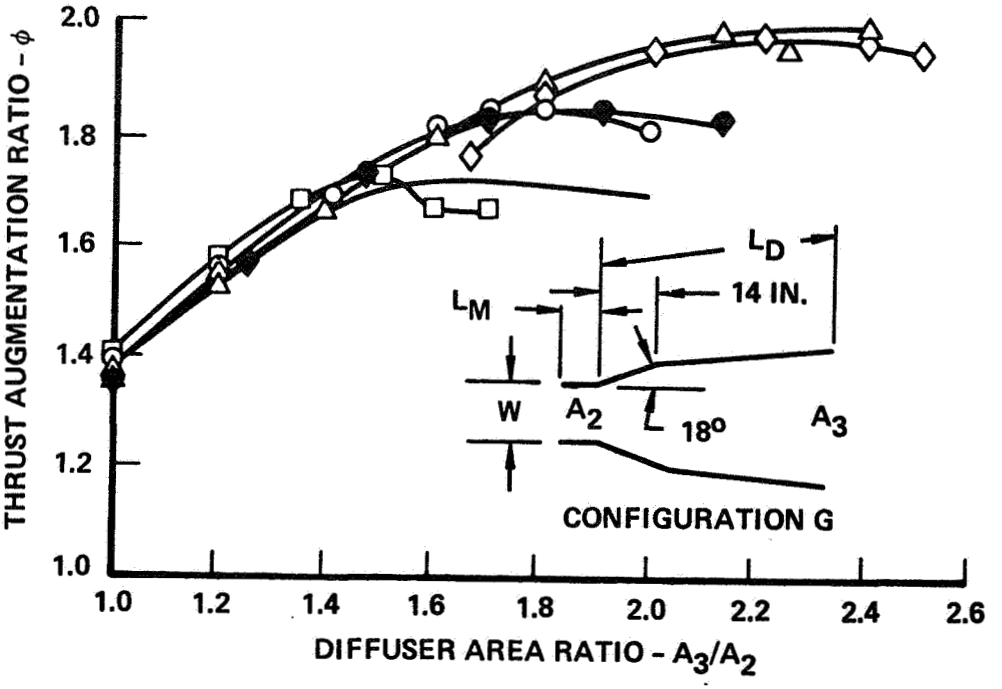

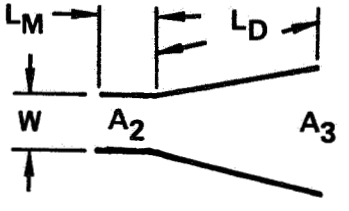

CONFIGS A - F

CONFIG	L_M	L_D	W	$L_{M/W}$	$L_{D/W}$
A ○	13	32.25	10	1.3	3.225
B □	13	15.25	10	1.3	1.525
C ●	5	23.0	10	0.5	2.30
D X	16	34.0	10	1.6	3.40
F △	5	45.0	10	0.5	4.50
G ◇	5	45.0	10	0.5	4.50

*QUINN, B. "COMPACT EJECTOR THRUST AUGMENTATION" JOURNAL OF AERONAUTICS VOL 10 NO. 8 AUGUST 1973

Figure 14.- Thrust augmentation of several ARL hypermixing configurations.*

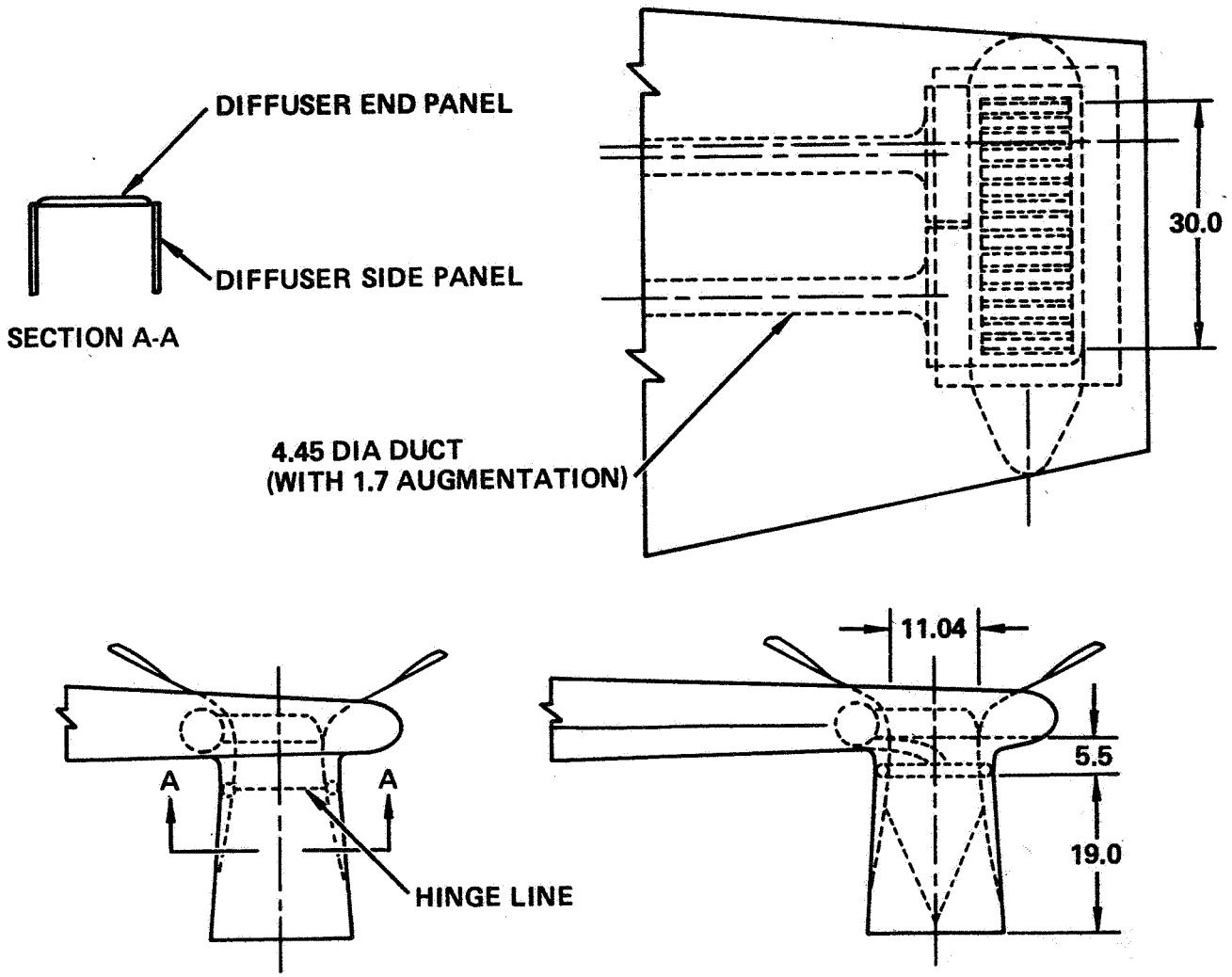

Figure 15.- Wing tip reaction control hypermixing ejector.

DESIGN AND TEST OF A PROTOTYPE SCALE EJECTOR WING

L. A. Mefferd, R. E. Alden and P. M. Bevilaqua
Rockwell International
Columbus Aircraft Division

Abstract

The use of analysis and scale model testing to design a full scale (prototype) ejector wing is described. A two-dimensional momentum-integral analysis was used to examine the effect of changing inlet area ratio, diffuser area ratio, and the ratio of ejector length to width. A relatively wide range of these parameters was considered. It was found that for constant inlet area ratio the augmentation increases with the ejector length, and for constant length: width ratio the augmentation increases with inlet area ratio. Scale model tests were used to verify these trends and to examine the effect of aspect ratio.

On the basis of these results, an ejector configuration was selected for fabrication and testing at a scale representative of an ejector wing aircraft designed to perform the U. S. Navy Type "A" mission. The test ejector was powered by a Pratt-Whitney F401 engine developing approximately 12,000 pounds of thrust. The results of preliminary tests indicate that the ejector is developing a thrust augmentation ratio better than $\phi = 1.65$. This is essentially the same level of augmentation obtained in the model scale tests. It is concluded that the combination of analysis and scale model testing can be used to design full size ejectors, although questions of scale and temperature effects remain.

INTRODUCTION

Since the cost of developing an aircraft at prototype scale is prohibitive, it has been usual to employ analytic methods and scale model testing in the initial stages of development. However, ejector development has been carried out largely by empirical and cut-and-try methods because suitable methods of ejector analysis and modelling had not been devised. Until recently only one-dimensional analyses of ejector performance were available.[1,2,3] These analyses were useful in identifying some of the factors that affect ejector performance and in establishing ideal levels of performance, but such parametric methods cannot be used for actual design purposes. For this it is necessary to predict the rate of entrainment due to the turbulent mixing within the ejector. Recently, Bevilaqua and McCullough[4] developed a two-dimensional, finite different analysis using integral methods for the jet entrainment, while Gilbert and Hill[5] used a mixing length model to calculate entrainment, and DeJoode and Patankar[6] used a two-equation turbulence model.

Various studies of ejector scale effects have given inconclusive results. The earliest study of aircraft ejector scale effect performed at the Pennsylvania State University[7] indicated that thrust augmentation increases with the ejector scale; however, aircraft scale ejectors built by Boeing[8] and DeHavilland[9] produced less augmentation than the laboratory models from which they were developed. Full scale Rockwell ejectors have generally performed as well as smaller models, but a limited study of the effects of size again suggested that augmentation increases with the scale.[10]

The purpose of this paper is to show that recently developed two-dimensional methods of analysis can be used with scale model testing to design prototype ejector wing aircraft. In the next section the use of the integral method to predict performance trends for a wide range of configurations is described. The results of scale model tests of three ejector configurations are compared to the analytic trends in the following section. In the last section test results from a prototype-scale ejector wing are compared to the analytic and scale models predictions.

METHOD OF ANALYSIS

We undertook to design a full scale ejector wing for a transport type aircraft such as that shown in Figure 1. The integral method of analysis[4] was used to make the initial trade-offs between ejector inlet area ratio and length to width ratio. Although the more sophisticated turbulence models[5,6] could be expected to give greater accuracy, such methods are too expensive and time consuming to use for parametric studies, which require many configurations to be analyzed. The integral method is a two-dimensional analysis in which the jet velocity profiles are assumed to have a self-preserving shape. Since there is a primary direction of flow (through the ejector) it is assumed that the thin shear layer approximation is applicable. This reduces the governing

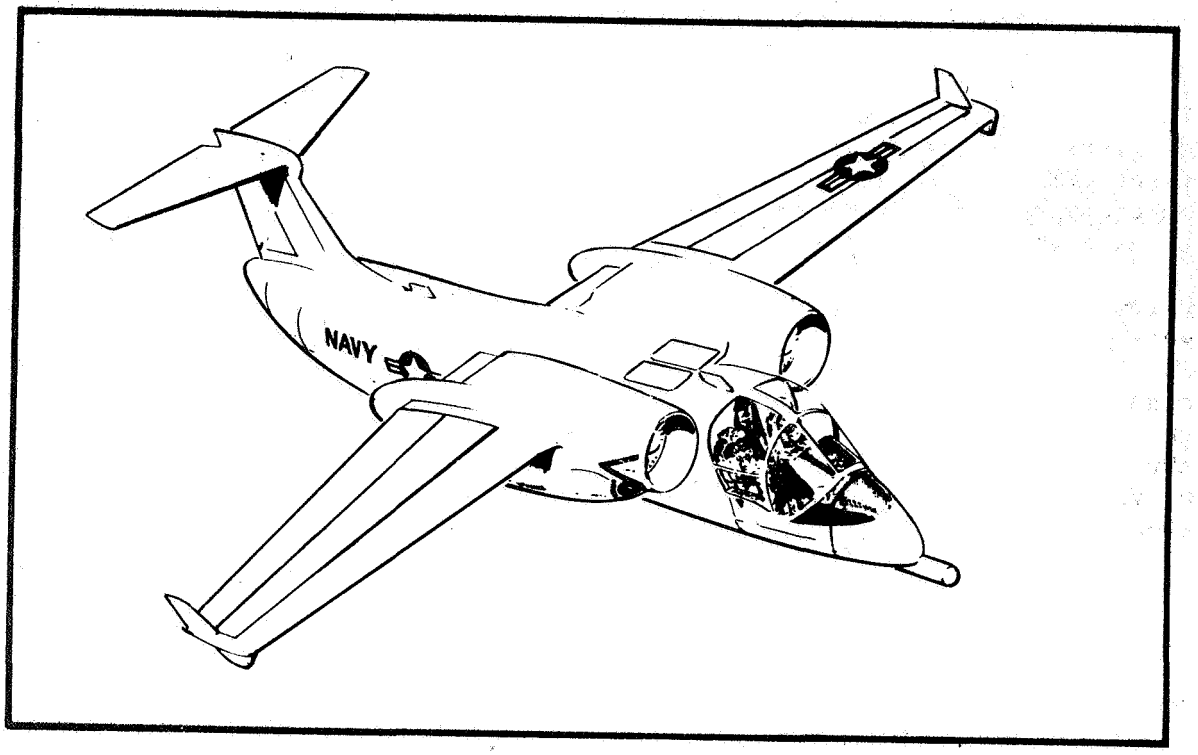

Figure 1. V/STOL aircraft utilizing ejector thrust augmentation in the wing.

elliptic equations to a parabolic set which can be solved by marching in the streamwise direction. A control volume approach was utilized to put the differential equations in finite difference form. The mass and momentum conservation equations are integrated over a control volume coinciding with the walls of the shroud and having length, dx, in the streamwise direction. Pressure and shearing stresses act on the fluid in the control volume at the walls and on the upstream and downstream faces.

The velocity distribution is represented by the superposition of a self-preserving jet velocity profile on a uniform stream. An explicit closure assumption relating the turbulent stresses to the mean flow was not made; however, the use of self-preserving mean velocity profiles is equivalent to an assumption that the stresses are proportional to the rate of strain. In this case the rate of entrainment can be specified by one empirical constant. These equations are solved simultaneously at each dx step through the ejector by straightforward algebraic procedures.

Although solution of the ejector equations has thus been transformed to an initial value problem that can be solved by a streamwise marching procedure, the basic elliptic character of the flow remains unchanged. This means that the velocities at the ejector inlet cannot be arbitrarily specified, but must be compatible with an outer flow that satisfies boundary conditions on the shroud and at infinity. Compatibility of the inner and outer flows is obtained by iterating on the inlet velocity until the exhaust pressure matches the static pressure outside the ejector exit.

This entrainment method provides a relatively simple procedure for calculating the turbulent mixing and entrainment within the ejector. It requires very short computing time, considerably less than one second on an IBM 370. Limitations of the program include the inability to compute compressibility effects and the influence of curvature on the turbulence in the Coanda jets.

Parametric trades between ejector throat width, W, and shroud length, L, were made by varying W at constant L/W, and by varying L/W at constant W. Results indicate that the larger inlet area ratios, A_2/A_0, at constant L/W consistently demonstrated higher levels of performance for the entire range of diffuser area ratios. A_2/A_0 was varied by changing the throat width, keeping A_0 constant. This was done for each of several different L/W's. A_2/A_0 is plotted against the maximum $\emptyset$ (thrust augmentation ratio) attainable at that L/W, Figure 2. Thrust augmentation ratio

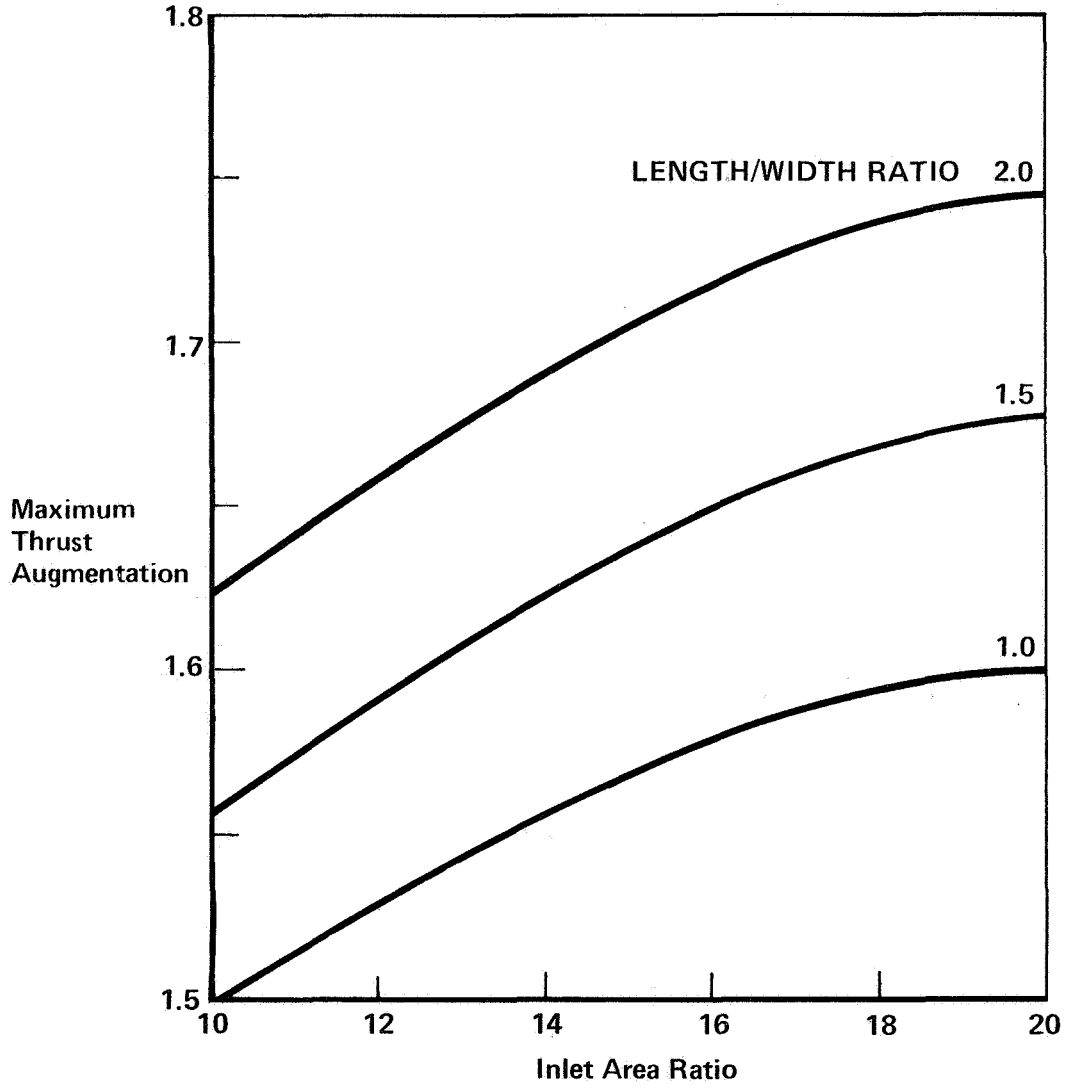

Figure 2. Predicted thrust augmentation ratio as a function of ejector geometry.

is defined as: total thrust/isentropic thrust. Since the computer program cannot predict separation, the diffuser area ratio which produced the peak performance was projected from previous emperical correlations between L/W and maximum diffuser area ratio, A_3/A_2, for rectangular augmenters. The analysis indicated:

- A change in A_2/A_0, in the A_2/A_0 = 10 to 16 range, has a sizable effect on augmentation.
- Augmentation is less sensitive to A_2/A_0 in the A_2/A_0 = 16 to 20 region; the percent increase with increasing A_2/A_0 begins to decline.
- An increase in L/W produces an increase in augmentation at each A_2/A_0. L/W testing performed shows that this rate of increase declines with increasing L/W.

MODEL TESTS

Testing to verify the analysis was carried out on the following three basic augmenter configurations. A typical configuration is shown in Figure 3.

Configuration	A_2/A_0	Average L/W	Average L (in)	W (in)	AR
1	13.1	1.53	6.15	4.02	8.488
2	17.3	1.55	8.2	5.32	6.415
3	17.3	1.73	9.22	5.32	6.415

As was done in the analysis, A_2/A_0 was varied by changing the throat width, keeping A_0 constant. In Figure 4 the measured change in augmentation with diffuser area ratio is shown for two inlet area ratios at L/W = 1.53 and for two shroud lengths at A_2/A_0 = 17.6.

The maximum performance from each of the test configurations was slightly below the predicted value; the trends produced compared favorably (Figure 5). The discrepancy in absolute values between the analysis and the test values is at least partly related to the fact that the analysis is for 2-D flow disregarding endwall effects. Local Ø values near the endwalls are considerably lower than midspan values, thus lowering the average value.

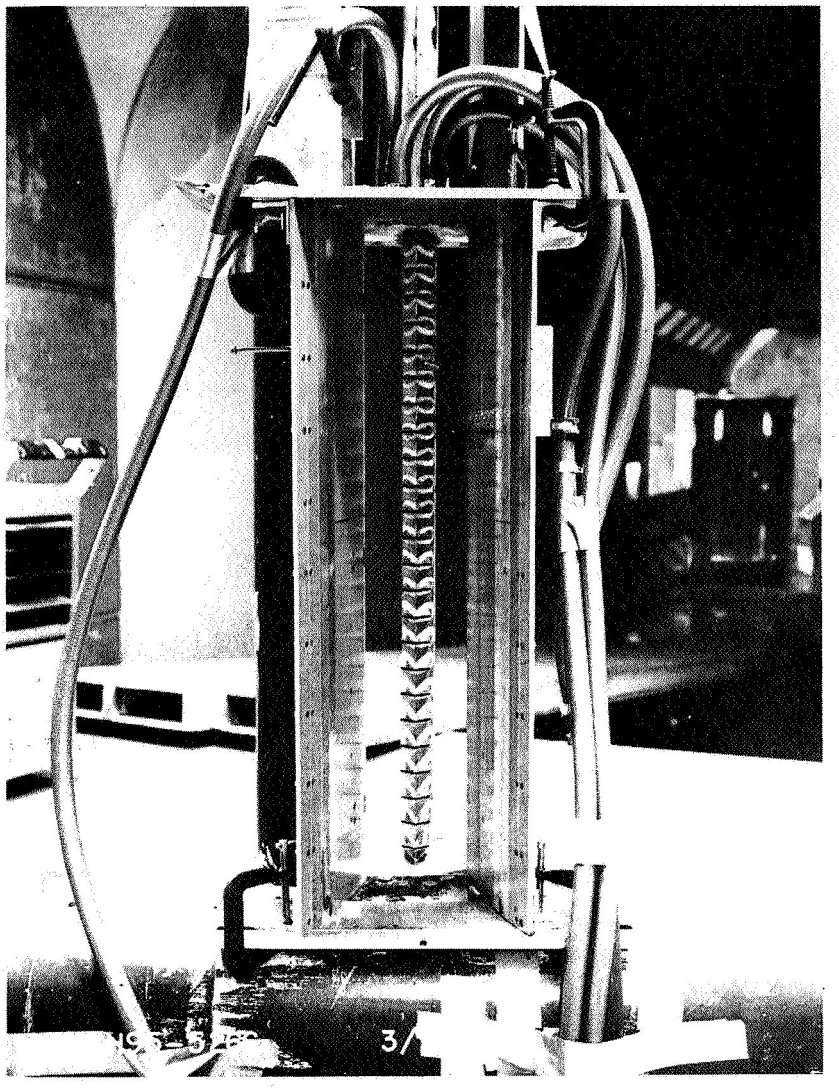

Figure 3. Scale model ejector utilized for all three test configurations.

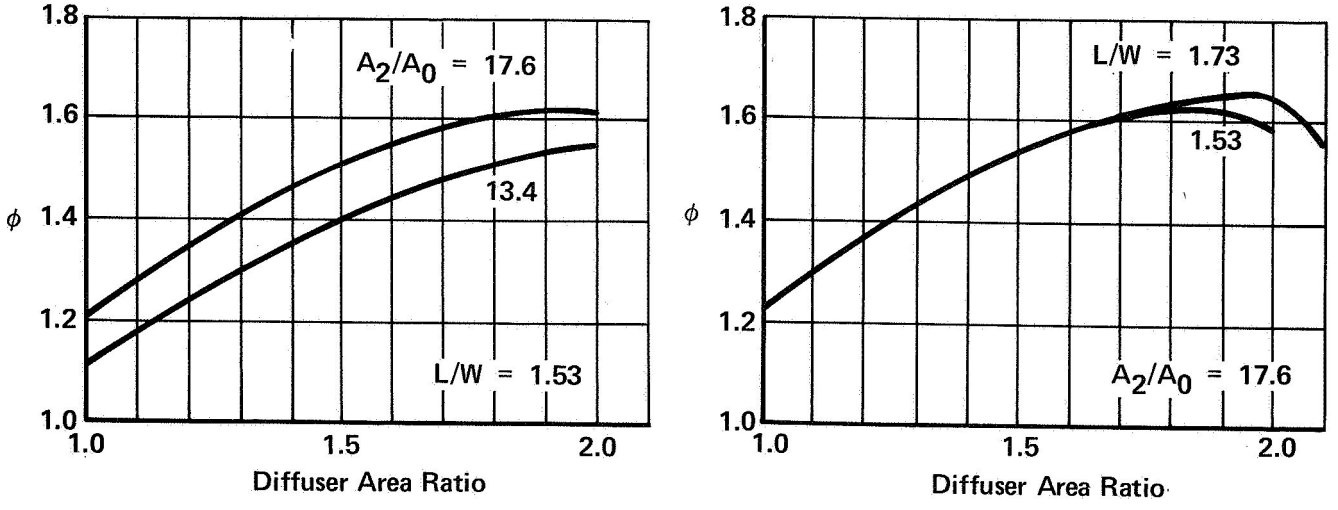

Figure 4. Thrust augmentation ratio measured for the scale model ejectors.

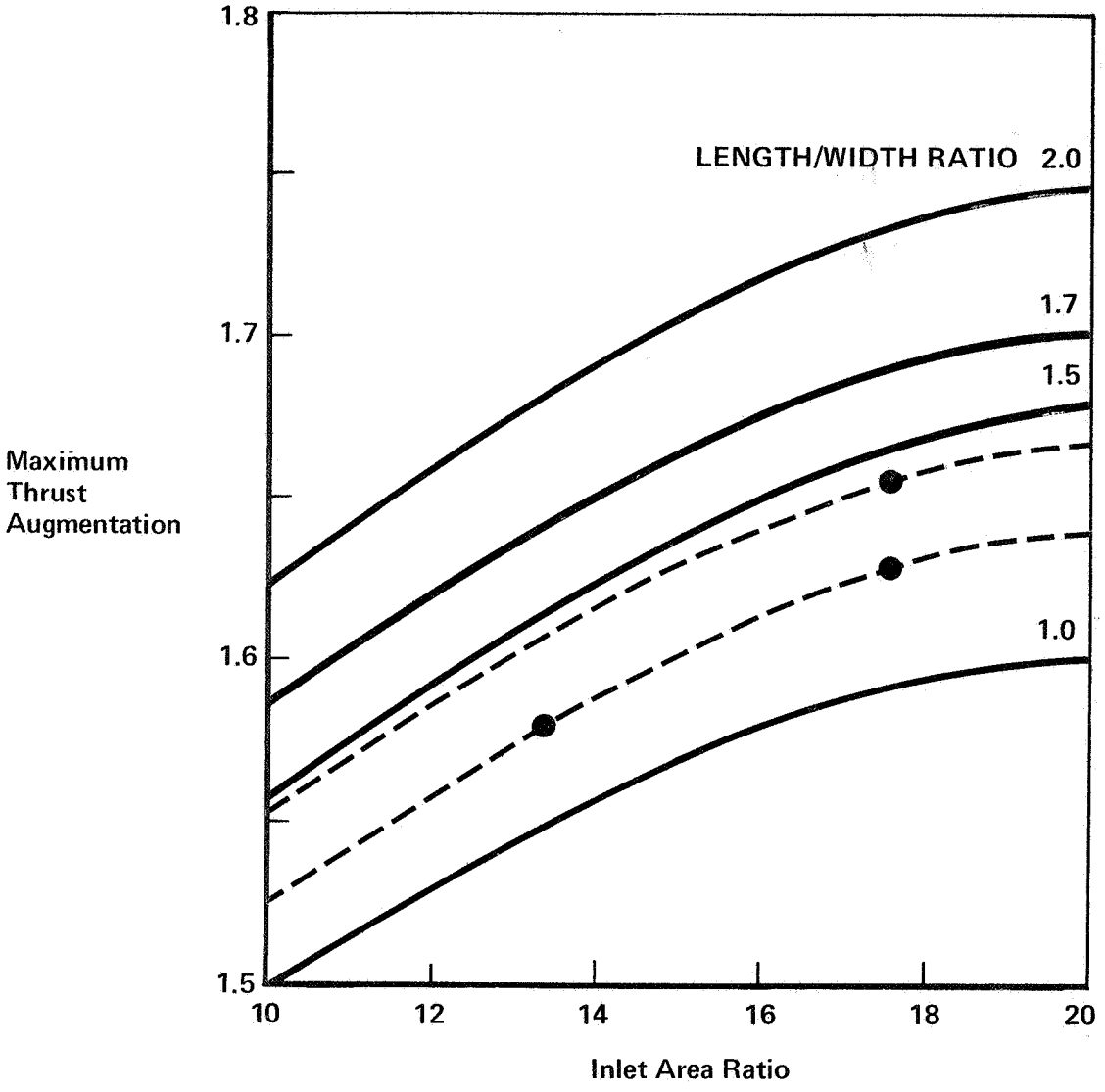

Figure 5. Comparison of predicted (———) and measured (- - -) thrust augmentation ratio.

FULL SCALE PROTOTYPE TESTS

Utilizing results from the analysis and from the small scale model testing, a full scale prototype ejector wing configuration was selected for fabrication and testing. A size was chosen that was representative of an ejector wing aircraft configured to perform the U. S. Navy Type A mission. A section through the full scale prototype augmenter wing is shown superimposed on the airplane ejector wing in Figure 6.

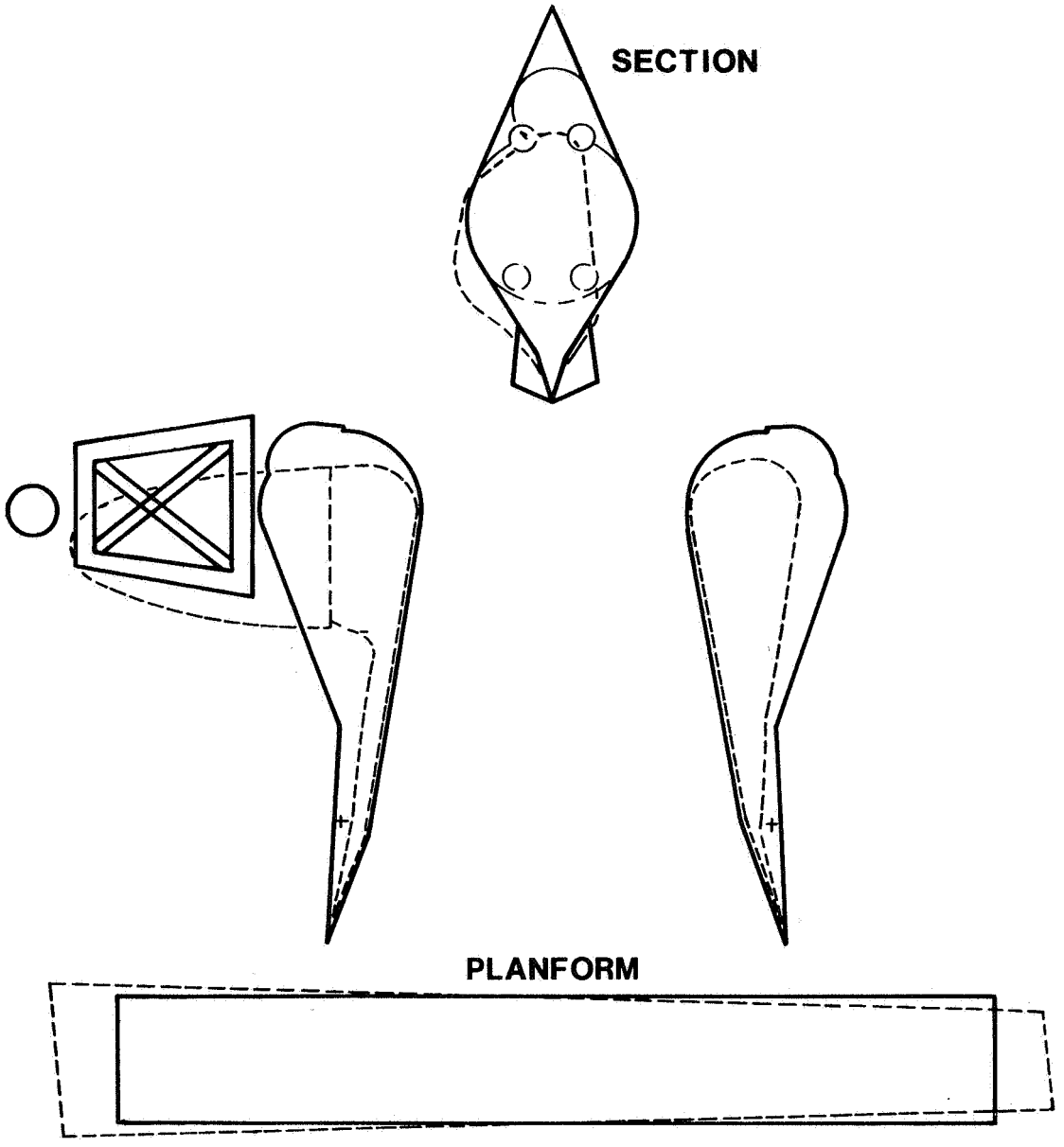

Figure 6. Comparison of aircraft wing design (- - -) and prototype ejector wing tested (———).

Particular attention was given to the design parameters which had been identified by both the analytical and empirical studies as producing significant effects on augmenter performance. This effort resulted in the augmenter wing which is shown in Figure 7.

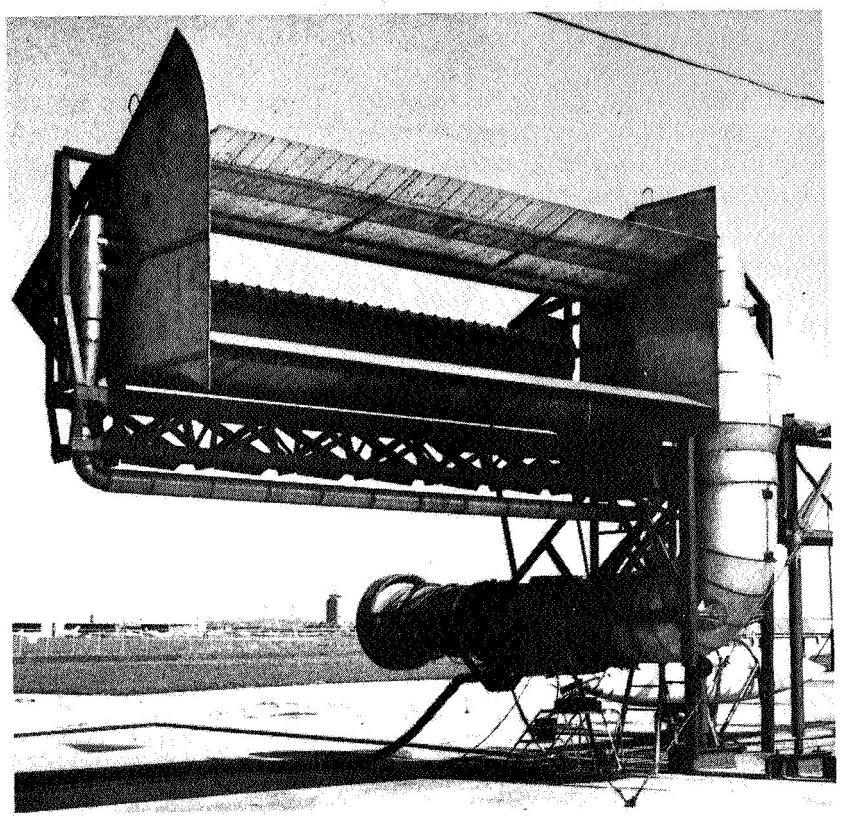

Figure 7. Prototype scale ejector wing shown rotated 90° to minimize ground effects.

The major parameters of the configuration are:

Span	245.8 inches
Throat (W)	38 inches
Flap Length (L)	60 inches
A_0	561 sq inches
Flow Split	(Coanda, 20%; Center Nozzle, 55%; Endwalls, 5%)

The large scale augmenter test facility was intentionally designed to feature a high degree of testing flexibility. This flexibility allows variations in a number of major augmenter geometric parameters such as throat width (W), flap length (L), Coanda nozzle gap (t), and diffuser flap angle (δ_F). The test facility as a whole also allows a great deal of testing flexibility and includes the capability to rotate the entire augmenter panel, vary the static height of the augmenter panel above the ground plane, and provisions for "taxi" and "flight" testing modes. Specific instrumentation and recording capability can be added as required.

The complete test article consists of a ninety (90) foot steel boom, a thirty (30) foot model support frame, engine mount facility for cradling the XF401 U. S. Navy engine (this engine being available on site for use), two twenty (20) foot flaps with both flaperon units and extender surfaces, the twenty (20) foot centerbody, the air distribution systems consisting of the plenum, and various pieces of ducting hardware, and the boom tie-down structure.

Initial testing of the full scale prototype augmenter wing has shown that the configuration is developing a thrust augmentation ratio in the $\phi = 1.65$ range.

Large scale performance measurements (throat velocity, flow quality) indicate that its overall performance level can be increased. Utilizing the flexibility built in the large scale augmenter evaluation will permit: (a) increasing L/W, (b) limited variations in A_2/A_0, and (c) increasing A_3/A_2 delaying flow separation to higher values of diffuser area ratio. Comparison of test results from this configuration with those obtained from its scale model counterpart indicate that the large scale ejector is currently obtaining augmentation ratios similar to the model at comparable A_3/A_2 ratios, all other design parameters being consistent (Figure 8).

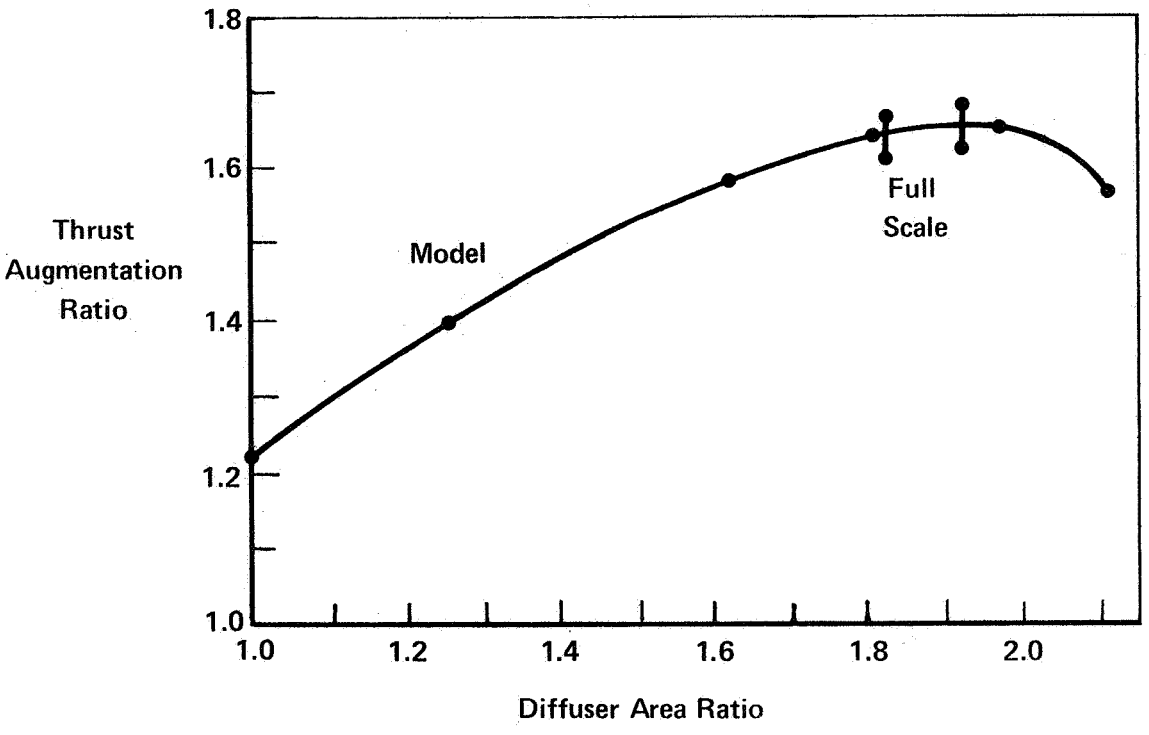

Figure 8. Comparison of measured thrust augmentation ratio at prototype and model scales.

This result suggests that apparent scale effects in previous tests were probably related to differences in internal ducting, primary jet temperature, method of construction, and other features that were not scaled. However, the present results should not be taken as proof that there are no scale effects. For example, in modeling the characteristics of jets, it is necessary that the Reynolds number be held constant. This is because small scale eddy motions are affected by Reynolds number; however, it is the large scale eddies that control the rate of entrainment and these are independent of Reynolds number. Thus, if the Reynolds numbers for both the original and model jets are large enough to insure that the flow is turbulent, equality of Reynolds number is not necessary to scale jet entrainment. On a more elementary level, the "square-cube law" for scaling implies that frictional effects are greater in small ejector models, because the model has greater wall surface (L^2) in relation to volume (L^3) than a full scale ejector. As long as the model is not made too small, frictional forces are almost negligible and may not reduce the augmentation significantly. Since the effect of increasing the temperature of the primary jet is to reduce the augmentation, these effects may have been equal and opposite in the present tests.

CONCLUSION

With the use of physical reasoning and mathematical analysis, scale model testing can be used for initial development of prototype scale ejectors. However, further study of ejector scale and temperature effects is needed to separate extraneous influences from true scale effects.

REFERENCES

1. von Karman, T., "Theoretical Remarks on Thrust Augmentation," in Contributions to Applied Mechanics, Reissner Anniversary Volume, pub. by J. W. Edwards, Ann Arbor, Michigan 1949, pp 461-468.

2. McCormick, B. W., "Aerodynamics of V/STOL Flight," Academic Press, New York, 1967.

3. Salter, G. R., "Method for Analysis of V/STOL Aircraft Ejector," Journal of Aircraft, Vol. 12, Dec. 1973, pp. 974-978.

4. Bevilaqua, P. M. and McCullough, J. K., "Entrainment Method for V/STOL Ejector Analysis," AIAA Paper 76-419, San Diego, CA, July 1976.

5. Gilbert G. E. and Hill, P. G., "Analysis and Testing of Two-Dimensional Slot Nozzle Ejectors with Variable Area Mixing Sections, NASA CR-3351, 1973.

6. DeJoode, A. D. and Patankar, S. V., "Prediction of Three-Dimensional Turbulent Mixing in an Ejector," AIAA Journal Vol. 16, Feb. 1978, pp. 145-150.

7. Fought, D., "Test and Analysis of a Coanda Thrust Augmentation Nozzle," M.S. Thesis, Penn State Univ., 1960.

8. Ashleman, R. H. and Skavdahl, "Development of an Augmenter Wing Jet STOL Research Airplane," NASA CR-114503, Aug. 1972.

9. Whittley, D. C., "Augmenter Wing Technology for STOL Transport Aircraft," VTSI Short Course, Oct. 1975.

10. Stewart, V. R., "A Study of Scale Effects on Thrust Augmenting Ejectors," NADC Contractor Report NR76H-2, Feb. 1976.

A Technical Note Entitled:

"The External Augmentor Concept for V/STOL Aircraft"

by

D.C. Whittley

The de Havilland Aircraft of Canada, Ltd.

THE EXTERNAL AUGMENTOR CONCEPT FOR V/STOL AIRCRAFT

(D. C. Whittley)

INTRODUCTION

The beneficial aspects of an ejector powered V/STOL concept have been well documented previously as follows:

- low temperature and low velocity of the lifting jet due to mixing which lessens the severity of ground erosion and makes handling of the aircraft easier - especially on a flight deck;
- augmentation of thrust which reduces powerplant size and weight;
- mixing of the jet within the augmentor which reduces noise;
- essential absence of rotating machinery which results in simplicity and low maintenance costs, etc.

Although these benefits are well recognized, there remains some doubt regarding the feasibility of satisfactorily incorporating an ejector system in a high performance V/STOL aircraft because the designer must solve the problems peculiar to the ejector concept as well as those generally associated with a VTOL design of any kind. In the "External Augmentor" concept, de Havilland engineers have attempted to avoid some of these major difficulties and make accommodation for others.

The concept is based on the use of chordwise ejector slots which are located adjacent to and on either side of the fuselage (Figure 1). The configuration is characterized by a marked absence of some of the classical aerodynamic interference problems which are associated with many low disc loading V/STOL configurations. Special consideration

has been given to the difficulties associated with integration of the ejector system which normally occupies a very large volume within the aircraft profile. The design of the ejector itself may be considered optional; however, a particular ejector has been designed as part of a research and evaluation program for the External Augmentor concept. A relatively low level research program to study the concept has been underway since 1966 funded by de Havilland, the Canadian Department of National Defence and NASA, Ames Research Center.

SOURCES OF EXPERIMENTAL DATA

(a) Small scale tests described in Reference 1 including both wind tunnel and ejector component tests.

(b) Large scale static tests described in Reference 2. A J-85 powered model was tested in ground effect.

(c) Small and large scale ejector development tests undertaken in the de Havilland Aerodynamics Research Laboratory.

(d) Static and wind tunnel tests of a large scale model in the NASA Ames 40' x 80' wind tunnel (Figure 2). It should be noted that 80% of the thrust issues from the fuselage ejector whereas the remaining 20% issues from an augmentor flap at the trailing edge.

AERODYNAMIC INTERFERENCE IN TRANSITION FLIGHT

The general trend of jet-induced aerodynamic interference effects has been described in Reference 3. Thiere is usually a loss in lift which tends to increase with forward velocity and an increment in nose-up pitching moment which increases with speed in a similar manner. These effects are evident in the absence of a horizontal tail - addition of the tail generates further increments, especially in pitching moment. It has been suggested that these adverse characteristics occur because the lifting jets roll up beneath the wing to form a pair of strong trailing vortices. This vortex pair causes an induced twist on the wing and an induced camber over the length of the fuselage (Reference 3).

In the case of the external augmentor, the two jets which issue from beneath the fuselage, coalesce to form a single keel-like jet which does not roll up to form a vortex pattern (or, which does so only at an appreciable distance downstream). In any event, test results have shown that lift loss effects are not apparent and pitching moment increments are small.

Based on early tests described in Reference 1, it was shown that, essentially, lift characteristics could be predicted simply by adding the appropriate static jet reaction to the "power-off" aerodynamic forces. Tests in the Ames 40' x 80' wind tunnel gave similar indications as shown in Figure 3. In this case, the wing is fitted with a powerful augmentor flap which generates supercirculation round the wing. The

aerodynamic lift, as represented by $C_{L_{aero}}$, is obtained by subtracting the appropriate static jet reaction of lift from the wind tunnel measurement of lift. It can be seen that values of $C_{L_{aero}}$ in excess of one were achieved at $\alpha = 0^{o}$ and that lift coefficient varies with blowing coefficient in the expected manner: by inference, it is concluded that aerodynamic interference effects are very small.

Similarly, pitching moment variations with forward velocity were small as shown in Figure 4. Normally, turning of airflow into the intake would create a large nose-up moment - as in the case of the fan-in-wing, for example. Flow visualization tests have shown that airflow to the intake of the chordwise ejector (with strake) follows a vortex pattern and enters from the side, as it were, rather than from the front (Figure 5). This may provide an explanation for the absence of large nose-up pitching moments.

Ingestion of the vortex (as depicted in Figure 5) has a beneficial effect in that both static longitudinal and lateral stability remain well ordered simply because flow over the wing is not upset by a streamwise vortex over the upper surface (which otherwise would be present). Power-on and power-off lateral characteristics are shown in Figure 6.

GROUND EFFECTS

Jet flow which strikes the ground generally adheres to it and spreads outward. Air becomes entrained into the spreading jet(s) setting up a flow field which creates a down load on the wing (a phenomenon known as suck-down). It was recognized that this effect is fundamental and little could be done to eliminate it; therefore, in the case of the "External Augmentor" it was decided to incorporate a ground cushion acting on the underside of the fuselage to offset lift loss on the wing. The magnitude of this fuselage ground cushion effect is shown in Figure 7 as measured on the J-85 powered rig.

Since there are no discreet jets, as such, it follows that the jet fountain effect is not encountered. Therefore it can be expected that hot-gas ingestion would be minimized. This has been demonstrated on the J-85 powered rig and it is expected to re-affirm this conclusion when static tests take place at Ames on the J-97 powered model.

INTEGRATION AND ACCOMMODATION OF THE EJECTOR SYSTEM

The designer is required to provide accommodation for ducting, nozzles and the diffuser passage which, taken together, occupy a large volume within the profile of the aircraft. In the de Havilland concept, the diffuser passage is situated external to the normal aircraft profile and is formed by doors, housed in the fuselage side, which are deployed to form the diffuser, (see Figure 8). By this means, the frontal area is kept to a minimum so as to reduce supersonic wave drag. With the same objective in mind, the exhaust gas pressure ratio of the engine should be about 3 to 3.5: in this way, the internal duct volume is kept reasonably low.

A general arrangement of a proposed supersonic V/STOL aircraft is shown in Figure 9.

THE EJECTOR

The ejector nozzle system for the large model is made up of a simple array of plain nozzles each having an aspect ratio of 60. Some details of the fuselage ejector are given as follows:

Chordwise length	98.0 in.
Throat width	10.5 in.
Exit width	16.8 in.
Diffuser length	34.0 in.
Number of nozzles per side	60

Performance of the fuselage ejector is shown in Figure 10 as measured on the large scale model. Thrust augmentation is defined in the following manner:

$$\text{Gross thrust augmentation, } \phi_G = \frac{\text{measured model thrust}}{\text{nozzle thrust}}$$

Performance of the system as a whole has been determined by measurement of model thrust with augmentor flap deflected to 90°. The ratio of model thrust to thrust of the bare engine is 1.52 at a pressure ratio of 3.

Figure 11 shows a comparison between cold flow tests in the DHC laboratory on an twelve nozzle segment of the augmentor and tests on the large scale model at a temperature of 700°C (approximately). Also shown, is the duct loss between the engine and the nozzle exit plane.

Some tests have been carried out at de Havilland on a similar ejector with a nozzle aspect ratio of 100. The model is half scale relative to the large scale wind tunnel model. Some results, shown in Figure 12, indicate the variation of augmentor performance with diffuser length and with pitch spacing ratio.

CONCLUSIONS AND RECOMMENDATIONS

It is believed that the External Augmentor concept has a basic inherent simplicity together with sufficient augmentor performance potential to make feasible a high performance V/STOL aircraft based on ejectors.

More research is required in a number of areas - the next major step in the development of the concept would be to design and build an piloted hovering test bed.

REFERENCES

1. Whittley, D.C. — Ejector Type Thrust Augmentors for VTOL. ICAS Paper 70-56, Rome 1970.

2. Whittley, D.C. — Ejector-Powered Lift Systems for V/STOL Aircraft. CASI Journal, May 1974.

3. Marguson, R.J. — Review of Propulsion-Induced Effects on Aerodynamics of Jet/STOL Aircraft. NASA TND-5617, February 1970.

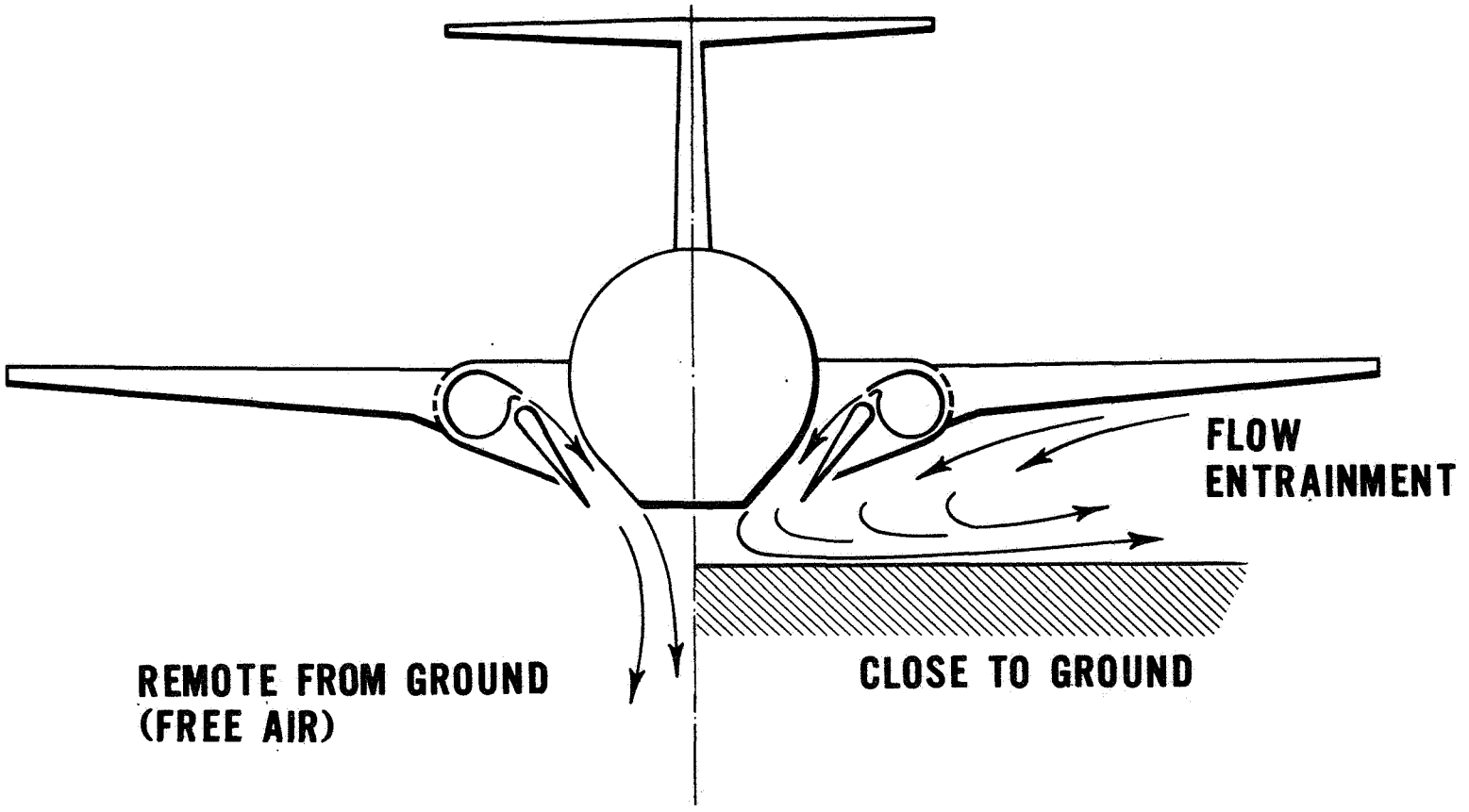

Figure 1.- External augmentor V/STOL concept flow patterns.

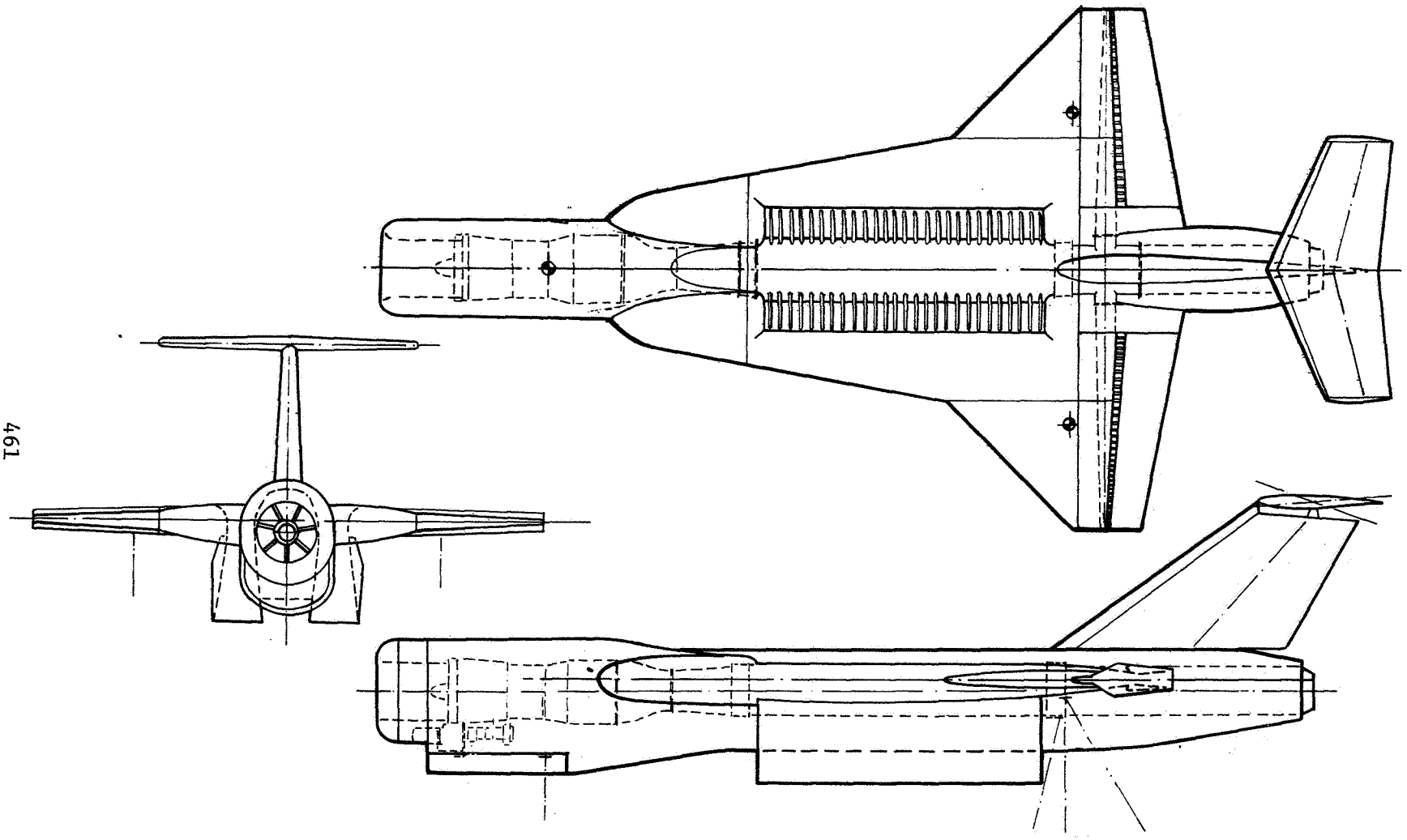

Figure 2.- DHC external augmentor V/STOL concept; G.A. of J-97 powered model.

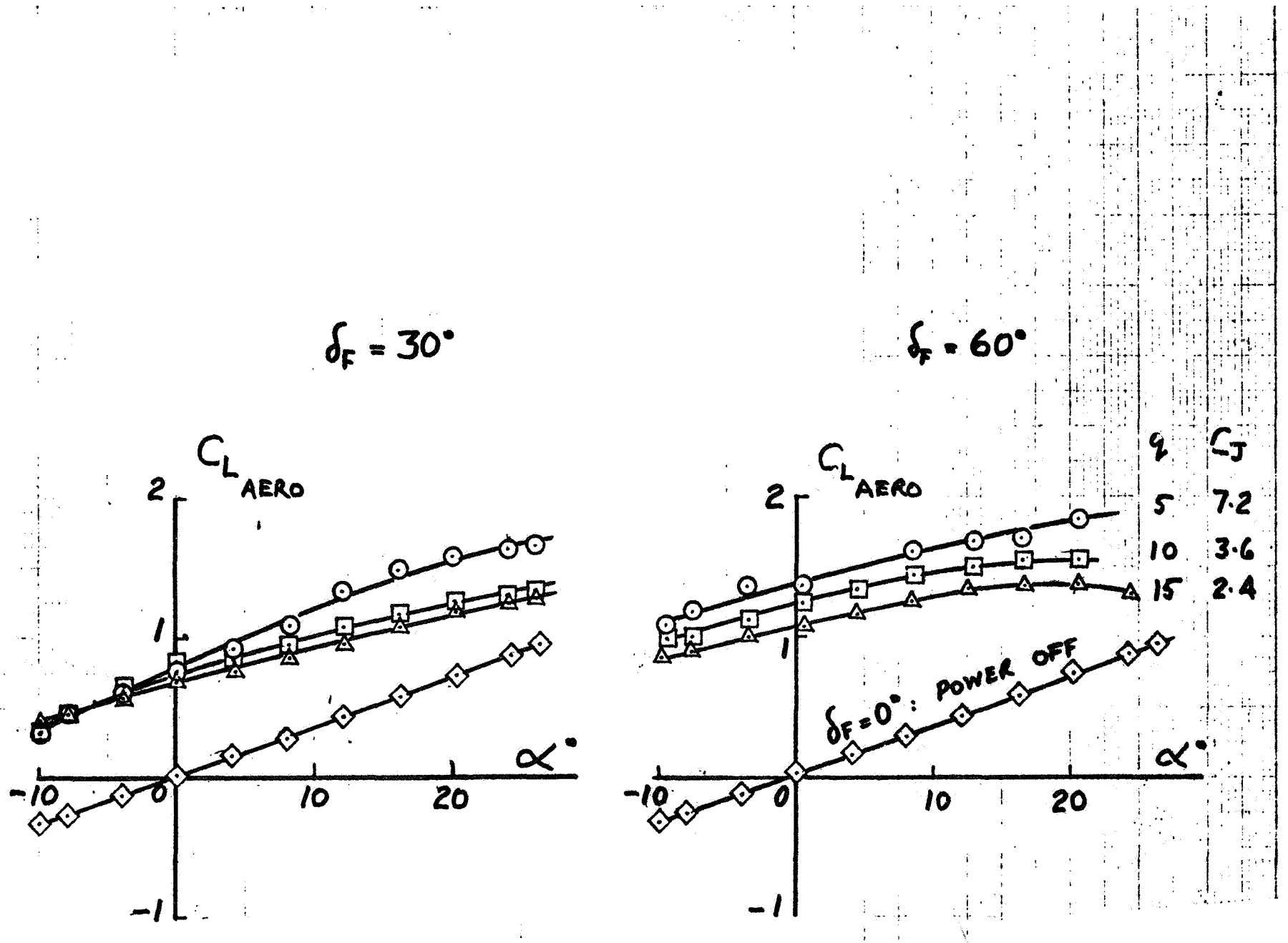

Figure 3.- Aerodynamic lift coefficient.

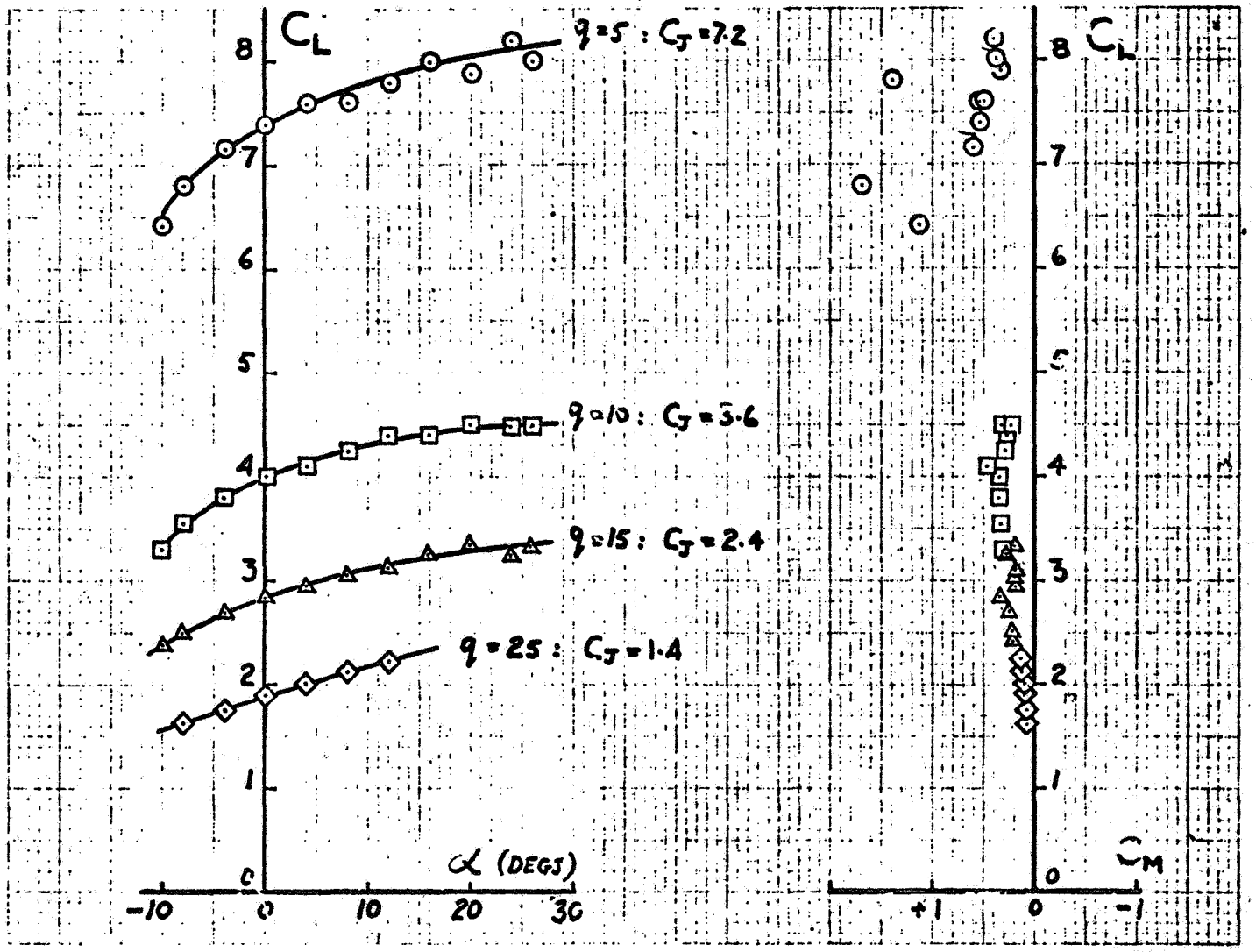

Figure 4.- Longitudinal characteristics; δ_F = 30°, NPR = 2.5.

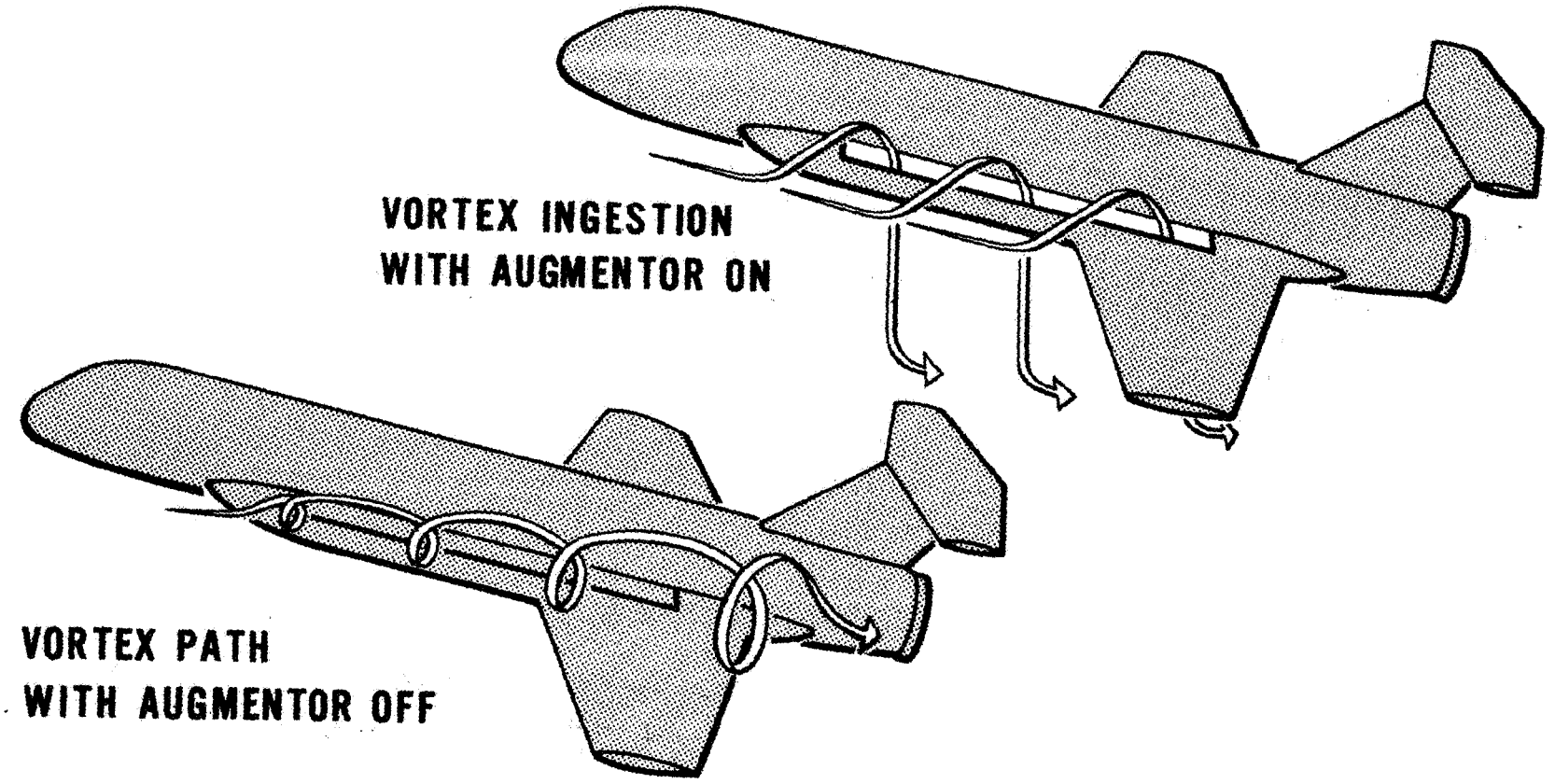

Figure 5.- Vortex behavior with augmentor.

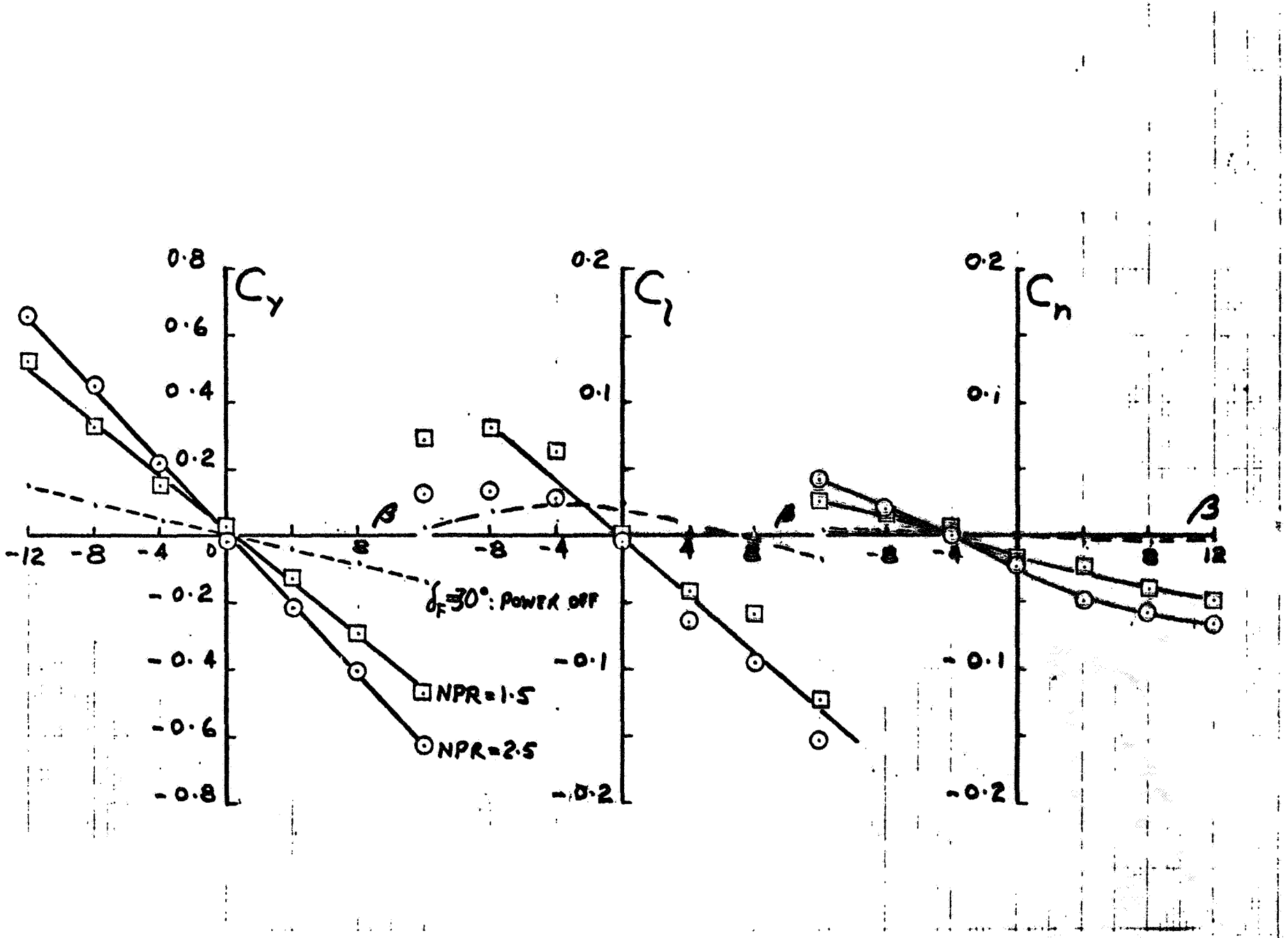

Figure 6.- Lateral directional characteristics; δ_F = 30°, q = 10 psf, α = 0°.

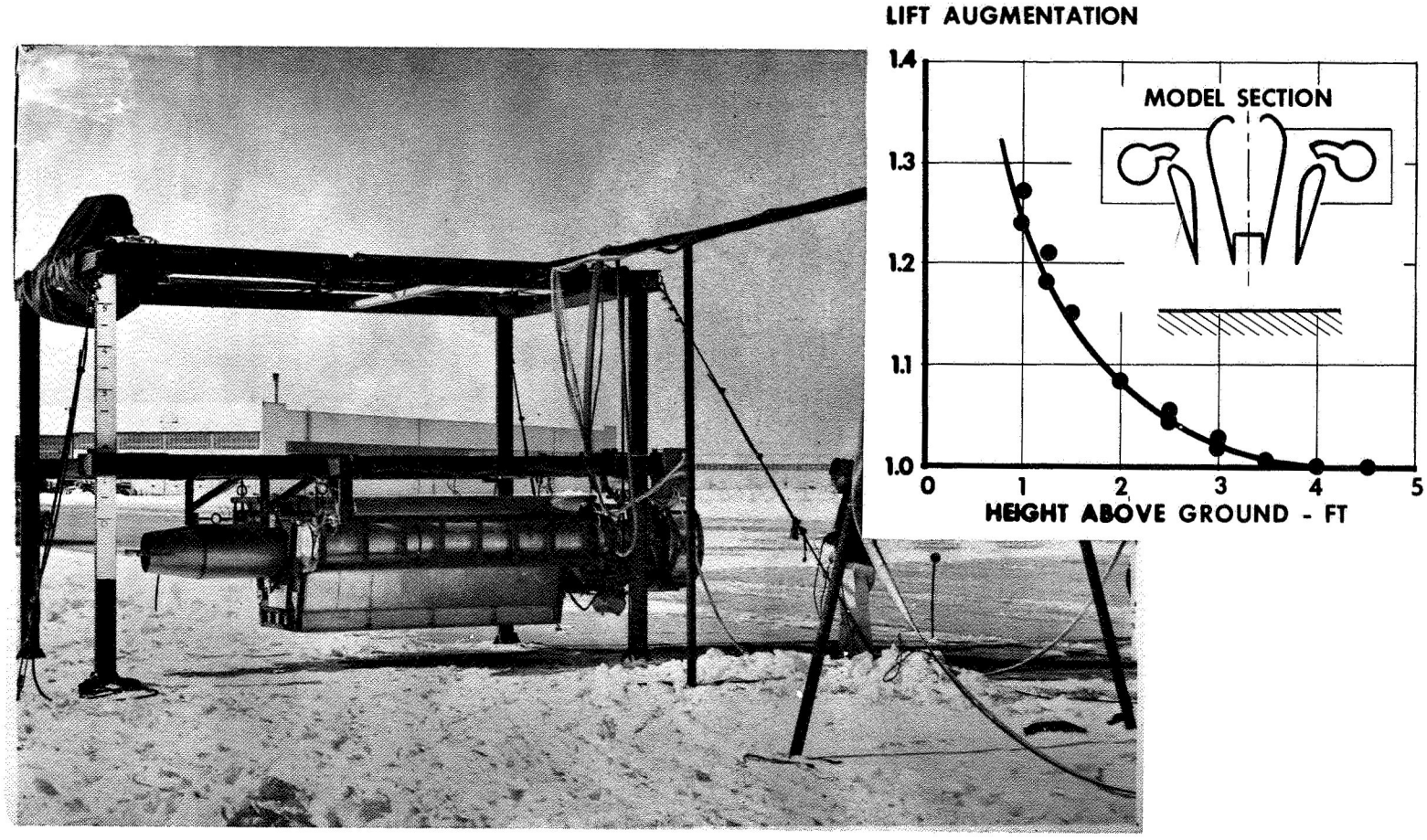

Figure 7.- Large-scale VTOL model mounted in variable height rig.

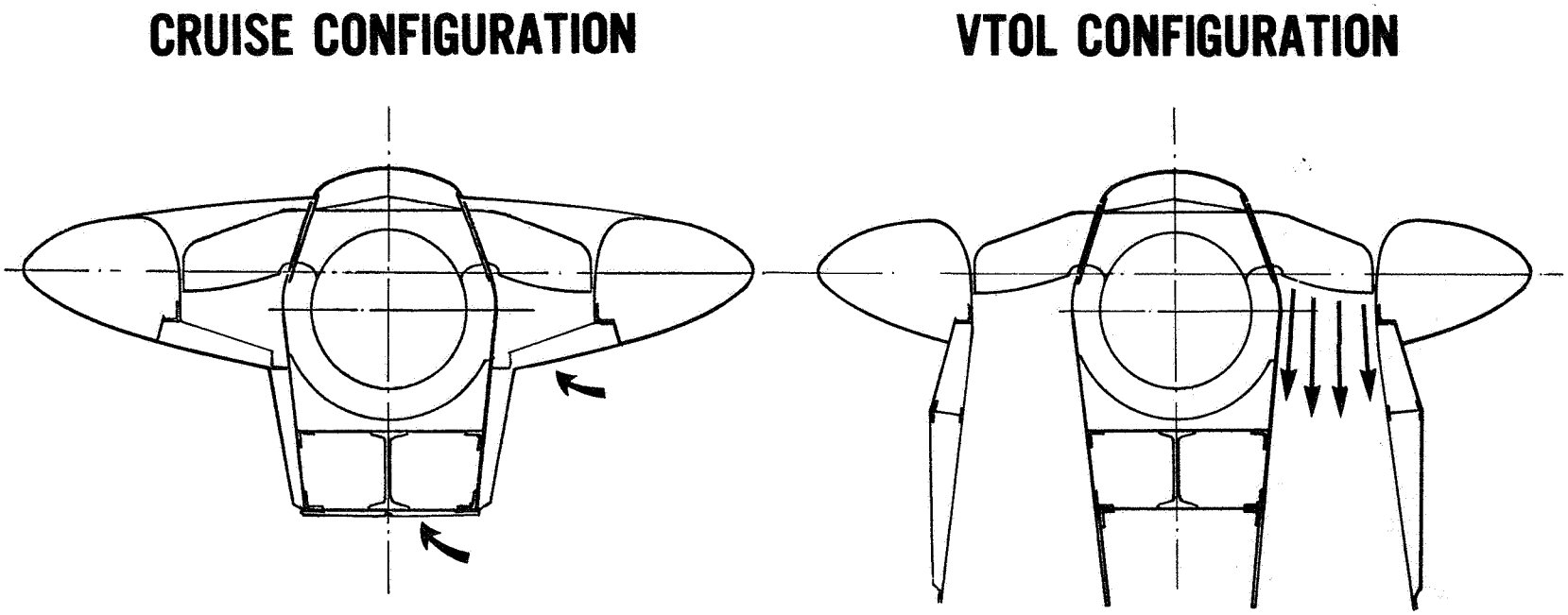

Figure 8.- DHC external augmentor; section of augmentor system.

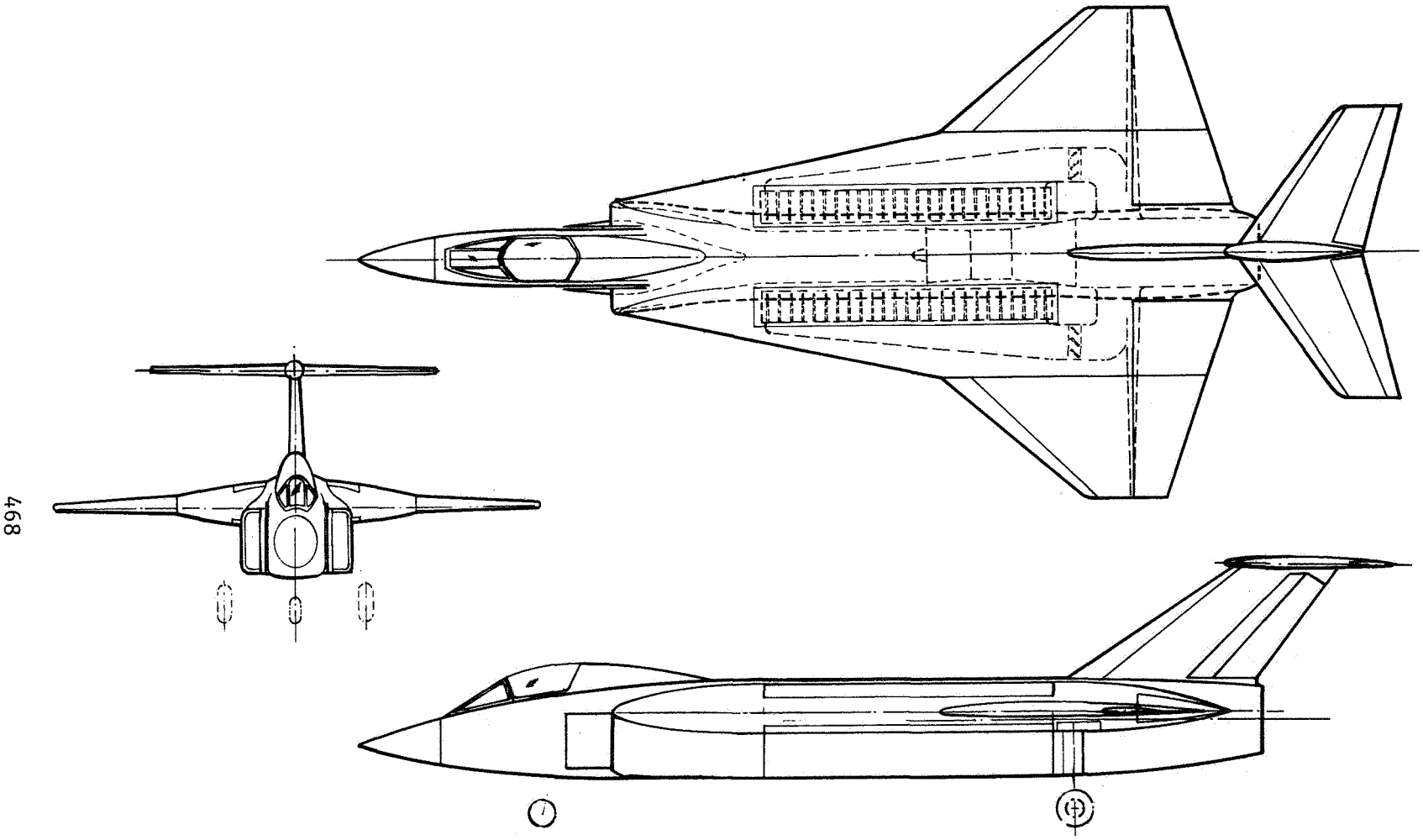

Figure 9.- DHC external augmentor V/STOL concept; "T"-tail configuration.

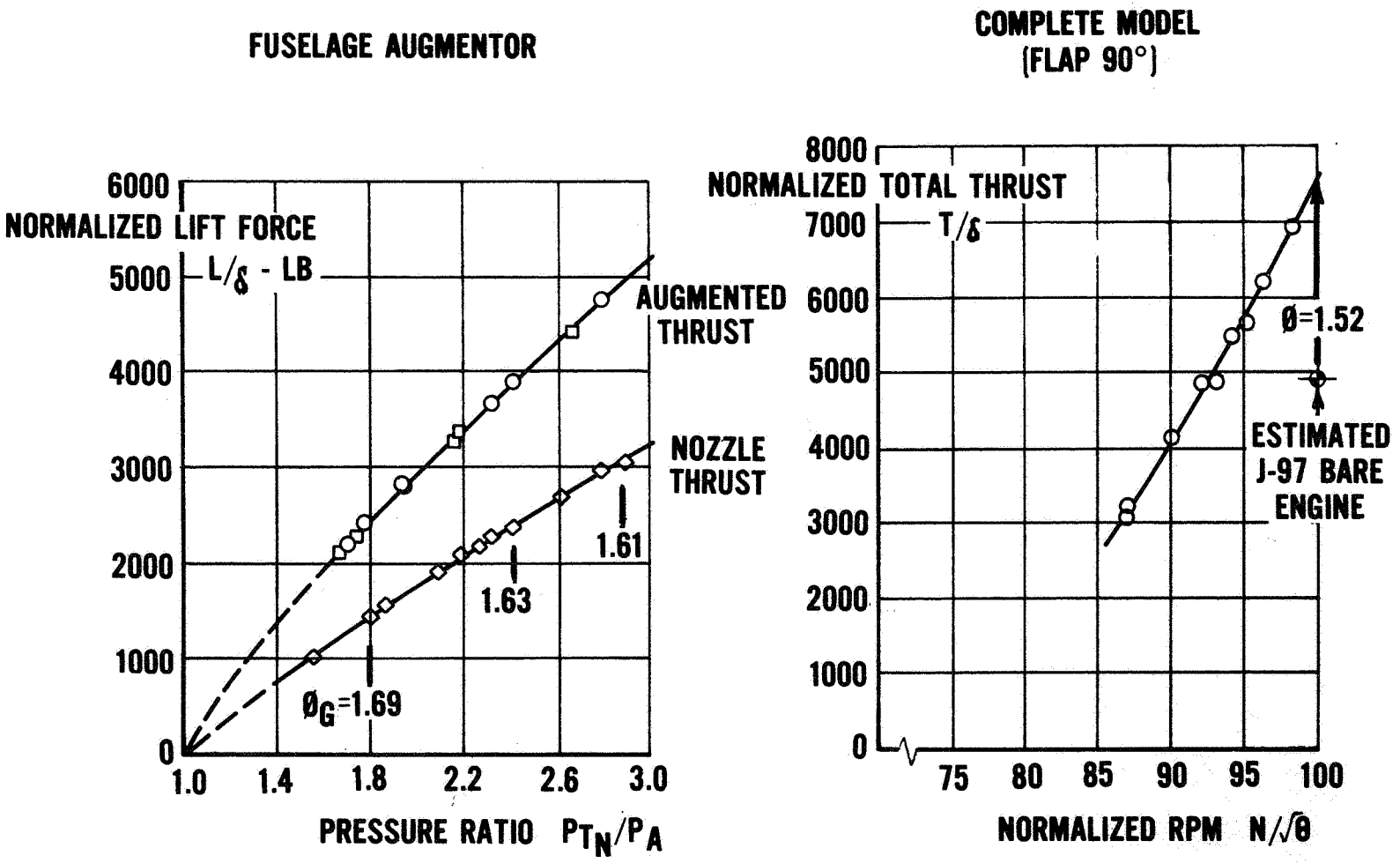

Figure 10.- Static thrust performance.

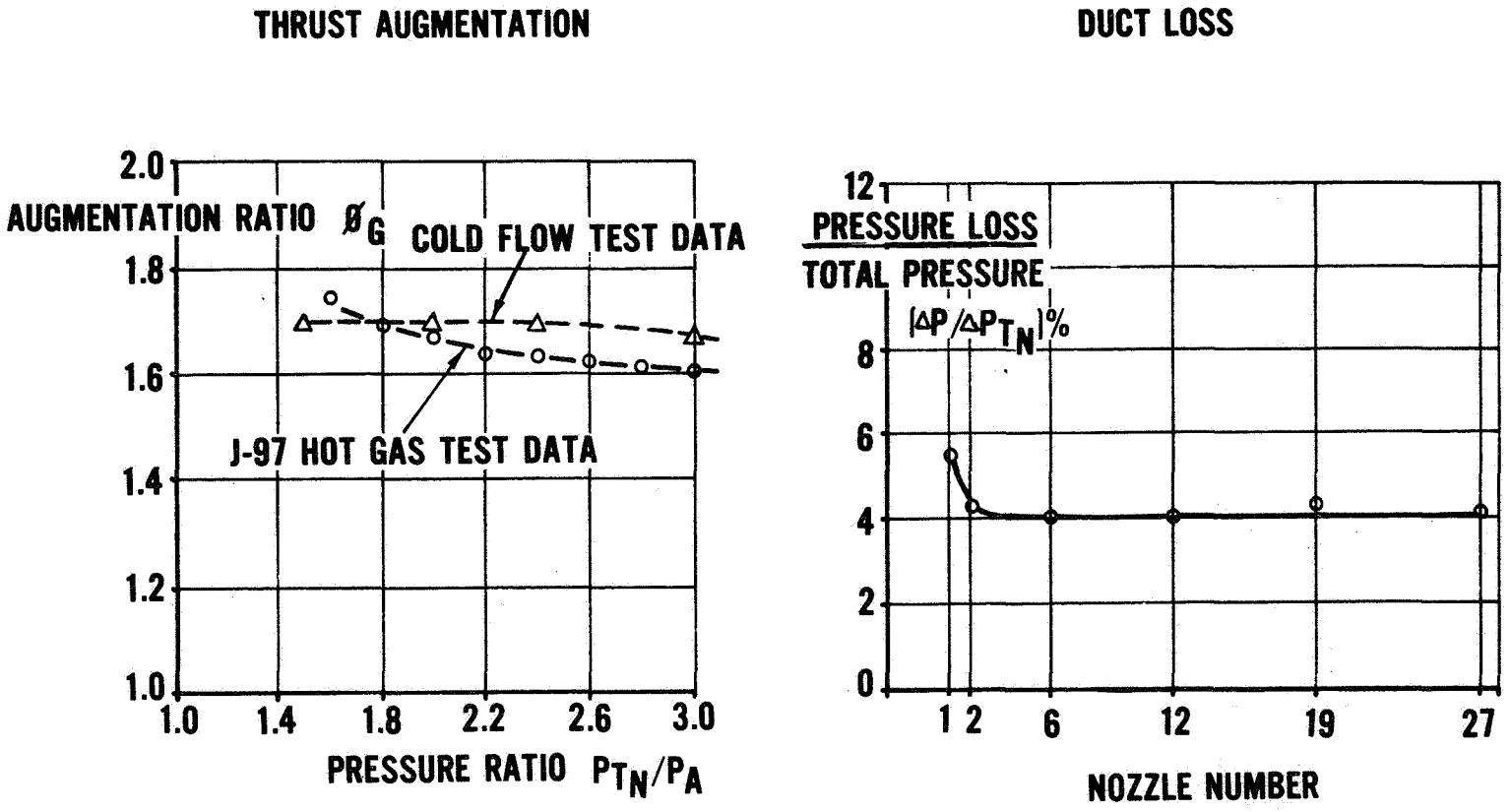

Figure 11.- External augmentor V/STOL model.

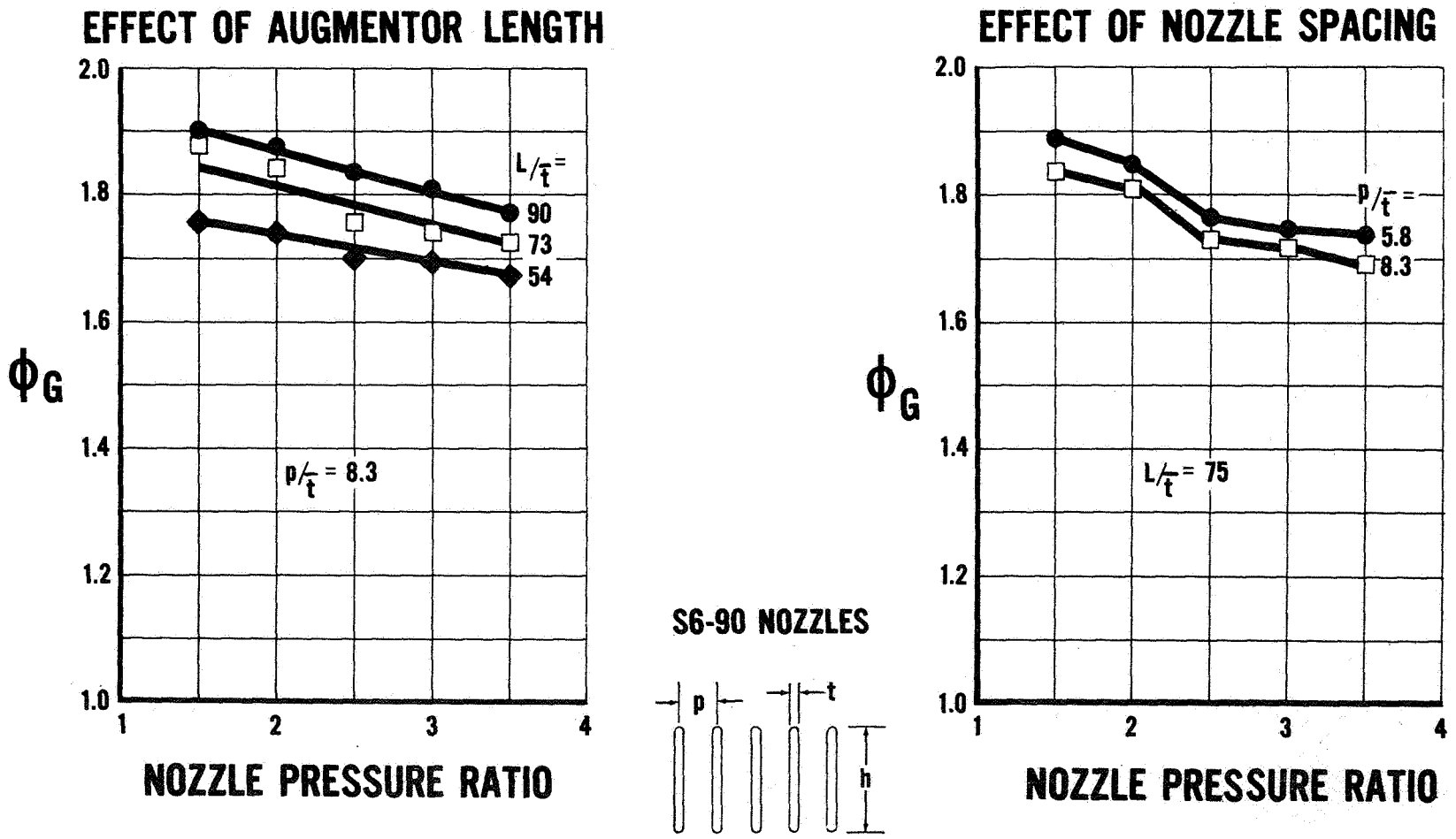

Figure 12.- Gross augmentation ratio ϕ_G; aspect ratio h/t = 100.

Mr. Ron Murphy
CDR Ernest L. Lewis
Naval Air Systems Command

XFV-12A
THRUST AUGMENTED WING (TAW)
PROTOTYPE AIRCRAFT

Introduction

The XFV-12A is a unique V/STOL technology prototype aircraft being developed for the Navy by the Columbus Aircraft Division of Rockwell International Corporation. This program is exploring the suitability of the thrust augmented wing/canard ejector concept to obtain a high performance aircraft with V/STOL capability. It is not intended that the XFV-12A program produce an operational production aircraft as the TAW is a research tool to explore ejector thrust augmentation technology. Of course the program goal is a flight-worthy vehicle to investigate and develop TAW aircraft characteristics in vertical, conversion and conventional flight modes.

TAW Concept

The innovative XFV-12A design features a high wing and low canard arrangement and is powered by a single Pratt & Whitney YF-401 engine. The air induction system includes two external compression inlets located along the sides of the fuselage and an auxiliary inlet located on top of the fuselage. Flow from the engine exits in to the diverter (consisting of a translating nozzle shroud, diverter doors and gas collector) which directs the engine exhaust flow aft through the plug nozzle for conventional flight or forward to the ducting/augmenter system in the wings and canards for V/STOL operation.

Thrust augmentation is directly proportional to the amount of secondary air flow. Variation of the diffuser flap angle modulates the amount of secondary airflow, which variest the lift created on each augmenter surface. With no change of engine thrust which is set at full-power height control is obtained by variation of the diffuser flaps on all four of the augmenters simultaneously. Attitude control is achieved by differential movement of the diffuser flaps on the wing and canard for pitch, the differential movement of the diffuser flaps on the right and left wings for roll, and the differential setting of the left and right wing mean augmenter angle for yaw.

Aircraft Development

The development of the XFV-12A progressed through the conceptual design, analysis, test and evaluation of major aircraft subsystems and suitability

of each for integration into the flight vehicle. Scaled models, flight and full scale test rigs, simulation and system integration tests were utilized in this development process. Wing and canard augmenters were tested in a unique facility, nicknamed the "whirl rig", which consists of a boom more than 100' long which is free to rotate. Jet efflux is ducted out the boom to the test augmenter which may then be "flown" remotely by the whirl rig operator. The test rig can be instrumented to measure performance and aerodynamic flow varibles. Concurrent with V/STOL system development, wind tunnel and free-flight testing of various scale models was conducted to define the aircraft characteristics in the powered lift mode, transition mode and the conventional flight mode.

Based on these system and vehicle integration tests, the sea level/standard day VTOL takeoff gross weight was estimated to be 19,130 lbs. For the VTOL mode, the engine exhaust gas is diverted to the wing and canard augmenters (47.5% and 52.5%, respectively). Thrust loss due to pressure loss and leakage was calculated to be 8% for the wing and 12% for the canard. Based on measurements from the whirl rig, the calculated free air augmentation ratios for the wing and canard are 1.51 and 1.31, respectively. With installed thrust of 16,500# from the YF401, approximately 10,850 lbs. of lift from the canard and 9,730 lbs. of lift from the wing, for a total of 20,580 lbs. of total lift is available. The 19,130 lbs. of VTOL takeoff gross weight allows for 500 lbs of lift due to trim and 5% lift loss for control.

Augmentation ratio is defined as the total lift developed from the wing and/or canard augmenters divided by the total thrust of the augmenter primary nozzles, including endwalls and dedicated corner blowers.

Fabrication and Structural Testing

Aircraft assembly was completed in early 1977. The XFV-12A proceeded through a series of structural proof and ground tests. Structural proof loading of the fuselage, vertical tail, wing and canard at critical design conditions was accomplished to define the CTOL flight envelope. The structural attach unit which would support the aircraft for static and dynamic tether tests at NASA Langley Research Center (LRC) was proof loaded at several critical conditions relating to fuselage bending which could occur during the static tests at LRC.

In addition to the proof loading tests, a ground vibration test was conducted to aid in evaluating the flutter characteristics of the aircraft. Vibrational effects on the hydraulic system were evaluated along with control system proof loading.

Functional Testing

Engine/ducting/augmenter functional tests were performed at ground level by placing the aircraft on three tie-down pads, each containing a lift and drag load cell. The objective of these tests was to functionally

evaluate the propulsion and control systems while in the vertical and horizontal (or conventional take-off) mode. Inasmuch as the aircraft was being tested for the first time as a complete article, it was not expected that the desired lift/control characteristics would be fully achieved with out minor modifications.

In addition to the basic functional tests, evaluation of temperature, velocity, noise, reingestion, cockpit procedures, and instrumentation and data reduction techniques were accomplished.

The structural proof and functional test results were reviewed by the Navy in November, 1977, and approval was granted to continue into the static tests tether at NASA LRC.

Performance and Control Testing

The Impact Dynamic Research Facility at NASA LRC was selected to conduct the XFV-12A static and dynamic tethered hover tests. This unique facility affords the capability of day to day testing in both static and dynamic modes. In addition, the facility permits static testing at any attitude and altitude in and out of ground effect, safe evaluation of large control movements, a good sized hover test envelope and, of course, pilot familiarization and training.

The tether system is based on a Navy varible speed shipboard underway replenishment winch. The hoist tether incorporates a 5 ft. stroke shock absorber which limits the cable forces to 40,000 lbf., a position sensor which drives the winch during dynamic operations, and a structural attach unit. Horizontal restraint cables are placed around the tether at the 100 ft. height in order to prevent lateral excursion of the aircraft which could result in contact with the gantry structure. For initial dynamic testing, a 5 ft. diameter ring around the tether cable minimizes lateral aircraft movement.

During static testing, the aircraft is hoisted to the desired test height by the safety tether and then restrained in the desired attitude by seven ground cables attached to the three landing gear. The upper tether and each of the lower restraint tethers contain load cells and the geometric summing of these load cell data provides lift and moment data.

For dynamic testing, the lower restraint cables are removed and the aircraft is free to maneuver within the constraints of the test site arrangement. During dynamic tests with lift to weight ratios greater than one, the position sensor signals the winch to track the vertical velocity of the aircraft. This will minimize impact of the tether on the aircraft handling qualities.

For both static and dynamic testing, instrumentation for aircraft loads, temperatures, and system performance are telemetered to the data station. Data from the cable loads, and extensive pressure instrumentation, are incorporated into the same transmissions.

Static testing at the Langley facility is directed towards developing the augmenters to their full potential, evaluating the resulting stability and control characteristics, and determing the external forces on the aircraft, both in and out of ground effect. Another important aspect of the static tests, is the evaluation of the structural integrity of the ducting and augmenter systems.

Dynamic tests will verify basic attitude and vertical control, both in and out of ground effect. The rate damping system and hover feel and trim will also be evaluated. The dynamic tests will, of course, provide pilot training and proficiency in VTOL operation.

Static Test Results

Initial static tether test results are summarized in the attached graphs. Rockwell has generated a method of estimating augmentation ratio (Φ) based on measuring the average velocity of the secondary air passing through the augmenter threat and correlationing this velocity with previous full scale test data. These "throat velocity (Φ)'s" indicate that the augmenters are performing close to the goal augmentation ratios. On the other hand, the augmentation ratios computed from load cell data indicate substantially less performance. The variance was reflected at all altitudes tested (0-30 feet). The project team expended considerable effort and time investigating the anomaly. By mechanically inducing loads into the tether arrangement and comparing the known input with the results of reduced load cell data the load measurement system was statically verified. In addition, tests of a scale augmenter model reflecting full scale conditions were run and additional instrumentation was placed on the aircraft to detect any unexpected external forces on the aircraft.

With the exception of the external forces, which resulted in a negligible amount of download on the aircraft at 30 feet, no definite conclusions could be drawn as to the validity of either set of augmentation ratio data.

After Navy and NASA review of the static test results, it was decided that an initial dynamic test should be approved in which the lower restraint cables would be removed and the aircraft would be suspended from the safety cable at a lift-to-weight ratio less than one. This would provide a qualitative assessment of control characteristics and a quantitative measurement of aircraft lift based on a single load cell. This lift measurement would serve to validate the lift measurement system.

These unrestrained tethered hover tests were accomplished on June 12, 13 and 14. Precision control of aircraft attitude was demonstrated and lift measurement system was validated.

Test Result Assessment

The static tethered hover tests have validated the TAW concept and quantified the propulsion system characteristics. The wing and canard augmentation ratios, are much less than goal values.

A comparison of a static and unrestrained test at approximately the same conditions tends to validate the lift measurement system. The comparative tests were accomplished with trim and power conditions that allowed the aircraft control system to operate within the linear portion of the augmenter lift curve slopes. This enabled very precise control of the aircraft during the unrestrained test.

A later test explored the higher lift/reduced control authority region by selecting a trim point which allowed the control system to operate in the non-linear range of the augmenter lift curve slope. Pilot work load for this test was higher; however, controlability was considered adequate.

In addition to these performance items a few comments should be made regarding other aircraft systems.

Total operating time for the XFV-12A in the VTOL mode has been approximately 46 hours with 7.5 hours at intermediate thrust throughout this tije period the Pratt and Whitney YF-401 engine has operated in a relatively flawless manner and at a performance level equal to, or greater than, original estimates. The structural integrity of the ducting system, with the exception of several internal vane failures and a rupture in one end wall blowing plenum, has been exceptional. The data acquisition system has proven very reliable and has demonstrated the degree of flexibility necessary for this type of testing.

Projections

Exit surveys of both the wing and canard at altitudes from 0-30 feet are currently being performed at NASA Langley, Research Center (LRC). This data will be evaluated and modifications incorporated into the augmenters. It is anticipated that several of the modifications can be tested at NASA LRC before the expiration of the current test phase in mid July.

After this test phase is complete, the augmenters will be removed from the aircraft and sent to Columbus to be tested on a full scale test stand. Analysis of the exit surveys and full scale tests will define the various augmenter problems. Modifications resulting from evaluation of these tests will be incorporated into the augmenters and tested as full scale flight hardware.

When demonstration of increased performance is achieved, the flight hardware will be incorporated into the aircraft for continued tethered hover testing at NASA LRC.

Several options for follow-on testing are being explored. Use of the full-scale tunnel here at NASA Ames for exploring the transition between VTOL and CTOL flight is being considered. Free flight is planned to follow tether and wind tunnel testing.

Features of the TAW approach to VSTOL, especially augmented thrust, a relatively benign exhaust "footprint" and greatly enhanced STOL performance due to circulation lift make the TAW a very attractive V/STOL concept which the NAVY will continue to explore.

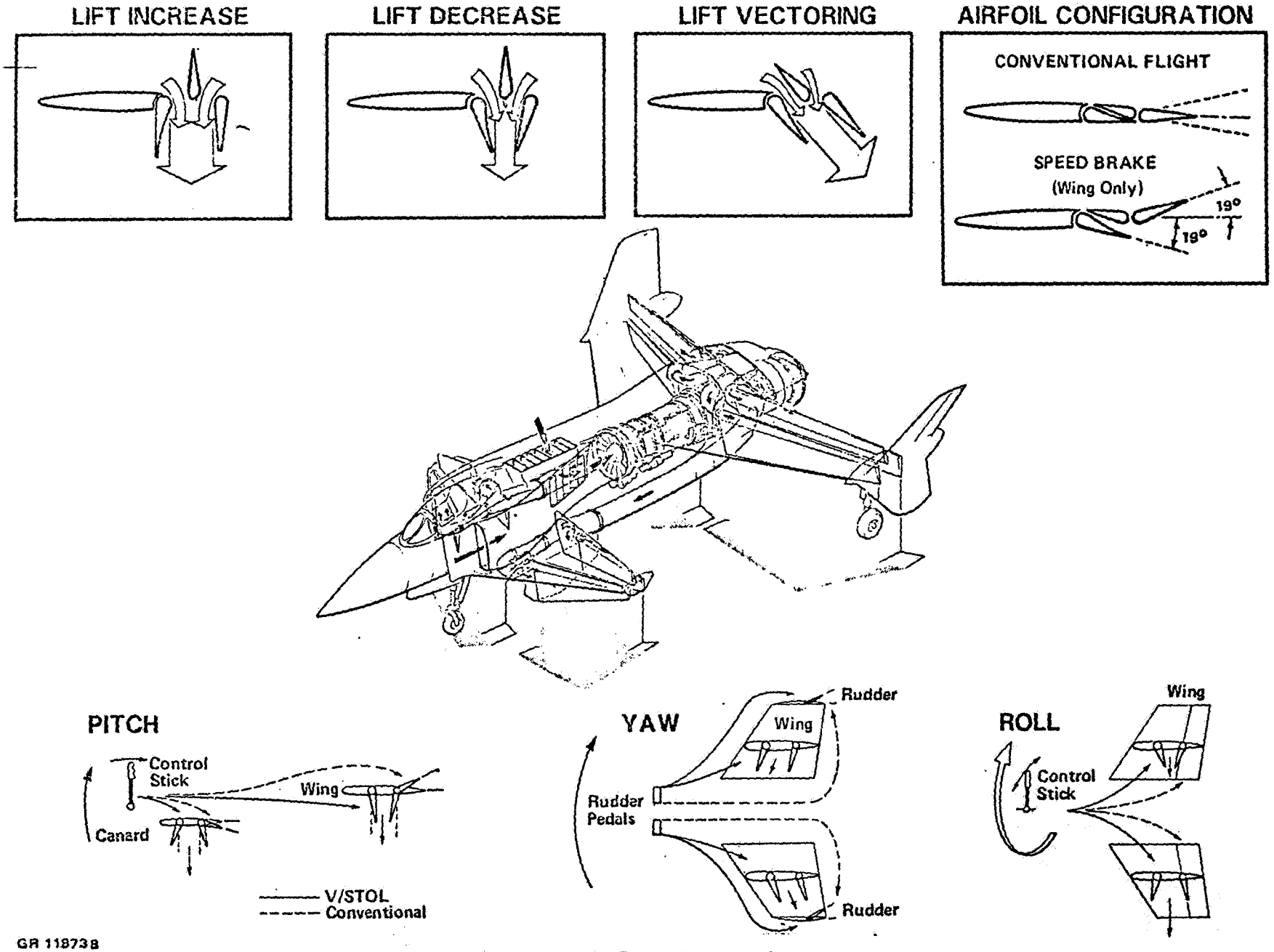

Figure 1.- Lift and control.

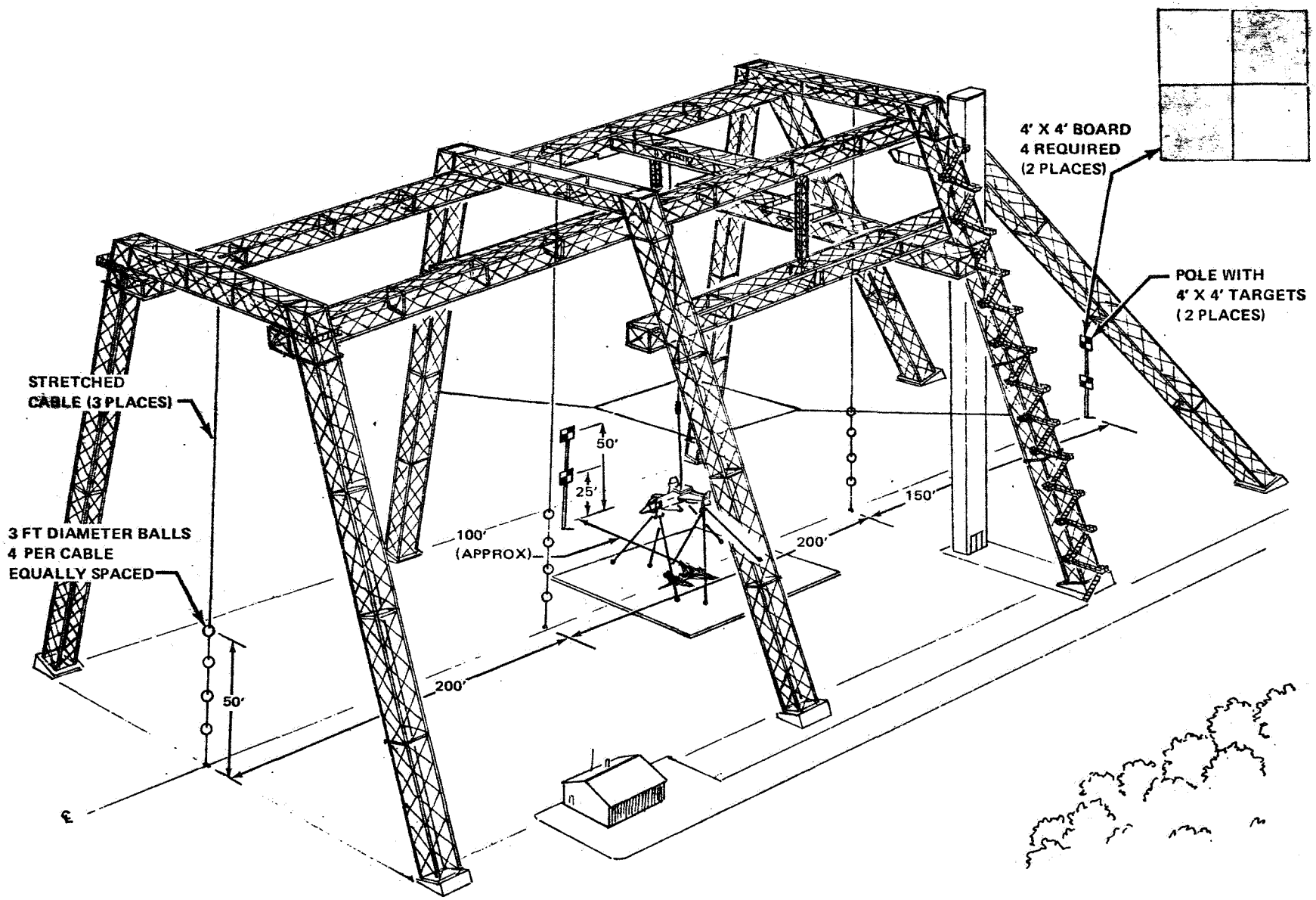

Figure 2.- NASA Langley test gantry.

PANEL DISCUSSION

Mr. Armando Lopez

This final session of the workshop will be devoted to a panel discussion summarizing the results and conclusions and to outline possible directions for new areas of research on thrust augmenting ejectors. The panel members are all researchers who have been instrumental in advancing technology for thrust augmenting ejectors. The panel members are: Harold Andrews from Naval Air Systems Command, Morten Alperin from Flight Dynamics Research Corps., Paul Bevelaqua from Rockwell International, Joseph Foa from George Washington University, Hans Von Ohain from Wright-Patterson Air Force Base and Donald Whittley from deHavilland Aircraft of Canada, Ltd. The panel will be moderated by Mr. Mark Kelly, Chief of the Large-Scale Aerodynamics Branch at Ames Research Center.

Mark Kelly

We will ask each of the panelists to give a 5-minute summary statement relative to the status of augmentor technology in the conference, and at the conclusion of their statements I'll give them the opportunity to question each other or comment on the statements that have been made by the panel. Then we'll proceed to take on the questions from you out there. As Mr. Lopez said, if you provide your questions in writing on a card and pass them either to Armando Lopez or get them up here to me, that will expedite handling those questions. I believe that everyone but Hal Andrews has been introduced. I think you probably all know Hal Andrews of Naval Air Systems Command, and the others have been introduced previously in connection with talks. Hal, do you want to go ahead then with your summary.

Hal Andrews

Panels are always good if they're somewhat informal, flexible, obviously we are ready to do it almost anyway, with or without members. I'd like to start! Are we geared up to have our viewgraph, please? You have all seen this before, as Commander Lewis stated in connection with our airplane, we're pretty good at borrowing things and the interservice cooperation is good and all that, so I borrowed Randy's viewgraph because it makes most of the points on an individual basis that I would try to make in my 5 minutes, and I don't need to make them over again; he has done it very well. What I would do is take from this chart and make the strong comment that all aircraft design, as you all know, is a compromise, and it's always a matter of balancing advantages and disadvantages, pluses and minuses and, of course, proving out the technology that's actual facts in areas where perhaps everything is not fully known. Of course, that's what we're involved with here. The advantages, particularly three of the advantages, first couple and the last one, are very important in terms of potential Navy use of V/STOL aircraft, and I think all of you that keep up with Aviation Week, Aerospace Daily or are otherwise involved

in what's going on in the Navy, are aware that the exact program content for the Navy is going through reorientation now, but I don't think that the thrust towards eventual application of V/STOL in the Navy is going to diminish except for perhaps in its intensity in specific aircraft developments sense in the near future. So I think that with that background in mind and with the obvious benefits of these advantages, we feel very strongly that we have to continue to keep the augmentor technology as an open one of the big types of things that we need to consider in our overall V/STOL picture. About a month or two ago on a little different basis from this meeting, the Navy did take a considerable look at where the augmentors were, with the cooperation of some of the people that are here today and a whole different format where we accepted a lot of information, but didn't interchange it the way we're doing here today. The objective of that was to look at where the real holes in technology were, where should we really be putting our efforts in connection with augmentors, and I think that the area that we sort of picked out from that is a major area. We skirted around it a bit in the last couple days, but I'd like to just underline it, and that is the transition from model test results, regardless of scale, even from full-scale models to the actual flight design hardware, seems to be where augmentors in general have come into some real problems that haven't been fully solved. Throughout the last couple days we've listened to papers addressing many of the different areas, and it's obvious that there are challenges all the way from flow phenomena on up through the final aircraft design application. There's plenty of room for people to apply their capabilities usefully in augmentor technology and its application. We hope that this will continue until we get a full final assessment of where the augmentor does fit into the total picture. You might recall a little story that some of you may or may not be familiar with, and I won't go through the whole story, but it concerns a couple of young lads, one of whom was the extreme optimist, and the other one an extreme pessimist, and their parents were a little concerned about that. They thought they ought to do something about the two boys and try to get them back a little towards the medium avenue. Without going into the whole story, I'll relate what they did with the young fellow that was such a complete optimist who really wanted a pony very badly. So what they decided to do was give him a special Christmas present and they built the barn and they got all set and he went out there at Christmas and opened the ribbon on the door, opened it up, and it was all full of horse manure, and they thought he would get the message from all that. They went out there halfway through the day and there he was digging through the horse manure. They said, "What in the world are you doing?" And he said, "With all this stuff around, there's got to be a pony in here somewhere." I wouldn't want to make the allusion that all that's been going on around here the last couple days is directly analagous, but I would like to say that we still feel there is a pony in there somewhere, and we have got to find it.

Mark Kelly

Thank you, Hal. Dr. Alperin, would you like to give a 5-minute summary of your views?

Morton Alperin

I haven't really thought about what I am going to say here. I thought I would be on the end of the line because Dr. Von Ohain just gave me a title of "Von" Alperin while we were out to lunch and that would set me back a little bit. One thing I would like to say perhaps is to straighten out some impressions that I may have left in the short talk I made here. The objective that I was trying to reach was that our research has indicated the fact that one may overdo the attempt to achieve complete mixing and that even achieving complete mixing to a certain extent is detrimental in terms of the total thrust one can get. But in the attempt to achieve more complete mixing, you may introduce additional losses in the form of nozzle losses or inlet losses, which are more detrimental than being satisfied with the incomplete mixing and making up for it with a small increase in diffuser area ratio. The other point which I didn't make very thoroughly is the fact that with a properly designed jet diffuser, the mixing process can occur far downstream of the solid surfaces and still be effective because the flow does not return to ambient pressure for quite a distance downstream. In the STAMP ejector that we developed with the jet diffuser, the region where the flow remained below ambient pressure was limited by the end effects, due to the flat ends that I showed on the drawing. A properly designed jet diffuser would have to have properly designed ends not only for the additional diffusion it gets, but for the additional space it makes available for the mixing process. That, in some cases, is even more important than the diffuser area ratio, particularly in the ejectors that are thrusting at high speeds which we didn't go into in this symposium. The additional room it provides for the mixing process can be such that the diffuser efficiency can easily exceed 90 to 95 percent. On the one we developed for the STAMP ejector, we had only 80 percent because of the flat ends. The diffuser deficiency was 80 percent. The one we just finished developing for the Naval Development Center is far superior to that, but we don't know what the efficiency was. We finished the work and really didn't have enough time to do a lot of detailed testing. We're hoping to do more of that, either on our own or, hopefully, with some Government support. But there is a lot of work to be done on jet diffusers, and we're still learning quite a bit about them all the time. The peripheral distribution of diffuser jet flow is a very difficult problem. It has to be quite uniform; otherwise, you get crossflows in the diffuser, and they always seem to be accompanied by pretty high losses in performance. I guess that takes care of my five minutes.

Mark Kelly

Thank you, Mort. Paul, would you like to take over the floor.

Paul Bevilaqua

First, let me say how much I have enjoyed being here these last two days, to see a lot of old friends, and to get a chance to meet some of you whose papers I've been reading for years and know only by reputation. To

summarize the impressions I get from the meeting here, I think it's still clear that we do not completely agree among ourselves even on some fundamentals. I've made a list of things that occurred to me while we were sitting here. For one thing, we still define augmentation ratio, ϕ in different ways. While it's helpful to identify the way in which ϕ is defined, and you can say this definition is a little more conservative or this one's a little more optimistic, it still makes it difficult to make comparisons from configuration to configuration. Also, I saw some papers showing advantages to leaving the ejector on in flight, and some showing that ram drag would prove disadvantageous. I guess some work I saw we don't really know if the von Karman analysis represents an absolute upper limit on the performance or if there is a possibility with some other mechanism to somehow exceed that limit. One other is, I guess, that we don't even agree on the importance in getting complete mixing in achieving augmentation. So these are just a few very fundamental subjects, and it seems to me that since this is the first time we've all been together here we ought to try to sort out among ourselves and then perhaps we can get on with the business of getting the ejector technology up to the same level as the rest of the airplane that is being designed. The augmentor I think, has the advantages and disadvantages. The advantages can be summed up in simplicity in smoothness, ease of conversion, etc., but the major disadvantage is the augmentation ratio. A fan or helicopter, or whatever, will always get you to higher augmentation. So the problem comes down to getting the augmentation in the practical installation in an aircraft. If we look at the level of technology and the kinds of questions we still disagree on, it's clear that there's a lot of room for growth. To get another small percentage increase in engine technology, get more engine thrust, will require millions and millions of dollars because it's so highly developed. Similarly, for fans. But I think the ejector technology still has a long way to go, and we have a tremendous opportunity to make that advance. Let me just close by saying that I wasn't around in those days, but I can imagine we must be something like the aircraft industry was when airplanes were first being developed. There were disagreeements as to whether you should put the tail in the front or the back, whether you wanted a biplane, or a ring wing or venetian-blind wing, or maybe more recently, when we started to go supersonic, there were all kinds of weird phenomena about control reversal and what we should do with the wings, etc. It's to be expected, I guess, and I would like to encourage you when we open the panel discussion up to ask some of those hard questions of us, and let's perhaps try to agree among ourselves on some of the fundamentals so we can get on with the job at hand.

Mark Kelly

Thank you, Paul; Dr. Foa.

Joseph Foa

I will try to limit myself to the general impressions of the meeting. It is sobering to reflect on the fact that the use of ejectors in steam

locomotives, to pump water into the boiler using steam from the boiler itself as a primary, can be traced as far back as 1859. Among the later ejectors, it was exhaust steam that was used for the same purpose. But by the same token, I found it refreshing to note how many new ideas and theories and suggestions for new applications have already generated in the wake of the recent renewal of interest in this very old technology. I think that the organizers of this workshop are to be congratulated, in fact, for giving us the experience of these two days. I have two comments to offer: one has to do with the evaluation procedures. I have felt much encouraged by what I have heard these two days, but I still have the impression that the evaluation of new ideas is still left very largely either to the originators of the idea itself or the originators of competing ideas. Now, in the former case, the use by different authors of different definitions, as Dr. Bevilaqua pointed out, different assumptions, different experimental situations, make it very difficult to arrive at valid comparison of the relative merits of different solutions. In the latter case, that is when ideas are left to be evaluated, or rather torn apart, by the competition, the evaluation is neither entirely unbiased nor always based on available information. What is worse, I think, is that neither of the two procedures is conducive to the kind of cooperation that one would like to find among people who share a potentially useful expertise. I also believe that the fragmentation of the research effort in this area may be blamed for the unfortunate fact that, apparently, very little attention has been given to the possibility of combining various solutions into a single device. For example, there is no reason why the best solution in a staged ejector should be the same for all stages. There is no reason why the primary, say, in a hypermixing wing ejector should not itself be the output of an augmentor of a different kind. There is no reason why a rotary jet and an operating diffuser shouldn't go well together or, at least, why that combination should not be worth looking into, etc. To fill these gaps and to work on the other difficulties that I mentioned, I would like to recommend that the evaluation of ideas and the determination of their most promising, either joined or combined applications, be carried out by an independent team or panel on a uniform basis; concurrently, of course, with the prosecution of separate research where warranted on the different ideas. In carrying out this task, the panel would inevitably develop standards and have to ask questions that, in turn, may give the researchers guidance and direction. I believe that the resulting feedback would improve the cost effectiveness of the program. Finally, I would like to point out that what I said about the solutions applies, in my opinion, also to the problems that each solution seems to generate. For example, in dealing with the mechanisms of energy transfer we have heard about within the last day and a half, we have heard advocates of steady, nonsteady, cryptosteady, oscillating, peristalic, intermittent and jet propulsion parameters. They certainly can't be all right. A comparison is very much in order. There are many such studies that should be carried out and, speaking as a disinterested party, I think universities should be given a greater role than they have at present in this task.

Mark Kelly

Thank you, Dr. Foa. Dr. Von Ohain

Hans Von Ohain

Gentlemen, let me try first to formulate the broad long-range goals of ejectors as I see it. It is in essence to transfer, efficiently, energy from a mass of a high energetic jet to a large mass with lower energy by immediate contact with the media. Now, as Bevilaqua already said, currently we do energy transfer of that nature by mechanical means, utilizing a turbine extracting the energy from the high-energy jet, feeding it possibly through a gear to a helicopter air screw which gives you a fantastic thrust augmentation or to a propeller or finally to a ducted fan. Now these are the current techniques of energy transfer which are extremely efficient, also lightweight. Now why in the world do we sink our teeth into something which is allegedly a very inefficient way or should be not a very efficient way. I should be careful here. I guess the answer is simply you would not like to have rotating machinery; of course, this is a weak argument because when you say, in the first place, that it's a rotating machinery somewhere, why not all the way and have other rotating machinery, and you make V/STOL, then, like the Harrier or like helicopters, and so on. It is a very difficult philosophical problem to make a good case for V/STOL ejectors. Now I would do it this way. I would say when you are rotating machinery and not only that it's not so nice to have rotating machinery for some reason or other, but you also have the disadvantage that you cannot build a rectangular compressor. Oh, they have been built with rectangular cross section, but not very good and not very efficient. I do believe, then, that is one of the advantages, that you are free in the way as to what cross section you choose. Furthermore, you can say you can make a point that I could have a very nonuniform velocity distribution and the ejector will work very well, but the total (?) machine wouldn't. So when used in V/STOL technology, it would invite the possibility for boundary-layer acceleration over the entire wing span, for example. Then you get the advantageous synergistic effect of a much higher jet or propulsive efficiency when you accelerate the boundary layer that way. The other way would be that you could make a point for supercirculation. Of course you can make supercirculation already with a normal engine probably mounted at the wing, but you could far more exploit the effect of supercirculation. So there are a number of reasons to go further. I should have also said you could have better actuation of control surfaces by this method of not to have too little mass of too high energy. You utilize the ejector for that purpose and make it locally distributed so that you get possibly better transitions. So all in all, you see not one major breakthrough-type advantage. That makes it so terribly difficult to sell the idea of ejector propulsion because you can always point and say you can do it that way but why, if we can do it with a more conventional fashion, maybe even more efficiently. So we have that fight, and therefore I do believe that what is required in that entire area of the ejector technology is, of course, new concepts aiming at asynergistics effects, as I mentioned boundary-layer circulation, energetic flows, and acceleration of boundary layer which would give you better propulsive efficiency. All these things, when you can

ultimately get the possibility of bringing these things together, then you will have better aircraft. Ultimately, the fan engine, even with a rectangular nozzle, with two-dimensional nozzles, will not quite be able to do what the ejector can do in combination with the whole thing. So it would call for new inventions, new ideas, new concepts which are refinements because we have already many, and, seemingly, we have pretty good concepts already in the making. It's tremendous difference today against about 10 or 15 years ago when we had industrial briefings of that nature. We didn't have them exactly like that, anyway; much fewer people were interested. The other thing is, if we ever want to be successful in this whole technology, it is my absolute belief that far more basic research is required. We have to look again to caution, and don't misunderstand me, I see a tremendous improvement in the understanding and interest of the scientific community in the basics of ejector technology. I heard a number of outstanding papers and excellent projection for the future. So I would say it will be a very hard thing to fight for the ejector technology. That with more basic research with better understanding and new concepts and patiently improving what we have, we will make step-by-step progress. Ultimately, I hope that ejector technology will bring you the following things: aircraft with advanced range, advance performance and added capabilities of STOL or V/STOL without a penalty. Right now we always say, yeah, when we want V/STOL or STOL — you have an added capability so you paid for that added capability. I believe if we have good ejector technology it will turn out that we have aircraft with STOL or V/STOL capability which may fall out as an additional bonus. That is enough of philosophy. I want to say a few points quickly about the current observations I could make. I said already outstanding fundamental approaches, and I believe we can strengthen that further more. As to the various aircraft which are now on the horizon, I would like to make one comment in the light of the philosophy I developed, namely, please consider that the subsonic aircraft is always much better suited from the standpoint of getting a high-thrust augmentation ratio because the inlets to the ejector are far more favorable. On the other hand, don't forget that the subsonic aircraft which usually may be a transport or what have you, has a much lower power to weight ratio than a supersonic aircraft. On the other hand, when you have a supersonic V/STOL aircraft utilizing ejector technology, you must consider that the thrust augmentation requirements are far lower than those of a subsonic transport. The most important thing to me and the most crucial point in the entire new crop of aircraft is that they prove not so much at the moment their thrust augmentation ratio, because we know that can be improved, but they show the operational characteristics, for example, that the guy doesn't have to climb up and make a controlled fall down, so to speak, and to pick up speed and then turn into normal flight transition capability. The control moment in hover, the transition from hover into flight, these are the most important things and not necessarily, at the moment, a particular thrust augmentation ratio. Otherwise, I would say in the future these stronger and stronger synergistic things look good to me.

Mark Kelly

Thank you. Thank you, Hans. Don?

Don Whittley

Seems to me, if we're talking about V/STOL fighters, we're talking first of all about V, then we start talking about supersonic fighters, and they have low frontal area and higher wing loadings. So, first and foremost, it seems that we do have to come back to the ejector itself and its hovering capability. We first should recognize that we're going to have to live with fairly high-pressure ratios. We can ask the engine manufacturers for the engine which will give us the highest pressure ratio available, 3, 3.5, something like that, and so, first of all, I would like to recommend that we should all perhaps pay more attention to the high-pressure ratio end in our studies and also the high-temperature end. When it comes to haggling about it, and so on, different ideas, that's fine; there's nothing wrong with that. Variety is the spice of life, and there is no reason why not, for instance, to incorporate an Alperin-type ejector in our wind-tunnel model. It seems to me that the ejector developments can go along in parallel, but I think it should be at high pressures and high temperatures. So then, having looked at that and having spent more time on that perhaps provides better understanding all around. Then we have the other side to the question and that's this question of integration and design synthesis. If we think or try to evaluate an ejector-powered V/STOL fighter, either in terms of flexibility or in terms of competitive position, I think that we must be very careful to separate features and/or problems associated with VTOL and features and/or problems associated with ejectors. It is going to be very easy if we're not careful to sort of mix them all up and blame an ejector-type airplane for some temperature ingestion, and all the VTOL airplanes have temperature ingestion. So, it seems to me, whatever you do for supersonic V/STOL, it's not going to be without its problems and your compromises. You will always face some fundamental problems, such as lift loss in ground effects, lift loss in transition, noseup pitching moment, hot-gas reingesting, and lateral stability in transition, engine-out control and survivability, and many others which Seth Anderson, here I am sure, could write a list three or four times as long as I could. But all these things are V/STOL-related matters and not ejector-related matters. So when it comes to an ejector, it seems to me that there are a number of features which are very much in its favor. Some of these have been listed on the viewgraphs: the mixing flow footprint, velocity and temperature, and then the ejector suction for flow control. I tried to indicate in some of my slides the way in which both advantages are in our ejector power-lifted augmentor wing STOL airplane. We use the ejector, and the inflow into the ejector with its flow control, all in a number of ways. In particular on the flight research airplane it permits us to achieve boundary-layer midchord control and highly satisfactory STOL characteristics. The airplane stalls at 40 knots, at 33° angle of attack, with a nosedown pitching moment. That's all due to the fact that we've integrated the ejector system into the wing. It's the suction into the ejector which is providing boundary-layer control effects. I think

that we can apply this with similar effects in our V/STOL line and that's another plus for the ejector. I believe the ejector flap can be used for high subsonic speeds and for high maneuverability, but certainly, further work is required there. So, as I say, I think there is a whole lot going for us, but, of course, a V/STOL configuration and ejector-powered V/STOL configuration, in particular, does require a very careful design synthesis. It will probably take some time to work out the best form for this synthesis or integration. This is where the thrust of research is required. If you take the recent last 15 years in power-lift STOL, we had a number of concepts: external blown flap, upper-surface blowing, augmentor wing, plus a few others. Much money and effort was spent in evaluating these concepts, particularly here at NASA-Ames, and particularly at large scale in the Ames 40- by 80-Foot Wind Tunnel. I think that we still have not arrived at the optimum configuration by any means. I think that it calls for a number of years of solid work in that area. As for the flight application there's one more observation worth making, I think, and it is certainly worth keeping in mind, and that is single-engine versus two-engine. Here again I think we ought to watch that we aren't looking at a two-engine ejector design, comparing it with an F-16 or some single-engine Harrier or something. Certainly a single-engine V/STOL concept is a lot easier than a twin because of the engine-out case and the particular cross ducting required in the case of augmentors to avoid upset and to provide survivability. That reminds me of a story that we once heard from Stanley Hawker. As you know, Stanley Hawker was involved in a debate for many years, arguing in favor of the single-engine Pegasus; that's the Harrier formula, as against the multi-engine lift concept which was being proposed at that time at Rolls Royce, and Hawker was with Bristol and other people at Rolls Royce. The remark that he made was that nothing comes down faster than a VTOL airplane upside down. I have never forgotten that remark. So, finally, there are two ejector-related matters. One is this, I think, in a powered-lift STOL work we found that there was one thing which singled out power-lift STOL from, say, 7-propeller-type STOL. That, of course, is as we were coming in on a steep gradient, it was the steep gradient and the thrust deflection or thrust vectoring requirements which singled out powered lift as different to any other STOL-type operation, and I think when it comes to ejectors, an ejector V/STOL design, I think there's one thing which singles out the ejector design from other designs, and that is the need to transfer from thrust to lift. The lift transfer or the thrust transfer, or whatever you call it, the fact that somewhere along the line we have to have a diverter valve or some kind to switch the gas from one system to another system. When it comes to ejectors, I think that's the one thing which can be singled out to sort of, from a design point of view at any rate, to make it different. The only other thing I was going to comment on is something that was only touched on latterly in the meeting, and that was by our friend from Lockheed and to some extent by myself, and that was this question of choking the throat of the ejector; personally, I believe that the throat-choking situation is a limiting factor. This is why it's so important that for future ejector we should be operating at pressure ratios with 3.5 and at temperatures of 700 °F. Thank you.

Mark Kelly

Do any of the panel members want to comment on what's been said at the panel? I guess I have one general question. I think I have heard two points of view expressed here into what really the thrust of research ought to be relative to ejector thrust augmentor technology: (1), fundamental study of the basics of the devices themselves, and (2), the design integration of these into aircraft. Looking at some of the theoretical papers here yesterday and the correlation with experiment, I had the impression that some of the basics were beginning to be pretty well understood in terms of getting thrust augmentation ratios of 1-1/2 to 2, and that where we were really in trouble is in trying to go from the idealized models to what you have to do to put it in the airplane. Could I get any of you to comment on that?

Paul Bevelaqua

I'll try. I guess what we're looking at is two separate problems there, really. We have ejectors of a given type that have been demonstrated at, say, model scale, and putting them into the airplane is a different problem, and now other compromises have to be made, brackets and supports, actuators in links, and that's a separate problem from developing a new concept for getting higher performance even out of the model at the original scale. I just remarked that it struck me that this being the first Ejector Workshop, even on the fundamentals we didn't agree yet.

Mark Kelly

That's true.

Paul Bevelaqua

I am not saying that existing model and existing levels of technology and model scale getting it to airplane scale is a separate problem; it should be addressed at the same time as the other and in theory you think about. First, you go to the basic research and then you go to the engineering handbook, and then you go to the airplane. But it's just as often, I think, what happened is some guy that didn't know it wasn't supposed to work, built something and got it to work, and then the theoreticians came back and explained why it should have all along. So we don't want to close off either possibility. Thank you.

Mark Kelly

I am sure we have a lot of tigers out there hungry for red meat, so I want to start with questions from the floor. First is from Ortwerth, AFWL, and addressed to Dr. H. Von Ohain and D. Whittley. It's on the XFV-12. What possible mechanisms can cause the loss of augmentation shown in the

paper (80%) (ejector mass flows apparently correct?) I think the question is referring to the fact that the pressure measurements indicated that the momentum flux is there, and yet the load cells are saying the augmentation is not there.

Paul Bevilaqua

That's the tough problem. I guess I can see the possibility that perhaps the primary thrust isn't being delivered. The augmentors are augmenting what they get, but it's not being delivered, which would be a leakage or duct loss or whatever question. The other possibility is that there is another force which we haven't anticipated or aren't aware of, although we looked at all of these things and can't find anything there and, lastly, there may be something wrong with our conclusion, our surveys. [There may be something wrong with the load cells.] It's not likely. There is only one load cell in the set of data taken in the last week.

Mark Kelly

There is another parenthetical remark I should have read. Are there global effects not considered? I presume this means interference effects such as suckdown on the airframe?

Hans Von Ohain

This is a very good point I believe. I wanted to ask you that question anyway. You see when you have that model, this ejector model which was for centrally oriented propulsive area of 1.6, couldn't be put, a big wing, so to speak, in the vertical position to find out if there is any negative interference up there.

Paul Bevilaqua

Another ejector?

Hans Von Ohain

No! Simulating a wing, so to speak, in which the ejector sits.

Paul Bevilaqua

It was done and it didn't have any negative effect.

Morton Alperin

I was wondering: you have end plates on the ejector in the airplane; is there any blowing on them?

Paul Bevilaqua

Yes, there is; there is end wall blowing on the airplane. I guess we are trying better systems. I am not the best one to ask all the airplane questions. Pete Marshall's been doing the work at Langley.

Morton Alperin

We have found that peripheral distribution of the blowing is pretty important that it should be uniform. When you blow in the corners only, you're going to get separation somewhere else or, if not separation, then crossflow. I just wonder how uniform your blowing was around at the ends. I know you have coanda jets for the sides. Does that end wall blowing match what you had on a scaled-down model or is it different on the airplane from the model?

Pete Marshall (from floor)

They are not very similar. They ended up quite differently.

Paul Bevilaqua

Let me just comment that one of the real insights that I have gotten from looking at your work is the distinction you don't make between side walls and end walls — that is, you treat all the surfaces as lifting surfaces; they all need to do their share of the work. Perhaps it's not right to talk about flaps or side walls and end walls. It's all ejector surface. It all needs to carry part of the lift.

Morton Alperin

Yes! We found that it has to be uniformly distributed, and that's the reason we had a ring vortex and constant circulation to avoid trailing vortices.

Paul Bevilaqua

The difficulty, of course, is folding that up?

Morton Alperin

I recognize the practical problems involved in doing that.

Mark Kelly

I think maybe the key point is that measurements that are really needed to answer the question are just in the process of being made, which would be a detailed exit momentum survey to answer the question of just how uniformly the augmentor is working. Perhaps we should go to the next question.

Question

Could I ask another question with regard to that same thing? Is separation a possible answer to that question?

Pete Marshall

Yes, it could.

Question

Could I ask another question relative to that same thing? What is the wing span? Those tests were made 30 ft above the ground?

Pete Marshall

28-1/2 ft.

Comment

I don't know what the mechanism was; but as far as I'm concerned, the reference length is the wing span, and that's the same order as the height above the ground. It is just not clear to me you are out of ground effect.

Pete Marshall

That is correct. It is not clear. We are out of ground effect.

Morton Alperin

I saw one paper saying that you get additional increased lift in the ground effect.

Paul Bevilaqua

The Hummingbird was that. That was the paper given this morning by Randy Lowry.

Ernest Lewis

That figures in the comment Dr. Von Ohain made about global effect. We are still very concerned with global effect that we have not yet measured.

Mark Kelly

We will move on to the next question, which not surprisingly is again related to the XFV-12, and this is addressed to Paul Bevilaqua and Hal Andrews, a two-part question: How significant is it to achieve successful test of the XFV-21 for maintaining continued interest in ejector studies per se?

Hal Andrews

I guess I can't find any place to hide. I think that we have long considered this a very necessary thing in terms of the overall thrust of our V/STOL activities in the past. I think today that part of it is probably more political than anything, as many things are. I think that we would tend to feel that the question, certainly from a technical standpoint, depends on a whole lot of other things. The effect in the high-level management political arena is, of course, something that none of us can predict, and in that sense we can all discuss it. There are certainly many people who would — and we have evidence from the past that when a major program to demonstrate technology has been completed unsuccessfully — write off that technology in total. There are certainly those people who would take that conclusion to XFV-12 to be the signal for that kind of action. We would hope that we can find enough other pieces of information, evidence, the kind of work that has been talked about today and yesterday, that things won't hang on the question of what finally comes from the XFV-12. But again, I would caution that in the environment that we all exist that certainly is one potential answer.

Paul Bevilaqua

Can I just make a comment? I want to repeat Hans' very insightful comment that the important thing about the XFV is the ejector wing and the ability to make a smooth conversion. The Hummingbird developed enough lift and demonstrated hover, but had quite an oscillation to go through conversion. The important thing at this stage, I think, for XFV-12 is the conversion characteristics. The augmentation can come with the technology.

Mark Kelly

The second part of the question is, "What are the specific problem areas we've ignored in the design of the XFV-12? For example, was the ejector airframe interference adequately studied or developed?"

Paul Bevilaqua

We had a session, as a matter of fact, last week, and we sat down and looked at all the problems here, the interference effect. We did make a study where we had an airplane, an XFV-12-like airplane, cut in half, where we could put the wings, for example, on a load cell but the canards weren't on the load cell. We looked at the interference effect. There didn't seem to be any. We looked at duct losses. They seem to be under control. We're looking at exit surveys, and they seem to be OK. So, we've considered everything, and the answer seems to be that there is no problem except for the load cells.

Pete Marshall

I think there was one significant thing that was not done during the development, for some rather obvious reasons; and that is that is would be very, very difficult. We had a full-span blowing augmentor model that was tested in the laboratory statically and in two different wind tunnels, as a matter of fact. What we never had was a full-span blowing augmentor model with sucking engine inlet systems because that was a very, very difficult model to execute, as you can imagine.

Questioner

I see.

J.A.C. Kentfield

Could I ask whether there was anything done to investigate the effect of that yellow girder work structure that appeared over the top, supporting the aircraft, distributing the load over the top of the fuselage. That looks like an unfaired object fairly close to the ejector inlets. Couldn't it possibly be the source of disturbances and vortex shedding and that sort of thing?

Paul Bevilaqua

It's a possibility, yes, but it's the only engine. And that is something borrowed, so we can't take any chances with it.

J.A.C. Kentfield

You can't get rid of that bit of structure from the top of it? One can't get rid of that yellow girder work structure and hang the airplane up on the fuselage itself?

Paul Bevilaqua

That's correct.

Mark Kelly

The next question is addressed to Dr. Von Ohain. Do you feel optimistic that if the right things are done in the optimum ejector design, ejector propulsion systems can become an attractive alternative device?

Hans Von Ohain

I think we all hopefully agree on that, or most of us. Yes!

Mark Kelly

Alright, the next question, addressed to Paul Bevilaqua, "What, in your opinion, are the most important new developments in our understanding of the detailed ejector parameters that may make them attractive for V/STOL applications?"

Paul Bevilaqua

Well, I can only speak personally. I think the greatest insight I obtained moving from the ARL configuration to the Rockwell configuration was the realization about how the lift is developed on the shrouds themselves — that they are the kind of wing with which we are trying to optimize the leading-end suction rather than normal force. There is a whole technology for airfoil sections. For what kind of airplane you want or what mission you want, you go to the NASA handbooks and pick out your airfoil. There is something we ought to do with proper shaping; also, the jet-flap diffuser effect. If you do not have complete mixing, I believe, you can make up for some of the inadequacies of the complete mixing. That is, you can begin treating it as an airfoil if you put a jet flap on it, which increases the lift and the suction. Those are areas where technology clearly is going to be applied. I think where a breakthrough can come would be in the turbulence. We have hypermixing, but really it's not a very effective or very large increase over the natural turbulence. I think if we really understood this — and I may be talking years down the line — if we really understood the turbulence mechanisms and developed some kind of a flash mixing nozzle, we could see a breakthrough in the development of the ejector.

Mark Kelly

This question is addressed to anyone on the panel that wants to field it: "Is the fluid-to-fluid interaction phenomena on the microscale understood well enough to allow the design of ejectors on the macroscale?" Mr. Sladky can correct me if I'm wrong, but I interpret that question to refer to the problem of whether you can go from first principles of the Navier-Stokes equations to solving the large eddy turbulence that you have in the ejector, or do you need to resort to empirical turbulence models? Is that the gist of the question?

J.F. Sladky

I suspect the entire question of the successful operation of the ejector depends on the way you transfer the energy from primary to secondary, and the question is — from all the papers we have seen today have addressed more or less a macroscopic view of that transfer. Perhaps only one paper, and that obliquely, specifically addressed that very small micro-interface between the two fluids. Now I wonder whether we understand that. I admit, though, that there has been alot of work done, but do we really understand how that transfer takes place?

Paul Bevilaqua

No, I would say we don't. I mean, that's a fundamental question being studied at universities, in government, all over. Einstein gave up on that problem. No, we don't really understand exactly how the energy is transferred from the primary to the secondary. That is why I say the hypermixing is a step in the right direction. But if we really did understand that, there might be the possibility of some sort of a flash mixing nozzle. And we don't understand that.

J.F. Sladky

Are we investigating in the wrong direction?

Paul Bevilaqua

It may be too tough a problem that we won't make a breakthrough on. There's enough going on, I think, in the turbulence area that if it's properly directed and the right questions are asked by the funding sources, maybe it would come from some work that is already going on.

Nagaraja

I have a question to Dr. Von Ohain. I had asked the question, whether he could consider the ejector as a valuable alternative if they are properly designed. The question I have is whether he would consider them (ejectors) as a viable alternative for propulsion even in cruise in subsonic speeds if they are properly designed?

Hans Von Ohain

Yes, I do believe that is definitely a possibility either within the engine in a way you know, like a fan engine or distributed with a wing. But as I pointed out, specifically the ejector offers a unique possibility of acceleration of the boundary layer of the wing. The boundary layer of the wing which is in essence of few centimeters, 5, 10. You could have a spanwise ejector which would operate in the boundary layer. In that case, you would then have the possibility of operating the ejector all the time in flying, as well as for takeoff. But I give the warning at the same time that these are concepts and are not very well understood things right now. I do believe there is very fundamental work necessary. Professor Mercy at Purdue University used the word, "functional integration," meaning, to get the integration of propulsion system with the airframe in such a manner that the functions of both are integrated. Not just simply that you integrate a propulsion system for many miles in the parasitic drag of the propulsion system, but here it is really the unique possibility to gain propulsive efficiency way over and above what propellers or the best fan engines could do. That's an optimistic view you know, as we had at the beginning of the panel.

Morton Alperin

We have done a lot of work in that area, Hans, on our ONR contract. I think you have seen the report in which we attempt to determine the performance of underwater ejectors which utilize the boundary layer.

Hans Von Ohain

Yes! That's a very good point.

Mark Kelly

The next question is from Mr. Streiff of Lockheed for Mort Alperin: "How do you think the Alperin jet diffuser ejector would perform as an axisymmetric ejector?"

Morton Alperin

We have actually built one jet diffuser axisymmetric ejector and one solid diffuser ejector and, although we haven't tested them in complete detail yet, we're still in the process of doing that. They seem to function better than the rectangular, in that these end-effect problems that I discussed don't seem to exist. The problem that we have in doing that work in that area is that it is much more difficult to change the configuration in an axisymmetric ejector than in a rectangular one. You have to build new parts every time you want to change dimension. You can't just open the diffuser. You can extend the walls a little bit, but even that requires special machining.

Mark Kelly

The next question is for Dr. Foa. It's from Dr. Nagaraja from the Air Force: "The rotary augmentor appears to have the potential of providing high-thrust augmentation. Have calculations been made of all the parametric effects such as the total conditions, geometry details on the performance? What are some of the things needed for establishing the liability of the concepts?"

Joseph Foa

Our studies on the early jet have been limited to conditions of forward motion, axial motion. Actually, our work has been on static augmentation, so many of the parameters have not been considered. Our task has been primarily involved in marine propulsion. Outside of those, yes, I think we have considered most of the geometric parameters which may have an effect on the performance. I am sure we haven't considered them all. There are some areas that we haven't investigated yet, for example, the possibility of eliminating the rotor. In fact, we have now an experimental setup which is completed at the Naval Academy where instead of using a rotor, we would utilize propagating stall through a very high-solidity cascade so that the unstalled regions would act like orifices on the rotor. That setup, if it works — as I said, the experiment is ready and we're going to work on it very soon — would make it possible to have a rectangular kind of rotary jet too. But, outside of that, we have only studied axial symmetric situations, mostly in static operation. We had some experiments with forward motion at Cornell many years ago. At that time, we worked both with ducted and unducted rotors. With ducted rotors, we found that the augmentation decreased to practically nothing at around 200 ft/sec; this was air-to-air. Without a duct, in other words, with a completely unducted rotor, there was produced, statically, an augmentation of 1.2 and, strangely enough, with a completely different model at McDonnell Aircraft a rotary jet was tested statically and got an augmentation at 1.2.

Mark Kelly

The next question is for Dr. Alperin from Kentfield of the University of Calgary: "How do you explain the great success of the jet diffuser system when it appears the diffuser area ratio is substantially less than for conventional diffuser, with consequently less surface for the pressure field within the ejector to act upon?"

Morton Alperin

When you say that the diffuser area ratio is substantially less than for a conventional diffuser, I don't know that there is any convention about the diffuser area ratio. Our jet diffuser ejectors have solid diffusers with area ratios up to three. The ones that I described in my paper had solid diffuser area ratios of 2.5. The reason they look smaller is because they diverge at half angles of 45^{o} at the end. So you can get quite a bit more diffuser area ratio in a given space. We've actually run diffusers with exit angles of 60^{o} without any separation. So, the answer to your question is that we don't have smaller diffuser area ratio. We have larger area ratios, because the effect of diffuser area ratio is larger than the geometric effect because of the jet diffusion.

Paul Bevilaqua

Mort, may I make a comment on that, because we do have small diffuser ratios. I think maybe you can visualize it in terms of the slide I had up yesterday, the vortex lattice analysis, where I went through a representation of the jet-flap diffuser as a vortex sheet, following Spence's model. If you consider the effect of a vortex in that sheet on a vortex bound into the shroud, it's to induce a velocity, V cross Gamma, which gives a leading-edge suction. So, in fact, the curvature of the jet sheet which, according to Spence, can be understood in terms of a vortex sheet, induces a velocity or pressure, if you will, on the solid shroud that appears as a force.

Morton Alperin

That can be thought of as a singularity or a supercirculation, or it can be thought of as a larger diffuser area ratio than the geometric — either one would cause that effect.

Mark Kelly

The next question is from Clint Hawkins, Liahona Aircraft Corporation. The question is for anyone on the panel: "With any given ejector configuration in a fixed volume of primary flow in a time frame, may one opt for a relatively large, low-velocity nozzle; and to what degree or range of tolerance may one operate?" Mr. Hawkins, do you want to elaborate on that question?

Hawkins

You have a primary flow source and an option of having a relatively large, low-velocity nozzle or a small-area, high-velocity nozzle, which would give you a better optimization of your mixing and your induced secondary flow.

Whittley

Assuming the same thrust, is that it? Well, I think it is fairly clear that higher augmentation ratios can be achieved at the low-pressure ratios than at high-pressure ratios. As I mentioned earlier, that, in the limit, the throat will choke, so you say you don't want to get a very high-pressure ratio. On the other hand, if you get a very low-pressure ratio, the thing becomes very bulky, so you have to keep in the low range. And I know what you're thinking about, whether 1.5 or 1.3 ratio, or something like that, is reasonable.

Morton Alperin

That's only true for stationary ejectors, wouldn't you say?

Mark Kelly

Static performance, Don?

Whittley

What do you mean by stationary?

Morton Alperin

Not moving.

Whittley

I thought you meant the jet was stationary, or not flapping, or not oscillating. Definitely stationary only — yes!

Paul Bevilaqua

There is a trade that has to be made. If you keep the size of your aircraft the same and you increase the nozzle area, you're decreasing the A2 to A0, or decreasing the area for the secondary so you entrain less air. And as you lower the pressure and increase the size of the nozzle, you're

lowering the ejector inlet area ratio. You're probably increasing the duct diameter — you're forced to — and it may not be the direction to go. It is the trade you have to make in your design.

Morton Alperin

Optimizations of that sort have to consider the machinery also. When you have low pressure, you're going to want a large mass flow to get a given thrust.

Mark Kelly

Do we have a question from the floor over here?

Paul Massier, JPL

Let's assume that we eventually get to the point to where we understand the fluid mechanics of the ejector and that we can achieve good performance. Say we understand the entrainment mechanism, be it steady-flow or pulsating-flow, whichever gives us the best, and we determine how to integrate into an airplane system taking into consideration the design. Is there any concern associated with the noise that might be created by these ejectors? Because, especially in the pulsating-flow situation, you know, you can have shock-associated noise, you can have screech, you can have jet crackle, you can have noise that's coming from the fine-scale turbulence jet noise. There's all kinds of things. I just wondered if you'd considered this?

Mark Kelly

Anyone want to take a shot at that?

Don Whittley

I think The Boeing Company did a lot of work for NASA on the noise of the ejector flap, and they found that it could be used to suppress noise. And basically what they found was that when you have a slot nozzle of some sort, you reduce the characteristic dimension of the jet. By the time you take the thrust, you distribute that along the wing — you think of the little narrow slot — and this pushes the frequency of the noise, the spectrum, to noise at high frequencies. And then what they did was to line the flaps, and they can then tune the lined flaps to suppress the noise. In actual fact, PNdB-wise, the noise increased by going to the slot, because it shot it up to the appropriate frequency, but they found that with lining the flaps this could be greatly reduced. So, a fair bit of work has been done on that and published.

Mark Kelly

Well, I know that the pulsed ejectors that were operated by Lockwood up at Hiller years ago were extremely noisy. That was an inspiring noise that they put out. They didn't really, I don't believe, make any attempt to quiet that or have the opportunity to try to quiet that, because the noise in that case is impulsive. There is a lot of high-frequency content, and you are running it by a lot of surface. So, it's not apparent to me that you couldn't at least alleviate that to some degree. But you're correct — the pulse ejectors that I have heard of are extremely noisy. On the other hand, the steady-flow ejectors can be made quiet, compared to conventional nozzle or even open-daisy nozzle.

Hans Von Ohain

I would like to make one comment to that. When we had ejectors and put these hypermixing devices on the primary nozzles, the noise was way down. Now, we couldn't explain it. Brian Quinn called me in and said, "Look, that's so low a noise." It worked wonderfully. And the moment that the ejector worked very well, then it was extremely low in noise. The other time, when we took these devices off, it screeched and was very high-pitched and a strong noise. So, we did not at that time investigate this point more, because we had other headaches. But that was an observation that I want to tell you.

Joseph Foa

May I add something to that? At Cornell many years ago, Cornell Laboratory worked on wave engines that are noisier than the pulse jet. When a shroud was placed around the exhaust of the wave engine along with the shroud acting as an ejector defector, the noise level went way down.

Pete Marshall

I could add to that a comment that we did have some experimental data at one point. In fact, at Columbus, we had a large, full-scale augmentor running which happens to be powered by two J-85 engines. We also happened to build the T-2 trainer which is powered by two J-85 engines. At one point, we made comparative noise measurements of the two, and the augmentor-powered version was 13 dB down from the ordinary airplane. The higher the augmentation the more the entrainment; the more the entrainment, the lower the exit velocity and, therefore, the noise. Steady flow.

Mark Kelly

Are there any other comments or questions?

Robert Weinraub

Just a question from an outsider to this whole area. Has anyone ever looked at the possibility of utilizing some combustion combination with the primary jet to enhance entrainment and, therefore, increase augmentation?

Morton Alperin

We studied the influence of temperature of the primary jet. Do you mean combustion in the ejector itself?

Robert Weinraub

For flame propagation as a mechanism for enhancing turbulence, and it's unsteady. I don't pretend to understand all of the ramifications, but has that ever been looked at?

Morton Alperin

I don't know whether you could burn in a primary jet, because the speed is at such a high velocity.

Robert Weinraub

I meant as a primary exit into the ejector itself and maybe have a slightly fuel-rich mixture that would utilize the secondary air to sustain combustion.

Morton Alperin

You get pretty high velocities in the ejector, even in the mixing section, if it's a well-designed ejector. Anything you put in there would give you trouble in the way of flame holders. I don't know. I have not heard of anyone doing it.

Paul Bevilaqua

Let me make a comment. We haven't done any experiments on that. But if you think about what happens when you add energy to the air stream by burning if you simply have a radiator or a burner in an air stream, the effect is to cause the stream to expand. But as you go downstream and it recovers back to atmospheric pressure, there is no net thrust added to a stream just by burning. Take a ram jet, for example. You have to have a duct around it, and the streamlines tend to expand behind the burner discs; it causes them to contract. So it works opposite to the way the ejector shroud works. It develops a lip thrust on the ram jet shroud. That's what really causes the

thrust in that case, by just the simple addition of heat. So in an ejector where you want to diffuse to get large augmentation, the effect of burning is going to be contrary to that, and then probably on those grounds would hurt you.

Robert Weinraub

I was thinking more in terms of a small amount of burning to enhance unsteadiness in the primary jet.

Paul Bevilaqua

We haven't performed an experiment. I'm just saying on those fundamental one-dimensional grounds would indicate that burning would hurt you.

Duvvuri

There was an Edwards Air Force Base contract some time back in 1965. It concerned itself with air-augmented-rocket combustion. That is essentially like an ejector, you see, except that the primary has the two-phase flow with particulates like aluminum and titanium, which were supposed to combust when they came into the duct. It was very much like the system that you are talking about, and there was theoretical as well as experimental work done. This was around 1966 or 1967, and some of this work was reported in AIAA journals. So that answers part of your question, whether this work has been done. Yes, it has been done. The other question about the ejector effect on noise — some work has been done at Rohr Industries on this also. Some of this work, in which I was involved, was on both of these things: the air-augmented-rocket combustion, as well as the ejector noise characteristics. There was also work done at Rohr Industries, where they were trying to find out if we could suppress the noise of a jet by using an ejector. This work is also part of what is recorded in the Journal of the Acoustical Society of America around 1970. There was some paperwork also done on how the ejector reduces the noise of the jet.

N. Malmuth

Just a question to the panel. We heard a lot about the adequacy of bringing subscale models and relating them to full-scale testing. I'm wondering what the overall opinion is as to the adequacy of theoretical modeling at this state. Are we satisfied with theoretical modeling — and I am not talking strictly of the microscopic processes and how they relate to macroscopic, but I am talking about such things as the unsteady flow effects, three-dimensional flow effects, and those kinds of things. Do we feel that we can adequately characterize what's going on? Also, some of the people talked about pressure ratio effects and temperature ratio effects. We know that there are unsteady one-dimensional models that handle compressible flow

effects, but what I am talking about is the development of two-dimensional shock wave or transonic patterns in these ejectors. Have they been adequately modeled? Can we understand what kind of processes they are?

Paul Bevilaqua

The ejector, of course — the classic viscid-inviscid interaction with streamwise stretching and compressibility effects and lateral gradients, and so forth. No, we are a long way from being able to compute the performance of a finite, three-dimensional ejector configuration. The furthest we have come is two-dimensional configuration — static — and then you add the wind on and the ground effects. And we can't do anything right now, really. There is a long way to go in that area.

Mark Kelly

The theory is a very useful guide, isn't it?

Paul Bevilaqua

Yes, the theory provides understanding to the designer. With the right combination of model tests and two-dimensional analysis, you can come up with a correction factor to the two-dimensional analysis to correct for taper, finite aspect ratio, and so forth. But it may be beyond the scope, although some of the people at the Ames Numerical Analysis Branch up here might disagree. But it may be beyond our present scope to try to compute a whole three-dimensional ejector airplane in ground effect during hover transitions.

N. Malmuth

I think, however, that we can make inroads in certain parts of the problems we have heard about. I think that work should continue.

C. Donaldson

I believe it's a major effort at the Ames Laboratory over the next ten years to be able to predict three-dimensional separation — and that's a real bear! I have worked on as complicated models of turbulent transport as there are; and at the present time, anybody who says that he has some scheme for computing three-dimensional separation is either lying or stupid. How soon we'll get to the ability to do that is a really long-range problem. In general, for diffusers, I have been trying to compute the performance of them for thirty-six years now. If it works, I can compute boundary at the layer end. If it doesn't work, I can't. And I don't know when it's not going to work, because my techniques aren't that good. And that's just about where it is. You cannot use these things as a diagnostic tool to tell you when it's going to not work. We can only give it some idea of why they work when they do.

Mark Kelly

That was Donaldson from ARAP who made that comment.

Dave Koenig

My question is addressed, I guess, to all the panel. I would like to know what are the real limits in thrust loading, since thrust loading is the key to packaging in the complete aircraft system. Are there other things besides sonic flow on the throat? Is that agreed upon by the panel?

Morton Alperin

You mean, is there an upper limit to the thrust-augmentation capability?

Dave Koenig

No, the actual thrust coming out the augmenter before the augmentation really drops off.

Morton Alperin

I think the answer to that involves some consideration of the losses that would occur if you were choked and what kind of shocks you would get in the diffuser. It's a pretty complicated subject. I don't think you can go much higher than the choking limit, though, as far as the thrust loading.

Paul Bevilaqua

I think that we would agree that secondary or compound choking can be a configuration limit, you know, that incompressible analysis wouldn't show. Another limit might be the suction that you can develop on the leading edges. If you make those leading edges too sharp, they won't develop any lift. With a sharp leading edge, you require infinite vacuum for zero radius that might be enough for fundamental limit, whereas the throat and nozzle area might suggest that you get a certain level of augmentation. If your upward-looking surfaces were too narrow, that might prevent you from reaching it. That would be another fundamental limit. It seems another fundamental limit might be thought of in terms of the diffuser area ratio or increasing the angle of attack of the flaps. As you increase the angle of the wing, the lift doesn't increase monotonically. You reach some point where you're 90^{o} to the relative wind, and you're not developing any circulation. It could be something analogous to that, fundamentally, limiting the ejector. We have seen in some of our experiments that we may be reaching that limit. That is, we continue to open the diffusers and the $\emptyset$ peaks and starts to fall, even though there's no separation occurring yet. I think what might be happening in there is

that the normal force or the download on the lower surface of the shroud is bigger than the upload, and we passed over a peak that's a fundamental limit on that configuration. Offhand, I can't think of any others, although there certainly are probably some.

Nagaraja

I have two questions. One is related to ejector application other than thrust augmentation, such as air-conditioning, cooling, heating of structures, and so on. Has any study been made on the potential of ejector application for pumping?

Morton Alperin

One of the first uses of ejectors were as pumps, as you know. For certain applications, they are without any competition. Now, in other cases, where efficiency and size are important, they're not as good as mechanical pumps.

Joseph Foa

May I add something to that? The oldest pumps were steam ejectors, and they were extremely effective. We did some work with rotary jet pumps, using water as a primary and water as a secondary, and they work quite well. Again, this kind of work was also done at McDonnell Aircraft and checked for what we have done. As far as other applications — other applications of the ejector, other applications on the same principle that we applied to the rotary jet, mainly utilizing the work for the interface pressure forces — as far as that is concerned, we have done some work too. We have a device which does what a Rank-Hilsch tube would do. In other words, given input flow of a certain temperature, you get two outputs: one with a higher temperature, and one with a lower temperature. The energy being transferred from one subflow to the other, not through viscous stresses but through interface pressure forces and the energy transfer efficiency, is very much greater than in the Rank-Hilsch tube. The dissipation is practically nil. So, there are many other applications in the same area.

Nagaraja

My next question is, how much of a practical gain can be made by putting more effort into understanding the basic turbulence mechanism into the nozzle design, and so on. Would it be practically meaningful for gaining the significant thrust augmentation? My feeling, as Dr. Von Ohain pointed out, maybe we need to develop new concepts of the configurations, rather than looking for fundamentals. It is useful to look more fundamentally into the effects of mixing processes, turbulent mechanism, and so on. But I think we need to spend more time and effort on the new concept developments for getting some significant gains in the thrust augmentation. Does any member of the panel have a comment on this?

Whittley

I am probably the most unqualified of most of the members on the panel to answer that question. But, nevertheless, I will have a go at it, because it seems to me that it has been explained and we all understand about the mixing process. In the mixing process, momentum is conserved. Thrust is momentum. So, it seems to me that very often we talk about promoting mixing, but all we really mean is distributing the jet more uniformly. Our experience has been that a jet — any kind of jet — entrains the flow and will give you interface mixing that you are looking for. We found that the important thing to do is to distribute the jet in the throat. You're looking for uniformity downstream, trying to achieve, at least to some extent, as uniform an exit distribution as possible. So, if that is one of the objectives, one of the easiest ways of achieving that is to distribute the jet as evenly as possible in the throat. And what we have found is that when you do that, you've got a built-in stability to the thing. This comes back to some of the discussion earlier. So, I would tend to think that you're right. There is a lot of work going on in study of turbulence, and certainly a lot on entrainment of coanda jets and things like that. By and large, even though we might not know the mechanisms — the detail mechanisms of it — we know the entrainment rates. So, all we need to know as engineers is that sort of entrainment rate of the secondary and the primary. Once we know that, we can then do some studies.

J.A.C. Kentfield

I would like to ask, if I may, what do the panel think about ejectors used for hot primary flows? I have heard several people express, during the last couple of days, some kind of satisfaction, I think, that thrust-gain-augmentation ratio didn't seem to fall off very much with increasing temperature, or fell off a little but not very significantly. But, in reality, one should get a thrust gain. The comparison between the ejector and some more reversible device becomes worse when you heat the primary flow and have a cool secondary flow. If the opposite is true and you're fortunate enough to have a cool primary flow and a hot secondary flow, the ejector comes out better or can come out better than, say, a turbine machine or an isentropic reversible ideal competing device. And if one takes reasonable compressor and turbine efficiencies for some sort of synthetic reversible machine, the comparison between that and the ejector worsens as the primary temperature increases.

Hans Von Ohain

Let me say one thing. When you heat at constant pressure the primary air, you must realize that you now reduce with the square root of the temperature inversely with the primary mass flow. Even so, energywise there is somewhat more energy now going through that nozzle. The mass flow is smaller; the velocity is higher. But in any event, the primary thrust is the same, because you have the same pressure and the same cross-sectional area. The primary thrust would be the same if you have constant pressures in the primary jet and start heating; and the thrust augmentation ratio goes down eventually, because the primary mass flow goes down.

Joseph Foa

Isn't it also true for nonsteady flow ejectors? The primary mass flow goes down; and yet, if the density ratio from secondary to primary is high, it's the other way around. It's only for a steady flow?

Hans Von Ohain

Right, because the nonsteady is a very good and highly efficient one, while the efficiency of the friction ejector was just based on the velocity differential in the mixing section increases.

J.A.C. Kentfield

I did some calculations on this, and I have converted something in my head. So, very roughly, for a temperature ratio of 1.6, one should expect 30% higher augmentation ratio as the result of doing this, if one is able to maintain the same efficiency, if you want to use that expression, of the ejector. In fact, the augmentation ratio remained about constant, which seems to indicate what one has to put up with — this unfortunate situation — for the other advantages of the device: no moving parts, and simplicity of it. Nevertheless, the comparison between the ejector and some potentially more reversible device worsens as you heat up the primary flow.

Hans Von Ohain

But you can make it more general. Say, with the primary medium having a higher sonic speed than the aspired medium, then the efficiency of the energy transfer force goes rapidly down. The other way around, if you take an ejector, let's say you use mercury vapor vs hydrogen as the expired medium, the efficiency is phenomenal. You have an efficiency of 90% energy-transfer-wise. Because the velocity differential in the mixing duct goes up in the case where you have a low sonic-speed medium and the efficiency, and it goes way down when you have a high speed, hydrogen vs mercury would be bad and mercury vs hydrogen would be good.

J.A.C. Kentfield

It seems to suggest that the case for the ejector is very good. When your engine is a turbofan and you're tapping off the fan flow as the primary stream, the case is at its best. If one has a turbojet or heated flow anyway, the justification is harder to make for the ejector other than its mechanical convenience.

Morton Alperin

There again, you're only talking about V/STOL ejectors. As a thruster, the situation is quite different. If you have a hot primary jet, the heat corresponding to the temperature above ambient is wasted; whereas if you put an ejector around it and utilize some of that heat to heat, the induced flow, the same total amount of heat is still ejected from the rear end but at a lower temperature. You recover some of the thermal energy in the form of thrust.

Joseph Foa

I recommend that, too. I think, here again, this applies only to steady-flow machine. In a nonsteady-flow machine, you can extract mechanical energy from the hot gas and expel it at a lower temperature. So, in that case, you can really take the exhaust of the turbojet and use that as the primary.

J.A.C. Kentfield

In other words, there does seem to be a case for looking at your pulsating device, the flip-flopping jet. Especially, there is a stronger case for doing this — for bothering with the things — if one's going to use a hot primary stream, I think.

Joseph Foa

May I ask one question, a very brief one? How is the augmentation defined in the case of the lifting ejector, that is, for motion? I heard Dr. Alperin gave some figures of augmentation in forward motion higher than in static operation. How does that happen? How is that defined?

Morton Alperin

The curve I showed, which showed an increase in augmentation, included the lift on a fairing which was attached to the leading edge of the ejector. The ejector was normal to the flow direction.

Joseph Foa

So, it was like a scoop, scooping air in from the free stream?

Morton Alperin

It was the upper surface of the wing. The inlet to the ejector was on the upper surface, and the leading edge of the wing developed a very high lift as a result of the supercirculation created by the flow through the ejector.

Joseph Foa

How would it be defined?

Morton Alperin

It is defined as the total lift force divided by the isentropic thrust of the jets, expanded to ambient pressure. We use only the total lift difference between the ejector-on and the ejector-off conditions in calculation of thrust augmentation ratio.

Joseph Foa

Suppose you had no primary and you had a scoop capturing free-stream air and deflecting vertically down. You would have an increase of lift.

Morton Alperin

You would have a moment. I don't know if you would have a lift — just vertically down. Yes.

Joseph Foa

You would have a lift without the primary?

Morton Alperin

That's right.

Joseph Foa

So, wouldn't that definition lead to the situation where you would have an infinite augmentation where you don't have a primary?

Morton Alperin

When the ejector is not powered, no augmentation can be calculated, and the forces are then considered as tare forces to be deducted from the total forces when the ejector is operational.

C. Donaldson

That's why they use the term, "supercirculation." It's the circulation you get in addition to what you get when the ejector isn't running.

Morton Alperin

The power-off lift would be subtracted from what you get when the ejector is in operation. That's exactly what we did.

Mark Kelly

I have a comment on your comment. I think that is to read very carefully the definitions by the man who runs the experiment, because he usually defines it in terms of what he can measure accurately. You have the same problem in all types of V/STOL aircraft, including helicopters. It is a very difficult thing to come out with a universal definition of something that is as complicated as thrust augmentation and supercirculation.

Morton Alperin

In addition to defining thrust augmentation, I think, whoever is writing the paper should give enough information to permit conversion to someone else's definition.

Mark Kelly

Gentlemen, we're well past 3 o'clock, and it looks like we could keep on going until midnight, so I'm going to put a stop to this. I want to thank the members of the panel and particularly the Navy and the North American people for bareing their souls on the XFV-12 at a time when all the cards aren't on the table yet and all the facts aren't in. And thanks to the members of the conference here for all their interest and their participation with the interesting questions here at the panel. I'll turn this back over to Mr. Lopez for some parting comments.

Armando Lopez

Just a couple of parting, quick comments. We now have some copies of Dr. Ortwerth's paper out in the lobby, in case somebody wants to pick them up; that is, copies of the viewgraphs. There is also in the lobby a list of attendees for everybody who wants them, and you can get them on the way out. For those of you who signed up for a tour of Ames tomorrow, I'll pick you up at the Visitor Center at about 9 o'clock. If anybody is interested in seeing the deHavilland augmentor model for the 40 by 80, Mr. Koenig has volunteered to take you over and show it to you. One parting comment — there is still some coffee out there if somebody still wants to drink a few cups. Thank you, gentlemen.

1. Report No.	2. Government Accession No.	3. Recipient's Catalog No.
NASA CP-2093		

4. Title and Subtitle	5. Report Date
WORKSHOP ON THRUST AUGMENTING EJECTORS*	6. Performing Organization Code

7. Author(s)	8. Performing Organization Report No.
Edited by A. E. Lopez and D. G. Koenig, Ames Research Center, Moffett Field, Calif.; D. S. Green, Naval Air Development Center, Warminster, Penn.; and K. S. Nagaraja, Air Force Flight Dynamics Laboratory, Wright-Patterson Air Force Base, Dayton, Ohio	A-7887
9. Performing Organization Name and Address	10. Work Unit No.
Ames Research Center, NASA Moffett Field, Calif 94035	505-10-31
	11. Contract or Grant No.
	13. Type of Report and Period Covered
12 Sponsoring Agency Name and Address	Conference Publication
National Aeronautics and Space Administration Washington, D.C. 20546	14. Sponsoring Agency Code

15 Supplementary Notes

*Cosponsored by NASA-Ames Research Center, Naval Air Development Center, and Air Force Flight Dynamics Laboratory, held at Ames Research Center, Moffett Field, California, June 28-29, 1978.

16. Abstract

The proceedings of the Workshop on Thrust Augmenting Ejectors held at Ames Research Center, Moffett Field, California, on June 28 and 29, 1978, are reported in this Conference Publication. This workshop was sponsored by NASA/Ames Research Center, Naval Air Development Center, and Air Force Flight Dynamics Laboratory.

The purpose of this workshop was the dissemination of progress and to point the desired direction of future studies in all aspects of Ejector Thrust Augmenting Systems. Following the presentation of the formal papers a panel composed of some advocates of Ejector Thrust Technology Development presented their impression of the workshop, reviewed briefly the state of the art in ejector technology, and pointed out the desired direction of future research.

Contributions to this workshop were made by representatives from NASA Ames and Lewis Research Centers, Boeing Aircraft Company, Rockwell International, Air Force, Navy, George Washington University, Wright State University, Duvvuri Associates, Vought Corporation, Jet Propulsion Laboratory, University of Calgary, Flight Dynamics Research Corporation, Lockheed California Company, The de Havilland Aircraft of Canada, Ltd., University of Queensland, and University of Virginia.

17. Key Words (Suggested by Author(s))	18. Distribution Statement
Ejectors Jets Thrust augmentation Powered lift V/STOL A/C	Unlimited STAR Category - 02

19. Security Classif. (of this report)	20. Security Classif. (of this page)	21. No. of Pages	22. Price*
Unclassified	Unclassified	520	$15.25

*For sale by the National Technical Information Service, Springfield, Virginia 22161

National Aeronautics and
Space Administration

Ames Research Center
Moffett Field, California 94035

Official Business
Penalty for Private Use. $300

THIRD-CLASS BULK RATE

Postage and Fees Paid
National Aeronautics and
Space Administration
NASA-451

U.S.MAIL

NASA

POSTMASTER: **If Undeliverable (Section 158 Postal Manual) Do Not Return**